Functional characterization of small non-coding RNAs of *Neisseria gonorrhoeae*

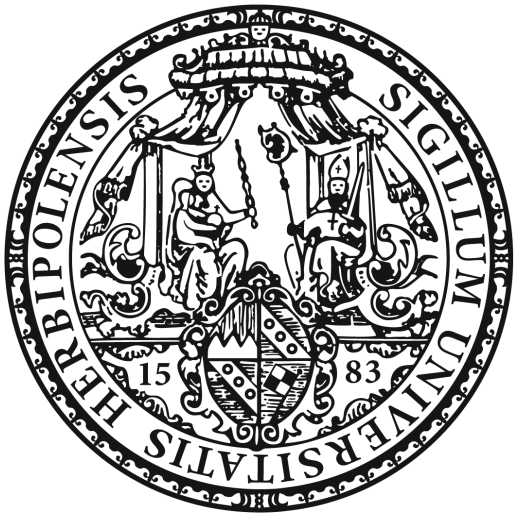

DISSERTATION

zur Erlangung des

naturwissenschaftlichen Doktorgrades

der Julius-Maximilians-Universität Würzburg

vorgelegt von

Marie Zachary

aus München

Würzburg, 2021

This document is licensed under the Creative Commons Attribution-NonCommercial-NoDerivatives 4.0 International License (CC BY-NC-ND 4.0): http://creativecommons.org/licenses/by-nc-nd/4.0 This CC license does not apply to third party material (attributed to another source) in this publication.

Eingereicht am:

Mitglieder der Prüfungskommision:

Vorsitzender:
Erstgutachter: Prof. Dr. Dagmar Beier
Zweitgutachter: Prof. Dr. Cynthia Sharma

Tag des Promotionskolloquiums:

Doktorurkunde ausgehändigt am:

TABLE OF CONTENT

SUMMARY

During infection, bacteria need to adapt to a changing environment and have to endure various stress conditions. Small non-coding RNAs are considered as important regulators of bacterial gene expression and so allow quick adaptations by altering expression of specific target genes. Regulation of gene expression in the human-restricted pathogen *Neisseria gonorrhoeae*, the causative agent of the sexually transmitted disease gonorrhoea, is only poorly understood. The present study aims a better understanding of gene regulation in *N. gonorrhoeae* by studying small non-coding RNAs.

The discovery of antisense RNAs for all *opa* genes led to the hypothesis of asRNA-mediated degradation of out-of-frame *opa* transcripts. Analysis of asRNA expression revealed a very low abundance of the transcripts and inclusion of another phase-variable gene in the study indicates that the asRNAs are not involved in degradation of out-of-frame transcripts.

This doctoral thesis focuses on the analysis of *trans*-acting sRNAs. The sibling sRNAs NgncR_162 and NgncR_163 were discovered as post-transcriptional regulators altering expression of genes involved in metabolic processes, amino acid uptake and transcriptional regulation. A more detailed analysis by *in silico* and transcriptomic approaches showed that the sRNAs regulate a broad variety of genes coding for proteins of central metabolism, amino acid biosynthesis and degradation and several transport processes. Expression levels of the sibling sRNAs depend on the growth phase of the bacteria and on the growth medium. This indicates that NgncR_162 and NgncR_163 are involved in the adaptation of the gonococcal metabolism to specific growth conditions.

This work further initiates characterisation of the sRNA NgncR_237. An *in silico* analysis showed details on sequence conservation and a possible secondary structure. A combination of *in silico* target prediction and differential RNA sequencing resulted in the identification of several target genes involved in type IV pilus biogenesis and DNA recombination. However, it was not successful to find induction conditions for sRNA expression. Interestingly, a possible sibling sRNA could be identified that shares the target interaction sequence with NgncR_237 and could therefore target the same mRNAs.

In conclusion, this thesis provides further insights in gene regulation by non-coding RNAs in *N. gonorrhoeae* by analysing two pairs of sibling sRNAs modulating bacterial metabolism or possibly type IV pilus biogenesis.

ZUSAMMENFASSUNG

Bakterien müssen sich während des Infektionsprozesses an eine sich veränderte Umgebung anpassen und sind dabei zahlreichen Stressfaktoren ausgesetzt. Kleine, nicht-kodierende RNAs gelten als wichtige Regulatoren der bakteriellen Genexpression und ermöglichen daher eine schnelle Anpassung durch eine Veränderung der Expression spezifischer Ziel-Gene. Die Regulation der Genexpression des Humanpathogens *Neisseria gonorrhoeae*, Auslöser der Geschlechtskrankheit Gonorrhö, ist bis jetzt kaum verstanden. Die vorliegende Studie soll durch die Analyse kleiner, nicht-kodierender RNAs zum besseren Verständnis der Genregulation in Gonokokken beitragen.

Durch die Entdeckung von antisense-RNAs für alle *opa* Gene wurde die Hypothese entwickelt, dass diese für den Abbau von *opa* Transkripten außerhalb des Leserahmens verantwortlich sind. Eine Analyse der asRNA Expression zeigte jedoch, dass diese sehr wenig exprimiert werden und auch die Untersuchung eines anderen phasenvariablen Gens weist darauf hin, dass die asRNAs keine Bedeutung für den Abbau von Transkripten außerhalb des Leserahmens haben.

Der Schwerpunkt der Doktorarbeit liegt auf der Untersuchung *trans*-codierter sRNAs. Die Zwillings-sRNAs NgncR_162 und NgncR_163 agieren als post-transkriptionelle Regulatoren, die die Expression von Genen verändern, die bei Stoffwechselprozessen, Aminosäureaufnahme und transkriptioneller Regulation eine Rolle spielen. Eine detailliertere Analyse durch *in silico*- und Transkriptom-Studien zeigte, dass die sRNAs ein großes Spektrum an Genen regulieren, die für Proteine des Zentralstoffwechsels, der Aminosäurebiosynthese und des –abbaus, sowie zahlreicher Transportprozesse kodieren. Die Expressionslevel der Zwillings-sRNAs hängen von der Wachstumsphase der Bakterien und dem Wachstumsmedium ab. Das weist darauf hin, dass NgncR_162 und NgncR_163 eine Rolle bei der Adaptation des Stoffwechsels von Gonokokken zu bestimmten Wachstumsbedingungen spielen.

In dieser Arbeit wird zudem die Charakterisierung der sRNA NgncR_237 initiiert. Im Rahmen von *in silico* Analysen wurde die Sequenzkonservierung und mögliche Sekundärstruktur untersucht. Eine Kombination aus *in silico* Zielgen-Vorhersage und differentieller RNA Sequenzierung führte zur Identifizierung zahlreicher Zielgene, die in der Biogenese von Typ IV Pili und DNA Rekombination eine Rolle spielen. Allerdings konnten keine Induktionsbedingungen für die sRNA Expression gefunden werden. Interessanterweise konnte eine mögliche Zwillings-sRNA identifiziert werden, die dieselbe Targetinteraktionsdomäne wie NgncR_237 hat und somit dieselben Zielgene regulieren könnte.

Zusammenfassend ermöglicht diese Arbeit neue Einblicke in die Genregulation durch nicht-kodierende RNAs in Gonokokken, indem zwei Paare Zwillings-sRNAs analysiert wurden, die den bakteriellen Stoffwechsel anpassen oder möglicherweise eine Rolle in der Typ IV Pilus Biogenese spielen.

1 INTRODUCTION

1.1 *Neisseria gonorrhoeae*

Neisseria gonorrhoeae was discovered in 1879 by the German physician Albert Neisser, who first called the bacterium *micrococcus* (Neisser 1879). The gram-negative diplococcus has a diameter of 0.6 to 1 µm and belongs to the family Neisseriaceae within the class of betaproteobacteria. The genus *Neisseria* comprises a great number of species of which eleven colonize humans. Most of the species are commensal bacteria like *N. lactamica* and *N. polysaccharea,* which can be isolated from the nasopharynx. Nevertheless, there exist also two pathogenic species, namely *N. gonorrhoeae* and *N. meningitidis* (Knapp 1988). *N. gonorrhoeae* are fastidious organisms that require enriched growth media (Spence et al. 2008). They were first considered to be obligate aerobe, however, if provided with nitrite as electron acceptor they are also able to grow under anaerobic conditions (Knapp and Clark 1984).

1.1.1 Pathogenesis and therapy

N. gonorrhoeae is the causative agent of the disease gonorrhoea, which is the second most common bacterial sexually transmitted disease worldwide. In 2012, there were approximately 78 million new cases of gonorrhoea in the world; between 2005 and 2008, the number of infections increased about 20 % (WHO 2016). The Center for Disease Control estimates that there are 820,000 infections in the US every year (CDC 2017). The reporting of gonorrhoea is incomplete since the highest incidence of disease occurs in less well developed countries (CDC 2001).

Another problem is the high number of carriers not showing any symptoms. Approximately 10 % of men and 50 % of women have an asymptomatic gonorrhoea (Creighton 2014). Infection occurs usually via unprotected sexual contact and so mainly affects the urogenital tract, but also the rectum or throat. Women suffer from vaginal discharge or lower abdominal pain caused by an inflammation of the uterine cervix. Untreated gonorrhoea can lead to complications like pelvic inflammatory disease and ectopic pregnancy, which possibly results in infertility. In men, uncomplicated infections mainly manifest as urethritis but they can also develop prostatitis (Smith and Angarone 2015). *N. gonorrhoeae* is in 0.5-3 % of the cases able to break through the epithelial barrier and spread within the human body. The disseminating gonococcal infection is characterized by a severe arthritic condition and can also manifest as meningitis or endocarditis (O'Brien et al. 1983).

Approximately 20-50 % of patients carrying *N. gonorrhoeae* are co-infected with *Chlamydia trachomatis,* which is the leading cause of bacterial sexually transmitted diseases in humans (Creighton et al. 2003, Kahn et al. 2005). Additionally, the presence of sexually transmitted

infections is increasing the likelihood of HIV transmission. An explanation would be that the produced chemokines and cytokines modulate HIV infectivity and it was further shown that gonococci recruit CD4+ T cells into the endocervix (Mabey 2000, reviewed in Jarvis and Chang 2014).

Infections with *N. gonorrhoeae* are diagnosed either by microbiological cultures or nucleic acid amplification tests of urine samples, urethral swab, or cervical swab; in men with urethritis also Gram staining is used (WHO 2016).

In the last decades, a broad range of antibiotics has been used to treat *N. gonorrhoeae* infections. However, due to easy availability and improper use of antibiotics combined with the natural competence of the bacteria, the number of still usable treatments is small and results in the classification of *N. gonorrhoeae* as a “superbug” (Goire et al. 2014, Unemo and Shafer 2014). The first used antimicrobiols were sulfonamides introduced in 1940, but already in the late 1940s more than 90 % of the gonococcal isolates were resistant (Kampmeier 1983). Starting from 1943 penicillin was used to treat gonorrhoea. First cases of antibiotic resistance were reported already in 1946; nevertheless, it took around 40 years until penicillin had to be abandoned. In the meantime also tetracycline and spectinomycin were applied, but for both high-level resistant strains started spreading in the 1980s (Unemo and Shafer 2014). Other and more recently used antibiotics - quinolones, macrolides and cephalosporins - also raised resistance in the 1990s. As the last line defence is now considered a dual therapy of 3rd generation cephalosporins and azithromycin. However, in 2010 the first ceftriaxon-resistant strain was isolated; in 2015 already 7 % of the analysed strains showed resistance to azithromycin and in 2017 a multidrug-resistant strain was found in France (Cole et al. 2017, Poncin et al. 2018). This is making the search for novel antimicrobials an urgent necessity and requires also a better understanding of the pathogen.

1.1.2 Major gonococcal virulence factors

Pathogens express virulence factors for efficient host colonization. Virulence factors are molecules important for attachment and invasion of host cells, obtainment of nutrients from the host or evasion of the immune system. *N. gonorrhoeae* expresses a wide range of virulence factors. Type IV pili play a role in the initial adhesion to the host cell, whereas opacity-associated proteins (Opa proteins) are important for tight binding and invasion of epithelial cells. Porins play a role in the passage of small molecules through the membrane as well as in the invasion of non-professional phagocytes. Lipooligosaccharides (LOS) and IgA1 protease are virulence factors for evasion of the host immune system.

1.1.2.1 Type IV pili

One of the major virulence factors of *N. gonorrhoeae* are type IV pili. Pili are hair-like appendages on the surface of bacteria (figure 1.1A) that can reach a length of several micrometers, in comparison to the diameter of gonococci, which is only approximately 1 µm (Craig et al. 2006). Type IV pili are important for various functions, including aggregation of bacteria (Swanson et al. 1971), adhesion to host cells (Virji et al. 1992), twitching motility (Henrichsen 1975), DNA transformation (Sparling 1966) and host cell cytotoxicity (Dunn et al. 1995). Though research on pili is done for several decades now, the assembly of the pilus apparatus and the mode of action is only poorly or not at all understood. This is especially true for DNA transformation, where DNA carrying a specific DNA uptake sequence (DUS) is recognized and taken up into the bacterial cell. A possible model for the type IV pilus apparatus is shown in figure 1.1B.

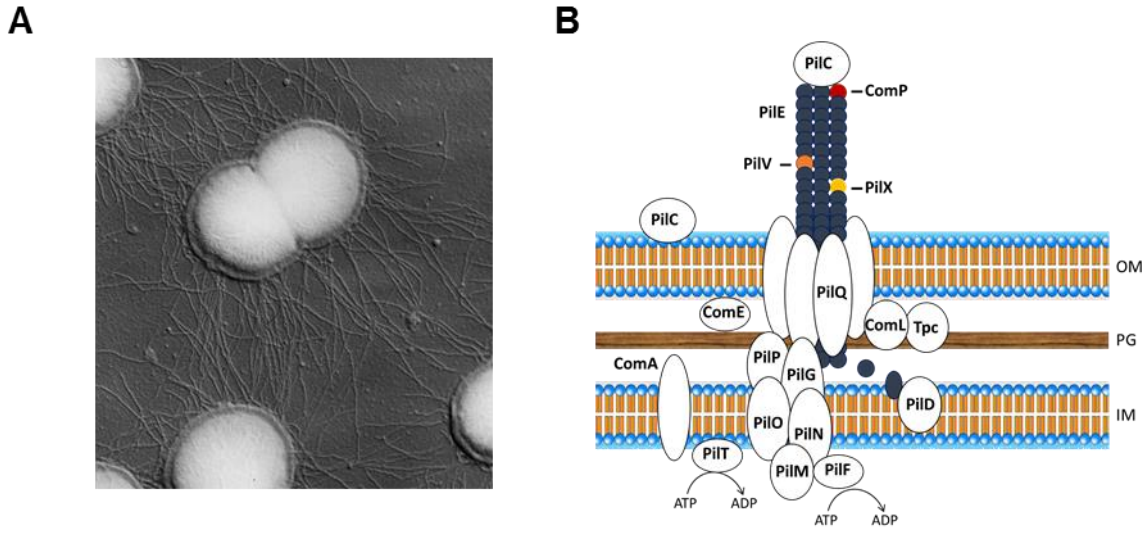

Figure 1.1: Pili of *Neisseria gonorrhoeae*. (A) Scanning electron microscopy of type IV pili *on N. gonorrhoeae* diplococci. The filaments reach a length of more than 1 µm. (Picture modified from http://www.medical-labs.net/neisseria-gonorrhoeae-in-electron-microscope-1581/). (B) Possible model of the type IV pilus apparatus. The model includes only proteins further described in the text. OM: outer membrane; PG: peptidoglycan; IM: inner membrane.

The major subunit of the visible pilus fiber is the pilin PilE. Since these proteins are surface exposed, the bacteria developed mechanisms for host immune response evasion, like antigenic variation (changes in the sequence of PilE) or phase variation (the on and off switch of pili). *N. gonorrhoeae* carries multiple copies of silent pilin gene loci necessary for antigenic variation (Meyer et al. 1984). Via RecA-mediated homologous recombination these gene loci can be exchanged and thereby generate a large sequence variability (Jonsson et al. 1992). PilE was shown to be necessary for the DNA binding step (Aas et al. 2002) and can play a role as an adhesin (Scheuerpflug et al. 1999). When assembled into the pilus fiber, the proteins build a three start helix containing charged patches (Craig et al. 2006). This led to the

hypothesis that these charged patches are able to bind DNA and the DNA could be pulled into the bacterial cell via the energy provided by the ATPase PilT. PilT is responsible for disassembly and thereby retraction of the pilus fiber. However, this theory could soon be disproved since first more energy would be required for pulling such big molecules through the membrane (Zaburdaev et al. 2014) and second it is not necessary to build up a visible pilus for successful DNA uptake (Long et al. 2003).

Freshly synthesised PilE is translocated into the inner membrane where it is N-terminally cleaved and methylated by the protease PilD (Jain et al. 2011). Subsequently, the pilus fiber itself is supposed to be assembled by the proteins PilM, PilN, PilO and PilP. This assembly complex is interacting with the integral membrane protein PilG and the ATPase PilF. The latter might generate the energy required for the process (Goosens et al. 2017). The exact role of PilG is not clear yet. It is essential for the assembly of the pilus subunits (Jain et al. 2011), but it was also shown to interact with the secretin PilQ and to be able to bind DNA, so PilG is possibly playing a role in mediating DNA transport through the inter-membrane space (Frye et al. 2015). The pilus passes the outer membrane through a channel formed by PilQ (Carbonnelle et al. 2006). The PilQ multimers are stabilized by PilP (Balasingham et al. 2007). On the tip of the pilus fiber, the adhesin PilC can be found, which mediates adhesion to epithelial cells and is addtionaly necessary for pilus extension (Rudel et al. 1995, Kirchner et al. 2005, Morand et al 2004). Three minor pilins are known to integrate at lower levels than PilE into the pilus fiber, ComP, PilV and PilX. DNA binding is mediated via ComP and PilV (Aas et al. 2002). ComP was shown to directly bind DNA, thereby displaying a preference for the DUS (Cehovin et al. 2013). PilV on the other hand only affects the levels of sequence specific DNA binding, but does not bind DNA itself. It is instead involved in the internalization into epithelial and endothelial cells (Takahashi et al. 2012). PilX plays a role in pilus aggregation and induces conformational changes within the pilus fiber to allow cell signalling (Helaine et al. 2005, Brissac et al. 2012). When the DNA has crossed the outer membrane, it is bound by the periplasmic protein ComE (Aas et al. 2002). The lipoproteins ComL and Tpc are associated with the peptidoglycan layer and might puncture the murein for facilitating transfer of DNA molecules (Fussenegger et al. 1996). The DNA finally crosses the inner membrane by the pore-forming protein ComA and could be integrated into the genome by homologous recombination in a RecA-dependent manner (Duffin and Seifert 2010).

Compared to DNA transformation, motility is much better understood. Due to the irregular character of the movements of *N. gonorrhoeae*, this motility was called “twitching”. Type IV pili prefer to adhere with their tip (Skerker and Berg 2001), which is stabilized by the adhesin PilC (Wolfgang et al. 2000). Adhesion often but not necessarily leads to subsequent pilus disassembly mediated by PilT and thereby pilus retraction. This generates a force pulling the gonococci in the direction of the cells and they thereby reach an average speed of 1.0-1.2 µm/s (Zaburdaev et al. 2014, Erikson et al. 2015). Since gonococci often move longer distances than the length of one pilus in one direction, they seem to have a directional memory. One explanation would be an immediate re-elongation of a pilus after complete retraction. This must

be mediated by a stable core complex at the base of the pilus probably consisting of PilG, PilQ and periplasmic proteins (Marathe et al. 2014). Further, the formation of pilus bundles increases the pulling force and bacteria are also able to organize their pili in a spatio-temporal manner by alternating the activity on different cell poles. Thereby they can change the direction of movement (Zaburdaev et al. 2014).

1.1.2.2 Opacity-associated proteins

The family of outer membrane proteins called opacity-associated (opa) proteins were identified due to the change of the opacity of colonies on agar plated when these proteins are expressed (Stern et al. 1986). Gonococcal strains can encode for up to 12 *opa* genes. They are integral outer membrane proteins consisting of eight membrane-spanning antiparallel β-sheets forming a β-barrel structure with four extracellular loops (Malorny et al. 1998).
The expression of Opa proteins undergoes phase variation, meaning a possible on or off switch of protein expression. This allows evasion of the host immune response. Within the coding region of the N-terminal leader sequence a pentameric repeat (CTCTT) is localized. During DNA replication, the number of repeats can change due to slipped strand mispairing. This modifies the open reading frame leading to a premature stop codon and consequently no functional Opa protein is expressed (reviewed in Palmer et al. 2016).
Another mechanism to evade detection by the host immune response is the highly variable sequence of the extracellular loops. Interestingly, interaction of Opa proteins with the host receptors also occurs via the hypervariable loops (Grant et al. 1999). Opa proteins are specific for two types of human surface receptors: the smaller group binds to heperansulfate proteoglycans (HSPG) and the larger group interacts with members of the carcinoembryonic antigen cell adhesion molecule (CEACAM) family (Dehio et al. 1998a, reviewed in Sadarangani et al. 2011).
HSPGs are localized on the cell surface or in the extracellular matrix and play a role in various processes like cell migration, proliferation or intercellular adhesion (Tumova et al. 2000). HSPG-binding Opa proteins mediate attachment to several epithelial cell types and the subsequent internalization process (Kupsch et al. 1993).
The human CEACAM family comprises seven members interacting with gonococci (CEACAM1, CEACAM3-8) and belong to the immunoglobulin superfamily. They modulate several cellular processes such as cell proliferation and motility, apoptosis and epithelial cell-cell interaction (Tchoupa et al. 2014). Every Opa protein has a binding specificity for a different subset of CEACAM receptors, showing a high affinity to compete with host factors (Martin et al. 2016). These CEACAM molecules can all mediate internalization of gonococci, but to a different level. The mechanism of bacterial engulfment and the cellular response to gonococcal infection depend on the kind of CEACAMs on the cells and the opa variants expressed by gonococci (McCaw et al. 2004). In contrast to HSPG, CEACAMs are also expressed on the apical side of polarized epithelial cells. They thereby allow transcytosis of epithelial cells and

so gonococci can reach the subepithelial space (reviewed in Hauck and Meyer 2003). Hence, it is not surprising that the majority of Opa proteins was found to be expressed in invasive disease-causing isolates, showing their importance for host invasion (Sadarangani et al. 2016).

1.1.2.3 Porins

Porins are the major class of neisserial outer membrane proteins (Lytton and Blake 1986). The porins comprise trimeric structures built from β-sheet rich polypeptides. These trimers function as pores mainly for the passage of ions and small macromolecules and are therefore essential for the survival of bacteria (Derrick et al. 1999, Zeth et al. 2013). Gonococcal porins can be divided into two serotypes, PorBIA and PorBIB, which have different structural and immunochemical characteristics. Most bacteria isolated from patients with disseminating gonococcal infection are positive for PorBIA, whereas bacteria expressing PorBIB are found in local urogenital infections (van Putten et al. 1998a).

Under low phosphate conditions, gonococci expressing PorBIA but not PorBIB are able to mediate uptake into their host cells. Low phosphate conditions can be found for example in the human blood stream and might therefore explain the higher abundance of PorBIA expressing bacteria in disseminating gonococcal infection (van Putten et al. 1998a, Kühlewein et al. 2006). The receptors, which are involved in invasion under low phosphate conditions, were identified as the glycoprotein Gp96 and the Scavenger Receptor expressed by Endothelial Cells (SREC) (Rechner et al. 2007).

N. gonorrhoeae is able to secrete PorB via outer membrane vesicles, which were shown to target mitochondria of immune cells (Deo et al. 2018). The porin is imported by host cell mitochondria and the pore formation in the inner membrane leads to a breakdown of the mitochondrial membrane potential, thereby causing cell death (Kozjak-Pavlovic et al. 2009).

Another effect of PorBIA is its association with higher serum resistance of gonococci. The fifth loop of PorBIA is able to bind factor H. Factor H is an essential regulator of the alternative pathway of the complement system being activated during infections. Consequently, by interfering with factor H activity, gonococci can decrease complement-mediated killing. However, it is the classical complement pathway, which is required for initiation of complement activation on gonococci and so also the proper function of the alternative pathway and the subsequent efficient clearance of gonococcal infection. It has been shown that PorBIA and some serotypes of PorBIB can bind the C4b-binding protein to their surface, which is mediating cleavage of the opsonin C4b and thereby inhibits the classical complement pathway (Chen and Seifert 2013).

Further porins can activate B cells, induce B cell proliferation and stimulate secretion of immunoglobulins, mostly IgM (Snapper et al. 1997). Nevertheless, gonococcal PorB suppresses the capacity of dendritic cells to induce CD4+ T cell proliferation (Zhu et al. 2018). On the other hand, the meningococcal porins bind to toll-like receptor TLR2. Its activation leads to an increased interleukin-8 (IL-8) secretion and an increased expression of the T cell

activating protein CD86 and of the antigen presenting complex MHCII on B cells, dendritic cells and other professional antigen-presenting cells (Massari et al. 2006). This is why PorB was tested as an adjuvant in a potential vaccine, thereby showing a strong induction of the T cell response (Mosaheb and Wetzler 2018).

1.1.2.4 Lipooligosaccharides

The major group of glycolipids found in the membrane of gram-negative bacteria are lipopolysaccharides. *Neisseria* colonize mucosal surfaces and so do not require protection from bile acids and therefore carry a truncated version of these molecules, the so-called lipooligosaccharides (LOS) (Griffiss et al. 1988). LOS in gonococci are built out of three oligosaccharide chains that are attached to a lipid A core embedded in the outer membrane. These chains branch from two heptose molecules attached to lipid A, but the number and length of the branches vary a lot (Apicella et al. 1987). LOS also undergo phase variation, which was first assumed as a loss or gain of LOS structures, but is more precisely a loss or gain of detection by monoclonal antibodies. The expression of different LOS structures is controlled by glycosyltransferase genes. Their expression is phase variable due to poly-G tracts that can cause slipped-strand mispairing and so non-functional enzymes. This results in truncated LOS structures (Gibson et al. 1993, Jennings et al. 1995).
LOS are structures easily recognized by the host immune system and so *Neisseria* developed several mechanisms for immune evasion. Gonococci can sialylate their LOS molecules by expressing a sialyltransferase and sialic acid substrates are present in the urogenital tract. Sialylation leads to the inhibition of all three complement pathways by independent mechanisms, decreases opsonic killing of bacteria and influences opa-mediated invasion of epithelial cells (Kim et al. 1992, Gill et al. 1996, van Putten 1993). Further, gonococci modify lipid A by adding molecules like phosphoethanolamine. This, on the one hand, enhances the activation of toll-like receptor TLR4 thereby triggering cytokine secretion and immune cell activation and on the other hand was shown to protect bacteria from the triggered immune response *in vivo* (Hobbs et al. 2013). There are various ways of modifying lipid A and all influence the immune response differently. It is hence not surprising that invasive strains have a predominantly altered modification pattern compared to non-invasive strains (John et al. 2016). LOS also induces pyroptosis of human macrophages after internalization of bacteria in a caspase-1-dependent manner (Ritter and Genco 2018). The presence of LOS in the cytosol of host cells triggers formation of the inflammasome, which is including activated caspase-1, after external TLR stimulation (Idosa et al. 2019).

1.1.2.5 IgA1 protease

IgA is the most common immunoglobulin found in mucous secretion and thereby also in the genitourinary tract. They are able to neutralize pathogens and exotoxins and are further

important to inhibit bacterial adherence (reviewd in Macpherson et al. 2007). Pathogenic Neisseria express a protease, which is secreted out of the cell and cleaving the proline-rich hinge region of the human IgA1 heavy chain (Mulks et al. 1980). Hence, the protease is supposed to play a role in the protection of gonococci from the host immune response. Another target of the protease was found to be LAMP1, which is the major lysosomal integral membrane protein (Hauck and Meyer 1997). The cleavage and subsequent degradation of LAMP1 causes alterations of the lysosomes and is so important for intracellular survival of *Neisseria*, but also affects the trafficking across polarized epithelial monolayers (Lin et al. 1997, Hopper et al. 2000). Nevertheless, gonococci do not seem to require IgA1 protease for successful colonization of the male urethra and for development of urethritis (Johannsen et al. 1999).
IgA1 protease is besides porins another component tested in possible vaccines. Mice treated with a recombinant IgA1 protease were shown to develop an immune response against this protein and be thereof protected against meningococcal and pneumococcal infections (Kotelnikova et al. 2019).

1.1.3 Host pathogen interactions

When entered the host, gonococci first establish contact to the mucosal epithelium. Therefore, they adhere to the epithelial cells. The above mentioned type IV pili, Opa proteins, porins and LOS play thereby an important role. Most *Neisseria* seem to stay attached to the cell surface, however, it was also shown that they invade nonciliated cervical epithelial cells and urethral epithelial cells of men after desialylation of LOS (reviewed in Edwards and Apicella 2004). This invasion and subsequent transcytosis can lead to the disseminating gonococcal infection. *Neisseria* avoid the host adaptive immune response and trigger a strong innate immune response instead. This is mainly characterized by the influx of polymorphonuclear leucocytes (PMNs), also known as neutrophils. However, these neutrophils are often not able to clear the infection and some bacteria were even found to survive within PMNs (reviewed in Criss and Seifert 2012). Figure 1.2 shows an overview of these host-pathogen interactions.

1.1.3.1 Invasion of epithelial cells

There are two characterized ways for invasion of epithelial cells, one is Opa-dependent and the other one PorBIA-dependent. The HSPG-binding protein Opa_{50} was found to be the major Opa protein for invasion of epithelial cells (Makino et al. 1991). Binding of HSPG results in the activation of several signalling cascades involving for example protein kinase C. This is finally leading to a remodelling of the actin cytoskeleton and so enables membrane engulfment and uptake of gonococci (Dehio et al. 1998b, Grassmé et al. 1996). Opa_{50} was also shown to interact with extracellular matrix proteins and thereby activate integrin-mediated uptake (van Putten et al. 1998b).

PorBIA mediates the invasion into different cell types under phosphate-free conditions. Its binding to SREC leads to the uptake of gonococci whereas interaction with the glycoprotein Gp96 seems to favour adherence over invasion (Rechner et al. 2007). The invasion process is depending on the formation of membrane rafts in which SREC is localized. Binding to SREC results in phosphorylation of caveolin-1 what activates a signalling cascade leading to cytoskeletal re-arrangements and so the uptake of bacteria (Faulstich et al. 2013). Host cells use the autophagy pathway in order to restrict intracellular growth and clear invading bacteria (reviewed in Shahnazari and Brumell 2011). Autophagy also affects survival of gonococci within epithelial cells. They are targeted by the autophagic pathway and captured in autophagosomes, where they are finally degraded. A small subpopulation of gonocooci was found to evade degradation and repress the autophagy pathway, allowing intracellular survival (Lu et al. 2019). A host factor important for bacterial survival is Folliculin. The protein downregulates autophagy, thereby supporting intracellular survival of gonococci in epithelial cells (Yang et al. 2020).

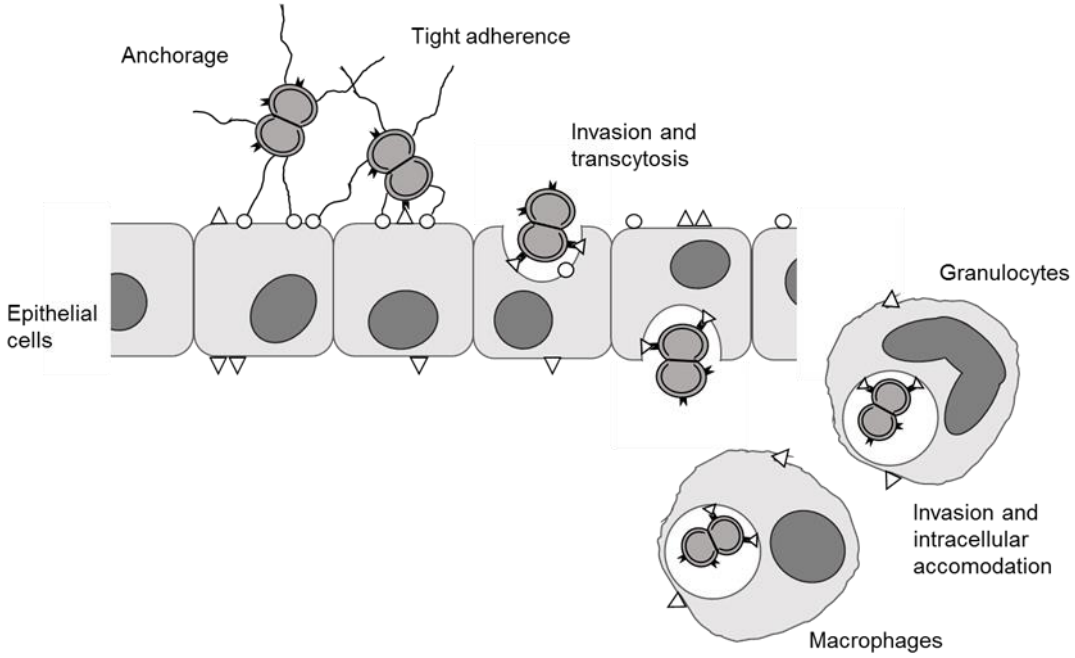

Figure 1.2: Model for host-pathogen interactions of *N. gonorrhoeae*. First contact to epithelial cells might be established by pili whereas the Opa proteins are used for a subsequent tight adherence. In some cases gonococci are taken up by cells in an Opa- or PorBIA-dependent manner. Transcytosis can lead to a systemic infection. Immune cells will be recruited to the site of infection, which can be also invaded by gonococci. In these cells, *Neisseria* can survive for a longer time period and so establish a persistent infection. Figure based on Dehio et al. 1998a.

1.1.3.2 Interaction with neutrophils

The infection of *N. gonorrhoeae* results in the activation of the innate immune response by mucosal epithelial cells and resident immune cells. The release of chemokines like IL-8, IL-6 and tumor necrosis factor α attracts the first line defence of the host immune system, neutrophils (Ramsey et al. 1995). The migration of PMNs from the blood stream into the infected tissue leads to an activation of the cells, which now have a higher killing potential. PMNs are phagocytes. They express receptors for binding complement or antibody opsonised particles or engulf unopsonised microbes via lectin-like interactions (Groves et al. 2008). Neutrophils have granules containing various antimicrobial substances like defensins or cathepsin G and also reactive oxygen species (ROS) generated by the NADPH oxidase. These granules can fuse with the phagosome and so kill the containing bacteria or can also degranulate to damage and kill cells in the proximity of the neutrophils (Borregaard et al. 2007). The so-called neutrophil extracellular traps are a further mechanism to kill extracellular bacteria and are DNA-rich and therefore sticky structures providing a high local concentration of antimicrobial peptides and proteins (Brinkmann et al. 2004).

Though PMNs have potent antimicrobial activities, it is still possible to isolate viable gonococci from gonorrhoeal exudates from infected men. Consequently, gonococci must have developed strategies to survive within this hostile environment.

The first step is to prevent uptake by neutrophils, mostly by interfering with opsonisation by the complement system or antibodies (reviewed in Ram et al. 1999). Nevertheless, *Neisseria* can still be efficiently taken up when expressing surface Opa proteins. Human PMNs express CEACAM1, 3 and 6 and the binding of any of these CEACAMs results in engulfment of the bacteria (McCaw et al. 2004). It has been reported that Opa-negative *Neisseria* survive better in the presence of neutrophils than gonococci expressing *opa* (Ball and Criss 2013). Especially, interaction with CEACAM3 leads to an efficiant phagocytosis of the opsonized bacterium and stimulates cytokine production by neutrophils (Johnson et al. 2015). Not surprisingly, Opa proteins expressed in strains isolated from patients with disseminating gonococcal infection failed to interact with CEACAM3 (Roth et al. 2013).

Even extracellular bacteria still need to defend themselves from the antimicrobial activities of PMNs. Gonococci have several mechanisms protecting themselves from the oxidative burst of neutrophils. First, lactate produced by PMNs during glycolysis increases oxygen consumption of gonococci, thereby reducing the available amount of oxygen for neutrophils (Britigan et al. 1988). Further, in response to ROS, *Neisseria* upregulate a large set of genes involved in detoxification or repair of oxidative damage including catalase, superoxide dismutase and peroxidases (reviewed in Seib et al. 2006). However, more important are the non-oxidative antimicrobial activities of PMNs since mutations in catalase or superoxide dismutase do not affect survival of gonococci (Criss et al. 2009). Pathogenic *Neisseria* express the efflux pump MtrCDE, which exports antimicrobial peptides and toxins from the bacterial cytoplasm (Handing et al. 2018). To limit exposure to antimicrobial substances, gonococci are able to

delay granule fusion with the phagosome, an effect caused by neisserial surface molecules (Johnson and Criss 2013). This might allow gonococci to adapt to the toxic environment. Modifications of LOS also positively influence intracellular survival, for example, changes in the surface charge on *Neisseria* reduce killing by cationic antimicrobial peptides (Kandler et al. 2014).

Principally, the strong recruitment of PMNs could promote neisserial pathogenesis. Neutrophil influx causes a lot of damage to the surrounding tissue thereby providing more nutrients for the bacteria and facilitating the migration into deeper tissues. Further, gonococci can survive within neutrophils what is offering them a protective niche and might help for the transmission to a new host (reviewed in Criss and Seifert 2012). A beneficial effect of neutrophil recruitment would also explain why gonococci strongly delay the phagocytosis-induced cell death of PMNs. They interfere with the activity of several caspases and thereby actively inhibit the intrinsic apoptosis pathway (Cho et al. 2020).

1.2 Small non-coding RNAs

Beside riboswitches and CRISPR RNAs (clustered regularly interspaced short palindromic repeats) small non-coding RNAs (sRNAs) form the biggest group of regulatory RNAs. A small number of sRNAs are responsible for housekeeping functions like the 4.5S RNA as a structural component of the signal recognition particle, but most sRNAs serve as regulators. They are usually synthesized in response to stress factors or a changing environment and many metabolic pathways are regulated by these molecules. Their transcripts are rather short with sizes between 50 and 300 nucleotides (reviewed in Storz et al. 2011).

1.2.1 Regulation by small non-coding RNAs

Good characterized ways of gene regulation are alternative sigma factors and transcriptional regulators. However, in *N. gonorrhoeae,* only three sigma factors were identified and also only a limited number of transcriptional regulators found in the genome. Consequently, regulatory RNAs are supposed to play an important role regarding gene regulation. Search for non-coding RNAs only came up in the early 2000s with the development of new bioinformatics techniques and computational predictions; some few discoveries before were rather serendipitously (reviewed in Gottesman 2005). Such a transcriptome analysis was also performed in *N. gonorrhoeae*, hereby identifying 253 new transcripts without annotation of a coding sequence (CDS) (Remmele et al. 2014).

Interestingly, a model shows that transcriptional regulation via small RNA is not significantly faster than via transcription factors under physiological conditions. Because of a fast mRNA turnover, fast transcription rates and the fact that translation occurs during transcription only minor advantages are given to sRNAs over transcription factors. In addition, the fast turnover

is not resulting in a clear advantage of sRNAs, since transcription factors can be easily inactivated by phosphorylation or binding of small molecules. Nevertheless, in comparison to transcription factors, sRNAs have the advantage of being better suited for a graded regulation (Hussein and Lim 2012).

Regulatory sRNAs can act on different target molecules, for example, one group is interacting with proteins, but a larger subset of sRNAs is basepairing with messenger RNAs. Examples for different ways of regulation by small RNAs are illustrated in figure 1.3.

Most RNAs acting on proteins that are characterized so far function by mimicking the structure of other nucleic acids. The RNAs CsrB and CsrC for example interact with CsrA, an RNA-binding protein involved in regulating mRNA stability after entry in stationary phase in *Escherichia coli*. Both regulatory RNAs contain several of the binding motifs CsrA is recognizing and so sequester the protein away from its target mRNAs. *CsrB* and *csrC* are transcribed in nutrient-poor conditions and their expression is regulated by a two-component system. This ensures CsrA inhibition only under specific conditions (Babitzke and Romeo 2007). Another well-studied example for an RNA modulating protein activity is the *E. coli* 6S RNA. The secondary structure mimics the conformation of DNA during transcription initiation and is therefore recognized by the σ^{70}-RNA polymerase. 6S RNA is abundant in stationary phase and so the housekeeping σ^{70}-RNA polymerase is mostly bound by the RNA, whereas the stationary phase σ^{S}-RNA polymerase is still active (Wassarman 2007, Trotochaud and Wassarman 2005).

RNAs that interact by basepairing with their target mRNAs can be divided into two groups, *cis*- and *trans*-acting small RNAs. *Cis*-encoded RNAs are transcribed from the opposite strand of their target mRNA and therefore have a long sequence homology, often more than 75 nucleotides. On the other hand, *trans*-encoded sRNAs are transcribed from a different genomic location. They share only limited complementarity with their targets, usually with the 5’ region of an mRNA. This offers the possibility of interacting with a large subset of different mRNAs.

Many of the *trans*-acting small RNAs require the RNA chaperone Hfq for proper function and often consist of three regions: a short “seed region” for interaction with target mRNAs, an AU-rich region for binding of Hfq, and a 3’ terminal loop for Rho-independent transcription termination and protection from exonuclease degradation (reviewed in Svensson and Sharma 2016 and in Waters and Storz 2009).

Most of the regulation of sRNAs reported so far is negative. For many sRNAs C- or CU-rich loops were found, which are able to interact with the ribosomal binding site (RBS) and thereby repressing translation or destabilizing the target mRNA by removing ribosomal protection. OxyS is a small RNA induced by oxidative stress in *E. coli* and is regulating several mRNAs like *fhlA*. The complementary region is overlapping with the RBS and so inhibiting binding of the 30S subunit (Altuvia et al. 1998). Further sRNAs are able to mediate RNase degradation of their target mRNAs. The RNAs SgrS and RhyB of *E. coli* stimulate the degradation of their targets by RNase E. Whether the mRNA itself gets more sensitive to degradation after sRNA

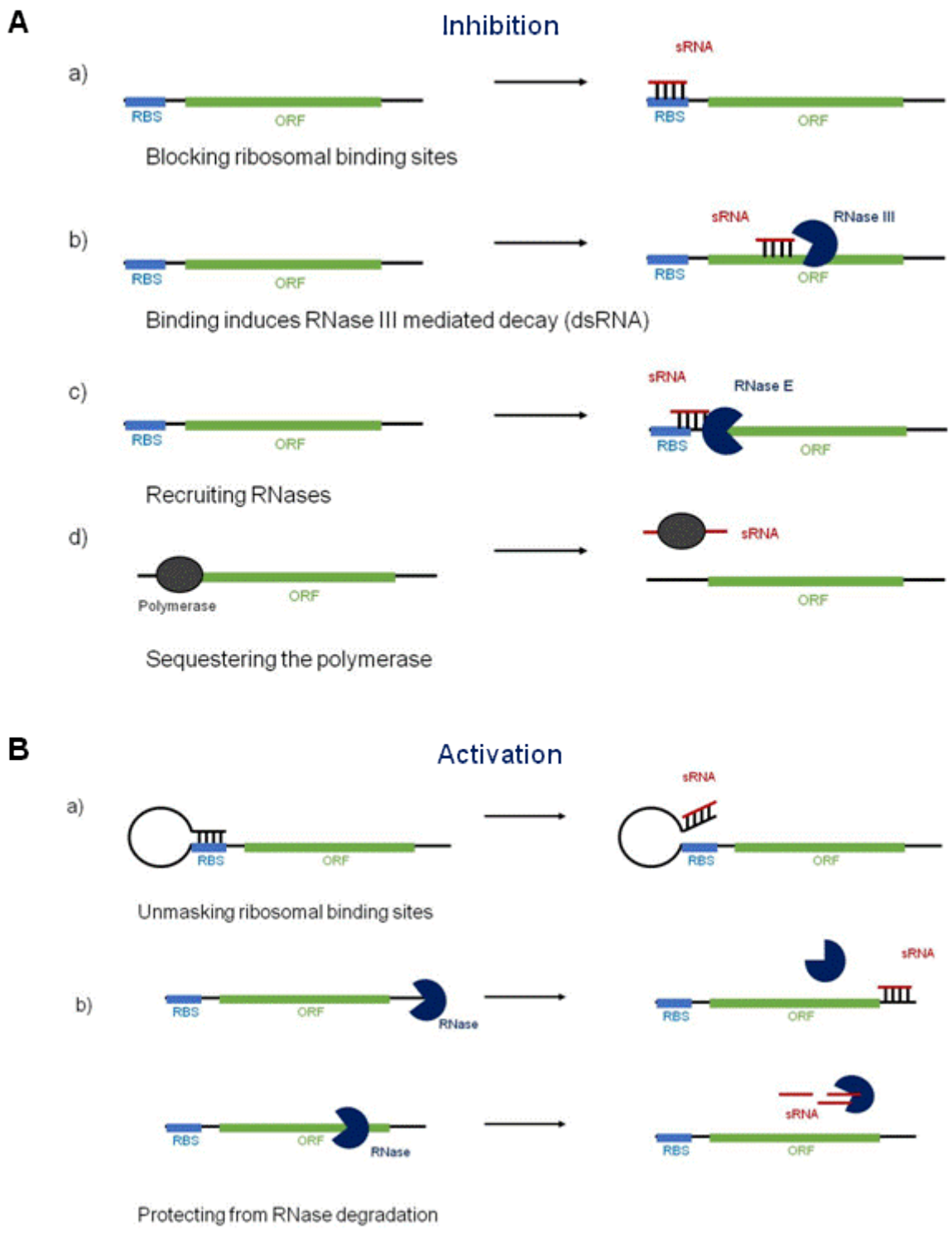

Figure 1.3: Examples of regulatory mechanisms by small non-coding RNAs. (A) Small RNAs can inhibit their target genes. Already observed mechanisms are blocking the ribosomal binding site (RBS), recruiting RNases and inducing RNase-mediated decay or sequestering the RNA polymerase. (B) Some sRNAs were also shown to have an activating effect. They unmask ribsosomal binding sites by changing the secondary srructure of the mRNA or protect their targets from RNase degradation by either masking RNase binding sites or sequestering the RNases.

binding or whether this is an effect of sRNA-dependent RNase recruitment could not be answered (Morita et al. 2005). Also RNase III, which is recognizing RNA duplex structures, can be recruited as a consequence of sRNA binding and lead to the degradation of both target and sRNA (Vogel et al. 2004). For one target gene, the *manX* mRNA, another regulatory mechanism of the sRNA SgrS is reported. Here, the sRNA is not the direct repressor. The binding of SgrS within the coding sequence of *manX* recruits Hfq to the mRNA. The Hfq binding site is located directly adjacent to the RBS and so Hfq interferes with ribosome binding (Azam and Vanderpool 2018). An unusual observation is the presence of secondary structures within the CDS of *fepA* mRNA involved in iron acquisition, which promote ribosome binding. The interaction of the sRNAs OmrA and OmrB with the coding sequence of the mRNA disrupts the stem-loop structures and thereby represses FepA synthesis (Jagodnik et al. 2017). Gene regulation by sRNAs does not necessarily have to be a post-transcriptional process. The sRNA ChiX downregulates the distal portion of the *chiPQ* operon cotranscriptionally. Binding of ChiX within the 5' untranslated region (UTR) inhibits translation; consequently, less ribosomes cover the Rho-utilization site in the *chiP* CDS leading to increased transcription termination (Bossi et al. 2012).

Comparably few sRNAs identified activate their targets. One mechanism is the improved accessibility of the mRNA to ribosomes, as it is the case for the *rpoS* mRNA. In the absence of sRNAs the 5' UTR of *rpoS* folds into a hairpin structure hiding the ribosomal binding site. The sRNAs bind the 5' UTR and are thereby changing the inhibitory structure and allowing ribosomal binding (Mika and Hengge 2014). The same mRNA is also subject to RNase III cleavage within the double-stranded sequences in the 5' UTR. One cleavage site is located next to the RBS and therefore cleavage could affect translation initiation. The binding of the sRNA DsrA redirects this cleavage in the 5' UTR and is so having a stabilizing effect on *rpoS* (Resch et al. 2008). The sRNAs RydC and ArrS protect *cfa* mRNA from degradation by RNase E. The sRNAs bind within the 5' UTR of *cfa*, thereby masking an RNase E cleavage site (Bianco et al. 2019). Consequently, influencing RNase cleavage can also lead to target activation. Influencing Rho-dependet transcription termination can also have a positive effect. Interaction of the sRNAs DsrA, ArcZ and RprA with the 5' UTR of *rpoS* directly interferes with Rho binding, stimulating transcription during the transition to the stationary growth phase (Sedlyarova et al. 2016). However, the mechanism of several activating sRNAs has not yet been discovered (reviewed in Papenfort and Vanderpool 2015).

1.2.2 The RNA chaperone Hfq

Trans-encoded RNAs have only a short and imperfect base-pairing with their target mRNAs and so often require help by an RNA chaperone. Hfq was discovered about 50 years ago in *E. coli* as *h*ost *f*actor of the bacteriophage *Q*β and is by now the best characterized RNA chaperone so far (reviewed in Vogel and Luisi 2011).

Hfq belongs to the (L)Sm protein superfamily. They share a characteristic fold of an N-terminal α-helix followed by five β-strands, which can be divided into two sequence motifs: Sm1 and Sm2. Sm1 is formed by the first three β-strands and can be found in all (L)Sm proteins whereas Sm2 encompasses the β-strands four and five and differ in bacterial Hfq proteins. In bacteria, Hfq usually assembles into homohexamers that form a ring-like structure. This assembly results in two faces for possible interactions with nucleic acids: The proximal face describes the surface of the ring of the N-terminal α-helix and the distal face is the opposite side (see figure 1.4A). Additionally, the outer ring is called the rim face or the lateral face (reviewed in Updegrove et al. 2016, Sauer 2013).

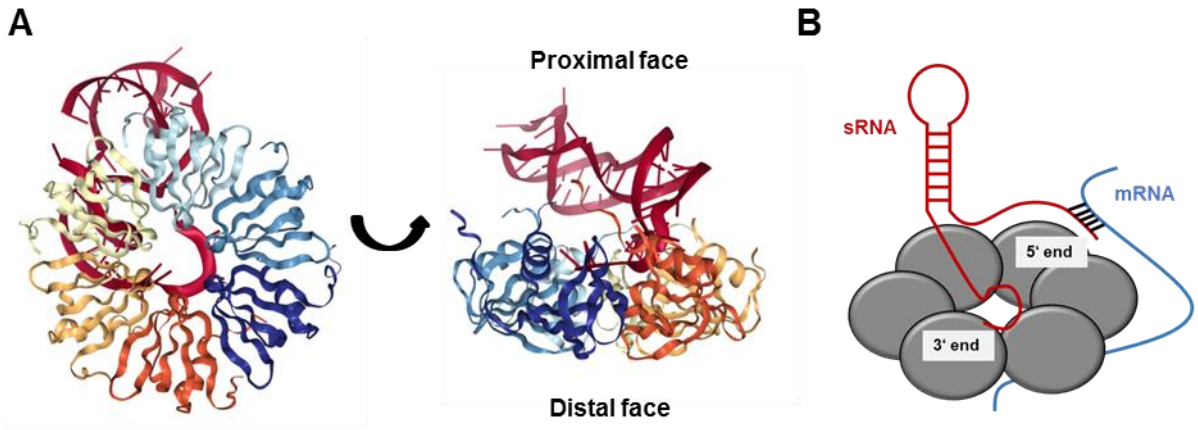

Figure 1.4: Structure of Hfq in complex with a regulatory RNA. (A) Crystal structure of Hfq in complex with the sRNA RydC. The structure was determined by x-ray diffraction with a resolution of 3.48 Å (PDB ID: 4V2S; deposited by Dimastrogiovanni et al. 2014). The structure shows the homohexameric structure of Hfq and the interaction of the sRNA with the central pore on the proximal face of Hfq via its 3' poly-U tail. (B) Schematic illustration of the interaction between two RNAs bound on Hfq (illustration based on Murina and Nikulin 2015).

The proximal face was shown to bind uridine-rich sequences, especially single-stranded A/U-rich sequences close to secondary structure elements. This kind of sequences is found in sRNAs with rho-independent terminators, comprising a hairpin loop with a poly-U tail at the 3' end of the sRNA. Experiments with sRNAs shortened at their 3' end showed that binding of this terminator sequence is essential for recognition by Hfq (Otaka et al. 2011).
However, the proximal face is not the only one important for sRNA binding. Each monomer has on its lateral side a patch of positively charged residues, which are able to interact with especially single-stranded, internal uridine-rich RNA sequences (Sauer et al. 2012).
The distal face on the other hand is binding rather A-rich sequences, further characterized as the ARN-motif (A is an adenosine, R is a purine and N any nucleotide). This site is assumed to be important for the interaction with internal purine-rich sequence of mRNAs and poly-A tracts (Salim et al. 2012, Soper and Woodson 2008). In contrast to the proximal site, where each protomer is pairing with only a single nucleotide, here every protomer binds one ARN-motif. Consequently, up to six different purine-rich sequences can be bound (Link et al. 2009).

Taken together the sRNA is recognized at its 3'end by the proximal face of Hfq and can be further stabilized by binding of internal poly-U sequences. One or several RNAs carrying the ARN-motif, mostly mRNAs, are bound on the distal site (see figure 1.4B). By providing a binding platform for RNAs, Hfq generates a high local concentration of RNAs. It also unfolds some RNA structures ensuring flexible RNAs for fast RNA-RNA interactions. However, Hfq only catalyses the interaction between the RNAs. Once the complex is formed, it is supposed to be released from the protein, since it is stable also in the absence of Hfq (reviewed in Wagner 2013 and Vogel and Luisi 2011).

Hfq facilitates not only the base-pairing between two RNAs. It can also protect RNAs from RNase degradation. In the case of the *ompA* mRNA the cleavage site for RNase E overlaps with the Hfq binding site so in the absence of Hfq mRNA stability is reduced (Moll et al. 2003). On the other side, Hfq can also induce degradation of RNAs. Hfq was found to bind components of the degradasome like the polynucleotide phosphorylase (PNPase) and poly(A) polymerase I (PAP I) (Mohanty et al. 2004). Though RNase E is also a component of the degradasome, it was shown to co-purify with the Hfq-RNA-complex independently of the other enzymes (Ikeda et al. 2011). This could bring the RNase into proximity when the mRNA is not protected by the ribosome anymore and so cleavage sites are accessible. Another possibility is that the sRNA is directly accelerating mRNA decay. It was shown that sRNAs can activate RNase E to cleave the mRNA six nucleotides downstream of the seed region. RNase E is activated by a 5' monophosphate, but mRNAs are synthesised with a 5' triphosphate. This is why cleavage by RNase E could not always be explained. By interacting with an sRNA providing a 5' monophosphate this problem can be solved (Bandyra et al. 2012).

Besides its function as sRNA regulators, Hfq is playing a role in ribosome biogenesis. It is involved in maturation of 16S rRNA and is therefore important for the correct assembly of the 30S subunit of the ribosome (Andrade et al. 2018).

Given the fact that Hfq fulfils an important role in the regulation by *trans*-acting RNAs, it is not surprising that - due to the lack of Hfq in some bacteria - other possible chaperones have been found. One of them is the FinO-domain containing protein ProQ, for which was already shown that it binds a large group of sRNAs and has a clear binding specificity for mRNAs and sRNAs (Holmqvist et al. 2018, reviewed in Olejniczak and Storz 2017). However, this group of proteins is not simply an alternative to Hfq. New sequencing approaches revealed that ProQ and Hfq compete for the same RNA-RNA pairs. Whereas one protein is promoting a negatively regulation, the other protein aims to block this regulation (Melamed et al. 2020). This shows that the regulatory network is far more complex than it has been thought before.

1.2.3 Degradation and turnover of RNAs

The rapid degradation of RNAs allows bacteria to quickly adapt to a changing environment. The control of the half-life of each RNA also results in controlling the protein levels and is so

an important step in the post-transcriptional regulation. Consequently, there are several enzymes required for proper degradation of RNAs. RNases can be divided into two groups depending on their site of cleavage: endonucleases and exonucleases. The most important endonucleases identified in gram-negative bacteria so far are RNase E and RNase III. RNase E plays a role in multiple RNA degradation and procession pathways and is responsible for initiating cleavage of more than half of *E. coli* mRNA transcripts during exponential growth (Stead et al. 2011, Clarke et al. 2014). It is also the scaffold enzyme of the degradasome, a multi-enzyme complex with the core enzymes RNase E, PNPase, the ATP-dependent helicase RhlB and the glycolytic enolase. Further enzymes can interact with the degradasome and so modulate its activity (Callaghan et al. 2004, Regonesi et al. 2006).

The other endonuclease, RNase III, is the primary enzyme for cleaving double-stranded RNA (Robertson et al. 1968). It mostly functions in maturation of ribosomal RNAs, but is also important for cleavage of stem-loop structures of mRNAs or digesting mRNA:sRNA duplexes (King et al. 1984, Aristarkhov et al. 1996, Vogel et al. 2004).

The exonucleases playing a role in mRNA and sRNA turnover are RNase II, RNase R and PNPase. All exonucleases characterized in gram-negative bacteria digest in 3' to 5' direction, whereas gram-positive bacteria also have enzymes digesting from 5' to 3' (reviewed in Bechhofer and Deutscher 2019). RNase II and RNase R belong to the RNR family of processive, nonspecific exonucleases cleaving their targets hydrolytically. RNase II is important for the digestion of a large number of mRNAs, but is strongly inhibited by secondary structures and stalls around seven nucleotides before reaching them (Cannistraro and Kennell 1999). RNase R on the other hand plays only a minor role in mRNA and sRNA turnover. Nevertheless, it can degrade RNAs with strong secondary structures because of its intrinsic helicase activity (Andrade et al. 2009, Cheng and Deutscher 2005).

PNPase is using inorganic phosphate as a nucleophile and is releasing nucleoside diphosphates instead of monophosphates. Diphosphates provide much more energy than monophosphates, which can be used to synthesize RNA as the reverse reaction of RNA degradation (reviewed in Bechhofer and Deutscher 2019). RNA degradation by PNPase is inhibited by RNA secondary structures, therefore the enzyme is often associated in complexes with a helicase like in the degradasome (Liou et al. 2002). PNPase was shown to interact with sRNAs not only in a degradative way, but also stabilzes them by direct interaction (Bandyra et al. 2016). RNase PH, which is closely related to PNPase, is also involved in the protection of some sRNAs when they are bound to Hfq (Cameron and De Lay 2016).

RNase II and PNPase have overlapping functions and the loss of one of both enzymes can be compensated by the upregulation of the other (Zilhão et al. 1996). The degradation by both enzymes is influenced by polyadenylation by PAP I since the poly-A tail offers a single-stranded region for efficient binding (Xu and Cohen 1995). This provides also possibilities for protection of RNAs from degradation. RNase II was shown to remove the poly-A tails and thereby inhibiting PNPase-dependent degradation of the transcript (Coburn and Mackie 1998).

All RNases mentioned so far release fragments of 2-5 nucleotides in length. However, the accumulation of these fragments results in a stop of cell growth (Ghosh and Deutscher 1999). The exoribonuclease oligoribonuclease is responsible for the degradation of these short fragments into mononucleotides. The enzyme hydrolyzes the oligoribonucleotides in 3' to 5' direction independently of the 5′-phosphorylation state of the RNA (Datta and Niyogi 1975). The main pathway for degradation of mRNAs seems to be first an endonucleic cleavage by RNase E followed by exonucleic degradation by RNase II and/or PNPase, which is often facilitated by addition of a poly-A tail by PAP I (Arraiano et al. 1993, Hajnsdorf et al. 1996).
Also degradation of sRNAs is initiated by endonucleic cleavage by either RNase E or RNase III when they are in complex with their target mRNA (Afonyushkin et al. 2005, Morita et al. 2005). This process is facilitated by the presence of Hfq (reviewed in Aiba 2007). These initially cleaved fragments are then further degraded by RNase II and PNPase. However, in the absence of Hfq the main degradation pathway seems to be independent of endonucleic cleavage and the major enzyme PNPase. PAP I can promote here RNA degradation but PNPase is not depending on it (Andrade et al. 2012). These most common degradation pathways are summarized in figure 1.5.

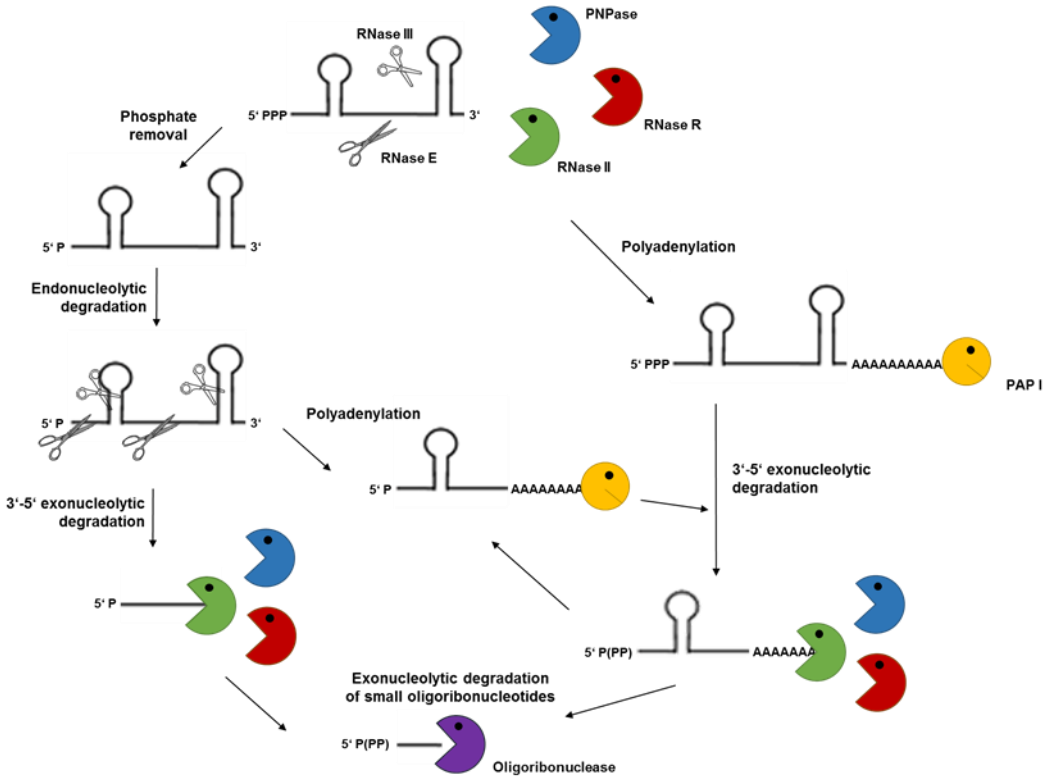

Figure 1.5: Overview on the main degradation pathways for mRNAs. The major nucleases involved in degradation of mRNAs are the endonucleases RNase E, which needs a 5' monophosphate for cleavage, and RNase III; and the exonucleases PNPase, RNase II and RNase R. The addition of poly-A tails by PAP I can facilitate exonucleolytic degradation. The enzyme oligoribonuclease cleaves the remaining oligoribonucleotides into mononucleotides. Figure based on Arraiano et al. 2010.

Nevertheless, an RNA is not limited to a single decay pathway, depending on the growth conditions they can be also degraded by other nucleases (Arraiano et al. 1997, Marujo et al. 2003).

1.2.4 Small RNAs in *Neisseria gonorrhoeae*

Until now, small RNAs in *N. gonorrhoeae* are only poorly characterized. The first sRNA analyzed in detail was NrrF, the *n*eisserial *r*egulatory *R*NA involved with iron [*F*e]. It was identified in *N. meningitidis* in the course of a bioinformatic screen for Fur-regulated sRNA molecules (Mellin et al. 2007). Fur, for ferric uptake regulator, is a transcriptional regulator forming complexes in the presence of iron, which are binding specific DNA sequences and thereby repressing transcription of several genes. NrrF was soon found to be expressed also in *N. gonorrhoeae*, where it is clearly upregulated under iron starvation (Ducey et al. 2009). In *N. meningitidis* a new screen for the identification of target genes was used showing that the succinate dehydrogenase genes *sdhA* and *sdhC* are regulated via an unknown mechanism (Mellin et al. 2007). These genes were chosen for further analysis because they are also posttranscriptionally regulated by the Fur-regulated RNA RyhB in *E. coli* (Massé and Gottesman 2002). However, in gonococci only *sdhA* but not *sdhC* was affected by the absence of NrrF. In return, several new target genes could be identified that are involved in DNA metabolism, amino acid biosynthesis or efflux of antibiotics. This led to the hypothesis that NrrF is on the one hand adapting gene expression to low iron conditions but is on the other hand also buffering Fur repression (Jackson et al. 2013). Further analysis of a screen for iron-regulated sRNAs revealed that NrrF seems to control expression of five iron-induced sRNAs (Jackson et al. 2017). Whether NrrF influences these sRNAs via a direct or indirect mechanism still needs to be determined.

Microarray experiments to determine the FNR regulon lead to the identification of an unknown transcript that was strongly induced by FNR (Whitehead et al. 2007). FNR is the regulator of fumarate and nitrate reduction and is an oxygen-sensing transcriptional regulator playing a role during anaerobic growth. This transcript was also found in a study looking for differential gene expression comparing aerobic with anaerobic conditions. The sRNA was therefore called FnrS and was shown to be strongly upregulated during anaerobic growth (Isabella and Clark 2011). Another study identified four target mRNAs, the cysteine desulfurase *iscS,* the RNA methyltransferase *yhhF, prlC* (encoding oligopeptidase A) and a hypothetical protein (Tanwer et al. 2017). These targets are functionally unrelated and interact with different regions of the sRNA and hence many questions regarding FnrS remain open.

During a transcriptome analysis in *N. meningitidis* two highly abundant sibling RNAs were identified, which were shown to regulate the putative colonization factor PrpB and therefore named RcoF1 and RcoF2 (for RNA regulating colonization factor; Heidrich et al. 2017). The same sRNAs were also found in another transcriptome study in *N. meningitidis*. The

identification of target genes was performed by comparing the protein expression profile of wildtype (WT) and sRNA deletion strains and the downregulation of several citric acid cycle enzyms could be confirmed. This led to the hypothesis that the sRNAs regulate the switch from cataplerotic to anaplerotic metabolism and the sibling RNAs were hence named $NmsR_A$ and $NmsR_B$ (Neisseria metabolic switch regulators; Pannekoek et al. 2017). These sRNAs correspond to the gonococcal NgncR_162 and NgncR_163. An initial analysis of the gonococcal homologues confirmed their regulation of citric acid cycle and methylcitrate cycle enzyms and included in the regulon a transcriptional regulator, an amino acid transporter and a gene involved in amino acid degradation (Bauer et al. 2017). This is suggesting a more complex function than stated before.

On the other side, the function of a *cis*-acting sRNA found in the upstream region of *pilE* seems rather clear. This non-coding RNA was shown to be essential for pilin antigenic variation and to be required for initiation of the homologous recombination leading to this antigenic variation (Cahoon and Seifert 2013). Upstream of *pilE* is located a DNA sequence containing 12 GC base pairs forming a guanine quadruplex (G4) structure necessary for antigenic variation (Cahoon and Seifert 2009). The non-coding RNA starts within this G4 sequence and only if this RNA is transcribed at this exact position and this orientation antigenic variation can take place (Cahoon and Seifert 2013). The frequency of antigenic variation is determined by the transcriptional initiation of the small RNA. Transcription of the non-coding RNA is opening the DNA duplex, what is subsequently allowing G4 structure formation, a process requiring single-stranded DNA (Prister et al. 2019). Therefore, it cannot be excluded that it is only the transcription and not the RNA itself being important for the process.

1.3 Aim of the thesis

Small RNAs play an important role in survival and pathogenicity of bacteria. They are often synthesized in response to environmental stimuli like limitation of nutrients or iron (Storz et al. 2011). A better understanding of virulence regulation becomes more and more important, especially regarding the decreasing possibilities for treatment of bacterial infections.

Previous work in our group identified two sibling sRNAs, NgncR_162 and NgncR_163 (Bauer et al. 2017), which were also shown to be expressed in the related *Neisseria meningitidis* (Heidrich et al. 2017, Pannekoek et al. 2017). They exhibit a sequence homology of 78 % and share the target interaction domain. First target genes for both sRNAs were identified with the help of bioinformatic tools. In this thesis, these sibling sRNAs should be further characterized. Also with the help of high-throughput techniques, the question is addressed why the expression of both sRNAs is conserved within *Neisseria*, but the function seems to be very redundant. The target genes identified so far give a hint of a role in metabolism, but this thesis should give a better idea about the possible physiological role of the sibling RNAs. Analysing sRNA expression under various conditions should further help to find clues for understanding the

function of the RNAs. A possible function in metabolic adaptations could play a role during infection processes. This hypothetesis was additionally addressed.

Another *trans*-acting small RNA was identified in a screen for transcripts upregulated in blood in *N. meningitidis* (Del Tordello et al. 2012). This RNA has a homologue in *N. gonorrhoeae*, NgncR_237 that has not been characterized so far. Initial *in silico* analysis give ideas on sequence conservation and possible interactions with target genes. The sRNA regulon can be expanded by high-throughput techniques and putative target gene candidates have to be validated. Not only analysis of target genes, but also of expression conditions help to characterize the function of non-coding RNAs, what is aimed by the study. The analysis of regulatory effects in a pathogen always rise the question about their function in pathogenesis and virulence and their role during infection shall be studied.

Until now most characterized small RNAs are *trans*-encoded (reviewed in Azhikina et al. 2015), rising interest in a further analysis of potential *cis*-encoded RNAs. Transcriptome studies on *N. gonorrhoeae* gave an idea of the presence of antisense transcripts for all *opa* genes (Remmele et al. 2014). In this work, the presence of these possible transcripts shall be confirmed. Since *opa* mRNAs can change between being in-frame or out-of-frame, also their influence on *opa* phase variation will be analysed.

In this work selected non-coding RNAs of *N. gonorrhoeae* are characterized, which is supposed to contribute to a better understanding of the pathogen and its virulence.

2 MATERIAL AND METHODS

2.1 Material

2.1.1 Bacterial strains

2.1.1.1 Neisseria gonorrhoeae strains

Table 2.1: *N. gonorrhoeae* strains used in this study

Strain	Description	Source
MS11	Clinical isolate	Laboratory strain collection
MS11 Δopa	Deletion of all *opa* genes	LeVan et al. 2012
MS11 2435lif	Δopa with NGFG_2435 locked in frame	Stefanie Schmitt
MS11 2435lof	Δopa with NGFG_2435 locked out of frame	Stefanie Schmitt
MS11 2258lif	Δopa with NGFG_2258 locked in frame	Stefanie Schmitt
MS11 2258lof	Δopa with NGFG_2258 locked out of frame	Stefanie Schmitt
MS11 P_{2435}-gfp	Fusion of NGFG_2435 promoter to *gfp*	Marc Kaethner
MS11 $P(as)_{2435}$-gfp	Fusion of NgncR_189 promoter to *gfp*	Marc Kaethner
MS11 P_{2258}-gfp	Fusion of NGFG_2258 promoter to *gfp*	Marc Kaethner
MS11 $P(as)_{2258}$-gfp	Fusion of NgncR_007 promoter to *gfp*	Marc Kaethner
MS11 342lif	NGFG_342 locked in frame	Susanne Bauer
MS11 342lof	NGFG_342 locked out of frame	Susanne Bauer
MS11 Δ162	MS11 with NgncR_162 substituted by a kanamycin resistance cassette	Bauer et al. 2017
MS11 Δ163	MS11 with NgncR_163 substituted by a kanamycin resistance cassette	Bauer et al. 2017
MS11 ΔΔ162/3	MS11 with NgncR_162 and NgncR_163 substituted by a kanamycin resistance cassette	Bauer et al. 2017
MS11 ΔΔc 162/3	MS11 ΔΔ162/163 with NgncR_162 and NgncR_163 inserted between iga and trpB	Bauer et al. 2017
MS11 ΔΔ162/3 AIE162	MS11 ΔΔ162/3 complemented with NgncR_162 under control of P_{tet} in iga-trpB locus	This study
MS11 ΔΔ162/3 AIE163	MS11 ΔΔ162/3 complemented with NgncR_163 under control of P_{tet} in iga-trpB locus	This study

MS11 45mut	MS11 expressing NGFG_0045 mutated in 3' region	This study
MS11 45mut ΔΔ162/163	MS11 ΔΔ162/163 expressing NGFG_0045 mutated in 3' region	This study
MS11 ΔgdhR	MS11 with GdhR substituted by a kanamycin resistance cassette	This study
MS11 Popa45	MS11 having the promoter region of NGFG_0045 exchanged by P_{opa}	Susanne Bauer
MS11 Popa45 ΔΔ162/3	MS11 Popa45 with NgncR_162 and NgncR_163 substituted by a kanamycin resistance cassette	Susanne Bauer
MS11 Popa45 ΔΔc162/3	MS11 Popa45 ΔΔ162/3 with NgncR_162 and NgncR_163 inserted in iga-trpB locus	Susanne Bauer
MS11 P_{162}-gfp	MS11 carrying a fusion of the NgncR162 promoter to gfp in iga-trpB	This study
MS11 P_{163}-gfp	MS11 carrying a fusion of the NgncR163 promoter to gfp in iga-trpB	This study
MS11 P_{163}2-gfp	MS11 carrying a fusion of the region comprising NgncR 162 and the intergenic region between NgncR162 and NgncR163 to gfp in iga-trpB	This study
MS11 ΔΔcs162	MS11 ΔΔ162/3 complemented with NgncR_162 under control of a truncated promoter	This study
MS11 ΔΔcs163	MS11 ΔΔ162/3 complemented with NgncR_163 under control of a truncated promoter	This study
MS11 Δ2170	MS11 with the region covering the first 47 codons of NGFG_2170 substituted by ermC	Bauer et al. 2017
MS11 ΔrelA	MS11 with RelA substituted by a erythromycin resistance cassette	This study
MS11 Δ1511	MS11 with NGFG_1511 substituted by a kanamycin resistance cassette	Susanne Bauer
MS11 ΔgntR	MS11 with GntR substituted by a kanamycin resistance cassette	Eva-Maria Hörner
MS11 Δhfq	MS11 with Hfq substituted by a kanamycin resistance cassette	Elisabeth Heinrichs
MS11 hfq-FLAG	MS11 containing 3xFLAG-tagged hfq	Elisabeth Heinrichs
MS11 P_{opa}162	MS11 expressing NgncR_162 under control of P_{opa} in iga-trpB locus	Johannes Kullmann

MS11 P_{opa}163	MS11 expressing NgncR_163 under control of P_{opa} in iga-trpB locus	Johannes Kullmann
MS11 1721-gfp	MS11 carrying a translational fusion of gfp to NGFG_1721 integrated between iga and trpB	Bauer et al. 2017
MS11 ΔΔ162/3 1721-gfp	MS11 ΔΔ162/3 carrying a translational fusion of gfp to NGFG_1721 integrated between iga and trpB	Bauer et al. 2017
MS11 Δopa ΔΔ162/3	MS11 Δopa with NgncR_162 and NgncR_163 substituted by a kanamycin resistance cassette	This study
MS11 Δopa ΔΔc 162/3	MS11 Δopa ΔΔ162/3 complemented with NgncR_162 and NgncR_163	This study
MS11 Δopa ΔΔ162/3 opa_{50}	MS11 Δopa ΔΔ162/3 expressing opa_{50}	Susanne Bauer
MS11 Δopa ΔΔc 162/3 opa_{50}	MS11 Δopa ΔΔc 162/3 expressing opa_{50}	Susanne Bauer
MS11 Δ237	MS11 with NgncR_237 substituted by a kanamycin resistance cassette	Julia Kirsch
MS11 Δ237 237AIE	MS11 Δ237 complemented with NgncR_237 under control of P_{tet} in iga-trpB locus	Julia Kirsch
MS11 P_{PilE}559gfp-AIE237	MS11 Δ237 with NGFG_559 under control of P_{PilE} fused to gfp and expressing NgncR237 under control of P_{tet} in iga-trpB locus	This study
MS11 Δ237 AIE237 P_{opa}1006gfp	MS11 Δ237 AIE237 with a translational fusion of gfp to NGFG_1721 integrated between LP and AA	This study
MS11 Δ237 AIE237 2119gfp	MS11 Δ237 AIE237 with a translational fusion of gfp to NGFG_2119	This study
MS11 Δopa Δ237	MS11 Δopa with NgncR_237 substituted by a kanamycin resistance cassette	This study
MS11 Δopa Δ237 c237	MS11 Δopa Δ237 complemented with NgncR_237 in iga-trpB	This study
MS11 Δopa Δ237 opa_{50}	MS11 Δopa Δ237 expressing opa_{50}	This study
MS11 Δopa Δ237 c237 opa_{50}	MS11 Δopa Δ237 c237 expressing opa_{50}	This study
MS11 Δopa ΔBns2-2	MS11 Δopa with Bns2-2 substituted by a kanamycin resistance cassette	This study
MS11 Δopa ΔBns2-2 opa_{50}	MS11 Δopa ΔBns2-2 expressing opa_{50}	This study

2.1.1.2 Escherichia coli strains

Table 2.2: *E. coli* strains used in this study

Strain	Description	Source
DH5α	Used for cloning	Thermo Scientific
TOP10	Used for 2-plasmid-system	Thermo Scientific

2.1.2 Cell lines

Chang (human conjunctiva epithelial cells): ATCC CCL20.2
Cultured in RPMI1640 (with glutamine and Hepes) supplemented with 10 % FCS.

HCET (human corneal epithelial cells): ATCC PCS-700-010
Cultured in DMEM (high glucose) supplemented with 10 % FCS.

2.1.3 Plasmids

Table 2.3: Plasmids

Plasmid	Description	Source
pSL1180	Cloning vector, derivate of pUC118, amp^R	Amersham Biosciences
pMR68	For integration in *N. gonorrhoeae iga-trpB* locus, kan^R, erm^R	Ramsey et al. 2012
pJV300	Plasmid expressing a nonsense sRNA	Urban and Vogel 2007
pXG10-SF	Standard plasmid for *gfp* fusion cloning	Corcoran et al. 2012
pXG30-SF	Plasmid for operonic *gfp* fusion cloning	Corcoran et al. 2012
pLAS::pPilE mCherry	Complementation vector for *N. gonorrhoeae*, for integration in NGFG_01468-NGFG_01471 locus, $spec^R$	Prof. Dr. Berenike Maier
pMR_AIE162	pMR68 with NgncR_162 placed immediately downstream of the -10 box of P_{tet}, used for construction of MS11 ΔΔ162/3 AIE162	This study
pMR_AIE163	pMR68 with NgncR_163 placed immediately downstream of the -10 box of P_{tet}, used for construction of MS11 ΔΔ162/3 AIE163	This study

pMR_P_{162}gfp	pMR68 containing 200 bp promoter region of NgncR_162 fused to *gfp,* used for construction of MS11 P_{162}-gfp	This study
pMR_P_{163}gfp	pMR68 containing 100 bp promoter region of NgncR_163 fused to *gfp,* used for construction of MS11 P_{163}-gfp	This study
pMR_P_{163}2gfp	pMR68 containing a fusion of NgncR_162 including the promoter and the intergenic region between the sRNA genes fused to *gfp,* used for construction of MS11 P_{163}2-gfp	This study
pMR_ΔΔcs162	pMR68 containing sRNA gene NgncR_162 and about 35 bp its upstream region, used for construction of MS11 ΔΔcs162	This study
pMR_ΔΔcs163	pMR68 containing sRNA gene NgncR_163 and about 35 bp its upstream region, used for construction of MS11 ΔΔcs163	This study
pMR-162/163	pMR68 containing sRNA genes NgncR_162 and NgncR_163 and the upstream region of NgncR_162, used for construction of MS11 Δopa ΔΔc	Bauer et al. 2017
pSLack-gfp	pSL1180 containing a translational *ack-gfp* fusion	Bauer et al. 2017
pMR-AIE237	pMR68 with NgncR_237 placed immediately downstream of the -10 box of P_{tet}	Julia Kirsch
pMR-237c	pMR68 containing sRNA gene NgncR_237, used for construction of MS11 Δopa Δ237c	Julia Kirsch
pMR-AIE237-559gfp	pMR-AIE237 containing the upstream region and the first codons of NGFG_0559 fused to *gfp* under control of P_{PilE}, used for construction of MS11 AIE237Δ P_{PilE}-559gfp	This study
pSL1006gfp	pSL1180 containing the upstream region and the first codons of NGFG_1006 fused to *gfp* under control of P_{opa}, used for construction of MS11 Δ237 AIE237 P_{opa}1006gfp	This study
pJV237	derivative of pJV300 expressing NgncR_237	This study
pJV237mut2	derivative of pJV300 expressing NgncR_237 with mut2 mutation	This study
pJV237mut3	derivative of pJV300 expressing NgncR_237 with mut3 mutation	Susanne Bauer

pXG-1006gfp	pXG10-SF derivative expressing a translational gfp-fusion of NGFG_01006 (pos. -185 to +66 relative to ATG)	This study
pXG-1006m2 gfp	pXG10-SF derivative expressing a translational gfp-fusion of NGFG_01006 (pos. -185 to +66 relative to ATG) with m2 mutation in the 5' UTR complementary to pJV237m2	This study
pXG-559gfp	pXG10-SF derivative expressing a translational gfp-fusion of NGFG_00559 (pos. -94 to +63 relative to ATG)	Susanne Bauer
pXG-559m3gfp	pXG10-SF derivative expressing a translational gfp-fusion of NGFG_00559 (pos. -94 to +63 relative to ATG) with m3 mutation in the 5' UTR complementary to pJV237m3	Susanne Bauer
pXG-693gfp	pXG30-SF derivative expressing a translational gfp-fusion of NGFG_00693 (pos. -136 to +105 relative to ATG)	This study
pXG-2119gfp	pXG10-SF derivative expressing a translational gfp-fusion of NGFG_02119 (pos. -127 to +87 relative to ATG)	Susanne Bauer

2.1.4 Oligonucleotides

Table 2.4: Oligonucleotides used for cloning

Sequences introduced for cloning purposes are given in lower case letters and restriction sites are underlined.

Name	Sequence 5'-3'	Amplification of
162-5(EcoRV)	tataatgatatcCCGTTGAGTTGCTTGATGCA	NgncR_162
162-2(SalI)	tataatgtcgac GGAACGAATTATGCAGCTTTTCC	NgncR_162
163-5(EcoRV)	tataatgatatcCGTTAGCTGGTTCGAGTAGT	NgncR_163
163-2(SalI)	tataatgtcgac TAACAACATCACGCACAGAGG	NgncR_163
45-3UTR-1	taatgaattcgccgtctgaa TTCGGTTCGCTGGTGTTCGC	3' region of *dinD*
45mut-1	tcatcacaatggcggaagtactca TTCGTCTTTGACATTAAAATCCTG	3' region of *dinD* delting the very 3' end

45mut-2	caggattttaatgtcaaagacgaa TGAGTACTTCCGCCATTGTGATGA	3' region of *dinD* delting the very 3' end
45mut-3	taatgtcgac GTGGAACGCGAATGGCAGCCGTA	3' region of *dinD*
45mut-spec-1	aatatggcggattaacaaaaaccg GTGGAACGCGAATGGCAGCCGTA	3' region of *dinD* with overlap to spec^R
spec-45mut-1	tacggctgccattcgcgttccac CGGTTTTTGTTAATCCGCCATATT	spec^R with overlap to 3' region of *dinD*
spec-45mut-2	ccggcagccttaacagggaaagc TTGTGTAGGGCTTATTATGCAGC	spec^R, overlap to down-stream region of *dinD*
45mut-spec2	gctgcataataagccctacacaa GCTTTCCCTGTTAAGGCTGCCGG	downstream region of *dinD,* overlap to spec^R
45mut-5	attatagagctc GGGGTGCAATATCTAAGGAATT	downstream region of *dinD*
C162-5	tataatgtcgacTGATTCTACCGCCCTAAAGG	Upstream region of NgncR_162
162gfp1	tatgtatatctccttcttaaatcta CGGTAATTATCCGCCGTTTCTT	Upstream region of NgncR_162 with overlap to *gfp*
162gfp2	aagaaacggcggataattaccg TAGATTTAAGAAGGAGATATACATA	*gfp*, overlap to upstream region of NgncR_162
PFcsiSgfp3	tataattctaga GCCGTCTGAAAACAGCCAAGCTTGCATGC	*gfp*
C163-5	tataatgtcgacTGTGTGCATTTTTTATCTCCGC	Upstream region of NgncR_163
163gfp1	tatgtatatctccttcttaaatcta AACGAATTATGCAGCTTTTCCGGTC	Upstream region of NgncR_163 with overlap to *gfp*
162-P5	tataatgaattcTGATTCTACCGCCCTAAAGG	Upstream region of NgncR_162
163gfp2	gaccggaaaagctgcataattcgtt TAGATTTAAGAAGGAGATATACATA	*gfp*, overlap to upstream region of NgncR_163
CS162-5	tataatgtcgac AATTGACAGCAGATAAGAAACGG	NgncR_162 with short promoter
162-22	tataattctaga GGAACGAATTATGCAGCTTTTCC	NgncR_162
CS163-5	tataatgtcgacGCTTGCTTTTTGACCGG	NgncR_163 with short promoter
163-2	tataattctagaTAACAACATCACGCACAGAGG	NgncR_163
relA-1	taaaggatccgccgtctgaa	Upstream region of *relA*

	GGCAAGGCATGAAATCGA	
relA-2	caattaaccctcactaaaggtacc TTCAGACGGCTTTCGGGATGTA	Upstream region of *relA* with overlap to ermC
relA-3	ttgttctttttcgtgtacctgca GCCTGTTAATCAAAAGGCAACC	Downstream region of *relA* with overlap to ermC
relA-4	tatttgagctcAGCCTTGATTCACGGACAGC	Downstream region of *relA*
relAermC1	tacatcccgaaagccgtctgaa GGTACCTTTAGTGAGGGTTAATTG	ermC with overlap to upstream region of *relA*
relAermC2	ggttgccttttgattaacagg CTGCAGGTACACGAAAAAGAACAA	ermC, overlap to down-stream region of *relA*
D1559-1	gccgtctgaaGTCCAGTGTAGCGTATGGG	Upstream region of *gdhR*
D1559-2	ttgagacacaattcatcgatgat CGTCAACGGCACTTACCTCG	Upstream region of *gdhR*, overhang to kan^R
D1559-3	tgcaggcatgcaagcttcag GGCGCAAAACGATTTGAAGCG	Downstream region of *gdhR*, overhang to kan^R
D1559-4	GAATATGCCGTCGACTTTGG	Downstream region of *gdhR*
1559kan-5’	cgaggtaagtgccgttgacg ATCATCGATGAATTGTGTCTCAAA	kan^R, overhang to upstream region of *gdhR*
1559kan-3’	cgcttcaaatcgttttgcgcc CTGAAGCTTGCATGCCTGCA	kan^R, overhang to downstream region of *gdhR*
162_up_s	gccgtctgaaGGCGATTTGTCCGCACAATG	Upstream region of NgncR_162
163_down_as	CCGTATCCCGATGACGGAGCT	Downstream region of NgncR_163
LP1	tataatgaattcAAACAGCTCGGAATCAAAGGC	lactate permease locus
LP2	tataatgatatcGTATCGGGTGTGTTGATTGG	lactate permease locus
AA-52	tataatctgcaggccgtctgaa TATCGGGCAGGCGTGATTGC	aspartate aminotransferase locus
AA-3(SpeI)	tataatactagtAAATCTTCAATCATGCCGTCC	aspartate aminotransferase locus
Popa5	tataatggtaccGGTTTTTGTTAATCCGCCA	P_{opa}
spec2	tataatctgcagTGTAGGGCTTATTATGCAGC	$Spec^r$
Popa(EcoRV)	tataatgatatcGGTTTTTGTTAATCCGCCA	P_{opa}
Popa1006-1	tttgtttcctgtgtgtattttgg ATTATATCGGGTTCCGGGCG	P_{opa}, overhang to upstream region of NGFG_1006

Popa1006-2	cgcccggaacccgatataat CCAAAATACACACAGGAAACAAA	Upstream region of NGFG_1006, overhang to P_{opa}
GfpSF-(KpnI)	tataatggtacc TTATTTGTAGAGCTCATCCATGC	*gfp*-SF
PpilE-5	tataatgtcgacAATCAACACACCCGATACC	P_{pilE} promoter
PpilE559-1	ggcctctttcccattcagttgt TGCGTATTATAAAGCAAGATTCGTGC	P_{pilE} promoter with overhang to *dinD*
PpilE559-2	cacgaatcttgctttataatacgca ACAACTGAATGGGAAAGAGGCC	Upstream region of *dinD*, overhang to P_{PilE}
gfp-SF(SalI)	tataatgtcgac TTATTTGTAGAGCTCATCCATGC	*gfp*-SF
237-1	tataatgaattcTTGTTTTAGCAATGTCTGTTTCG	NgncR_237
237-2	tataattctaGATGTAACCTTAATCAGTCGGAC	NgncR_237
237mut-3	CGTTTTCCCCGTAcgcgcTTTGGCCGTC	NgncR_237 with mutation m2
237mut-4	GACGGCCAAAgcgcgTACGGGGAAAACG	NgncR_237 with mutation m2
6935UTR1	tataatatgcatGATATAGGCGGCAAAAGCGTC	5'end of NGFG_0693
6935UTR2	tataatgctagcGATTTTGTTGCCCTCCTCTTCC	5'end of NGFG_0693
10065UTR1	tcacatatgcat CCAAAATACACACAGGAAACAAA	5'end of NGFG_1006
10065UTR2	tataatgctagc ATTCGCACCCAATGGGCTTGAA	5'end of NGFG_1006
1006UTR_m1	ATTATCCGAATATCAAAGCGCGTATG	5'end of NGFG_1006, with mutation m2
1006UTR_m2	CATACGCGCTTTGATATTCGGATAAT	5'end of NGFG_1006, with mutation m2

Table 2.5: Oligonucleotides used for quantitative real time PCR

Name	Sequence 5'-3'	Target
qRT2435-1	TACCCACGATTATCCGAAACC	NGFG_2435/NgncR_189
qRT2435-2	AAGTCGTAGCCAACCGACAC	NGFG_2435/NgncR_189
qRT2435-3	CCTGAAGACGGAAAATCAGG	NGFG_2435
qRT2435-4	AATCGATGCTGTGTCTGACG	NGFG_2435
qRT2258-1	TACCCACGATTATCCGGAAC	NGFG_2258/NgncR_007
qRT2258-2	AAGTCGTAGCCGACCGACAC	NGFG_2258/NgncR_007
qRT2258-3	TCACTCGGCTTATCCGCTAT	NGFG_2258
qRT2258-4	TTGCTGGGGACGGTAGTAAC	NGFG_2258

qRTgfp-1	GGTGATGCAACATACGGAAA	*gfp*
qRTgfp-2	CTGGGTATCTCGCAAAGCAT	*gfp*
qRT342-1	GGGTTCGGCGTGTAATAAGA	NGFG_342
qRT342-2	GTTGCCGCATTAAACAACCT	NGFG_342
qRT2048-1	CCCTTCCTCGAACACATGAT	NGFG_2048 (*hisB*)
qRT2048-2	GATTGCTTGTCCGAGTGTGA	NGFG_2048 (*hisB*)
qRT349-1	GTCGGTGCGCAACTTTTATT	NGFG_0349 (*hisH*)
qRT349-2	ATATGCGGGACTTTCAGACG	NGFG_0349 (*hisH*)
qRT1965-1	CCGACAATATCGGCAACTTT	NGFG_1965
qRT1965-2	GACGACGGTAAAGGGCAGTA	NGFG_1965
qRT1349-1	TGGAGAACGAATCCAAATCC	NGFG_1349
qRT1349-2	ATTGCCAAATTCAGGCTCAG	NGFG_1349
qRT1133-1	CGCTTTACCTTGACCTGACC	NGFG_1133
qRT1133-2	TGCCCAAAACCTTCAATAGC	NGFG_1133
1721qRT-1	AAAAGGCTTGGGCAAAAACT	NGFG_1721
1721qRT-2	ATACCGAAGCTGGTTTGCAC	NGFG_1721
qRTprpC-1	CGCTTAAAGGTCCGAAACAC	NGFG_1404 (*prpC*)
qRTprpC-2	ACCGATCACGATTTCTTTGC	NGFG_1404 (*prpC*)
qRTack-1	TGGGTATGCTGTTGAACGAA	NGFG_1411 (*ack*)
qRTack-2	AGGACGTCTTGGTCGATGAG	NGFG_1411 (*ack*)
qRT45-1	TCAGGACAAGCTGAACATCG	NGFG_0045
qRT45-2	TTTGTCCATCACGTCCAAAA	NGFG_0045
qRT254-1	GAAAATCCTCGTCGATTCCA	NGFG_0254 (*secB*)
qRT254-2	TTCGATGTTGTGGGTTTCAA	NGFG_0254 (*secB*)
qRT1146-1	TGGCGCAACCGTTGATCATA	NGFG_1146
qRT1146-2	GCAATTTCCGCCGGAAAGGT	NGFG_1146
qRT1353-1	GATGGCGTTGGCGATATCGT	NGFG_1353
qRT1353-2	ATGGGGACGTTTGTGTTTGC	NGFG_1353
qRT1728-1	GACCAATCCTGAGGTTTCCA	NGFG_1728 (*minD*)
qRT1728-2	ACACGTTCGGGAGAATAACG	NGFG_1728 (*minD*)
qRT2039-1	GCTGCCAACCTGAAAGATTC	NGFG_2039 (*ilvC*)
qRT2039-2	CAGCAGCAGCATAACAACAT	NGFG_2039 (*ilvC*)
qRT2111-1	CAACTGGGATACGGAACGAT	NGFG_2111 (*gloA*)
qRT2111-2	GTTGTGCCGTGTTTCATCAG	NGFG_2111 (*gloA*)
qRT2263-1	GGCAAAGTCGGCTACAAAAA	NGFG_2263
qRT2263-2	CCGGAAGCCAAAATAAACAA	NGFG_2263
qRT881-1	AAAAACGCATCCACACCTTC	NGFG_0881 (*leuA*)
qRT881-2	GCAGGAAAATTCCACATCGT	NGFG_0881 (*leuA*)
qRTiscR-1	CCTCCCGCACAAATCAACAT	NGFG_1163 (*iscR*)
qRTiscR-2	AATTCTCCCAAAGGTCGTGC	NGFG_1163 (*iscR*)

qRT1407-1	TACCACCTGTAACGGCATGA	NGFG_1407 (*acn*)
qRT1407-2	AGGAAAGCCTGTTTCGCATA	NGFG_1407 (*acn*)
qRT1491-1	AAAACCGTTCTGAAGCCAAA	NGFG_1491
qRT1491-2	TGATGTCGCATTCTTTGGAA	NGFG_1491
qRT1722-1	CAATAAAGAGCGCATGGTCA	NGFG_1722 (*dadA*)
qRT1722-2	GCTTCGACTTCTTCGGTTTG	NGFG_1722 (*dadA*)
qRT1842-1	GCGAAATCATGAAGGCGTAT	NGFG_1842 (*thiC*)
qRT1842-2	ACGCTTTATCGGTCAATTCG	NGFG_1842 (*thiC*)
qRT2102-1	TTATTACGGCACACGGATGA	NGFG_2102
qRT2102-2	TTCAGGATTGAACGGGTTTC	NGFG_2102
qRT2343-1	ATTTGGCCGGGTTAAGTTCT	NGFG_2343
qRT2343-2	ATCAATTCCGCCAGACAATG	NGFG_2343
qRTNgncR201-1	GCCGAAATCAACAAACAAAGA	NgncR_201
qRTNgncR201-2	CCTGCCTTTTGTGTTTCAGG	NgncR_201
qRT1514-1	CCGTCGGTATTACCCATCAC	NGFG_1514 (*gcvH*)
qRT1514-2	TGCGGCTTTTACATACTCAA	NGFG_1514 (*gcvH*)
qRT2042-1	ATTTTGTCCGAGATGGTTGC	NGFG_2042 (*ilvB*)
qRT2042-2	GATAATTTCGCTGCCGTTGT	NGFG_2042 (*ilvB*)
qRT2153-1	GCCCAACATAAAGATGGCGG	NGFG_2153 (*norB*)
qRT2153-2	CTGTGGGTGGAAGGCTTCTT	NGFG_2153 (*norB*)
qRT93-1	TGGACATCAACGTCTTCCAA	NGFG_0093
qRT93-2	GATTTCAGTTTGCCCGGATA	NGFG_0093
qRT249-1	CGATGATAGGCGGTTTGATT	NGFG_0249
qRT249-2	CGACCGATAAAAACGTCGTC	NGFG_0249
qRT1471-1	ATTGGCGATGGTCAACGAAG	NGFG_1471
qRT1471-2	CCATTCTTCTTTGCTGGTCAAA	NGFG_1471
qRT1564-1	ACCTCTTGGTTTCCCTGCTT	NGFG_1564
qRT1564-2	GTACCGAACGGCATTTTCAT	NGFG_1564
qRT1937-1	AGAAGCCGCCGATATTGATG	NGFG_1937
qRT1937-2	TATTCATCGCATTGGGCAGC	NGFG_1937
2049qRT-1	CAAATGGGTCTGCCTATGGT	NGFG_2049
2049qRT-2	GCTGCCGTAAACTTTTGCTC	NGFG_2049
qRT1697-1	GCATTCAGGACGTGCTCAAAG	NGFG_1697 (RNase E)
qRT1697-2	CGGATTGTTCGGCATCAATAC	NGFG_1697 (RNase E)
qRT1624-1	TTGCCGCCATCGAACGCAAA	NGFG_1624 (RNase II)
qRT1624-2	TGTAGGTCAGCGACTGTTTG	NGFG_1624 (RNase II)
qRT2278-1	TGAATTATACGGTGGCGCGG	NGFG_2278 (RNase III)
qRT2278-2	AGACCGTCGCCGACATTCAT	NGFG_2278 (RNase III)
qRT2082-1	AGGAAGAACACAACAGCGCC	NGFG_2082 (PNPase)
qRT2082-2	CGCCGCGATTCGATGTGTTT	NGFG_2082 (PNPase)

qRT569-1	GTGCGAAGGTTCATCAGAAC	NGFG_0569 (PAP)
qRT569-2	CCCGTTGTGGAAATCCAAAATC	NGFG_0569 (PAP)
qRTgltA-1	GAGCAAAACGCCTCAACTTC	NGFG_0814 (*gltA*)
qRTgltA-2	CCGATTTCATCCAGCATTTT	NGFG_0814 (*gltA*)
qRT2171-1	AAGCATTCGATTTGGGTACG	NGFG_2171 (*alr*)
qRT2171-2	AAATGCCGTATAACGCCAAG	NGFG_2171 (*alr*)
qRT1948-1	AAAGGTAGAAGGACGCAACG	NGFG_1948
qRT1948-2	TCGTCTTCGGCGTTTCTATT	NGFG_1948
qRT664-1	CACAATGTAAGCCTTTATGAA	NGFG_0664
qRT664-2	AAGCTATCTTCCTTATCCTCA	NGFG_0664
qRT1160-1	GTGGAAGACCGCAAATCAAT	NGFG_1160
qRT1160-2	TGCGGTCAAAAATCACAAAA	NGFG_1160
qRT2344-1	AACTTCATCAGCATTGAGTCTG	NGFG_2344
qRT2344-2	CCAATTTTCAATTCCTTCATCC	NGFG_2344
qRTpilEN-1	GAGGCATTTCCCCTTTCAAT	NGFG_1821 (*pilE*)
qRTpilEN-2	GCGGTGTAGTCTTGGTAGGC	NGFG_1821 (*pilE*)
qRT193-1	ATTACAATGACGGCGGTTGC	NGFG_0193 (*hpaC*)
qRT193-2	ATCCTGATGTTCGTCCGCCA	NGFG_0193 (*hpaC*)
qRT252-1	GAAAATCCTCGTCGATTCCA	NGFG_0252 (*rng*)
qRT252-2	TTCGATGTTGTGGGTTTCAA	NGFG_0252 (*rng*)
qRT319-1	ATATTGACCCCGACGGGGGT	NGFG_0319 (*tatC*)
qRT319-2	GAAAAACGCCTGATTACGCC	NGFG_0319 (*tatC*)
qRT515-1	CCGTCTATGTTTCCCCCTTT	NGFG_0515
qRT515-2	GTTCCGTGCTATCCCAAAAA	NGFG_0515
qRT559-1	CGCCAAACACATCGACGAAA	NGFG_0559 (*dinD*)
qRT559-2	TTCCTGATGTTTCGCAAGCG	NGFG_0559 (*dinD*)
qRT609-1	AGGGGGTCCGCACTGTTTAT	NGFG_0609 (*pilX*)
qRT609-2	CTCGGCTAAAGACAAAGCCA	NGFG_0609 (*pilX*)
qRT693-1	ATCACGTCCAAAACCAAAGC	NGFG_0693 (*alaT*)
qRT693-2	TCGGCGAAAATAATCAAACC	NGFG_0693 (*alaT*)
qRT914-1	GGTATGGCGGAAGACTTGAA	NGFG_0914 (*bioB*)
qRT914-2	GACTTTGCCCAAGGTATCCA	NGFG_0914 (*bioB*)
qRT1006-1	CCGTCTAAAAGCTGCCACTC	NGFG_1006
qRT1006-2	TGACCGGGGCTTTATATTTG	NGFG_1006
qRT1290-1	GAAAACGGCGGTATGGAGTA	NGFG_1290
qRT1290-2	AACTCGTTTACGGACGCCTT	NGFG_1290
qRT1338-1	ATGAACGCGTCAAACTGGAG	NGFG_1338
qRT1338-2	GGGTATATTTCGCGCCTTTT	NGFG_1338
qRT1380-1	GCAGCCTGCAGAAACGGAAA	NGFG_1380 (*ftsN*)
qRT1380-2	TCGGCAGCTTTTTCCGCATC	NGFG_1380 (*ftsN*)

qRT1479-1	TTTACGCTGCTCGAGCTGAT	NGFG_1479
qRT1479-2	TCCAAGTTTTGCGCGTTCAC	NGFG_1479
qRT1617-1	TCAAAGTTTTCCGCCAAGTC	NGFG_1617
qRT1617-2	TGTTGTGGTGCAGGAGTTTG	NGFG_1617
qRT1941-1	AACGGGGAGAATTGGTTTTC	NGFG_1941
qRT1941-2	CCAAACCCAAAAGCAACAGT	NGFG_1941
qRT1964-1	CCGTGTCCCTATTGGAAGAA	NGFG_1964 (*arsC*)
qRT1964-2	AATCATCTTTCACGCGCATC	NGFG_1964 (*arsC*)
qRT2119-1	GGGGGATTTTCTTTGTTCGC	NGFG_2119 (*pilG*)
qRT2119-2	GGATGCCGCGTTTTGCCAGT	NGFG_2119 (*pilG*)

Table 2.6: Northern Blot probes

Name	Sequence 5'-3'	Target
5S RV	TTGGCAGTGACCTACTTTCG	5S rRNA
MS11_1.249.008	TGTGTGCCAAGTCGACAAAGGAGA	NgncR_162/163
NBS162	AATCAAGCTGCATCAAGCAACTCAA	NgncR_162
NBS163	TATTAACTGACTACTCGAACCAGCT	NgncR_163
NBStAla	CAAAGCAGGTGCTCTACCAACTGA	Alanine tRNA
NB237-1	CACATTACGGGGAAAACGTCTTACTCAATGAG	NgncR_237 and Bns2-2
NB237-2	TGCGAAACAGACATTGCTAAAACA	NgncR_237
Bns22NB	GCTCATAATCCTGCTTGAACAGG	Bns2-2

2.1.5 Media and buffers

Table 2.7: Bacterial culture media

Medium	Ingredients
GC agar	36.23 g GC agar base (Oxoid) in 1 l H_2O, after autoclaving 1 % (v/v) vitamin mix is added
Graver-Wade medium	1 l M199 cell culture medium (with Earle's salts, without glutamine), supplemented with 500 ml solution containing 10 g glucose, 2 g ammonium bicarbonate, 1 g sodium acetate, 0.75 g L-glutamine, 0.2 g spermidine, 0.1 g L-arginine, 0.05 g hypoxanthine, 0.05 g uracil, 0.05 g oxaloacetate, 0.05 g thiamine hydrochloride, 0.01 g L-ornithine, 0.01 g NAD, 2.5 ml 60 % (w/w) DL-lactate; hypoxanthine and uracil were dissolved in 1 N NaOH; pH was adjusted to 6.8 and the medium was sterile filtered

Hepes medium	50 ml solution I, 10 ml solution II, 200 µl solution III, 3 ml solution IV/V, 5 ml solution VI, 50 ml solution VII, 50 ml solution VIII; fill up to 500 ml with dH_2O, adjust pH to 7.3, sterile filter
Hepes solution I	0.1 % (w/v) L-alanine, 0.15 % (w/v) L-arginine, 0.025 % (w/v) L-asparagine, 0.025 % (w/v) L-glycine, 0.018 % (w/v) L-histidine, 0.05 % (w/v) L-lysine, 0.015 % (w/v) L-methionine, 0.05 % (w/v) L-proline, 0.05 % (w/v) L-serine, 0.05 % (w/v) L-threonine, 0.061 % (w/v) L-cysteine, 0.036 % (w/v) L-cystine, 0.05 % (w/v) L-glutamine, 0.046 % (w/v) glutathione reduced, 0.0032 % (w/v) hypoxanthine, 0.008 % (w/v) uracil and 0.004 % (w/v) D-biotin are dissolved in 18 % 1 N NaOH and 82 % dH_2O, pH adjusted to 7.2
Hepes solution II	37.5 % (w/v) glucose
Hepes solution III	1 % (w/v) $Fe(NO_3)_3 \times 9H_2O$
Hepes solution IV/V	0.33 % (w/v) NAD, 0.33 % (w/v) cocarboxylase, 0.33 % (w/v) thiamine, 0.33 % (w/v) calcium panthotenate, 0.188 % (w/v) $CaCl_2 \times 2H_2O$, 4.17 % (w/v) sodium lactate, 15.33 % (w/v) glycerol, 3.33 % (w/v) oxaloacetate
Hepes solution VI	5 % (w/v) $MgCl_2 \times 7H_2O$
Hepes solution VII	5 % (w/v) NaCl, 3.4 % (w/v) sodium acetate
Hepes solution VIII	2.38 % (w/v) Hepes
CDM-10	25 ml 4x stock, 71 ml ddH_2O, 4 ml 500 mM $NaHCO_3$; add 100 µl 1 M $MgCl_2$, stir, then add 25 µl 1 M $CaCl_2$ and 100 µl 10 mM $Fe(NO_3)_3$, sterile filter
CDM-10 4x stock	Combine solutions I to VI, add 20 g Hepes, adjust pH to 7.5, add ddH_2O to 500 ml, sterile filter
CDM-10 solution I	0.006 g Na_2EDTA in 25 ml 0.1 N NaOH, add 11.7 g NaCl, 2 g K_2SO_4, 0.44 g NH_4Cl; up to 50 ml with ddH_2O
CDM-10 solution II	0.696 g K_2HPO_4, 0.544 g KH_2PO_4, dissolve in 4 ml ddH_2O
CDM-10 solution III	Dissolve 0.2 g L-alanine, 0.3 g L-arginine, 0.05 g L-asparagine and 1 g L-aspartic acid in 25 ml 0.2 N NaOH; dissolve 0.11 g L-cysteine and 0.07 g L-cystine in 25 ml 1 % HCl; dissolve 2.6 g L-glutamic acid, 0.1 g L-glutamine, 0.05 g L-glycine, 0.05 g L-histidine, 0.06 g L-isoleucine, 0.18 g L-leucine and 0.1 g L-lysine in 25 ml 4 % HCl; dissolve 0.03 g L-methionine, 0.05 g L-phenylalanine, 0.1 g L-proline, 0.1 g L-serine, 0.1 g L-threonine in 25 ml ddH_2O; dissolve 0.16 g L-tryptophan and 0.12 g L-valine in 25 ml ddH_2O; dissolve 0.09 g glutathione and 0.14 g L-tyrosine in 0.2 N NaOH; combine all fractions and fill up to 250 ml with ddH_2O
CDM-10 solution IV	0.004 g thiamine HCl, 0.001 g thiamine pyrophosphate, 0.0038 g pantothenic acid, 0.006 g d-biotin; dissolve in 20 ml 50 % ethanol

CDM-10 solution V	10 g glucose in 50 ml ddH_2O
CDM-10 solution VI	0.1 g hypoxanthine, 0.1 g uracil; dissolve in 20 ml 0.1 N NaOH
LB medium	10 g tryptone, 5 g yeast extract, 10 g NaCl in 1 l dH_2O
LB agar	10 g tryptone, 5 g yeast extract, 10 g NaCl, 15 g agar in 1 l dH_2O
Proteose Peptone Medium (PPM)	15 g proteose peptone No. 3, 5 g NaCl, 0.5 g soluble starch, 1 g KH_2PO_4, 4 g K_2HPO_4 in 1 l dH_2O
PPM+	PPM supplemented with 1 % (v/v) vitamin mix, 0.5 % (w/v) $NaHCO_3$
Vitamin mix	Solutions I and II are combined to 2 l with dH_2O, sterile filtered
Vitamin mix solution I	200 g glucose, 20 g L-glutamine, 52 g L-cysteine x HCl, 0.2 g cocarboxylase, 0.04 g iron(III)nitrate x 9H_2O, 0.006 g thiamine x HCl, 0.026 g 4-aminobenzoic acid, 0.5 g NAD, 0.02 g vitamin B12; dissolve in 1 l H_2O
Vitamin mix solution II	2.2 g L-cystine, 2 g adenine hemisulfate, 0.06 g guanine x HCl, 0.3 g L-arginine x HCl, 1 g uracile; dissolve in 600 ml dH_2O and 30 ml 32 % HCl

Table 2.8: Buffers used for DNA extraction, agarose gels and Northern Blots

Buffer	Composition
Blue juice	65 % (w/v) sucrose, 10 mM Tris HCl pH 7.5, 10 mM EDTA, 0.3 % (w/v) xylene cyanol and 0.3 % (w/v) bromphenol blue
GTE buffer	50 mM glucose, 25 mM Tris HCl pH 8, 10 mM EDTA
10x MOPS buffer	10 mM EDTA, 200 mM MOPS, 50 mM sodium acetate, pH 7 with NaOH
Northern transfer buffer	175.5 g NaCl, 0.62 g N-Lauroylsarcosine sodium salt, 0.32 g NaOH in 1 l DEPC-treated water
Northern wash buffer	2x SSC, 0.1 % (w/v) SDS
PBS	137 mM NaCl, 2.7 mM KCl, 10 mM Na_2HPO_4, 1.8 mM KH_2PO_4, pH 7.4
5x Phosphate buffer	79.25 g Na_2HPO_4, 60.25 g NaH_2PO_4 in 1 l DEPC-treated water
RNA loading buffer	750 µl formamide, 150 µl 10x MOPS buffer, 262 µl 37 % formaldehyde solution, 5 µl 1 % ethidium bromide solution
2x RNA loading dye	95 % (v/v) formamide, 18 mM EDTA, 0.025 % (w/v) SDS, traces of xylene cyanol and bromphenol blue
20x SSC	175.3 g NaCl, 88.2 g sodium citrate to 1 l dH_2O, pH 7 with HCl
TBE buffer	1.1 M Tris, 900 mM boric acid, 25 mM EDTA pH 8

Table 2.9: Buffers used for SDS PAGE and Western Blotting

Buffer	Composition
ECL-1	1 ml luminol, 0.44 ml cumaric acid, 10 ml 1 M Tris HCl pH 8.5 up to 100 ml with dH_2O
ECL-2	10 ml 1 M Tris HCl pH 8.5, 62 µl 30 % H_2O_2 up to 100 ml with dH_2O
2x Lämmli	125 mM Tris-HCl (pH 6,8), 20 % (w/v) glycerol, 4 % (w/v) SDS, 0.04 % (w/v) bromphenolblue, 10 % (v/v) β-mercaptoethanol
10x SDS running buffer	30 g Tris, 144 g glycine and 10 g SDS to 1l dH_2O
TBS	20 mM Tris, 150 mM NaCl, pH 7.6 with HCl
TBS-T	1 l TBS with 1 ml Tween-20
Western Blot transfer buffer	5.3 g Tris, 2.9 g glycine, 0.37 g SDS, 100 ml ethanol in 1l dH_2O

Table 2.10: Buffers and solution used for immunuefluorescent staining

Buffer	Composition
Blocking solution	1 % (w/v) BSA in 1x D-PBS
Mowiol mounting medium	35 g glycerol, 12 g Mowiol, 30 ml dH_2O, 60 ml 0.2 M Tris-HCl pH 8.5
Permeabilization solution	0.2 % (v/v) Triton-100 in 1 x D-PBS

2.1.6 Antibiotics and additives

Table 2.11: Concentration of antibiotics used

Name	Final concentration	Source
Ampicillin	100 µg/ml (*E. coli*)	Sigma-Aldrich
Anhydrotetracycline	2 ng/ml (*N. gonorrhoeae*)	Acros Organics
Chloramphenicol	30 µg/ml (*E. coli*)	Fluka
Erythromycin	200 µg/ml (*E. coli*)	Sigma-Aldrich
	7 µg/ml (*N. gonorrhoeae*)	
Gentamicin	50 µg/ml (*N. gonorrhoeae*)	Sigma-Aldrich
Kanamycin	30 µg/ml (*E. coli*)	Carl Roth
	40 µg/ml (*N. gonorrhoeae*)	
Spectinomycin	50 µg/ml (*E. coli*)	Sigma-Aldrich
	40 µg/ml (*N. gonorrhoeae*)	

Tetracycline	10 µg/ml (*N. gonorrhoeae*)	AppliChem

2.1.7 Antibodies and dyes

Table 2.12: Antibodies and fluorescent dyes

Name	Origin	Dilution	Manufacturer
αGFP	mouse	1:1000	Santa Cruz
αHsp60	mouse	1:1000	Santa Cruz
αFlag	rabbit	1:500	Sigma
αmouse-HRP	goat	1:3000	Santa Cruz
αrabbit-HRP	goat	1:3000	Santa Cruz
αNeisseria	rabbit	1:300	US Biological
αrabbit-Cy5	goat	1:100	Dianova
αrabbit-Cy2	goat	1:100	Dianova
Phalloidin555	-	1:100	Invitrogen

2.1.8 Enzymes

Table 2.13: Enzymes used in this study

Enyzme	Manufacturer
FastAP	Thermo Scientific
ReproFast Polymerase	Genaxxon Bioscience
Restriction enzymes	Thermo Scientific
RNase A	Thermo Scientific
T4 Ligase	Thermo Scientific
T4 Polynucleotide Kinase (PNK)	Thermo Scientific
Taq Polymerase	Genaxxon Bioscience

2.1.9 Kits

Table 2.14: Commercial Kits

Name	Purpose	Manufacturer
GeneJet Gel Extraction Kit	PCR purification	Thermo Scientific
Invitrogen™ Decade™ Markers System	RNA ladder labelling	Thermo Scientific
miRNeasy micro Kit	RNA extraction	Qiagen

NucleoSpin Plasmid Kit	Plasmid preparation	Macherey-Nagel
Random Primer DNA Labeling Kit Ver. 2	Radioactive labelling	Takara
RevertAid first strand cDNA synthesis Kit	cDNA synthesis	Thermo Scientific
RNase-free DNase Set	DNase digestion	Qiagen

2.1.10 Chemicals and size standards

Acrylamide Rotiphorese 30 (Carl Roth), Acrylamide Rotiphorese 40 (Carl Roth), agar (BD), D-alanine (Carl Roth), D-alanine-$^{13}C_3$ (Sigma), L-alanine (Sigma), adenine hemisulfate (Sigma), 4-aminobenzoic acid (Merck), ammonium bicarbonate (Roth), L-arginine monohydrochloride (Sigma), L-asparagine (Sigma), [γ-^{32}P] ATP (Hartmann Analytic), Bacto™ Proteose Peptone No. 3 (BD), calcium chloride (Carl Roth), calcium panthotenate (Sigma), cocarboxylase (Sigma), [α-^{32}P] CTP (Hartmann Analytic), L-cysteine hydrochloride (Sigma), L-cystine (Sigma), dipotassium phosphate (Roth), desoxyribonucleic acid triphosphates (dNTPs) (Genaxxon), diethyl pyrocarbonate (Carl Roth), DMEM with 4500 mg/L glucose + L-glutamine + sodium pyruvate + sodium bicarbonate (Sigma), 6x DNA loading dye (Thermo Scientific), D-PBS (Gibco), fetal calf serum (FCS) (Gibco), Ficoll (GE Healthcare), GC agar base (Oxoid), GeneRuler™ 1 kb DNA ladder (Thermo Scientific), D(+)glucose (Carl Roth), L-glutamine (Sigma), glycine (Carl Roth), glycerol (Carl Roth), guanine hydrochloride (Roth), HBSS medium (Gibco), HD Green DNA dye (Intas), Hepes (Sigma), High ROX Sybr Green Master Mix (Genaxxon), L-histidine (Sigma), hydrochloric acid 37 % (Merck), hypoxanthine (Sigma), iron (III) nitrate 9H_2O (Sigma), M199 cell culture medium with Earle's salts without glutamine (Sigma), magnesium chloride (Merck), nicotinamide adenine dinucleotide (NAD) (Sigma), L-ornithine (Sigma), oxaloacetate (Sigma), PAGEruler Prestained Protein ladder (Thermo Scientific), Potassium dihydrogen phosphate (Roth), RiboRuler High Range RNA Ladder (Thermo Scientific), RiboRuler Low Range RNA Ladder (Thermo Scientific), rifampicin (Roth), RPMI 1640 with glutamine and Hepes (Gibco), saponin (Sigma), sodium acetate (Sigma), sodium chloride (VWR), sodium hydrogen carbonate (Merck), sodium lactate (Roth), sodium pyruvate (PAA), soluble starch (Sigma), tetramethylethylenediamine (TEMED) (Fluka Analytics), thiamine hydrochloride (Sigma), tryptone (BD), ULTRAhyb Ultrasensitive Hybridization Buffer (Thermo Scientific), uracil (Sigma), vitamin B12 (Sigma), yeast extract (Carl Roth)

All other chemical were purchased from Carl Roth, Serva, Sigma or Merck if not stated otherwise.

2.1.11 Technical equipment

Table 2.15: Technical equipment

Equipment	Manufacturer
Centrifuge 5415R (cooling centrifuge)	Eppendorf
Chemiluminescence camera system (Chemostar)	Intas
Gel Imager (Biostep Dark hood DH 40-50)	Biostep
HeraCell 240i incubator	Thermo Scientific
Megafuge 1.0R	Heraeus
Microcentrifuge Mikro 2000	Hettich
NanoDrop 1000 spectrophotometer	Peqlab Biotechnology
PCR Thermocycler T3	Biometra
Photometer Ultrospec 3100 pro	Amersham Biosciences
PerfectBlue™ Doppel-Gelsystem Twin S	Peqlab Biotechnology
PerfectBlue Semi-Dry Elektroblotter	Peqlab Biotechnology
pH electrode SenTix	WTW series inolab
StepOne Plus real-time PCR system	Life technologies
TCS SP5 confocal microscope	Leica
TCS SPE confocal microscope	Leica
Tecan Infinite M Plex plate reader	Tecan
Typhoon 9200 Imager	GE Healthcare

2.1.12 Software and webtools

Table 2.16: Software and webtools

Software	Company/homepage
ApE A plasmid editor 8.5.2.0	Wayne Davis (University of Utah)
Argus x1 version 7.6.17	Biostep
CopraRNA	University of Freiburg (Wright et al. 2014): http://rna.informatik.uni-freiburg.de/CopraRNA/Input.jsp
GraphPad Prism 5	GraphPad Software, Inc.
ImageJ	National Institutes of Health (Schneider et al. 2012)
IntaRNA	University of Freiburg (Mann et al. 2017): http://rna.informatik.uni-freiburg.de/IntaRNA/Input.jsp
Integrated Genome Browser	BioViz (Freese et al. 2016)
LabImage Chemostar	Intas
Leica LAS AF confocal microscope software	Leica microsystems

MAFFT Alignment Tool	European Bioinformatics Institute (Madeira et al. 2019): https://www.ebi.ac.uk/Tools/msa/mafft/
MView	European Bioinformatics Institute (Madeira et al. 2019): https://www.ebi.ac.uk/Tools/msa/mview/
NCBI blast	National Center for Biotechnology Information: https://blast.ncbi.nlm.nih.gov/Blast.cgi
ND-100 V3.7.1	NanoDrop Technologies, Inc. Wilmington
Office 2016	Microsoft
RNAfold	University of Vienna: http://rna.tbi.univie.ac.at/cgi-bin/RNAWebSuite/RNAfold.cgi
StepOne Software v2.3	Life Technologies
TargetRNA2	Wellesley College (Kery et al. 2014): http://cs.wellesley.edu/~btjaden/TargetRNA2/
Tecan I control	Tecan

2.2 Methods

2.2.1 Cultivation of bacteria

2.2.1.1 Cultivation of *E. coli*

E. coli were grown overnight on LB agar at 37 °C or in LB broth at 37 °C and 180 rpm supplement with the required antibiotics for selection. Bacteria were stocked in LB with 25 % glycerol at -80 °C.

2.2.1.2 Cultivation of *N. gonorrhoeae*

General cultivation

N. gonorrhoeae were grown on GC agar plates with appropriate antibiotics at 37 °C with 5 % CO_2. For multiday culture bacteria were transferred every 24 h to a new plate, for transfer in liquid cultivation growth was limited to a maximum of 16 h to ensure viability. Liquid cultures were usually performed in PPM+ at 37 °C and 120 rpm. Gonococci were transferred from plate to a pre-culture with an optical density (OD) at 550 nm of 0.15 to synchronize growth, whereas the main culture was inoculated at an OD_{550} 0.1. Overnight cultures were started from 6-8 h cultured bacteria at an OD_{550} 0.07 and shaken at 30 °C and 120 rpm. For stocking the bacteria were frozen in PPM supplemented with 23 % glycerol at -80 °C.

Cultivation under various conditions

In the case bacteria needed to be cultured under different conditions then the standard growth conditions stated above, the following changes were made. To change the growth medium for the main culture, the pre-culture was centrifuged at 4000 rpm for 5 min and the pellet resuspended in the new medium. The OD was measured from a 1:20 dilution and the main culture inoculated with an OD_{550} 0.1 or 0.15.
When bacteria were cultured in different versions of the chemically defined medium CDM-10, the changes are listed in table 2.17.

Table 2.17: Different media based on CDM-10

Medium	Description
CDM-10 Lac	Glucose is exchanged by sodium lactate to a final concentration of 5 g/l
CDM-10 Pyr	Glucose is exchanged by sodium pyruvate to a final concentration of 5 g/l
CDM-10 Glc+	Glucose concentration is increased to 10 g/l
CDM-10 w/o Ala	CDM-10 without alanine
CDM-10 D-Ala	CDM-10 without L-alanine containing 0.05 g/l D-alanine
CDM-10 D-Ala+	CDM-10 without L-alanine containing 0.5 g/l D-alanine
CDM-10 L-Ala+	CDM-10 with 0.5 g/l L-alanine
CDM-10 Prop	Sodium propionate is added to a final concentration of 5 mM

The substances listed in table 2.18 were directly added to the main culture in PPM+ for 1 h when bacteria were in mid-log phase, the pooled human serum was added to RPMI medium. The concentration of all substances except serum was determined by growth tests before, gonococci were supposed to still grow, but retarded compared to non-treated condition. Human serum was heat-inactivated for 30 min at 56 °C before use.

Table 2.18: Media supplements to PPM+/RPMI

Substance	Final concentration used
H_2O_2	5 mM and 15 mM
MMS	0.05 % (v/v)
Nalidixic acid	10 µg/ml
Pooled human serum (heat inactivated)	2 % (v/v)

Growth of gonococci in a plate reader

In order to pursuit growth in a plate reader, the pre-culture was diluted to an OD_{550} 0.1 and pipetted into a 48-well-plate with 400 µl per well. Every strain was inoculated in triplicates, including a medium control. The plate was set in a pre-warmed Tecan Infinite M Plex plate reader, where it was incubated for 6 h under shaking. The OD_{550} and GFP fluorescence (excitation 488 nm, emission 518 nm) was measured every 10 min.

^{13}C labelling experiment for isotopolologue profiling

The pre-culture was centrifuged and the pellet resuspended in CDM-10 without alanine. *Neisseria* were inoculated at an OD_{550} 0.1 in CDM-10 without alanine supplemented with 5.6 mM $^{13}C_3$-D-alanine. Gonococci were harvested at an OD_{550} 0.5 and the pellet resuspended in 1 ml PBS. Bacteria were inactivated for 3 h at 56 °C, which was verified by plating an aliquot of each sample. The samples were centrifuged and flash-frozen in liquid nitrogen before storage at -80 °C. The samples were sent to Thomas Steiner (Chair of biochemistry, TU München) for isolation of amino acids and metabolites for GC/MS analysis.

2.2.2 Genetic manipulation of bacteria

2.2.2.1 Preparation of chemically competent *E. coli*

For the generation of chemically competent *E. coli,* 0.5 ml of an overnight culture were inoculated in 100 ml LB medium and grown until an OD_{600} of approximately 0.6. Bacteria were harvested by 10 min centrifugation at 4000 rpm, 4 °C. The pellet was resuspended in 20 ml ice-cold 0.1 M $CaCl_2$ and chilled on ice for 30 min. Bacteria were centrifuged again and resuspended in 10 ml of a solution containing 0.1 M ice-cold $CaCl_2$ and 20 % (v/v) glycerol. 200 µl aliquots were stored at -80 °C.

2.2.2.2 Transformation of chemically competent *E. coli*

To each aliquot of chemically competent bacteria 7.5 µl ligation mix or 150 ng of plasmid DNA were added, carefully mixed and chilled on ice for 30 min. Bacteria were heat-shocked at 42 °C for 90 s and transferred back to ice. For expression of the antibiotic resistance, bacteria were incubated at 37 °C for 1 h while shaking. Afterwards they were spin down (8000 g, 2 min), resuspended in 100 µl LB medium, plated on LB agar containing the respective antibiotics and incubated overnight at 37 °C.

2.2.2.3 Transformation of naturally competent *N. gonorrhoeae*

N. gonorrhoeae take up DNA containing a DNA uptake sequence via their type IV pili. According to their morphology, 15-16 h before transformation pili positive colonies were picked and transferred to a new GC agar plate.
Bacteria were collected from the plate into a tube with 1 ml PPM+ containing additionally 10 mM $MgCl_2$. To 50 µl bacteria solution of an OD_{550} 0.32 were added 200 ng plasmid DNA or 10 ng linear DNA. The mixture was dropped on a GC agar plate and incubated 5-6 h at 37 °C, 5 % CO_2. Afterwards, the bacteria were taken up in PPM+ and pelleted with 5000 g, 5 min. The pellet was resuspended in 100 µl PPM+ and plated on GC agar containing the respective antibiotics. After 2-3 days colonies appeared.
In case of neisserial strains with low pilus expression, transformation was performed in liquid culture. An overnight culture was diluted to an OD_{550} 0.07 with PPM+ containing additionally 10 mM $MgCl_2$. To 1 ml bacteria 1 µg of plasmid DNA or 50 ng of linear DNA was added and the bacteria were incubated for 5-6 h at 37 °C, 120 rpm. The follow-up process was the same as for transformation on plate.

2.2.2.4 Conjugation between *N. gonorrhoeae*

For conjugation experiments the donor and acceptor strains were collected from plate. They were cultured not longer than 16 h on plate. Both strains were adjusted to an OD_{550} of 0.32 in PPM+ containing additionally 10 mM $MgCl_2$. Equal volumes of donor and acceptor were mixed and 50 µl were dropped on a GC agar plate without antibiotics and incubated 5-6 h at 37 °C and 5 % CO_2. Then the bacteria were collected from the plate and a 1:10 dilution was plated on a GC agar plate containing antibiotics of both plasmid and acceptor strain. The remaining bacteria were centrifuged for 5 min at 5000 rpm and the pellet resuspended in 100 µl PPM+ containing additionally 10 mM $MgCl_2$. The solution was plated as the dilution before. After 2 days of incubation at 37 °C and 5 % CO_2, colonies were picked.

2.2.2.5 Construction of *N. gonorrhoeae* mutants

In order to generate *N. gonorrhoeae* mutant strains, all cloning steps were performed in *E. coli* DH5α. Proper integration of the DNA was verified by sequencing.
For construction of strains MS11 ΔΔ162/3 AIE162 and AIE163, strain MS11 ΔΔ162/163 was transformed with plasmids pMR-AIE162 and pMR-AIE163, respectively. Plasmids are based on vector pMR-AIE237 and the sRNA sequence was exchanged by EcoRV/SalI cloning. NgncR_162 and NgncR_163 sRNA sequences were amplified with primer pairs 162-5(EcoRV)/162-2(SalI) and 163-5(EcoRV)/163-2(SalI), respectively.
Deletion of the very 3’ end of NGFG_0045 was achieved via subsequent steps of overlap extension PCR. The first fragments comprising the new 3’ end of NGFG_0045 were amplified

with primer pairs 45-3UTR-1/45mut-1 and 45mut-2/45mut-3. Both fragments were combined and amplified with 45-3UTR-1/45mut-spec-1, creating an overlap to the spectinomycin resistance cassette amplified with primer pairs spec-45mut-1/spec-45mut-2. The downstream region was amplified with 45mut-spec2/45mut-5. All fragments were combined and transformed into strains MS11 and MS11 ΔΔ162/3, yielding strains MS11 45mut and MS11 45mut ΔΔ.

Strains carrying sRNA promoter-gfp fusions: The promoter of NgncR_162 was amplified with primer pairs C162-5/162gfp1 from MS11 genomic DNA, creating an overlap to the *gfp* fragment, amplified with 162gfp2/PFcsiSgfp3 from plasmid pSLack-gfp. The PCR fragments were combined with overlap extention PCR and integrated into vector pMR68 with SalI/XbaI cloning. The resulting plasmid was transformed into strain MS11, yielding MS11 P_{162}-gfp. Comparably, strains MS11 P_{163}-gfp and MS11 P_{163}2-gfp were generated, only the selected primer pairs differed: The promoter region was amplified with primer pairs C163-5/163gfp1 (P_{163}-gfp) or 162-P5/163gfp1 (P_{163}2-gfp) and fused to *gfp*, amplified with primer pairs 163gfp2/PFcsiSgfp3.

Strains carrying the sibling sRNA genes with truncated promoter regions comprising only the -10 promoter element and the region comprising the -35 box were generated based on pMR68. Sequences of NgncR_162 and NgncR_163 were amplified from MS11 genomic DNA with primer pairs CS162-5/162-22 and CS163-5/163-2, respectively. Each fragment was cloned with XbaI/SalI digestion in vector pMR68 and the resulting plasmids transformed in strain MS11 ΔΔ162/3, yielding strains MS11 ΔΔcs162 and MS11 ΔΔcs163.

For deletion of *relA*, its sequence was replaced by an erythromycin resistance cassette. The up- and downstream flanking regions were amplified from MS11 genomic DNA with primer pairs relA-1/relA-2 and relA-3/relA-4, respectively. The erythromycin resistance cassette was amplified from pMR68 with primer pair relAermC1/relAermC2. The three fragments were assembled with overlap extension PCR and transformed into strain MS11.

Comparably, *gdhR* was replaced by a kanamycin resitance cassette. The three fragments covering the upstream flanking region (D1559-1/D1559-2 on MS11 genomic DNA), the kanamycin resistance cassette (1559kan-5'/1559kan-3' on MS11 ΔΔ162/3 genomic DNA) and the downstream flanking region (D1559-3/D1559-4 on MS11 genomic DNA) were assembled with overlap extension PCR. Selection of kanamycin-resistant clones after transformation of strain MS11 resulted in strain MS11 ΔgdhR.

In order to generate strain MS11 Δopa ΔΔ162/3, strain MS11 Δopa was transformed with a PCR fragment harbouring a kanamycin cassette flanked by the upstream and downstream region of the sRNA sequences. The fragment was amplified with primer pairs 162_up_s/ 163_down_as from genomic DNA isolated from strain MS11 ΔΔ162/3. The resulting strain MS11 Δopa ΔΔ162/3 was transformed with plasmid pMR-162/163 and erythromycin-resistant clones selected, yielding MS11 Δopa ΔΔc.

Three strains carry translational target-*gfp* fusions with inducible overexpression of NgncR_237. Strain MS11 Δ237 AIE237 was transformed with a DNA fragment comprising the

up- and downstream regions of NGFG_2119, *gfp*-SF and a spectinomycin resistance cassette, which was assembled via overlap extension PCR by Susanne Bauer. Spectinomycin-resistant transformants were selected yielding MS11 Δ237 AIE237 2119gfp.

NGFG_1006-*gfp* was integrated between the genes encoding lactate permease and aspartate aminotransferase. Regions flanking the integration site were amplified from MS11 genomic DNA with primer pairs LP1/LP2 and AA-52/AA-3(SpeI), respectively. The fragments were digested with EcoRI/EcoRV and PstI/SpeI and cloned into vector pSL1180. The spectinomycin resistance cassette was amplified from pLAS::pPilEmCherry using primer pairs Popa5/spec2 and integrated into the vector with KpnI/PstI cloning. pLAS::pPilEmCherry was used as template for amplification of P_{opa} (primer pairs Popa(EcoRV)/Popa1006-1), thereby Popa1006-1 generated an overlap to a fragment that comprised the 5'-UTR and first 22 codons of NGFG_1006 fused to *gfp*-SF. This fragment was amplified from vector pXG-1006gfp with primer pairs Popa1006-2/GfpSF-(KpnI) and assembled with the P_{opa}-fragment via overlap extension PCR. The resulting P_{opa}1006gfp fragment was ligated into the plasmid and the resulting vector transformed into strain MS11 Δ237 AIE237, thereby yielding strain MS11 Δ237 AIE237 P_{opa}1006gfp.

For chromosomal integration of a translational NGFG_0559-*gfp* fusion in *iga-trpB* locus 559-gfp under control *pilE* promoter was cloned into pMR-AIE237. P_{PilE} was amplified using primer pairs PpilE-5/PpilE559-1 from template pLAS::pPilEmCherry creating an overlap to a fragment comprising the 5'-UTR and the first 21 codons of NGFG_0559 fused to *gfp*-SF amplified with primer pair PpilE559-2/gfp-SF(SalI) from plasmid pXG-559gfp. Both fragments were combined with overlap extension PCR and cloned into pMR-AIE237 via SalI digestion.The resulting plasmid was transformed into strain MS11 Δ237, yielding MS11 P_{PilE}559gfp-AIE237.

The NgncR_237 deletion mutant MS11 Δopa Δ237 was obtained by transformation of MS11 Δopa with a DNA fragment composed of a kanamycin resistance cassette and approximately 500 bp from the 5' and 3' sRNA-flanking regions. The fragment was generated by Julia Kirsch (Bachelor thesis). Transformation of this strain with plasmid pMR-237c yielded erythromycin-resistant strain MS11 Δopa Δ237 c237.

Strain MS11 Δopa ΔBns2-2 was generated by transformation of strain MS11 Δopa with a DNA fragment assembled by Katharina Wagler (Master thesis) harbouring a kanamycin cassette flanked by the upstream and downstream region of the sRNA locus. Kanamycin-resistant transformants were selected.

2.2.3 Cell culture techniques

2.2.3.1 Cultivation of cell lines

Cell lines were cultured in 75 cm^2 cell culture flasks at 37 °C and 5 % CO_2. Cells were passaged to prevent them reaching 100 % confluency in the flasks. Chang cells had to be passaged

every two to three days, Cornea cells only once a week. After removal of the medium, the cells were washed with PBS and detached from the flask by adding 1 ml trypsin-EDTA solution per flask and subsequent incubation at 37 °C. The digestion could be stopped by adding fresh medium and the desired amount of cells could be transferred to a new cell culture flask.

2.2.3.2 Freezing and thawing of cells

For freezing, cells of a nearly confluent flask were detached by trypsin and some fresh medium was added. The cells were transferred to a 15 ml tube and centrifuged for 5 min at 800 g at room temperature. The pellet was resuspended in 3 ml of a solution containing 90 % (v/v) FCS and 10 % (v/v) DMSO and pipetted into cryotubes. A styrofoam box was filled with tissues, the tubes were added and the closed box frozen at -80 °C. After 2-3 days the tubes could be transferred into a normal box.
When the cells were thawed, first the DMSO had to be removed by washing. The thawed cells of one tube were taken up in 9 ml fresh medium and centrifuged for 5 min at 800 g at room temperature. The pellet could be resuspended in fresh medium and transferred to a cell culture flask.

2.2.4 Desoxyribonucleic acid techniques

2.2.4.1 Isolation of plasmid DNA from *E. coli*

Plasmid DNA isolation was performed with the NucleoSpin Plasmid Kit from Macherey-Nagel according to the manufacturer's instructions. For high copy plasmids DNA was isolated from 5 ml *E. coli* overnight culture whereas for low copy plasmids 10 ml cultures were used.

2.2.4.2 Polymerase chain reaction (PCR)

ReproFast polymerase is a proof-reading polymerase and was therefore used for amplification of fragments needed for cloning. The reaction mix was in total 50 µl consisting of 50 ng chromosomal DNA or 10 ng plasmid DNA, 5 µl 10x buffer, 1 µl each primer (10 µM), 1 µl dNTPs (10 mM), 0.5 µl polymerase and ddH_2O.
For colony PCR, the non-proofreading polymerase Taq was used in a 20 µl reaction mix. The template was 2 µl of bacterial lysate generated by adding a few cells into 50 µl dH_2O and boiling them 5 min at 100 °C. Further 2 µl 10x buffer, 1 µl each primer (10 µM), 1 µl dNTPs (10 mM), 0.2 µl polymerase and ddH_2O were added to the reaction mix.
For both polymerases the PCR program started with 2 min initial denaturation at 95 °C, followed by 30 cycles with 30 s 95 °C, 30 s 55 °C and 1 min/1 kb elongation at 72 °C. A final elongation step for 10 min at 72 °C was added.

In order to link two DNA fragments the overlap extension PCR was used. In an initial hybridization step 100 ng of the larger fragment and an equimolar amount of the smaller fragment were mixed with 5 µl 10x ReproFast buffer, 2 µl dNTPs (10 mM), 0.5 µl ReproFast polymerase, 0.2 µl Taq polymerase and filled up with ddH_2O to 50 µl. The following PCR program was reduced to 10 cycles with an elongation time of 30 s. Afterwards 1 µl each primer (10 µM) was added followed by a normal PCR program.
PCR fragments were analyzed on 1 % (w/v) agarose gels run in 1x TBE buffer. 5 µl of DNA were mixed with 1 µl 6x Loading Dye and run 60 min at 120 V before being visualized under UV light. Correct products were purified with the GeneJet gel extraction kit by diluting the PCR reaction with the same amount of binding buffer. After loading the mixture onto a column, the manufacturer's protocol was followed. The DNA was eluted in 25 µl ddH_2O.

2.2.4.3 Ligation of insert DNA into vector

Plasmid and insert DNA were digested with the respective restriction enzymes following the manufacturer's instruction. Afterwards the DNA was purified with the GeneJet gel extraction kit as mentioned in 2.2.3.2. 100 ng vector DNA with an 5x molar excess of insert DNA were mixed with 2 µl ligation buffer and 0.2 µl T4 DNA ligase in a total volume of 20 µl. Ligation was performed either overnight at 16 °C or 2 h at 22 °C.

2.2.4.4 Sequencing

DNA fragments or plasmids used for transformation were verified by sequencing. Sanger sequencing of DNA was performed by Microsynth Seqlab in Göttingen.

2.2.4.5 Isolation of genomic DNA from *N. gonorrhoeae*

Genomic DNA was isolated from bacteria grown on GC agar plates overnight. One inoculation loop of bacteria was resuspended in 500 µl PBS. The solution was centrifuged at 5000 rpm for 5 min. The pellet was resuspended in 500 µl GTE buffer and 5 µl 20 mg/ml RNase and 5 µl 10 % (w/v) SDS were added. The solution was incubated for 10 min at 42 °C. Then 500 µl of a 1:1 mixture of phenol and Chloroform were added. The phases were separated by centrifugation (3 min, 10000 rpm) and the upper watery phase transferred to a fresh tube. This step was repeated once. Finally, the DNA was precipitated by adding 1/10 volume 3 M sodium acetate and 2.5 volume ethanol and pelleted at 10000 rpm for 2 min. The pellet was dried and resuspended in 100 µl ddH_2O.

2.2.4.6 Radioactive labelling of DNA fragments

For labelling of oligonucleotides at their 5' end, 1 µl of the oligo (100 µM) was mixed with 2 µl PNK A buffer, 1 µl T4 PNK and 10-20 µCi γ^{32}P-ATP to a final reaction volume of 20 µl. The solution was incubated at 37 °C for 1 h and was boiled at 95 °C for 5 min before usage.

Longer DNA fragments were generated by PCR and random labelled with α^{32}P-dCTP with the Takara Random Primer DNA Labeling Kit Ver. 2 according to manufacturer's instructions. Briefly, 10-30 ng of template DNA were mixed with 2 µl Random Primer in a reaction volume of 14 µl and heated at 95 °C for 3 min before cooling down on ice for 5 min. Then 2.5 µl 10x buffer, 2.5 µl dNTP mixture, 5 µl α^{32}P-dCTP (50 µCi) and 1 µl Exo-free Klenow Fragment were added and incubated 10 min at 37 °C. Finally, the reaction mix was boiled at 95 °C for 3-5 min.

2.2.5 Ribonucleic acid techniques

2.2.5.1 RNA isolation

For RNA isolation from *N. gonorrhoeae*, bacteria were harvested by centrifugation of 5-10 ml bacteria liquid culture (5 min, 4000 rpm) or directly from plate by resuspending one inoculation loop of bacteria in 1 ml PPM and spinning it down for 5 min, 5000 rpm. If not directly used, the pellet was flash-frozen in liquid nitrogen and stored at -80 °C.
RNA was isolated using the miRNeasy Micro Kit from Qiagen following manufacturer's instructions including removal of traces of DNA by on-column digestion with the RNase-free DNase Kit.

2.2.5.2 cDNA synthesis

RNA was transcribed into cDNA with the help of the RevertAid first strand cDNA synthesis Kit (Thermo Scientific) according to manufacturer's instructions. Briefly, 1 µg of RNA with 1 µl Random Hexamer Primer or 1 µl each specific primer (10 µM) were mixed in a reaction volume of 12 µl with RNase-free water and heated up to 65 °C for 5 min. While the samples cooled down to 4 °C, 4 µl 5x reaction buffer, 2 µl 10 mM dNTP mix, 1 µl RNase inhibitor and 1 µl reverse transcriptase were added per sample. The mixture was heated to 25 °C for 5 min, 42 °C for 60 min. The reaction was terminated by heating at 70 °C for 5 min.
cDNA was stored at -20 °C for a maximum of 2-3 weeks.

2.2.5.3 Quantitative real time PCR (qRT PCR)

For quantification of gene expression, the High ROX Sybr Green Master Mix was used on a StepOnePlus Real-Time PCR System in 96 well plates. For each reaction, 1.8 µl each forward

and reverse primer (10 µM) and 1.4 µl ddH_2O were mixed with 10 µl Sybr Green master mix and 5 µl 1:20 diluted cDNA were added. The reactions were performed in triplicates.
An initial reaction step for 10 min at 95 °C was followed by 40 PCR cycles 15 s at 95 °C and 1 min at 60 °C. The PCR reaction was followed by a primer melt curve. Results were normalized to the 5S rRNA gene and analyzed using StepOne software by the $2^{-\Delta\Delta CT}$ method (Livak and Schmittgen 2001).

2.2.5.4 Northern Blotting

Small RNAs were analyzed on 8 M urea gels containing 15 % acrylamide. For this 24 g urea were dissolved in 5 ml 5x TBE and 16.8 ml 40 % acrylamide solution in a total volume of 50 ml. Before horizontally casting the gel, 250 µl 10 % APS and 50 µl TEMED were added. All plates, combs and spacer were DEPC-treated to prevent RNase contamination.
The RNA ladder Decade™ Marker was labelled with γ^{32}P-ATP according to manufacturer's protocol. 5-15 µg RNA were mixed with 2x RNA Loading Dye and boiled for 5 min at 95 °C before loading the gel. The gel was pre-run for 1 h at 10 mA with 0.5x TBE and after loading the RNA samples currency was increased to 12 mA for another 1.5 h.
After separation the RNA was transferred to a positively charged nylon membrane in a wet transfer chamber in 0.5x TBE for 2 h at 400 mA. Afterwards RNA was crosslinked to the membrane with UV light for 3 min.

Longer RNAs were separated in agarose gels. To prepare one gel, 1.2 g agarose were boiled in 102 ml DEPC-treated water and, when cooled down, 12 ml 10x MOPS buffer and 7.5 ml 37 % formaldehyde solution were added. RNA samples were mixed with 3x volume of RNA loading buffer and incubated at 65 °C for 15 min. Then 1/6 volume of blue juice were added.
RNA was separated in MOPS buffer at 55 V for approximately 4 h. The RNA was transferred to a positively charged nylon membrane via alkaline transfer using capillary force in Northern Blot transfer buffer for 2.5 h. Transfer and position of the marker bands on the membrane were verified under UV light. The membrane was washed for 5 min in phosphate buffer and then the RNA was crosslinked to the membrane with UV light for 3 min.

For hybridization of radioactively labelled probes the membranes were incubated with Invitrogen™ ULTRAhyb™ Ultrasensitive Hybridization Buffer for 1 h at 42 °C, then 5 µl of the respective probe were added and incubated overnight. The membrane was washed 3 times with Northern Blot wash buffer for 10-15 min each and then exposed to a phosphor screen.
For stripping of membranes, they were incubated for 15 min with boiling 0.1 % SDS. After washing, the membrane was again incubated with hybridization buffer and a new probe could be added.

2.2.5.5 Determination of RNA stability by Rifampicin Assay

Half-life of RNA was determined by using a rifampicin assay. *N. gonorrhoeae* pre-cultures were diluted to a 50 ml culture of an OD_{550} 0.15 and grown to mid-log growth phase. RNA synthesis is then blocked by adding rifampicin to a final concentration of 100 µg/ml. Bacteria are harvested at time point zero and at further indicated time points by taking 5 ml bacteria culture to a tube containing 1 ml stop solution (95 % (v/v) ethanol, 5 % (v/v) phenol) and immediate freezing in liquid nitrogen. Prior to RNA isolation, the samples were centrifuged for 5 min at 4000 rpm, 4 °C.

2.2.5.6 Transcriptome sequencing (RNAseq)

10 µg of DNase-treated RNAs were sent in biological triplicates for further processing to the Max Planck-Genome-Centre in Cologne. RNAs were converted into a cDNA library including rRNA depletion. Samples were sequenced on an Illumina HiSeq12 2500 machine with single reads with a length of 150 bp and five million reads per sample.
Data analysis was performed by Maximilian Klepsch (chair of microbiology, university of Würzburg). Briefly, low-quality ends and adapters were removed using cutadapt (Martin 2011). Reads with a minimum length of 15 bp were then mapped to the genome of MS11 using Bowtie2 (Langmead and Salzberg, 2012) und gene quantification and identification of differentially regulated transcripts was performed with the help of featureCounts (Liao et al. 2014) and Deseq2 (Love et al. 2014), respectively.

2.2.6 Protein techniques

2.2.6.1 Generation of bacterial lysates

To prepare bacterial lysates from *Neisseria gonorrhoeae* for protein analysis bacteria were either cultivated on plate or in liquid culture until respective OD was reached. Bacteria were collected in 1 ml PBS to a final OD_{550} 0.5. When the culture was in Hepes medium, the OD_{550} was 1 to get the same amount of bacteria. The tubes were centrifuged (14000 rpm, 2 min) and the pellet resuspended in 25 µl PBS. After addition of 25 µl 2x Lämmli buffer the samples were boiled for 5 min at 95 °C.

E. coli were grown in 20 ml LB medium with the respective antibiotics out of 200 µl overnight culture. The flasks were incubated at 37 °C and 180 rpm until an OD_{600} of 1 was reached. 2 ml of bacteria suspension were harvested by centrifugation (8000 g, 2 min) and the pellet resuspended in 100 µl ddH_2O. 100 µl 2x Lämmli buffer were added and the samples boiled for 5 min at 95 °C.

2.2.6.2 SDS Polyacrylamide gel electrophoresis (PAGE)

For separation of proteins in an electric field, 10-15 µl *N. gonorrhoeae* lysates or 20 µl *E.coli* lysates were loaded onto acrylamide gels. Depending on the size of analyzed proteins, 12-15 % running gels with 5 % stacking gels were used. The gels were run in SDS PAGE running buffer beginning with 100 V and after reaching the running gel the voltage was increased to 120-150 V.

2.2.6.3 Western Blot

After separation, the proteins were transferred to a nitrocellulose membrane. The membrane and filter papers were soaked in blotting buffer before stacked in the transfer chamber with the SDS gel. The transfer was performed in a semi dry transfer chamber at 1 mA per cm² of membrane.
After transfer, the membrane was incubated for at least 1 h in 5 % skim milk solution. Primary antibody was added over night at 4 °C. Membranes were washed three times for 15 min with TBS-T and incubated with the secondary antibody for 2 h. Before developing blots were again washed three times. Developing solutions ECL-1 and 2 were mixed 1:1 and dispersed over the membrane. The signal was detected on an Intas LabImage Chemostar system.

2.2.7 Infection assays

2.2.7.1 Gentamicin protection assay

This assay shows bacterial adherence to the host cell and invasion into the cells. Chang or Cornea cells were seeded in two 24-well plates, per condition in triplicates on each plate. The cells grew overnight to approximately 80 % confluency. Bacteria were grown in overnight cultures and on the day of infection diluted to OD_{550} 0.1 and cultured until mid-log phase. The medium of the cells was changed to cell culture medium without FCS and cells were infected with MOI 50. After 3 h of infection, cells were washed three times with cell culture medium. In the first plate, the cells were lysed with 1 % (w/v) saponin for 7-10 min at 37 °C for comparing adherence of the different gonococcal mutant strains. Bacteria were plated in different dilutions (10^{-1} to 10^{-3}) on GC agar plates. The cells in the second plate were treated with 50 µg/ml gentamicin to kill extracellular bacteria and incubated for further 2 h. Afterwards cells were washed another three times to remove remaining gentamicin and lysed with 1 % (w/v) saponin for 7-10 min at 37 °C. Again, a serial dilution was generated (10^{0} to 10^{-2}) and bacteria were plated on GC agar plates. The plates were incubated for 20 h at 37 °C and 5 % CO_2 for determination of the colony forming units (cfu).

2.2.7.2 Infectivity Assay and differential *Neisseria* staining

Cells were seeded in a 24-well plate containing a 10 mm diameter coverslip per well so that they grew overnight to approximately 80 % confluency. *Neisseria gonorrhoeae* strains were grown in liquid culture until mid-log phase. The medium of the cells was changed to cell culture medium without FCS and cells were infected with MOI 10. After 3 h of infection cells were washed three times with cell culture medium and once with PBS. Then the cells were fixed with 350 µl 4 % (w/v) paraformaldehyde (PFA) per well for 15 min at RT. The plate with PBS could be stored at 4 °C for several days.
Staining of the infected cells was performed at room temperature was as little light as possible. For staining of extracellular *Neisseria,* cells were first incubated with blocking solution for 30-60 min. Then the BSA was removed and 25 µl anti-*Neisseria* antibody, which was diluted in blocking solution, were pipetted carefully on each coverslip. After 1 h, the cells were washed three times with PBS and once with blocking solution before adding 25 µl secondary antibody per coverslip for again 1 h (anti-rabbit Cy5, diluted in blocking solution). In order to stain also intracellular bacteria cells were permeabilized by adding 500 µl permeabilization solution per well for 15 min. Then blocking and addition of the primary antibody was repeated as before. The secondary antibody anti-rabbit Cy2 was mixed with DAPI and Phalloidin-555 prior to pipetting it on the coverslips. After 1 h incubation, the samples were washed four times with PBS and were fixed with 350 µl 4 % (w/v) PFA per well for 15 min at RT. The samples were washed another three times with PBS. For mounting, a drop of Mowiol solution was pipetted on a glass slide and the coverslip carefully added on the drop upside-down. The slides had to dry overnight before imaging of on a SPE or SP5 confocal microscope.
The amount of intracellular and extracellular bacteria was determined by manual counting.

2.2.7.3 Isolation and infection of polymorphonuclear leukocytes from human blood

Polymorphonuclear leukocytes (PMNs) were isolated from lithium heparin blood from healthy donors. Each tube of blood was carefully layered on 15 ml Ficoll without mixing the layers. After a centrifugation step (1500 rpm, 30 min, 22 °C, no brakes) the blood was separated into five distinct bands. Since the PMN layer was located directly on top of the red blood cells, all top layers were soaked up and in the next steps the red blood cells had to be removed. Each tube was carefully mixed with 30 ml PVA and incubated for 30 min at room temperature. This led to the formation of two layers, one light red containing the PMNs on the top and a dark red at the bottom. The upper part was transferred to a new tube and remaining red blood cells lysed via osmosis: After centrifugation (5 min, 1000 rpm, RT) the pellet was resuspended in 16 ml sterile ddH_2O and after 30 s 4 ml 5x PBS were added. The next centrifugation step (5 min, 1000 rpm, RT) was leading to a white pellet which was resuspended in 5 ml HBSS medium. PMNs could be used for a maximum of 8 h after isolation.

For infection of PMNs, bacteria from overnight cultures were diluted to OD_{550} 0.1 and cultured until mid-log phase. PMNs were diluted with RPMI medium, seeded into 24 well plates with $3x10^5$ cells per well and the plates were centrifuged for 5 min at 1000 rpm. Infection was performed in duplicates or triplicates with MOI 25. The plates were centrifuged for 5 min at 1000 rpm and incubated 5 min at 37 °C. Then the plates were washed three times with RPMI and the first plate lysed with 1 % (w/v) saponin for 7 min at 37 °C (time point zero). Bacteria were plated in different dilutions (10^{-1} to 10^{-3}) on GC agar plates. The procedure was repeated for the second plate after 2 h incubation at 37 °C, 5 % CO_2. The GC agar plates were incubated for 20 h at 37 °C and 5 % CO_2 for determination of number of cfu.

2.2.7.4 Isolation of bacterial RNA from infected cells

Cells were seeded in 3-4 150 mm dishes with a density of $5x10^6$ cells per dish and incubated overnight. The following day, cells were infected with the same procedure as for gentamicin protection assay with an MOI 50 (see 2.2.6.1).
Cell lysis was performed in a way to limit contamination with eukaryotic RNA on the one hand and to stabilize bacterial RNA on the other hand. Cells were washed with RPMI and incubated for 30 min on ice covered with 10 ml lysis buffer per tray containing 0.1 % (w/v) SDS, 1 % (v/v) phenol and 19 % (v/v) ethanol. Afterwards cells were scratched and pooled in a falcon tube. The suspension was centrifuged for 20 min, 4000 rpm at 4 °C. RNA was isolated from the pellet using the miRNeasy Micro Kit from Qiagen following manufacturer's instructions including removal of traces of DNA by on-column digestion with the RNase-free DNase Kit.

2.2.8 Statistical analysis

Statistical significance was calculated using Student's t-test. The asterisks correspond to the following p-values: *: $p < 0.05$, **: $p < 0.01$, ***: $p < 0.001$.

3 RESULTS

3.1 *Cis*-acting small RNAs: *opa* antisense RNAs

The Opa proteins of *Neisseria gonorrhoeae* are phase variable, meaning the expression can be switched on and off. This is possible due to a pentameric repeat sequence, CTCTT, in the leader region of the mRNA. When the DNA polymerase encounters such a repeat sequence, it can change the number of repeats. This slipped strand mispairing can lead to out-of-frame transcripts with a premature stop codon shortly after the pentameric repeats. Most *opa* genes are out-of-frame and, since they have a strong promoter, this would lead to the massive accumulation of useless mRNAs (Remmele et al. 2014). Interestingly, data shows that the amount of out-of-frame RNAs is smaller than the amount of full-length transcripts (Belland et al. 1997). Therefore, a rapid degradation mechanism is necessary specifically for out-of-frame transcripts allowing their fast recycling. However, so far there is no explanation for this observation. Then transcriptome analysis of *N. gonorrhoeae* revealed the presence of antisense transcripts for all eleven *opa* genes of which nine exhibited strong antisense transcription (Remmele et al. 2014). This gave rise to the idea that these antisense RNAs (asRNAs) could initiate degradation of out-of-frame transcripts. A fully transcribed *opa* mRNA is covered by ribosomes translating it into a protein. In the case of an out-of-frame RNA this protection is lost due to the early stop codon (see figure 3.1). This allows the binding of the antisense transcript resulting in the formation of an RNA:RNA duplex. RNase III, which is specific for double-stranded RNAs, recognizes these structures and degrades both RNAs.

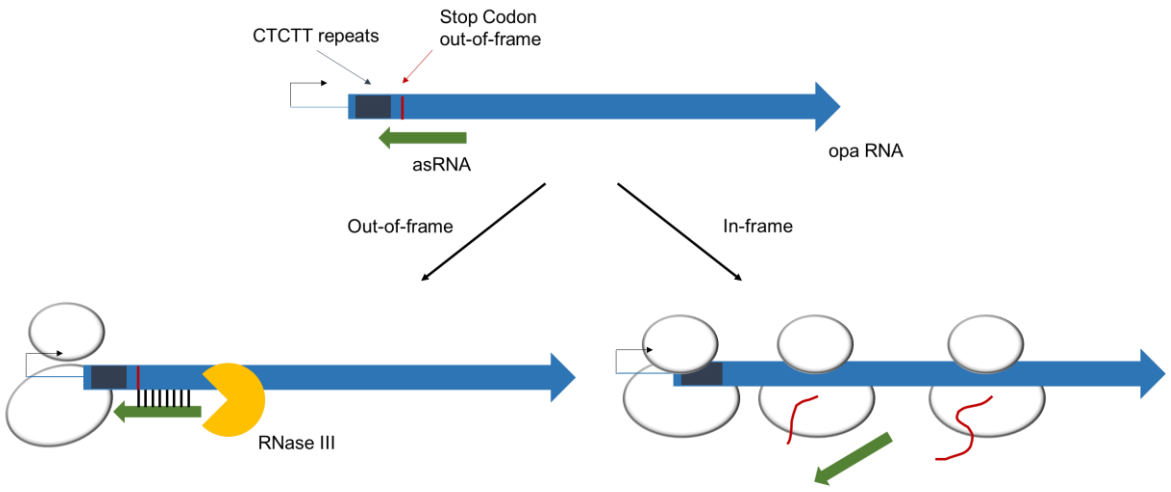

Figure 3.1: Model for specific degradation of out-of-frame transcripts via asRNAs. *Opa* transcripts are either in-frame or out-of-frame depending on the number of CTCTT repeats. In the case of in-frame transcripts, the binding site for an asRNA is blocked by ribosomes, which are not present in out-of-frame transcripts with premature stop codon. The RNA:RNA duplex will then be degraded by RNase III.

In order to test this hypothesis, the sequence of two exemplary *opa* genes was modified in a way that they are either locked in-frame (lif) or locked out-of-frame (lof). This allows the differentiation between these different states and the analysis of the influence of the asRNAs. These modified *opa* genes were cloned in a Δopa background, meaning a deletion of all eleven *opa* genes, to exclude unspecific effects of other *opa* genes due to their sequence similarity. The analysed Opa proteins are NGFG_2435 and NGFG_2258, which are named here due to the non-standardized nomenclature by their genomic locus in strain MS11 (see table 3.1), and their respective asRNAs NgncR_189 and NgncR_007.

Table 3.1: Opa nomenclature of NGFG_2435 and NGFG_2258

Locus	Bhat et al. 1991	Kupsch et al. 1993	Belland et al. 1997	LeVan et al. 2012	Roth et al. 2013
NGFG_2435	opaC	opa_{50}	opaA	opa5	opa_{HSPG}
NGFG_2258	opaH	opa_{60}	opaI	opa6	$opa_{CEA\text{-}e}$

In a first approach, these modified strains were used to test the published observation by Hogan and co-workers that there is less out-of-frame RNA compared to full-length transcripts. This confirmation is necessary for further usage of these strains. Therefore, for both tested Opa proteins, NGFG_2435 and NGFG_2258, the transcript amount of the locked in-frame strains was compared with the amount of the locked out-frame strains by qRT PCR (figure 3.2). In a first experiment, randomly primed cDNA (left side) was measured and, in order to exclude detection of the asRNAs, additionally cDNA specifically primed for the respective *opa* gene (right side) was measured. The data confirms that both NGFG_2435 and NGFG_2258 have clearly reduced amounts of out-of-frame transcripts compared to in-frame transcripts.

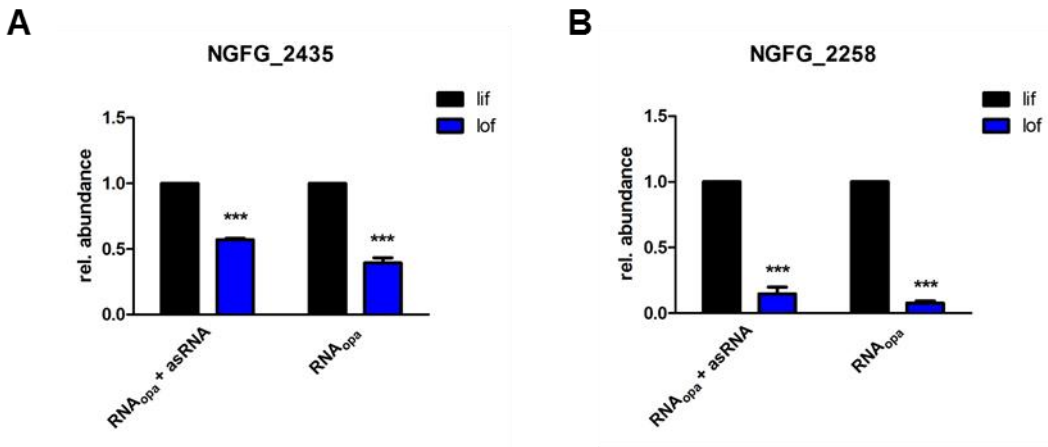

Figure 3.2: Comparison of the relative amount of in-frame and out-of-frame transcripts. For the tested *opa* genes *NGFG_2435* (A) and *NGFG_2258* (B) the amount of locked out-of-frame *opa* transcripts was measured relative to the amount of locked in-frame transcripts by qRT PCR. The used cDNA was either randomly primed (RNA_{opa} + asRNA) or primed specifically for the respective *opa* gene (RNA_{opa}).

In figure 3.2, there is a visible but small difference between the unspecific samples and those measuring only the *opa* transcripts. The antisense RNAs can only have the postulated effect on the out-of-frame transcripts when both have a similar abundance. Therefore, the expression of the antisense RNAs was further analysed. In order to compare the promoter strength, the promoter region of the reporter gene *gfp* was exchanged by the promoter of the *opa* gene or the asRNA. When regarding *gfp* expression on mRNA level, the data shows that the strength of the antisense promoters for both NGFG_2435 and NGFG_2258 is strongly reduced compared to the respective *opa* promoters (figure 3.3A). This observation was validated on protein level, but here no signal could be detected for the antisense promoters as well. These data indicate that the antisense promoters are hardly active and so give rise to the question whether this low activity is sufficient to generate the amount of asRNAs needed for degradation of *opa* out-of-frame RNAs. In a next step, the asRNA levels should be directly determined. The amount of *opa* and antisense RNA in two different strain backgrounds was compared (figure 3.3B). First in strain MS11 WT background, further the transcript amounts were also compared in the Δopa background with the specific *opa* sequence locked in-frame. In order to

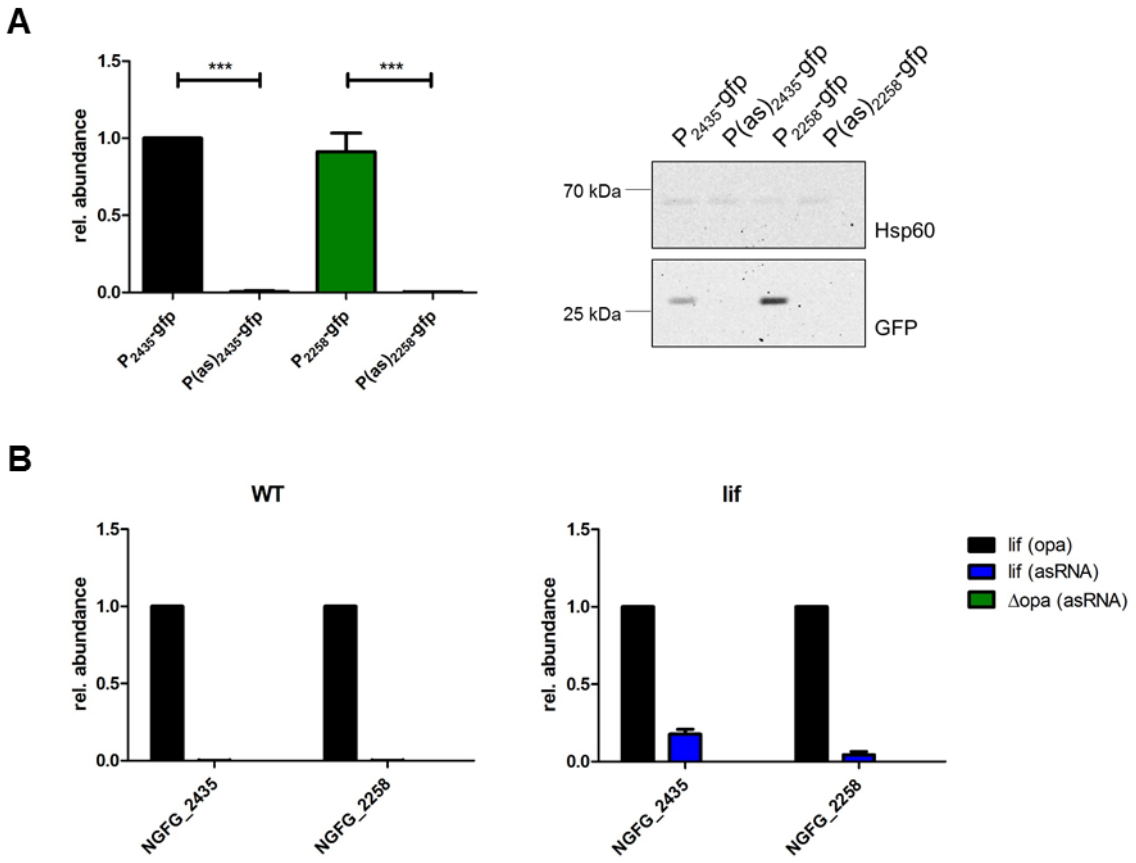

Figure 3.3: Low expression of antisense transcripts. (A) Comparison of promoter activity between *opa* promoter and antisense promoter. The mapped promoter region was cloned upstream of the reporter gene and the *gfp* expression was measured by qRT PCR (n=3). The amount of GFP was determined by Western Blot. (B) Abundance of *opa* and antisense transcripts in WT and the strains having the respective *opa* gene locked in-frame (n=2). Strain Δopa was used as a negative control. The cDNA was primed to quantify only *opa* or antisense RNA.

differentiate between sense and antisense transcripts, the cDNA was primed specifically for the respective target. For better comparison, also the Δopa strain was included as a negative control since here neither *opa* nor antisense transcripts should be detected. Both graphs show that the abundance of antisense RNA was much lower than the abundance of *opa* RNA and the signal is only slightly higher than the one in total absence of all *opa* genes in strain Δopa. To confirm this data, the antisense RNAs should be also detected on a Northern Blot, however, even after long exposure times, no bands for these transcripts were visible. Regarding the low promoter activity and the resulting low expression of asRNAs, it is questionable whether these transcripts are abundant enough to cause such a great effect on the out-of-frame transcripts.

As a control experiment, another phase-variable gene was tested: NGFG_342, the glycosyl-transferase *pglE*. There is no antisense transcript annotated for *pglE*, therefore no difference in abundance between in-frame and out-of-frame transcripts is expected in case asRNAs are responsible for this effect. Consequently, here also two different strains were generated were *pglE* is either locked in-frame or locked out-of-frame. However, when comparing these two strains, the amount of out-of-frame transcripts was significantly reduced compared to in-frame transcripts (figure 3.4). This effect is comparable to the one observed for the analysed *opa* genes. In summary, these data suggest that the lower abundance of out-of-frame transcripts compared to in-frame transcripts is not due to the binding of antisense RNAs.

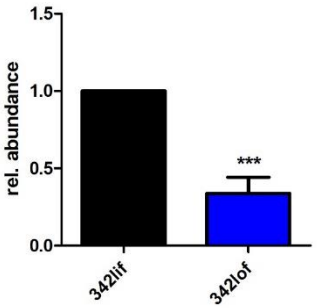

Figure 3.4: Less out-of-frame transcripts for NGFG_342. The phase-variable protein NGFG_342 (glycosyl-transferase pglE) was as well as the before tested *opa* genes locked in-frame and locked out-of-frame. The relative amount of transcripts in these two strains was compared by qRT PCR (n=3).

3.2 *Trans*-acting small RNAs: NgncR_162 and NgncR_163

3.2.1 Sequence conservation and genomic locus

In *N. meningitidis* two sibling sRNAs were identified, named RcoF1/F2 (Heidrich et al. 2017) or $NmsR_A/R_B$ (Pannekoek et al. 2017). The same paralogous sRNAs were also found during transcriptome analysis of *N. gonorrhoeae* strain MS11 as NgncR_162 and NgncR_163 (Remmele et al. 2014). The RNAs have a length of 88 and 91 nucleotides, respectively. They

exhibit 78 % sequence identity, which is why they have similar secondary structures. Both small RNAs fold into three stem-loops (SL1-3) connected by single stranded regions (figure 3.5). Sequence variation between NgncR_162 and NgncR_163 is highest in the SL1 stem loop, whereas SL2 is identical.

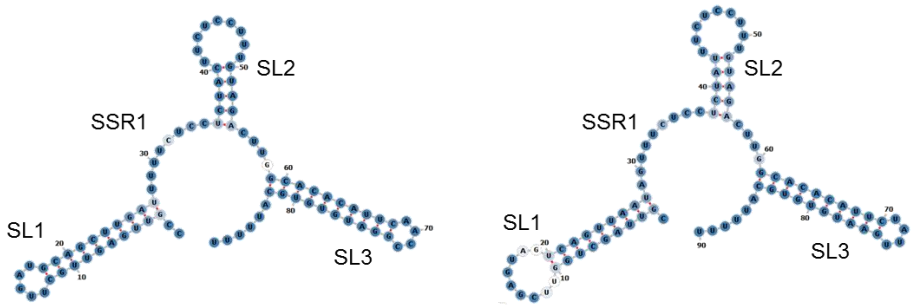

NgncR_162 NgncR_163

Figure 3.5: Secondary structure prediction of NgncR_162 and NgncR_163. The sRNAs have a similar secondary structure consisting of three stem-loops (SL1-3) which are separated by single-stranded regions (SSR). SL2 is identical for both sRNAs. The minimum free energy structure was predicted with the webserver of Vienna RNAfold (http://rna.tbi.univie.ac.at/cgi-bin/RNAWebSuite/RNAfold.cgi). Nucleotides coloured in brighter blue have a lower base-pair probability.

Investigating the sequence conservation of NgncR_162 and NgncR_163 in other *Neisseria*, pathogenic or commensal species, can give hints on a conserved function of both sRNAs. This is why available neisserial genomes were analysed using nucleotide BLAST from NCBI (https://blast.ncbi.nlm.nih.gov/Blast.cgi) for presence of the sibling sRNAs. This analysis revealed that the sibling sRNAs are conserved in many other neisserial species, not only in the closely related *N. meningitidis*, but also in human commensal and zoonotic species. A copy of at least one of the sibling sRNAs could be detected in 23 out of the 29 *Neisseria* species for which whole genome sequences are available at NCBI Genome. The resulting sequences were aligned with the MAFFT (*m*ultiple *a*lignment using *f*ast *F*ourier *t*ransform) high speed multiple sequence alignment program of the European Bioinformatics Institute. Standard settings were applied, meaning a gap open penalty of 1.53 and a gap extension penalty of 0.123. Interestingly, not all species harbour both copies of the sibling sRNAs and NgncR_163 is the more common sibling. The sequences of the sibling RNAs are nearly completely conserved between the most closely related strains, *N. gonorrhoeae*, *N. meningitidis*, *N. polysaccharea* and *N. lactamica* (figure 3.6). Even in the other analysed commensal or zoonotic strains the sequence conservation is striking. The sequence conservation of NgncR_162 is in most strains between 80 % and 90 % and lowest in *N. wadsworthii* (71 %), which has a prolonged CT-rich region. NgncR_163 shows a higher sequence conservation, only eight of the 24 sequences have a percentage identity below 90 %. Compared to the sRNA sequence, the flanking regions show a highly variable sequence. Only the four closely related

strains have also conserved flanking regions. The SL2 sequence of NgncR_162 and NgncR_163 is identical, whereas the other structural elements show some sequence variability between the siblings. In line with this observation, the sequence of SL2 is fully conserved in the NgncR_162 and NgncR_163 homologues of the other members of the genus *Neisseria* and sequence variability is restricted to the SL1 and SL3 sequences of the homologous sRNAs. This second stem loop was already confirmed to be involved in target regulation (Bauer et al. 2017) and these results hence suggest an important role of SL2 for sRNA function.

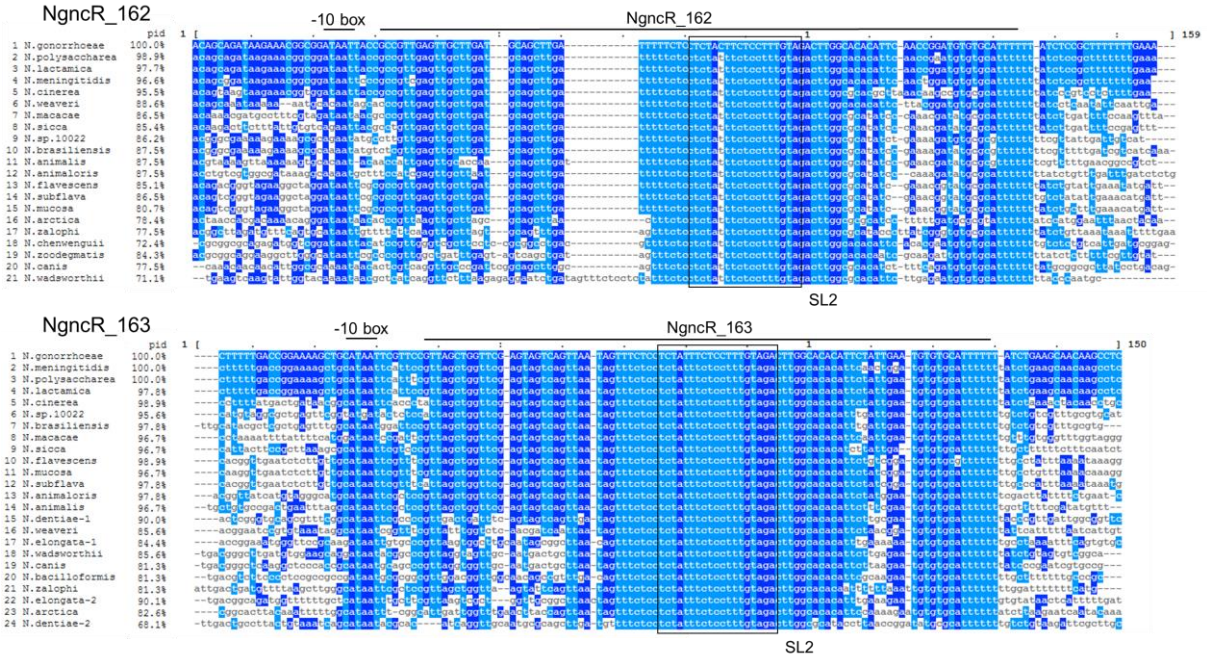

Figure 3.6: Sequence conservation of NgncR_162 and NgncR_163. The sequence alignments were created with the high speed multiple sequence alignment program MAFFT (https://www.ebi.ac.uk/Tools/msa/mafft/) and visualized with the alignment editor MView (https://www.ebi.ac.uk/Tools/msa/mview/). The percentage identity (pid) is given for each strain only for the sRNA sequence. The sequence is coloured according to nucleotide identity with *N. gonorrhoeae* MS11 as reference strain, for better visualization purine and pyrimidine nucleotides are coloured differently. Strains used in the study: *N. meningitidis* MC58, *N. polysaccharea* ATCC 43768, *N. lactamica* 020-06, *N. cinerea* ATCC 14685, *N. weaveri* NCTC13585, *N. macacae* ATCC 33926, *N. sicca* FDAARGOS_260, *N. brasiliensis* N.177.16, *N. animalis* ATCC 49930, *N. animaloris* NCTC12227, *N. flavescens* SK114, *N. subflava* NJ9703, *N. mucosa* C6A, *N. arctica* KH1503, *N. zalophi* ATCC BAA-2455, *N. chenwenguii* 10023, *N. zoodegmatis* NCTC12230, *N. canis* NCTC10296, *N. wadsworthii* DSM 22245, *N. dentiae* DSM 19151, *N. elongata subsp. glycolytica* ATCC 29315, *N. bacilliformis* DSM 23338.

NgncR_162 and NgncR_163 are located in the intergenic region between the disulfide bond formation protein DsbB and an Lrp/AsnC family transcriptional regulator. An alanine racemase encoded in opposite direction is found downstream of this regulator. Sequence comparisons with other *Neisseria* revealed that this gene arrangement is conserved in the most highly related species *N. gonorrhoeae, N. meningitidis, N. polysaccharea* and *N. lactamica* (figure 3.7). In all analysed species, NgncR_162 and NgncR_163 are located in intergenic regions.

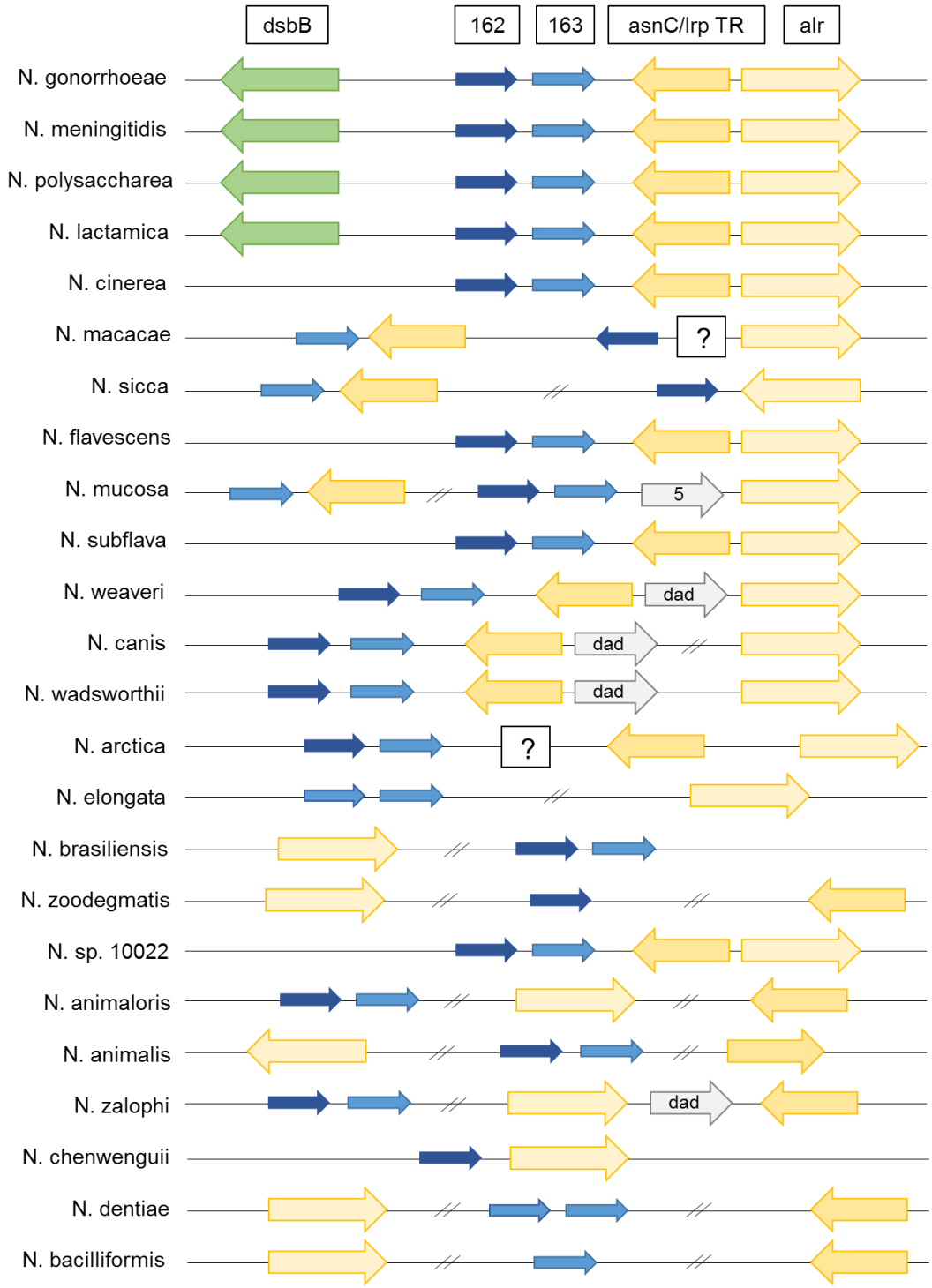

Figure 3.7: Conservation of the genomic locus of NgncR_162 and NgncR_163. The location of the sRNAs and their flanking genes is mapped schematically. When there is no complete genome available and the respective genes are located on different contigs, the distance between the genes is marked by question marks. Flanking genes: disulfide bond formation protein *dsbB* (green arrow), Lrp/AsnC family transcriptional regulator (yellow arrow) and alanine racemase *alr* (pale yellow arrow). Two slashes indicate longer distances in the genome. *N. weaveri, N. canis, N. wadsworthii* and *N. zalophi* encode a D-amino acid dehydrogenase (dad) downstream of the AsnC family transcriptional regulator. In *N. mucosa*, five further genes are encoded between NgncR_163 and the alanine racemase.

Interestingly, most analysed strains had both copies of the sibling RNAs. Only six out of 24 strains showed a different arrangement. *N. mucosa* harbours an additional copy of NgncR_163, in *N. elongata* and *N. dentiae* NgncR_162 is replaced by a second copy of NgncR_163 and there are only three species coding for one of the sibling RNAs, NgncR_162 (*N. zoodegmatis* and *N. chenwenguii)* or NgncR_163 (*N. bacilliformis*). The disulfide bond formation protein DsbB is located upstream of the sRNAs only in the closely related species. According to annotations, many analysed species encode upstream of the sRNAs a DUF domain-containing protein or genes coding for proteins with completely different function. The genetic linkage between the sRNA genes and the ORFs encoding the transcriptional regulator and the alanine racemase seems to be more conserved. In 14 of the analysed strains, these genes are encoded in the same location and orientation downstream of the sRNAs. Therefore, their function could be linked to the physiological role of NgncR_162 and NgncR_163. Mostly zoonotic species differ in the gene arrangement next to the sRNAs and the Lrp/AsnC family transcriptional regulator and alanine racemase are not encoded in proximity of the sibling RNAs. These species are more distant relatives to *N. gonorrhoeae* and could require different host adaptations. Four species encode a D-amino acid dehydrogenase in proximity to the transcriptional regulator, a gene that is also linked to the sRNAs, as it is a target gene of the sibling sRNAs in gonococci.

3.2.2 Identification of new sRNA targets

Previously, an *in silico* prediction for potential target genes was performed using the tool targetRNA2. Thereby, several genes could be identified and subsequently validated as actual target genes of the sibling sRNAs (Bauer et al. 2017). Expression of NGFG_1721, annotated as a sodium-alanine symporter, was most strongly affected by the sRNAs. Further validated genes are involved in amino acid degradation (NGFG_2049), the methylcitrate cycle (*prpB, prpC, ack*), the citric acid cycle (*sucC, sdhC, fumC, gltA*) and transcriptional regulation (*gdhR*). All of these genes are predicted to be downregulated by the sRNAs via an interaction of the SL2 domain of the sRNA and the Shine Dalgarno sequence of the target mRNA, thereby inhibiting ribosome binding. This hypothesis was validated for a subset of these genes. The SL2 domain is identical between NgncR_162 and NgncR_163 and it was shown that the presence of one of the sibling RNAs is sufficient for full regulation of target gene expression in the case of NGFG_01721 and *ack* (Bauer et al. 2017). Therefore, the function of NgncR_162 and NgncR_163 might be redundant, however, target genes controlled by only one of the sibling sRNAs or sRNA-specific regulatory mechanisms might exist. This study aims to define the complete regulon of each of the sibling sRNAs, thereby addressing the question on a redundant function of the sRNAs. Identified sRNA regulons also help understanding the physiological role of a sRNA within regulatory networks. The characterized target genes are mostly involved in metabolic processes, but do not allow association to a clear physiological function.

3.2.2.1 Validation of selected putative target genes predicted by *in silico* analysis

Therefore, it was searched for further potential target genes. Studies conducted on the homologous sRNAs in *N. meningitidis* and the analysis of genetic arrangements of validated target genes suggested the possibility that the sRNAs play a role in histidine biosynthesis. NGFG_2048, coding for *hisB*, is located in an operon with the validated target NGFG_2049 (figure 3.8A) and might be regulated by the sRNAs as well. NGFG_2049 is coding for the enzyme 3-hydroxyisobutyrate dehydrogenase, which is participating in the degradation of branched-chain amino acids. In a study addressing the interactome of the RNA chaperone Hfq, *hisH* was listed as possible target for the NgncR_162 homologue RcoF2 (Heidrich et al. 2017). Within this study, the sibling sRNAs were identified to co-precipitate with Hfq. The CopraRNA algorithm was applied for identification of target mRNAs and the list further filtered for enrichment according to the Hfq RIP-seq data to reduce false-positive predictions. This resulted in a list of ten putative target mRNAs, of which one is the imidazole glycerol phosphate synthase subunit HisH. In another study, the protein expression profile in presence or absence of the meningococcal sRNA homologues was compared by mass spectrometry (Pannekoek et al. 2017). Applying a 1.5-fold up- or downregulation as a cutoff for differential expression led to a list of 18 proteins with increased expression and ten proteins with decreased expression in the KO strains. This list includes the enzyme 1-(5-phosphoribosyl)-5-[(5-phosphoribosylamino) methylideneamino] imidazole-4-carboxamide isomerase HisA, showing a more than twofold increase in protein expression in the absence of the sibling sRNAs.
Since *hisA* and *hisH* are encoded in the same operon (figure 3.8A) only *hisH* was chosen for validation. The effect of NgncR_162 and NgncR_163 on gene expression of *hisH* and *hisB* was assessed in full medium. Expression levels were compared by qRT PCR between strains MS11 WT, the gonococcal strain with deletion of both NgncR_162 and NgncR_163 (ΔΔ162/3) and the complemented KO strain expressing both sRNA genes in *trans* (ΔΔc) (figure 3.8B). Transcript levels of both *hisH* and *hisB* were significantly upregulated in the double KO strain and the effect was complemented by sRNA expression in *trans*, though the absolute fold change was rather small. To further analyse the regulation of the histidine biosynthesis genes by the sibling sRNAs, the interacting regions between NgncR_162 and the target mRNA were predicted using the webtool IntaRNA (figure 3.8C). NgncR_162 is predicted to interact with the *hisH* mRNA in the region upstream of the start codon, which is including the RBS. Inhibiting ribosome binding is a common regulatory mechanism of non-coding RNAs and hence explains downregulation of target gene expression. This regulatory mechanism was also confirmed for other target genes of the sibling RNAs (Bauer et al. 2017). NgncR_162 is predicted to interact with *hisH* by its SSR1 region, which was also already postulated to be involved in target gene regulation (Bauer et al. 2017). This sequence involved in regulation is identical between NgncR_162 and NgncR_163, therefore both sRNAs are likely to have the predicted regulatory effect. The prediction for interaction of NgncR_162 with the *hisB* mRNA is more unusual. The sRNA is supposed to bind *hisB* at the end of its coding region by its SL1 domain. The sequence

of this stem loop differs between NgncR_162 and NgncR_163 and therefore NgncR_163 could not cause a negative effect in *hisB* expression. Nevertheless, here the observed downregulation could be a consequence of the sRNAs interacting with the 5' UTR of NGFG_2049, which might lead to a destabilization of the bicistronic mRNA.

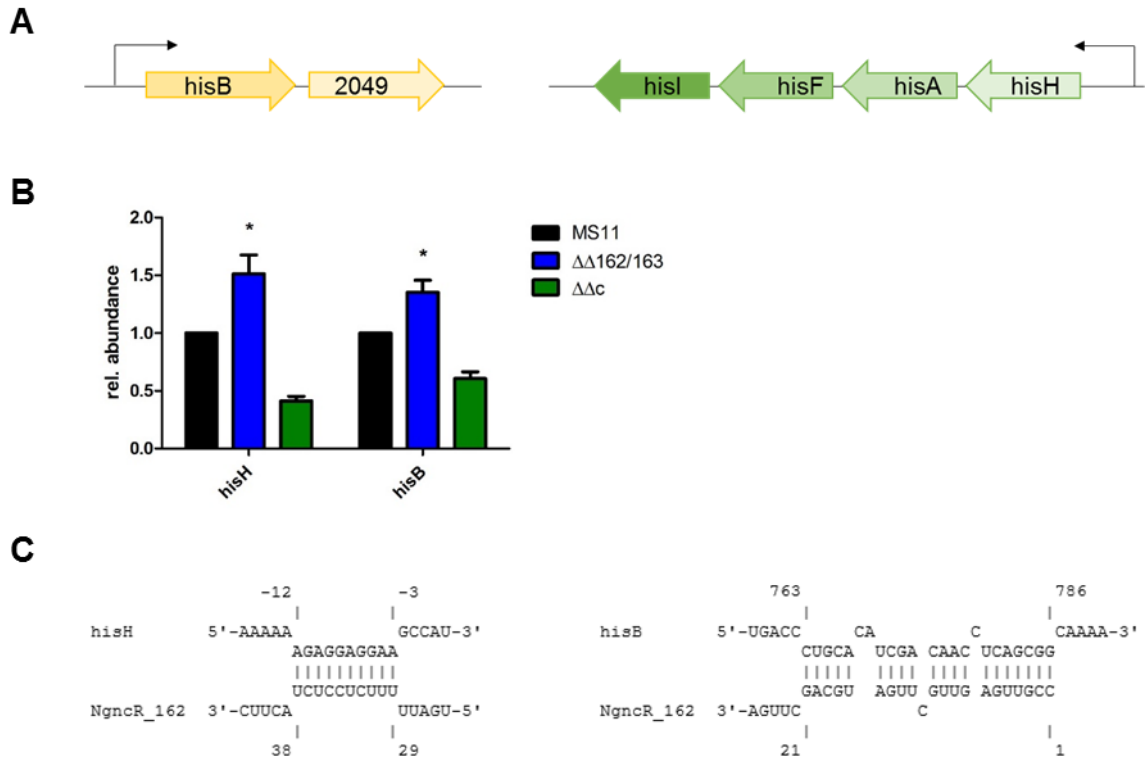

Figure 3.8: Role of sRNAs in histidine biosynthesis. (A) The genes involved in the biosynthesis of histidine are encoded in operons. *HisB* is located upstream of the target gene NGFG_2049 whereas *hisH* and *hisA* are in an operon with *hisF* and *hisI*. (B) Gene expression analysis of *hisH* and *hisB* in MS11 WT, the double KO ΔΔ162/3 and the complementation strain ΔΔc with both NgncR_162 and NgncR_163 by qRT PCR (n=3). (C) Prediction via intaRNA of the interaction sequence between NgncR_162 and *hisH* and *hisB*, respectively. Numbers refer to the nucleotide position with respect to the start codon (+1) or in the case of NgncR_162 the transcriptional start site.

The initial approach for prediction of target genes was an *in silico* analysis. The bioinformatics tool TargetRNA was applied using default settings by matching the sequence of NgncR_162 with the genome of *N. gonorrhoeae* strain FA 1090. This resulted in a list of 43 putative target genes with a p-value <0.05, which included eight genes predicted to be regulated at the RBS (Bauer et al. 2017). Unexpectedly, two other genes, NGFG_1965 and NGFG_1349, exhibited complementarity of the 5' UTR with the conserved SL2 region of the sRNA when targetRNA2 analysis was performed with NgncR_163. NGFG_1965 codes for thioredoxin, whereas NGFG_1349 is a hypothetical protein. The target gene prediction for the *N. meningitidis* homologues RcoF2 and RcoF1 was adjusted using Hfq RIP-seq data and are therefore more robust (Heidrich et al. 2017). Due to the high sequence conservation between the gonococcal and meningococcal sRNAs, besides *hisH* another candidate from this list was included in the study. NGFG_1133 is the homologue of NMV_1044, which is predicted to be regulated by both

RcoF2 and RcoF1 with a high statistical significance. NGFG_1133 is annotated as the multiple antibiotic resistance membrane protein MarC, but a note is added that it is identical to the small neutral amino acid transporter SnatA, so the function of the protein is unclear.

To test the influence of the sRNAs on these genes, their expression levels were compared between MS11 WT, the double KO strain and the complementation strain with both NgncR_162 and NgncR_163 by qRT PCR (figure 3.9A). The data shows that NGFG_1349 and NGFG_1133, but not NGFG_1965, are significantly upregulated in the absence of the sRNAs. Especially NGFG_1349 mRNA levels were increased more than three-fold in the double KO strain compared to the WT, suggesting a regulation of the gene also in *N. gonorrhoeae*. Both NGFG_1133 and NGFG_1349 were analysed *in silico* for their respective target interaction region with the sRNA NgncR_163 with the webtool IntaRNA (figure 3.9B). NgncR_163 engages the same single-stranded domain for the interaction with NGFG_1133 and NGFG_1349 as with the previously validated target genes. It is predicted to interact with the loop region of SL2, which is containing an anti-Shine–Dalgarno sequence, with the target mRNAs. The mRNAs of NGFG_1133 and NGFG_1965 are bound directly upstream of the start codon, a sequence including the RBS. The sRNAs would thereby apply their usual regulatory mechanism as post-transcriptional regulators by interfering with ribosome binding.

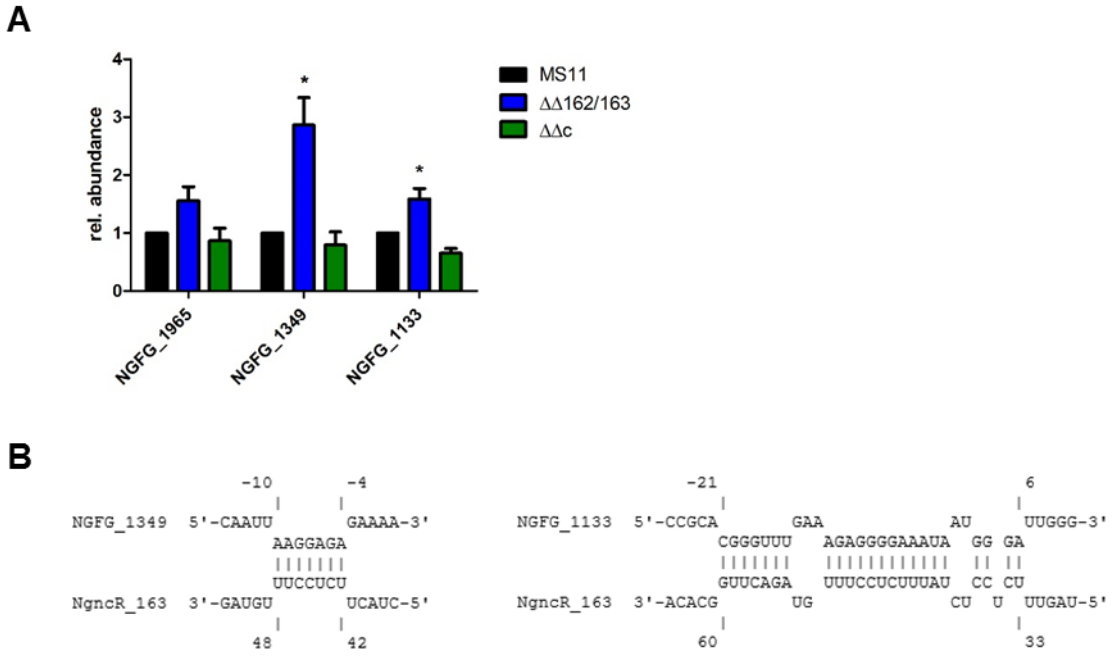

Figure 3.9: Validation of further sRNA targets. (A) Gene expression analysis of NGFG_1965, NGFG_1349 and NGFG_1133 in MS11 WT, the double KO ΔΔ162/3 and the complementation strain with both NgncR_162 and NgncR_163 by qRT PCR (n=4). (B) Prediction of the potential interacting region was performed with the webtool intaRNA. The interaction sequence was determined between NgncR_163 and NGFG_1349 and NGFG_1133, respectively. Numbers refer to the nucleotide position with respect to the start codon (+1) or in the case of NgncR_162 the transcriptional start site.

3.2.2.2 Characterization of the NgncR_162/163 regulon via pulse expression of the individual sRNAs

The target genes reported above were mostly identified by an *in silico* analysis. Computational approaches often do not result in a fully defined sRNA regulon and the data analysis is biased. In the study on NgncR_162 and NgncR_163 only potential target genes were considered for further analysis, which are predicted to be regulated by the sRNAs at the RBS. This is the best characterized regulatory mechanism of non-coding RNAs, however, many more were shown to exist. The validation of the potential target genes suggested a redundant function of the sibling sRNAs since the target mRNAs were predicted to be regulated by the common loop region of SL2 of both NgncR_162 and NgncR_163. This raised the question whether unique target genes might exist. In order to address this question, a transcriptome analysis was applied after pulse expression of the individual sibling sRNAs.

Appropriate *N. gonorrhoeae* strains were generated by transforming the gonococcal strain ΔΔ162/3 with a modified version of the shuttle vector pMR68 developed by Ramsey et al. (2012). The plasmid was initially designed for expression of protein coding genes under control of the P_{tet} promoter. An EcoRV restriction site was added immediately downstream of the -10 box of P_{tet} to allow integration of any sRNA gene by simple EcoRV/SalI cloning (figure 3.10A). The localization of the EcoRV restriction site ensures proper transcriptional initiation. With the help of this plasmid, the tet repressor and the respective sRNA gene under control of the anhydrotetracycline (AHT)-inducible P_{tet} promoter is integrated in the intergenic region between *iga* and *trpB* genes. The resulting strains were termed AIE for AHT-inducible expression. Ramsey et al. (2012) determined 2 ng/ml AHT as sufficient amount for full activity and an induction time of 2 h as optimal time range for protein expression. For an initial testing of the new strains ΔΔ162/3 AIE162 and ΔΔ162/3 AIE163 these settings were applied to verify sRNA expression. Strains MS11, ΔΔ162/3 AIE162 and ΔΔ162/3 AIE163 were cultured in PPM+ until early log phase, when 2 ng/ml AHT were added to the medium and bacteria were incubated for another 2 h. Expression of the sRNAs was analysed by Northern Blot (figure 3.10B). The presence of AHT in the medium does not have an effect on sRNA expression in strain MS11 WT. In both strains with inducible sRNA expression, hardly any sRNA transcripts were detected in the absence of AHT, whereas upon induction in both strains the respective sRNA was transcribed abundantly. However, NgncR_162 and NgncR_163 were slightly less efficiently transcribed under control of P_{tet} than under control of their native promoters.

The new developed strains were used for sRNA pulse expression and subsequent differential RNAseq analysis. Expressing a regulatory sRNA only for a short time period allows excluding indirect effects. The regulatory role of sRNAs on transcriptional regulator would also affect their regulon and therefore the induction time should be reduced to a minimum. To find optimal experimental conditions for pulse expression still resulting in post-transcriptional regulation of validated target genes, expression of several transcripts was analysed in a time course experiment. Bacteria were cultured to early or mid-log phase before adding AHT for 15 min,

30 min or 60 min. The expression of NGFG_1721 (figure 3.10C), *ack* and *prpC* was analysed in strains ΔΔ162/3 AIE162 and ΔΔ162/3 AIE163 at the respective time points with strain MS11 as control sample after 60 min induction. For each time point, transcript amounts present in the absence and presence of AHT were compared. Transcript levels of NGFG_1721 were already downregulated after 15 min induction with NgncR_162 or NgncR_163. Downregulation of *prpC* and *ack* was observed after 30 min of sRNA pulse expression (data not shown)

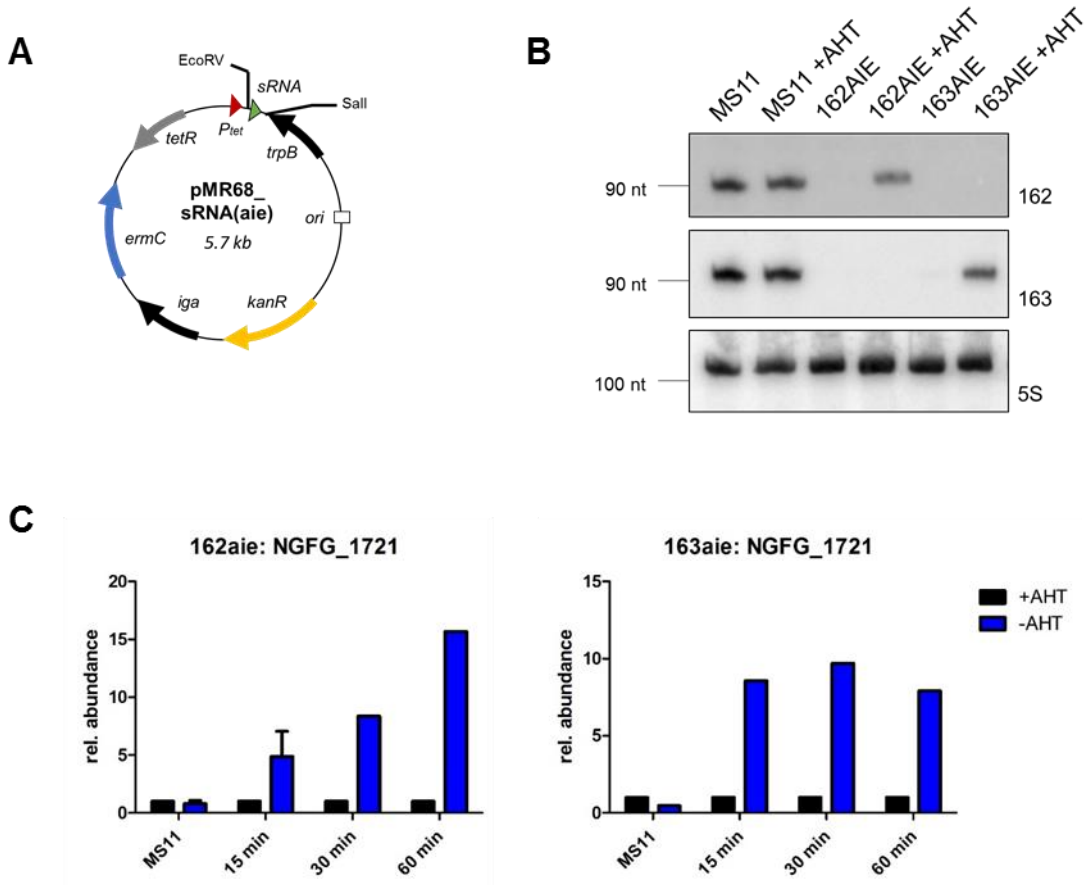

Figure 3.10: Establishing a system for inducible expression of sRNAs. (A) The system is based on the plasmid pMR68 (Ramsey et al. 2012). The sRNA can be exchanged by EcoRV/SalI restriction enzyme digestion. (B) sRNA expression was verified after 2 h induction with AHT for both NgncR_162 and NgncR_163 in a Northern Blot. (C) The minimal needed time of induction was determined in a time course experiment by testing the effect on the validated target gene NGFG_1721 (162aie: n=2, 163aie: n=1). Strain MS11 was included as control.

For transcriptome analysis, strains MS11 WT, ΔΔ162/3, ΔΔ162/3 AIE162 and ΔΔ162/3 AIE163 were grown until mid-log phase and 2 ng/µl AHT were added for 30 min. All strains were cultured in presence of AHT in order to exclude false-positive hits caused by regulatory effects of the compound. RNA was isolated directly after the bacteria were harvested. Samples were tested for post-transcriptional regulation of the target genes NGFG_1721, *prpC* and *ack* by the sRNAs before library preparation and sequencing. Library preparation of three biological replicates each and Illumina sequencing was performed at the Max-Planck-Genome-Centre

Cologne in collaboration with Bruno Hüttel. Analysis of raw sequencing data and identification of differentially expressed genes using DESeq2 was done by Maximilian Klepsch (University of Würzburg). Pairwise comparison of the respective datasets was performed in the following combinations: ΔΔ162/3 AIE162 versus ΔΔ162/3, ΔΔ162/3 AIE163 versus ΔΔ162/3 and ΔΔ162/3 versus MS11 WT. The complete lists of all three datasets showing the logarithmic fold change, p-value and adjusted p-value can be found in the appendix (table A.2). In the following only genes with an adjusted p-value <0.05 were considered as significantly regulated. Initially, no cut-off of the fold change was applied. This resulted in 57 (ΔΔ162/3 AIE162 versus ΔΔ162/3), 30 (ΔΔ162/3 AIE163 versus ΔΔ162/3) or 128 (ΔΔ162/3 versus MS11 WT) significantly regulated genes. In table 3.2 significantly regulated transcripts of both datasets ΔΔ162/3 AIE162 versus ΔΔ162/3 and ΔΔ162/3 AIE163 versus ΔΔ162/3 are summarized. Genes, which show no significant differential regulation in one of the datasets, are marked in italics and coloured grey in the respective column. The 128 differentially regulated genes of dataset ΔΔ162/3 versus MS11 WT are listed in the appendix (table A.1).

Not surprisingly, NGFG_1721 showing the highest ratio of differential expression in qRT PCR exhibited also the highest fold change in every RNAseq data set. Other validated target genes such as *prpB*, *gdhR* or *gltA* show only weak regulation and do not appear as significantly regulated upon pulse-expression of the sRNAs. Also *prpC* (NGFG_1404) results only in dataset ΔΔ162/3 versus MS11 in a significant fold change, although every sample was tested for *prpC* expression by qRT PCR before. This indicates limitations in the detection of subtle differences in posttranscriptional regulation of the applied experimental approach.

Table 3.2: Comparison of significant RNAseq results for 162AIE and 163AIE versus ΔΔ

Locus	Functional category	162AIE versus ΔΔ		163AIE versus ΔΔ	
		Adjusted p-value	Fold change	Adjusted p-value	Fold change
NGFG_00033	Hypothetical proteins	0.0000	1.4897	0.0000	1.4917
NGFG_00039	Transport and binding proteins	0.0372	0.6134	*0.3640*	*0.7749*
NGFG_00045	Transport and binding proteins	*0.0523*	*1.4540*	0.0113	1.6178
NGFG_00091	Transport and binding proteins	0.0110	0.6969	*0.0707*	*0.7516*
NGFG_00100	Energy metabolism	0.0272	1.4928	0.0294	1.4886
NGFG_00101	Energy metabolism	0.0471	1.3472	*0.1450*	*1.2754*
NGFG_00171	Biosynthesis of cofactors, prosthetic groups, and carriers	0.0103	0.7438	*0.1150*	*0.8094*
NGFG_00247	Energy metabolism	0.0372	1.6211	*0.4950*	*1.2193*
NGFG_00254	Transport and binding proteins	0.0342	1.4152	*0.1150*	*1.3315*
NGFG_00321	Protein fate	0.0372	1.4692	*0.1170*	*1.3765*
NGFG_00414	Hypothetical proteins	0.0000	2.7702	*0.0985*	*1.6449*
NGFG_00415	Amino acid biosynthesis	0.0000	1.9159	*0.2870*	*1.2553*

NGFG_00441	Protein synthesis	0.0252	1.3538	*0.1210*	*1.2658*
NGFG_00442	Protein synthesis	*0.0968*	*1.3041*	0.0221	1.4152
NGFG_00452	Mobile and extrachromosomal element functions	0.0429	1.5411	*0.7900*	*1.0981*
NGFG_00617	Cellular processes	0.0100	1.4499	0.0303	1.3822
NGFG_00658	Energy metabolism	0.0277	1.2995	*0.2870*	*1.1663*
NGFG_00703	Cell envelope	0.0030	0.6653	0.0237	0.7115
NGFG_00839	Energy metabolism	0.0476	0.7280	*0.1930*	*0.7879*
NGFG_00881	Amino acid biosynthesis	0.0372	0.7862	0.0221	0.7684
NGFG_00897	Fatty acid and phospholipid metabolism	*0.0642*	*0.7684*	0.0294	0.7412
NGFG_00941	Cell envelope	0.0038	1.4845	0.0221	1.4035
NGFG_01012	DNA metabolism	*0.1200*	*1.4280*	0.0292	1.6066
NGFG_01027	Transcription	*0.0523*	*0.7615*	0.0199	0.7235
NGFG_01046	Amino acid biosynthesis	0.0376	0.6422	*0.0702*	*0.6588*
NGFG_01122	Transcription	0.0160	1.4113	*0.1000*	*1.3077*
NGFG_01146	Hypothetical proteins	0.0376	1.5508	*0.2800*	*1.3186*
NGFG_01160	DNA metabolism	0.0342	1.6200	*0.1170*	*1.4856*
NGFG_01163	Biosynthesis of cofactors, prosthetic groups, and carriers	0.0376	0.5590	*0.1260*	*0.6194*
NGFG_01176	Transcription	0.0144	0.7351	*0.1000*	*0.7922*
NGFG_01204	Protein fate	0.0025	1.4540	0.0125	1.4054
NGFG_01289	Mobile and extrachromosomal element functions	0.0160	0.6439	*0.1830*	*0.7479*
NGFG_01353	Transport and binding proteins	*0.3250*	*1.3426*	0.0173	1.8570
NGFG_01369	Hypothetical proteins	0.0099	0.7081	*0.1430*	*0.7933*
NGFG_01407	Energy metabolism	0.0160	0.6303	0.0160	0.6242
NGFG_01411	Energy metabolism	0.0012	0.5872	0.0016	0.5897
NGFG_01422	DNA metabolism	0.0448	0.7225	*0.1510*	*0.7711*
NGFG_01491	Hypothetical proteins	0.0476	0.6263	*0.0855*	*0.6471*
NGFG_01567	Fatty acid and phospholipid metabolism	0.0376	0.7781	*0.0707*	*0.7917*
NGFG_01568	Fatty acid and phospholipid metabolism	0.0232	0.7225	0.0267	0.7275
NGFG_01569	Hypothetical proteins	0.0271	0.6364	*0.0990*	*0.6916*
NGFG_01571	Hypothetical proteins	0.0376	0.7305	*0.4010*	*0.8556*
NGFG_01618	DNA metabolism	*0.1260*	*1.3500*	0.0452	1.4651
NGFG_01721	Transport and binding proteins	0.0000	0.3231	0.0000	0.2717
NGFG_01722	Energy metabolism	0.0000	0.5381	0.0000	0.4698
NGFG_01727	Cellular processes	0.0160	1.5812	*0.0727*	*1.4610*

NGFG_01728	Cellular processes	0.0186	1.5390	0.0392	1.4835
NGFG_01732	Protein synthesis	0.0413	1.3708	0.0303	1.3899
NGFG_01770	Protein synthesis	0.0297	1.4172	0.0294	1.4172
NGFG_01771	Protein synthesis	0.0272	1.4419	0.0259	1.4469
NGFG_01772	Transcription	0.0335	1.3278	0.0160	1.3717
NGFG_01842	Biosynthesis of cofactors, prosthetic groups, and carriers	0.0042	0.5441	0.0119	0.5602
NGFG_01935	Hypothetical proteins	0.0342	0.8106	*0.1150*	*0.8403*
NGFG_02039	Amino acid biosynthesis	0.0099	1.4201	*0.0717*	*1.3140*
NGFG_02040	Hypothetical proteins	0.0272	1.4763	*0.0707*	*1.4132*
NGFG_02102	Mobile and extrachromosomal element functions	0.0160	0.6139	0.0303	0.6399
NGFG_02106	Hypothetical proteins	0.0049	1.4682	*0.0636*	*1.3435*
NGFG_02107	Regulatory functions	0.0011	1.6245	0.0249	1.4590
NGFG_02111	Central intermediary metabolism	0.0000	2.2501	0.0000	2.1287
NGFG_02237	Cell envelope	0.0450	0.5696	#NV	#NV
NGFG_02263	Transport and binding proteins	0.0238	1.4671	0.0127	1.5273
NGFG_02426	Hypothetical proteins	0.0238	0.5426	0.0135	0.5116
NGFG_02496	Cellular processes	0.0413	1.5878	*0.1700*	*1.4241*
NGFG_02500	Mobile and extrachromosomal element functions	0.0417	0.6181	*0.0852*	*0.6448*

Comparison of the datasets ΔΔ162/3 AIE162 versus ΔΔ162/3 and ΔΔ162/3 AIE163 versus ΔΔ162/3 should allow finding unique target genes for the individual sibling sRNA. 23 genes are significantly differentially regulated in both datasets with pulse expression of one of the sibling sRNAs. Seven genes show significant regulation in ΔΔ162/3 AIE163 versus ΔΔ162/3 but not in ΔΔ162/3 AIE162 versus ΔΔ162/3 and 33 genes in AIE162 but not in AIE163. Nevertheless, these genes have the same trend in regulation when overexpressing the other sibling RNA, although the adjusted p-value is above cut-off. The only exception is NGFG_0452, which is 1.5-fold upregulated upon overexpression of NgncR_162, but not upon overexpression of NgncR_163. However, no inverse regulation can be observed in dataset ΔΔ162/3 versus MS11. The data is hence suggesting a redundant function of NgncR_162 and NgncR_163. Analysis of dataset ΔΔ162/3 versus MS11 serves as control since here the possible target genes are expected to be inversely regulated compared to the other two datasets. A fold change of >1.2 in dataset ΔΔ162/3 versus MS11 is considered as negative regulation and <0.85 as positive regulation by the sibling RNAs. Considering these ratios, only 15 of the 23 genes significantly differentially regulated in the datasets with pulse expression of one sibling sRNA show inverse regulation.

Inverse regulation was considered as criterium for further target gene validation. Ten genes are significantly regulated in all three datasets (table 3.3). Only two (NGFG_1721 and *ack*) are already characterized target genes. Besides protein-encoding genes, the list also comprises several copies of the alanine tRNA, which are here summarized and the values for locus NGFG_6033 are given, and the non-coding RNA NgncR_201. Fourteen genes have an adjusted p-value <0.05 in two of the datasets and still show regulation in the third one, considering the cut-offs of >1.2 and <0.85 mentioned above.

Table 3.3: Selected differentially expressed transcripts in ΔΔ162/3 AIE162 and ΔΔ162/3 AIE163 versus ΔΔ162/3 and ΔΔ162/3 versus MS11 WT

Locus	Gene	AIE162 vs ΔΔ		AIE163 vs ΔΔ		ΔΔ vs MS11	
		adjusted p-value	fold change	adjusted p-value	fold change	adjusted p-value	fold change
Significantly differentially regulated in all three datasets							
NGFG_00881	leuA	0.0372	0.7862	0.0221	0.7684	0.0153	1.2772
NGFG_01407	acn	0.0160	0.6303	0.0160	0.6242	0.0056	1.5900
NGFG_01411	ack	0.0012	0.5872	0.0016	0.5897	0.0000	1.9079
NGFG_01721		0.0000	0.3231	0.0000	0.2717	0.0000	6.4531
NGFG_01722	dadA	0.0000	0.5381	0.0000	0.4698	0.0000	3.2266
NGFG_01728	minD	0.0186	1.5390	0.0392	1.4835	0.0175	0.6736
NGFG_01842	thiC	0.0042	0.5441	0.0119	0.5602	0.0064	1.7088
NGFG_02102		0.0160	0.6139	0.0303	0.6399	0.0000	2.1435
NGFG_02111	gloA	0.0000	2.2501	0.0000	2.1287	0.0256	0.6657
NGFG_02263		0.0238	1.4671	0.0127	1.5273	0.0452	0.7265
NgncR_201		0.0160	0.5422	0.0002	0.4444	0.0000	2.9282
tRNA Ala (e.g. NGFG_06033)		0.0000	0.4033	0.0000	0.4147	0.0000	3.2944
Significantly differentially regulated in two datasets							
NGFG_00045		0.0523	1.4540	0.0113	1.6178	0.0000	0.2553
NGFG_00100	atpF	0.0272	1.4928	0.0294	1.4886	0.3200	0.8117
NGFG_00254	secB	0.0342	1.4152	0.1150	1.3315	0.0006	0.6346
NGFG_00703		0.0030	0.6653	0.0237	0.7115	0.1180	1.2614
NGFG_01146		0.0376	1.5508	0.2800	1.3186	0.0000	0.5126
NGFG_01163	iscR	0.0376	0.5590	0.1260	0.6194	0.0105	1.8635
NGFG_01204	clpP	0.0025	1.4540	0.0125	1.4054	0.2200	0.8339
NGFG_01353		0.3250	1.3426	0.0173	1.8570	0.0161	0.5736
NGFG_01491		0.0476	0.6263	0.0855	0.6471	0.0018	1.8366
NGFG_01727	minE	0.0160	1.5812	0.0727	1.4610	0.0123	0.6498
NGFG_02039	ilvC	0.0099	1.4201	0.0717	1.3140	0.0000	0.6268

NGFG_02040	0.0272	1.4763	0.0707	1.4132	0.0017	0.6298
NGFG_02426	0.0238	0.5426	0.0135	0.5116	0.2050	1.4449
NGFG_02500	0.0417	0.6181	0.0852	0.6448	0.0050	1.7569

Eight positively regulated and eight negatively regulated genes were selected for validation, as well as NgncR_201 and the alanine tRNAs. These include eight genes significantly regulated in all datasets; NGFG_1721 and *ack* are already confirmed target genes. Seven other genes were chosen for their strong differential regulation or high statistical significance in dataset ΔΔ162/3 versus MS11 WT, provided that they also show significance in one of the other data sets. NGFG_1727 (*minE*) was not included in the analysis although it fulfils these criteria since it is encoded in an operon with NGFG_1728 (*minD*), a gene listed as significant in all three datasets. Instead, the hypothetical protein NGFG_2343 was analysed due to its high statistical significance (adjusted p-value of 0.0000009) and a fold change of more than two in dataset ΔΔ162/3 versus MS11 WT. Although statistical significance is not reached in the other datasets, the gene still seemed regulated upon pulse-expression of the sRNAs.

The positively regulated potential new target genes comprise the NSS-family neurotransmitter sodium symporter NGFG_0045. It belongs to a protein family of which the best characterized bacterial member is the amino acid transporter LeuT (Quick et al. 2018). Further possible positively regulated targets are NGFG_0254 encoding the protein-export protein SecB, the hypothetical protein NGFG_1146, NGFG_1353 coding for a PiT-family inorganic phosphate transporter, the septum site-determining protein MinD (NGFG_1728) and the ketol-acid reductoisomerase IlvC (NGFG_2039), an enzyme, which plays a role in the biosynthesis of branched-chain amino acids (Kim et al. 2017). The lactoylglutathione lyase GloA encoded at locus NGFG_2111 is also known under the name glyoxalase I and is involved in methylglyoxal detoxification (Sukedo et al. 2004), whereas NGFG_2263 encodes a potential glucose/galactose transporter protein.

Among the analysed negatively regulated genes were NGFG_0881 encoding the 2-isopropylmalate synthase LeuA, which is involved in the synthesis of L-leucine, and NGFG_1163 coding for the iron-sulfur cluster regulator IscR. Aconitate hydratase (*acn*, NGFG_1407) is a citric acid cycle enzyme, which is also involved in the propionate catabolism (Horswill and Escalante-Semerena 2001) and NGFG_1407 is encoded in the same gene cluster as *prpB*, *prpC* and *ack*. NGFG_1491 is a hypothetical protein, BLAST analysis showed that it is a conserved protein, which is putatively secreted. NGFG_1722 codes for the D-amino acid dehydrogenase *dadA*, which probably converts D-alanine to its respective oxoacid pyruvate. NGFG_1842 encodes the phosphomethylpyrimidine synthase ThiC, which is part of the thiamine biosynthesis, and NGFG_2102 is a phage protein.

Expression levels of the candidate genes were compared by qRT PCR in strains MS11 WT, ΔΔ162/3 and the complemented strain ΔΔc (figure 3.11A). Despite the high significance in the RNAseq data, only seven out of sixteen genes show also significant differential regulation in the qRT PCR data. Transcript levels of both analysed non-coding RNAs, the small RNA

NgncR_201 and the alanine tRNAs, are not affected by the absence of NgncR_162 and NgncR_163 (figure 3.11A+B). The alanine tRNAs are encoded within rRNA operons, therefore the high fold change in the RNAseq data might be a result of ribodepletion. The data confirms four positively regulated target genes: The transport proteins NGFG_0045 and NGFG_1353, the hypothetical protein NGFG_1146, and the lactoylglutathione lyase GloA. Three genes were validated as negatively regulated: aconitase, the hypothetical NGFG_1491 and the D-amino acid dehydrogenase *dadA*. A differential regulation of *dadA* (NGFG_1722) was expected since it is co-transcribed with the transporter NGFG_1721, which is known to be strongly regulated by the sibling RNAs (Bauer et al. 2017). In the case of NGFG_1491, the complementation did not recover the phenotype completely. Two genes, *thiC* and NGFG_2102, have a p-value just slightly above threshold (0.0594 and 0.0568, respectively) and therefore cannot be ruled out as potential new target genes.

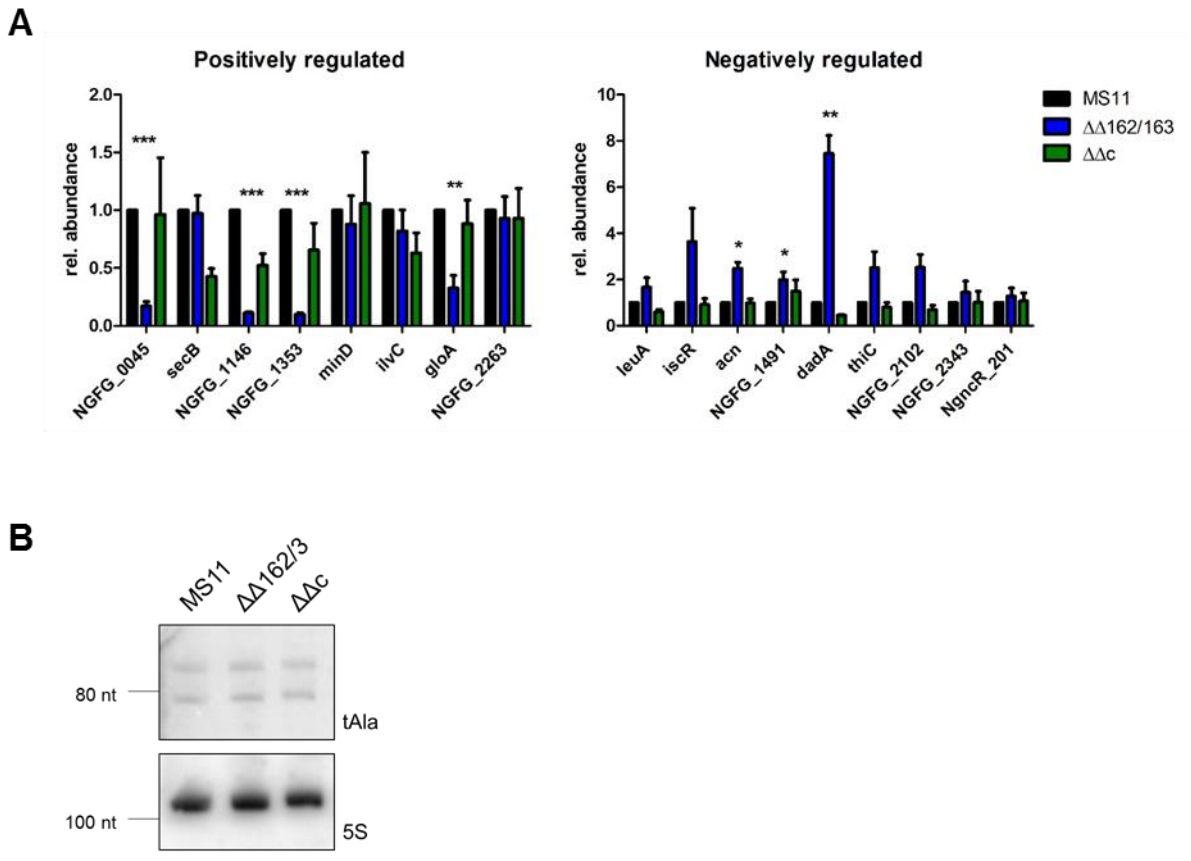

Figure 3.11 Validation of target genes from the RNAseq screen. Selected hits from the RNAseq screen were tested by qRT PCR (A) for differential expression in the absence of NgncR_162 and NgncR_163 (n=3-4). The graph includes data obtained by Susanne Bauer to allow statistical evaluation. (B) Expression of alanine tRNA was compared in MS11 WT, sRNA double KO and complementation strain by Northern Blot.

In dataset ΔΔ162/3 versus MS11, 128 genes have an adjusted p-value <0.05 and are therefore considered as significantly regulated. Applying a cut-off of >1.5 for negative regulation and <0.6 for positive regulation still results in a list of 55 possibly negatively and six possibly

positively regulated genes. Many transcript levels significantly regulated in ΔΔ162/3 remain unchanged upon pulse-expression of the individual sibling sRNAs. Considering the cut-offs for inverse regulation set before (>1.2; <0.85), only 35 negatively regulated and three positively regulated genes fulfil these criteria for inverse regulation. Analysis of validated target genes suggested that expression of one sibling RNA is sufficient for full regulation of transcript levels (Bauer et al. 2017), but here genes are differentially regulated in the double KO, but not upon pulse-expression of a single sRNA. Thus, three genes exhibiting strong differential regulation in dataset ΔΔ162/3 versus MS11, but not showing inverse regulation upon pulse-expression of NgncR_162 or NgncR_163, were further analysed (table 3.4). The tested genes include NGFG_1514, coding for the glycine cleavage system H protein GcvH, a component of a degradation machinery triggered by high glycine concentration (reviewed in Kikuchi et al. 2008). NGFG_2042 is encoding the acetolactate synthase IlvB and NGFG_2153 the nitric oxide reductase subunit B (NorB). Transcript levels of *gcvH*, *ilvB* and *norB* were compared by qRT PCR in WT, ΔΔ162/3 and the complemented strain ΔΔc (figure 3.12). All three tested genes are significantly differentially regulated in the absence of the sibling RNAs. However, only for *gcvH* and *norB* WT transcript levels were restored in the complemented strain. The downregulation of *ilvB* transcript levels in a ΔΔ162/3 strain background could be explained by

Table 3.4: Genes differentially expressed according to dataset ΔΔ162/3 versus MS11, but not according to ΔΔ162/3 AIE162 and ΔΔ162/3 AIE163 versus ΔΔ162/3

Locus	Gene	ΔΔ vs MS11		AIE162 vs ΔΔ		AIE163 vs ΔΔ	
		adjusted p-value	fold change	adjusted p-value	fold change	adjusted p-value	fold change
NGFG_01514	gcvH	0.0000	2.2191	0.3600	1.2719	0.8670	1.0666
NGFG_02042	ilvB	0.0000	0.4796	0.6640	1.1011	0.4870	1.1551
NGFG_02153	norB	0.0000	0.5897	0.2680	1.1900	0.2790	1.1966

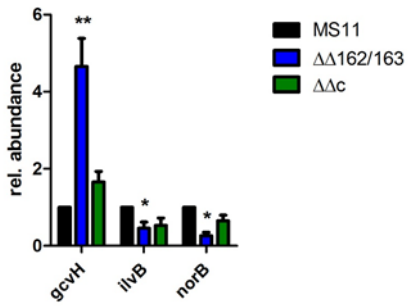

Figure 3.12: Analysis of RNAseq hits of dataset ΔΔ162/3 versus MS11 not differentially regulated in the other datasets. Expression levels of genes NGFG_1514 (*gcvH*), NGFG_2042 (*ilvB*) and NGFG_2153 (*norB*) were analysed in strains MS11, ΔΔ162/3 and complementation strain ΔΔc by qRT PCR (n=3). The graph includes data from experiments performed by Susanne Bauer.

secondary mutations occurring during mutagenesis. Both *gcvH* and *norB* might require presence of both sRNAs for full regulation, but further experiments are required to prove this hypothesis. It also needs to be considered that not all genes known to be targets of NgncR_162 and NgncR_163 appear regulated in all datasets, what might the case here as well.

Validation of putative sRNA targets differentially expressed in a Δhfq mutant of *N. meningitidis*

In a study investigating global transcription profile differences in *N. meningitidis* expressing or lacking the RNA chaperone Hfq, 152 genes were found to be differentially regulated (Fantappiè et al. 2011). Not only the meningococcal sibling sRNAs RcoF2/F1 were shown to interact with Hfq (Heidrich et al. 2017), but also NgncR_162 and NgncR_163 (Heinrichs and Rudel, unpublished). Several genes identified to be differnentially regulated in the absence of Hfq in *N. meningitidis* are validated targets of NgncR_162/NgncR_163. These genes include the transport proteins NGFG_1721, NGFG_0045 and NGFG_2263. Interestingly, five other genes encoding transport proteins were significantly regulated upon deletion of *hfq* in *N. meningitidis* (Fantappiè et al. 2011) and these genes show also significant differential regulation in dataset ΔΔ162/3 versus MS11 (table 3.5). Inverse regulation upon pulse-expression of NgncR_162 or NgncR_163 can be observed for NGFG_1471 and NGFG_1564, whereas NGFG_0093, NGFG_0249 and NGFG_1937 show inverse regulation only in dataset ΔΔ162/3 AIE163 versus ΔΔ162/3. NGFG_0093 codes for a methionine transport protein, NGFG_0249 for a citrate transporter, NGFG_1471 is annotated as lactate permease, NGFG_1564 belongs like NGFG_0045 to the NSS family neurotransmitter Na+ symporter family of transport proteins

Table 3.5: RNAseq results of genes differentially expressed in a Δhfq mutant of *N. meningitidis*

Locus	ΔΔ vs MS11		AIE162 vs ΔΔ		AIE163 vs ΔΔ	
	adjusted p-value	fold change	adjusted p-value	fold change	adjusted p-value	fold change
NGFG_00093	0.0000	1.6369	0.8340	0.9602	0.2290	0.8299
NGFG_00249	0.0000	2.9282	0.7230	0.9013	0.1610	0.7150
NGFG_01471	0.0191	0.7658	0.0783	1.2666	0.0704	1.2861
NGFG_01564	0.0087	0.7061	0.1850	1.2518	0.2040	1.2570
NGFG_01937	0.0000	1.8700	0.9950	0.9970	0.2640	0.7770

and NGFG_1937 codes for a peptide transporter. Transcript levels of all five genes were compared in strains MS11 WT, ΔΔ162/3 and ΔΔc by qRT PCR (figure 3.13A). Negative regulation by the sibling sRNAs could be confirmed for NGFG_0249 and NGFG_1937, positive regulation for NGFG_1471 and NGFG_1564. NGFG_0093 levels are not significantly affected. Regulation of NGFG_1471 might be an indirect regulatory effect. Expression of lactate

permease was reported to be inhibited by GdhR (Ayala and Shafer 2019), what could be confirmed in strain MS11 (figure 3.13B). GdhR itself is downregulated by the sibling RNAs (Bauer et al. 2017) and hence the absence of NgncR_162 and NgncR_163 would explain a decrease in NGFG_1471 transcript levels.

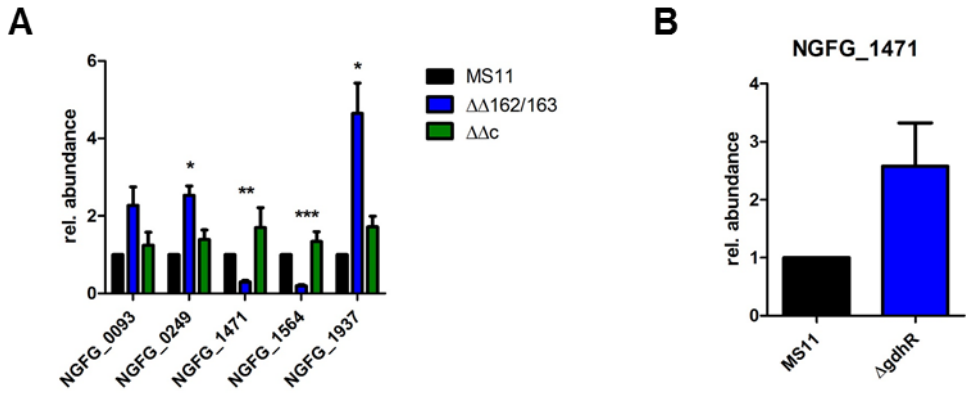

Figure 3.13: Validation of putative targets differentially expressed in a meningococcal Δhfq mutant. (A) Transcript levels of genes NGFG_0093, NGFG_0249, NGFG_1471, NGFG_1564 and NGFG_1937 were compared in strains MS11 WT, ΔΔ162/3 and complementation strain ΔΔc by qRT PCR (n=3). The graph includes data from experiments performed by Susanne Bauer. (B) Comparison of NGFG_1471 transcript levels in strains MS11 WT and ΔgdhR by qRT PCR (n=3).

In silico prediction of sRNA-mRNA interactions

Genes which showed also significant regulation by the sRNAs in the qRT PCR analysis were analysed for possible sRNA-mRNA interaction regions. IntaRNA (Mann et al. 2017) was applied using standard settings for prediction of the interaction region between the target mRNA and NgncR_162. The results are shown in figure 3.14. Previously validated target genes of NgncR_162 and NgncR_163 are all negatively regulated by interaction with the SL2 loop or SSR1 of the sRNA with the RBS (Bauer et al. 2017). From the six newly identified negatively regulated genes only two, NGFG_0249 and NGFG_1937, are predicted to be regulated by the same mechanism. *DadA* is co-transcribed with NGFG_1721, but seems to be regulated itself by interaction of the sRNA SSR1 domain with the RBS. The SSR1 sequence is also conserved between NgncR_162 and NgncR_163. In case of *acn*, NGFG_1491 and *gcvH* mRNAs sRNA binding is predicted to occur within the coding sequence. Interaction sites were found in the middle of the CDS for *acn* and NGFG_1491 and at the 3' end of the coding sequence in case of *gcvH*. NGFG_1491 and *gcvH* exhibit sequence complementarity to the SL2 loop of NgncR_162 and NgncR_163, whereas *acn* might interact with the SL1 loop of NgncR_162. This stem loop shares no sequence homology between NgncR_162 and NgncR_163 and therefore is unlikely to interact with the *acn* mRNA, since regulation of this transcript was also observed upon pulse-expression of NgncR_163. When repeating the IntaRNA prediction with NgncR_163, the SSR1/SL2 of the sRNA is predicted to interact with the *acn* mRNA (figure 3.14C). NgncR_162 differs only in one nucleotide from NgncR_163 in

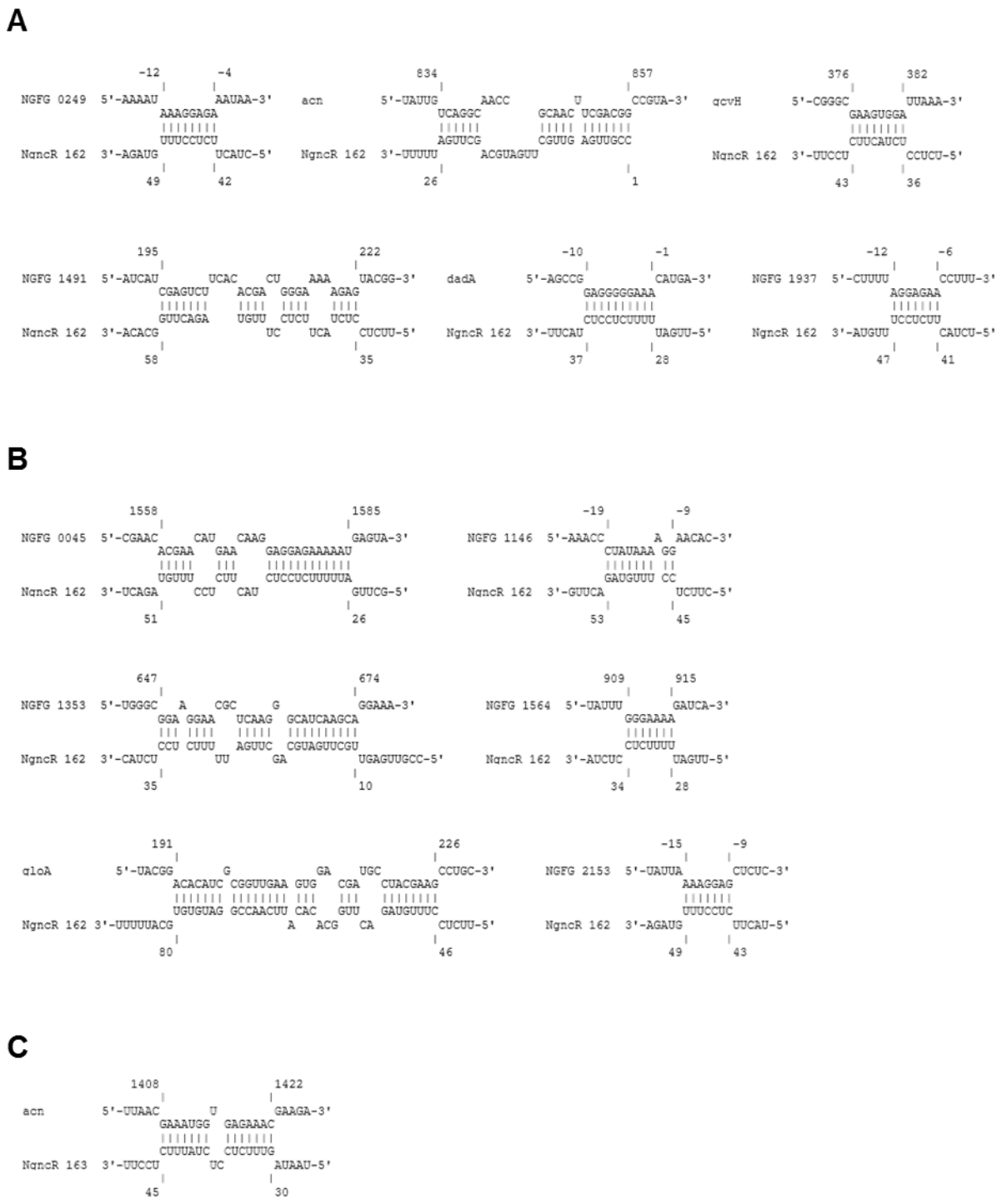

Figure 3.14: Prediction of sRNA:mRNA interactions between NgncR_162/163 and their target genes. Interactions between negatively regulated target genes NGFG_0249, *acn*, *gcvH*, NGFG_1491, dadA and NGFG_1937 (A) or positively regulated target genes NGFG_0045, NGFG_1146, NGFG_1353, NGFG_1564, *gloA* and NGFG_2153 (B) and the sRNA NgncR_162 was predicted with the webtool IntaRNA. *Acn* was additionally tested for interaction with NgncR_163 (C). Numbers refer to the nucleotide position with respect to the start codon (+1) or in the case of the sRNA the transcriptional start site.

this sequence and so possibly could also bind the respective mRNA sequence. Further, it needs to be considered that *acn* is part of the *prpB/C/ack* operon and hence *acn* transcript levels might be affected by regulation of these mRNAs.

Positive regulation by sRNAs seems more diverse. Two mRNAs, NGFG_1146 and NGFG_2153, show interaction with the SL2 loop of the sRNAs with the 5' UTR including the RBS. This interesting since interaction with the RBS is usually associated with negative regulation. NGFG_1353, NGFG_1564 and *gloA* mRNAs are bound in the middle of the CDS, but via different regions of the sRNA. They are predicted to interact with the SL1 loop including SSR1, the SSR1 sequence or SL2 including SL3 loop, respectively. NgncR_162 and NgncR_163 differ in the SL1 and SL3 sequence, therefore regulation of NGFG_1353 and *gloA* mRNA by NgncR_163 would be questionable, however, both appear regulated in dataset AIE163 vs ΔΔ. NGFG_0045 mRNA is predicted to be bound by the SL2 loop of the sRNAs with the very 3' end of its coding sequence. Binding of the sRNA within the coding sequence of their target mRNA for positive regulation has been reported for several non-coding RNAs.

3.2.2.3 Positive target regulation by NgncR_162 and NgncR_163

A more detailed analysis of positively regulated genes is required for better understanding of the regulatory mechanism. Binding of the sRNA within the coding region could result in protection of the target transcript from degradation by RNases like RNase E or RNase III. Northern Blot analysis was performed to check for specific cleavage patterns of the target mRNAs NGFG_0045 and *gloA* in the absence of the sibling RNAs. Northern Blotting confirmed positive regulation of NGFG_0045 and *gloA* by the sibling sRNAs. For NGFG_0045 degradation products of the transcript are visible, however, they do not differ in strains MS11 WT and ΔΔ162/163 (figure 3.15). No degradation products could be detected for *gloA* mRNA and transcript size did not differ in the different strains.

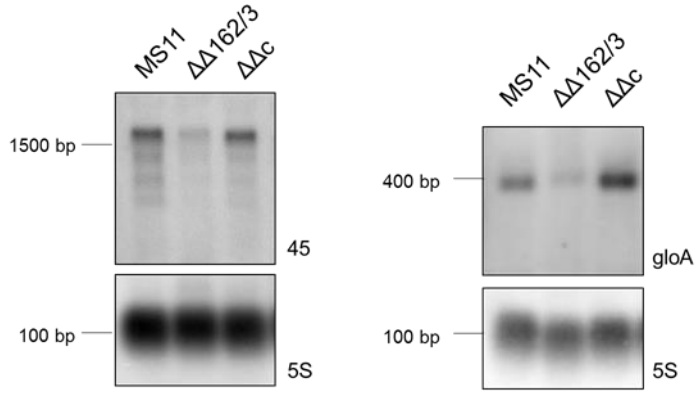

Figure 3.15: Regulation of NGFG_45 and *gloA* by NgncR_162 and NgncR_163. The effect of the absence of the sibling sRNAs on NGFG_0045 and *gloA* transcript levels was examined by analysing RNAs from strains MS11, ΔΔ162/3 and complemented strain ΔΔc by Northern Blot.

The transcriptional regulator GdhR is involved in indirect regulation of the lactate permease NGFG_1471 (figure 3.13B). Although NGFG_0045 is regulated upon pulse-expression of NgncR_162 and NgncR_163 and experimental conditions were supposed to exclude indirect regulatory effects in these datasets, transcriptional regulation by a transcription factor like GdhR whose expression is controlled by the sibling sRNAs cannot be excluded. NgncR_162 and NgncR_163 downregulate GdhR. If an increased GdhR expression in the absence of the sRNAs were responsible for the decreased transcript amounts of NGFG_0045, an increase in NGFG_0045 transcript level would be expected in a GdhR knockout strain due to the loss of transcriptional repression. However, the opposite effect was observed and Northern Blots as well as qRT PCR experiments showed a decrease of the amount of NGFG_0045 transcripts in the absence of GdhR (figure 3.16A+B). The sRNAs seem to downregulate a transcription factor, which is having the same regulatory effect on NGFG_0045 than the sRNAs. In order to assess whether the sibling sRNAs regulate their target directly or indirectly, the promoter region of NGFG_0045 was exchanged by the *opa* promoter in strains MS11 WT, ΔΔ162/3 and ΔΔc. The respective mutants were analysed for NGFG_0045 expression (figure 3.16C). The regulation pattern was unaltered by the exchange of the promoter region. This indicates that NGFG_0045 is directly regulated by the sRNAs acting on the NGFG_0045 mRNA. Furthermore, the promoter region of NGFG_0045 including its 5‘ UTR was fused to *gfp* in MS11 WT and ΔΔ162/3. Equal amounts of transcript were detected in presence and absence of the sibling sRNAs (experiments performed by Susanne Bauer). This data further confirm direct regulation by the sibling sRNAs and suggest that post-transcriptional regulation of NGFG_0045 does not involve its 5’ UTR. Direct regulation by the sRNAs could be assessed by measuring the mRNA half-life in the presence and absence of the sibling RNAs. However, determination of NGFG_0045 half-life in strain ΔΔ162/3 by Northern Blot failed due to the very low amount of NGFG_00045 transcript. For the same reason, an alternative strategy by performing transcript quantification with qRT PCR did not result in reliable data.

A possible direct interaction site between NgncR_162 and NGFG_0045 was predicted to be at the 3’ end of the coding region of NGFG_0045. The codons encompassing the putative interacting region were deleted and the native NGFG_0045 sequence was replaced by the truncated version in strains MS11 WT (45mut) and ΔΔ162/3 (45mut ΔΔ). According to RNAseq data, NGFG_0045 is co-transcribed with a small gene encoding a hypothetical protein, whose open reading frame overlaps by four nucleotides with the open reading frame of NGFG_0045 (Remmele et al. 2014). Overlap of the two open reading frames (ORFs) remained unaltered in the truncated version of NGFG_0045. Expression of mutated NGFG_0045 was tested in presence and absence of the sibling sRNAs by qRT PCR and Northern Blot (figure 3.16D+E). However, in the absence of the sibling sRNAs transcript levels of the mutated NGFG_0045 decreased to a similar extent than that of WT NGFG_0045. This result suggests that NgncR_162 and NgncR_163 do not regulate expression of NGFG_0045 via the predicted region of complementarity between sRNA and mRNA.

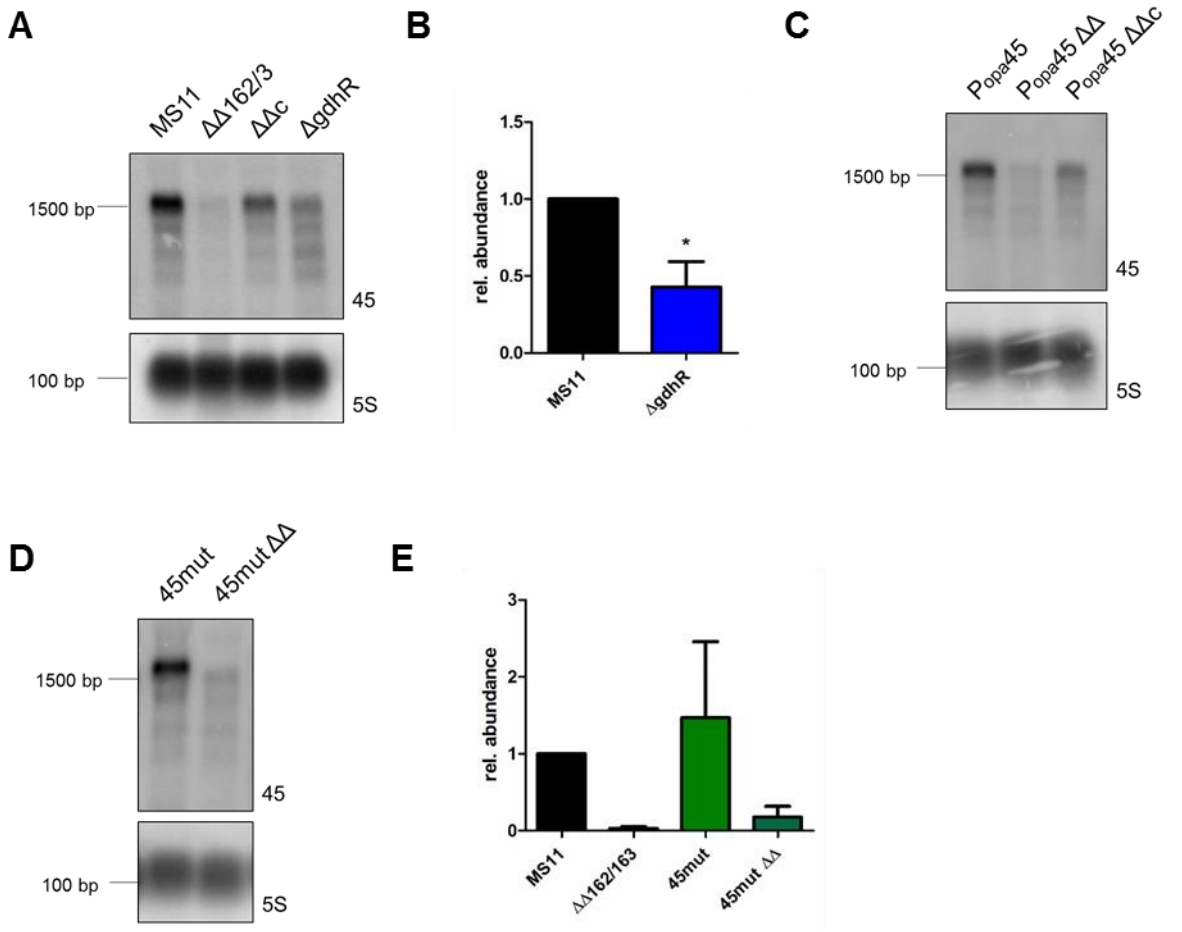

Figure 3.16: Analysis of positive regulation by NgncR_162 and NgncR_163 on NGFG_45. (A+B) The possible influence of the transcriptional regulator GdhR on expression of NGFG_45 was analysed by Northern Blot (A) and qRT PCR (B). (C) The promoter region of NGFG_45 was exchanged by the *opa* promoter in WT, sRNA KO and complementation strain background and subsequent the expression of NGFG_45 analysed by Northern Blot. (D+E) In order to find the interaction site between target gene and sRNAs, the predicted interacting region in NGFG_45 was mutated. Expression of NGFG_45 carrying the mutation was compared in presence (45mut) and absence of the sRNAs (45mut ΔΔ) by Northern Blot (D) and qRT PCR (E) (n=2).

3.2.3 Differential expression of NgncR_162 and NgncR_163

The transcriptome analysis in *N. gonorrhoeae* suggested higher abundance of NgncR_163 compared to NgncR_162 (Remmele et al. 2014). Also in meningococci, the sRNAs RcoF1 and RcoF2 are not expressed in same amounts under standard growth conditions (Heidrich et al. 2017). For comparison of the expression of the homologous sRNAs in *N. gonorrhoeae*, NgncR_162 and NgncR_163, a Northern Blot probe was used that is binding in the conserved region, which is identical between both sRNAs. In strain MS11 WT the hybridization signal corresponding to NgncR_163 was stronger than that corresponding to NgncR_162 and this effect was also observed with RNA from the individual deletion mutants MS11 ∆162 and MS11

Δ163 (figure 3.17). This data indicates higher abundance of NgncR_163 compared to NgncR_162 in *N. gonorrhoeae* under standard growth conditions.

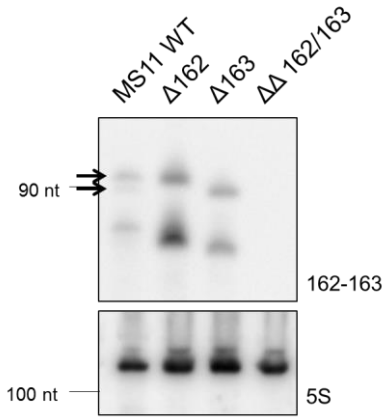

Figure 3.17: Differential expression of NgncR_162 and NgncR_163. Comparison of the expression of NgncR_162 and NgncR_163 in a Northern Blot using a probe binding to both sRNAs. The arrows mark bands for NgncR_162 (lower band) and NgncR_163 (upper band).

A higher stability of NgncR_163 compared to NgncR_162 would explain the difference in sRNA abundance. The sRNA stability can be analysed by comparing the respective half-lives of both sRNAs with a rifampicin assay. Rifampicin is an antibiotic interfering with the bacterial DNA-dependent RNA polymerase and thereby inhibiting RNA synthesis. By comparing the amount of transcripts at different time points after addition of rifampicin, it is possible to draw conclusions about transcript stability. The time point, at which 50 % of the RNA is degraded, determines the half-life of the RNA. Northern Blot analysis of RNA extracted from samples taken at different time points after rifampicin addition by Northern Blots show a half-live for NgncR_162 of 58 min and for NgncR_163 of 56 min (figure 3.18). Considering experimental variability, an identical half-life for both sRNAs could be determined.

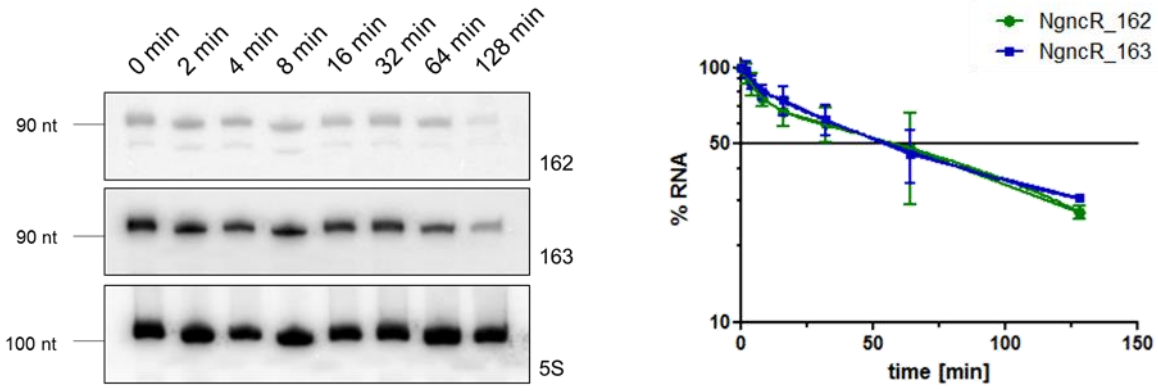

Figure 3.18: Identical half-lives of the sRNAs. The stability of the sRNAs was determined in a rifampicin assay and the relative amount of RNA was determined by quantification of Northern Blots. Three independent experiments were performed for determination of the respective half-lives. The half-life of NgncR_162 is 58 min and the half-life of NgncR_163 56 min.

Differences in abundance of the sibling sRNAs could also result from differences in promoter strength. Therefore, promoter activity of both sRNAs was compared using reporter gene fusions. The upstream region of NgncR_162 comprising approximately 200 nucleotides was fused to *gfp*, resulting in strain P_{162}-gfp. In strain P_{163}1-gfp the intergenic region between NgncR_162 and NgncR_163 comprising about 100 nucleotides is fused to *gfp*. Since regulatory elements for NgncR_163 could be present in the sequence of NgncR_162, a second P_{163} construct was designed, P_{163}2-gfp, which additionally comprises the sequence and upstream region of NgncR_162. The amount of *gfp* transcripts under control of the different promoter regions was compared in all three strains, showing higher *gfp* expression for both P_{163} strains compared to the P_{162} strain (figure 3.19A). These results were confirmed on protein level, by comparing the GFP signal of the different bacterial lysates by Western Blot (figure 3.19B). For better comparison, the promoter regions were aligned showing the sequence 100 bp upstream of each sRNA gene as well as the first ten nucleotides of the sRNA (figure 3.19C). The alignment of the promoter region of both sRNAs reveals that the sequence is only poorly conserved and hence offers different binding possibilities for transcriptional regulators. Taken together, the data indicate that higher abundance of NgncR_163 results from a difference in promoter strength.

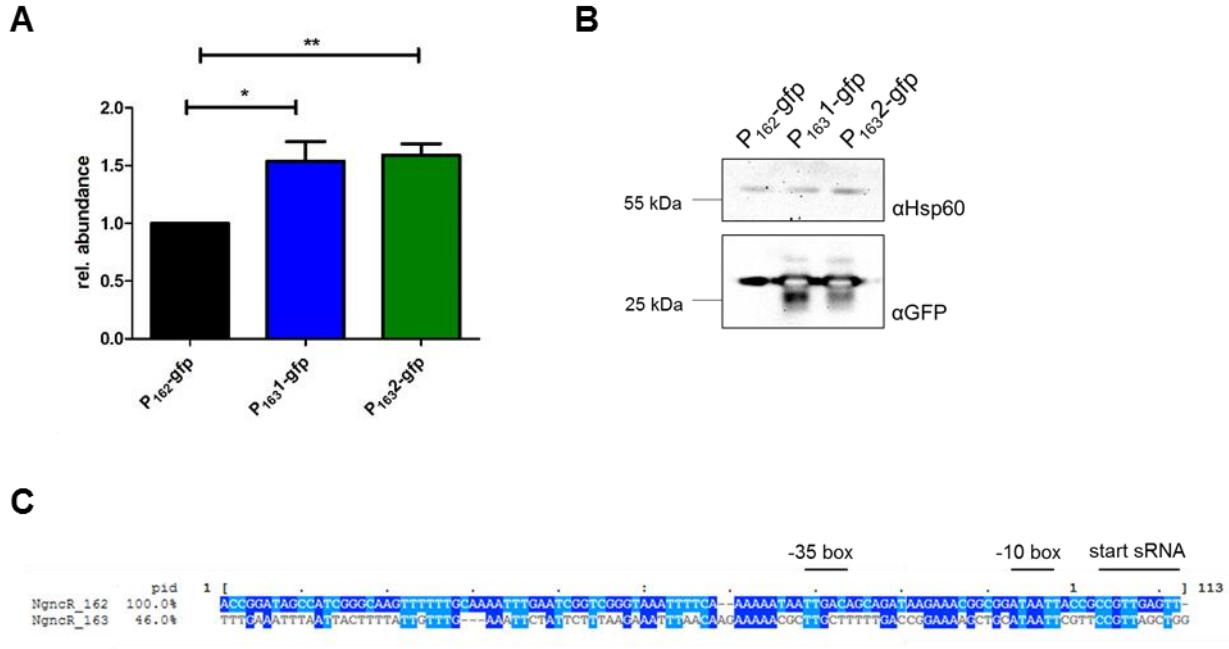

Figure 3.19: Difference in promoter activity between NgncR_162 and NgncR_163. The upstream regions of NgncR_162 and NgncR_163 were combined with the reporter gene *gfp*, For NgncR_163 a shorter (P_{163}1) and longer (P_{163}2) upstream region was used, (A) Transcript amounts were determined by qRT PCR (n=6). (B) The protein levels of the reporter gene fusions were analysed with Western Blots with Hsp60 as loading control. (C) Comparison of the promoter sequence between NgncR_162 and NgncR_163. The sequence alignments were created with the high speed multiple sequence alignment program MAFFT (https://www.ebi.ac.uk/Tools/msa/mafft/) and visualized with the alignment editor MView (https://www.ebi.ac.uk/Tools/msa/mview/). The sequence percentage identity is given in reference to NgncR_162.

Differences in expression of NgncR_162 and NgncR_163 could be the result of different transcriptional regulators binding upstream of the RNA polymerase binding site. Therefore, sRNA genes with truncated promoter regions comprising only the -10 promoter element and the region comprising the -35 box were integrated into strain MS11 ΔΔ162/3 (ΔΔcs162 or ΔΔcs163). In addition, sRNA genes with an upstream region comprising approximately 200 bp were used for complementation (ΔΔc162 or ΔΔc163). sRNA levels of these complemented strains were compared by Northern Blot (figure 3.20A). Expression of both NgncR_162 and NgncR_163 was clearly reduced in strains carrying the truncated promoter variants limited to the -35 region compared to strains with the full-length promoter sequence. However, the effect was more pronounced in the case of NgncR_163, indicating that the region upstream of the RNA polymerase binding site is required for efficient initiation of transcription. This data was confirmed by analysing target gene expression by qRT PCR. mRNA levels of NGFG_1721 and NGFG_2049 were compared in WT, double KO and the different complemented strains (figure 3.20B). A complementation with sRNAs having a full length promoter sequence restores WT

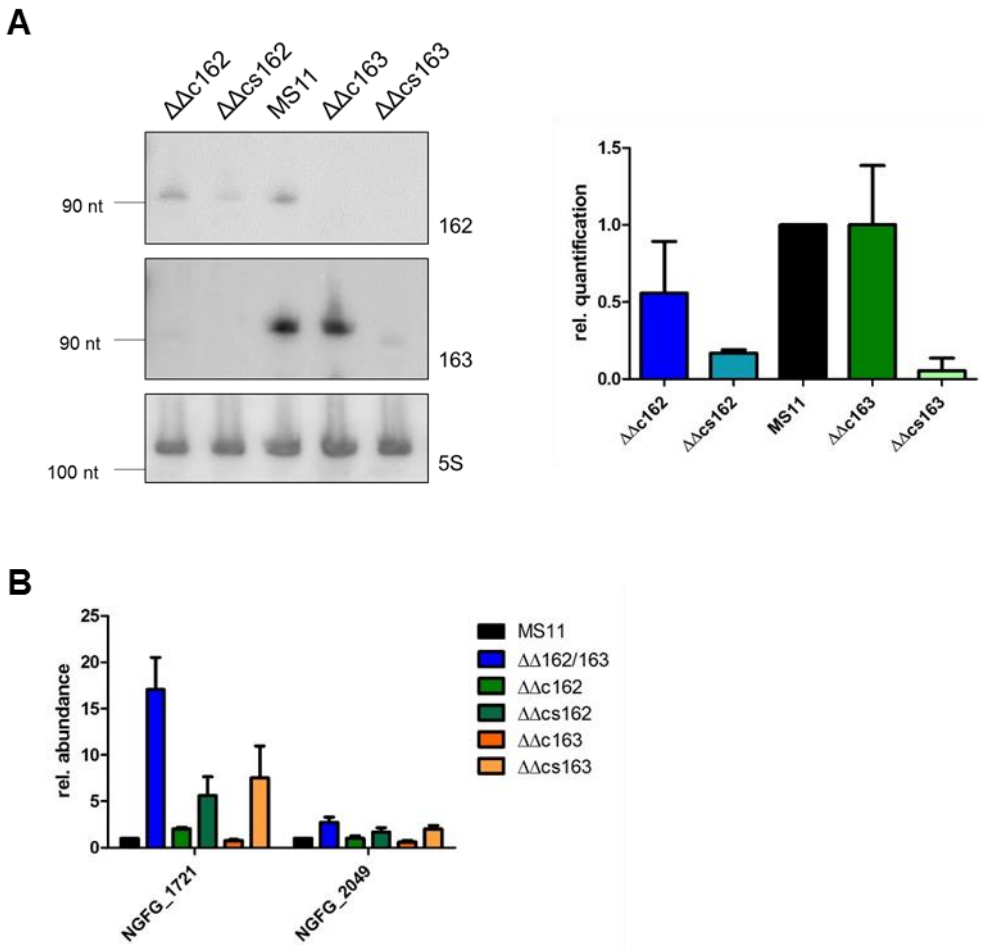

Figure 3.20: Analysis of sRNAs carrying a minimal promoter region. (A) The double KO strain is complemented with the sRNA with normal promoter length (ΔΔc) and the minimal promoter (ΔΔcs), implying only the sequence from the transcription start site to the putative -35 box. The graph shows the quantification of three Northern Blots. (C) Testing the sRNA complementation strains on NGFG_1721 and NGFG_2049 target gene expression by qRT PCR (n=3).

transcript levels, whereas truncation of the promoter sequence results in higher target mRNA levels. This effect can be easily explained by the lower abundance of the sibling RNAs.

Some transcriptional regulators could be promising candidates in affecting sRNA transcript levels and therefore deletion mutations of these regulators were analysed for sRNA expression. GdhR is a GntR-type transcriptional regulator regulating mostly membrane proteins (Ayala and Shafer 2019). It was validated as target gene of the sibling RNAs (Bauer et al. 2017) and so GdhR could play a role in regulation of NgncR_162 and NgncR_163 via a feedback loop. NGFG_2170 encodes an Lrp/AsnC family transcriptional regulator and is located directly downstream of the sRNAs (see figure 3.7). This genomic organization is rather conserved within *Neisseria* and therefore function of NGFG_2170 could be connected to the sRNAs. Another regulator, RelA, was reported to influence the expression of the homologous sibling RNAs in *N. meningitidis* (Pannekoek et al. 2017). In *N. gonorrhoeae* RelA is the sole producer of (p)ppGpp and therefore activator of the stringent response (Fisher et al. 2005). In meningococci grown on a nutrient-rich medium, RelA was suggested to downregulate sibling sRNA expression by direct interaction with a GC-rich sequence within the $NmsR_A$ promoter sequence (Pannekoek et al. 2017). In addition, two KO strains available in the laboratory were included in the study, NGFG_1511 is another Lrp/AsnC family transcriptional regulator in strain MS11 and GntR (NGFG_2027), like GdhR a GntR family transcriptional regulator. GntR was

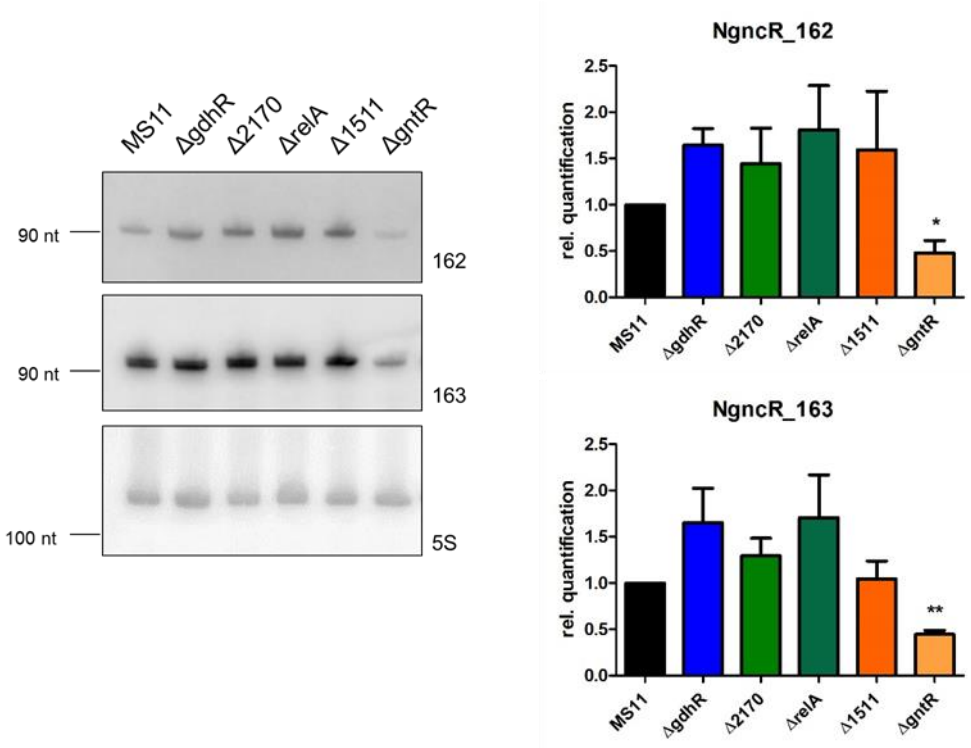

Figure 3.21: Influence of the deletion of several transcriptional regulators on sRNA expression. The expression of NgncR_162 and NgncR_163 was analysed on Northern Blots after deletion of the transcriptional regulators GdhR, NGFG_2170, RelA, NGFG_1511 and GntR. The diagrams show the quantification of three independent experiments for each sRNA.

reported to repress the meningococcal sRNA Bns1 under glucose-limiting conditions (Fagnocchi et al. 2015). Expression levels of NgncR_162 and NgncR_163 were compared in strain MS11 WT and the five regulator KO strains by Northern Blot (figure 3.21). The analysis revealed the same expression pattern for both NgncR_162 and NgncR_163. With the exception of GntR, the tested transcriptional regulators have no significant effect on sRNA expression. Deletion of GntR resulted in reduced levels of both NgncR_162 and NgncR_163. Binding motifs of the GntR family are conserved, varying only little within the subfamilies, and reported consensus sequences are $N_yGTM\text{-}N_{0-1}\text{-}KACN_y$ or $N_yGTMTAKACN_y$. Especially the GT/AC pairs are conserved and surrounded by A and T residues (Suvorova et al. 2015). However, such a binding motif is not conserved in the promoter region between NgncR_162 and NgncR_163.

3.2.4 Influence of the growth phase on sRNA expression

It has been shown for several small RNAs that they are differentially regulated in the different growth phases of bacteria thereby adapting to the changing needs depending on the growth phase (reviewed in Wassarman 2002). To test whether expression levels of NgncR_162 and NgncR_163 are influenced by the growth phase, samples were taken from a bacterial culture at three different time points and the isolated RNA was analysed by Northern Blot. Bacteria were harvested during logarithmic and during stationary growth phase and at the transition between the two phases. The time points are illustrated in the growth curve in figure 3.22B. Both sibling sRNAs are strongly downregulated in stationary phase (figure 3.22A). There is no effect detectable at the transition between logarithmic and stationary growth phase. However, this result is not surpsrising considering the long half-lifes of the sRNAs. Lower sRNA levels would result in a less efficient target mRNA regulation. NGFG_1721 is negatively regulated by NgncR_162 and NgncR_163 and hence a decrease in sRNA levels should cause an increase in mRNA levels. Therefore, expression of NGFG_1721 was tested in logarithmic and stationary growth phase by qRT PCR (figure 3.22C). In line with the downregulation of the sibling sRNAs, NGFG_1721 was clearly upregulated in stationary phase.

Several factors could influence the expression of small RNAs and so cause a lower abundance of sRNA transcripts in stationary phase. One possibility is a transcriptional regulation of sRNA expression. Therefore, reporter gene expression of the sRNA promoter-*gfp* fusions were analysed in the different growth phases by qRT PCR (data not shown) and in the case of NgncR_163 additionally by Western Blot (figure 3.23). The expected downregulation of *gfp* expression in stationary growth phase could not be observed, indicating no impact of transcriptional regulation on downregulation of sRNA expression.

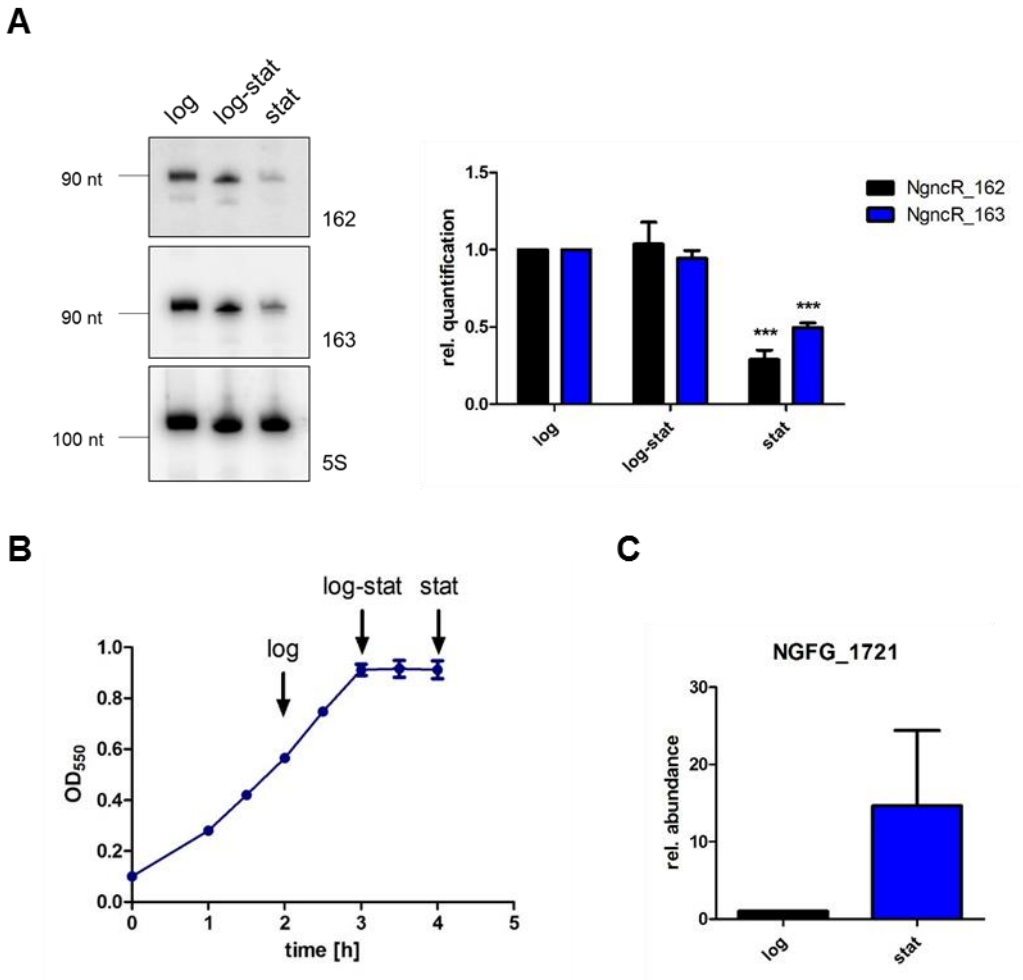

Figure 3.22: Downregulation of sRNA expression in stationary phase. (A) Northern Blot for sRNA expression at the different growth phases: logarithmic, transition between logarithmic and stationary phase and stationary phase. The diagram shows the quantification of four experiments. (B) Summary of the growth curves of the experiments showing the time points for sampling. (C) The abundance of the target gene NGFG_1721 was determined by qRT PCR comparing logarithmic and stationary growth phase (n=2).

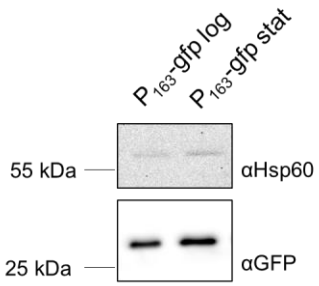

Figure 3.23: NgncR_163 promoter activity in logarithmic and stationary growth phase. The NgncR_163 promoter-*gfp* fusion was analysed in the two growth phases for GFP abundance by Western Blot.

A decrease in the stability of the sibling sRNAs could cause their downregulation in stationary phase. Both NgncR_162 and NgncR_163 were shown to co-immunoprecipitate with the RNA chaperone Hfq (Heinrichs and Rudel, unpublished). Hfq is known to be an important factor for the stability of several small RNAs. In order to test whether Hfq impacts on sibling sRNA abundance, the expression levels of both sibling sRNAs were compared in presence and absence of the RNA chaperone by Northern Blot (figure 3.24A). Both sRNAs are clearly less abundant in the absence of Hfq confirming that their stability is depending on the RNA chaperone. Thus, expression of *hfq* was analysed in logarithmic and stationary growth phase by Northern Blot (figure 3.24B). The amount of *hfq* transcripts is noticeably decreased in stationary growth phase. However, more relevant is an analysis of the amount of Hfq on protein level. By using a strain carrying a Flag-tagged version of Hfq, the protein can be detected by an anti-Flag antibody in Western Blot (figure 3.24C). The difference between logarithmic and stationary growth phase is less pronounced on protein level than on transcript level, but still detectable. A reduced amount of the RNA chaperone could explain the difference in sRNA abundance in the different growth phases.

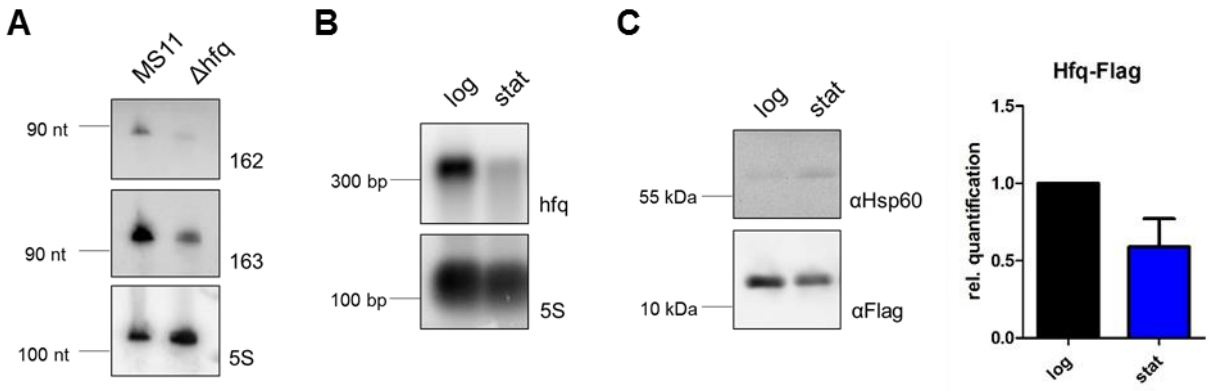

Figure 3.24: Hfq-dependent downregulation of NgncR_162 and NgncR_163 in stationary phase. (A) Expression of both sRNA in presence and absence of Hfq. (B) Comparison of the expression of *hfq* in logarithmic versus stationary growth phase in Northern Blot. (C) A Flag-tagged Hfq was used for measuring the protein level of Hfq by detection with an anti-Flag antibody. The quantification of three Western Blots is shown in the graph on the right.

Enzymes involved in degradation of sRNAs could also influence the abundance of NgncR_162 and NgncR_163. The endonuclease RNase III is known for degradation of sRNA:mRNA complexes, but also RNase E is associated with sRNA degradation (Afonyushkin et al. 2005). The major exonucleases in *E. coli* are RNase II and PNPase. Especially PNPase is reported to be essential for regulating the expression of a small RNA (Andrade and Arraiano 2008). PAP I can promote RNA degradation by exonucleases (Xu and Cohen 1995), therefore this enzyme was included in the study. The expression of these RNA degrading enzymes was compared in logarithmic and stationary growth phase by qRT PCR (figure 3.25). Trancript levels of all five enzymes were strongly upregulated in stationary growth phase, especially RNase II and RNase III, which show a more than 40-fold increase of mRNA levels. In summary,

this data supports the hypothesis that a higher abundance of the nucleases leads to a higher degree of sRNA degradation and thereby causes the decreased amounts of NgncR_162 and NgncR_163.

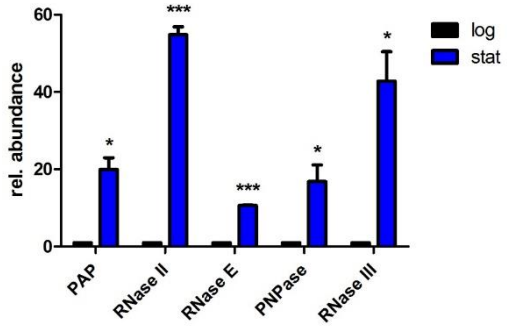

Figure 3.25: Upregulation of enzymes involved in RNA degradation in stationary phase. The expression of five different enzymes important for degradation of mRNAs and sRNAs was compared by qRT PCR in logarithmic and stationary growth phase (n=3).

3.2.5 Influence of the growth medium composition on sRNA expression

3.2.5.1 Analysis of sRNA expression in various culture media

According to the literature, many sRNAs are involved in regulation of metabolic processes and adaptation to environmental changes. The list of target mRNAs of NgncR_162 and NgncR_163 comprises several genes coding for transport proteins or that are directly involved in metabolic processes. Hence, the nutrient availability could affect target regulation by the sRNAs. Every growth medium has a unique composition of nutrients and previous results on the meningococcal homologous $NmsR_A$ and $NmsR_B$ revealed an impact of the selected growth medium on sRNA regulation (Pannekoek et al. 2017). Therefore, several chemically defined media were analysed for sibling sRNA expression: the phosphate-free Hepes infection medium, the cell culture medium RPMI, the cell culture medium-based Graver-Wade medium (Wade and Graver 2007) and the chemically defined medium CDM-10 (Dyer et al. 1987).
Comparing the growth of MS11 WT, the sRNA double KO strain and the complementation strain in four of the media already reveals huge growth differences (figure 3.26). All three tested strains grew well in the full medium PPM+, which is rich in nutrients. In the chemically defined media, the OD_{550} reached after 5 hours of growth is lower compared to the full medium. In Hepes medium, hardly any growth of gonococci was observed. Interestingly, the double KO strain ΔΔ162/3 behaved differently when compared to the WT strain in the tested media. Whereas in PPM+ and RPMI medium the mutant strain grew like the WT, in Hepes and CDM-10 the growth rate was significantly lower. There is no obvious link to the medium composition, all three chemically defined media vary quite a lot in their exact composition, but the amount of many nutrients is in the same range (see table A.3).

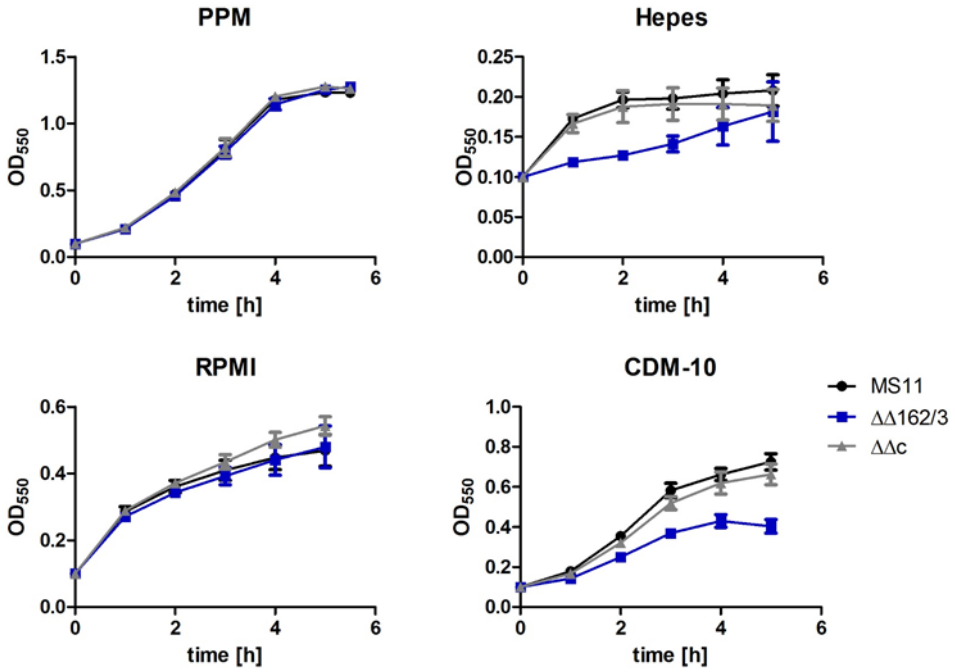

Figure 3.26: Comparing the growth of WT versus ΔΔ162/3 in different media. Growth of strains MS11 WT, double KO ΔΔ162/3 and complementation strain ΔΔc was monitored over 5 h by measuring the OD_{550} in the full medium PPM+ or the chemically defined media Hepes, RPMI or CDM-10 (n=3).

The growth curves show that NgncR_162 and NgncR_163 influence gonococcal growth depending on the media composition. To test whether medium composition affects expression of the sibling sRNAs, abundance of NgncR_162 and NgncR_163 was compared in the five different growth media by Northern Blot (figure 3.27A). The expression of the sibling RNAs is clearly downregulated in Hepes medium and RPMI, whereas expression in Graver-Wade medium is similar to PPM+. In CDM-10 medium, only a small downregulation can be observed for NgncR_162, which is negligible in the case of NgncR_163. These data reveal no link between a growth defect and altered sRNA expression in the respective growth medium. The results were confirmed by comparing gene expression of the target gene NGFG_1721 in the different media by qRT PCR (figure 3.27B). As expected, expression of NGFG_1721 significantly increases in Hepes medium and RPMI and shows a smaller increase in CDM-10. NGFG_1721 transcript levels in Graver-Wade medium correspond to those in the rich medium, confirming the Northern Blot data on sRNA abundance. As control experiment, expression of alanine racemase was analysed. Alanine racemase is not listed as target gene of the sibling RNAs and qRT PCR experiments confirmed that alanine racemase mRNA levels remain unchanged upon deletion of the sibling sRNAs (figure 3.27C). Nevertheless, the pattern is similar to NGFG_1721; transcript levels are also increased in Hepes medium, RPMI and CDM-10. These results suggest that medium shift also results in transcriptional regulation of a subset of genes.

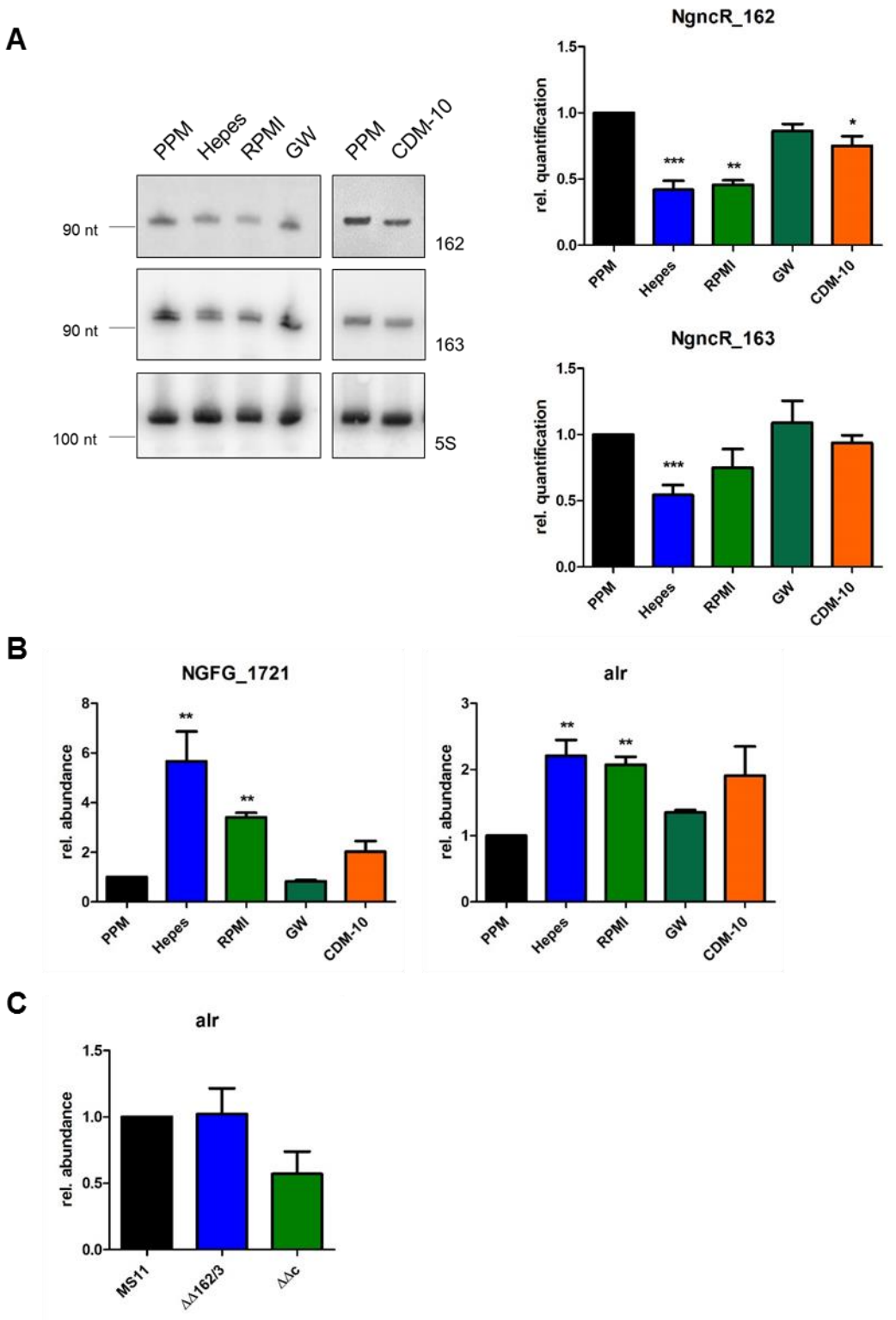

Figure 3.27: Difference of sRNA expression in various media. Gonococci were grown in a pre-culture in PPM before being shifted in the main culture to the different media. Samples from mid-log cultures were analysed for sRNA expression by Northern Blot (A) and the expression of the target gene NGFG_1721 and of the alanine racemase by qRT PCR (B). Northern Blot quantifications are shown on the right (qRT PCR and Northern Blot: n=6 Hepes, n=3 for the other media). (C) Transcript levels of alanine racemase were analysed in strains MS11 WT, ΔΔ162/3 and ΔΔc by qRT PCR (n=5).

Downregulation of sRNA expression is most pronounced in Hepes medium, raising questions about the cause for this observation. If the observed effect were sRNA dependent, also expression levels of the other sRNA target genes should be affected. Therefore, the transcript amounts of three further negatively regulated target genes, NGFG_1722, *ack* and *prpC*, and the positively target gene NGFG_0045 were compared in Hepes medium and PPM+ by qRT PCR (figure 3.28A). NGFG_1722, *ack* and *prpC* are all as expected upregulated in Hepes medium, whereas mRNA levels of the positively regulated target NGFG_0045 decrease.
It could be shown that the alanine racemase gene is not regulated by the sibling sRNAs, but still its mRNA levels significantly increase upon shift to Hepes medium. In order to ensure target gene regulation is due to the decrease of sRNA levels, expression of NGFG_1721 was compared in both media in a sRNA KO background (figure 3.28B). NGFG_1721 mRNA levels only increase upon shift to Hepes medium in WT strain background, but not in the absence of the sibling sRNAs, confirming a sRNA-dependent upregulation of NGFG_1721 expression in Hepes medium. Levels of alanine racemase mRNA are upregulated in Hepes medium even in the absence of NgncR_162 and NgncR_163, suggesting an sRNA-independent regulatory mechanism.

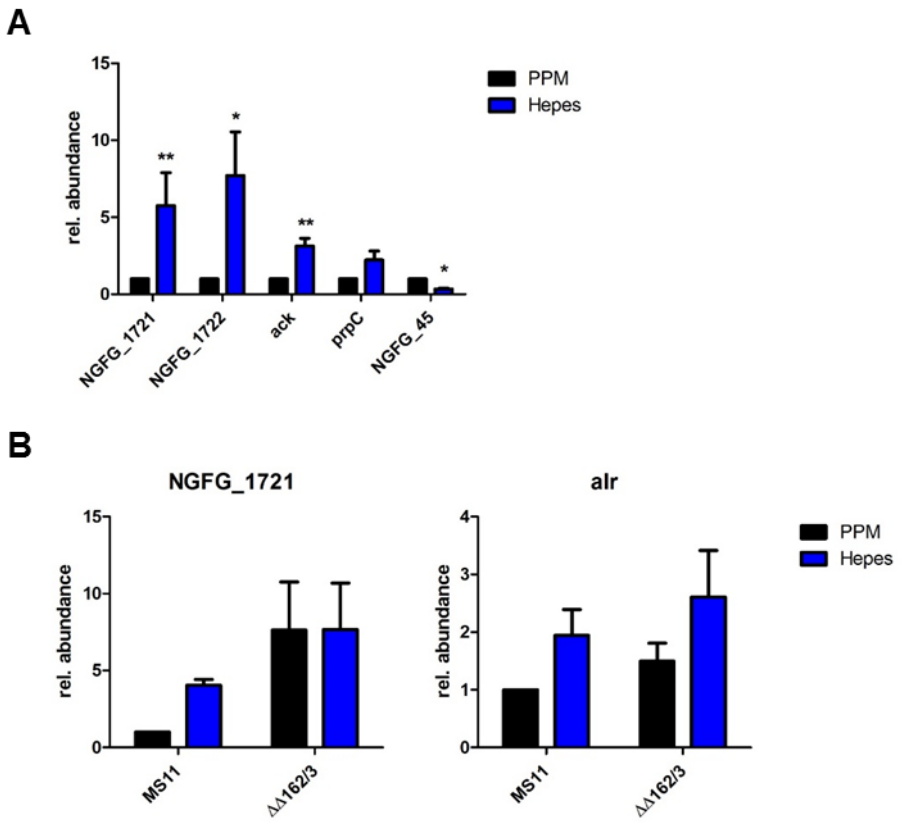

Figure 3.28: sRNA-dependent regulation in Hepes medium. (A) Comparison of the expression of several target genes between PPM+ and Hepes medium by qRT PCR. (B) Expression of NGFG_1721 and alanine racemase was analysed in the double KO in comparison to MS11 WT in PPM and Hepes medium (n=5).

To test whether downregulation of the sibling sRNAs is due to transcriptional regulation, the gonococcal mutants carrying the sRNA promoter-*gfp* fusions introduced in chapter 3.2.3 were analysed. Strains P_{162}gfp, P_{163}1gfp and P_{163}2gfp were incubated in main culture either in PPM+ or shifted to Hepes medium and *gfp* expression in mid-logarithmic phase cultures analysed by qRT PCR. For all three strains the amount of *gfp* transcripts was clearly reduced in Hepes medium (figure 3.29A). Promoter activity in Hepes medium is approximately half than in PPM+ what corresponds to the ratio of sRNA downregulation. Nevertheless, the complemented strains carrying the sRNA genes under control of the truncated promoters (ΔΔcs) were tested as control. Due to the truncated promoter region, binding of a transcriptional regulator to the upstream region is not expected. However, the data show a clear downregulation of sRNA expression for both complementated strains in Hepes medium (figure 3.29B). The ratio is similar to the WT strain and so rather indicates a promoter-independent regulation. Therefore, sRNA expression was analysed in PPM+ and Hepes medium in strains AIE, since they are ΔΔ162/3 strains complemented with one of the sRNA under control of an anhydrotetracycline-inducible and so foreign promoter. Gonococci were grown in the presence of AHT for 1 h and then shifted to the different media. After 2 h in the respective medium without AHT, samples were taken and analysed for sRNA expression by Northern Blot (figure 3.29C). Even under control of a different promoter the downregulation of the sRNAs in Hepes medium is comparable to the one observed under WT conditions. In addition, the expression of the target gene NGFG_1721 is significantly increased in an AIE strain background in Hepes medium compared to PPM+ and the regulatory effect is comparable to that caused by both NgncR_162 and NgncR_163 with their native promoter (figure 3.29D). All this data indicates that the decreased amount of NgncR_162 and NgncR_163 in Hepes medium is due to a lower sRNA stability, wheras the initial data in figure 3.29A suggests a lower promoter activity. Therefore, decreased sRNA levels in Hepes medium might be explained by a combined effect of transcriptional regulation and reduced sRNA stability.

Transcriptional regulation could result in a reduced promoter activity of NgncR_162 and NgncR_163. The sRNAs and the alanine racemase are both encoded next to the transcriptional regulator NGFG_2170. It belongs to the AsnC family of transcriptional regulators that usually do not act in a global manner and consequently could target genes in proximity. It did not have any impact on sRNA expression when tested in PPM medium (see figure 3.21). However, this family of transcription factors requires the binding of a specific small molecule for activity, which might not be abundant in PPM+. Since both the sRNAs and alanine racemase are subject to regulation in Hepes medium, the influence of NGFG_2170 on sRNA and mRNA expression was tested in the new medium by Northern Blot and qRT PCR (figure 3.30A and B). However, the sRNAs are still downregulated to the same extent in absence of the transcriptional regulator. Both alanine racemase and the target gene NGFG_1721 have higher transcript levels in Hepes medium compared to PPM in a NGFG_2170 KO background as it is the case in WT gonococci. Thus, the change in RNA levels of both sRNAs, NGFG_1721

and alanine racemase mRNA in Hepes medium is not depending on the transcriptional regulator NGFG_2170.

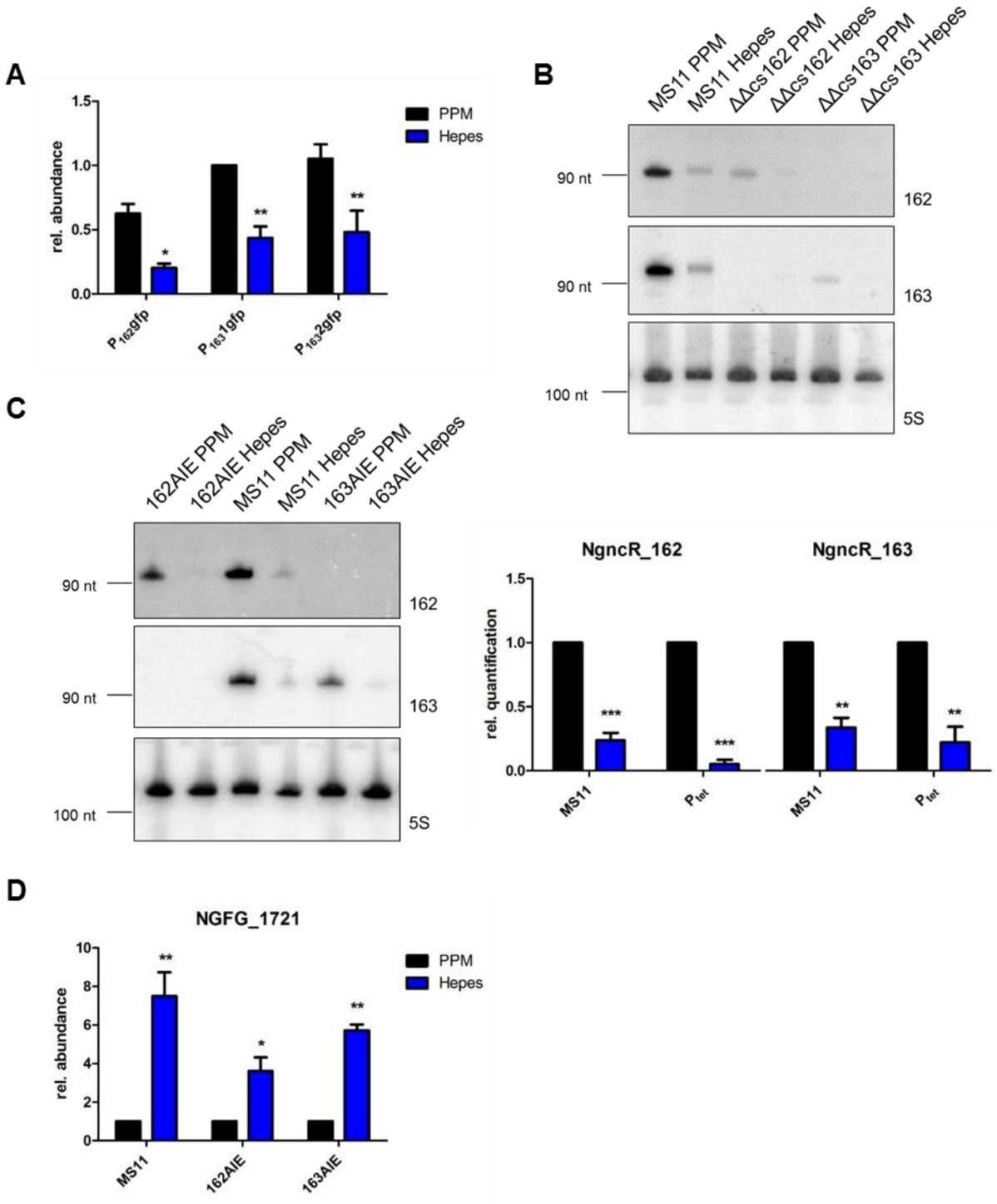

Figure 3.29: Influence of the sRNA promoter on Hepes-dependent downregulation. (A) Reporter gene expression was analysed for sRNA promoter fusions in PPM and Hepes medium by qRT PCR. The effect of Hepes-medium on different sRNA complementation strains was analysed by Northern Blot. First, strains in which the sRNAs carry only a truncated promoter comprising only the -10 box and the -35 region (B) and further in which the promoter region is exchanged by the AHT-inducible promoter (C). The diagrams on the right (C) show the quantification of three Northern Blots. The graph in (D) compares the expression of the target NGFG_1721 in PPM+ and Hepes medium in MS11 WT and the strains in which the sRNAs are fused to the AHT-inducible promoter.

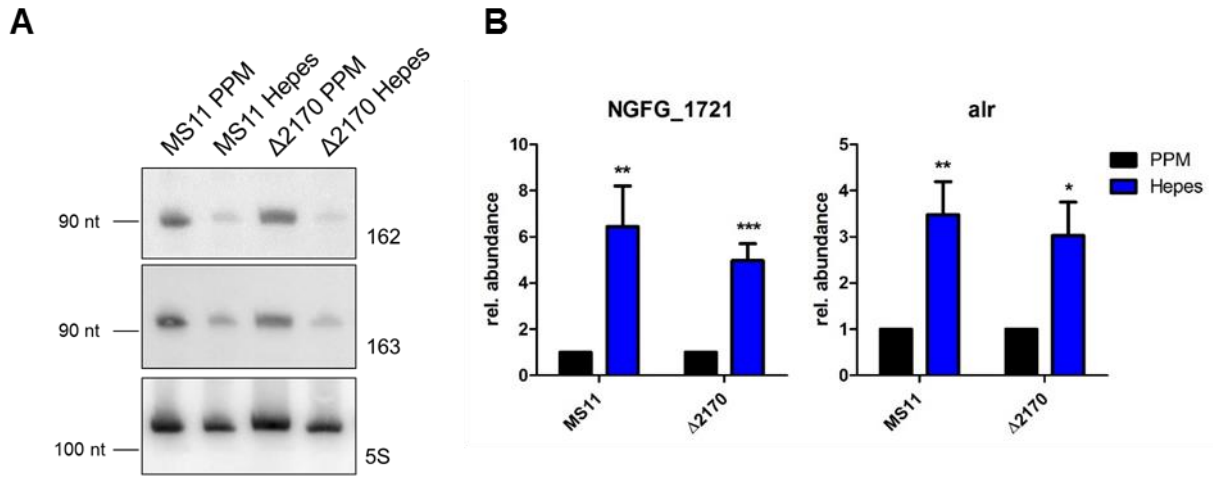

Figure 3.30: Influence of NGFG_2170 on RNA expression in Hepes medium. In order to assess whether the difference in expression levels in Hepes medium compared to PPM+ is mediated by NGFG_2170, expression of the sRNAs (A) and expression of NGFG_1721 and alanine racemase (n=3) (B) was analysed in strain Δ2170.

A lower abundance of NgncR_162 and NgncR_163 in Hepes medium could be the result of lower sRNA stability. Thus, the half-life of the sibling RNAs was determined in Hepes medium with a rifampicin assay (figure 3.31). Stability of NgncR_162 and NgncR_163 is clearly reduced in Hepes medium compared to PPM+; nevertheless, the half-lives are still identical for both sRNAs. Half-lifes declined from almost 60 min in PPM+ to >10 min in Hepes medium, meaning a significant decrease in sRNA stability.

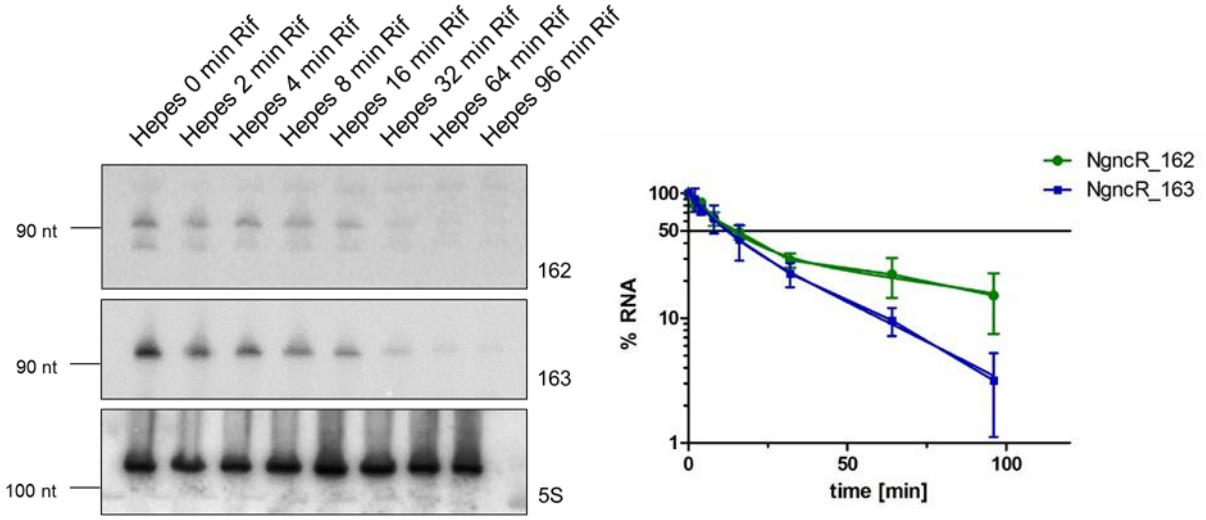

Figure 3.31: Determination of sRNA half-life in Hepes medium. The half-life of NgncR_162 and NgncR_163 was determined by Rifampicin assay and subsequent Northern Blot quantification. Fifty percent of NgncR_162 was degraded after 14 min, of NgncR_163 after 12 min.

In stationary growth phase, the data revealed a decreased expression of the RNA chaperone Hfq, which is known to stabilize the sibling RNAs. The reduced amount of Hfq protein during stationary phase could explain the decreased sRNA levels in this growth phase. Gonococci hardly grow in Hepes medium and so regulatory mechanisms acting during stationary growth might act during growth in Hepes medium as well. Transcript levels of *hfq* were analysed in PPM+ and Hepes medium by Northern Blot (figure 3.32A). However, expression of *hfq* does not change upon media change. Analysing Hfq protein expression by comparing the Flag-tagged version of Hfq between Hepes medium and PPM+ also did not reveal any differences (figure 3.32B). The chaperone is hence not responsible for reduced sRNA stability in Hepes medium. Nevertheless, in stationary phase not only *hfq* expression was affected, but also several enzymes involved in the degradation of mRNAs and sRNAs. These enzymes include the endonucleases RNase III and RNase E, the exonucleases RNase II and PNPase and Poly-A polymerase I. Transcript levels of the five enzymes were analysed in PPM+ and Hepes medium by qRT PCR (figure 3.32C). Interestingly, also in Hepes medium the expression of all tested enzymes is upregulated. The effect is not as pronounced as in stationary phase, but still significant. Like in stationary phase, the strongest regulated enzymes are RNase II and RNase III.

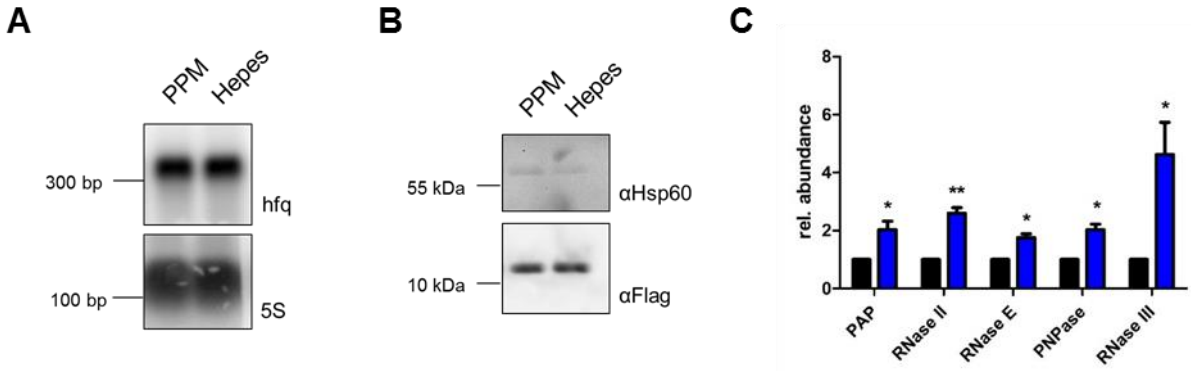

Figure 3.32: Abundance of Hfq and enzymes involved in RNA degradation in Hepes medium. The abundance of the RNA chaperone Hfq was analysed in Hepes medium and PPM+ on transcript level by Northern Blot (C) and on protein level by Western Blot with the help of a Flag-tagged Hfq (D). The expression level of enzymes involved in RNA degradation (E) and transcriptional regulation (F) was determined by qRT PCR (n=3).

It is striking that the degree of sRNAs downregulation reflects the growth rate in the respective medium (figure 3.33A). The downregulation is strongest in Hepes medium and RPMI and these are the media with the lowest growth rate. Growth in CDM-10 is only slightly slower than in PPM+ and here also the downregulation of sRNA expression is not very pronounced. Since the sRNA expression is also downregulated in stationary phase, the observed regulatory effects might be due to a reduced growth rate. Thus, gonococcal growth was inhibited with tetracycline (figure 3.33B). Two different concentrations of tetracycline were chosen: By adding 0.31 µg/ml tetracycline the growth is already clearly impaired, whereas with 0.62 µg/ml tetracycline bacteria grow very poorly and so better mimicks growth rate in Hepes medium.

Samples were taken after 3 h growth and analysed for expression of NGFG_1721 and alanine racemase by qRT PCR. However, no differences between the samples could be observed, the growth defect caused by tetracycline did not affect gene expression of NGFG_1721 and alanine racemase. Therefore, it might not be the growth rate per se, which is causing the observed downregulation of sRNA expression.

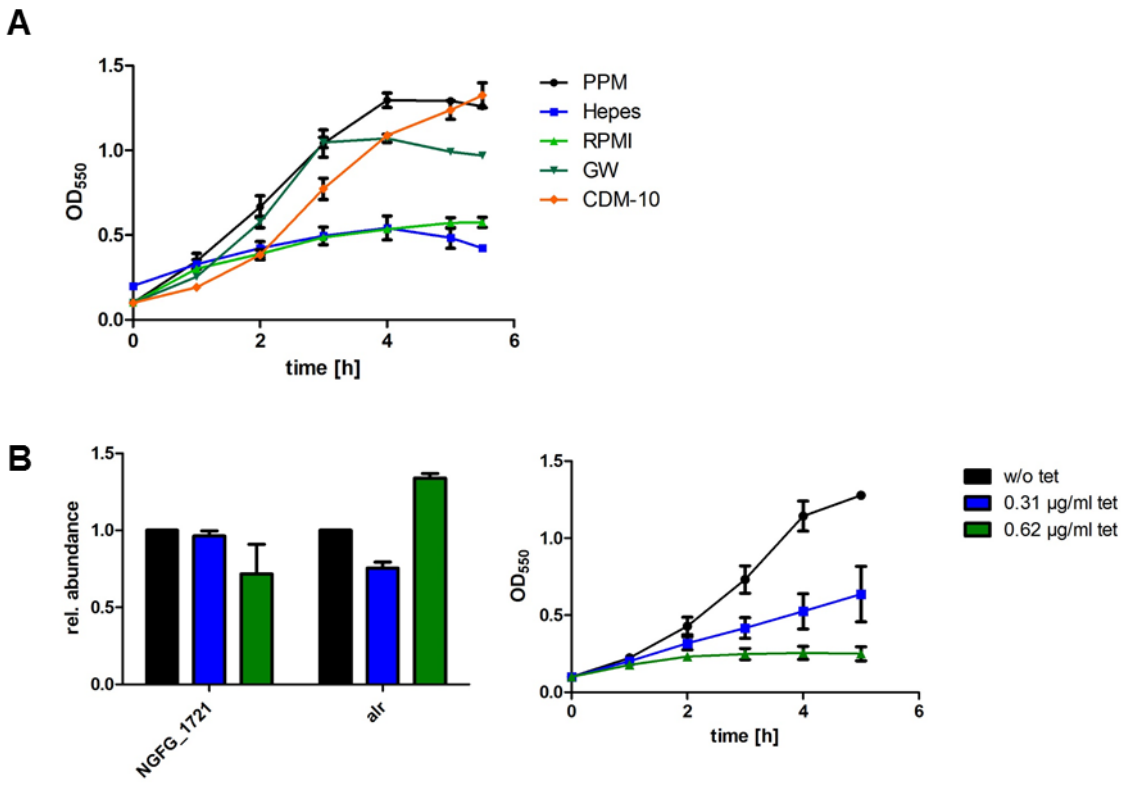

Figure 3.33: Impact of the growth rate on expression of NGFG_1721 and alr. (A) The growth curve shows the different growth rates of strain MS11 in the various media (n=3). (B) Growth of strain MS11 is impaired by the addition of 0.31 µg/ml and 0.62 µg/ml tetracycline and the effects on mRNA expression of NGFG_1721 and alanine racemase were analysed by qRT PCR (n=3).

3.2.5.2 Influence of the carbon source

Many of the target genes identified for NgncR_162 and NgncR_163 play a role in basic metabolic pathways, like the methylcitrate and the citrate cycle or amino acid uptake and metabolism. The sRNAs could help adapting the activity of bacterial metabolism to a change of the availability of specific nutrients. It is of interest to see whether the loss or gain of specific medium components influences sRNA expression and so elucidate their potential role in metabolism. The use of a chemically defined medium allows selecting specific components for that purpose. In CDM-10, gonococcal growth is only slightly reduced compared to rich medium and the sibling RNAs are abundantly expressed. Therefore, the medium was selected for the following experiments.

The list of validated target genes encompasses several genes encoding enzymes involved in carbon metabolism, especially in the citric acid cycle like *gltA* (citrate synthase) and *sdhC* (succinate dehydrogenase complex). It was reported that *N. gonorrhoeae* uses besides glucose only lactate and pyruvate as sole carbon and energy source (Morse and Bartenstein 1974). The available carbon source influences gene expression and the choice of metabolic pathways in *N. gonorrhoeae*. Glucose is largely catabolised by a combination of the Entner-Doudoroff and pentose phosphate pathways, resulting in accumulation of acetate in the medium. Levels of citric acid cycle enzymes are markedly reduced in the presence of glucose (Morse and Hebeler 1978).

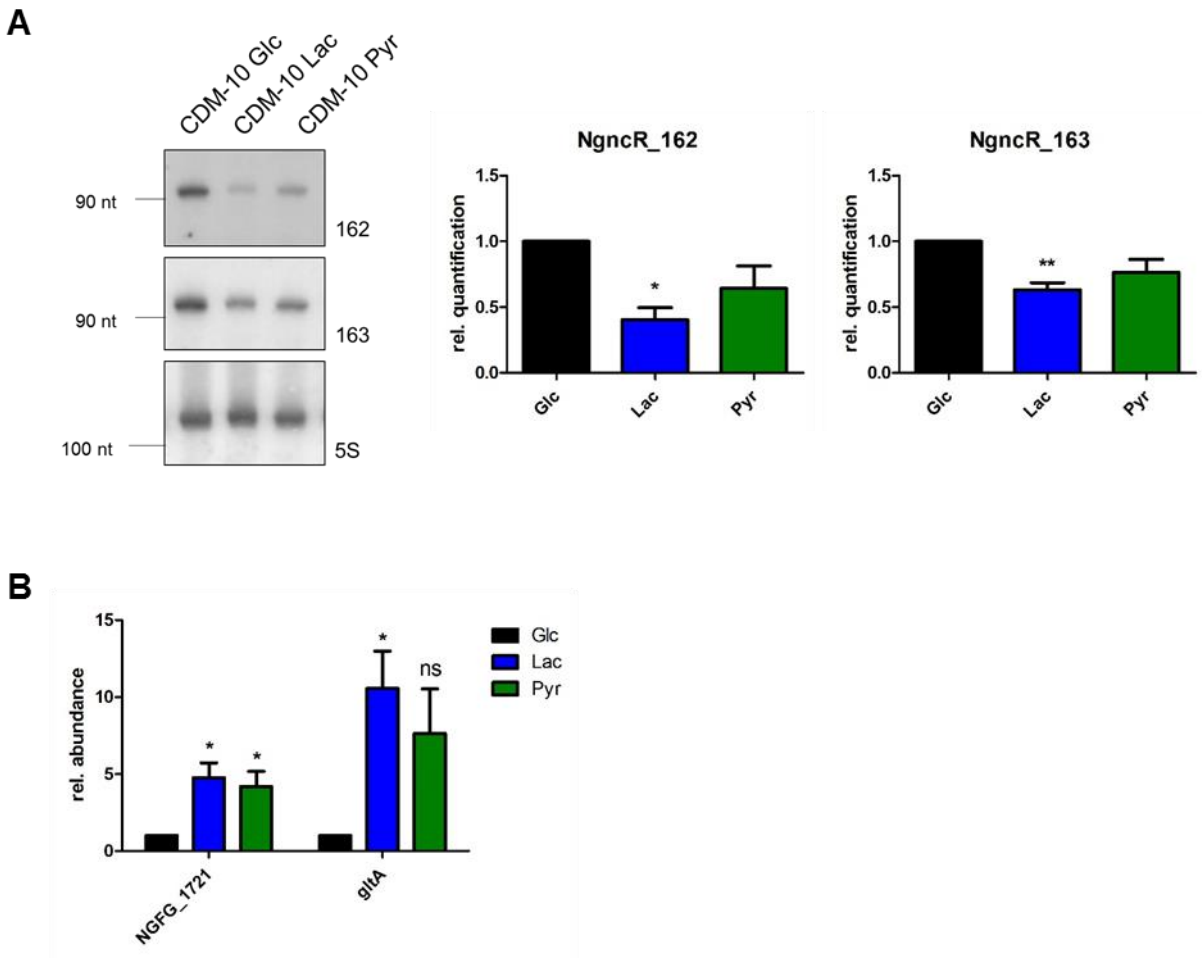

Figure 3.34: Influence of carbon source on sRNA expression. (A) Neisseria were grown in CDM-10 exclusively containing one of the carbon sources glucose, lactate or pyruvate. Expression of NgncR_162 and NgncR_163 was compared by Northern Blot. The quantification of four Northern Blots is shown on the right for both sRNAs. (B) Comparison of target gene expression (NGFG_1721 and *gltA*) by qRT PCR in media containing glucose, lactate or pyruvate (n=3).

In order to test the impact of the available carbon source on the sRNAs, the chemically defined medium CDM-10 was modified. CDM-10 contains 5 g/l glucose as carbon source (CDM-10 Glc), which was replaced in alternative media by lactate (CDM-10 Lac) or pyruvate (CDM-10 Pyr). The pre-culture was grown on glucose and it was divided into three cultures containing either glucose, lactate or pyruvate and incubated until mid-log phase before taking samples. Samples were analysed for sRNA expression by Northern Blot. The results show that both sRNAs are significantly downregulated when growing on lactate compared to growth on glucose (figure 3.34A). In the presence of pyruvate only a minor and not significant effect on sRNA expression was detected, especially in the case of NgncR_162. The downregulation of the sRNAs should lead to an upregulation of their target genes. Expression levels of NGFG_1721 and *gltA* were analysed in the different media by qRT PCR. Both tested genes are upregulated in the absence of glucose confirming the previous results (figure 3.34B). NGFG_1721 is stronger regulated by the sRNAs than *gltA*, nevertheless *gltA* mRNA levels are more affected by the presence of glucose in the medium, suggesting additional regulatory mechanisms acting on *gltA*.

The observed downregulation of NgncR_162 and NgncR_163 in medium containing only lactate as energy source could be promoter-dependent or an effect of decreased sRNA stability. To address the question the strains carrying the sRNA promoter-reporter gene fusions were grown in media with glucose, lactate or pyruvate and the amount of GFP was determined by Western Blot (figure 3.35A). For both sRNA promoters, GFP levels did not change in the different media. Also on transcript level, *gfp* expression was not significantly altered between glucose, lactate and pyruvate containing media (figure 3.35B). This data suggests that the decrease of sRNA levels during growth on lactate is promoter-independent. In order to validate this observation, expression of NgncR_162 and NgncR_163 was analysed in the different media with strains, in which the respective sRNA is under control of the *opa* promoter (figure 3.35C). The sequence of the *opa* promoter was fused directly to the transcriptional start site of NgncR_162 (P_{opa}162) or NgncR_163 (P_{opa}163) and the resulting sequence integrated in the *iga-trpB* locus in the sRNA double KO strain. Comparably to the WT, also these strains show a downregulation of sRNA expression during growth on lactate. This confirms that the decrease of sibling aRNA levels in media with lactate as carbon source is promoter-independent.

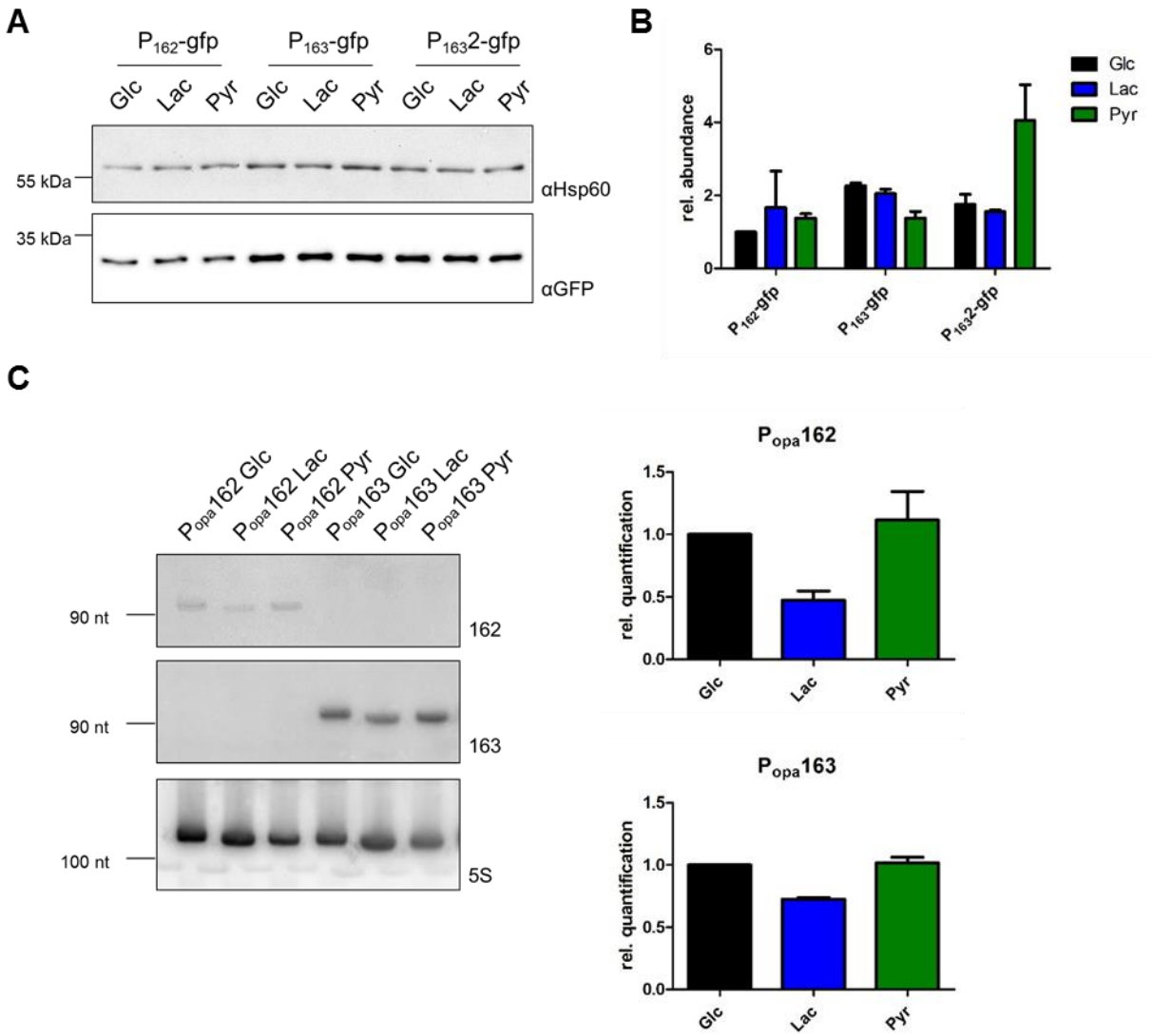

Figure 3.35: Promoter-independent downregulation of sRNA expression in the presence of lactate. The reporter gene *gfp* is under control of the respective sRNA promoter region and its expression is analysed in chemically defined media containing glucose, lactate or pyruvate as carbon source. Expression of *gfp* is analysed on protein level by Western Blot (A) and on transcript level by qRT PCR (n=2) (B). (C) The respective promoter region of the sRNA was exchanged by the *opa* promoter (P_{opa}) and sRNA expression monitored in glucose, lactate or pyruvate containing media. The diagrams show the quantification of two Northern Blots.

Since the expression of NgncR_162 and NgncR_163 is changing depending on the available carbon source, they could also influence growth and survival of gonococci in the respective medium. Growth of WT *Neisseria* is not impaired by a change of the carbon source (figure 3.36). However, in the sRNA double KO strain, growth differs in the three media. In all conditions, this strain did not reach the same maximal OD than the WT and entered earlier into stationary growth phase. Interestingly, this effect was much stronger when growing on glucose compared to growth on lactate or pyruvate as carbon source. However, the complementated strain did not completely recover the growth phenotype. Nevertheless, the differences between the different carbon sources were much smaller than in the ΔΔ162/3 strain, so it cannot be excluded that the sibling RNAs play a role in the efficient usage of glucose as energy source.

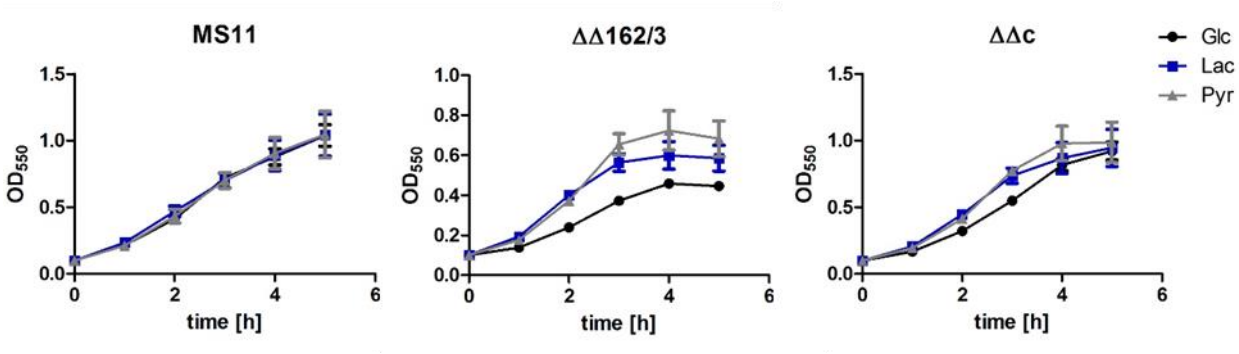

Figure 3.36: Influence of sRNAs on growth on different carbon sources. The pre-cultures of strains MS11 WT, double KO ΔΔ162/3 and complementation strain ΔΔc were divided into three different main-cultures containing either glucose, lactate or pyruvate as carbon source and growth was monitored over 5 h by measuring the OD_{550}. The graphs summarize the growth curves of three experiments.

3.2.5.3 Role of propionic acid

Three other validated target genes of NgncR_162 and NgncR_163, namely *prpB*, *prpC* and *ack*, encode enzymes of another metabolic pathway, the methylcitrate cycle. Hereby propionic acid is catabolized and finally converted into pyruvate and succinate. In order to elucidate a potential link between propionate catabolism and the sibling RNAs, the influence of propionic acid in the medium was tested on growth and sRNA and target gene expression. 5 mM propionate were added to the main culture and transcript levels of the target genes NGFG_1721 and *prpC*, which is involved in propionate catabolism, compared in presence and absence of propionate by qRT PCR. Expression of NGFG_1721 and *prpC* was not altered by the presence of 5 mM propionate in the medium (figure 3.37A). The samples were also analysed for sRNA expression by Northern Blot. The detected amount of both NgncR_162 and NgncR_163 remained unchanged (figure 3.37B). Consequently, the presence of propionate does not influence the expression of the sibling sRNAs. On the other hand, when comparing the growth between MS11 WT and the double KO strain, it seems that propionic acid stronger impairs growth of the KO strain than of the WT (figure 3.37C). Propionic acid had a negative effect on growth of all tested strains, but the impact on strain ΔΔ162/3 was higher. However, the difference is not significant.

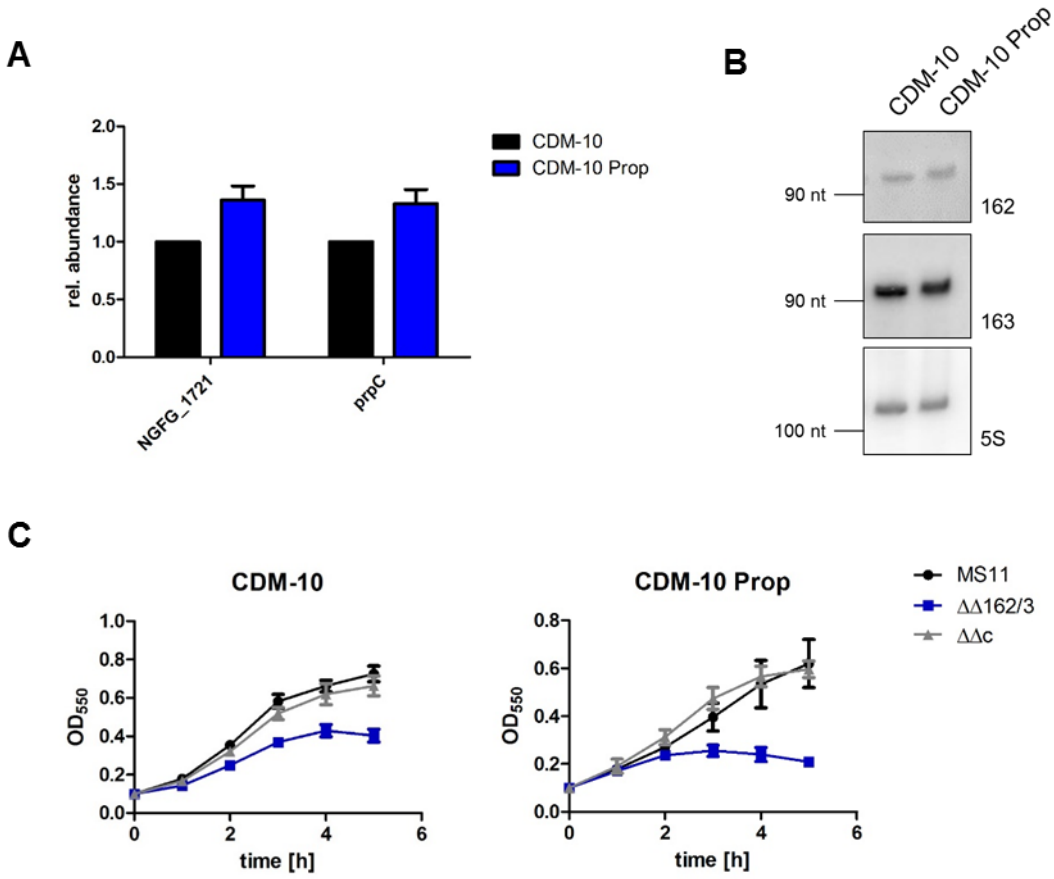

Figure 3.37: Impact of propionic acid on the expression of NgncR_162 and NgncR_163. Gonococci were grown either in normal CDM-10 medium or in CDM-10 supplemented with 5 mM propionic acid. Differences in target gene expression (n=3) (A) and sRNA expression (B) were analysed. Further, the growth of strains MS11 WT, double KO ΔΔ162/3 and complementation strain ΔΔc was monitored over 5 h by measuring the OD_{550} in both media (n=3) (C).

3.2.5.4 Role of alanine

NgncR_162 and NgncR_163 regulate also several genes involved in amino acid metabolism. The target genes showing the highest degree of regulation by the sibling sRNAs are NGFG_1721 and NGFG_1722, a sodium alanine symporter and a D-amino acid dehydrogenase, which is most likely catalysing the reaction between D-alanine and pyruvate (figure 3.38). The genomic organization of the sRNAs is quite conserved between different *Neisseria* (figure 3.7). Strikingly, they are located in several species in proximity of an Lrp/AsnC family transcriptional regulator and an alanine racemase. Lrp/AsnC family transcriptional regulators are proteins known to regulate the “feast/famine” amino acid metabolism and need to bind a specific amino acid for full function. NGFG_2170 belongs to the AsnC-type regulators, which are rather specific regulators compared to the Lrp-type, which act globally (reviewed in Deng et al. 2011). Although a connection between NGFG_2170 and the sibling sRNAs or the alanine racemase was not proven yet, it needs to be considered that the activator of the

transcriptional regulator is still unknown and might not have been present in sufficient amount under the applied experimental conditions. D-alanine is mostly used by *N. gonorrhoeae* in peptidoglycan and the pathogen is known for its unusual low recycling efficiency of peptidoglycan fragments, which are transported back to the cytoplasm and broken down (Chan and Dillard 2016). Here, the released D-alanine can be recycled into peptidoglycan, or further metabolized requiring enzymes like alanine racemase or D-alanine dehydrogenase.

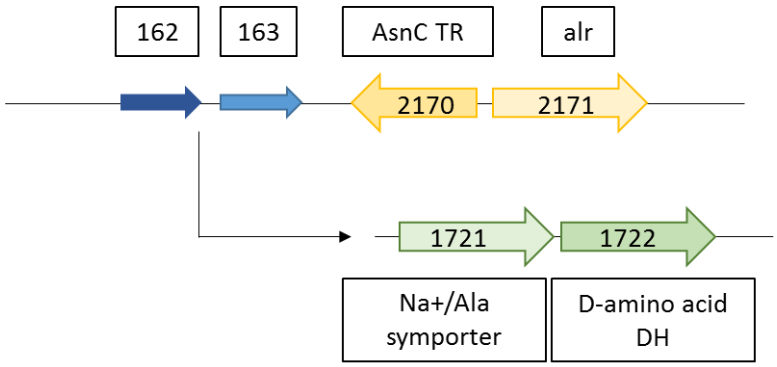

Figure 3.38: Schematic view of the connection between NgncR_162/NgncR_163 and alanine-associated genes. The sRNAs are encoded downstream of an AsnC-type transcriptional regulator and the alanine racemase and they regulate the expression of an alanine transporter and a D-amino acid dehydrogenase

The availability of alanine might hence influence the growth of gonococci. Therefore, growth of MS11 WT, the double KO and the complementation strain was monitored in media with different amounts of D- and L-alanine (figure 3.39). The absence of alanine did not influence the growth of any of the analysed strains compared to standard CDM-10. However, increasing the concentration of L-alanine led to a better growth of all strains, but to a smaller extent for the sRNA KO. The fold change of MS11 versus ΔΔ162/3 after 5 h in CDM-10 is 1.8, whereas it is 2.2 in CDM-10 with a higher concentration of L-alanine. The exchange of L-alanine to D-alanine resulted in a decreased growth rate of the sRNA KO strain, but also for the complementation strain. All analysed strains reached a much lower OD in a medium with a high D-alanine concentration. This effect is even stronger for the sRNA KO strain, which reached a 2.6 fold lower OD compared to the WT, which is significantly less than in standard CDM-10 medium (p-value 0.025). Thus, a high amount of D-alanine seems to be rather harmful to gonococci, especially in the absence of NgncR_162 and NgncR_163, in contrast to the beneficial effect of an increased amount of L-alanine.

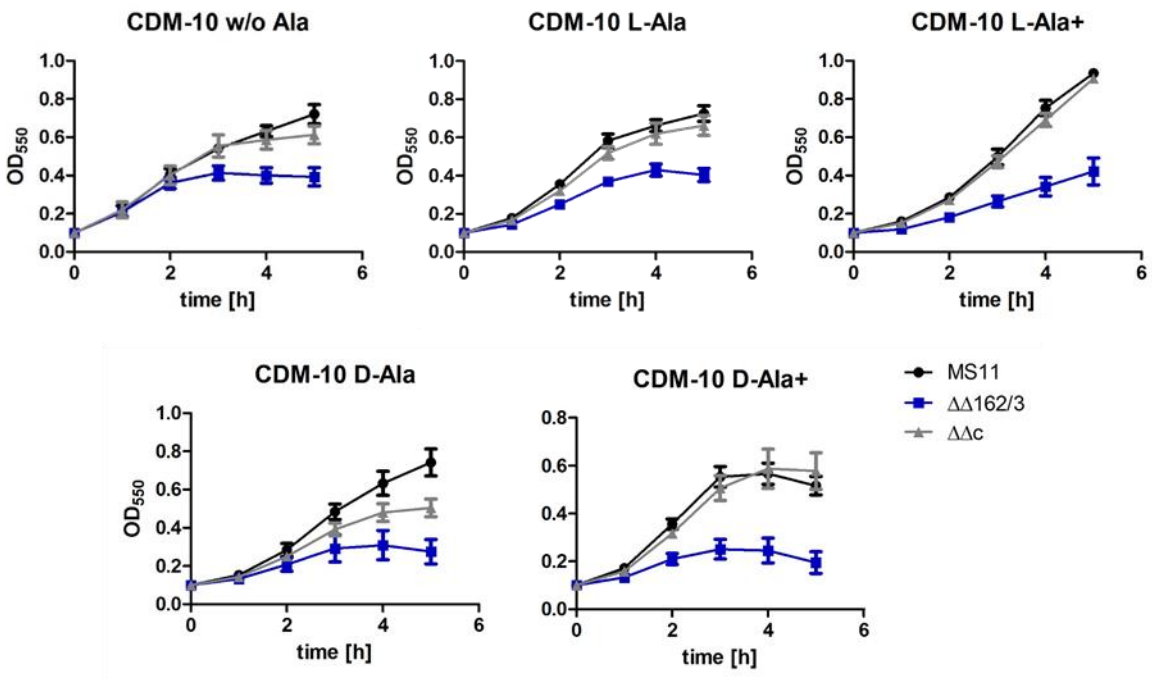

Figure 3.39: Growth in media containing different D- and L-alanine concentrations. Growth of strains MS11 WT, double KO ΔΔ162/3 and complementation strain ΔΔc was monitored over 5 h by measuring the OD_{550}. Gonococci were grown in modified CDM-10 media without alanine, with normal or with increased alanine concentration. The graphs summarize the growth curves of three experiments.

The abundance of L-alanine or D-alanine could influence expression of NgncR_162 and NgncR_163, therefore several media containing different concentrations of L-alanine or D-alanine were tested for changes in sRNA or target gene expression. To analyse activity of D-alanine dehydrogenase in other bacteria, significantly higher D-alanine concentrations were used than the normal alanine concentration in CDM-10 (He et al. 2011). Hence, a medium was included in the study in which the D-alanine amount was five-fold increased to a final concentration of 0.5 g/l (D-Ala+). sRNA expression was compared in media containing no alanine, L-alanine, D-alanine or increased amount of D-alanine. However, the data did not reveal any effect of the alanine availability in the medium on sRNA expression (figure 3.40A). The influence of the different media on mRNA levels of the target gene NGFG_1721 and alanine racemase was next analysed by qRT PCR (figure 3.40B). Whereas alanine racemase might be downregulated in the absence of alanine, there is no effect on the expression of NGFG_1721.

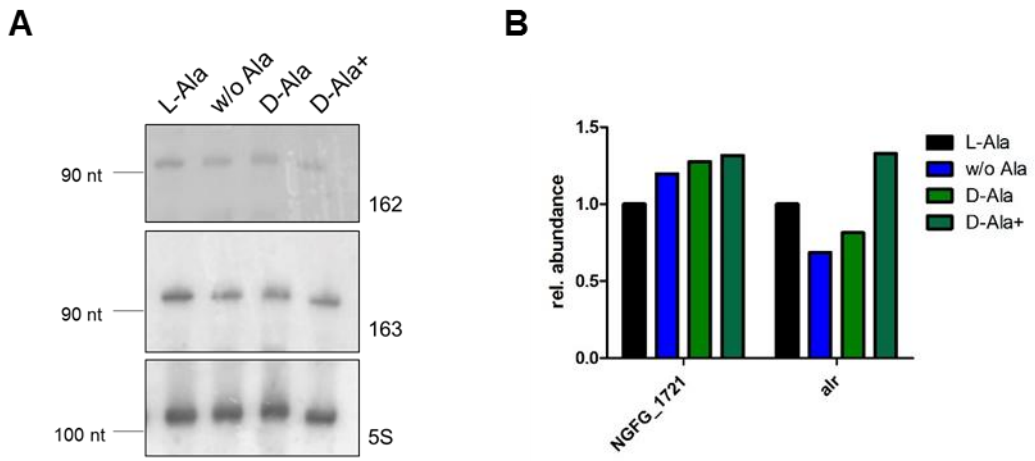

Figure 3.40: Impact of alanine on sRNA expression. (A) Comparison of sRNA expression in media containing different amounts of L-alanine or D-alanine by Northern Blot (n=2). (B) Comparison of the expression of the target gene NGFG_1721 and the alanine racemase NGFG_2171 in media containing different amounts of L-alanine or D-alanine by qRT PCR (n=1).

Nevertheless, the fact that an alanine-transporter and an enzyme for conversion of D-alanine are the strongest regulated target genes of the sibling RNAs, still suggests that NgncR_162 and NgncR_163 are associated with alanine metabolism. Hence, *N. gonorrhoeae* cultures were fed with $^{13}C_3$-D-alanine and the samples were analysed for ^{13}C enrichments and isotopologue patterns by Thomas Steiner at the chair of biochemistry, TUM. The ^{13}C excess was determined in two fractions, the soluble components in the cytosol (polar metabolites) and the utilized amino acids, which are mostly derived from proteins, but could also be derived from the peptidoglycan layer in the cell wall. Most of the alanine found in the cytosol is labelled, showing efficient uptake of the $^{13}C_3$-D-alanine from the medium. Despite the strong upregulation of the alanine transporter NGFG_1721 in the absence of the sRNAs, there is no difference in alanine uptake between MS11 WT and the double KO strain (figure 3.41A). The analysis of metabolites shows that the D-alanine taken up by the *Neisseria* was not further metabolized. D-alanine can be converted into pyruvate and consequently used for fermentation, the citric acid cycle or fatty acid synthesis. However, none of the products of these metabolic pathways was noteworthy labelled with ^{13}C. The isotopologue profile (IP) on the right gives further information on the metabolization of alanine. M stands for the molar mass of alanine, which is higher depending on the number of heavy carbon atoms. In the experiment, gonococci were fed with $^{13}C_3$-D-alanine and most of the alanine found in the cytosol is still labelled on all three carbon atoms. Only a small part is labelled on only two carbon atoms, showing that alanine was processed to a C_2 molecule. Since D-alanine is metabolised via pyruvate, this molecule is most likely acetyl-CoA. Nevertheless, there was no ^{13}C detected in citric acid cycle products or fatty acids, so acetyl-CoA seems not to be further metabolised. Furthermore, we could not detect significant amounts of ^{13}C in other proteinogenic amino acids, showing no conversion of alanine (figure 3.41B). This is also confirmed by the isotopologue profile. Comparable to the polar metabolites, also here most of

the detected alanine is having three heavy carbon atoms and was therefore not converted before into different molecules. For the measurements of the proteinogenic amino acids, the samples were lysed and peptide bonds broken to isolate only utilized amino acids. Interestingly, here is a clear difference in labelled alanine between WT and sRNA KO strain. The data show that in absence of NgncR_162 and NgncR_163 more alanine is used than in

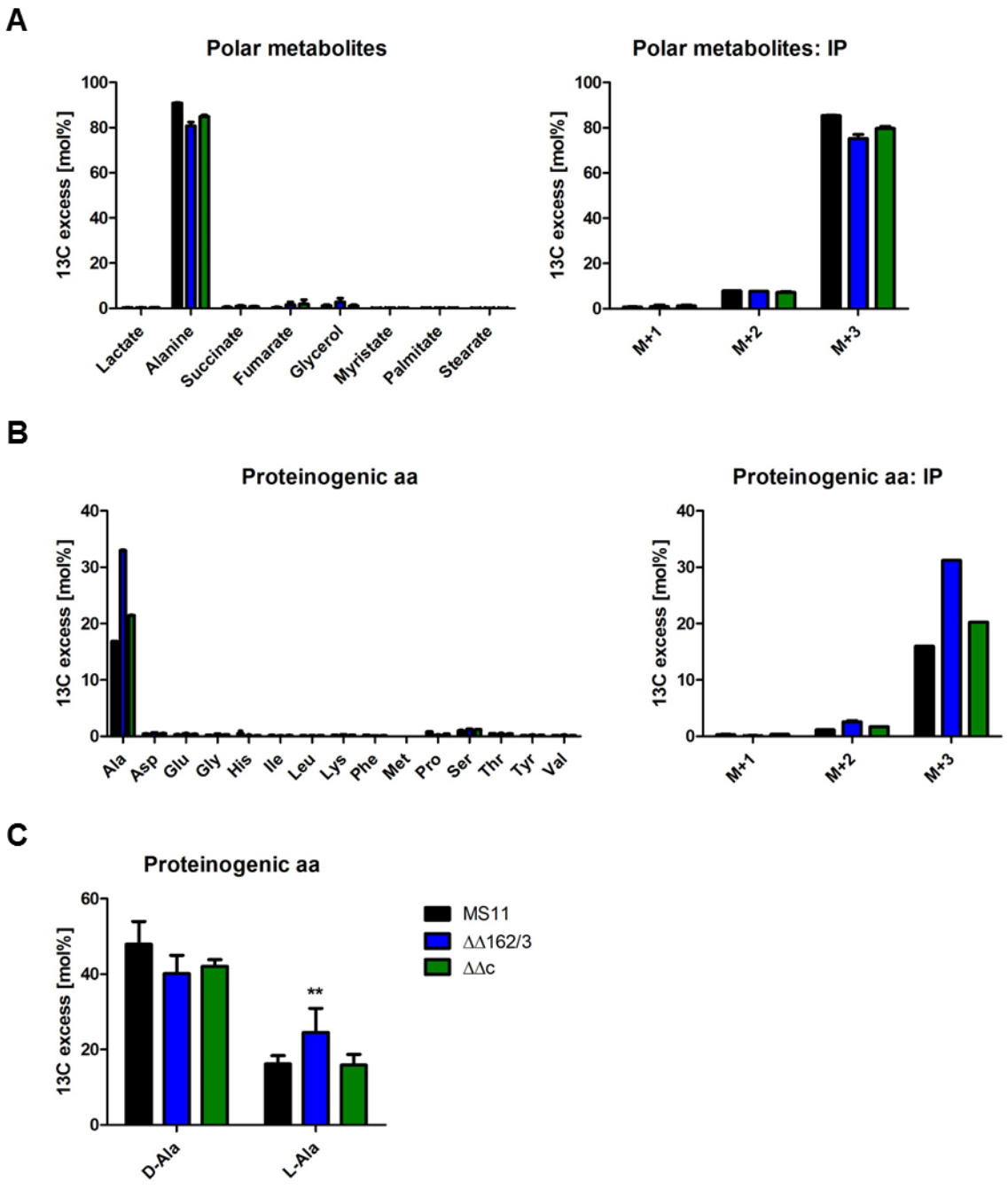

Figure 3.41: Assessing the influence of the sRNAs on alanine metabolism by isotopologue profiling. MS11 WT, the double KO and complementation strain were fed with ^{13}C-labelled D-alanine in CDM-10 medium without further alanine. The bacterial pellets were analysed for ^{13}C incorporation in protein-derived amino acids (B+C) and metabolites present in the cytosol (A). For experiments A and B, the isotopologue profile (IP) shows the distribution of heavy C-atoms, whereby M+1, 2 or 3 corresponds to one, two or three heavy carbon atoms, respectively. Alanine was derivatized in order to differentiate between D-alanine and L-alanine (C).

the WT and complementation strain. The measurement here cannot distinguish between D-alanine and L-alanine; consequently, it is not possible to draw conclusions about the usage of the alanine. Whereas L-alanine is used for protein biosynthesis, D-alanine is incorporated in the cell wall, which usually contains D-alanyl-D-alanine dipeptides. Therefore, the alanine was derivatized in a following experiment (figure 3.41C). The data show that most of the taken up D-alanine was directly incorporated in the peptidoglycan layer and only a smaller part was converted into L-alanine and so used in proteins. The levels of labelled D-alanine between WT and sRNA KO strain are similar, so there were no differences in integration of D-alanine into the cell wall. However, in the mutant strain clearly elevated levels of ^{13}C labelled L-alanine can be observed. A reason for this should be a higher alanine racemase activity in the absence of the sRNAs. The analysis of the alanine metabolome shows that *N. gonorrhoeae* hardly metabolises alanine and the sRNAs have also no impact on alanine uptake, but rather on the conversion of D-alanine to L-alanine. Previous data shows that at least transcript levels of alanine racemase are not affected by NgncR_162 and NgncR_163, raising the question on how D-alanine conversion is altered by the sibling RNAs.

3.2.5.5 Role of histidine

In section 3.2.2.1, two genes involved in the biosynthesis of histidine were tested as potential targets for NgncR_162 and NgncR_163, suggesting a role of the sRNAs in histidine metabolism. The influence of the sRNAs on target gene expression was rather small, however significant, so the absence of histidine and the thereafter need for biosynthesis of the amino acid might also influence expression of the sRNAs. Therefore, mRNA levels of two target genes, NGFG_1721 as strongest regulated target and *hisH* as target involved in histidine biosynthesis, were compared in the chemically defined medium CDM-10 with and without histidine (figure 3.42). However, none of the analysed genes changed its expression significantly upon media change, even *hisH* expression is not increased in the absence of histidine. Although it could be possible that longer periods of histidine starvation are necessary, the data do not suggest that sRNA abundance is influenced by the absence of histidine.

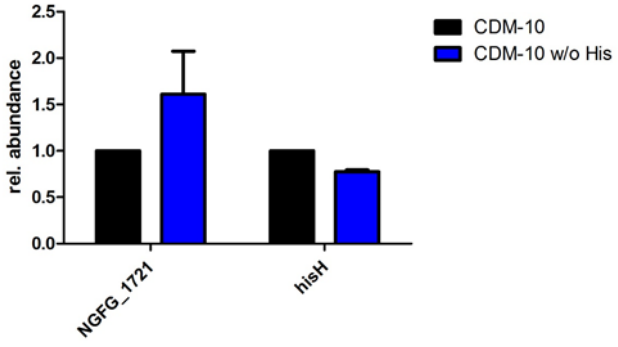

Figure 3.42: Influence of histidine on target gene expression. The expression of the target genes NGFG_1721 and *hisH* was compared in CDM-10 medium with and without histidine by qRT PCR (n=3).

3.2.6 Role of the sibling sRNAs during infection

Infection conditions require metabolic adaptations from both sides, pathogen and host. Bacteria need to adapt to the changed environment and try to benefit from host nutrients. On the other hand, the host cells try to prevent this and eliminate the pathogen. Since NgncR_162 and NgncR_163 are involved in metabolic pathways and are important for growth in some tested media, their function could be also important for successful host colonisation.
Their role was first tested by infecting epithelial Chang conjunctiva cells with strains MS11, ΔΔ162/3 and the complementation strain ΔΔc. Since infection also depends on expression of some variable surface proteins, all infection experiments were carried out with strains in Δopa background, to rule out experimental variability due to changes in *opa* expression. Here bacteria express exclusively opa_{50} in order to select for a specific invasion pathway. The gentamicin protection assay performed by Susanne Bauer showed reduced amounts of invasive bacteria in the absence of the sRNAs. In this assay, adherent bacteria are determined after the infection period, whereas for invasive bacteria cells are treated for another 2 h with gentamicin. Consequently, a reduced number of invasive bacteria could mean that either less bacteria enter the cells or bacteria survive less within the cells. To discriminate between the two options, a differential *Neisseria* staining can be applied. Here, the number of invasive and adherent bacteria is determined at the same time point of the same sample by first staining only extracellular gonococci and then permeabilizing the cells and staining all gonococci. Counting bacteria shows that also in this experiment, the number of invasive bacteria is significantly reduced in the sRNA KO strain compared to the WT (figure 3.43). NgncR_162 and NgncR_163 do not influence adherence to the host cell, but clearly play a role in invasion of epithelial cells.

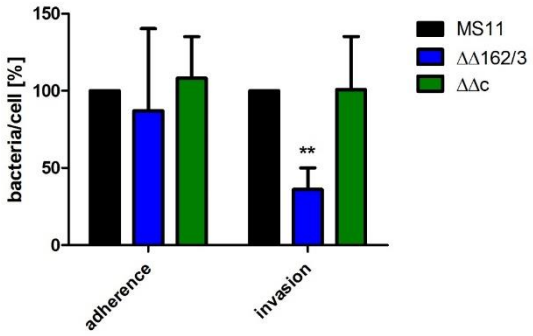

Figure 3.43: Influence of NgncR_162 and NgncR_163 on infection of Chang cells. After infection, cells were stained for intracellular and extracellular *Neisseria*. The number of bacteria per cell was determined by counting and subsequently normalized to the WT (n=3).

Beside epithelial cells, gonococci are also known to invade neutrophils. Pathogenic *Neisseria* are reported to trigger a strong recruitment of neutrophils, which are often not able to clear the infection. *Neisseria* were shown to survive within these cells and inhibit apoptosis of neutrophils for prolonged survival (reviewed in Criss and Seifert 2012). Survival within PMNs requires very specific adaptations, which might involve the sibling sRNAs. Therefore, invasion and survival

within human neutrophils was analysed. Since the fate of *N. gonorrhoeae* within neutrophils strongly depends on the *opa* expression patterns (Ball and Criss 2013), the sRNA double deletion was introduced into strain MS11 ∆opa lacking all *opa* genes. Furthermore, this strain was complemented by insertion of the sibling sRNAs into the *iga-trpB* locus. Neutrophils were freshly isolated from human blood and directly infected with strains MS11 ∆opa, ∆opa ΔΔ162/3 and ∆opa ΔΔc. After 5 min of incubation, all wells were stringently washed and the first wells lysed and plated as time point 0. After 2 h the rest of the wells were plated (t = 2 h). Data was plotted by giving the survival ratio and additionally the normalized bacteria counts at both time points (figure 3.44). For most experiments, the number of bacteria after 2 h was higher than at time point 0, suggesting bacterial replication within PMNs. Nevertheless, the absence of NgncR_162 and NgncR_163 does not significantly influence neither adhesion to nor invasion of or survival within human neutrophils.

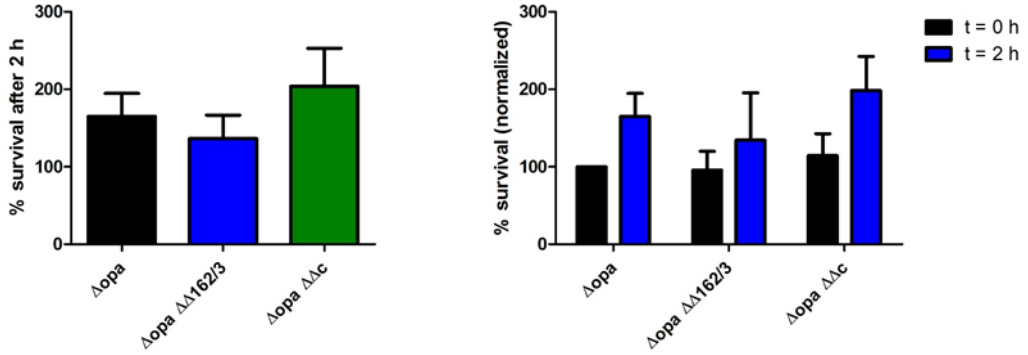

Figure 3.44: Influence of NgncR_162 and NgncR_163 on infection of neutrophils. PMNs were isolated from human blood and infected with gonococci. Cells were lysed to plate bacteria 5 min after infection (t = 0 h) and 2 h after infection. The number of bacteria was determined by cfu counting. The graphs show the survival ratio of the selected strains and the relative bacteria number at the two time points of five independent experiments.

3.3 *Trans*-acting small RNAs: NgncR_237 (Bns2)

A transcriptome analysis in *N. meningitidis* for transcripts differentially regulated in human blood revealed several highly regulated transcripts, including seven small RNAs thereafter called Bns (for *b*lood-induced *n*eisserial *s*RNA; Del Tordello et al. 2012). Bns2, corresponding to NgncR_237 in *N. gonorrhoeae*, is only very poorly analysed. Therefore, in this study the characterization of the gonococcal homologue of Bns2 was initiated.

3.3.1 Structure prediction and sequence conservation

According to RNAseq data, the sRNA NgncR_237 has a length of 99 nucleotides (Remmele et al. 2014). The sRNA could be detected in Northern Blots, albeit the signal was very weak

and did not correspond perfectly to the predicted length (figure 3.45A). Its putative secondary structure was predicted using the RNAfold WebServer of the University of Vienna. Default settings minimum free energy and partition function at 37 °C and the function to avoid isolated base pairs were applied. The sequence input results in two structure predictions, the minimum free energy (MFE) structure and the centroid structure, which considers additionally the probability of the occurrence of a secondary structure. Both calculation methods resulted in the same secondary structure (figure 3.45B). The predicted secondary structure of NgncR_237 has a free energy of -32.40 kcal/mol. It consists of two stem loops, including a Rho-independent transcription termination stem-loop, which are connected by a single stranded region ranging from nucleotide 43 to nucleotide 62 that probably serves for interaction with the target mRNAs.

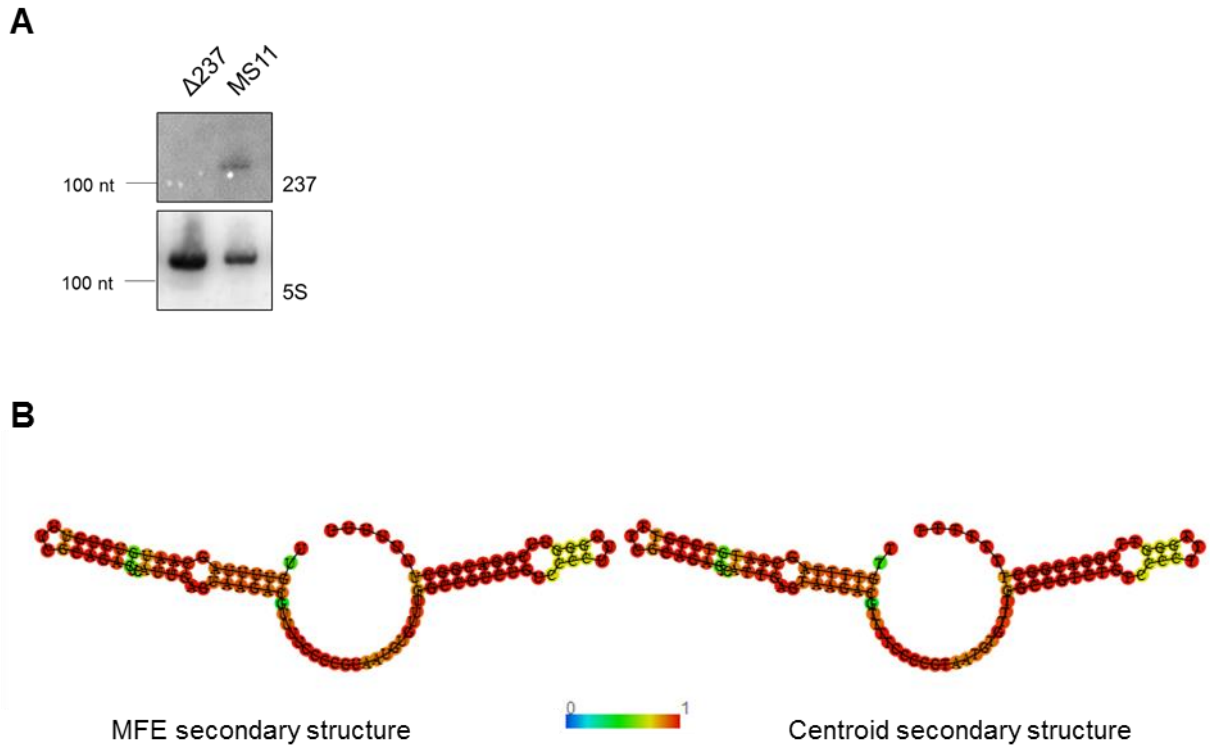

Figure 3.45: Verification of NgncR_237 expression and secondary structure prediction. (A) Expression of NgncR_237 was verified with a Northern Blot probe binding to 5' end of the sRNA. Size was determined with a decade marker. (B) The minimum free energy (MFE) structure and the centroid secondary structure of the sRNA NgncR_237 were predicted with the webserver of Vienna RNAfold (http://rna.tbi.univie.ac.at/cgi-bin/RNAWebSuite/RNAfold.cgi). Nucleotides are coloured according to base-pair probabilities.

According to BLAST analysis, the sRNA is only found in the closest related species *N. meningitidis*, *N. lactamica* and *N. polysaccharea.* The respective sRNA sequences were aligned to the reference sequence of NgncR_237 from *N. gonorrhoeae* using the multiple sequence alignment program MAFFT. The alignment shows that the sRNA sequences of *N. lactamica* and *N. polysaccharea* are 100 % identical to NgncR_237 (figure 3.46), while in *N.*

meningitidis one nucleotide exchange can be found, which is located at the end of the potential first stem loop. The alignment includes the 30 nucleotides upstream of the sRNA sequence, which is also highly conserved in the analysed strains.

The NgncR_237 gene is located 109 nucleotides downstream of the gene *thiF* encoding a thiazole biosynthesis adenylyltransferase. Downstream of NgncR_237 is located in opposite direction a gene coding for SlyX protein. This genomic localization is conserved in the four neisserial strains.

Figure 3.46: Sequence conservation of NgncR_237. The sequence alignment of NgncR_237 of *N. gonorrhoeae* MS11 and its homologues in strains *N. meningitidis* MC58, *N. lactamica* Y92-1009 *and N. polysaccharea* M18661 was created with the high speed multiple sequence alignment program MAFFT (https://www.ebi.ac.uk/Tools/msa/mafft/) and visualized with the alignment editor MView (https://www.ebi.ac.uk/Tools/msa/mview/). The sequence is coloured according to nucleotide identity with *N. gonorrhoeae* as reference strain.

3.3.2 Target prediction and validation

3.3.2.1 *In silico* target prediction

In order to find potential target genes regulated by NgncR_237, an *in silico* prediction was applied using the webtools TargetRNA2 and CopraRNA. The webserver TargetRNA2 (Kery et al. 2014) is a tool to identify mRNA targets of sRNAs in bacteria considering sRNA conservation and secondary structures. The sequence of NgncR_237 was matched with the genome of *N. gonorrhoeae* strain FA 1090 using default settings. A total of 56 genes were predicted to be targets of NgncR_237 (complete list see table A.4). Of these genes, only hits were taken into consideration for further target validation that show complementarity between the single stranded region of NgncR_237 and the region of the 5'-UTR which is located immediately upstream of the start codon, which is a common interaction region for sRNAs. Additionally, NGFG_1338 was included in the analysis, although the predicted region of complementarity is further upstream of the RBS. This results in a list of four candidates (table 3.6). NGFG_1006 is annotated as a hypothetical protein. BLAST search showed that the gene is conserved among *Neisseria* and probably encodes a periplasmic protein. A recent study identified this protein to be involved in type IV pilus stability (Hu et al. 2020). NGFG_0515 and NGFG_1338 are both coding for endonucleases, whereas NGFG_0693 encodes the aminotransferase AlaT, which is involved in the conversion of pyruvate to L-alanine.

Table 3.6: Selected hits from the TargetRNA2 screen of NgncR_237 on *N. gonorrhoeae* FA1090

Rank	Energy [kcal/mol]	p-value	Locus FA1090	Locus MS11	Gene
12	-15.46	0.000	NGO0783	NGFG_01006	
24	-12.21	0.007	NGO0364	NGFG_00515	
43	-10.15	0.022	NGO1598	NGFG_01338	
51	-8.7	0.042	NGO1047	NGFG_00693	alaT

A second *in silico* target prediction was performed using the webserver CopraRNA. CopraRNA, short for Comparative prediction algorithm for small RNA targets, combines distinct whole genome IntaRNA predictions (Wright et al. 2014). CopraRNA is a comparative method and requires the input of at least three homologous sRNA sequences from at least three different organisms, the species of interest is chosen as reference. *N. gonorrhoeae* MS11 was selected as reference genome and *N. meningitidis* MC58, *N. polysaccharea* and *N. lactamica* were added for comparison. The prediction was made using default settings. The output is a list of 200 potential target genes and can be found in the annex (table A.6). Here nearly all mRNAs are predicted to interact with the single-stranded region of NgncR_237. Nineteen putative target mRNAs exhibit complementarity with NgncR_237 within the region including the RBS. Ten of these genes have a p-value < 0.05 and are listed in table 3.7. NGFG_1006 and *alaT* are common hits of both screens, TargetRNA2 and CopraRNA. NGFG_0914 encodes *bioB*, the biotin synthase catalysing the key step in biotin biosynthesis. PilX is a protein associated with the type IV pilus. It is a minor pilin, which is found to be crucial for bacterial aggregation and adhesion to host cells (Helaine et al. 2007). According to annotation, NGFG_2119 encodes the type IV pilus assembly protein PilC; however, considering a protein BLAST search and the genomic organization of the ORF, it seems much more likely to be the pilus assembly protein PilG. TatC is part of the twin-arginine translocation system that transports large folded proteins containing a twin-arginine motif in their signal peptide across membranes (Holzapfel et al. 2007). NGFG_1479 is coding for a prepilin-type N-terminal cleavage/methylation domain-containing protein. This protein family comprises pilin-like inner membrane proteins, which could be minor pilins or pseudopilins (Cisneros et al. 2012). NGFG_0559 encodes the DNA-damage inducible protein DinD, NGFG_0193 the 4-hydroxyphenylacetate 3-monooxygenase reductase component *hpaC* involved in the reduction of flavins. The last candidate FtsN is a cell division protein activating septal peptidoglycan synthesis and constriction of the cell (Addinall et al. 1997).

Table 3.7: Selected hits from the CopraRNA screen of NgncR_237

Rank	Energy [kcal/mol]	p-value CopraRNA	p-value IntaRNA	Locus MS11	Gene
9	-13.71	0.003599	0.012430	NGFG_01006	
13	-13.61	0.00481	0.013359	NGFG_00693	alaT
14	-13.25	0.004884	0.017070	NGFG_00914	bioB
15	-12.60	0.005379	0.026207	NGFG_00609	pilX
18	-12.76	0.00721	0.023684	NGFG_02119	pilG
38	-14.30	0.01484	0.008128	NGFG_00319	tatC
55	-11.45	0.02489	0.053049	NGFG_01479	
60	-10.77	0.02668	0.078070	NGFG_00559	dinD
64	-9.34	0.02794	0.162271	NGFG_00193	hpaC
101	-10.57	0.04764	0.087018	NGFG_01380	ftsN

3.3.2.2 RNAseq after pulse expression of NgncR_237

In order to define the NgncR_237 regulon, a transcriptome analysis was performed after pulse expression of the sRNA. Hence, NgncR_237 was cloned in the modified vector pMR68 described in chapter 3.2.2.2. The resulting plasmid was transformed into strain MS11 Δ237 and sRNA expression confirmed by Northern Blot (figure 3.47). Since no target genes are validated yet, conditions for pulse-expression were adapted from the sRNAs NgncR_162 and NgncR_163 and expression of NgncR_237 in strain Δ237 AIE237 was induced by addition of 2 ng/µl AHT for 30 min. The reference strain Δ237 was similarly treated with AHT to ensure identical growth conditions. Samples were tested for NgncR_237 expression prior to library preparation. Samples were processed by using high throughput Illumina sequencing by the group of Bruno Hüttel (Max-Planck-Genome-Centre Cologne) and data was analysed by Maximilian Klepsch (University of Würzburg). Dataset Δ237 AIE237 versus Δ237 was analysed for differential expression. The results can be found in the appendix (table A.5). Overall 13 genes are significantly differentially regulated in strain Δ237 AIE237 compared to strain Δ237. The list does contain neither NGFG_1006 nor *alaT*, although the genes appear in both the TargetRNA2 screen and the CopraRNA screen. Applying a cut-off of >1.5 fold for positive or <0.75 fold for negative regulation results in a list of eleven candidates. Additionaly, NGFG_0559 and NGFG_1290 were considered for further target validation since they show a strong differential regulation, though the adjusted p-value is above cut-off. This results in a list of 13 potential target genes (table 3.8). Eight of these genes are negatively regulated, including NGFG_1479, NGFG_0559 and NGFG_2119, which are also listed in the CopraRNA data. NGFG_1941 and NGFG_1964 encode both oxidoreductases, NGFG_1290 codes for a phage protein. NGFG_1617 encodes a LysR-family transcriptional regulator, the most abundant type

of transcriptional regulator in prokaryotes regulating a diverse set of genes (Maddocks and Oyston 2008). NGFG_0252 is annotated as cytoplasmic axial filament protein CafA, a gene that was later renamed in ribonuclease G. The five putative positively regulated genes include three hypothetical proteins, NGFG_1948, NGFG_0664 and NGFG_2345, whereas NGFG_0664 and NGFG_2345 are part of a Maf operon. Maf genes (*m*ultiple *a*dhesin *f*amily) are encoded in genomic islands and are characterized by modules of toxins and immunity proteins (Jamet et al. 2015). NGFG_1160 codes for a type III restriction enzyme, a group of endonucleases that recognize a non-palindromic sequence. The last potential target gene is *pilE*, the major pilin of the type IV pilus.

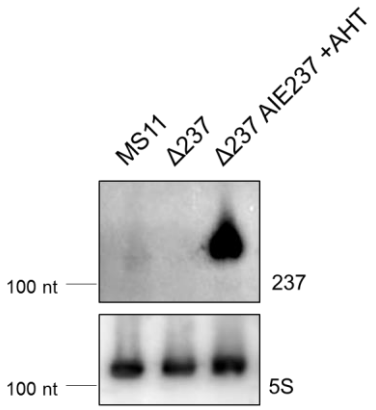

Figure 3.47: Induced overexpression of NgncR_237. Expression of NgncR_237 is strongly increased compared to WT conditions after 2 h induction with AHT.

Table 3.8: Selected differentially expressed genes in Δ237 AIE237 versus Δ237

Locus	Gene	Functional category	Adjusted p-value	Fold change
NGFG_01479		Protein fate	0.023	0.5676
NGFG_01941		Cellular processes	0.0000227	0.6025
NGFG_01964	arsC	Cellular processes	0.0371	0.6250
NGFG_01290		Mobile and extrachromosomal element functions	0.187	0.6417
NGFG_01617		Regulatory functions	0.0193	0.6713
NGFG_00559	dinD	DNA metabolism	0.0596	0.6854
NGFG_00252	rng	Transcription	0.0268	0.7260
NGFG_02119	pilG	Cell envelope	0.0181	0.7295
NGFG_01948		Hypothetical proteins	0.0268	1.5605
NGFG_00664		Hypothetical proteins	0.041	1.6460
NGFG_01160		DNA metabolism	0.0371	1.6947
NGFG_02345		Hypothetical proteins	0.0224	1.7544
NGFG_01821	pilE	Cell envelope	0.0000465	2.5140

3.3.2.3 Target validation on mRNA level

Summarizing potential target genes of the *in silico* analysis with TargetRNA2 and CopraRNA and the RNAseq screen results in five positively and 17 putatively negatively regulated transcripts. The coding sequence of NGFG_2345 is very short and since the adjacent ORF NGFG_2344, which is located in the same Maf operon, seems also regulated by NgncR_237 (adjusted p-value 0.0514), NGFG_2344 was chosen for validation. Of 22 tested genes, nine are significantly regulated in absence of NgncR_237 according to qRT PCR data (figure 3.48). Most of these genes are negatively regulated. Transcript levels of *rng*, *alaT*, NGFG_1338, NGFG_1479 and NGFG_1617 are about twofold, of *dinD*, NGFG_1006 and *pilG* about threefold upregulated in the absence of the sRNA. The only gene significantly upregulated by NgncR_237 is *pilE*. However, the extent of upregulation is surprisingly high.

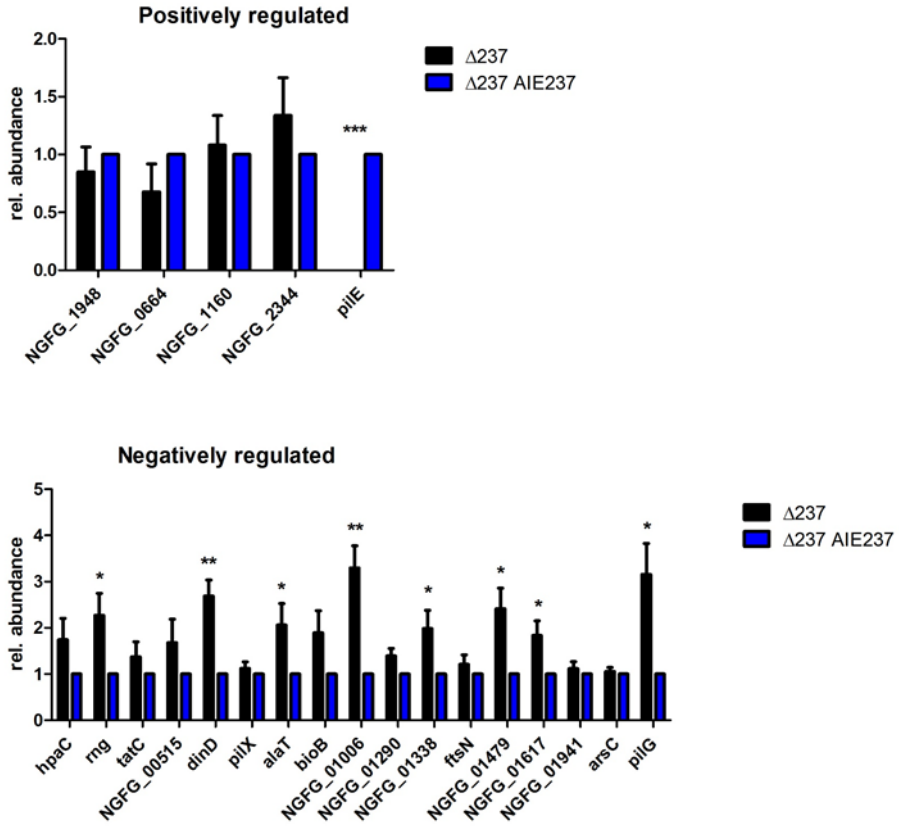

Figure 3.48: Validation of NgncR_237 target genes by qRT PCR. All potential target genes resulting from the TargetRNA2, CopraRNA and RNAseq data were analysed for differential expression in strains Δ237 and Δ237 AIE237 (n=3-6). Both strains were cultured in presence of 2 ng/µl AHT. The graph include data from experiments performed by Eva-Maria Hörner and Susanne Bauer.

The high ratio of differential expression of *pilE* is striking, especially since *pilE* is known for its antigenic variation. The primers used in qRT PCR were derived from the conserved N-terminal sequence of the pilin to avoid effects of antigenic variation. Nevertheless, the observed differences might be due to differences in the strain background. Thus, expression of *pilE*, NGFG_1479, *dinD*, *rng* and *pilG* was compared in the same genetic background, in strain

Δ237 AIE237 with and without induction with AHT (figure 3.49). The differential regulation is here for all tested genes less pronounced compared to the differential expression with the KO strain. Only NGFG_1479, *dinD* and *pilG* can still be considered as differentially regulated by the sRNA. The massive upregulation of *pilE* cannot be observed in this experiment, arguing against regulation of the pilin by NgncR_237.

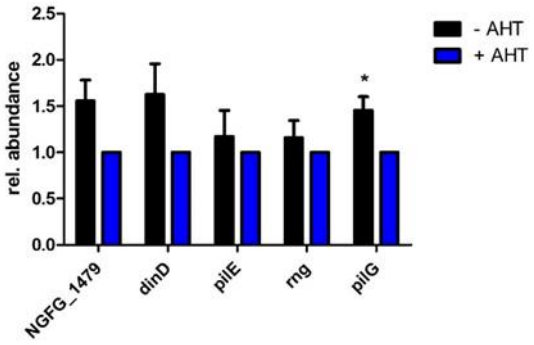

Figure 3.49: Verification of post-transcriptional regulation by NgncR_237. Strain Δ237 AIE237 was cultivated in presence and absence of AHT and samples analysed for expression of NGFG_1479, dinD, pilE, rng and pilG by qRT PCR (n=3).

3.3.2.4 Target validation in *E. coli* and analysis on sRNA:mRNA interactions

The webtool IntaRNA is designed for the prediction of RNA-RNA interactions considering accessibility and the existence of a seed interaction (Mann et al. 2017). Here it was applied for prediction of the mRNA sequence of the eight remaining target genes bound by NgncR_237 (figure 3.50). The nucleotide positions of the mRNA are given relative to the start codon (+1). All genes are predicted to interact with the single-stranded region of the sRNA. However, different regions of the single-stranded region are engaged. NGFG_0252 (*rng*), NGFG_0559 (*dinD*), NGFG_1338 and NGFG_1617 are predicted to interact with the first half of the single-stranded region, whereas NGFG_0693 (*alaT*), NGFG_1006 and NGFG_2119 (*pilG*) with the second half. The interaction region of NGFG_1479 covers almost the complete length of the single-stranded region. Most mRNAs are bound at the sequence around or directly upstream of the start codon including the RBS (NGFG_0559, NGFG_0693, NGFG_1006, NGFG_1479 and NGFG_2119). Interfering with ribosomal binding is a well-described mechanism of sRNA for negative target gene regulation. NGFG_252 and NGFG_1617 are predicted to be bound within the coding sequence and NGFG_1338 in the 5' UTR upstream of the RBS.

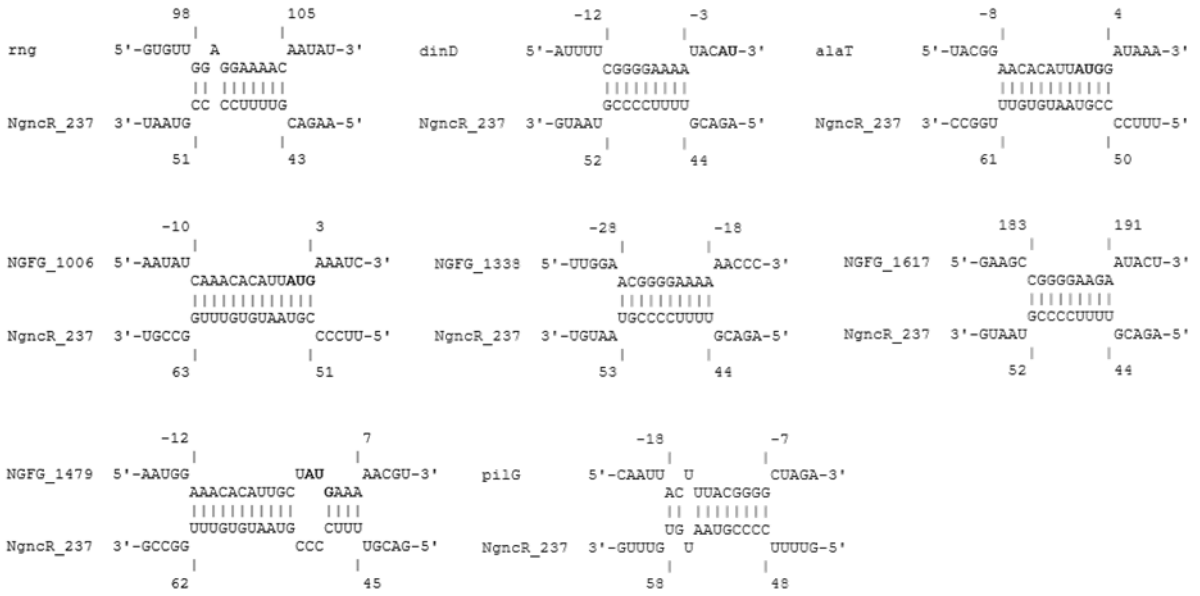

Figure 3.50: Prediction of sRNA:mRNA interactions between NgncR_237 and its target genes. Interactions between *rng*, *dinD*, *alaT*, NGFG_1006, NGFG_1338, NGFG_1617, NGFG_1479 and *pilG* and the sRNA NgncR_237 was predicted with the webtool IntaRNA. Numbers refer to the nucleotide position with respect to the start codon (+1) or in the case of the sRNA the transcriptional start site. The start codon (AUG) if shown is in bold.

To further validate post-transcriptional regulation of the postulated target genes by NgncR_237, the two-plasmid *gfp* reporter system was used, which was developed for detection of sRNA target interactions in *E. coli* (Urban and Vogel 2007). The sequence of the 5' UTR including and the first few codons of the putative target gene is fused to *gfp* in the low-copy vectors pXG10 or pXG30. Vector pXG10 is designed for genes with known transcription start site, whereas pXG30 mimics an intra-operonic target arrangement. The sRNA is cloned in vector pJV300, which is co-transformed with the target-*gfp* fusion in *E. coli* Top10. The empty vector pJV300 expresses a nonsense sRNA and so serves as negative control. Both the sRNA and the target-*gfp* fusion are under control of constitutive phage-derived promoters. Five of the target genes differentially regulated according to qRT PCR data have a predicted interaction sequence around the start codon and therefore fulfil criteria for use as target-*gfp* fusion in *E. coli*. In the case of NGFG_1479 and *pilG,* the transcriptional start site was annotated (Remmele et al. 2014) and so the complete 5' UTR including the first codons of the gene were cloned into plasmid pXG10. NGFG_1006 and *dinD* do not have an annotated transcriptional start site and so 185 and 94 nucleotides from the upstream sequence of NGFG_1006 and *dinD*, respectively, were arbitrarily cloned in the vector. Regarding *alaT*, the stop codon of the neighbouring locus NGFG_0692 is located only 88 nucleotides upstream of the start codon of *alaT*. Since no promoter elements are obvious in the upstream region of *alaT*, a polycistronic organization cannot be excluded. Therefore, this gene was cloned into vector pXG30. Post-transcriptional regulation can be confirmed by the translational *gfp*-fusions for target genes *dinD*, *alaT*, NGFG_1006 and *pilG* (figure 3.51). For NGFG_1479 no effects of NgncR_237 on the amount of GFP could be detected. The effect of plasmid pJV237 in comparison to control plasmid

pJV300 expressing a non-sense RNA is well pronounced for target genes *dinD*, NGFG_1006 and *pilG*, for *alaT* a weaker, though reproducible effect can be observed.

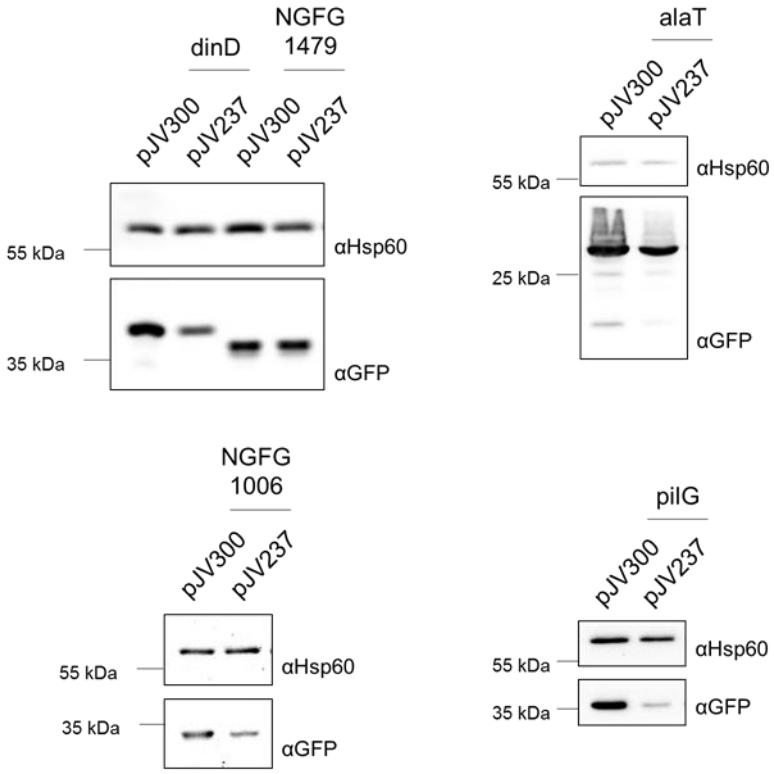

Figure 3.51: Validation of NgncR_237 target genes in *E. coli* using translational *gfp*-fusions. *E. coli* Top10 was co-transformed with plasmids expressing translational gfp fusions pXG10_dinD-gfp, pXG10_1479-gfp, pXG30_alaT-gfp, pXG10_1006-gfp or pXG10_pilG-gfp and a plasmid expressing either no functional RNA (pJV300) or NgncR_237 (pJV237). The Western Blot showing pXG10_pilG-gfp was performed by Katharina Wagler.

All target mRNAs were predicted to interact with the single-stranded region of NgncR_237 (figure 3.50), however, the region of complementarity differs between the predicted target genes. Thus, two mutants of the sRNA were constructed and cloned in vector pJV300, resulting in pJV237mut3 having nucleotides 44-46 and 50-51 mutated and pJV237mut2 having nucleotides 55-59 mutated. The location of the mutations within the NgncR_237 sequence is schematically illustrated in figure 3.52A. Regulation of NGFG_1006 and *dinD* by the sRNA could be confirmed with the translational *gfp*-fusions in *E. coli*. Both mRNAs are predicted to interact with different parts of the single-stranded region of NgncR_237: NGFG_1006 with nucleotides 51 to 63 and *dinD* with nucleotides 44 to 52. Complementary mutations to the respective pJV237mut were introduced in the 5' UTR of NGFG_1006 and *dinD* cloned in plasmid pXG10, generating plasmids pXG10_1006mut2-gfp and pXG10_dinDmut3-gfp. NGFG_1006 is regulated by NgncR_237, but not by 237mut2 and 237mut3 (figure 3.52B). Regulation by 237mut3 was still expected since here the mutated nucleotides hardly interfere with the predicted binding region (figure 3.52C). 1006mut2-gfp is not regulated by NgncR_237 anymore, but restoring complementarity to the sRNA resulted again in decreased GFP levels,

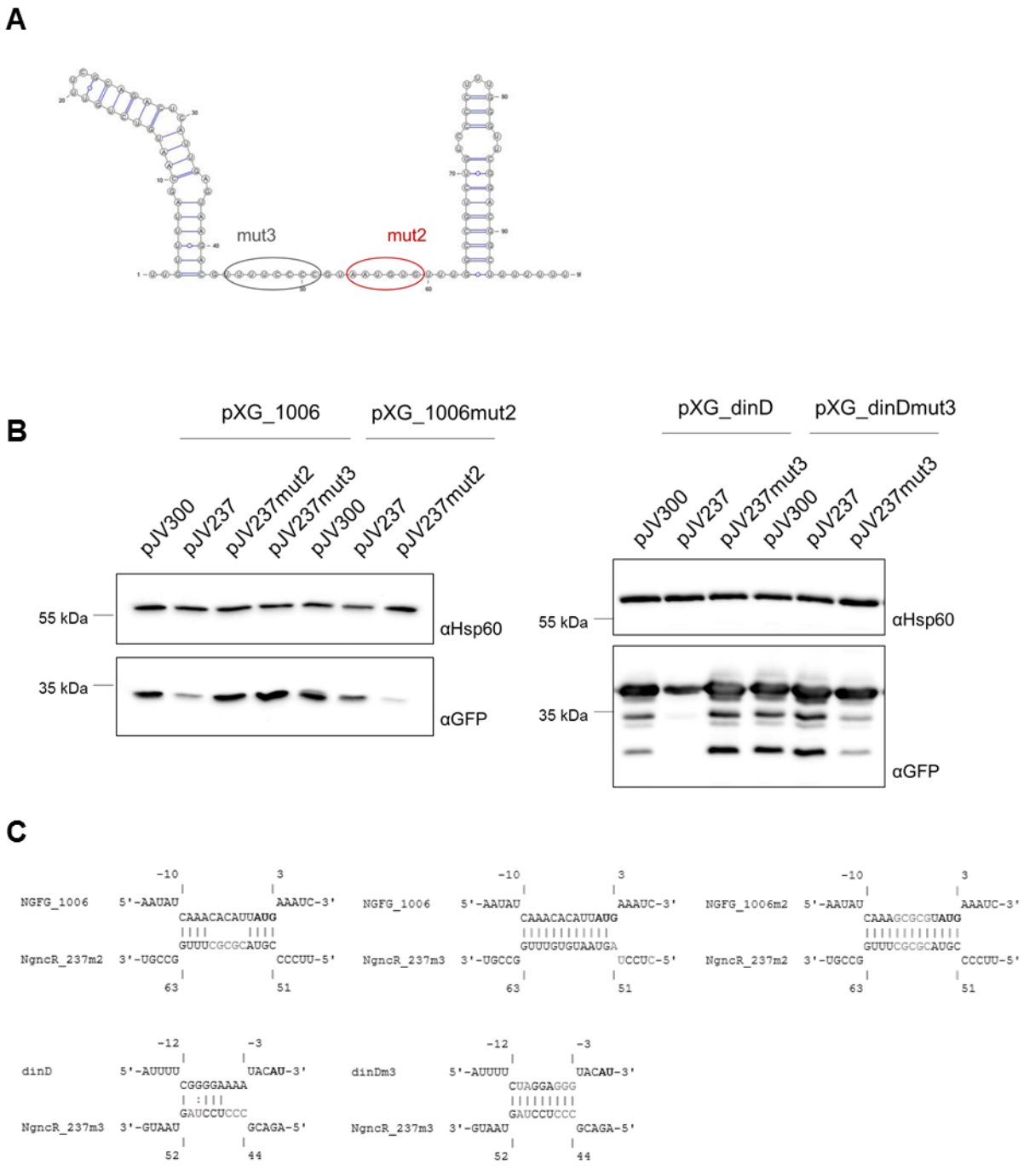

Figure 3.52: Validation of predicted interaction domains between NGFG_1006 or *dinD* and NgncR_237. (A) The picture shows schematically the location of the mutations in the single stranded region of NgncR_237 in pJV237mut2 and pJV237mut3. (B) Testing the predicted interaction region between NGFG_1006/*dinD* and NgncR_237 in *E. coli* using translational *gfp*-fusions. *E. coli* was co-transformed with plasmids pXG_1006-gfp/pXG_dinD-gfp and pXG_1006mut-gfp/pXG_dinDmut-gfp and a plasmid expressing either no functional RNA (pJV300), NgncR_237 (pJV237) or variants of NgncR_237 (pJV237mut2/3). The mutation in pXG_1006mut-gfp is complementary to those in pJV237mut2, the mutation in pXG_dinDmut-gfp complementary to pJV237mut3. The Western Blot testing the *dinD* plasmids was performed by Susanne Bauer. (C) Illustration of the interactions between NgncR_237 derivates and NGFG_1006 or *dinD*. Nucleotides that differ from the native sRNA or mRNA are coloured in grey.

confirming the predicted interaction sequence within the NGFG_1006 mRNA. Similar results were obtained for *dinD*. 237mut3 did no longer downregulate GFP, but clearly decreased GFP levels when the complementary mutation in pXG10_dinD-gfp was introduced. This data confirms the predicted binding regions by NgncR_237 within the 5' UTRs of NGFG_1006 and *dinD*.

3.3.2.5 Target validation on protein level in *N. gonorrhoeae*

The regulatory role of NgncR_237 was further investigated on protein level. To prove post-transcriptional regulation by NgncR_237 in *N. gonorrhoeae* target-*gfp* fusions in strain Δ237 237AIE were constructed. Since NGFG_1006 and *dinD* are weakly transcribed according to transcriptome data (Remmele et al. 2014), they were replaced by the stronger neisserial promoter P_{opa} (NGFG_1006) or P_{PilE} (*dinD*) to allow detection of the GFP signal. Artificial increase of the sRNA target should not affect post-transcriptional regulation due to overexpression of NgncR_237. The gene of *pilG* was replaced by the *gfp* fusion covering also the first codons of the target gene, whereas the *dinD* fusion was integrated downstream of the sRNA in the *iga-trpB* locus and 1006-gfp was integrated in the intergenic region between lactate permease and aspartate aminotransferase, leaving an intact copy of the original locus. The expression of GFP was compared with and without induction of the sRNA expression with AHT. Strains were grown on plates in presence and absence of the inducer before shifted to liquid culture. GFP detection in a plate reader allows analysing GFP expression in a time-dependent manner, whereas Western Blots show end-point results. However, only the *pilE* promoter results in a strong enough GFP expression to be detected in a TECAN plate reader. This is why the *dinD* fusion was analysed in a plate reader and the other two strains by Western Blot. GFP expression was reproducibly reduced for P_{PilE}559gfp, the translational fusion of *dinD* to *gfp* (figure 3.53A). This effect was mostly visible when bacteria enter stationary phase. This could mean that regulation by NgncR_237 is rather weak during exponential growth phase, but is more probably due to detection limits. Experiments in a TECAN plate reader with other bacteria than gonococci showed that detection of the GFP signal starts being reliable around an OD_{600} 0.3, so when gonococci enter stationary phase.
Both other translational *gfp* fusions, with NGFG_2119 (*pilG*) and NGFG_1006, confirm also a downregulation by the sRNA (figures 3.53B+C). Quantification of the Western Blots show that the effect is approximately 1.5 fold compared to induced samples.
In all analysed target genes, the differential regulation by the sRNA is significant, but rather small. Nevertheless, also in the qRT PCR experiments comparing target gene expression in strain Δ237 237AIE with and without induction the differences were small. Consequently, these data confirm that NgncR_237 acts as post-transcriptional regulator by inhibiting expression of the analysed target genes.

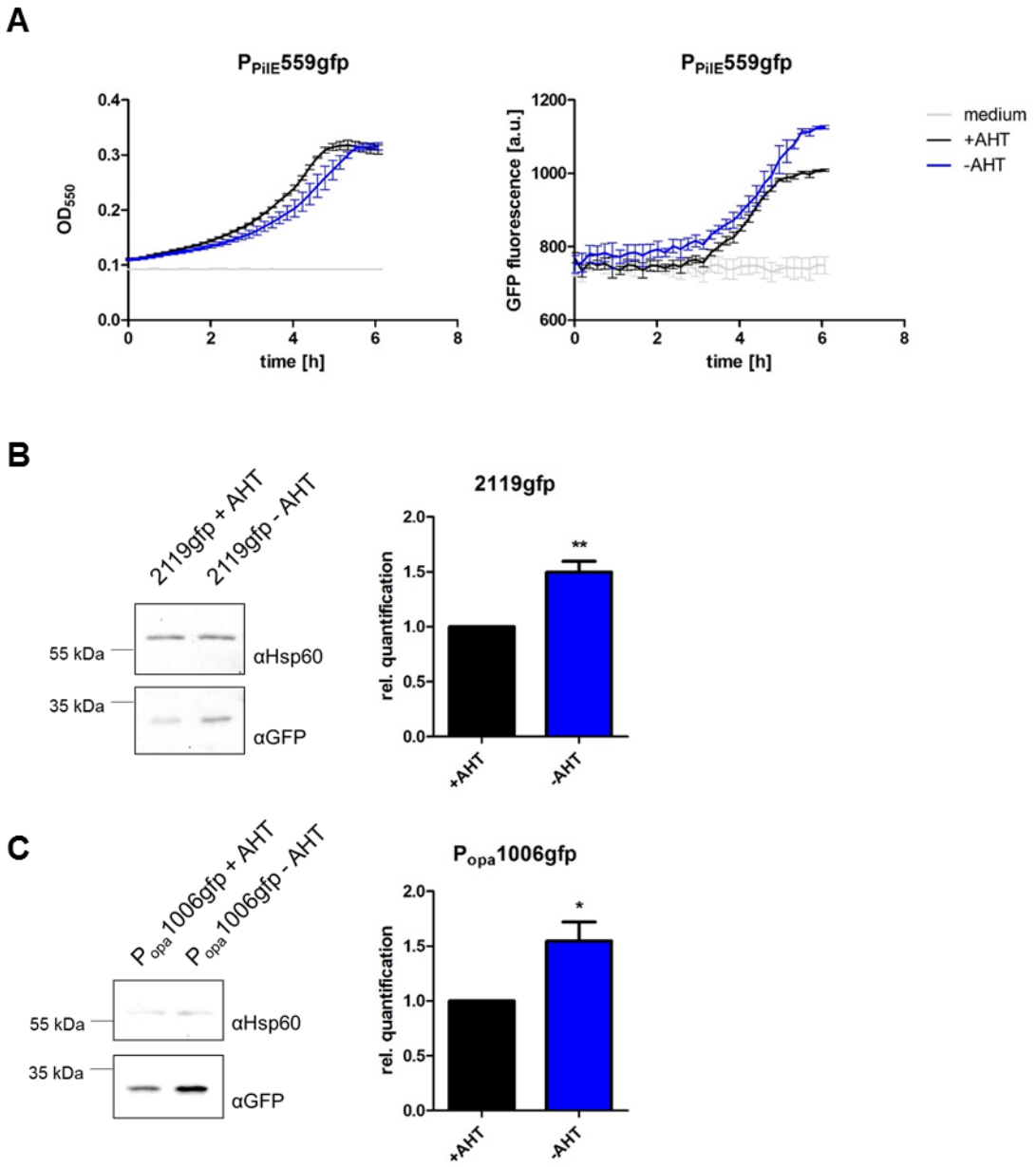

Figure 3.53: Validation of target genes of NgncR_237 on protein level in *N. gonorrhoeae*. Gonococci express translational target-*gfp* fusions derived from strain Δ237 AIE237. GFP abundance was compared in absence and presence of the inducer AHT. (A) The translational fusion of NGFG_0559 (*dinD*) is under control of *pilE* promoter due to the weak native promoter of the target gene. OD_{550} and GFP emission were measured over a time course of more than 6 h in a TECAN plate reader. (B) The translational fusion of NGFG_2119 (*pilG*) is analysed by Western Blot. The diagram shows the quantification of five Western Blots. (C) The translational fusion of NGFG_1006 is under control of *opa* promoter due to the weak native promoter of the target gene. GFP expression is analysed by Western Blots and the quantification of four Western Blots is shown.

3.3.3 Expression conditions for NgncR_237

The Northern Blot experiments showed that NgncR_237 is hardly expressed under standard growth conditions. It has been reported for the meningococcal homologue Bns2 that several conditions can induce expression of the sRNA.

Transcriptional regulators might repress expression of NgncR_237. The effect of the deletion of five DNA binding proteins, GdhR, NGFG_2170, RelA, GntR and NGFG_1511, was tested. None of the analysed KO strains had an effect of sRNA expression (figure 3.54A). Due to the very weak expression of the sRNA and thus difficult detection of NgncR_237, band intensity seems more variable. These effects are not reproducible.

Meningococcal Bns2 is hardly expressed during exponential growth phase, but the sRNA could be clearly detected during stationary phase (Fagnocchi et al. 2015). Since a change in the growth phase causes deregulation of several sRNAs, including the sibling sRNAs NgncR_162 and NgncR_163, expression of NgncR_237 was compared in logarithmic and stationary growth (figure 3.54B). However, expression levels do not increase upon entry of stationary phase.

In case sRNA expression is only induced upon host cell infection, epithelial Chang conjunctiva cells were infected with gonococci and RNA isolated from the lysed cells. Cell lysis was performed in a way to strongly reduce the amount of eukaryotic RNA, which would be otherwise too dominant to analyse bacterial RNAs. The comparison of NgncR_237 transcript levels by Northern Blot shows that under the chosen infection conditions no increase in sRNA expression can be observed (figure 3.54C). The sample extracted from infected cells still contained remaining levels of eukaryotic RNA and so a lower amount of bacterial RNA was loaded on the gel compared to the control sample, resulting in a weaker band.

Bns2 was identified as an sRNA to be upregulated in blood in *N. meningitidis* (Del Tordello et al. 2012). Due to the bactericidal activity of human blood against many gonococcal strains, analysis of NgncR_237 expression was not performed in whole blood, but by supplementation of serum. RPMI medium supplemented with 10 % (v/v) fetal calf serum or with 2 % (v/v) pooled human serum were used to compare sRNA expression (figure 3.54D). Before sample analysis, it was verified that survival of gonococci was not significantly affected at these serum concentrations. Nevertheless, also the presence of serum did not induce sRNA expression.

Another factor reported to influence meningococcal Bns homologues is the carbon source availability. Increased levels of glucose in the medium induced expression of Bns1 and Bns2 (Fagnocchi et al. 2015). Therefore, gonococci were grown in CDM-10 containing either glucose, lactate or pyruvate as carbon source. Additionally, a medium was tested in which the glucose concentration was elevated to 10 g/l. However, none of the tested carbon sources has an effect on NgncR_237 levels (figure 3.54E).

The *din* genes respond in *E. coli* to oxidative stress or DNA damage (Oh et al. 1999). Since *dinD* is a validated target gene of NgncR_237, the sRNA might be involved in the SOS

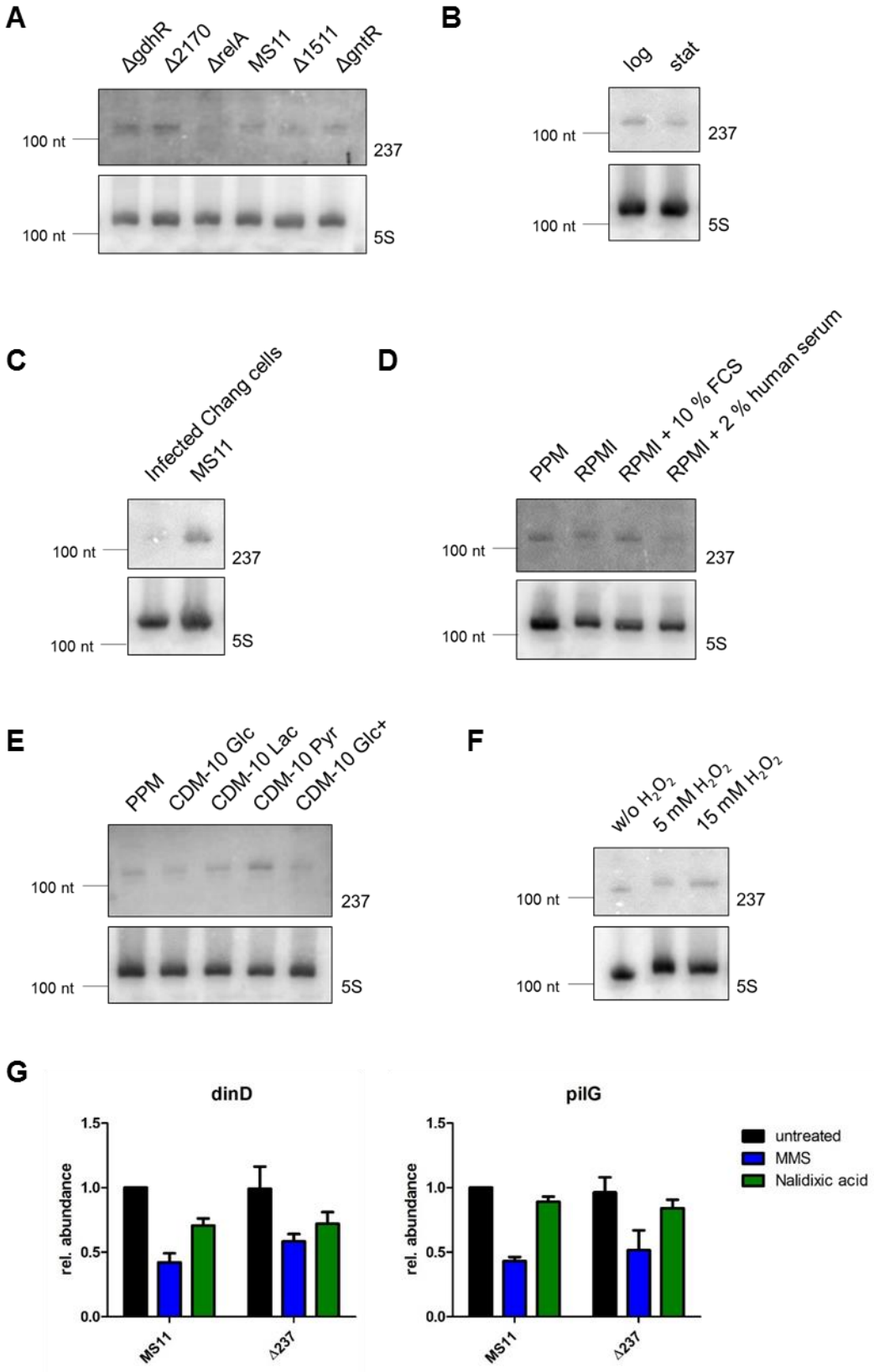

Figure 3.54: Testing induction conditions for NgncR_237. Expression of NgncR_237 was monitored by Northern Blot under various conditions. The influence of the impact of the DNA-binding proteins GdhR, NGFG_2170, RelA, NGFG_1511 and GntR was tested with the help of KO strains (A), as well as the growth phase by comparing logarithmic with stationary phase (B). Further Chang conjunctiva cells were infected with gonococci and the resulting RNA compared with the RNA of flask-grown bacteria (C).To test the effect of serum either 10 % FCS or 2 % pooled human serum was added to the growth

medium (D). The influence of the carbon source was determined by growth in CDM-10 media containing either glucose, lactate, pyruvate or an increased amount of glucose as carbon source (E) and the influence of H_2O_2 by adding 5 mM or 15 mM H_2O_2 for 1 h to the medium (F). The effect of MMS and nalidixic acid was analysed by comparing the expression of the target genes *dinD* and *pilG* in presence and absence of the damaging agent in strains MS11 WT and Δ237 by qRT PCR (n=2) (G).

response. Thus, several inducers were tested: H_2O_2, the DNA alkylating agent methyl methanesulfonate (MMS) and the gyrase inhibitor nalidixic acid. For all substances, first growth experiments were performed to determine the optimal concentration: 5 mM and 15 mM H_2O_2, 0.05 % MMS and 10 µg/ml nalidixic acid. Growth of gonococci was supposed to be only slightly reduced by addition the substance. The effect of H_2O_2 on sRNA expression was determined by Northern Blot (figure 3.54F). However, none of the used concentrations affected expression of NgncR_237. MMS and nalidixic acid were tested indirectly by measuring target gene expression by qRT PCR in strains MS11 WT and Δ237 (figure 3.54G). The data suggest no influence of NgncR_237 in presence of MMS and nalidixic acid since the downregulation observed for *dinD* and *pilG* is also present in strain Δ237.
Taken together, expression of NgncR_237 was not induced under the conditions tested.

3.3.4 Role of NgncR_237 in infection

In order to assess whether NgncR_237 plays a role during infection, epithelial cell lines were infected with strains Δopa, Δopa Δ237 and the complementation strain Δopa Δ237c. All strains expressed *opa*$_{50}$ from a plasmid, the presence of Opa$_{50}$ was verified by Western Blot. Chang conjunctiva cells were infected in a gentamicin protection assays, resulting in cfu counts of adherent and invasive bacteria (figure 3.55A). However, NgncR_237 does not influence infection of Chang cells. No difference in the number of adherent or invasive bacteria could be detected between strains Δopa and Δopa Δ237.
Since several of the validated target genes are associated with type IV pili, the infection experiment was repeated with Cornea epithelial cells, which are known to be infected by pilus-expressing bacteria (Scheuerpflug et al. 1999). Genes like *pilG,* NGFG_1006 or NGFG_1479 are downregulated by NgncR_237, hence more adherent bacteria would be expected in the absence of NgncR_237. Nevertheless, no influence of NgncR_237 on infection of Cornea epithelial cells could be observed, since neither levels of adherent nor invasive bacteria change significantly (figure 3.55B).

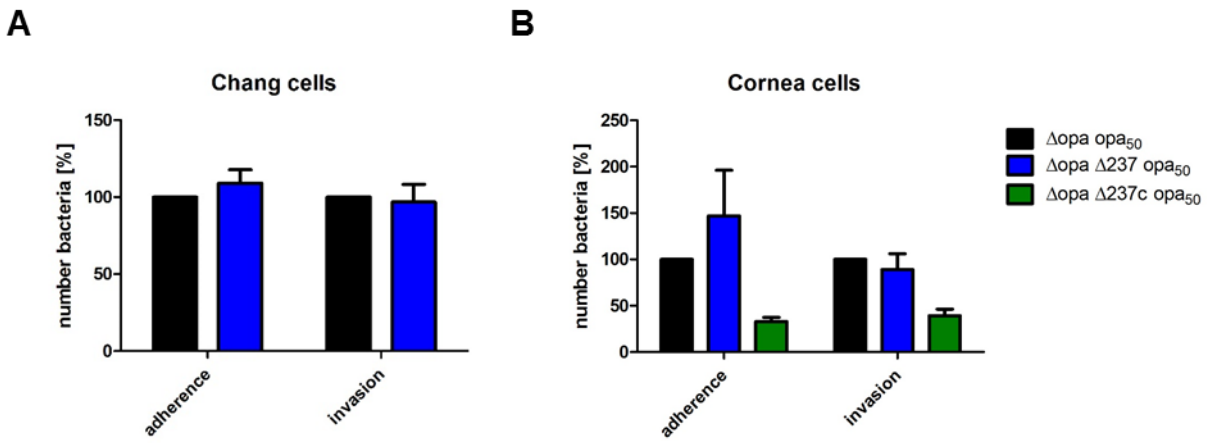

Figure 3.55: Role of NgncR_237 in infection of epithelial cells. The influence of NgncR_237 on Chang conjunctiva cells (A) or Cornea cells (B) was determined in a gentamicin protection assay. Cells were infected with gonococcal strains with Δopa background expressing opa_{50}, either the WT, NgncR_237 KO strain or the complementation strain (n=3).

NgncR_237 could also play a role during infection of immune cells. PMNs were infected directly after isolation from fresh human blood from healthy donors. At time point zero, corresponding to 5 min after infection, the cells were stringently washed to remove extracellular bacteria. Half of the wells were lysed, the remaining cells were incubated for another 2 h. Bacteria from both time points were plated at different dilutions on GC agar to determine the cfu at each time point. The number of bacteria was normalized to the WT and the survival ratio determined (figure 3.56). The results show that the number of invasive and tightly adherent bacteria at time point zero is the same for both strains. Strain Δ237 seems to show a better survival in the presence of neutrophils compared to the WT strain, however, this result is not significant. Therefore, the data do not reveal a role of NgncR_237 during infection.

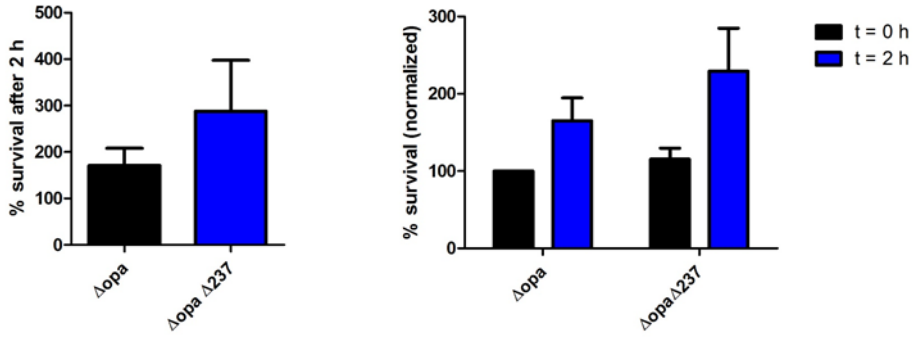

Figure 3.56: Influence of NgncR_237 on infection of neutrophils. PMNs were isolated from human blood and infected with gonococci. Cells were lysed to plate bacteria 5 min after infection (t = 0 h) and 2 h after infection. The number of bacteria was determined by cfu counting. The graphs show the survival ratio of the selected strains (left) and the relative bacteria number at the two time points (right) of five independent experiments.

3.3.5 Identification of a possible sibling sRNA

3.3.5.1 *In silico* analysis of sRNA structure and sequence conservation

Initially, for detection of NgncR_237 in Northern Blots a probe was used, which is binding the single-stranded region of the sRNA. However, this probe was not specific and detected another transcript of slightly smaller size, which was also present in strain Δ237 (figure 3.57A). Since the analysis of sequence conservation of NgncR_237 in different *Neisseria* revealed that the three closely related species *N. meningitidis, N. lactamica* and *N. polysaccharea* harbour two distinct copies of the sRNA at distant genomic loci, it seemed possible that the second transcript is a sibling of NgncR_237. This second sRNA is also present in *N. gonorrhoeae*, though it was not found in the transcriptome screen of the bacterium (Remmele et al. 2014). Interestingly, the single stranded region of NgncR_237, which is responsible for target gene regulation, is identical in the second sRNA (figure 3.57B). This is suggesting a similar function of both sRNAs and they might be therefore considered as sibling RNAs.

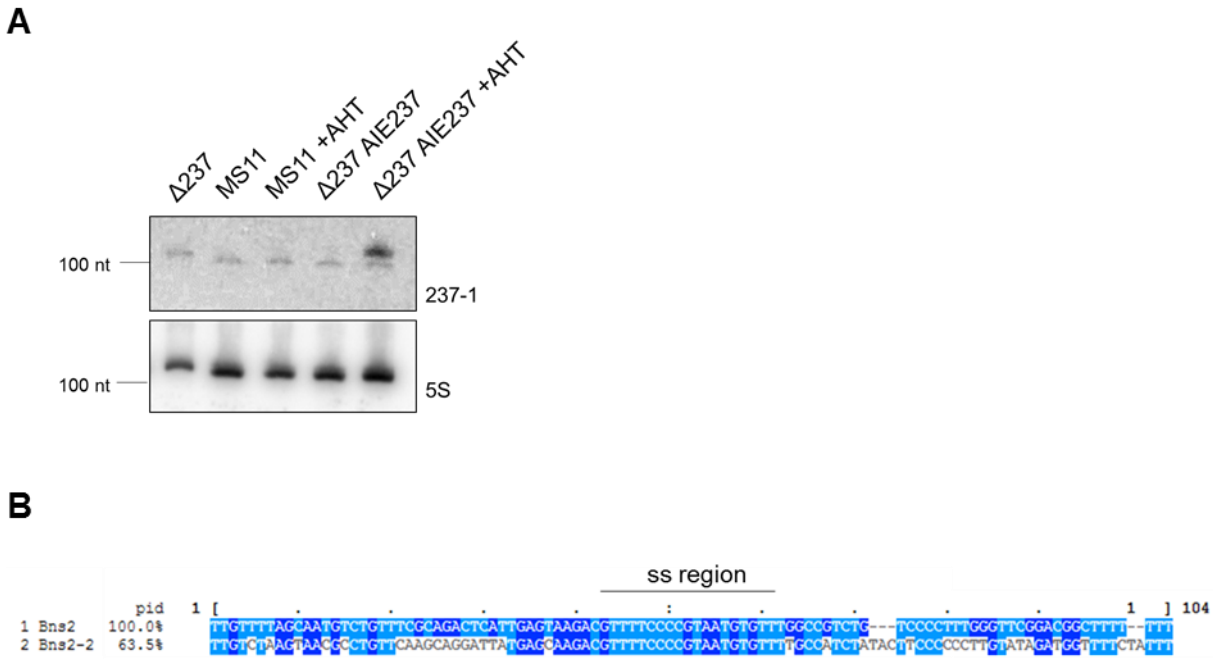

Figure 3.57: Sequence similarity between NgncR_237 and Bns2-2. (A) RNA of strains Δ237, MS11 and Δ237 AIE237 with and without induction with AHT was analysed by Northern Blot. The probe 237-1 binds the single stranded region of both NgncR_237 and Bns2-2. (B)The sequence of NgncR_237 (Bns2) was aligned to the potential sibling RNA Bns2-2 with the high speed multiple sequence alignment program MAFFT (https://www.ebi.ac.uk/Tools/msa/mafft/) and visualized with the alignment editor MView (https://www.ebi.ac.uk/Tools/msa/mview/). The sequence is coloured according to nucleotide identity and the single stranded region in NgncR_237 is annotated.

Since Bns2-2 was not annotated in the transcriptome analysis, the sRNA sequence was assumed to start with the same set of nucleotides than NgncR_237 and end with a Rho-independent transcription termination stem-loop common for *trans*-acting sRNAs. This would

result in an sRNA of 104 nucleotides in length. Detection of Bns2-2 in Northern Blot results in a clear band appearing around 100 bp, confirming the assumed sRNA sequence (figure 3.58). Bns2-2 seems stronger expressed under standard growth conditions than NgncR_237 (figure 3.57A), however the signal is still weak. Transcript levels of Bns2-2 were compared in both MS11 WT and Δ237 in order to elucidate whether the absence of NgncR_237 influences the expression of Bns2-2 (figure 3.58). However, the Northern Blot shows that this is not the case.

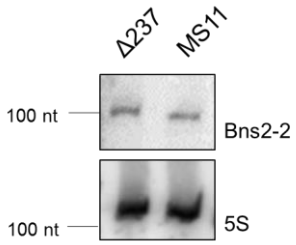

Figure 3.58: Specific detection of Bns2-2 in Northern Blot. Total RNA from strains MS11 WT and Δ237 were loaded on a poly-acrylamide gel. The membrane was probed specificly for Bns2-2 and bands could be detected at 100 bp.

NgncR_237 is predicted to fold into two stem loops separated by a single-stranded region. The RNAfold WebServer of the University of Vienna was applied for secondary structure prediction of Bns2-2, using default settings minimum free energy and partition function at 37 °C and the function to avoid isolated base pairs. The sequence input here resulted in two different structure predictions; the MFE structure is distinct from the centroid secondary structure (figure 3.59). The MFE structure is highly similar to the predicted structure of NgncR_237, the single stranded region is identical. The calculated free energy of this structure prediction is -24.1 kcal/mol. The centroid secondary structure has a much smaller first stem loop, resulting in a longer single-stranded region. The free energy of the predicted structure is -19.0 kcal/mol, less than the MFE prediction.

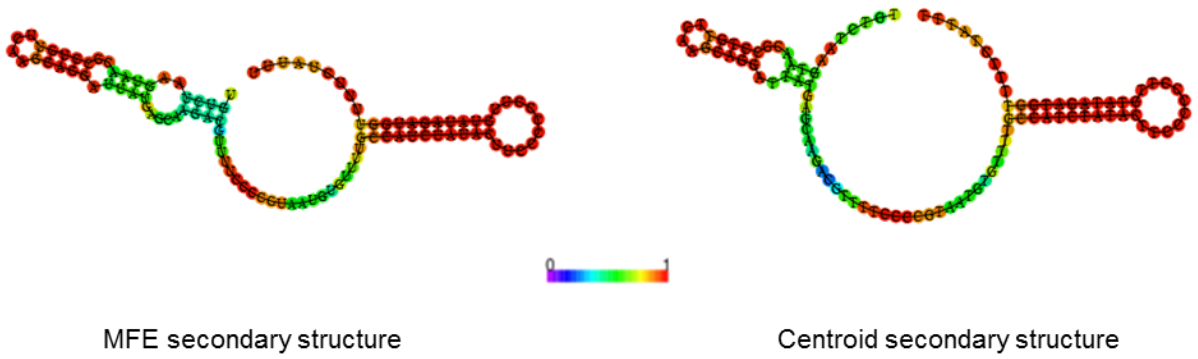

Figure 3.59: Predicted secondary structure of Bns2-2. The minimum free energy (MFE) structure and the centroid secondary structure of the sRNA Bns2-2 were predicted with the webserver of Vienna RNAfold (http://rna.tbi.univie.ac.at/cgi-bin/RNAWebSuite/RNAfold.cgi). Nucleotides are coloured according to base-pair probabilities.

NgncR_237 was rather poorly conserved among *Neisseria* and a copy of the sRNA is only present in the three closest related species. Performing a nucleotide BLAST analysis of Bns2-2 using blastn algorithm revealed the presence of the sRNA in 22 of the 29 at NCBI available genomes. The sequence of Bns2-2 of several neisserial species was aligned with the multiple sequence alignment program MAFFT to the reference sequence from *N. gonorrhoeae* strain MS11. The alignment shows that the sequence of Bns2-2 shares around 75 % sequence identity in the analysed strains (figure 3.60). The single-stranded region and so the possible target interaction domain is identical in all analysed strains, except a single nucleotide deletion in *N. elongata*. The sequence of the second stem loop, a putative Rho-independent transcription termination stem loop, is also conserved within *Neisseria*, whereas the first stem loop has a more variable sequence.

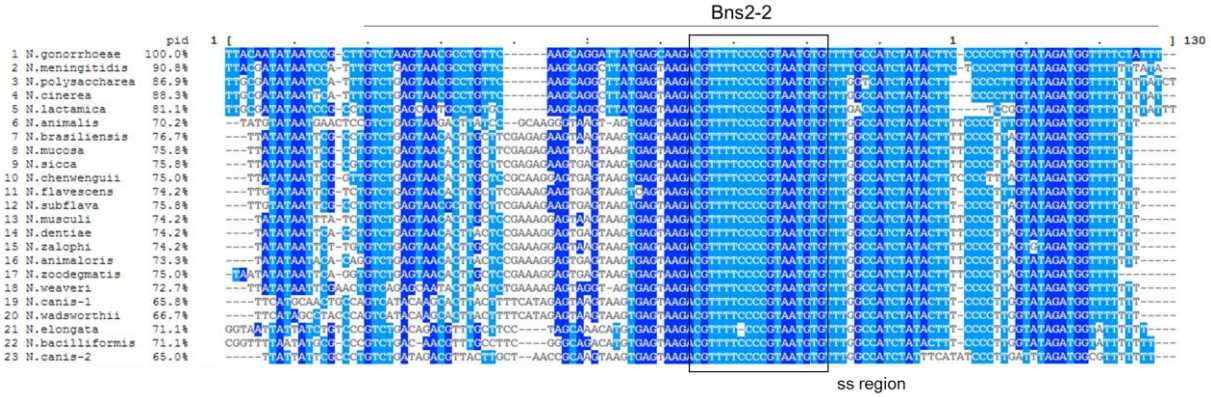

Figure 3.60: Sequence conservation of Bns2-2. The sequence alignment comprising the putative sequence of Bns2-2 and additional 20 nucleotides upstream was created with the high speed multiple sequence alignment program MAFFT (https://www.ebi.ac.uk/Tools/msa/mafft/) and visualized with the alignment editor MView (https://www.ebi.ac.uk/Tools/msa/mview/). The predicted single-stranded region is enframed. The sequence is coloured according to nucleotide identity with *N. gonorrhoeae* MS11 as reference strain. The possible single-stranded region is annotated. Strains used in the analysis: *N. meningitidis* MC58, *N. polysaccharea* ATCC 43768, *N. cinerea* ATCC 14685, *N. lactamica* 020-06, *N. animalis* ATCC 49930, *N. brasiliensis* N.177.16, *N. mucosa* C6A, *N. sicca* DSM 17713, *N. chenwenguii* 10023, *N. flavescens* SK114, *N. subflava* ATCC 49275, *N. musculi* NW831, *N. dentiae* DSM 19151, *N. zalophi* ATCC BAA-2455, *N. animaloris* NCTC12227, *N. zoodegmatis* NCTC12230, *N. weaveri* NCTC13585, *N. canis* NCTC10296, *N. wadsworthii* DSM 22245, *N. elongata subsp. glycolytica* ATCC 29315, *N. bacilliformis* DSM 23338.

Bns2-2 is located in the intergenic region between NGFG_1192 coding for a NSS-family neurotransmitter sodium symporter and NGFG_1191 encoding a pseudouridine synthase. NGFG_1192 belongs to the same family of transporters like the previously analysed NGFG_0045, target gene of NgncR_162 and NgncR_163, and is so most likely an amino acid transporter. Pseudouridine synthases convert uridine to pseudouridine, the most common posttranscriptional modification of cellular RNAs. The genomic localisation of the sRNA is quite conserved among *Neisseria* (figure 3.61). Bns2-2 is located upstream of a pseudouridine synthase in every analysed neisserial species and in nine species also downstream of a sodium transporter.

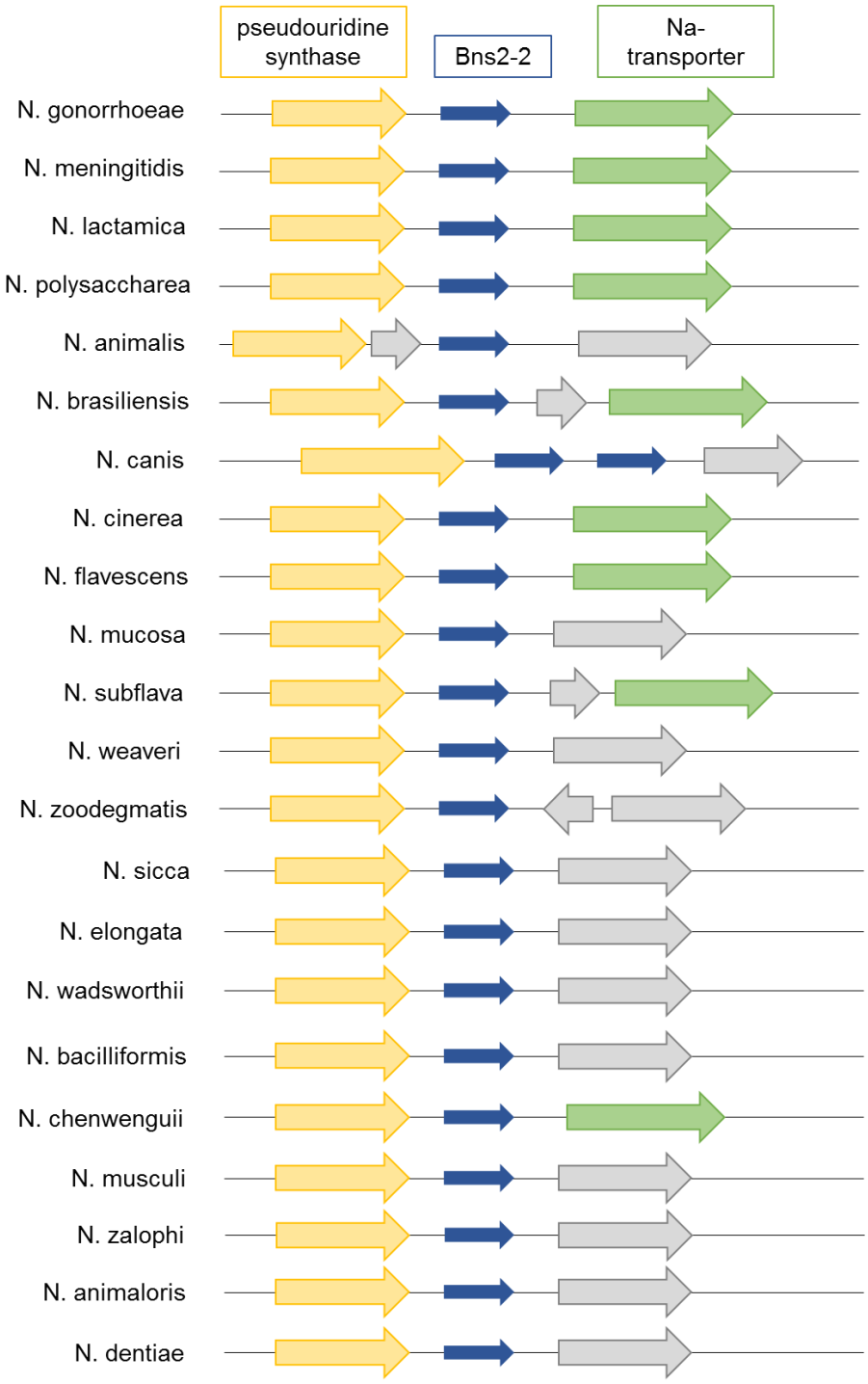

Figure 3.61: Conservation of the genomic locus of Bns2-2. The location of the sRNA and its flanking genes is mapped schematically. Pseudouridine synthase is marked with a yellow arrow, the sodium transporter with a green arrow. Non-conserved genes are shown with a grey arrow.

3.3.5.2 Analysis of the expression of Bns2-2

Although the expression of Bns2-2 is stronger than of NgncR_237 under standard growth conditions, the sRNA is still comparably low abundant. Therefore, several conditions were tested for induction of Bns2-2 expression.

Transcriptional regulators can also strongly influence sRNA expression. The impact of the two GntR-family transcriptional regulators GdhR and GntR, the two AsnC/Lrp family transcriptional regulators NGFG_1511 and NGFG_2170 and the stringent response regulator RelA was analysed (figure 3.62A). The data could not show an effect of the transcriptional regulators.

The influence of the growth phase on sRNA expression was of special interest, since results for Bns2 in *N. meningitidis* detecting induction of sRNA expression in stationary phase were obtained with a probe that could also detect Bns2-2 (Fagnocchi et al. 2015). However, Northern Blot analysis could not detect an induction of Bns2-2 expression in stationary growth phase (figure 3.62B).

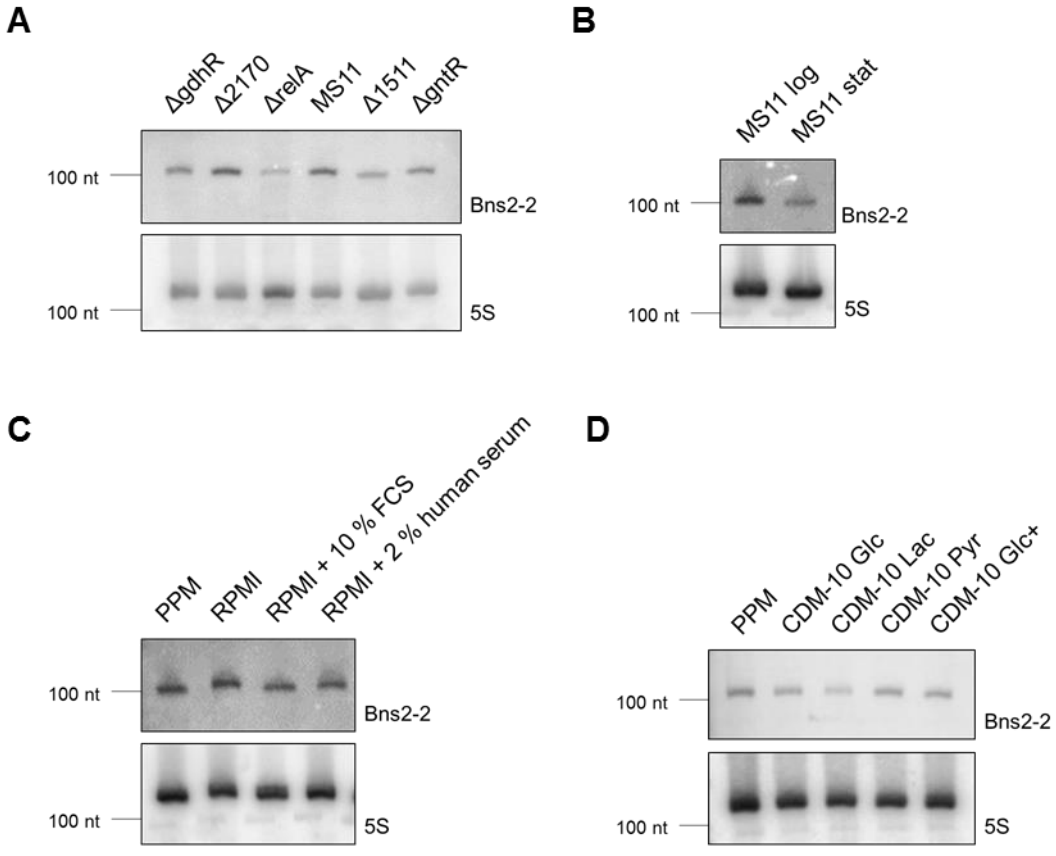

Figure 3.62: Analysing expression conditions for Bns2-2. To assess changes in the expression of Bns2-2, abundance of the sRNA was compared under various conditions by Northern Blot. Bns2-2 was analysed in the absence of several transcriptional regulators (A), under logarithmic and stationary growth (B), in presence of serum (C), and with different available carbon sources (D).

Since Bns2-2 might be as well part of the meningococcal blood-induced sRNAs, the effect of serum was tested (figure 3.62C). 10 % (v/v) fetal calf serum and 2 % (v/v) heat-inactivated human serum were added to the medium. However, none of the two substances had an effect on Bns2-2 expression.
Finally, the role of the available carbon source was analysed, since a transcript corresponding to Bns2-2 in *N. meningitidis* was shown to be affected by glucose levels (Fagnocchi et al. 2015). Bacteria were grown in a chemically defined medium containing either glucose, lactate or pyruvate or increased levels of glucose (10 g/l) as carbon source. However, the carbon source availability did not influence expression levels of Bns2-2 (figure 3.62D).

3.3.5.3 Role of Bns2-2 in infection

Bns2-2 shares the target interaction domain with NgncR_237 and so likely also targets genes involved in the formation and function of type IV pili. Therefore, Cornea epithelial cells were selected as infection model. Cells were infected with gonococci with Δopa background to avoid variability in *opa* expression, but constitutively expressing opa_{50} to enable cell invasion in the presence of phosphate. Bns2-2 does not significantly affect infection of Cornea cells (figure 3.63). The number of adherent bacteria did not change in comparison to the WT strain. Levels of invasive bacteria were slightly, however not significantly, reduced.

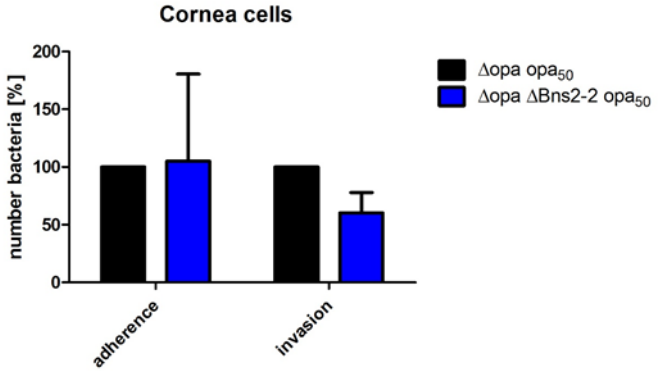

Figure 3.63: Influence of Bns2-2 on the infection of epithelial cells. Cornea epithelial cells were infected with gonococcal strains expressing no *opa* genes except opa_{50} in WT and ΔBns2-2 background. The number of bacteria was determined by cfu counting in a gentamicin protection assay (n=3).

4 DISCUSSION

Within the last years, it became clear that non-coding RNAs are important factors regarding gene regulation and adaptation to a changing environment and that they were largely underestimated before. In bacteria, they are shown to be involved in a variety of processes like virulence or respond to factors important for survival, like altered iron levels or changes in oxygen availability (reviewed in Waters and Storz 2009). Many small RNAs were found to regulate levels of outer membrane proteins, which are important for pathogenesis since they are main targets of the host immune system. Well characterized examples are the sRNAs MicA and RybB, which are both translational inhibitors of protein synthesis for a broad range of porins, including OmpA and OmpW (Udekwu et al. 2005, Papenfort et al. 2010). Most sRNAs characterized so far react to a changing environment. GcvB plays an important role during amino acid starvation (Pulvermacher et al. 2008), RyhB is activated under iron-limiting conditions (Masse and Gottesman 2002) or OxyS is produced upon oxidative stress (Altuvia et al. 1997). Nevertheless, the number of functionally characterized sRNAs is rather small, despite the strong increase of identified transcripts. The steady improvement of sequencing techniques allowed the identification of hundreds of new potential non-coding RNAs. Most of these large data sets were never analysed and so the majority of sRNAs remain uncharacterized. The transcriptome studies on *N. gonorrhoeae* revealed the presence of 253 new transcripts, which do not have a coding sequence annotation and hence could be possible non-coding RNAs (Remmele et al. 2014). In contrast to this number is the amount of characterized sRNAs in gonococci: The iron-regulated RNA NrrF (Ducey et al. 2009), FnrS responding to anaerobic growth (Isabella and Clark 2011), a cis-regulating RNA acting on *pilE* (Cahoon and Seifert 2013) and the sibling RNAs NgncR_162 and NgncR_163 (Bauer et al. 2017), which were analysed in this study. This shows that gonococcal non-coding RNAs need to be analysed in more detail for a better understanding of the role of these transcripts.

4.1 Regulation by antisense RNAs

Most of the characterized non-coding RNAs are *trans*-encoded, which further emphasizes the importance of studying *cis*-encoded antisense RNAs. They are transcribed from the same locus but in opposite orientation to their target gene and therefore share a long region of perfect complementarity. Besides sharing extended regions of complementarity, asRNAs have the advantage of being transcribed in proximity to their target gene and hence are more effective (Georg and Hess 2018). Several of the characterized asRNAs are also involved in virulence and metabolism, like the IsrR asRNA in iron metabolism of cyanobacteria (Dühring et al. 2006) or AmgR, which is associated with survival of *Salmonella* in macrophages (Lee and Groisman 2010). The discovery that nine out of eleven *opa* genes have an antisense transcript encoded on the opposite strand was striking (Remmele et al. 2014). All *opa* genes are transcribed from

a constitutive promoter, however, most of the genes are out of frame due to a change in the number of pentameric repeats caused by slipped strand mispairing. The observation that out-of-frame transcripts have a clearly reduced stability compared to in-frame transcripts (Belland et al. 1997) raised the question for the reason for this observation. Since the interaction of the predicted asRNAs with the *opa* mRNA could be inhibited by the presence of ribosomes, a negative regulatory mechanism by the asRNAs seemed an explanation for the reduced amount of out-of-frame transcripts. The regulatory mechanism that asRNAs induce cleavage of their target mRNAs by RNase III is not unusual and has been reported for several asRNAs so far (Gerdes et al. 1992, Blomberg et al. 1990, Vogel et al. 2003). However, the experiments within this study on the promoter activity and expression of the *opa* asRNAs showed that they are hardly detectable (figure 3.3). This was surprising because in the transcriptome analysis a strong expression of the *opa* asRNAs was reported (Remmele et al. 2014). Possibly, the data obtained by Remmele et al. might be a result of the high sequence conservation between all *opa* genes. The strong discrepancy in the abundance of asRNAs compared to their target mRNAs does not make an efficient regulation very likely. Additionally, the data shows that the other phase variable gene NGFG_0342 has the same decrease in abundancy of out-of-frame transcripts than the *opa* RNAs even in the absence of asRNAs (figure 3.4). This raises the question why it is possible to detect antisense transcripts for all *opa* genes when they do not seem to have a function. Transcriptome studies in several bacteria revealed that 20 % - 50 % of the protein-coding genes encode asRNAs (Dornenburg et al. 2010, Sharma et al. 2010, Mitschke et al. 2011). Nevertheless, these antisense transcripts are not conserved between related bacteria like *E.coli* and *Salmonella*. Even when comparing different *E. coli* strains, most of these RNAs are not conserved (Raghavan et al. 2012). Therefore, the authors of the study suggested that most of the antisense transcripts detected in bacterial genomes are non-functional. Further analysis of bacterial transcriptomes resulted in a simulation of asRNA-mediated regulation (Lloréns-Rico et al. 2016). The authors show that asRNA expression needs to overcome a certain threshold to achieve a regulatory effect on their target mRNA. Many asRNAs are expressed in a too low abundance to have this effect and therefore need to be considered as transcriptional noise arising from spurious promoters. This low-level expression costs very little energy and is not harmful to the bacteria. Point mutations are sufficient to generate promoter-like sequences since the σ^{70} factor binding sites have a low information content (Stone and Wray 2001). The conclusion might be that the analysed asRNAs arose from spurious promoters and are no functional transcripts. Another study tried to reproduce the data from Lloréns-Rico et al. (Michaelsen et al. 2020). They could confirm that an increase of the AT content in the bacterial genome leads to an increase of spurious promoters, but there is no correlation between occurrence of spurious promoters and the number of antisense transcripts. The conclusion is that antisense RNA expression seems to be caused by different factors and cannot be traced back to a single event like the occurrence of spurious promoters and several of these factors still need to be elucidated.

Other factors can influence the abundance of out-of-frame transcripts. Most likely, the decreased stability is caused by the loss of ribosomal protection. Ribosomes are known to protect bacterial RNAs from cleavage by nucleases and so influence mRNA decay (Deana and Belasco 2005).

4.2 The sibling sRNAs NgncR_162 and NgncR_163: regulators of bacterial metabolism

The analysis of the gonococcal transcriptome by Remmele et al. (2014) allowed the identification of several new putative non-coding RNAs, 59 of these transcripts are located in intergenic regions and therefore supposed to be *trans*-acting regulatory sRNAs. The analysis of these transcripts by co-immunoprecipitation revealed that 19 putative sRNAs are associated with Hfq, among these are NgncR_162 and NgncR_163 (Heinrichs and Rudel, unpublished). The RNA chaperone is strongly associated with the function of regulatory RNAs in bacteria by facilitating the interaction between the sRNA and the target (reviewed in Vogel and Luisi 2011). Hence, an interaction of a putative sRNA with Hfq is another indication for its regulatory function. Validation of an *in silico* prediction of possible target genes confirmed the regulation of several transcripts by NgncR_162 and NgncR_163: the amino acid transporter NGFG_1721, the transcriptional regulator GdhR, the three genes *prpB*, *prpC* and *ack* involved in propionate catabolism, NGFG_2049 associated with the degradation of valine and the citric acid cycle genes *sucC*, *sdhC*, *fumC* and *gltA* (Bauer et al. 2017). At the same time, these sRNAs were also identified in *N. meningitidis* as RcoF1/F2 (Heidrich et al. 2017) or $NmsR_A/R_B$ (Pannekoek et al. 2017). The meningococcal protein expression profile was analysed in the presence and absence of $NmsR_A/R_B$, thereby confirming regulation of the citric acid cycle genes and *prpB* and *prpC*. Heidrich et al. also confirmed *prpB* and *prpC* as targets of RcoF1/F2 and suggested according to their Hfq RIP-seq data a NGFG_1721 homologue as target gene.

The RNAseq approach led to the identification of several new target genes. High-throughput sequencing of the transcriptome of a cell was first decribed for eukaryotic cells, since working with bacterial RNA is more challenging in comparison to eukaryotic RNA. Problems are the high content of rRNA and tRNA in the RNA preparations or the very short half-life of bacterial mRNAs (reviewed in Condon 2007). To reduce detection of ribosomal RNA, samples were rRNA depleted prior to library preparation. This had the consequence that several 16S and 23S ribosomal RNAs appeared highly significantly regulated in all datasets what could not be validated by qRT PCR (data not shown). Further, several alanine tRNA loci can be found as significant hits in the RNAseq data. Since this differential regulation was not confirmed in Northern Blot experiments (figure 3.11) and these tRNAs are encoded directly upstream of 23S rRNAs, it is very likely that the postulated regulation is an artefact of ribodepletion. Another problem of the experimental approach seems to be the sensitivity. Of all genes identified by *in*

silico approaches as target genes of the sibling sRNAs, only NGFG_1721, NGFG_1722 and *ack* would fulfil the criteria set for further analysis of potential new targets. Hence, the RNAseq study allows identification of several new target genes, but does not cover the complete regulon of NgncR_162 and NgncR_163.

The initial idea of the transcriptome study was besides a better understanding of the sRNA regulon the discovery of unique target genes of NgncR_162 and NgncR_163. For all of the previously reported target genes regulation by both sRNAs is either confirmed or assumed due to predicted interaction of the common SL2 domain. Further, it could be shown that the presence of one of the sibling sRNAs is sufficient for full target regulation when tested for NGFG_1721, *gdhR*, *prpC* and *ack* (Bauer et al. 2017, Master Thesis Jonas Helmreich). This would suggest a redundant function of NgncR_162 and NgncR_163 since additionally both siblings seem to be expressed under the same growth conditions. Several other sibling sRNA were discovered in different bacteria until now and they usually do not show redundant functions. The sRNAs RfrA and RfrB in *Salmonella enterica* were both reported to be repressed under iron-limiting conditions and have a clearly overlapping role in pathogenesis (Ellermeier and Slauch 2008, Ortega et al. 2012). However, detailed analyses revealed that only RfrB is activated by the stationary phase sigma factor and targets genes only inefficiently regulated by RfrA (Padalon-Brauch et al. 2008, Kim and Kwon 2013). Only on the first glance, these sRNAs seemed to share the regulon. The analysed target genes of NgncR_162 and NgncR_163 are expected to be regulated by both sRNA since regulation of most target genes is predicted via the SL2 stem loop. It needs to be considered that the predicted interaction domain of NGFG_0045 could not be validated and therefore the sRNA region responsible for target regulation is still unknown. Especially in the case of positive regulation, for which no interaction with the Shine-Dalgarno-sequence is predicted, also different regions of the sRNAs might be applied. OmrA and OmrB in *E. coli* are both activated by a two-component system and regulate the expression of several surface proteins, but only OmrB is additionally regulated by the stress sigma factor σ^S (Guillier and Gottesman 2006, 2008, Peano et al. 2015). Members of the LhrC family comprising the seven siblings LhrC1-5, Rli22 and Rli33-1 negatively regulate expression of the genes *lapB*, *oppA* and *tcsA* in *Listeria monocytogenes*. Target regulation indicates that they act in a functionally redundant manner; however, they show differential expression profiles under infection-relevant conditions, such as induction of LhrC1-5 and Rli33-1 expression within macrophages, whereas only Rli22 is activated in the intestinal lumen of mice (Mollerup et al. 2016, Ross et al. 2019). Expression NgncR_162 and NgncR_163 was mostly analysed in rich culture media, which do not resemble most growth conditions during infection. Therefore, the expression profile of the sibling sRNAs could vary more than detected here and explain the presence of a second sRNA copy. Even under standard growth conditions, NgncR_163 is more abundant than NgncR_162 (figure 3.17). This did not seem to have a clear effect on target gene regulation as observed so far. Nevertheless, preliminary data obtained by Susanne Bauer analysing NGFG_0045 regulation indicate that complementation with NgncR_162 is not sufficient for restoring WT expression levels. It is

interesting that dataset ΔΔ162/3 versus MS11 WT of the RNAseq data includes several hits, which are highly significantly regulated, but do not show any regulation upon pulse-expression of a single sRNA. These could be possibly indirectly regulated genes and the time period after induction with AHT in strains 162AIE and 163AIE is too short to detect this effect. Other options could be that for some genes the presence of both sibling sRNAs is required for efficient regulation or the effect results from unintended genetical differences in strain ΔΔ162/3, which are not detected upon pulse-expression since both 162AIE and 163AIE are derived from strain ΔΔ162/3. This might be the case for NGFG_2042, since here complementation with both sRNAs did not result in restoring wildtype mRNA levels (figure 3.12).
The data obtained here does not allow conclusions on a redundant function of NgncR_162 and NgncR_163. They seem to be expressed under the same conditions and all initially tested target genes were regulated by both sRNAs. However, many target genes were never tested for regulation with the individual sibling sRNA and it was just assumed that both sRNAs are involved since regulation is predicted via the SL2 stem loop. The analysis of NGFG_0045 shows that NgncR_162 and NgncR_163 might also have unique functions.

4.2.1 Influence of NgncR_162/163 on amino acid metabolism and transport

The presence of new datasets of potential target genes of the meningococcal homologues allowed initial progression in the search for further transcripts regulated by NgncR_162 and NgncR_163. Comparing both lists of potential target genes for the meningococcal homologues revealed a common feature: histidine biosynthesis (Heidrich et al. 2017, Pannekoek et al. 2017). Out of the seven transcripts suggested to be regulated by RcoF1, one is the imidazole glycerol phosphate synthase HisH (Heidrich et al. 2017). Pannekoek et al. observed the 1-(5-phosphoribosyl)-5-[(5-phosphoribosylamino)-methylideneamino] imidazole-4-carboxamide isomerase HisA to be differentially regulated in the absence of $NmsR_A$ and $NmsR_B$. HisH and HisA catalyse subsequent steps in the biosynthesis of histidine and are encoded together with *hisF* and *hisI* in an operon. Interestingly, also HisB, which is catalysing the step after HisH in histidine biosynthesis, came into focus since its gene is co-transcribed with the validated target gene NGFG_2049. The pathway for histidine biosynthesis is conserved among all organisms. Histidine biosynthesis is linked to the synthesis of pyrimidine nucleotides, purine nucleotides and tryptophan and the accumulation of intermediates was shown to activate the stringent response in *E. coli* (reviewed in Winkler and Ramos-Montañez 2009). HisH and HisB were analysed for potential regulation by NgncR_162 and NgncR_163. The fold change detected in qRT PCR experiments in presence and absence of the sibling sRNAs is rather small, nevertheless significant (figure 3.8). Since cultivating gonococci in a medium without histidine did not result in any changes in target gene expression, although it might be possible that stringent washing or longer starvation times are required, a role of the sRNAs in histidine biosynthesis remains unclear. Nevertheless, the number of target genes related with histidine

biosynthesis appearing in the context of the sibling sRNAs is striking. According to the RNAseq data in dataset ΔΔ162/3 versus MS11, also *hisG* is significantly regulated by NgncR_162 and NgncR_163. In the other two datasets the gene also seems regulated, but statistical significance was missed. Regulation of *hisG* by the sibling sRNAs was not experimentally validated, but would increase the number of genes of the histidine biosynthesis pathway.

Several genes appearing to be differentially regulated by the sibling sRNAs are also suggested to be targeted by sRNAs in *N. meningitidis*. The comparison of the protein expression profile by mass spectrometry in presence and absence of the meningococcal sRNA homologues $NmsR_A$ and $NmsR_B$ resulted in a list comprising ten genes putatively positively regulated by the sibling sRNAs (Pannekoek et al. 2017). These genes include leucine tRNA synthetase *leuS* and two genes involved in branched-chain amino acid synthesis, *ilvD* and *ilvA*. Isoleucine, leucine and valine biosynthetic genes, therefore called *ilv* genes, are clustered in several operons and whereas *ilvA* is only involved in isoleucine biosynthesis, the other genes are required for all three amino acids (Vitreschak et al. 2004). Changes of intracellular concentrations of branched-chain amino acids are linked to important physiological responses like virulence gene expression and therefore the biosynthetic genes are subject of transcriptional regulation (reviewed in Kaiser and Heinrichs 2018). Other sRNAs were already shown to regulate branched-chain amino acid synthesis. In *Listeria monocytogenes*, the sRNA Rli47 is responsible for specific repression of *ilvA* by direct binding of the RBS. The sRNA is activated under stress conditions and might serve to block growth (Marinho et al. 2019). According to RNAseq data, in gonococci three other genes of the branched chain amino acid biosynthesis pathway, but not *ilvA* and *ilvD*, are positively regulated by the sRNAs: *ilvB*, *ilvC* and *ilvH*. All three genes are highly significantly regulated according to dataset ΔΔ162/3 versus MS11; only *ilvC* is also regulated upon pulse-expression of the sibling sRNAs. The three genes are encoded in loci NGFG_2039 (*ilvC*), NGFG_2041 (*ilvH*) and NGFG_2042 (*ilvB*) and might be part of an operon, though individual transcriptional start sites are annotated for NGFG_2040 and NGFG_2042 (Remmele et al. 2014). Additionally, NGFG_2040, encoding a hypothetical protein that is most likely an antibiotic biosynthesis monooxygenase, reaches statistical significance in two datasets and is just above cut-off in dataset AIE163 versus ΔΔ162/3. According to IntaRNA analysis, NgncR_162 is predicted to interact with its SL2 stem loop within the coding region of NGFG_2042 (*ilvB*) and with its SSR1 region directly upstream of the start codon of NGFG_2040 (data not shown). Regulation of *ilvC* was tested, but could not be confirmed by qRT PCR; nevertheless, the number of genes is noticeable. A positive regulation of branched-chain amino acid synthesis by NgncR_162 and NgncR_163 would fit to negative regulation of degradation of branched-chain amino acids, since downregulation of NGFG_2049 by the sibling sRNAs was already confirmed (Bauer et al. 2017).

Several other putative target genes of NgncR_162 and NgncR_163 from the RNAseq data are differentially expressed in an *hfq* deletion mutant of *N. meningitidis* (Fantappie et al. 2011).

Stability of the sibling sRNAs is largely affected by Hfq in both gonococci and meningococci (Heinrichs and Rudel, unpublished; Heidrich et al. 2017) and hence target genes of the sibling sRNAs are also expected to be differentially regulated in an *hfq* deletion mutant. Interestingly, many of the common differentially regulated genes encode transport proteins. These include the amino acid transporters NGFG_1721, NGFG_0045, NGFG_0093 and NGFG_1564, the citrate transporter NGFG_0249, the peptide transporter NGFG_1937, the glucose/galactose transporter NGFG_2263 and lactate permease NGFG_1471. Significant differential expression of all of genes except NGFG_0093 and NGFG_2263 was confirmed by qRT PCR (figure 3.13). Regulation of outer membrane or transport proteins is well-reported for non-coding RNAs, although this might be due to easy detection of these proteins (reviewed in Waters and Storz 2009). The sRNA GcvB in *E. coli* targets the periplasmic-binding protein components of the two major peptide transport systems DppA and OppA and the amino acid transporter SsT. Since their expression is repressed in full medium, it is suggested that GcvB negatively regulates peptide and amino acid transport under nutrient-rich conditions (Pulvermacher et al. 2008 and 2009). SR1 in *Bacillus subtilis* is expressed under gluconeogenic conditions and negatively regulates the arginine catabolic operons, which also encode a transport protein (Heidrich et al. 2007, Gimpel et al. 2012). Phosphosugar stress induces expression of SgrS sRNA in *E. coli*, which is subsequently downregulating the major glucose transporter protein, PtsG, by reducing translation and stability of the mRNA (Kawamoto et al. 2005 and 2006). Such clear relationships cannot be postulated for NgncR_162 and NgncR_163, the functions of the regulated genes are too divers. Nevertheless, most regulated transport proteins are involved in amino acid transport and several other validated target genes regulate pathways in amino acid metabolism, hence a connection between both processes seems likely. Adaptation of citrate transport also matches downregulation of several citric acid enzymes including citrate synthase. The results show that the sibling sRNAs are able to coordinate several different metabolic processes.

Genes most strongly regulated by NgncR_162 and NgncR_163 are the alanine transporter NGFG_1721 and D-amino acid dehydrogenase *dadA* (NGFG_1722). NGFG_1722 is co-transcribed with NGFG_1721, nevertheless IntaRNA predictions indicate direct regulation by the sibling RNAs by interaction of the sRNAs with the RBS of the gene. Eva-Maria Hörner confirmed direct regulation during her bachelor thesis. The D-amino acid dehydrogenase DadA was shown to be essential for D-alanine catabolism in gram-negative bacteria and was shown to have a broad subsrate specificity: D-histidine, D-phenylalanine, D-serine, D-threonine and D-valine can be used as substrated as well (He et al. 2011). Regarding its localisation in an operon with the alanine transporter NGFG_1721, a role of DadA in D-alanine metabolism seems quite likely. According to the KEGG pathway database, *N. gonorrhoeae* metabolises D-alanine to L-alanine via alanine racemase or to D-alanyl-D-alanine for peptidoglycan metabolism (Kanehisa and Goto 2000). Peptide chains attached to the N-acetylmuramic acid consist of two to five amino acids of the sequence L-Ala-D-Glu-meso-Dap-D-Ala-D-Ala in *N.*

gonorrhoeae. During growth, gonococci release an unusual amount of peptidoglycan fragments, which are inducing an inflammatory response in the human host. 15 % of peptidoglycan monomers are released by gonococci, making uptake and racemisation of alanine even more important (reviewed in Schaub and Dillard 2019). In 13 of the analysed genomes, the sibling sRNAs are encoded in close proximity to an alanine racemase (figure 3.7). Hence, the conserved localization of alanine racemase downstream of the sibling sRNAs was considered in this context as interesting. Nevertheless, it was not possible to show regulation of alanine racemase by NgncR_162 and NgncR_163. Further, an AsnC/Lrp-family transcriptional regulator is located between the sRNAs and alanine racemase. The protein family is involved in regulation of amino acid metabolism and binding of a ligand influences activation or repression of some target promoters (Thaw et al. 2006). In *E. coli*, an AsnC/Lrp-family transcriptional regulator was shown to regulate the *dadAX* operon and binding affinity is influenced by the presence of leucine and alanine (Zhi et al. 1999). However, a regulatory network including the transcriptional regulator NGFG_2170 could not be confirmed. Expression levels of *dadA* remained unchanged upon deletion of NGFG_2170 and also mRNA levels of NGFG_1721 and alanine racemase did not alter significantly when cultured in PPM+ or Hepes medium (data not shown). Whether there is a connection between these genes and the sRNAs remains unclear.

Although NgncR_162 and NgncR_163 do not seem to be influenced by D- or L-alanine in the growth medium, metabolome analyses revealed a connection between the sibling sRNAs and alanine metabolism. Due to the strong regulation of the alanine transporter NGFG_1721, differences in alanine uptake were expected in the absence of the sRNAs, which could not be observed after feeding bacteria with ^{13}C-labeled D-alanine. In some bacteria, amino acid transporters exhibit a stereo-specificity what is also true for some alanine transport proteins (Sidiq et al. 2020). Thus, it might be possible that NGFG_1721 is not involved in D-alanine import. Analysis of spent culture media at the department of botany (Markus Krischke, University of Würzburg) showed that L-alanine levels do not change upon deletion of NgncR_162 and NgncR_163, giving rise to the question why downregulation of an alanine transporter does not influence alanine uptake. NGFG_1721 is annotated as an alanine transporter and doing a BLAST analysis on the amino acid sequence showed that the homologues in related species are annotated as alanine transporters as well. Nevertheless, this was never confirmed and the data could be explained if NGFG_1721 were a transporter for another amino acid. Metabolome analysis also revealed that D-alanine is not further metabolised in gonococci. Alanine can be converted into pyruvate and subsequently be used in fatty acid synthesis, the citric acid cycle and synthesis of other amino acids. The observation that alanine is not feeding the citric acid cycle to a great extent is not surprising considering that the amino acid cannot be used as energy source (Hebeler and Morse 1976), nevertheless it is interesting that alanine is converted at least in small parts to acetyl-CoA, as indicated the isotopologue profile, but not further metabolised. Derivatisation of the incorporated alanine uncovered that the sibling sRNAs influence conversion of D-alanine to L-alanine. The enzyme

responsible for this reaction step is alanine racemase. The gene is listed in the RNAseq analysis in dataset ΔΔ162/3 versus MS11 as significantly regulated, however, the fold change is comparably small and it was shown to be not affected by the absence of NgncR_162 and NgncR_163 in qRT PCR analysis (figure 3.28). Consequently, alanine racemisation should not differ in the sRNA KO strain. A conversion of D-alanine to L-alanine via pyruvate seems possible and at least one of the involved enzymes, DadA, is a confirmed target gene of the sibling sRNAs.

Validation of RNAseq data revealed an influence of the sibling sRNAs on the metabolism of another amino acid. Levels of *gcvH* mRNA significantly increase in strain ΔΔ162/3 (figure 3.11). The glycine cleavage system is composed of four proteins, including the carrier protein GcvH, and degrades glycine to CO_2, NH_4^+ and a methylene group accepted by tetrahydrofolate (reviewed in Kikuchi et al. 2008). Interestingly, it was already reported for the meningococcal homologues $NmsR_A$ and $NmsR_B$ to downregulate serine hydroxymethyltransferase GlyA (Pannekoek et al. 2017). The reaction catalysed by the enzyme is linked to glycine cleavage, since GlyA reversibly converts glycine to serine and thereby recovers tetrahydrofolate required as carbon carrier for glycine cleavage (Bang and Lee 2018). In the absence of Hfq, mRNA levels of both *glyA* and *gcvT* are significantly upregulated in meningococci (Fantappie et al. 2011). GcvT is one of the four proteins of the glycine cleavage complex and required for the tetrahydrofolate-dependent reaction (reviewed in Kikuchi et al. 2008). Post-transcriptional regulation of both reactions, glycine cleavage and the GlyA-mediated reaction, makes an influence of the sRNAs on glycine metabolism more likely.
NgncR_162 and NgncR_163 seem to be associated mostly with the metabolism of non-polar amino acids, meaning the three branched-chain amino acids and alanine and glycine. Interestingly, the analysis of culture supernatants revealed a connection to another non-polar amino acid, proline. According to data obtained by Susanne Bauer in cooperation with the department of botany (Markus Krischke, University of Würzburg), proline levels in the spent culture media decreased for strain ΔΔ162/3 and especially for a knockout mutant of the amino acid transporter NGFG_0045. An increased uptake of proline might be a compensation for reduced uptake of another amino acid. According to KEGG pathways, *Neisseria* metabolise proline by converting it to glutamate, which can subsequently be integrated in the citric acid cycle or be used for other amino biosynthesis pathways. Levels of glutamate in the spent culture media did not differ in the mutant strains in comparison to the WT. Thus, the amino acid transported by NGFG_0045 requires further investigation as well as the cause for differences in proline uptake.

4.2.2 Role of the sRNAs in central metabolism

The RNAseq screen allowed identification of another target gene, aconitate hydratase, which is involved in both citric acid and methylcitrate cycle. Considering that already several enzymes of both the citric acid and methylcitrate cycle are confirmed as target genes of the sibling sRNAs, like citrate synthase, fumarate hydratase or acetate kinase, role of NgncR_162 and NgncR_163 in central metabolism seems likely. All these genes, including aconitate hydratase, are also suggested as target genes of the sibling sRNAs in meningococci, leading to the hypothesis that the sRNAs generally control metabolic switches (Pannekoek et al. 2017).
It has been reported that growth on glucose reduces levels of citric acid cycle enzymes in gonococci and these enzymes are also downregulated in meningococci upon incubation in glucose-rich human blood (Morse and Hebeler 1978, Echenique-Rivera et al. 2011). Adaptations to available carbon sources are important for successful colonization of different niches within the human host, since for example blood and the female genital tract contain high levels of both glucose and lactate, whereas glucose levels in oral cavities are rather low (reviewed in Quillin and Seifert 2018). According to literature, gonococci can use only glucose, lactate and pyruvate as sole carbon source (Morse and Bartenstein 1974). Testing sRNA expression in media containing one of the three carbohydrates, glucose, lactate or pyruvate, revealed a promoter-independent downregulation of sRNA levels in media containing exclusively lactate as carbon source compared to glucose (figures 3.34+35). *Neisseria* take up lactate via lactate permease, a transporter significantly downregulated in the absence of the sibling sRNAs. This regulation is most likely indirectly via the transcriptional regulator GdhR (figure 3.13) as lactate permease was confirmed as target gene of GdhR (Ayala and Shafer 2019). The taken up lactate is subsequently oxidized to pyruvate and gonococci possess at least three distinct lactate dehydrogenases (Atack et al. 2014). Studies in *N. meningitidis* showed that growth on glucose results in the highest growth yield since lactate and pyruvate need to feed additionally into the gluconeogenesis pathway, nevertheless, growth on lactate seems less favourable than growth on pyruvate (Leighton et al. 2001). Comparably, sRNA levels were highest during growth on glucose and lowest during growth on lactate. In meningococci, one sRNA was identified to be affected by the carbon source availability. Bns1, corresponding to NgncR_152 in gonococci, was shown to be differentially induced by glucose and to regulate several genes of the methylcitrate cycle, which are targets of NgncR_162 and NgncR_163 as well (Fagnocchi et al. 2015). Transcriptome analysis in meningococci in presence and absence of glucose revealed differential regulation of 82 genes (Antunes et al. 2016). The strongest regulated genes include several genes targeted by NgncR_162 and NgncR_163. In the presence of glucose, all genes of the tricarboxylic acid cycle are downregulated, as well as *prpB*, *prpC* and *ack*. Interestingly, also mRNA levels of the transcriptional regulator GdhR are clearly downregulated. Transcriptome profiles of *E. coli* cells were compared by microarray analysis after growth on media supplemented with either pyruvate or glucose (Kaberdina et al. 2019). This led to the detection of differential regulation

not only of genes involved in central carbon metabolism, but also of several sRNAs including CyaR, RyhB, GcvB and RyeA, showing that adaptations of sRNA levels depending on available metabolites is not unusual in bacteria. CyaR is an sRNA activated by Crp under conditions in which cAMP levels are high, so when glucose levels are low. The sRNA regulates a variety of target genes, including several outer membrane proteins (De Lay and Gottesman 2009). Another sRNA is negatively regulated by Crp and so cAMP. Spot 42 is involved in regulation of various metabolic processes including central metabolism and was shown to reduce bacterial growth in the presence of several non-preferred carbon sources, which are transported or metabolised by its target genes (Beisel and Storz 2011). NgncR_162 and NgncR_163 might play a role in metabolic adaptations to growth on glucose, considering regulation of several genes in central metabolism and the limited growth of strain ΔΔ162/3 in a medium containing exclusively glucose as carbon source.

The newly identified target gene of the sibling sRNAs, aconitate hydratase, is found in the same genomic localisation as *prpB* or *prpC* and is hence most likely part of the methylcitrate cycle. The methylcitrate cycle is tightly linked to the citric acid cycle and converts propionate and oxaloacetate into pyruvate and succinate. Propionate is a short chain fatty acid that is toxic for bacteria in higher concentrations (reviewed in Dolan et al. 2018). It was shown for *Mycobacterium tuberculosis* that the cycle can operate in reverse to generate propionyl-CoA for fatty acid biosynthesis when bacteria grow on lactate or pyruvate (Serafini et al. 2019). In meningococci, the utilisation of propionate as a supplementary carbon source is reported to support growth particularly under nutrient-limiting conditions (Catenazzi et al. 2014). Addition of propionate to the growth medium led to a negative effect on bacterial growth, what was expected due to its cytotoxicity. However, no effect on mRNA expression of methylcitrate cycle enzymes or sRNA expression could be observed (figure 3.37). In strain MS11, like in several other gonococcal strains, *prpB* is split into two ORFs due to a stop codon in the 5’ region of the gene. Therefore, these gonococcal strains might not have a functional methylcitrate cycle what would explain why enzyme levels do not increase upon incubation with propionate. Meningococci code for another sRNA, Bns1, which also regulates the *prpB-prpC* gene cluster (Del Tordello et al. 2012). Regulation of these genes by the gonococcal homologous sRNA, NgncR_152, however, could not be confirmed (Eva-Maria Hörner, bachelor thesis). The data indicate that the methycitrate cycle plays a minor role in gonococci compared to meningococci.

4.2.3 sRNA expression in various chemically defined media

Chemically defined media allow the analysis of the impact of single medium components on sRNA or gene expression and therefore are indispensable for studies of metabolic regulations. Interestingly, sRNA levels were decreased in a subset of the selected chemically defined media as well as the respective change in target gene expression could be observed (figure

3.27). The most obvious explanation for these results was an impact of the growth rate, since the sibling sRNAs are downregulated during stationary growth phase and the growth rate of gonococci is clearly reduced in both RPMI and Hepes medium. The growth rate was artificially decreased by addition of antibiotics (figure 3.33) or by testing mutant strains with growth defect (data not shown); however, no effect on NGFG_1721 mRNA levels could be observed. In both conditions, stationary phase and growth in Hepes medium, sRNA stability is affected and transcript levels of RNase II and RNase III are significantly increased. Thus, there might still be a connection between a reduced growth rate and sRNA expression. On the other hand, other factors influencing sRNA levels, like *hfq* expression or the relative promoter activity, differ in the tested conditions. Since NgncR_162 and NgncR_163 seem to be involved in the adaptation of the gonococcal metabolism to a changing environment, this regulation might not be required during growth in minimal media that probably lack nutrients inducing sRNA-dependent regulation and therefore sRNA levels are downregulated. It has been shown for other bacteria that a switch from nutrient rich growth conditions to a minimal medium results in differential expression of several sRNAs (Mohd-Padil et al. 2017). Even the NgncR_163-homologue $NmsR_B$ is differentially expressed in Jyssum medium compared to nutrient-rich TSB medium, although here an upregulation is observed (Pannekoek et al. 2017). Gonococci are fastidious organisms with complex nutritional requirements (Spence et al. 2008) and hence growth in minimal media could cause a reduced growth rate. Four chemically defined media were analysed and growth was only affected in RPMI and Hepes medium, but not in Graver-Wade medium or CDM-10. This allows the conclusion that the nutrient composition of both Graver-Wade medium and CDM-10 seem to better correspond to the requirements of gonococci. Comparing the media composition did not allow any conclusions on the compounds responsible for the growth phenotype since all tested media vary in their composition. Adding several components of Graver-Wade medium to Hepes medium, as additional inorganic salts, amino acids and vitamins, did not recover gonococcal growth (data not shown). Hepes medium also contains a comparibly high amount of acetate. *Neisseria* were shown to secrete acetate into the medium, especially during growth on glucose (Baart et al. 2007). High acetate concentrations in the growth medium can cause acid stress and gonococcal growth can be inhibited by acetate (Negrete and Shiloach 2015, Breshears et al. 2015). Therefore, in addition to supplementing Hepes medium with further nutrients, acetate levels were reduced. Nevertheless, this did not have any effects on gonococcal growth (data not shown). The most striking component of CDM-10 is the high glutamate level: 1.3 g/l in comparison to 0.04 g/l in Graver-Wade medium and 0.02 g/l in RPMI, whereas Hepes medium does not contain any glutamate at all. Addition of glutamate to Hepes medium did alter neither the growth phenotype, nor sRNA expression levels (data not shown). Due to the different composition of CDM-10 and Graver-Wade medium or RPMI and Hepes medium, it seems unlikely that a single compound causes the growth defect and more knowledge on gonococcal nutrient requirements is necessary to identify the factors responsible for changes in gonococcal growth and sibling sRNA expression.

4.3 Growth phase dependency of NgncR_162 and NgncR_163 expression

When nutrient availability is not sufficient to sustain steady growth, bacteria enter stationary phase, which is a tightly regulated process (reviewed in Navarro Llorens et al. 2010). Not surprisingly also sRNA regulators are involved in this process. *Salmonella enterica* serovar Typhimurium was reported to express 140 sRNAs at early stationary phase (Kröger et al. 2012) and a screen for identification of novel sRNA in *E. coli* showed that most detected sRNAs have increased expression levels upon entry into stationary phase (Argaman et al. 2001). Even in *N. gonorrhoeae*, several sRNAs were shown to be induced in late log through stationary phase (Jackson et al. 2017). Entry in stationary phase requires adaptations to reduced nutrient availability and hence adaptation of bacterial metabolism. The sRNA RsaE in *Staphylococcus aureus* accumulates in late exponential growth phase and targets various metabolic pathways, including amino-acid transport and metabolism, carbohydrate metabolism and energy production (Geissmann et al. 2009). Unlike most of the reported sRNAs differentially expressed in the growth phases, RNA levels of NgncR_162 and NgncR_163 decrease upon entry in stationary phase (figure 3.22). Since sRNA levels are also reduced during growth in minimal media, NgncR_162 and NgncR_163 seem to be important during growth in nutrient-rich conditions. Downregulation of sibling sRNA levels seems to be promoter-independet (figure 3.23) and hence is rather caused by a decrease in sRNA stability due to reduced Hfq levels or increased RNase activity. Transcript amounts of both NgncR_162 and NgncR_163 clearly decrease in the absence of Hfq and transcript levels of the RNA chaperone significantly decrease upon entry in stationary phase (figure 3.24). Downregulaion of Hfq in stationary phase was already reported for *E. coli* (Ali Azam et al. 1999) and it was suggested that the reduced amount of Hfq affects the stability of the regulatory RNA MicA (Andrade and Arraiano 2008). Interestingly, also mRNA levels of several enzymes involved in RNA degradation are upregulated in stationary phase, mostly affected is RNase II mRNA (figure 3.25). SRNAs are mostly degraded by RNase E and PNPase or, if bound to its target mRNA, by RNase III (reviewed in Saramago et al. 2014). Transcript levels of all three enzymes are upregulated in stationary phase in gonococci (figure 3.25) and an increased activity could therefore affect NgncR_162 and NgncR_163. In *E. coli*, a higher enzymatic activity of RNase II, RNase R and PNPase was observed in stationary phase, suggesting a role of PNPase in the degradation of free sRNAs (Pobre et al. 2019). A possible role of PNPase in degradation of the sibling sRNAs could not be tested since all attempts constructing a PNPase mutant failed.

4.4 Positive regulation by NgncR_162 and NgncR_163

Transcriptome analysis resulted in the identification of several positively regulated target genes. Neither for NgncR_162 and NgncR_163, nor for the meningococcal homologues

RcoF2 and RcoF1 any positively regulated target genes are reported (Bauer et al. 2017, Heidrich et al. 2017). Only for $NmsR_A$ and $NmsR_B$ a group of putatively positively regulated target genes was reported, however, these were not validated (Pannekoek et al. 2017). Most negatively regulated target genes seem to be regulated by interference with ribosome binding, the mechanism of positive regulation of the validated target genes is, however, unclear. NGFG_0045 was selected as example for studying the regulatory mechanism. Nevertheless, data only suggest a direct post-transcriptional regulation of NGFG_0045 not involving its 5' UTR, since an exchange of the promoter region did not alter regulation of the NGFG_0045 mRNA (figure 3.16), but an impact of the sibling sRNAs on mRNA stability could not be experimentally confirmed. The predicted interaction region at the 3' end of the coding sequence seems not be targeted by the sibling sRNAs. Truncated versions of NGFG_0045 lacking two or six N-terminal transmembrane domains out of twelve transmembrane domains in total were analysed for NgncR_162- and NgncR_163-dependent regulation (experiments performed by Susanne Bauer). However, this analysis did not result in the identification of the sequence interacting with the sRNAs. The deletions cover overall large parts of the coding sequence of NGFG_0045, nevertheless, the interaction sequence could not be identified. Binding within the coding sequence of a target transcript can be associated with interference with RNase-dependent degradation. The coding sequence of *rbn* mRNA harbours several RNase E cleavage sites within the region of greatest complementarity to the sRNA GcvB and the binding of Hfq additionally increases transcript stability (Chen et al. 2019). Another possible regulatory mechanism could be the interaction of NgncR_162 and NgncR_163 within the 3' UTR of NGFG_0045 mRNA. The sRNA GadY was suggested to base pair with the 3' UTR of *gadX* mRNA, thereby increasing transcript stability by interfering with exonucleic degradation (Opdyke et al. 2004). However, IntaRNA analysis predicted besides the region at the 3' end of the coding sequence only one alternative binding site at the 5' end with negative minimal energy when the analysis was repeated with NgncR_163. Since this region was covered by the truncations examined by Susanne Bauer, positive regulation of NGFG_0045 remains enigmatic.

4.5 Influence of NgncR_162 and NgncR_163 on invasion of epithelial cells and PMNs

Small RNAs are also associated with virulence and pathogenicity. The pathogenicity island-encoded sRNA IsrM of *Salmonella* is necessary for invasion of epithelial cells or replication within immune cells (Gong et al. 2011). Other sRNAs regulate virulence genes like the antisense RNA AmgR (Lee and Groisman 2010) or are important at early or late infection times upon entry into the host cell (Ortega et al. 2012). To investigate the role of the sibling sRNAs in infection, epithelial cells were infected with WT, double KO and complementation strain and Opa_{50}-dependent invasion analysed. Susanne Bauer detected in a Gentamicin protection

assay a reduced number of invasive gonococci in the absence of NgncR_162 and NgncR_163. The same effect was observed by differential immuno-staining, indicating reduced invasion but not reduced survival of the double KO strain (figure 3.43). Regarding the validated target genes of the sibling sRNAs, this result is rather surprising. Most of the mRNAs differentially regulated by NgncR_162 and NgncR_163 are involved in metabolic and transport processes and there are no hints of genes important for cell contact or bacterial uptake. It is hypothesised that gonococci trigger influx of neutrophils into infected tissues to promote nutrient acquisition and gain access to intracellular nutrient pools (reviewed in Quillin and Seifert 2018). Nutrient levels within the cells are expected to differ from the surrounding culture medium. Therefore, the presence of the sibling sRNAs could be of importance for intracellular survival. Literature for infection of epithelial cells by gonococci is quite diverse and infection times vary from 1 h (Solger et al. 2020) to 6 h (Bauer et al. 1999). Hence, the chosen infection time of 3 h might be too long to clearly differentiate between reduced invasion and survival of gonococci in the absence of the sibling sRNAs and NgncR_162 and NgncR_163 could still influence gonococcal survival within epithelial cells.

Gonococci are also known to invade neutrophils and to survive and replicate within these cells (reviewed in Johnson and Criss 2011). Consequently, survival of gonococci in PMNs could be also influenced by the sibling sRNAs. Nevertheless, the data did not show any significant effect of NgncR_162 and NgncR_163 on the survival rate (figure 3.44). This might be due to the high experimental variability, since gonococci also need to adapt their metabolism to the different milieu in presence of neutrophils (reviewed in Johnson and Criss 2011). Several factors influence immune cells like the nutritional status or hormone levels of the donor and variations increase when different donors are used for the experiment (Kleiveland 2015). Therefore, several more replicates might be needed to see an effect. In the presence of neutrophils, gonococci are exposed to high concentrations of lactate produced by PMNs during glycolysis, which stimulates gonococcal metabolic activity and oxygen consumption increases (Britigan et al. 1988). Since the sibling sRNA levels are downregulated in media containing lactate instead of glucose, NgncR_162 and NgncR_163 might not be important for survival in the presence of neutrophils. For other bacteria it has been shown that they display stationary phase physiology when residing within immune cells (Wang et al. 2015, reviewed in Wayne and Sohaskey 2001), so another condition in which sRNA levels are decreased. Hence, NgncR_162 and NgncR_163 seem not to play a role for gonococcal survival within human neutrophils.

4.6 A gonococcal homologue of the sRNA Bns2

The analysis of the meningococcal transcriptome in a time-course experiment upon incubation in whole-blood led to the detection of a set of sRNAs, termed Bns, upregulated in human blood (Del Tordello et al. 2012). Analysis of the gonococcal homologue of Bns2, NgncR_237, was initiated here. Bsn2 is reported with a length of 85 nucleotides and runs in Northern Blot

beneath 100 nt (Del Tordello et al. 2012). Bns2 binds strongly to the RNA chaperone Hfq (Heidrich et al. 2017) and since sequence comparison shows that Bns2 and NgncR_237 are 99 % identical, it can be assumed that NgncR_237 interacts with Hfq as well.

4.6.1 Target genes of NgncR_237: influence of NgncR_237 on type IV pilus biogenesis

The application of two *in silico* target prediction tools, TargetRNA2 and CopraRNA, as well as a differential RNAseq analysis allowed the identification of several target genes of NgncR_237. The validated target genes NGFG_1006 and *alaT* of the *in silico* approaches do not appear as regulated in the RNAseq data. This indicates that the aim finding the complete regulon of NgncR_237 by transcriptome analysis failed. Potential target genes were validated in both *E. coli* and in *N. gonorrhoeae*. Nine genes were significantly regulated according to qRT PCR analysis (figure 3.48), however, two of these genes, *pilE* and *rng*, were not further analysed due to loss of regulation upon comparison in the same genetic background, in strain Δ237 AIE237 with and without induction with AHT (figure 3.49). The seven remaining genes are all negatively regulated by the sRNA. Katharina Wagler (University of Würzburg) performed during her Master thesis additional validation experiments in *E. coli*. She could confirm regulation of four genes showing significant differential expression in qRT PCR experiments (*dinD*, *alaT*, NGFG_1006 and *pilG*) and observed further regulation for *pilX*, *hpaC* and NGFG_0515. In contrast to *pilX, hpaC* and NGFG_0515 show some regulation by NgncR_237 in the qRT PCR experiments, though not significant, and therefore cannot be ruled out as potential target genes. NGFG_1617 was not analysed in *E. coli* due to its predicted interaction site within the coding sequence. NGFG_1479 and NGFG_1338 do not seem regulated in the *E.coli* two-plasmid system. The result for NGFG_1479 was surprising since the gene is significantly regulated in the qRT PCR data and has an extended complementarity of its 5' UTR to the single-stranded region of NgncR_237. It was reported for another sRNA target gene, *gdhR,* that regulation by NgncR_162 and NgncR_163 could not be detected in the *E. coli* system (Bauer et al. 2017) and therefore NGFG_1479 cannot be ruled out as target gene. Post-transcriptional regulation of *dinD*, NGFG_1006 and *pilG* could be confirmed on protein level. Efforts of testing NGFG_1479 on protein level were not successful due to problems generating a mutant strain.

Regulation of these genes is negative. Pairing between the sRNA and its target mRNA mostly involves a seed region of six to eight base pairs. Therefore, sRNAs often have a conserved, single-stranded region for target interaction (reviewed in Gottesman and Storz 2011). The single-stranded region flanked by two hairpin loops of NgncR_237 was predicted to base pair with the target mRNAs. The target mRNAs interact with different parts of the sRNA, either with the CU-rich first part or with the GU-rich second part of the single-stranded region. The prediction was validated for NGFG_1006 and *dinD*, both interacting with different parts of the single-stranded region of NgncR_237. Despite of the sequence differences within the single-

stranded region of NgncR_237, both target mRNAs, NGFG_1006 and *dinD*, are regulated by interaction with the sequence upstream of the start codon, which is usually comprising the Shine-Dalgarno sequence. However, the sRNA binding sites of neither NGFG_1006 nor *dinD* contain the AGGAGG consensus sequence. Therefore, it can be only assumed that NgncR_237 negatively regulates the target genes by interfering with initiation of translation.

A great number of predicted target genes is associated with type IV pili and regulation of three genes, *pilG,* NGFG_1006 and NGFG_1479, could be confirmed by qRT PCR. Therefore, NgncR_237 might be important during processes in which type IV pili play a role. Pili are involved in adherence to epithelial cells and piliated gonococci were shown to strongly interact with cornea epithelial cells (Scheuerpflug et al. 1999). However, no significant impact of NgncR_237 on adherence to cornea cells could be observed (figure 3.55). The number of adherent bacteria was though quite variable. Since the impact of NgncR_237 on pilus function was analysed, gonococci were not selected according to their piliation status before infection. Therefore, the changes in pilus expression could have caused the experimental variability. To further address the question about the influence of NgncR_237 on type IV pili, an aggregation assay was performed (data not shown). However, this experiment was not sensitive enough to detect differences between low piliation and loss of piliation. Nevertheless, pilus-related differences could be observed in the absence of NgncR_237. Transformation efficiency of strain Δ237 was very low and it was difficult to generate mutants based on strain Δ237. To test whether the effect is caused by secondary mutations, Susanne Bauer generated a new Δ237 strain, which had the same low transformation efficiency. The same effect was observed by Katharina Wagler for strain ΔBns2-2. Since Bns2-2 was shown to regulate the NgncR_237 target genes *pilG*, *dinD,* NGFG_1006 and the prepilin-type cleavage/methylation domain-containing protein NGFG_1479 on mRNA level, the sRNAs might be involved in regulation of DNA uptake and transformation.

PilG encoded by NGFG_2119 is an essential type IV pilus component. The protein spanning the inner membrane might provide a link between cytoplasmic and periplasmic components of the pilus (Collins et al. 2007). The cytoplasmic domain of PilG is able to bind DNA DUS-independently and since PilG was also shown to interact with the membrane-spanning pore protein PilQ, PilG is supposed to play a role in the guidance of DNA into the cytoplasm (Frye et al. 2015). NGFG_1006 is a hypothetical protein containing a conserved domain of unknown function (DUF4124) that, according to the NCBI structure database, may have an Ig-fold. The protein has a Sec-dependent, cleavable signal sequence and is predicted to localize in the periplasm. Recent analysis revealed that NGFG_1006 is important for stabilizing the pilus in in an extended state and its deletion resulted in a non-piliated colony morphology (Hu et al. 2020). NGFG_1479 is annotated as prepilin-type N-terminal cleavage/methylation domain-containing protein. Prepilin proteins still harbour the N-terminal leader peptide cleaved by the peptidase PilD (reviewed in Chen and Dubnau 2004). Proteins expressing this domain were described as minor pilins or pseudopilins (Cisneros et al. 2012, Dickey et al. 2018).

Interestingly, the minor pilin PilX, although no regulation by NgncR_237 could be observed in the qRT PCR analysis, showed decreased fluorescence in the presence of the sRNA in the *E. coli* system (Katharina Wagler, Master Thesis).

Other target genes are linked to DNA recombination. NGFG_0559 encodes the DNA-damage inducible protein DinD, a not very well characterized member of the bacterial SOS response. The SOS system of *E. coli* includes genes involved in DNA damage repair such as *recA*, *umuCD*, *uvrAB* and several *din* genes, which are controlled by the repressor LexA, and is induced if progression of an active replication fork is blocked by DNA damage or mutations (reviewed in Maslowska et al. 2019). The gonococcal SOS system seems not to be comparable to that of *E. coli*, the observation that *recA* and *uvrAB* genes do not react to stimuli like MMS or UV light led to the hypothesis that gonococci do not have an SOS system (Black et al. 1998). Also in the experiments here, *dinD* expression levels did not increase upon incubation with MMS or nalidixic acid (figure 3.54). Nevertheless, expression of the gonococcal LexA-ortholog is upregulated by stimulation with hydrogen peroxide, indicating the presence of an SOS system. However, gonococcal LexA regulates only three genes, which do not include *dinD* (Schook et al. 2011). NGFG_0515 encodes another enzyme linked to DNA uptake, a restriction endonuclease. Gonococci use these proteins to protect themselves from parasitic DNA taken up by transformation or conjugation (Stein et al. 1992). During infection, endonucleases are also released into the host cell, where they can cross the nuclear membrane to digest methylated human DNA (Weyler et al. 2014).

Hence, NgncR_237 could control several steps in DNA uptake and recombination. Pilin proteins can influence binding and uptake of foreign DNA. PilG is part of the pilus apparatus and was reported to interact with DNA and was therefore suggested to be involved in the DNA uptake process (Frye et al. 2015). The newly acquired DNA can be integrated in the genome by homologous recombination in a RecA-dependent manner (reviewed in Hamilton and Dillard 2005). RecA was shown to co-localize with the competence machinery of *Bacillus subtilis* and hence DNA uptake and recombination seems closely linked (Kidane and Graumann 2005). Since the DNA-binding N-terminal domains of PilG are found in the cytoplasm, the protein could provide a link from DNA uptake to recombination (Frye et al. 2015). PilG also binds DprA, a protein required for DNA transformation that interacts with RecA, and a role of PilG in DNA processing was proposed (Beyene et al. 2017). Interestingly, also the SOS response gene *dinD* is involved in DNA recombination. DinD targets RecA filaments bound to duplex DNA, causes their disassembly and thereby allows recycling of RecA (Uranga et al. 2011). Consequently, the absence of NgncR_237 or Bns2-2 could cause a deregulation of DNA uptake and recombination and hence influence transformation efficiency.

4.6.2 Induction of NgncR_237 expression in comparison to Bns2

NgncR_237 was determined to be sufficiently expressed in the transcriptome study of *N. gonorrhoeae* (Remmele et al. 2014). Nevertheless, according to Northern Blot analysis expression levels of NgncR_237 are very low under standard growth conditions. Since sRNAs often regulate cell responses to various stress factors, expression of these sRNAs is most likely induced under specific conditions. The meningococcal homologue Bns2 was found to be expressed upon incubation in human blood (Del Tordello et al. 2012). Gonococci rarely enter the bloodstream and not all strains have the ability to survive in human blood (reviewed in Edwards and Apicella 2004). MS11 is s strain isolated from a patient with uncomplicated gonorrhoea and therefore gonococci were incubated with heat-inactivated serum instead of full blood. Neither FCS nor human serum had any effect on sRNA expression (figure 3.54). Blood has a specific nutrient composition and additionally contains cellular components as well as the complement system, which is inactivated upon incubation at 65 °C. Since the trigger for Bns2 expression was not determined, several factors could play a role in sRNA induction. Human blood is known for its high glucose concentrations and also contains considerable amounts of lactate (reviewed in Smith et al. 2001). Bns2 was found to be differentially induced by glucose (Fagnocchi et al. 2015), which is not the case for NgncR_237. Growth phase dependent expression could also not be confirmed for NgncR_237, although Bns2 is hardly detectable in exponential phase, though strongly expressed in stationary phase (Fagnocchi et al. 2015). However, the growth phase dependent expression of the sRNA is questionable, since the putative Bns2 transcript upregulated in stationary phase has a size around 400 nucleotides (Fagnocchi et al. 2015), but Bns2 was before reported with a size about 100 nucleotides (Del Tordello et al. 2012). Nevertheless, NgncR_237 shows altered expression compared to Bns2 and so the data suggest a different role of NgncR_237 in gonococci than Bns2 in meningococci. Comparing the sequence upstream of the -10 box of the respective sRNA promoter in the four different neisserial species shows that the A-rich sequence is rather short in *N. gonorrhoeae* in comparison to *N. meningitidis*, *N. lactamica* and *N. polysaccharea*. This could influence regulation of sRNA expression in gonococci and play a role in the altered induction conditions compared to the meningococcal homologue.

4.6 A new sibling sRNA: Bns2-2

Northern Blot analysis of NgncR_237 using a probe directed against the single-stranded region of the sRNA resulted in detection of two RNA species, of which one is slightly shorter than the other and is also present in a NgncR_237 deletion strain (figure 3.57). After BLAST analysis, the putative new sRNA could be localised in the intergenic region of a pseudouridine synthase and a sodium-dependent transporter and the presence of the approximately 100 nt long sRNA could be confirmed with specific probes by Northern Blot (figure 3.58). Interestingly, the sRNA

was not detected in a transcriptome analysis of *N. gonorrhoeae* (Remmele et al. 2014), in contrast to NgncR_237, although the new sRNA is more abundant under standard growth conditions. However, the sRNA was detected in transcriptome studies in *N. meningitidis*. When searching for transcripts upregulated upon incubation in human blood, the sRNA with the number IG44 showed also a significant differential regulation after 30 min incubation, but was not further analysed (Del Tordello et al. 2012). The putatively 68 nucleotides long sRNA is also described in a transcriptome study analysing the effect of sRNAs on the meningococcal response to stress signals (Fagnocchi et al. 2015). The sRNA 1298-1299_F is regulated similarly to Bns2 and was therefore assigned to the same cluster. Its expression level is increased upon incubation with glucose and decreased in absence of the chaperone Hfq, indicating Bns2-2 might be an Hfq-dependent *trans*-acting sRNA. The upregulation in stationary phase is less pronounced for 1298-1299_F compared to Bns2. However, as it was already observed for NgncR_237, expression of Bns2-2 was not induced upon incubation with serum or increased levels of glucose and also transition to stationary growth phase did not alter transcript levels of the sRNA (figure 3.62).
Interaction of Bns2-2 with Hfq could be confirmed since the sRNA co-precipitated with Hfq in a RIP-seq analysis (Heidrich et al. 2017).

Bns2-2 shares the single-stranded region with NgncR_237. Since this region is responsible for NgncR_237-target mRNA interaction, it seems likely that Bns2-2 regulate the same target genes. In fact, genes significantly regulated by NgncR_237 like *dinD*, NGFG_1006, *pilG*, *alaT* and NGFG_1479 could be confirmed to be differentially regulated by Bns2-2 (Katharina Wagler, Master Thesis).
Non-coding RNAs are designated as sibling sRNAs when they show a high degree of sequence relatedness (reviewed in Caswell et al. 2014). Bns2-2 shows 63.5 % sequence identity with NgncR_237 and shares the target interaction region. Both sRNAs regulate a common set of target genes, but due to the unknown induction conditions, they might act under different conditions. The meningococcal homologues, however, are induced by similar triggers and hence suggest action of both sRNAs in response to comparable environmental cues (Fagnocchi et al. 2015). The effect of the reduced transformation efficiency could be observed for both Δ237 and ΔBns2-2, indicating a related function of NgncR_237 and Bns2-2. In summary, NgncR_237 and Bns2-2 can be considered as sibling sRNAs.

4.7 Conclusion and outlook

This study aimed a better understanding of small non-coding RNAs in *N. gonorrhoeae*. The first project was about the role of antisense RNAs in the degradation of out-of-frame *opa* transcripts. Since expression levels of the asRNAs are in the range of transcriptional noise and other phase variable genes show reduced amounts of out-of-frame transcripts independently of asRNAs, the hypothesis could not be confirmed. Therefore, the project can be considered as completed.

The work mostly focused on *trans*-acting sRNAs. Identification of new target genes of NgncR_162 and NgncR_163 gave further hints that the sibling sRNAs are involved in regulation of metabolic processes. However, the exact nature of these processes is not known yet. The obtained data indicate that they play a role in amino acid and central metabolism and NgncR_162 and NgncR_163 were shown to regulate expression of several amino acid transporters. However, the kind of amino acid transported by these proteins is mostly unknown**.** Identification of the amino acids transported and a better understanding of the subsequent metabolism of the taken up amino acids would help elucidating the role of the sibling sRNAs in amino acid metabolism. Especially considering that some amino acid transporters are upregulated whereas others are downregulated shows the importance of a better understanding of the involved metabolic processes to get an idea of the function of NgncR_162 and NgncR_163. Analysis of sRNA levels in various growth media shows that their expression is downregulated in two of the selected growth media. Hence, more studies are required to find out which nutrients are required for sRNA expression.

The identification of new target mRNAs allowed validation of positively regulated genes. However, when exemplarily studying NGFG_0045 it was not possible to identify the regulatory mechanism. The data only indicate that the gene is directly regulated by the sibling sRNAs and the interaction site is still unknown. To find the respective sequence, further truncations within the locus of NGFG_0045 are required, also including the 3' UTR. If the interaction site were known, it would be possible to prove the binding of the sRNA with its target gene. Positve regulation by the sibling sRNAs was validated for more genes. More analysis was done in the case of *gloA*. Its coding sequence is short in comparison to NGFG_0045 and its transcription start and end sites are annotated (Remmele et al. 2014). Hence, it might be worth characterizing mRNA:sRNA interactions with *gloA*.

The other *trans*-acting sRNA analysed was NgncR_237. With different approaches, both *in silico* and experimentally, potential target genes were identified. Interestingly, the number of target genes involved in type IV pilus biogenesis and DNA recombination is noteworthy. Nevertheless, a pilus-related phentotype in the absence of NgncR_237 could not be experimentally proven. Since strain Δ237 also showed a reduced transformation efficiency, the impact of NgncR_237 on transformation should be confirmed experimentally. A problem could be that generation of a double mutant Δ237 ΔBns2-2 failed and therefore the presence of the other sibling sRNA prevents detection of a clear phenotype. More efforts might be required to

generate this strain. Induction conditions of NgncR_237 are still unknown. A more extensive target validation could help getting new ideas about potential inducers of sRNA expression. The sibling sRNA Bns2-2 shares the single-stranded region with NgncR_237. Therefore, all validated target genes of NgncR_237 should be tested for regulation by Bns2-2. Since Bns2-2 is more conserved in *Neisseria* than NgncR_237, the sRNA might have an individual role. Therefore, an *in silico* target prediction could be performed specifically for Bns2-2 to identify individual target genes.

Within this work, small non-coding RNAs were studied. It shows new insights into their expression conditions and regulon, contributing to a better understanding of sRNA function and gene regulation by sRNAs in gonococci.

5 REFERENCES

Aas FE, Wolfgang M, Frye S, Dunham S, Løvold C, Koomey M (2002). Competence for natural transformation in Neisseria gonorrhoeae: components of DNA binding and uptake linked to type IV pilus expression. *Mol Microbiol* **46**(3):749-60.

Addinall SG, Cao C, Lutkenhaus J (1997). FtsN, a late recruit to the septum in Escherichia coli. *Mol Microbiol* **25**(2):303-9.

Afonyushkin T, Vecerek B, Moll I, Bläsi U, Kaberdin VR (2005). Both RNase E and RNase III control the stability of sodB mRNA upon translational inhibition by the small regulatory RNA RyhB. *Nucleic Acids Res* **33**(5):1678-89.

Aiba H (2007). Mechanism of RNA silencing by Hfq-binding small RNAs. *Curr Opin Microbiol* **10**(2):134-9.

Ali Azam T, Iwata A, Nishimura A, Ueda S, Ishihama A (1999). Growth phase-dependent variation in protein composition of the Escherichia coli nucleoid. *J Bacteriol* **181**(20):6361-70.

Andrade JM, Arraiano CM (2008). PNPase is a key player in the regulation of small RNAs that control the expression of outer membrane proteins. *RNA* **14**(3):543-51.

Andrade JM, Hajnsdorf E, Régnier P, Arraiano CM (2009). The poly(A)-dependent degradation pathway of rpsO mRNA is primarily mediated by RNase R. *RNA* **15**(2):316-26.

Andrade JM, Pobre V, Matos AM, Arraiano CM (2012). The crucial role of PNPase in the degradation of small RNAs that are not associated with Hfq. *RNA* **18**(4):844-55.

Andrade JM, Dos Santos RF, Chelysheva I, Ignatova Z, Arraiano CM (2018). The RNA-binding protein Hfq is important for ribosome biogenesis and affects translation fidelity. *EMBO J* **37**(11):e97631.

Antunes A, Golfieri G, Ferlicca F, Giuliani MM, Scarlato V, Delany I (2015). HexR Controls Glucose-Responsive Genes and Central Carbon Metabolism in Neisseria meningitidis. *J Bacteriol* **198**(4):644-54.

Altuvia S, Weinstein-Fischer D, Zhang A, Postow L, Storz G (1997). A small, stable RNA induced by oxidative stress: role as a pleiotropic regulator and antimutator. *Cell* **90**(1):43-53.

Altuvia S, Zhang A, Argaman L, Tiwari A, Storz G (1998). The Escherichia coli OxyS regulatory RNA represses fhlA translation by blocking ribosome binding. *EMBO J* **17**(20):6069-75.

Apicella MA, Shero M, Jarvis GA, Griffiss JM, Mandrell RE, Schneider H (1987). Phenotypic variation in epitope expression of the Neisseria gonorrhoeae lipooligosaccharide. *Infect Immun* **55**(8):1755-61.

Argaman L, Hershberg R, Vogel J, Bejerano G, Wagner EG, Margalit H, Altuvia S (2001). Novel small RNA-encoding genes in the intergenic regions of Escherichia coli. *Curr Biol* **11**(12):941-50.

Aristarkhov A, Mikulskis A, Belasco JG, Lin EC (1996). Translation of the adhE transcript to produce ethanol dehydrogenase requires RNase III cleavage in Escherichia coli. *J Bacteriol* **178**(14):4327-32.

Arraiano CM, Yancey SD, Kushner SR (1993). Identification of endonucleolytic cleavage sites involved in decay of Escherichia coli trxA mRNA. *J Bacteriol* **175**(4):1043-52.

Arraiano CM, Cruz AA, Kushner SR (1997). Analysis of the in vivo decay of the Escherichia coli dicistronic pyrF-orfF transcript: evidence for multiple degradation pathways. *J Mol Biol* **268**(2):261-72.

Arraiano CM, Andrade JM, Domingues S, Guinote IB, Malecki M, Matos RG, Moreira RN, Pobre V, Reis FP, Saramago M, Silva IJ, Viegas SC (2010). The critical role of RNA processing and degradation in the control of gene expression. *FEMS Microbiol Rev* **34**(5):883-923.

Atack JM, Ibranovic I, Ong CL, Djoko KY, Chen NH, Vanden Hoven R, Jennings MP, Edwards JL, McEwan AG (2014). A role for lactate dehydrogenases in the survival of Neisseria gonorrhoeae in human polymorphonuclear leukocytes and cervical epithelial cells. *J Infect Dis* **210**(8):1311-8.

Ayala JC, Shafer WM (2019). Transcriptional regulation of a gonococcal gene encoding a virulence factor (L-lactate permease). *PLoS Pathog* **15**(12):e1008233.

Azam MS, Vanderpool CK (2018). Translational regulation by bacterial small RNAs via an unusual Hfq-dependent mechanism. *Nucleic Acids Res* **46**(5):2585-2599.

Azhikina TL, Ignatov DV, Salina EG, Fursov MV, Kaprelyants AS (2015). Role of Small Noncoding RNAs in Bacterial Metabolism. *Biochemistry (Mosc)* **80**(13):1633-46.

Baart GJ, Zomer B, de Haan A, van der Pol LA, Beuvery EC, Tramper J, Martens DE (2007). Modeling Neisseria meningitidis metabolism: from genome to metabolic fluxes. *Genome Biol* **8**(7):R136.

Babitzke P, Romeo T (2007). CsrB sRNA family: sequestration of RNA-binding regulatory proteins. *Curr Opin Microbiol* **10**(2):156-63.

Balasingham SV, Collins RF, Assalkhou R, Homberset H, Frye SA, Derrick JP, Tønjum T (2007). Interactions between the lipoprotein PilP and the secretin PilQ in Neisseria meningitidis. *J Bacteriol* **189**(15):5716-27.

Ball LM, Criss AK (2013). Constitutively Opa-expressing and Opa-deficient neisseria gonorrhoeae strains differentially stimulate and survive exposure to human neutrophils. *J Bacteriol* **195**(13):2982-90.

Bandyra KJ, Said N, Pfeiffer V, Górna MW, Vogel J, Luisi BF (2012). The seed region of a small RNA drives the controlled destruction of the target mRNA by the endoribonuclease RNase E. *Mol Cell* **47**(6):943-53.

Bandyra KJ, Sinha D, Syrjanen J, Luisi BF, De Lay NR (2016). The ribonuclease polynucleotide phosphorylase can interact with small regulatory RNAs in both protective and degradative modes. *RNA* **22**(3):360-72.

Bang J, Lee SY (2018). Assimilation of formic acid and CO2 by engineered Escherichia coli equipped with reconstructed one-carbon assimilation pathways. *Proc Natl Acad Sci USA* **115**(40):E9271-E9279.

Bauer FJ, Rudel T, Stein M, Meyer TF (1999). Mutagenesis of the Neisseria gonorrhoeae porin reduces invasion in epithelial cells and enhances phagocyte responsiveness. *Mol Microbiol* **31**(3):903-13.

Bauer S, Helmreich J, Zachary M, Kaethner M, Heinrichs E, Rudel T, Beier D (2017). The sibling sRNAs NgncR_162 and NgncR_163 of Neisseria gonorrhoeae participate in the expression control of metabolic, transport and regulatory proteins. *Microbiology* **163**(11):1720-1734.

Bechhofer DH, Deutscher MP (2019). Bacterial ribonucleases and their roles in RNA metabolism. *Crit Rev Biochem Mol Biol* **54**(3):242-300.

Beisel CL, Storz G (2011). The base-pairing RNA spot 42 participates in a multioutput feedforward loop to help enact catabolite repression in Escherichia coli. *Mol Cell* **41**(3):286-97.

Belland RJ, Morrison SG, Carlson JH, Hogan DM (1997). Promoter strength influences phase variation of neisserial opa genes. *Mol Microbiol* **23**(1):123-35.

Beyene GT, Kalayou S, Riaz T, Tonjum T (2017). Comparative proteomic analysis of Neisseria meningitidis wildtype and dprA null mutant strains links DNA processing to pilus biogenesis. *BMC Microbiol* **17**(1):96.

Bhat KS, Gibbs CP, Barrera O, Morrison SG, Jähnig F, Stern A, Kupsch EM, Meyer TF, Swanson J (1991). The opacity proteins of Neisseria gonorrhoeae strain MS11 are encoded by a family of 11 complete genes. *Mol Microbiol* **5**(8):1889-901.

Bianco CM, Fröhlich KS, Vanderpool CK (2019). Bacterial Cyclopropane Fatty Acid Synthase mRNA Is Targeted by Activating and Repressing Small RNAs. *J Bacteriol* **201**(19):e00461-19.

Black CG, Fyfe JA, Davies JK (1998). Absence of an SOS-like system in Neisseria gonorrhoeae. *Gene* **208**(1):61-6.

Blomberg P, Wagner EGH, Nordström K (1990). Control of replication of plasmid R1: the duplex between the antisense RNA, CopA, and its target, CopT, is processed specifically in vivo and in vitro by RNase III. *EMBO J* **9**:2331–40.

Borregaard N, Sørensen OE, Theilgaard-Mönch K (2007). Neutrophil granules: a library of innate immunity proteins. *Trends Immunol* **28**(8):340-5.

Bossi L, Schwartz A, Guillemardet B, Boudvillain M, Figueroa-Bossi N (2012). A role for Rho-dependent polarity in gene regulation by a noncoding small RNA. *Genes Dev* **26**(16):1864-73.

Breshears LM, Edwards VL, Ravel J, Peterson ML (2015). Lactobacillus crispatus inhibits growth of Gardnerella vaginalis and Neisseria gonorrhoeae on a porcine vaginal mucosa model. *BMC Microbiol* **15**:276.

Brinkmann V, Reichard U, Goosmann C, Fauler B, Uhlemann Y, Weiss DS, Weinrauch Y, Zychlinsky A (2004). Neutrophil extracellular traps kill bacteria. *Science* **303**(5663):1532-5.

Britigan BE, Klapper D, Svendsen T, Cohen MS (1988). Phagocyte-derived lactate stimulates oxygen consumption by Neisseria gonorrhoeae. An unrecognized aspect of the oxygen metabolism of phagocytosis. *J Clin Invest* **81**(2):318-24.

Brissac T, Mikaty G, Duménil G, Coureuil M, Nassif X (2012). The meningococcal minor pilin PilX is responsible for type IV pilus conformational changes associated with signaling to endothelial cells. *Infect Immun* **80**(9):3297-306.

Britigan BE, Klapper D, Svendsen T, Cohen MS (1988). Phagocyte-derived lactate stimulates oxygen consumption by Neisseria gonorrhoeae. An unrecognized aspect of the oxygen metabolism of phagocytosis. *J Clin Invest* **81**(2):318-24.

Cahoon LA, Seifert HS (2009). An alternative DNA structure is necessary for pilin antigenic variation in Neisseria gonorrhoeae. *Science* **325**(5941):764-7.

Cahoon LA, Seifert HS (2013). Transcription of a cis-acting, noncoding, small RNA is required for pilin antigenic variation in Neisseria gonorrhoeae. *PLoS Pathog* **9**(1):e1003074.

Callaghan AJ, Aurikko JP, Ilag LL, Günter Grossmann J, Chandran V, Kühnel K, Poljak L, Carpousis AJ, Robinson CV, Symmons MF, Luisi BF (2004). Studies of the RNA degradosome-organizing domain of the Escherichia coli ribonuclease RNase E. *J Mol Biol* **340**(5):965-79.

Cameron TA, De Lay NR (2016). The Phosphorolytic Exoribonucleases Polynucleotide Phosphorylase and RNase PH Stabilize sRNAs and Facilitate Regulation of Their mRNA Targets. *J Bacteriol* **198**(24):3309-3317.

Cannistraro VJ, Kennell D (1999). The reaction mechanism of ribonuclease II and its interaction with nucleic acid secondary structures. *Biochim Biophys Acta* **1433**(1-2):170-87.

Carbonnelle E, Helaine S, Nassif X, Pelicic V (2006). A systematic genetic analysis in Neisseria meningitidis defines the Pil proteins required for assembly, functionality, stabilization and export of type IV pili. *Mol Microbiol* **61**(6):1510-22.

Catenazzi MC, Jones H, Wallace I, Clifton J, Chong JP, Jackson MA, Macdonald S, Edwards J, Moir JW (2014). A large genomic island allows Neisseria meningitidis to utilize propionic acid, with implications for colonization of the human nasopharynx. *Mol Microbiol* **93**(2):346-55.

Cehovin A, Simpson PJ, McDowell MA, Brown DR, Noschese R, Pallett M, Brady J, Baldwin GS, Lea SM, Matthews SJ, Pelicic V (2013). Specific DNA recognition mediated by a type IV pilin. *Proc Natl Acad Sci USA* **110**(8):3065-70.

Centers for Disease Control and Prevention (2001). Summary of notifiable diseases—United States, 2001. *Morb Mortal Wkly Rep* **50**:1-108.

Centers for Disease Control and Prevention (2019). Sexually transmitted disease surveillance 2017: Gonococcal Isolate Surveillance Project (GISP) supplement and profiles. Atlanta: US Department of Health and Human Services.

Chan JM, Dillard JP (2016). Neisseria gonorrhoeae Crippled Its Peptidoglycan Fragment Permease To Facilitate Toxic Peptidoglycan Monomer Release. *J Bacteriol* **198**(21):3029-3040.

Chen A, Seifert HS (2013). Structure-Function Studies of the Neisseria gonorrhoeae Major Outer Membrane Porin. *Infect Immun* **81**(12): 4383–4391.

Chen H, Previero A, Deutscher MP (2019). A novel mechanism of ribonuclease regulation: GcvB and Hfq stabilize the mRNA that encodes RNase BN/Z during exponential phase. *J Biol Chem* **294**(52):19997-20008.

Chen I, Dubnau D (2004). DNA uptake during bacterial transformation. *Nat Rev Microbiol* **2**(3):241-9.

Cheng ZF, Deutscher MP (2005). An important role for RNase R in mRNA decay. *Mol Cell* **17**(2):313-8.

Cho C, Teghanemt A, Apicella MA, Nauseef WM (2020). Modulation of phagocytosis-induced cell death of human neutrophils by Neisseria gonorrhoeae. *J Leukoc Biol* **108**(5):1543-1553.

Cisneros DA, Pehau-Arnaudet G, Francetic O (2012). Heterologous assembly of type IV pili by a type II secretion system reveals the role of minor pilins in assembly initiation. *Mol Microbiol* **86**(4):805-18.

Clarke JE, Kime L, Romero AD, McDowall KJ (2014). Direct entry by RNase E is a major pathway for the degradation and processing of RNA in Escherichia coli. *Nucleic Acids Res* **42**(18):11733-51.

Coburn GA, Mackie GA (1998). Reconstitution of the degradation of the mRNA for ribosomal protein S20 with purified enzymes. *J Mol Biol* **279**(5):1061-74.

Cole MJ, Spiteri G, Jacobsson S, Woodford N, Tripodo F, Amato-Gauci AJ, Unemo M; Euro-GASP network (2017). Overall Low Extended-Spectrum Cephalosporin Resistance but high Azithromycin Resistance in Neisseria gonorrhoeae in 24 European Countries, 2015. *BMC Infect Dis* **17**(1):617.

Collins RF, Saleem M, Derrick JP (2007). Purification and three-dimensional electron microscopy structure of the Neisseria meningitidis type IV pilus biogenesis protein PilG. *J Bacteriol* **189**(17):6389-96.

Condon C (2007). Maturation and degradation of RNA in bacteria. *Curr Opin Microbiol* **10**(3):271-8.

Corcoran CP, Podkaminski D, Papenfort K, Urban JH, Hinton JC, Vogel J (2012). Superfolder GFP reporters validate diverse new mRNA targets of the classic porin regulator, MicF RNA. *Mol Microbiol* **84**(3):428-45.

Cornelissen CN, Kelley M, Hobbs MM, Anderson JE, Cannon JG, Cohen MS, Sparling PF (1998). The transferrin receptor expressed by gonococcal strain FA1090 is required for the experimental infection of human male volunteers. *Mol Microbiol* **27**(3):611-6.

Craig L, Volkmann N, Arvai AS, Pique ME, Yeager M, Egelman EH, Tainer JA (2006). Type IV pilus structure by cryo-electron microscopy and crystallography: implications for pilus assembly and functions. *Mol Cell* **23**(5):651-62.

Creighton S, Tenant-Flowers M, Taylor CB, Miller R, Low N (2003). Co-infection with gonorrhoea and chlamydia: how much is there and what does it mean? *Int J STD AIDS* **14**(2):109-13.

Creighton S (2014). Gonorrhea. *BMJ Clin Evid* 2014 pii 1604.

Criss AK, Seifert HS (2012). A bacterial siren song: intimate interactions between Neisseria and neutrophils. *Nat Rev Microbiol* **10**(3):178-90.

Datta AK, Niyogi K (1975). A novel oligoribonuclease of Escherichia coli. II. Mechanism of action. *J Biol Chem* **250**(18):7313-9.

Deana A, Belasco JG (2005). Lost in translation: the influence of ribosomes on bacterial mRNA decay. *Genes Dev* **19**(21):2526-33.

Dehio C, Gray-Owen SD, Meyer TF (1998a). The role of neisserial Opa proteins in interactions with host cells. *Trends Microbiol* **6**(12):489-95.

Dehio C, Freissler E, Lanz C, Gómez-Duarte OG, David G, Meyer TF (1998b). Ligation of cell surface heparan sulfate proteoglycans by antibody-coated beads stimulates phagocytic uptake into epithelial cells: a model for cellular invasion by Neisseria gonorrhoeae. *Exp Cell Res* **242**(2):528-39.

De Lay N, Gottesman S (2009). The Crp-activated small noncoding regulatory RNA CyaR (RyeE) links nutritional status to group behavior. *J Bacteriol* **191**(2):461-76.

Del Tordello E, Bottini S, Muzzi A, Serruto D (2012). Analysis of the Regulated Transcriptome of Neisseria Meningitidis in Human Blood Using a Tiling Array. *J Bacteriol* **194**(22):6217-32.

Deng W, Wang H, Xie J (2011). Regulatory and pathogenesis roles of Mycobacterium Lrp/AsnC family transcriptional factors. *J Cell Biochem* **112**(10):2655-62.

Deo P, Chow SH, Hay ID, Kleifeld O, Costin A, Elgass KD, Jiang JH, Ramm G, Gabriel K, Dougan G, Lithgow T, Heinz E, Naderer T (2018). Outer membrane vesicles from Neisseria gonorrhoeae target PorB to mitochondria and induce apoptosis. *PLoS Pathog* **14**(3):e1006945.

Derrick JP, Urwin R, Suker J, Feavers IM, Maiden MC (1999). Structural and evolutionary inference from molecular variation in Neisseria porins. *Infect Immun* **67**(5):2406-13.

Dickey AM, Schuller G, Loy JD, Clawson ML (2018). Whole genome sequencing of Moraxella bovoculi reveals high genetic diversity and evidence for interspecies recombination at multiple loci. *PLoS One* **13**(12):e0209113.

Dimastrogiovanni D, Fröhlich KS, Bandyra KJ, Bruce HA, Hohensee S, Vogel J, Luisi BF (2014). Recognition of the small regulatory RNA RydC by the bacterial Hfq protein. *Elife* **3**:e05375.

Dolan SK, Wijaya A, Geddis SM, Spring DR, Silva-Rocha R, Welch M (2018). Loving the poison: the methylcitrate cycle and bacterial pathogenesis. *Microbiology (Reading)* **164**(3):251-259.

Dornenburg JE, Devita AM, Palumbo MJ, Wade JT (2010). Widespread antisense transcription in Escherichia coli. *mBio* **1**(1):e00024-10.

Ducey TF, Jackson L, Orvis J, Dyer DW (2009). Transcript analysis of nrrF, a Fur repressed sRNA of Neisseria gonorrhoeae. *Microb Pathog* **46**(3):166-70.

Duffin PM, Seifert HS (2010). DNA uptake sequence-mediated enhancement of transformation in Neisseria gonorrhoeae is strain dependent. *J Bacteriol* **192**(17):4436-44.

Dühring U, Axmann IM, Hess WR, Wilde A (2006). An internal antisense RNA regulates expression of the photosynthesis gene isiA. *Proc Natl Acad Sci USA* **103**:7054–8.

Dunn KL, Virji M, Moxon ER (1995). Investigations into the molecular basis of meningococcal toxicity for human endothelial and epithelial cells: the synergistic effect of LPS and pili. *Microb Pathog* **18**(2):81-96.

Dyer DW, West EP, Sparling PF (1987). Effects of serum carrier proteins on the growth of pathogenic neisseriae with heme-bound iron. *Infect Immun* **55**(9):2171-2175.

Echenique-Rivera H, Muzzi A, Del Tordello E, Seib KL, Francois P, Rappuoli R, Pizza M, Serruto D (2011). Transcriptome analysis of Neisseria meningitidis in human whole blood and mutagenesis studies identify virulence factors involved in blood survival. *PLoS Pathog* **7**(5):e1002027.

Edwards JL, Apicella MA (2004). The molecular mechanisms used by Neisseria gonorrhoeae to initiate infection differ between men and women. *Clin Microbiol Rev* **17**(4):965-81.

Ellermeier JR, Slauch JM (2008). Fur regulates expression of the Salmonella pathogenicity island 1 type III secretion system through HilD. *J Bacteriol* **190**(2):476-86.

Eriksson J, Eriksson OS, Maudsdotter L, Palm O, Engman J, Sarkissian T, Aro H, Wallin M, Jonsson AB (2015). Characterization of motility and piliation in pathogenic Neisseria. *BMC Microbiol* **15**:92.

Fagnocchi L, Bottini S, Golfieri G, Fantappiè L, Ferlicca F, Antunes A, Guadagnuolo S, Del Tordello E, Siena E, Serruto D, Scarlato V, Muzzi A, Delany I (2015). Global transcriptome analysis reveals small RNAs affecting Neisseria meningitidis bacteremia. *PLoS One* **10**(5):e0126325.

Fantappiè L, Oriente F, Muzzi A, Serruto D, Scarlato V, Delany I (2011). A novel Hfq-dependent sRNA that is under FNR control and is synthesized in oxygen limitation in Neisseria meningitidis. *Mol Microbiol* **80**(2):507-23.

Faulstich M, Böttcher JP, Meyer TF, Fraunholz M, Rudel T (2013). Pilus phase variation switches gonococcal adherence to invasion by caveolin-1-dependent host cell signaling. *PLoS Pathog* **9**(5):e1003373.

Fisher SD, Reger AD, Baum A, Hill SA (2005). RelA alone appears essential for (p)ppGpp production when Neisseria gonorrhoeae encounters nutritional stress *FEMS Microbiol Lett* **248**(1):1-8

Freese NH, Norris DC, Loraine AE (2016). Integrated genome browser: visual analytics platform for genomics. *Bioinformatics* **32**(14):2089-95.

Frye SA, Lång E, Beyene GT, Balasingham SV, Homberset H, Rowe AD, Ambur OH, Tønjum T (2015). The Inner Membrane Protein PilG Interacts with DNA and the Secretin PilQ in Transformation. *PLoS One* **10**(8):e0134954.

Fussenegger M, Facius D, Meier J, Meyer TF (1996). A novel peptidoglycan-linked lipoprotein (ComL) that functions in natural transformation competence of Neisseria gonorrhoeae. *Mol Microbiol* **19**(5):1095-105.

Geissmann T, Chevalier C, Cros MJ, Boisset S, Fechter P, Noirot C, Schrenzel J, François P, Vandenesch F, Gaspin C, Romby P (2009). A search for small noncoding RNAs in Staphylococcus aureus reveals a conserved sequence motif for regulation. *Nucleic Acids Res* **37**(21):7239-57.

Georg J, Hess WR (2018). Widespread Antisense Transcription in Prokaryotes. *Microbiol Spectr* **6**(4).

Gerdes K, Nielsen A, Thorsted P, Wagner EGH (1992). Mechanism of killer gene activation. Antisense RNA-dependent RNase III cleavage ensures rapid turn-over of the stable Hok, SrnB and PndA effector messenger RNAs. *J Mol Biol* **226**:637–49.

Ghosh S, Deutscher MP (1999). Oligoribonuclease Is an Essential Component of the mRNA Decay Pathway. *Proc Natl Acad Sci USA* **96**(8):4372-7.

Gibson BW, Melaugh W, Phillips NJ, Apicella MA, Campagnari AA, Griffiss JM (1993). Investigation of the structural heterogeneity of lipooligosaccharides from pathogenic

Haemophilus and Neisseria species and of R-type lipopolysaccharides from Salmonella typhimurium by electrospray mass spectrometry. *J Bacteriol* **175**:2702–12.

Gill MJ, McQuillen DP, van Putten JP, Wetzler LM, Bramley J, Crooke H, Parsons NJ, Cole JA, Smith H (1996). Functional characterization of a sialyltransferase-deficient mutant of Neisseria gonorrhoeae. *Infect Immun* **64**:3374–8.

Gimpel M, Preis H, Barth E, Gramzow L, Brantl S (2012). SR1--a small RNA with two remarkably conserved functions. *Nucleic Acids Res* **40**(22):11659-72.

Goire N, Lahra MM, Chen M, Donovan B, Fairley CK, Guy R, Kaldor J, Regan D, Ward J, Nissen MD, Sloots TP, Whiley DM (2014). Molecular approaches to enhance surveillance of gonococcal antimicrobial resistance. *Nat Rev Microbiol* **12**(3):223-9.

Gong H, Vu GP, Bai Y, Chan E, Wu R, Yang E, Liu F, Lu S (2011). A Salmonella small non-coding RNA facilitates bacterial invasion and intracellular replication by modulating the expression of virulence factors. PLoS Pathog 7(9):e1002120.

Gottesman S (2005). Micros for microbes: non-coding regulatory RNAs in bacteria. *Trends Genet* **21**(7):399-404.

Gottesman S, Storz G (2011). Bacterial small RNA regulators: versatile roles and rapidly evolving variations. *Cold Spring Harb Perspect Biol* **3**(12):a003798.

Grant CC, Bos MP, Belland RJ (1999). Proteoglycan receptor binding by Neisseria gonorrhoeae MS11 is determined by the HV-1 region of OpaA. *Mol Microbiol* **32**(2):233-42.

Grassmé HU, Ireland RM, van Putten JP (1996). Gonococcal opacity protein promotes bacterial entry-associated rearrangements of the epithelial cell actin cytoskeleton. *Infect Immun* **64**(5):1621-30.

Griffiss JM, Schneider H, Mandrell RE, Yamasaki R, Jarvis GA, Kim JJ, Gibson BW, Hamadeh R, Apicella MA (1988). Lipooligosaccharides: the principal glycolipids of the neisserial outer membrane. *Rev Infect Dis* **10** Suppl 2:S287-95.

Groves E, Dart AE, Covarelli V, Caron E (2008). Molecular mechanisms of phagocytic uptake in mammalian cells. *Cell Mol Life Sci* **65**(13):1957-76.

Guillier M, Gottesman S (2006). Remodelling of the Escherichia coli outer membrane by two small regulatory RNAs. *Mol Microbiol* **59**(1):231-47.

Guillier M, Gottesman S (2008). The 5' end of two redundant sRNAs is involved in the regulation of multiple targets, including their own regulator. *Nucleic Acids Res* **36**(21):6781-94.

Hajnsdorf E, Braun F, Haugel-Nielsen J, Le Derout J, Régnier P (1996). Multiple degradation pathways of the rpsO mRNA of Escherichia coli. RNase E interacts with the 5' and 3' extremities of the primary transcript. *Biochimie* **78**(6):416-24.

Hamilton HL, Dillard JP (2006). Natural transformation of Neisseria gonorrhoeae: from DNA donation to homologous recombination. *Mol Microbiol* **59**(2):376-85.

Handing JW, Ragland SA, Bharathan UV, Criss AK (2018). The MtrCDE Efflux Pump Contributes to Survival of Neisseria gonorrhoeae From Human Neutrophils and Their Antimicrobial Components. *Front Microbiol* **9**:2688.

Hauck CR, Meyer TF (1997). The lysosomal/phagosomal membrane protein h-lamp-1 is a target of the IgA1 protease of Neisseria gonorrhoeae. *FEBS Lett* **405**(1):86-90.

Hauck CR, Meyer TF (2003). 'Small' talk: Opa proteins as mediators of Neisseria-host-cell communication. *Curr Opin Microbiol* **6**(1):43-9.

He W, Li C, Lu CD (2011). Regulation and characterization of the dadRAX locus for D-amino acid catabolism in Pseudomonas aeruginosa PAO1. *J Bacteriol* **193**(9):2107-15.

Hebeler BH, Morse SA (1976). Physiology and metabolism of pathogenic neisseria: tricarboxylic acid cycle activity in Neisseria gonorrhoeae. *J Bacteriol* **128**(1):192-201.

Heidrich N, Moll I, Brantl S (2007). In vitro analysis of the interaction between the small RNA SR1 and its primary target ahrC mRNA. *Nucleic Acids Res* **35**(13):4331-46.

Heidrich N, Bauriedl S, Barquist L, Li L, Schoen C, Vogel J (2017). The primary transcriptome of Neisseria meningitidis and its interaction with the RNA chaperone Hfq. *Nucleic Acids Res* **45**(10):6147-6167.

Helaine S, Carbonnelle E, Prouvensier L, Beretti JL, Nassif X, Pelicic V (2005). PilX, a pilus-associated protein essential for bacterial aggregation, is a key to pilus-facilitated attachment of Neisseria meningitidis to human cells. *Mol Microbiol* **55**(1):65-77.

Helaine S, Dyer DH, Nassif X, Pelicic V, Forest KT (2007). 3D structure/function analysis of PilX reveals how minor pilins can modulate the virulence properties of type IV pili. *Proc Natl Acad Sci USA* **104**(40):15888-93.

Helmreich JK (2017). Charakterisierung der twin-sRNAs NgncR_162 und NgncR_163 von Neisseria gonorrhoeae. *Master Thesis, Universität Würzburg, Lehrstuhl für Mikrobiologie*.

Henrichsen J (1975). The occurrence of twitching motility among gram-negative bacteria. *Acta Pathol Microbiol Scand B* **83**(3):171-8.

Hobbs MM, Anderson JE, Balthazar JT, Kandler JL, Carlson RW, Ganguly J, Begum AA, Duncan JA, Lin JT, Sparling PF, Jerse AE, Shafer WM (2013). Lipid A's structure mediates Neisseria gonorrhoeae fitness during experimental infection of mice and men. *mBio* **4**(6):e00892-13.

Holmqvist E, Li L, Bischler T, Barquist L, Vogel J (2018). Global Maps of ProQ Binding In Vivo Reveal Target Recognition via RNA Structure and Stability Control at mRNA 3' Ends. *Mol Cell* **70**(5):971-982.e6.

Holzapfel E, Eisner G, Alami M, Barrett CM, Buchanan G, Lüke I, Betton JM, Robinson C, Palmer T, Moser M, Müller M (2007). The entire N-terminal half of TatC is involved in twin-arginine precursor binding. *Biochemistry* **46**(10):2892-8.

Hopper S, Vasquez B, Merz A, Clary S, Wilbur JS, So M (2000). Effects of the immunoglobulin A1 protease on Neisseria gonorrhoeae trafficking across polarized T84 epithelial monolayers. *Infect Immun* **68**(2):906-11.

Hörner EM (2018). Analyse kleiner regulatorischer RNAs aus Neisseria gonorrhoeae. *Bachelor Thesis, Universität Würzburg, Lehrstuhl für Mikrobiologie.*

Horswill AR, Escalante-Semerena JR (2001). In vitro conversion of propionate to pyruvate by Salmonella enterica enzymes: 2-methylcitrate dehydratase (PrpD) and aconitase enzymes catalyze the conversion of 2-methylcitrate to 2-methylisocitrate. *Biochemistry* **40**(15):4703-13.

Hu LI, Yin S, Ozer EA, Sewell L, Rehman S, Garnett JA, Seifert HS (2020). Discovery of a New Neisseria gonorrhoeae Type IV Pilus Assembly Factor, TfpC. *mBio* **11**(5):e02528-20.

Hussein R, Lim HN (2012). Direct comparison of small RNA and transcription factor signaling. *Nucleic Acids Res* **40**(15):7269-79.

Idosa BA, Kelly A, Jacobsson S, Demirel I, Fredlund H, Särndahl E, Persson A (2019). Neisseria meningitidis-Induced Caspase-1 Activation in Human Innate Immune Cells Is LOS-Dependent. *J Immunol Res* **2019**:6193186.

Ikeda Y, Yagi M, Morita T, Aiba H (2011). Hfq binding at RhlB-recognition region of RNase E is crucial for the rapid degradation of target mRNAs mediated by sRNAs in Escherichia coli. *Mol Microbiol* **79**(2):419-32.

Isabella VM, Clark VL (2011). Deep sequencing-based analysis of the anaerobic stimulon in Neisseria gonorrhoeae. *BMC Genomics* **12**:51.

Jackson LA, Pan JC, Day MW, Dyer DW (2013). Control of RNA stability by NrrF, an iron-regulated small RNA in Neisseria gonorrhoeae. *J Bacteriol* **195**(22):5166-73.

Jackson LA, Day M, Allen J, Scott E 2nd, Dyer DW (2017). Iron-regulated small RNA expression as Neisseria gonorrhoeae FA 1090 transitions into stationary phase growth. *BMC Genomics* **18**(1):317.

Jagodnik J, Chiaruttini C, Guillier M (2017). Stem-Loop Structures within mRNA Coding Sequences Activate Translation Initiation and Mediate Control by Small Regulatory RNAs. *Mol Cell* **68**(1):158-170.e3.

Jain S, Mościcka KB, Bos MP, Pachulec E, Stuart MC, Keegstra W, Boekema EJ, van der Does C (2011). Structural characterization of outer membrane components of the type IV pili system in pathogenic Neisseria. *PLoS One* **6**(1):e16624.

Jamet A, Jousset AB, Euphrasie D, Mukorako P, Boucharlat A, Ducousso A, Charbit A, Nassif X (2015). A new family of secreted toxins in pathogenic Neisseria species. *PLoS Pathog* **11**(1):e1004592.

Jarvis GA, Chang TL (2012). Modulation of HIV Transmission by Neisseria gonorrhoeae: Molecular and Immunological Aspects. *Curr HIV Res* **10**(3):211-217.

Jennings M, Hood D, Peak R, Virji M, Moxon E (1995). Molecular analysis of a locus for the biosynthesis and phase-variable expression of the lacto-N-neotetraose terminal lipopolysaccharide structure in Neisseria meningitidis. *Mol Microbiol* **18**:729–40.

Johannsen DB, Johnston DM, Koymen HO, Cohen MS, Cannon JG (1999). A Neisseria gonorrhoeae immunoglobulin A1 protease mutant is infectious in the human challenge model of urethral infection. *Infect Immun* **67**(6):3009-13.

John CM, Phillips NJ, Din R, Liu M, Rosenqvist E, Høiby EA, Stein DC, Jarvis GA (2016). Lipooligosaccharide Structures of Invasive and Carrier Isolates of Neisseria meningitidis Are Correlated with Pathogenicity and Carriage. *J Biol Chem* **291**(7):3224-38.

Johnson MB, Criss AK (2011). Resistance of Neisseria gonorrhoeae to neutrophils. *Front Microbiol* **2**:77.

Johnson MB, Criss AK (2013). Neisseria gonorrhoeae phagosomes delay fusion with primary granules to enhance bacterial survival inside human neutrophils. *Cell Microbiol* **15**(8):1323-40.

Johnson MB, Ball LM, Daily KP, Martin JN, Columbus L, Criss AK (2015). Opa+ Neisseria gonorrhoeae exhibits reduced survival in human neutrophils via Src family kinase-mediated bacterial trafficking into mature phagolysosomes. *Cell Microbiol* **17**(5):648-65.

Jonsson AB, Pfeifer J, Normark S (1992). Neisseria gonorrhoeae PilC expression provides a selective mechanism for structural diversity of pili. *Proc Natl Acad Sci USA* **89**(8):3204-8.

Kaberdina AC, Ruiz-Larrabeiti O, Lin-Chao S, Kaberdin VR (2019). Reprogramming of gene expression in Escherichia coli cultured on pyruvate versus glucose. *Mol Genet Genomics* **294**(5):1359-1371.

Kahn RH, Mosure DJ, Blank S, Kent CK, Chow JM, Boudov MR, Brock J, Tulloch S (2005). Chlamydia trachomatis and Neisseria gonorrhoeae prevalence and coinfection in adolescents entering selected US juvenile detention centers 1997-2002. *Sex Transm Dis* **32**(4):255-259.

Kaiser JC, Heinrichs DE (2018). Branching Out: Alterations in Bacterial Physiology and Virulence Due to Branched-Chain Amino Acid Deprivation. *mBio* **9**(5):e01188-18.

Kampmeier RH (1983). Introduction of sulfonamide therapy for gonorrhea. *Sex Transm Dis* **10**(2):81-84.

Kandler JL, Joseph SJ, Balthazar JT, Dhulipala V, Read TD, Jerse AE, Shafer WM (2014). Phase-variable expression of lptA modulates the resistance of Neisseria gonorrhoeae to cationic antimicrobial peptides. *Antimicrob Agents Chemother* **58**(7):4230-3.

Kanehisa M, Goto S (2000). KEGG: Kyoto Encyclopedia of Genes and Genomes. *Nucleic Acids Res* **28**:27-30.

Kawamoto H, Morita T, Shimizu A, Inada T, Aiba H (2005). Implication of membrane localization of target mRNA in the action of a small RNA: mechanism of post-transcriptional regulation of glucose transporter in Escherichia coli. *Genes Dev* **19**(3):328-38.

Kawamoto H, Koide Y, Morita T, Aiba H (2006). Base-pairing requirement for RNA silencing by a bacterial small RNA and acceleration of duplex formation by Hfq. *Mol Microbiol* **61**(4):1013-22.

Kery MB, Feldman M, Livny J, Tjaden B (2014). TargetRNA2: identifying targets of small regulatory RNAs in bacteria. *Nucleic Acids Res* **42**:W124-9.

Kidane D, Graumann PL (2005). Intracellular protein and DNA dynamics in competent Bacillus subtilis cells. *Cell* **122**(1):73-84.

Kikuchi G, Motokawa Y, Yoshida T, Hiraga K. Glycine cleavage system: reaction mechanism, physiological significance, and hyperglycinemia (2008). *Proc Jpn Acad Ser B Phys Biol Sci* **84**(7):246-263.

Kim GL, Lee S, Luong TT, Nguyen CT, Park SS, Pyo S, Rhee DK (2017). Effect of decreased BCAA synthesis through disruption of ilvC gene on the virulence of Streptococcus pneumonia. *Arch Pharm Res* **40**(8):921-932.

Kim JN, Kwon YM (2013). Genetic and phenotypic characterization of the RyhB regulon in Salmonella Typhimurium. *Microbiol Res* **168**(1):41-9.

King TC, Sirdeshmukh R, Schlessinger D (1984). RNase III cleavage is obligate for maturation but not for function of Escherichia coli pre-23S rRNA. *Proc Natl Acad Sci USA* **81**(1):185-8.

Kirchner M, Heuer D, Meyer TF (2005). CD46-independent binding of neisserial type IV pili and the major pilus adhesin, PilC, to human epithelial cells. *Infect Immun* **73**(5):3072-82.

Kleiveland CR (2015). Peripheral Blood Mononuclear Cells. In: Verhoeckx K et al. (eds) The Impact of Food Bioactives on Health. *Springer*, Cham.

Knapp JS, Clark VL (1984). Anaerobic growth of Neisseria gonorrhoeae coupled to nitrite reduction. *Infect Immun* **46**(1)176-181.

Knapp JS (1988). Historical perspectives and identification of Neisseria and related species. *Clin Microbiol Rev* **1**(4):415-31.

Kotelnikova O, Alliluev A, Zinchenko A, Zhigis L, Prokopenko Y, Nokel E, Razgulyaeva O, Zueva V, Tokarskaya M, Yastrebova N, Gordeeva E, Melikhova T, Kaliberda E, Rumsh L (2019). Protective potency of recombinant meningococcal IgA1 protease and its structural derivatives upon animal invasion with meningococcal and pneumococcal infections. *Microbes Infect* **21**(7):336-340.

Kozjak-Pavlovic V, Dian-Lothrop EA, Meinecke M, Kepp O, Ross K, Rajalingam K, Harsman A, Hauf E, Brinkmann V, Günther D, Herrmann I, Hurwitz R, Rassow J, Wagner R, Rudel T (2009). Bacterial porin disrupts mitochondrial membrane potential and sensitizes host cells to apoptosis. *PLoS Pathog* **5**(10):e1000629.

Kröger C, Dillon SC, Cameron AD, Papenfort K, Sivasankaran SK, Hokamp K, Chao Y, Sittka A, Hébrard M, Händler K, Colgan A, Leekitcharoenphon P, Langridge GC, Lohan AJ, Loftus B, Lucchini S, Ussery DW, Dorman CJ, Thomson NR, Vogel J, Hinton JC (2012). The transcriptional landscape and small RNAs of Salmonella enterica serovar Typhimurium. *Proc Natl Acad Sci USA* **109**(20):E1277-86.

Kühlewein C, Rechner C, Meyer TF, Rudel T (2006). Low-phosphate-dependent invasion resembles a general way for Neisseria gonorrhoeae to enter host cells. *Infect Immun* **74**(7):4266-73.

Kupsch EM, Knepper B, Kuroki T, Heuer I, Meyer TF (1993). Variable opacity (Opa) outer membrane proteins account for the cell tropisms displayed by Neisseria gonorrhoeae for human leukocytes and epithelial cells. *EMBO J* **12**(2):641-50.

Langmead B, Salzberg SL (2012). Fast gapped-read alignment with Bowtie 2. *Nat Methods* **9**(4):357-9.

Lee EJ, Groisman EA (2010). An antisense RNA that governs the expression kinetics of a multifunctional virulence gene. *Mol Microbiol* **76**:1020–33.

Leighton MP, Kelly DJ, Williamson MP, Shaw JG (2001). An NMR and enzyme study of the carbon metabolism of Neisseria meningitidis. *Microbiology (Reading)* **147**(Pt 6):1473-1482.

LeVan A, Zimmerman LI, Mahle AC, Swanson KV, DeShong P, Park J, Edwards VL, Song W, Stein DC (2012). Construction and characterization of a derivative of Neisseria gonorrhoeae strain MS11 devoid of all opa genes. *J Bacteriol* **194**(23):6468-78.

Liao Y, Smyth GK, Shi W (2014). featureCounts: an efficient general purpose program for assigning sequence reads to genomic features. *Bioinformatics* **30**(7):923-30.

Lin L, Ayala P, Larson J, Mulks M, Fukuda M, Carlsson SR, Enns C, So M (1997). The Neisseria type 2 IgA1 protease cleaves LAMP1 and promotes survival of bacteria within epithelial cells. *Mol Microbiol* **24**(5):1083-94.

Link TM, Valentin-Hansen P, Brennan RG (2009). Structure of Escherichia coli Hfq bound to polyriboadenylate RNA. *Proc Natl Acad Sci USA* **106**(46):19292-7.

Liou GG, Chang HY, Lin CS, Lin-Chao S (2002). DEAD box RhlB RNA helicase physically associates with exoribonuclease PNPase to degrade double-stranded RNA independent of the degradosome-assembling region of RNase E. *J Biol Chem* **277**(43):41157-62.

Livak KJ, Schmittgen TD (2001). Analysis of relative gene expression data using real-time quantitative PCR and the 2(-Delta Delta C(T)) Method. *Methods* **25**(4):402-8.

Lloréns-Rico V, Cano J, Kamminga T, Gil R, Latorre A, Chen WH, Bork P, Glass JI, Serrano L, Lluch-Senar M (2016). Bacterial antisense RNAs are mainly the product of transcriptional noise. *Sci Adv* **2**(3):e1501363.

Long CD, Tobiason DM, Lazio MP, Kline KA, Seifert HS (2003). Low-level pilin expression allows for substantial DNA transformation competence in Neisseria gonorrhoeae. *Infect Immun* **71**(11):6279-91.

Love M, Huber W, Anders S (2014). Moderated estimation of fold change and dispersion for RNA-seq data with DESeq2. *Genome Biol* **15**(12):550.

Lu P, Wang S, Lu Y, Neculai D, Sun Q, van der Veen S (2019). A Subpopulation of Intracellular Neisseria gonorrhoeae Escapes Autophagy-Mediated Killing Inside Epithelial Cells. *J Infect Dis* **219**(1):133-144.

Lytton EJ, Blake MS (1986). Isolation and partial characterization of the reduction-modifiable protein of Neisseria gonorrhoeae. *J Exp Med* **164**(5):1749-59.

Mabey D (2000). Interactions between HIV infection and other sexually transmitted diseases. *Trop Med Int Health* **5**(7):A32–6.

Macpherson AJ, McCoy KD, Johansen FE, Brandtzaeg P (2007). The immune geography of IgA induction and function. *Mucosal Immunity* **1**:11-22.

Madeira F, Park YM, Lee J, Buso N, Gur T, Madhusoodanan N, Basutkar P, Tivey ARN, Potter SC, Finn RD, Lopez R (2019). The EMBL-EBI search and sequence analysis tools APIs in 2019. *Nucleic Acid Res* **47** (W1):W636-W641.

Maddocks SE, Oyston PCF (2008). Structure and function of the LysR-type transcriptional regulator (LTTR) family proteins. *Microbiology (Reading)* **154**(Pt 12):3609-3623.

Makino S, van Putten JP, Meyer TF (1991). Phase variation of the opacity outer membrane protein controls invasion by Neisseria gonorrhoeae into human epithelial cells. *EMBO J* **10**(6):1307-15.

Malorny B, Morelli G, Kusecek B, Kolberg J, Achtman M (1998). Sequence diversity, predicted two-dimensional protein structure, and epitope mapping of neisserial Opa proteins. *J Bacteriol* **180**(5):1323-30.

Mann M, Wright PR, Backofen R (2017). IntaRNA 2.0: enhanced and customizable prediction of RNA–RNA interactions. *Nucleic Acids Res* **45**(W1):W435-W439.

Marathe R, Meel C, Schmidt NC, Dewenter L, Kurre R, Greune L, Schmidt MA, Müller MJ, Lipowsky R, Maier B, Klumpp S (2014). Bacterial twitching motility is coordinated by a two-dimensional tug-of-war with directional memory. *Nat Commun* **5**:3759.

Marinho CM, Dos Santos PT, Kallipolitis BH, Johansson J, Ignatov D, Guerreiro DN, Piveteau P, O'Byrne CP (2019). The σB-dependent regulatory sRNA Rli47 represses isoleucine biosynthesis in Listeria monocytogenes through a direct interaction with the ilvA transcript. *RNA Biol* **16**(10):1424-1437.

Martin JN, Ball LM, Solomon TL, Dewald AH, Criss AK, Columbus L (2016). Neisserial Opa protein – CEACAM interactions: competition for receptors as a means for bacterial invasion and pathogenesis. *Biochemistry* **55**(31):4286–4294.

Martin M (2011). Cutadapt removes adapter sequences from high-throughput sequencing reads. *EMBnet.journal* **17**(1):10-12.

Marujo PE, Braun F, Haugel-Nielsen J, Le Derout J, Arraiano CM, Régnier P (2003). Inactivation of the decay pathway initiated at an internal site by RNase E promotes poly(A)-dependent degradation of the rpsO mRNA in Escherichia coli. *Mol Microbiol* **50**(4):1283-94.

Maslowska KH, Makiela-Dzbenska K, Fijalkowska IJ (2019). The SOS system: A complex and tightly regulated response to DNA damage. *Environ Mol Mutagen* **60**(4):368-384.

Massari P, Visintin A, Gunawardana J, Halmen KA, King CA, Golenbock DT, Wetzler LM (2006). Meningococcal porin PorB binds to TLR2 and requires TLR1 for signaling. *J Immunol* **176**(4):2373-80.

Massé E, Gottesman S (2002). A small RNA regulates the expression of genes involved in iron metabolism in Escherichia coli. Proc *Natl Acad Sci USA* **99**(7):4620-5.

McCaw SE, Liao EH, Gray-Owen SD (2004). Engulfment of Neisseria gonorrhoeae: revealing distinct processes of bacterial entry by individual carcinoembryonic antigen-related cellular adhesion molecule family receptors. *Infect Immun* **72**(5):2742-52.

Melamed S, Adams PP, Zhang A, Zhang H, Storz G (2020). RNA-RNA Interactomes of ProQ and Hfq Reveal Overlapping and Competing Roles. *Mol Cell* **77**(2):411-425.

Mellin JR, Goswami S, Grogan S, Tjaden B, Genco CA (2007). A novel fur- and iron-regulated small RNA, NrrF, is required for indirect fur-mediated regulation of the sdhA and sdhC genes in Neisseria meningitidis. *J Bacteriol* **189(**10):3686-94.

Meyer TF, Billyard E, Haas R, Storzbach S, So M (1984). Pilus genes of Neisseria gonorrheae: chromosomal organization and DNA sequence. *Proc Natl Acad Sci USA* **81**(19):6110-4.

Michaelsen TY, Brandt J, Singleton CM, Kirkegaard RH, Wiesinger J, Segata N, Albertsen M (2020). The Signal and the Noise: Characteristics of Antisense RNA in Complex Microbial Communities. *mSystems* **5**(1):e00587-19.

Mika F, Hengge R (2014). Small RNAs in the control of RpoS, CsgD, and biofilm architecture of Escherichia coli. *RNA Biol* **11**(5):494-507.

Mitschke J, Georg J, Scholz I, Sharma CM, Dienst D, Bantscheff J, Voss B, Steglich C, Wilde A, Vogel J, Hess WR (2011). An experimentally anchored map of transcriptional start sites in the model cyanobacterium Synechocystis sp. PCC6803. *Proc Natl Acad Sci USA* **108**(5):2124-9.

Mohanty BK, Maples VF, Kushner SR (2004). The Sm-like protein Hfq regulates polyadenylation dependent mRNA decay in Escherichia coli. *Mol Microbiol* **54**(4):905-20.

Mohd-Padil H, Damiri N, Sulaiman S, Chai SF, Nathan S, Firdaus-Raih M (2017). Identification of sRNA mediated responses to nutrient depletion in Burkholderia pseudomallei. *Sci Rep* **7**(1):17173.

Moll I, Afonyushkin T, Vytvytska O, Kaberdin VR, Bläsi U (2003). Coincident Hfq binding and RNase E cleavage sites on mRNA and small regulatory RNAs. *RNA* **9**(11):1308-14.

Mollerup MS, Ross JA, Helfer AC, Meistrup K, Romby P, Kallipolitis BH (2016). Two novel members of the LhrC family of small RNAs in Listeria monocytogenes with overlapping regulatory functions but distinctive expression profiles. *RNA Biol* **13**(9):895-915.

Morand P, Bille E, Morelle S, Eugène E, Beretti JL, Wolfgang M, Meyer T, Koomey M, Nassif X (2004). Type IV pilus retraction in pathogenic Neisseria is regulated by the PilC proteins. *EMBO J* **23**:2009–2017

Morita T, Maki K, Aiba H (2005). RNase E-based ribonucleoprotein complexes: mechanical basis of mRNA destabilization mediated by bacterial noncoding RNAs. *Genes Dev* **19**(18):2176-86.

Morse SA, Bartenstein L (1974). Factors affecting autolysis of Neisseria gonorrhoeae. *Proc Soc Exp Biol Med* **145**(4):1418-21.

Morse SA, Hebeler BH (1978). Effect of pH on the growth and glucose metabolism of Neisseria gonorrhoeae. *Infect Immun* **21**(1):87-95.

Mosaheb M, Wetzler LM (2018). Meningococcal PorB induces a robust and diverse antigen specific T cell response as a vaccine adjuvant. *Vaccine* **36**(50):7689-7699.

Murina VN, Nikulin AD (2014). Bacterial small regulatory RNAs and Hfq protein. *Biochemistry (Mosc)* **80**(13):1647-54.

Navarro Llorens JM, Tormo A, Martínez-García E (2010). Stationary phase in gram-negative bacteria. *FEMS Microbiol Rev* **34**(4):476-95.

Negrete A, Shiloach J (2015). Constitutive expression of the sRNA GadY decreases acetate production and improves E. coli growth. *Microb Cell Fact* **14**:148.

Neisser A (1879). Ueber eine der Gonorrhoe eigentümliche Micrococusform. *Centralblatt für die medizinischen Wissenschaften* **17**(28):497-500.

O'Brien JP, Goldenberg DL, Rice PA (1983). Disseminated gonococcal infection: a prospective analysis of 49 patients and a review of pathophysiology and immune mechanisms. *Medicine (Baltimore)* **62**(6):395-406.

Oh TJ, Lee CW, Kim IG (1999). The damage-inducible (din) genes of Escherichia coli are induced by various genotoxins in a different way. *Microbiol Res* **154**(2):179-83.

Olejniczak M, Storz G (2017). ProQ/FinO-domain proteins: another ubiquitous family of RNA matchmakers? *Mol Microbiol* **104**(6):905-915.

Opdyke JA, Kang JG, Storz G (2004). GadY, a small-RNA regulator of acid response genes in Escherichia coli. *J Bacteriol* **186**(20):6698-705.

Ortega AD, Gonzalo-Asensio J, García-del Portillo F (2012). Dynamics of Salmonella small RNA expression in non-growing bacteria located inside eukaryotic cells. *RNA Biol* **9**(4):469-88.

Otaka H, Ishikawa H, Morita T, Aiba H (2011). PolyU tail of rho-independent terminator of bacterial small RNAs is essential for Hfq action. *Proc Natl Acad Sci USA* **108**(32):13059-64.

Padalon-Brauch G, Hershberg R, Elgrably-Weiss M, Baruch K, Rosenshine I, Margalit H, Altuvia S (2008). Small RNAs encoded within genetic islands of Salmonella typhimurium show host-induced expression and role in virulence. *Nucleic Acids Res* **36**(6):1913-27.

Palmer GH, Bankhead T, Seifert HS (2016). Antigenic Variation in Bacterial Pathogens. *Microbiol Spectr* **4**(1).

Pannekoek Y, Huis In 't Veld RA, Schipper K, Bovenkerk S, Kramer G, Brouwer MC, van de Beek D, Speijer D, van der Ende A (2017). Neisseria meningitidis Uses Sibling Small Regulatory RNAs To Switch from Cataplerotic to Anaplerotic Metabolism. *mBio* **8**(2):e02293-16.

Papenfort K, Bouvier M, Mika F, Sharma CM, Vogel J (2010). Evidence for an autonomous 5' target recognition domain in an Hfq-associated small RNA. *Proc Natl Acad Sci USA* **107**(47):20435-40.

Papenfort K, Vanderpool CK (2015). Target activation by regulatory RNAs in bacteria. FEMS *Microbiol Rev* **39**(3):362-78.

Peano C, Wolf J, Demol J, Rossi E, Petiti L, De Bellis G, Geiselmann J, Egli T, Lacour S, Landini P (2015). Characterization of the Escherichia coli σ(S) core regulon by Chromatin Immunoprecipitation-sequencing (ChIP-seq) analysis. *Sci Rep* **5**:10469.

Pobre V, Barahona S, Dobrzanski T, Steffens MBR, Arraiano CM (2019). Defining the impact of exoribonucleases in the shift between exponential and stationary phases. *Sci Rep* **9**(1):16271.

Poncin T, Fouere S, Braille A, Camelena F, Agsous M, Bebear C, Kumanski S, Lot F, Mercier-Delarue S, Ngangro NN, Salmona M, Schnepf N, Timsit J, Unemo M, Bercot B (2018). Multidrug-resistant Neisseria gonorrhoeae failing treatment with ceftriaxone and doxycycline in France, November 2017. *Euro Surveill* **23**(21).

Prister LL, Ozer EA, Cahoon LA, Seifert HS (2019). Transcriptional initiation of a small RNA, not R-loop stability, dictates the frequency of pilin antigenic variation in Neisseria gonorrhoeae. *Mol Microbiol* **112**(4):1219-1234.

Pulvermacher SC, Stauffer LT, Stauffer GV (2008). The role of the small regulatory RNA GcvB in GcvB/mRNA posttranscriptional regulation of oppA and dppA in Escherichia coli. *FEMS Microbiol Lett* **281**(1):42-50.

Pulvermacher SC, Stauffer LT, Stauffer GV (2009). The small RNA GcvB regulates sstT mRNA expression in Escherichia coli. *J Bacteriol* **191**(1):238-48.

Quick M, Abramyan AM, Wiriyasermkul P, Weinstein H, Shi L, Javitch JA (2018). The LeuT-fold neurotransmitter:sodium symporter MhsT has two substrate sites. *Proc Natl Acad Sci USA* **115**(34): E7924–E7931.

Quillin SJ, Seifert HS (2018). Neisseria gonorrhoeae host adaptation and pathogenesis. *Nat Rev Microbiol* **16**(4):226-240.

Raghavan R, Sloan DB, Ochman H (2012). Antisense transcription is pervasive but rarely conserved in enteric bacteria. *mBio* **3**(4):e00156-12.

Ram S, Mackinnon FG, Gulati S, McQuillen DP, Vogel U, Frosch M, Elkins C, Guttormsen HK, Wetzler LM, Oppermann M, Pangburn MK, Rice PA (1999). The contrasting mechanisms of serum resistance of Neisseria gonorrhoeae and group B Neisseria meningitidis. *Mol Immunol* **36**(13-14):915-28.

Ramsey KH, Schneider H, Cross AS, Boslego JW, Hoover DL, Staley TL, Kuschner RA, Deal CD (1995). Inflammatory cytokines produced in response to experimental human gonorrhea. *J Infect Dis* **172**(1):186-91.

Ramsey ME, Hackett KT, Kotha C, Dillard JP (2012). New complementation constructs for inducible and constitutive gene expression in Neisseria gonorrhoeae and Neisseria meningitides. *Appl Environ Microbiol* **78**(9):3068-78.

Rechner C, Kühlewein C, Müller A, Schild H, Rudel T (2007). Host glycoprotein Gp96 and scavenger receptor SREC interact with PorB of disseminating Neisseria gonorrhoeae in an epithelial invasion pathway. *Cell Host Microbe* **2**(6):393-403.

Regonesi ME, Del Favero M, Basilico F, Briani F, Benazzi L, Tortora P, Mauri P, Dehò G (2006). Analysis of the Escherichia coli RNA degradosome composition by a proteomic approach. *Biochimie* **88**(2):151-61

Remmele CW, Xian Y, Albrecht M, Faulstich M, Fraunholz M, Heinrichs E, Dittrich MT, Müller T, Reinhardt R, Rudel T (2014). Transcriptional landscape and essential genes of Neisseria gonorrhoeae. *Nucleic Acids Res* **42**(16):10579-95.

Resch A, Afonyushkin T, Lombo TB, McDowall KJ, Bläsi U, Kaberdin VR (2008). Translational activation by the noncoding RNA DsrA involves alternative RNase III processing in the rpoS 5'-leader. *RNA* **14**(3):454-9.

Ritter JL, Genco CA (2018). Neisseria gonorrhoeae-Induced Inflammatory Pyroptosis in Human Macrophages is Dependent on Intracellular Gonococci and Lipooligosaccharide. *J Cell Death* **11**:1179066017750902.

Robertson HD, Webster RE, Zinder ND (1968). Purification and properties of ribonuclease III from Escherichia coli. *J Biol Chem* **243**(1):82-91.

Ross JA, Thorsing M, Lillebæk EMS, Teixeira Dos Santos P, Kallipolitis BH (2019). The LhrC sRNAs control expression of T cell-stimulating antigen TcsA in Listeria monocytogenes by decreasing tcsA mRNA stability. *RNA Biol* **16**(3):270-281.

Roth A, Mattheis C, Muenzner P, Unemo M, Hauck CR (2013). Innate recognition by neutrophil granulocytes differs between Neisseria gonorrhoeae strains causing local or disseminating infections. *Infect Immun* **81**(7):2358-70.

Rudel T, Scheurerpflug I, Meyer TF (1995). Neisseria PilC protein identified as type-4 pilus tip-located adhesin. *Nature* **373**(6512):357-9.

Sadarangani M, Pollard AJ, Gray-Owen SD (2011). Opa proteins and CEACAMs: pathways of immune engagement for pathogenic Neisseria. *FEMS Microbiol Rev* **35**(3):498-514.

Sadarangani M, Hoe CJ, Makepeace K, van der Ley P, Pollard AJ (2016). Phase variation of Opa proteins of Neisseria meningitidis and the effects of bacterial transformation. *J Biosci* **41**(1):13-9.

Salim NN, Faner MA, Philip JA, Feig AL (2012). Requirement of upstream Hfq-binding (ARN)x elements in glmS and the Hfq C-terminal region for GlmS upregulation by sRNAs GlmZ and GlmY. *Nucleic Acids Res* **40**(16):8021-32.

Saramago M, Bárria C, Dos Santos RF, Silva IJ, Pobre V, Domingues S, Andrade JM, Viegas SC, Arraiano CM (2014). The role of RNases in the regulation of small RNAs. *Curr Opin Microbiol* **18**:105-15.

Sauer E, Schmidt S, Weichenrieder O (2012). Small RNA binding to the lateral surface of Hfq hexamers and structural rearrangements upon mRNA target recognition. *Proc Natl Acad Sci USA* **109**(24):9396-401.

Sauer E (2013). Structure and RNA-binding properties of the bacterial LSm protein Hfq. *RNA Biol* **10**(4):610-8.

Scheuerpflug I, Rudel T, Ryll R, Pandit J, Meyer TF (1999). Roles of PilC and PilE proteins in pilus-mediated adherence of Neisseria gonorrhoeae and Neisseria meningitidis to human erythrocytes and endothelial and epithelial cells. *Infect Immun* **67**(2):834-43.

Schneider CA, Rasband WS, Eliceiri KW (2012). NIH Image to ImageJ: 25 years of image analysis. *Nature methods* **9**(7): 671-675.

Schook PO, Stohl EA, Criss AK, Seifert HS (2011). The DNA-binding activity of the Neisseria gonorrhoeae LexA orthologue NG1427 is modulated by oxidation. *Mol Microbiol* **79**(4):846-60.

Sedlyarova N, Shamovsky I, Bharati BK, Epshtein V, Chen J, Gottesman S, Schroeder R, Nudler E (2016). sRNA-Mediated Control of Transcription Termination in E. coli. *Cell* **167**(1):111-121.e13.

Seib KL, Wu HJ, Kidd SP, Apicella MA, Jennings MP, McEwan AG (2006). Defenses against oxidative stress in Neisseria gonorrhoeae: a system tailored for a challenging environment. *Microbiol Mol Biol Rev* **70**(2):344-61.

Serafini A, Tan L, Horswell S, Howell S, Greenwood DJ, Hunt DM, Phan MD, Schembri M, Monteleone M, Montague CR, Britton W, Garza-Garcia A, Snijders AP, VanderVen B, Gutierrez MG, West NP, de Carvalho LPS (2019). Mycobacterium tuberculosis requires glyoxylate shunt and reverse methylcitrate cycle for lactate and pyruvate metabolism. *Mol Microbiol* **112**(4):1284-1307.

Shahnazari S, Brumell JH (2011). Mechanisms and consequences of bacterial targeting by the autophagy pathway. *Curr Opin Microbiol* **14**(1):68-75.

Sharma CM, Hoffmann S, Darfeuille F, Reignier J, Findeiss S, Sittka A, Chabas S, Reiche K, Hackermüller J, Reinhardt R, Stadler PF, Vogel J (2010). The primary transcriptome of the major human pathogen Helicobacter pylori. *Nature* **464**(7286):250-5.

Sidiq KR, Chow MW, Zhao Z, Daniel RA (2020). Alanine metabolism in Bacillus subtilis. *Mol Microbiol*, Epub ahead of print.

Skerker JM, Berg HC (2001). Direct observation of extension and retraction of type IV pili. *Proc Natl Acad Sci USA* **98**(12):6901-4.

Smith L, Angarone MP (2015). Sexually Transmitted Infections. *Urol Clin North Am* **42**(4):507-18.

Snapper CM, Rosas FR, Kehry MR, Mond JJ, Wetzler LM (1997). Neisserial porins may provide critical second signals to polysaccharide-activated murine B cells for induction of immunoglobulin secretion. *Infect Immun* **65**(8):3203-8.

Solger F, Kunz TC, Fink J, Paprotka K, Pfister P, Hagen F, Schumacher F, Kleuser B, Seibel J, Rudel T (2020). A Role of Sphingosine in the Intracellular Survival of Neisseria gonorrhoeae. *Front Cell Infect Microbiol* **10**:215.

Soper TJ, Woodson SA (2008). The rpoS mRNA leader recruits Hfq to facilitate annealing with DsrA sRNA. *RNA* **14**(9):1907-17.

Sparling PF (1966). Genetic transformation of Neisseria gonorrhoeae to streptomycin resistance. *J Bacteriol* **92**(5):1364-71.

Spence JM, Wright L, Clark VL (2008). Laboratory maintenance of Neisseria gonorrhoeae. *Curr Protoc Microbiol* Chapter 4:Unit 4A.1.

Stead MB, Marshburn S, Mohanty BK, Mitra J, Pena Castillo L, Ray D, van Bakel H, Hughes TR, Kushner SR (2011). Analysis of Escherichia coli RNase E and RNase III activity in vivo using tiling microarrays. *Nucleic Acids Res* **39**(8):3188-203.

Stein DC, Chien R, Seifert HS (1992). Construction of a Neisseria gonorrhoeae MS11 derivative deficient in NgoMI restriction and modification. *J Bacteriol* **174**(15):4899-906.

Stern A, Brown M, Nickel P, Meyer TF (1986). Opacity genes in Neisseria gonorrhoeae: Control of phase and antigenic variation. *Cell* **47**:61-71.

Stone JR, Wray GA (2001). Rapid evolution of cis-regulatory sequences via local point mutations. *Mol Biol Evol* **18**(9):1764-70.

Storz G, Vogel J, Wassarman KM (2011). Regulation by small RNAs in bacteria: expanding frontiers. *Mol Cell* **43**(6):880-91.

Sukedo N, Clugston SL, Daub E, Honek JF (2004). Distinct classes of glyoxalase I: metal specificity of the Yersinia pestis, Pseudomonas aeruginosa and Neisseria meningitidis enzymes. *Biochem J* **384**:111–117

Suvorova IA, Korostelev YD, Gelfand MS (2015). GntR Family of Bacterial Transcription Factors and Their DNA Binding Motifs: Structure, Positioning and Co-Evolution. *PLoS One* **10**(7):e0132618.

Svensson SL, Sharma CM (2016). Small RNAs in Bacterial Virulence and Communication. *Microbiol Spectr* **4**(3): VMBF-0028-2015.

Swanson J, Kraus SJ, Gotschlich EC (1971). Studies on gonococcus infection. I. Pili and zones of adhesion: their relation to gonococcal growth patterns. *J Exp Med* **134**(4):886-906.

Takahashi H, Yanagisawa T, Kim KS, Yokoyama S, Ohnishi M (2012). Meningococcal PilV potentiates Neisseria meningitidis type IV pilus-mediated internalization into human endothelial and epithelial cells. *Infect Immun* **80**(12):4154-66.

Tanwer P, Bauer S, Heinrichs E, Panda G, Saluja D, Rudel T, Beier D (2017). Post-transcriptional regulation of target genes by the sRNA FnrS in Neisseria gonorrhoeae. *Microbiology* **163**(7):1081-1092.

Tchoupa AK, Schuhmacher T, Hauck CR (2014). Signaling by epithelial members of the CEACAM family - mucosal docking sites for pathogenic bacteria. *Cell Commun Signal* **12**:27.

Thaw P, Sedelnikova SE, Muranova T, Wiese S, Ayora S, Alonso JC, Brinkman AB, Akerboom J, van der Oost J, Rafferty JB (2006). Structural insight into gene transcriptional regulation and effector binding by the Lrp/AsnC family. *Nucleic Acids Res* **34**(5):1439-49.

Trotochaud AE, Wassarman KM (2005). A highly conserved 6S RNA structure is required for regulation of transcription. *Nat Struct Mol Biol* **12**(4):313-9.

Tumova S, Woods A, Couchman JR (2000). Heparan sulfate proteoglycans on the cell surface: versatile coordinators of cellular functions. *Int J Biochem Cell Biol* **32**(3):269-88.

Udekwu KI, Darfeuille F, Vogel J, Reimegård J, Holmqvist E, Wagner EG (2005). Hfq-dependent regulation of OmpA synthesis is mediated by an antisense RNA. *Genes Dev* **19**(19):2355-66.

Unemo M, Shafer WM (2014). Antimicrobial resistance in Neisseria gonorrhoeae in the 21st century: past, evolution, and future. *Clin Microbiol Rev* **27**(3):587-613.

Updegrove TB, Zhang A, Storz G (2016). Hfq: the flexible RNA matchmaker. *Curr Opin Microbiol* **30**:133-138.

Uranga LA, Balise VD, Benally CV, Grey A, Lusetti SL (2011). The Escherichia coli DinD protein modulates RecA activity by inhibiting postsynaptic RecA filaments. *J Biol Chem* **286**(34):29480-91.

Urban JH, Vogel J (2007). Translational control and target recognition by Escherichia coli small RNAs in vivo. *Nucleic Acids Res* **35**(3):1018-37.

van Putten JP (1993). Phase variation of lipooligosaccharide directs interconversion of invasive and immuno-resistant phenotypes of Neisseria gonorrhoeae. *EMBO J* **12**:4043–51.

van Putten JP, Duensing TD, Carlson J (1998a). Gonococcal invasion of epithelial cells driven by P.IA, a bacterial ion channel with GTP binding properties. *J Exp Med* **188**(5):941-52.

van Putten JP, Duensing TD, Cole RL (1998b). Entry of OpaA+ gonococci into HEp-2 cells requires concerted action of glycosaminoglycans, fibronectin and integrin receptors. *Mol Microbiol* **29**(1):369-79.

Virji M, Alexandrescu C, Ferguson DJ, Saunders JR, Moxon ER (1992). Variations in the expression of pili: the effect on adherence of Neisseria meningitidis to human epithelial and endothelial cells. *Mol Microbiol* **6**(10):1271-9.

Vitreschak AG, Lyubetskaya EV, Shirshin MA, Gelfand MS, Lyubetsky VA (2004). Attenuation regulation of amino acid biosynthetic operons in proteobacteria: comparative genomics analysis. *FEMS Microbiol Lett* **234**(2):357-70.

Vogel J, Bartels V, Tang TH, Churakov G, Slagter-Jäger JG, Hüttenhofer A, Wagner EG (2003). RNomics in Escherichia coli detects new sRNA species and indicates parallel transcriptional output in bacteria. *Nucleic Acid Res* **31**:6435–43.

Vogel J, Argaman L, Wagner EG, Altuvia S (2004). The small RNA IstR inhibits synthesis of an SOS-induced toxic peptide. *Curr Biol* **14**(24):2271-6.

Vogel J, Luisi BF (2011). Hfq and its constellation of RNA. *Nat Rev Microbiol* **9**(8):578-89.

Wade JJ, Graver MA (2007). A fully defined, clear and protein-free liquid medium permitting dense growth of Neisseria gonorrhoeae from very low inocula. *FEMS Microbiol Lett* **273**(1):35-7.

Wagler K (2021). Identifying target genes of the sRNAs NgncR 237 and Bns2-2 of Neisseria gonorrhoeae. *Master Thesis, Universität Würzburg, Lehrstuhl für Mikrobiologie*.

Wagner EG (2013). Cycling of RNAs on Hfq. *RNA Biol* **10**(4):619-26.

Wang Y, Ke Y, Xu J, Wang L, Wang T, Liang H, Zhang W, Gong C, Yuan J, Zhuang Y, An C, Lei S, Du X, Wang Z, Li W, Yuan X, Huang L, Yang X, Chen Z (2015). Identification of a Novel Small Non-Coding RNA Modulating the Intracellular Survival of Brucella melitensis. *Front Microbiol* **6**:164.

Wassarman KM (2002). Small RNAs in bacteria: diverse regulators of gene expression in response to environmental changes. *Cell* **109**(2):141-4.

Wassarman KM (2007). 6S RNA: a regulator of transcription. *Mol Microbiol* **65**(6):1425-31.

Waters LS, Storz G (2009). Regulatory RNAs in bacteria. *Cell* **136**(4):615-28.

Wayne LG, Sohaskey CD (2001). Nonreplicating persistence of mycobacterium tuberculosis. *Annu Rev Microbiol* **55**:139-63.

Weyler L, Engelbrecht M, Mata Forsberg M, Brehwens K, Vare D, Vielfort K, Wojcik A, Aro H (2014). Restriction endonucleases from invasive Neisseria gonorrhoeae cause double-strand breaks and distort mitosis in epithelial cells during infection. *PLoS One* **9**(12):e114208.

Whitehead RN, Overton TW, Snyder LA, McGowan SJ, Smith H, Cole JA, Saunders NJ (2007). The small FNR regulon of Neisseria gonorrhoeae: comparison with the larger Escherichia coli FNR regulon and interaction with the NarQ-NarP regulon. *BMC Genomics* **8**:35.

Winkler ME, Ramos-Montañez S (2009). Biosynthesis of Histidine. *EcoSal Plus* **3**(2):10.1128

Wolfgang M, van Putten JP, Hayes SF, Dorward D, Koomey M (2000). Components and dynamics of fiber formation define a ubiquitous biogenesis pathway for bacterial pili. *EMBO J.* **19**(23):6408-18.

World Health Organization (WHO) (2016). WHO guidelines for the treatment of Neisseria gonorrhoeae.

Wright, PR, Georg, J, Mann, M, Sorescu, DA, Richter, AS, Lott, S, Kleinkauf, R, Hess, WR, Backofen, R (2014). CopraRNA and IntaRNA: predicting small RNA targets, networks and interaction domains. *Nucleic acids research*, **42**:W119–W123.

Xu F, Cohen SN (1995). RNA degradation in Escherichia coli regulated by 3' adenylation and 5' phosphorylation. *Nature* **374**(6518):180-3.

Yang T, Heydarian M, Kozjak-Pavlovic V, Urban M, Harbottle RP, Rudel T (2020). Folliculin Controls the Intracellular Survival and Trans-Epithelial Passage of Neisseria gonorrhoeae. *Front Cell Infect Microbiol* **10**:422.

Zaburdaev V, Biais N, Schmiedeberg M, Eriksson J, Jonsson AB, Sheetz MP, Weitz DA (2014). Uncovering the mechanism of trapping and cell orientation during Neisseria gonorrhoeae twitching motility. *Biophys J* **107**(7):1523-31.

Zeth K, Kozjak-Pavlovic V, Faulstich M, Fraunholz M, Hurwitz R, Kepp O, Rudel T (2013). Structure and function of the PorB porin from disseminating Neisseria gonorrhoeae. *Biochem J* **449**(3):631-42.

Zhi J, Mathew E, Freundlich M (1999). Lrp binds to two regions in the dadAX promoter region of Escherichia coli to repress and activate transcription directly. *Mol Microbiol* **32**(1):29-40.

Zhu W, Tomberg J, Knilans KJ, Anderson JE, McKinnon KP, Sempowski GD, Nicholas RA, Duncan JA (2018). Properly folded and functional PorB from Neisseria gonorrhoeae inhibits dendritic cell stimulation of CD4(+) T cell proliferation. *J Biol Chem* **293**(28):11218-11229.

Zilhão R, Cairrão F, Régnier P, Arraiano CM (1996). PNPase modulates RNase II expression in Escherichia coli: implications for mRNA decay and cell metabolism. *Mol Microbiol* **20**(5):1033-42.

6 APPENDIX

6.1 List of abbreviations

Abbreviation	Meaning
AHT	Anhydrotetracycline
asRNA	Antisense RNA
cDNA	Complementary DNA
CDS	Coding sequence
CEACAM	Carcinoembryonic antigen cell adhesion molecule
Cfu	Colony forming unit
DNA	Desoxyribonucleic acid
ddH_2O	Double-distilled water (milliQ)
dNTP	Desoxyribonucleosid phosphate
DUS	DNA uptake sequence
E. coli	Escherichia coli
FCS	Fetal calf serum
G4	Guanine quadruplex
HRP	Horseradish peroxidase
HSPG	Heperansulfate proteoglycans
IL	Interleukin
IP	Isotopologue profile
kb	Kilo base
LB	Luria Bertani
lif	Locked in-frame
lof	Locked out-of-frame
LOS	Lipooligosaccharides
M	Molar
MMS	Methylmethanesulfonate
mRNA	Messenger RNA
N. gonorrhoeae	Neisseria gonorrhoeae
OD	Optical density
Opa	Opacity-associated
ORF	Open reading frame
PAGE	Polyacrylamide gel electrophoresis
PAP	Poly(A) polymerase
PCR	Polymerase chain reaction
PFA	Paraformaldehyde
PMN	Polymorphonuclear leukocytes
PNK	Polynucleotide kinase
PNPase	Polynucleotide phosphorylase
PPM	Proteose peptone medium
qRT PCR	Quantitative real time PCR
RBS	Ribosomal binding site
RNA	Ribonucleic acid
ROS	Reactive oxygen species
rpm	Revolutions per minute
rRNA	Ribosomal RNA
SREC	Scavenger Receptor expressed by Endothelial Cells
sRNA	Small RNA
TLR	Toll-like receptor
UTR	Untranslated region

6.2 List of figures

6.3 List of tables

6.4 Supplementary information

Table A.1: Significantly regulated RNAseq hits in dataset ΔΔ versus MS11

	Gene	q-value	Fold change		Gene	q-value	Fold change
NGFG_00045		0.0000	0.2553	NGFG_01497	grpE	0.0271	0.7387
NGFG_00052	luxS	0.0442	0.7351	NGFG_01514	gcvH	0.0000	2.2191
NGFG_00070		0.0088	1.4191	NGFG_01516		0.0081	0.6471
NGFG_00072	mce	0.0271	1.3398	NGFG_01528		0.0191	1.4661
NGFG_00093		0.0000	1.6369	NGFG_01536		0.0076	1.6876
NGFG_00116	fabG	0.0419	0.7770	NGFG_01544		0.0008	0.6816
NGFG_00126		0.0147	0.7511	NGFG_01564		0.0087	0.7061
NGFG_00249		0.0000	2.9282	NGFG_01710	rrf	0.0011	0.6511
NGFG_00252	rng	0.0001	0.6598	NGFG_01711	uppS	0.0278	0.8185
NGFG_00254	secB	0.0006	0.6346	NGFG_01715	omp85	0.0073	0.7647
NGFG_00343		0.0133	1.5551	NGFG_01721		0.0000	6.4531
NGFG_00360	ppa	0.0487	0.6602	NGFG_01722	dadA	0.0000	3.2266
NGFG_00366		0.0011	1.9265	NGFG_01727	minE	0.0123	0.6498
NGFG_00423	rlpB	0.0002	0.6718	NGFG_01728	minD	0.0175	0.6736
NGFG_00447		0.0118	1.7839	NGFG_01810	galE	0.0017	0.6950
NGFG_00448		0.0035	1.6806	NGFG_01821	pilE	0.0438	1.6609
NGFG_00480	txn	0.0002	1.7950	NGFG_01842	thiC	0.0064	1.7088
NGFG_00507		0.0001	1.7740	NGFG_01865	thiF	0.0453	0.8022
NGFG_00551	adss	0.0278	0.8061	NGFG_01897		0.0322	1.3899
NGFG_00557	hldD	0.0134	0.7485	NGFG_01898	rsm	0.0175	1.5444
NGFG_00658	hsdM	0.0008	1.4015	NGFG_01937		0.0000	1.8700
NGFG_00662		0.0419	1.4814	NGFG_01941		0.0053	0.7101
NGFG_00666		0.0089	1.3679	NGFG_01955	waaC	0.0020	1.3861
NGFG_00670		0.0190	1.7041	NGFG_01956	pncA	0.0002	1.4083
NGFG_00671		0.0217	1.6044	NGFG_02039	ilvC	0.0000	0.6268
NGFG_00699		0.0021	1.8239	NGFG_02040		0.0017	0.6298
NGFG_00708	fumC	0.0012	1.4938	NGFG_02041	ilvH	0.0000	0.5385
NGFG_00720		0.0010	1.8378	NGFG_02042	ilvB	0.0000	0.4796
NGFG_00721		0.0001	1.9212	NGFG_02044	hisG	0.0002	0.6502
NGFG_00765	rpiA	0.0159	0.6930	NGFG_02049		0.0037	1.8075
NGFG_00779	lysC	0.0083	0.6792	NGFG_02050		0.0312	1.6178
NGFG_00814	cs	0.0000	1.8596	NGFG_02056	pcaC	0.0113	0.6143
NGFG_00824		0.0031	0.6722	NGFG_02057	mtrA	0.0253	0.7610
NGFG_00825		0.0256	0.6194	NGFG_02065	gpmA	0.0026	0.6426
NGFG_00831	greA	0.0164	1.4459	NGFG_02066	parC	0.0064	0.7371
NGFG_00881	leuA	0.0153	1.2772	NGFG_02090		0.0271	1.3746
NGFG_00893		0.0137	0.6625	NGFG_02102		0.0000	2.1435
NGFG_00906		0.0229	0.7542	NGFG_02111	gloA	0.0256	0.6657
NGFG_00952	ssb	0.0012	1.8201	NGFG_02144	aroF	0.0104	0.7727
NGFG_00953	topB	0.0191	1.6598	NGFG_02153	norB	0.0000	0.5897

NGFG_00962		0.0022	1.3651	NGFG_02154	nirK	0.0113	0.6457
NGFG_00963		0.0442	1.5326	NGFG_02170		0.0000	1.8751
NGFG_00971		0.0043	1.6806	NGFG_02171	alr	0.0104	1.3957
NGFG_00981	traH	0.0100	1.7888	NGFG_02204		0.0170	1.6166
NGFG_01146		0.0000	0.5126	NGFG_02205		0.0128	1.5011
NGFG_01163	iscR	0.0105	1.8635	NGFG_02209		0.0402	1.5834
NGFG_01166	fic	0.0242	1.4389	NGFG_02237		0.0363	1.7076
NGFG_01216	trxB	0.0368	0.7961	NGFG_02247		0.0216	1.5379
NGFG_01303		0.0002	1.6358	NGFG_02259		0.0493	0.7076
NGFG_01311		0.0247	1.7605	NGFG_02263		0.0452	0.7265
NGFG_01315		0.0438	1.4530	NGFG_02284	htpX	0.0025	1.4682
NGFG_01323		0.0113	0.7240	NGFG_02342		0.0006	1.9494
NGFG_01349		0.0064	1.8075	NGFG_02343		0.0000	2.1585
NGFG_01351	anmK	0.0342	0.7526	NGFG_02345		0.0064	1.6853
NGFG_01353		0.0161	0.5736	NGFG_02348		0.0004	1.7851
NGFG_01354	hemN	0.0472	0.7443	NGFG_02349		0.0002	1.9319
NGFG_01356	cysB	0.0113	0.7526	NGFG_02363		0.0453	1.6234
NGFG_01404	prpC	0.0053	1.5900	NGFG_02407	psaT	0.0068	0.7366
NGFG_01407	acn	0.0056	1.5900	NGFG_02415		0.0000	2.5140
NGFG_01411	ack	0.0000	1.9079	NGFG_02419		0.0033	0.7320
NGFG_01445	bioF	0.0255	1.3131	NGFG_02439		0.0371	1.5966
NGFG_01471	lctP	0.0191	0.7658	NGFG_02463		0.0089	1.6290
NGFG_01486		0.0170	0.8106	NGFG_02499		0.0105	1.7171
NGFG_01491		0.0018	1.8366	NGFG_02500		0.0050	1.7569

Table A.2: Complete list of the results of the RNAseq screen on NgncR_162 and NgncR_163

	162AIE versus ΔΔ			163AIE versus ΔΔ			ΔΔ versus MS11		
	logFC	p-value	q-value	logFC	p-value	q-value	logFC	p-value	q-value
NGFG_00001	-0.0737	0.7230	0.8970	0.1150	0.5780	0.8360	0.4280	0.0412	0.2420
NGFG_00002	0.1900	0.3270	0.6430	0.1370	0.4790	0.7880	-0.0060	0.9760	0.9940
NGFG_00003	-0.1340	0.5960	0.8230	#NV			0.0591	0.8150	0.9440
NGFG_00006	-0.0819	0.7290	0.9000	-0.1200	0.6100	0.8480	0.4020	0.0893	0.3620
NGFG_00007	0.1540	0.5400	0.8020	#NV			0.0957	0.7020	0.9010
NGFG_00008	0.1420	0.5720	0.8160	0.0913	0.7170	0.9020	0.1200	0.6330	0.8690
NGFG_00009	0.0684	0.7830	0.9140	#NV			-0.0855	0.7300	0.9110
NGFG_00010	0.0045	0.9850	0.9950	#NV			0.1760	0.4750	0.7850
NGFG_00014	-0.0799	0.6500	0.8530	0.1180	0.4990	0.7940	-0.1550	0.3690	0.7150
NGFG_00017	-0.1140	0.3930	0.7070	-0.0816	0.5410	0.8120	0.2640	0.0478	0.2620
NGFG_00018	-0.3920	0.0151	0.1610	-0.4760	0.0033	0.0922	0.2280	0.1540	0.4850
NGFG_00021	0.0651	0.7190	0.8940	-0.0249	0.8910	0.9780	-0.0776	0.6670	0.8870
NGFG_00022	-0.3300	0.1280	0.4190	-0.2970	0.1700	0.4950	0.2200	0.3080	0.6570
NGFG_00023	-0.1540	0.3180	0.6340	0.0221	0.8860	0.9770	-0.0518	0.7350	0.9110
NGFG_00024	0.3620	0.0681	0.3160	0.3250	0.1020	0.4090	-0.5750	0.0037	0.0538

NGFG_00025	-0.3460	0.0059	0.0995	-0.2680	0.0319	0.2630	-0.3390	0.0047	0.0620
NGFG_00027	-0.1070	0.6580	0.8580	-0.0460	0.8480	0.9610	-0.0346	0.8850	0.9670
NGFG_00028	-0.0233	0.8740	0.9510	-0.2070	0.1600	0.4860	0.0673	0.6450	0.8760
NGFG_00029	-0.2360	0.0855	0.3510	-0.1460	0.2870	0.6400	-0.0337	0.8030	0.9370
NGFG_00030	-0.0785	0.6690	0.8650	-0.1120	0.5410	0.8120	0.0050	0.9780	0.9950
NGFG_00031	-0.0305	0.7790	0.9130	-0.0516	0.6350	0.8600	-0.1940	0.0721	0.3260
NGFG_00032	-0.0350	0.8690	0.9500	0.0508	0.8100	0.9470	0.1840	0.3840	0.7240
NGFG_00033	0.5750	0.0000	0.0000	0.5770	0.0000	0.0000	-0.2290	0.0148	0.1270
NGFG_00034	0.1510	0.3050	0.6210	0.1080	0.4610	0.7770	0.0387	0.7920	0.9340
NGFG_00035	0.0248	0.8950	0.9600	-0.1210	0.5190	0.8030	0.2560	0.1730	0.5180
NGFG_00036	-0.1370	0.5700	0.8160	#NV			0.1340	0.5800	0.8390
NGFG_00037	-0.0897	0.6160	0.8310	-0.1670	0.3520	0.7020	-0.2320	0.1890	0.5390
NGFG_00038	-0.3490	0.0248	0.2100	-0.1740	0.2590	0.6100	-0.2750	0.0671	0.3170
NGFG_00039	-0.7050	0.0008	0.0372	-0.3680	0.0763	0.3640	0.2930	0.1560	0.4880
NGFG_00041	-0.0169	0.9020	0.9620	0.0649	0.6360	0.8600	-0.1420	0.2960	0.6470
NGFG_00042	0.0592	0.7340	0.9000	0.2100	0.2240	0.5690	-0.0856	0.6210	0.8640
NGFG_00043	0.3450	0.0476	0.2720	0.4710	0.0069	0.1320	0.0783	0.6530	0.8800
NGFG_00044	0.0501	0.7740	0.9120	0.0000	1.0000	1.0000	-0.0660	0.7050	0.9010
NGFG_00045	0.5400	0.0017	0.0523	0.6940	0.0001	0.0113	-1.9700	0.0000	0.0000
NGFG_00046	0.1570	0.4450	0.7390	-0.0056	0.9780	0.9980	-0.3410	0.0931	0.3660
NGFG_00048	0.1190	0.3420	0.6590	0.0859	0.4920	0.7930	-0.3540	0.0045	0.0602
NGFG_00049	#NV			#NV			0.1600	0.4900	0.7950
NGFG_00050	-0.0803	0.6800	0.8720	-0.0039	0.9840	0.9990	0.1370	0.4800	0.7860
NGFG_00051	0.3030	0.0999	0.3770	0.1830	0.3200	0.6800	-0.3380	0.0660	0.3160
NGFG_00052	0.3400	0.0225	0.2000	0.2720	0.0689	0.3470	-0.4440	0.0028	0.0442
NGFG_00054	-0.1160	0.4310	0.7270	-0.0760	0.6070	0.8480	-0.1670	0.2570	0.6130
NGFG_00055	0.1880	0.3390	0.6540	0.0819	0.6760	0.8850	0.1130	0.5630	0.8340
NGFG_00056	0.0120	0.9290	0.9760	0.0027	0.9840	0.9990	-0.1000	0.4530	0.7720
NGFG_00058	-0.2530	0.1980	0.5070	-0.2290	0.2430	0.5900	0.1460	0.4580	0.7740
NGFG_00062	-0.4640	0.0031	0.0757	-0.2390	0.1230	0.4440	0.0380	0.8030	0.9370
NGFG_00063	-0.4950	0.0084	0.1190	-0.5490	0.0036	0.0979	0.2150	0.2390	0.5970
NGFG_00064	-0.1450	0.1860	0.4930	-0.0891	0.4160	0.7500	-0.0972	0.3670	0.7130
NGFG_00065	-0.3010	0.0418	0.2600	-0.2360	0.1090	0.4210	0.1490	0.3120	0.6610
NGFG_00067	-0.1610	0.2710	0.5950	-0.3490	0.0177	0.2040	-0.0674	0.6400	0.8730
NGFG_00068	-0.1370	0.5480	0.8060	#NV			-0.0843	0.7080	0.9010
NGFG_00069	0.0022	0.9900	0.9950	-0.0362	0.8290	0.9500	-0.3460	0.0375	0.2300
NGFG_00070	-0.4110	0.0032	0.0769	-0.4240	0.0024	0.0759	0.5050	0.0003	0.0088
NGFG_00071	-0.3030	0.0568	0.2900	-0.2120	0.1830	0.5070	0.3870	0.0148	0.1270
NGFG_00072	-0.1120	0.3980	0.7090	-0.0534	0.6860	0.8860	0.4220	0.0015	0.0271
NGFG_00073	0.0078	0.9600	0.9880	-0.0994	0.5180	0.8030	0.1580	0.3040	0.6540
NGFG_00074	-0.1880	0.1570	0.4590	-0.2590	0.0515	0.3090	0.3810	0.0042	0.0579
NGFG_00075	0.0007	0.9960	0.9980	-0.0512	0.7410	0.9140	0.1460	0.3470	0.6930
NGFG_00076	0.2030	0.3000	0.6160	0.2830	0.1480	0.4710	-0.2670	0.1720	0.5170
NGFG_00077	-0.0705	0.7070	0.8880	0.0082	0.9650	0.9950	0.0945	0.6130	0.8600
NGFG_00078	-0.1040	0.3960	0.7080	-0.1330	0.2760	0.6310	0.2570	0.0357	0.2250
NGFG_00081	0.0518	0.8120	0.9260	0.2570	0.2390	0.5880	0.5020	0.0215	0.1660
NGFG_00082	0.2360	0.2720	0.5960	0.4380	0.0418	0.2870	0.1140	0.5970	0.8490

NGFG_00083	0.1680	0.1540	0.4570	0.2250	0.0555	0.3200	-0.1630	0.1660	0.5070
NGFG_00084	0.1350	0.4760	0.7630	0.0695	0.7140	0.9010	-0.0078	0.9670	0.9940
NGFG_00085	0.0648	0.7630	0.9100	0.1130	0.5980	0.8480	-0.0039	0.9860	0.9970
NGFG_00087	0.0740	0.6050	0.8250	-0.0418	0.7710	0.9260	-0.1350	0.3440	0.6900
NGFG_00088	0.3570	0.0154	0.1620	0.3720	0.0116	0.1670	0.0040	0.9790	0.9950
NGFG_00089	-0.1790	0.2760	0.5980	-0.2230	0.1750	0.4990	-0.0036	0.9830	0.9960
NGFG_00091	-0.5210	0.0001	0.0110	-0.4120	0.0021	0.0707	0.2030	0.1220	0.4250
NGFG_00092	-0.1380	0.4120	0.7180	-0.2540	0.1330	0.4550	0.0753	0.6520	0.8800
NGFG_00093	-0.0585	0.6220	0.8340	-0.2690	0.0236	0.2290	0.7110	0.0000	0.0000
NGFG_00094	-0.0959	0.5640	0.8160	-0.1960	0.2390	0.5880	0.2030	0.2210	0.5840
NGFG_00095	-0.0936	0.2920	0.6100	-0.0568	0.5220	0.8030	-0.1230	0.1620	0.5000
NGFG_00097	-0.1100	0.6360	0.8450	-0.0100	0.9660	0.9950	0.2930	0.2090	0.5660
NGFG_00098	0.1260	0.3770	0.6910	0.1920	0.1790	0.5030	-0.0205	0.8860	0.9670
NGFG_00099	0.2910	0.1250	0.4130	0.5790	0.0022	0.0729	-0.1550	0.4120	0.7450
NGFG_00100	0.5780	0.0005	0.0272	0.5740	0.0005	0.0294	-0.3010	0.0685	0.3200
NGFG_00101	0.4300	0.0013	0.0471	0.3510	0.0089	0.1450	-0.2040	0.1290	0.4340
NGFG_00102	0.3420	0.0062	0.1020	0.2780	0.0263	0.2380	-0.2190	0.0793	0.3430
NGFG_00103	0.2420	0.0318	0.2330	0.1760	0.1190	0.4400	-0.1290	0.2510	0.6080
NGFG_00104	0.2720	0.1020	0.3810	0.1950	0.2410	0.5900	-0.1010	0.5440	0.8220
NGFG_00105	0.3520	0.0371	0.2460	0.2420	0.1510	0.4720	-0.1560	0.3560	0.7000
NGFG_00106	0.0505	0.7470	0.9040	0.0141	0.9280	0.9830	-0.0613	0.6950	0.8970
NGFG_00107	-0.0930	0.5620	0.8160	-0.0790	0.6230	0.8510	-0.1600	0.3190	0.6660
NGFG_00109	0.0548	0.6960	0.8810	0.0023	0.9870	0.9990	-0.1710	0.2220	0.5840
NGFG_00110	-0.0707	0.5750	0.8160	-0.0599	0.6350	0.8600	-0.1680	0.1810	0.5310
NGFG_00113	-0.3950	0.0017	0.0523	-0.2930	0.0194	0.2070	0.1330	0.2830	0.6320
NGFG_00114	-0.2060	0.1200	0.4040	-0.1880	0.1560	0.4830	0.1850	0.1610	0.5000
NGFG_00115	-0.0473	0.8110	0.9260	-0.0606	0.7600	0.9230	0.3000	0.1300	0.4360
NGFG_00116	0.1940	0.1090	0.3910	0.1710	0.1580	0.4840	-0.3640	0.0026	0.0419
NGFG_00117	-0.0035	0.9860	0.9950	-0.0029	0.9890	0.9990	-0.1420	0.4790	0.7860
NGFG_00118	-0.0235	0.8630	0.9490	-0.1260	0.3560	0.7100	-0.0213	0.8760	0.9650
NGFG_00119	0.1930	0.3670	0.6820	0.2000	0.3490	0.7010	-0.2480	0.2470	0.6030
NGFG_00120	-0.1190	0.5210	0.7920	0.0923	0.6160	0.8480	-0.3080	0.0913	0.3620
NGFG_00121	-0.0578	0.6710	0.8680	-0.0100	0.9420	0.9880	-0.3760	0.0055	0.0677
NGFG_00124	0.0831	0.6350	0.8450	0.0526	0.7640	0.9240	0.2170	0.2200	0.5830
NGFG_00125	-0.0818	0.6080	0.8260	-0.1900	0.2340	0.5820	-0.0297	0.8510	0.9570
NGFG_00126	0.2410	0.0480	0.2720	0.2120	0.0819	0.3660	-0.4130	0.0006	0.0147
NGFG_00127	0.0677	0.7570	0.9080	0.0122	0.9550	0.9930	0.2500	0.2530	0.6090
NGFG_00128	0.0563	0.7080	0.8880	-0.0019	0.9900	0.9990	0.1240	0.4100	0.7440
NGFG_00129	-0.1460	0.4260	0.7230	-0.0597	0.7450	0.9160	0.4620	0.0123	0.1160
NGFG_00130	0.3020	0.0149	0.1610	0.2550	0.0400	0.2870	0.1270	0.3080	0.6570
NGFG_00131	0.0165	0.8510	0.9450	-0.0327	0.7100	0.8970	-0.0619	0.4810	0.7880
NGFG_00133	-0.4260	0.0399	0.2570	-0.5460	0.0087	0.1430	0.3870	0.0616	0.3060
NGFG_00134	-0.1020	0.4330	0.7270	-0.0303	0.8150	0.9480	-0.0787	0.5400	0.8180
NGFG_00135	-0.0090	0.9720	0.9930	#NV			-0.0656	0.7960	0.9350
NGFG_00137	-0.3750	0.0247	0.2100	-0.3400	0.0414	0.2870	0.1520	0.3600	0.7050
NGFG_00138	0.1290	0.2020	0.5100	0.1390	0.1700	0.4950	-0.1210	0.2300	0.5880
NGFG_00139	-0.3230	0.1140	0.3970	-0.2490	0.2220	0.5660	0.0143	0.9440	0.9880

NGFG_00140	-0.2090	0.3160	0.6330	-0.1050	0.6150	0.8480	0.0606	0.7710	0.9240
NGFG_00143	-0.2410	0.1570	0.4590	-0.2550	0.1330	0.4540	0.0136	0.9360	0.9850
NGFG_00149	0.0147	0.9440	0.9830	0.0127	0.9520	0.9930	-0.2280	0.2760	0.6280
NGFG_00152	-0.1170	0.4830	0.7660	-0.0122	0.9420	0.9880	0.1140	0.4940	0.7960
NGFG_00153	-0.0823	0.5660	0.8160	-0.1160	0.4170	0.7500	-0.1850	0.1950	0.5500
NGFG_00154	-0.3630	0.1350	0.4340	-0.1250	0.6050	0.8480	0.1820	0.4500	0.7700
NGFG_00155	0.0427	0.7560	0.9080	0.0699	0.6110	0.8480	-0.1720	0.2090	0.5660
NGFG_00156	0.1930	0.3950	0.7080	0.1960	0.3870	0.7270	-0.2570	0.2530	0.6090
NGFG_00157	-0.3250	0.0334	0.2350	-0.2480	0.1040	0.4150	0.1420	0.3490	0.6940
NGFG_00158	-0.2920	0.1230	0.4080	-0.1170	0.5320	0.8100	-0.0802	0.6600	0.8840
NGFG_00159	-0.3460	0.1190	0.4040	-0.2440	0.2690	0.6240	0.1220	0.5780	0.8380
NGFG_00160	-0.6380	0.0036	0.0783	-0.3350	0.1220	0.4430	-0.0398	0.8520	0.9570
NGFG_00161	-0.1760	0.2220	0.5340	-0.2730	0.0581	0.3240	-0.1160	0.4150	0.7460
NGFG_00162	-0.3750	0.0020	0.0595	-0.2680	0.0265	0.2390	-0.0731	0.5370	0.8150
NGFG_00163	0.1090	0.6140	0.8300	0.0163	0.9400	0.9870	-0.0282	0.8960	0.9720
NGFG_00164	0.1400	0.4250	0.7230	0.1570	0.3700	0.7150	-0.2590	0.1380	0.4510
NGFG_00165	-0.3490	0.0092	0.1220	-0.1810	0.1720	0.4950	-0.0485	0.7100	0.9010
NGFG_00166	-0.4880	0.0304	0.2320	-0.2550	0.2560	0.6060	0.0597	0.7880	0.9330
NGFG_00167	-0.2730	0.1870	0.4940	-0.1960	0.3440	0.6970	0.0243	0.9060	0.9720
NGFG_00169	-0.0286	0.7900	0.9150	-0.1230	0.2510	0.6000	-0.1660	0.1200	0.4200
NGFG_00170	-0.3010	0.0790	0.3380	-0.2320	0.1740	0.4970	-0.2970	0.0754	0.3360
NGFG_00171	-0.4270	0.0001	0.0103	-0.3050	0.0052	0.1150	-0.0248	0.8190	0.9470
NGFG_00172	-0.0980	0.5990	0.8230	-0.0824	0.6580	0.8750	0.3290	0.0781	0.3400
NGFG_00174	-0.0193	0.8420	0.9410	-0.0032	0.9740	0.9960	-0.0302	0.7550	0.9190
NGFG_00175	0.0903	0.5470	0.8060	0.0892	0.5520	0.8190	-0.1500	0.3150	0.6640
NGFG_00176	-0.1280	0.5480	0.8060	-0.2770	0.1930	0.5230	0.0519	0.8070	0.9390
NGFG_00177	-0.1980	0.2780	0.6010	-0.2250	0.2170	0.5580	0.0292	0.8730	0.9630
NGFG_00178	-0.1050	0.6500	0.8530	-0.0517	0.8230	0.9500	-0.0097	0.9670	0.9940
NGFG_00180	-0.2070	0.0546	0.2880	-0.2520	0.0194	0.2070	-0.0351	0.7420	0.9140
NGFG_00181	0.0198	0.9050	0.9630	-0.0049	0.9760	0.9980	-0.1800	0.2780	0.6310
NGFG_00182	0.2640	0.2080	0.5190	0.3220	0.1240	0.4470	-0.0821	0.6950	0.8970
NGFG_00183	0.2970	0.1750	0.4790	0.3670	0.0937	0.3950	-0.1590	0.4690	0.7820
NGFG_00184	-0.3110	0.0631	0.2990	-0.2950	0.0778	0.3640	0.3390	0.0418	0.2440
NGFG_00186	-0.2120	0.1370	0.4360	-0.0985	0.4880	0.7900	0.1780	0.2100	0.5670
NGFG_00187	-0.3420	0.1070	0.3870	-0.3340	0.1150	0.4350	0.2630	0.2130	0.5710
NGFG_00189	0.0612	0.6950	0.8810	0.0417	0.7890	0.9340	-0.2760	0.0757	0.3370
NGFG_00190	-0.1990	0.3840	0.6980	-0.1180	0.6070	0.8480	0.3870	0.0906	0.3620
NGFG_00192	0.3360	0.1360	0.4340	0.3560	0.1150	0.4340	-0.1970	0.3820	0.7240
NGFG_00193	-0.2620	0.1070	0.3870	-0.2700	0.0961	0.3990	0.0991	0.5380	0.8160
NGFG_00194	-0.4620	0.0083	0.1170	-0.4280	0.0143	0.1830	0.1870	0.2830	0.6320
NGFG_00195	-0.3920	0.0103	0.1300	-0.3300	0.0305	0.2560	0.2690	0.0761	0.3370
NGFG_00196	-0.1520	0.3510	0.6680	-0.1100	0.5010	0.7940	-0.0415	0.7990	0.9360
NGFG_00197	-0.2450	0.0448	0.2690	-0.2470	0.0430	0.2880	0.2150	0.0787	0.3410
NGFG_00199	-0.5310	0.0048	0.0898	-0.3820	0.0417	0.2870	0.4590	0.0144	0.1270
NGFG_00200	-0.2060	0.0515	0.2830	-0.2060	0.0513	0.3090	0.0272	0.7960	0.9350
NGFG_00203	-0.1810	0.1750	0.4790	-0.0465	0.7260	0.9080	-0.1170	0.3770	0.7220
NGFG_00204	0.0804	0.3060	0.6220	0.0858	0.2750	0.6300	-0.1960	0.0125	0.1160

NGFG_00207	-0.0359	0.8400	0.9390	0.0677	0.7030	0.8960	-0.2180	0.2170	0.5800
NGFG_00208	-0.0981	0.3550	0.6700	-0.1610	0.1290	0.4520	-0.1380	0.1920	0.5420
NGFG_00209	-0.5250	0.0038	0.0805	-0.4470	0.0134	0.1810	0.3360	0.0611	0.3040
NGFG_00214	-0.2930	0.0033	0.0780	-0.2550	0.0105	0.1600	-0.0876	0.3760	0.7210
NGFG_00217	0.0337	0.8950	0.9600	#NV			-0.0689	0.7870	0.9330
NGFG_00218	-0.0102	0.9460	0.9830	-0.2700	0.0766	0.3640	0.2430	0.1100	0.3980
NGFG_00219	-0.1860	0.1890	0.4970	-0.3090	0.0299	0.2530	0.2590	0.0659	0.3160
NGFG_00220	-0.2730	0.0601	0.2920	-0.2040	0.1590	0.4850	0.1770	0.2200	0.5830
NGFG_00221	0.0727	0.6390	0.8470	0.0198	0.8980	0.9800	-0.1270	0.4070	0.7410
NGFG_00222	-0.2380	0.1620	0.4660	-0.4030	0.0187	0.2070	0.0306	0.8550	0.9580
NGFG_00223	0.0409	0.7570	0.9080	-0.1080	0.4150	0.7500	-0.2310	0.0776	0.3390
NGFG_00224	-0.1160	0.4810	0.7660	-0.0879	0.5920	0.8460	0.0017	0.9920	0.9990
NGFG_00225	-0.2180	0.3360	0.6530	-0.1700	0.4520	0.7710	-0.0862	0.7030	0.9010
NGFG_00226	-0.1850	0.4160	0.7200	-0.3280	0.1510	0.4720	0.3410	0.1340	0.4450
NGFG_00227	0.0859	0.4670	0.7580	0.1220	0.3020	0.6600	-0.1510	0.1970	0.5500
NGFG_00230	-0.0493	0.7960	0.9190	-0.0381	0.8410	0.9580	-0.0499	0.7930	0.9340
NGFG_00231	-0.3310	0.0168	0.1680	-0.1310	0.3360	0.6900	0.0770	0.5670	0.8370
NGFG_00232	0.0688	0.6800	0.8720	-0.0192	0.9080	0.9820	-0.1340	0.4210	0.7510
NGFG_00233	0.2330	0.0979	0.3760	0.1230	0.3820	0.7270	-0.1760	0.2100	0.5670
NGFG_00234	0.0384	0.8310	0.9350	0.0207	0.9080	0.9820	-0.0056	0.9750	0.9940
NGFG_00235	0.2160	0.1600	0.4650	0.1010	0.5130	0.8000	-0.1640	0.2860	0.6340
NGFG_00236	0.1900	0.2730	0.5960	0.1840	0.2870	0.6400	-0.0502	0.7710	0.9240
NGFG_00237	0.2390	0.0587	0.2920	0.2010	0.1120	0.4270	0.0845	0.5040	0.8000
NGFG_00238	0.1840	0.2220	0.5340	0.1640	0.2770	0.6320	-0.1530	0.3080	0.6570
NGFG_00239	0.4450	0.0170	0.1690	0.4190	0.0248	0.2330	-0.4060	0.0295	0.2020
NGFG_00240	-0.0178	0.8660	0.9490	0.0228	0.8290	0.9500	-0.0637	0.5460	0.8240
NGFG_00241	0.1640	0.0893	0.3580	0.1650	0.0871	0.3810	-0.0943	0.3270	0.6730
NGFG_00242	-0.3570	0.0259	0.2140	-0.2560	0.1090	0.4210	0.2640	0.0980	0.3730
NGFG_00243	-0.1680	0.2470	0.5700	-0.2110	0.1460	0.4680	0.1330	0.3560	0.7000
NGFG_00245	-0.1760	0.2460	0.5690	-0.1420	0.3510	0.7020	0.1550	0.3060	0.6550
NGFG_00246	-0.2070	0.1400	0.4360	-0.1940	0.1670	0.4940	0.1340	0.3380	0.6850
NGFG_00247	0.6970	0.0008	0.0372	0.2860	0.1690	0.4950	0.4040	0.0527	0.2750
NGFG_00249	-0.1500	0.4250	0.7230	-0.4840	0.0109	0.1610	1.5500	0.0000	0.0000
NGFG_00250	-0.0969	0.7030	0.8850	#NV			0.0987	0.6980	0.8980
NGFG_00251	-0.2410	0.1730	0.4750	-0.1230	0.4840	0.7900	-0.1490	0.3910	0.7300
NGFG_00252	-0.0312	0.7980	0.9200	-0.1080	0.3760	0.7210	-0.6000	0.0000	0.0001
NGFG_00253	-0.0955	0.6490	0.8530	0.1760	0.4000	0.7370	0.0432	0.8360	0.9520
NGFG_00254	0.5010	0.0007	0.0342	0.4130	0.0052	0.1150	-0.6560	0.0000	0.0006
NGFG_00255	-0.3370	0.0030	0.0752	-0.3150	0.0055	0.1170	0.0146	0.8970	0.9720
NGFG_00256	-0.2560	0.1550	0.4570	-0.1420	0.4320	0.7550	0.2650	0.1410	0.4600
NGFG_00257	-0.4560	0.0697	0.3180	#NV			-0.1030	0.6790	0.8930
NGFG_00259	-0.0623	0.7380	0.9000	0.0182	0.9220	0.9820	0.2240	0.2290	0.5880
NGFG_00260	0.1440	0.5320	0.7960	0.2260	0.3240	0.6830	0.3070	0.1840	0.5340
NGFG_00262	0.3110	0.0276	0.2210	0.1970	0.1640	0.4920	-0.3330	0.0178	0.1460
NGFG_00263	0.0059	0.9800	0.9950	#NV			0.2610	0.2670	0.6210
NGFG_00264	-0.0781	0.7400	0.9000	#NV			0.4370	0.0648	0.3140
NGFG_00266	0.1380	0.1840	0.4900	0.0424	0.6840	0.8860	-0.1470	0.1560	0.4880

NGFG_00267	-0.1600	0.2990	0.6160	-0.2530	0.1000	0.4050	0.0338	0.8250	0.9500
NGFG_00268	-0.1030	0.4390	0.7330	-0.1190	0.3740	0.7210	-0.0898	0.4960	0.7960
NGFG_00269	0.0829	0.5030	0.7800	0.0771	0.5330	0.8100	-0.1160	0.3450	0.6900
NGFG_00270	0.1420	0.3570	0.6700	0.3040	0.0467	0.2960	0.1010	0.5150	0.8030
NGFG_00271	0.1500	0.3190	0.6350	0.1280	0.3960	0.7360	0.0029	0.9850	0.9970
NGFG_00272	0.0336	0.8640	0.9490	0.0337	0.8640	0.9700	0.0121	0.9510	0.9910
NGFG_00273	-0.0539	0.6110	0.8290	-0.0621	0.5580	0.8210	0.0077	0.9420	0.9880
NGFG_00275	-0.0117	0.9180	0.9690	-0.0715	0.5330	0.8100	-0.1040	0.3600	0.7050
NGFG_00276	-0.4330	0.0180	0.1750	-0.2480	0.1730	0.4950	0.0790	0.6600	0.8840
NGFG_00277	-0.3180	0.1890	0.4960	#NV			0.1260	0.5990	0.8500
NGFG_00281	0.0805	0.4470	0.7430	0.1070	0.3120	0.6700	-0.2350	0.0261	0.1880
NGFG_00282	-0.0576	0.7180	0.8940	-0.1540	0.3360	0.6900	-0.2550	0.1080	0.3930
NGFG_00283	-0.1390	0.5440	0.8050	0.0880	0.6980	0.8940	-0.2130	0.3450	0.6900
NGFG_00284	-0.0108	0.9460	0.9830	-0.0357	0.8210	0.9500	0.1560	0.3250	0.6700
NGFG_00286	0.0421	0.8100	0.9260	0.1020	0.5610	0.8230	-0.3530	0.0437	0.2500
NGFG_00287	-0.0328	0.8460	0.9430	-0.0995	0.5560	0.8210	-0.2320	0.1680	0.5110
NGFG_00289	-0.4310	0.0078	0.1150	-0.3760	0.0201	0.2090	0.3250	0.0444	0.2520
NGFG_00291	-0.0016	0.9920	0.9960	0.0578	0.7270	0.9080	0.2450	0.1410	0.4600
NGFG_00292	-0.0764	0.5900	0.8190	-0.1580	0.2670	0.6220	-0.2030	0.1460	0.4680
NGFG_00293	-0.0626	0.6840	0.8750	-0.0421	0.7840	0.9320	0.3020	0.0505	0.2720
NGFG_00295	0.0045	0.9800	0.9950	0.0625	0.7250	0.9070	-0.3530	0.0469	0.2590
NGFG_00297	-0.0947	0.5760	0.8160	-0.0364	0.8300	0.9500	-0.1730	0.3050	0.6540
NGFG_00300	0.2490	0.3070	0.6230	-0.1070	0.6620	0.8770	0.4120	0.0939	0.3670
NGFG_00301	0.1760	0.4730	0.7620	0.2300	0.3500	0.7010	0.2310	0.3490	0.6940
NGFG_00302	0.0870	0.7050	0.8870	0.2040	0.3750	0.7210	0.1630	0.4800	0.7860
NGFG_00303	0.1340	0.5840	0.8160	#NV			-0.0297	0.9030	0.9720
NGFG_00305	-0.1860	0.4040	0.7110	-0.2160	0.3340	0.6900	0.1180	0.5980	0.8490
NGFG_00306	0.0844	0.7270	0.9000	-0.0857	0.7230	0.9060	-0.0122	0.9600	0.9940
NGFG_00307	-0.0610	0.6940	0.8810	0.0097	0.9500	0.9930	-0.2560	0.0940	0.3670
NGFG_00308	0.4350	0.0296	0.2320	0.3570	0.0740	0.3580	-0.1460	0.4660	0.7800
NGFG_00309	-0.1220	0.4290	0.7260	-0.1580	0.3060	0.6620	0.3310	0.0321	0.2110
NGFG_00310	-0.0433	0.7740	0.9120	-0.1410	0.3480	0.7010	0.0321	0.8310	0.9520
NGFG_00311	-0.1180	0.6040	0.8240	0.1660	0.4650	0.7820	0.0572	0.8010	0.9370
NGFG_00313	-0.2820	0.0669	0.3130	-0.2140	0.1640	0.4920	0.1510	0.3250	0.6700
NGFG_00314	-0.0147	0.9010	0.9610	-0.0178	0.8800	0.9740	-0.1260	0.2820	0.6320
NGFG_00316	0.1760	0.2760	0.5980	0.0313	0.8470	0.9610	0.0971	0.5490	0.8260
NGFG_00317	0.2090	0.4100	0.7150	#NV			-0.0156	0.9510	0.9910
NGFG_00318	-0.0179	0.8980	0.9600	-0.0054	0.9690	0.9960	-0.1640	0.2370	0.5960
NGFG_00319	0.1070	0.4250	0.7230	0.0480	0.7210	0.9050	0.0926	0.4900	0.7950
NGFG_00320	0.2670	0.0456	0.2690	0.2270	0.0894	0.3850	-0.1600	0.2290	0.5880
NGFG_00321	0.5550	0.0008	0.0372	0.4610	0.0054	0.1170	-0.3580	0.0309	0.2050
NGFG_00322	0.3840	0.0131	0.1500	0.1610	0.3000	0.6600	-0.0401	0.7960	0.9350
NGFG_00323	-0.1320	0.4810	0.7660	-0.2940	0.1170	0.4370	0.4540	0.0155	0.1310
NGFG_00324	0.2560	0.1390	0.4360	0.2520	0.1450	0.4670	-0.2270	0.1910	0.5410
NGFG_00325	-0.1890	0.2690	0.5940	-0.2670	0.1200	0.4400	0.1420	0.4020	0.7370
NGFG_00326	0.0856	0.6610	0.8600	0.1660	0.3940	0.7360	0.0025	0.9900	0.9980
NGFG_00327	0.2060	0.0817	0.3450	0.1370	0.2470	0.5950	-0.1000	0.3960	0.7310

NGFG_00328	0.3060	0.0368	0.2460	0.3260	0.0263	0.2380	-0.0850	0.5620	0.8340
NGFG_00329	-0.0611	0.7950	0.9190	0.0491	0.8350	0.9540	0.0455	0.8470	0.9550
NGFG_00330	0.0432	0.6030	0.8240	0.0154	0.8530	0.9650	0.0317	0.7030	0.9010
NGFG_00331	0.1070	0.3100	0.6280	0.1640	0.1180	0.4370	0.0826	0.4320	0.7600
NGFG_00332	0.2860	0.0514	0.2830	0.2970	0.0428	0.2870	-0.0195	0.8940	0.9710
NGFG_00333	-0.0449	0.6430	0.8500	-0.1050	0.2790	0.6340	0.1050	0.2760	0.6280
NGFG_00334	-0.2530	0.0836	0.3500	-0.1640	0.2620	0.6150	0.3250	0.0263	0.1880
NGFG_00335	-0.2210	0.2460	0.5690	-0.3090	0.1050	0.4170	0.2890	0.1280	0.4340
NGFG_00336	0.0901	0.5690	0.8160	0.0513	0.7460	0.9160	-0.1750	0.2670	0.6210
NGFG_00337	0.0543	0.6540	0.8550	0.0690	0.5690	0.8260	-0.1340	0.2650	0.6190
NGFG_00338	-0.0338	0.8440	0.9420	0.0566	0.7410	0.9140	-0.2740	0.1050	0.3900
NGFG_00339	-0.3290	0.0431	0.2660	-0.3690	0.0235	0.2290	-0.0182	0.9090	0.9730
NGFG_00340	0.0910	0.4170	0.7210	0.1690	0.1290	0.4520	-0.1870	0.0912	0.3620
NGFG_00341	0.0795	0.5860	0.8170	-0.0026	0.9860	0.9990	-0.3140	0.0308	0.2050
NGFG_00343	0.3430	0.0626	0.2990	-0.1030	0.5740	0.8320	0.6370	0.0005	0.0133
NGFG_00345	-0.1920	0.1650	0.4710	-0.2440	0.0777	0.3640	0.0778	0.5720	0.8370
NGFG_00346	-0.2430	0.1720	0.4750	-0.2690	0.1300	0.4520	0.2040	0.2500	0.6060
NGFG_00347	-0.1920	0.4000	0.7100	-0.3120	0.1720	0.4950	0.3090	0.1750	0.5190
NGFG_00348	-0.2070	0.3800	0.6940	-0.1760	0.4560	0.7730	0.4060	0.0849	0.3540
NGFG_00349	-0.1160	0.5780	0.8160	-0.2360	0.2590	0.6100	-0.1060	0.6110	0.8590
NGFG_00350	0.2190	0.3450	0.6620	0.2200	0.3440	0.6970	-0.2160	0.3520	0.6960
NGFG_00351	-0.1960	0.2890	0.6070	-0.2180	0.2410	0.5900	0.0465	0.8000	0.9370
NGFG_00352	0.0244	0.8610	0.9480	0.0699	0.6150	0.8480	-0.0335	0.8090	0.9400
NGFG_00353	-0.1090	0.6170	0.8310	-0.1260	0.5640	0.8250	0.1760	0.4220	0.7510
NGFG_00355	-0.0744	0.7350	0.9000	0.0442	0.8400	0.9570	-0.0725	0.7390	0.9110
NGFG_00356	-0.0117	0.9560	0.9870	-0.2030	0.3450	0.6980	-0.0219	0.9190	0.9780
NGFG_00357	-0.1350	0.5360	0.8000	-0.3740	0.0861	0.3790	0.2430	0.2630	0.6190
NGFG_00358	-0.1200	0.4380	0.7330	-0.1040	0.5030	0.7940	-0.1590	0.2970	0.6470
NGFG_00359	0.0757	0.7370	0.9000	0.1070	0.6340	0.8600	-0.2670	0.2330	0.5910
NGFG_00360	0.3290	0.1060	0.3870	0.2590	0.2040	0.5380	-0.5990	0.0033	0.0487
NGFG_00361	-0.3170	0.1140	0.3970	-0.3320	0.0979	0.4020	0.1360	0.4950	0.7960
NGFG_00362	0.1290	0.3550	0.6700	0.0038	0.9780	0.9980	-0.0178	0.8980	0.9720
NGFG_00363	0.3490	0.1370	0.4360	0.3650	0.1200	0.4400	0.4250	0.0705	0.3250
NGFG_00364	0.4860	0.0326	0.2350	0.4960	0.0292	0.2510	0.5690	0.0125	0.1160
NGFG_00366	0.4820	0.0294	0.2310	0.3380	0.1270	0.4510	0.9460	0.0000	0.0011
NGFG_00368	0.1370	0.4890	0.7700	0.2400	0.2270	0.5720	-0.2140	0.2810	0.6320
NGFG_00369	-0.0632	0.7460	0.9030	-0.0624	0.7490	0.9180	-0.3170	0.1040	0.3870
NGFG_00371	-0.2340	0.2500	0.5730	-0.3550	0.0825	0.3670	0.0699	0.7300	0.9110
NGFG_00372	-0.3530	0.0317	0.2330	-0.3890	0.0178	0.2040	0.1590	0.3320	0.6780
NGFG_00373	0.0215	0.8930	0.9600	0.0625	0.6960	0.8920	0.0212	0.8940	0.9710
NGFG_00374	-0.2050	0.1620	0.4660	-0.2900	0.0480	0.3000	-0.1890	0.1870	0.5390
NGFG_00375	-0.1790	0.1950	0.5010	-0.1330	0.3360	0.6900	-0.0575	0.6750	0.8930
NGFG_00376	-0.1200	0.3360	0.6530	-0.1060	0.3950	0.7360	-0.2540	0.0385	0.2320
NGFG_00377	-0.0472	0.7560	0.9080	-0.0333	0.8260	0.9500	-0.0509	0.7370	0.9110
NGFG_00378	-0.1020	0.5780	0.8160	0.0162	0.9300	0.9830	0.1220	0.5060	0.8000
NGFG_00379	-0.0520	0.7620	0.9100	-0.0474	0.7830	0.9320	-0.0265	0.8770	0.9650
NGFG_00381	0.0027	0.9810	0.9950	-0.0158	0.8880	0.9780	-0.1120	0.3160	0.6640

NGFG_00383	-0.1720	0.2980	0.6160	-0.0115	0.9440	0.9890	0.4580	0.0058	0.0697
NGFG_00384	0.0726	0.7070	0.8880	0.0253	0.8960	0.9800	0.0260	0.8930	0.9710
NGFG_00385	0.1270	0.2020	0.5100	0.0877	0.3780	0.7220	-0.2120	0.0327	0.2140
NGFG_00386	0.1000	0.5750	0.8160	0.0121	0.9460	0.9900	0.2090	0.2430	0.6000
NGFG_00387	-0.3580	0.1400	0.4360	-0.1790	0.4600	0.7760	0.3040	0.2100	0.5670
NGFG_00390	-0.1850	0.3130	0.6290	-0.0692	0.7040	0.8960	0.0809	0.6560	0.8820
NGFG_00391	-0.0109	0.9490	0.9830	-0.1580	0.3620	0.7130	0.2170	0.2080	0.5660
NGFG_00392	0.3560	0.0385	0.2520	0.1850	0.2830	0.6380	-0.3020	0.0782	0.3400
NGFG_00393	-0.3490	0.1560	0.4590	#NV			0.2980	0.2250	0.5870
NGFG_00396	-0.3310	0.0430	0.2660	-0.3460	0.0341	0.2740	0.0296	0.8550	0.9580
NGFG_00398	-0.0524	0.7710	0.9110	-0.1150	0.5230	0.8030	0.1100	0.5390	0.8160
NGFG_00400	-0.3010	0.0316	0.2330	-0.2780	0.0467	0.2960	0.1060	0.4450	0.7670
NGFG_00401	-0.3870	0.0299	0.2320	-0.3450	0.0525	0.3120	0.0393	0.8220	0.9490
NGFG_00402	-0.3010	0.1400	0.4360	-0.0949	0.6380	0.8620	-0.2350	0.2350	0.5960
NGFG_00403	-0.3070	0.0144	0.1600	-0.2370	0.0584	0.3240	0.0201	0.8720	0.9630
NGFG_00405	-0.0278	0.8790	0.9560	-0.0705	0.7010	0.8950	0.0028	0.9880	0.9980
NGFG_00406	0.0652	0.6770	0.8720	-0.0364	0.8170	0.9490	-0.1210	0.4410	0.7640
NGFG_00407	-0.0616	0.6970	0.8810	-0.1050	0.5090	0.7960	-0.1760	0.2640	0.6190
NGFG_00408	-0.1430	0.2970	0.6140	-0.0974	0.4760	0.7870	0.0891	0.5120	0.8020
NGFG_00409	0.1300	0.5080	0.7840	0.0576	0.7700	0.9260	-0.1330	0.4980	0.7960
NGFG_00410	0.0028	0.9860	0.9950	-0.1150	0.4860	0.7900	-0.1460	0.3760	0.7210
NGFG_00411	0.1190	0.4360	0.7310	0.0622	0.6830	0.8850	-0.0526	0.7300	0.9110
NGFG_00412	0.2370	0.0881	0.3540	0.0763	0.5840	0.8400	-0.3470	0.0123	0.1160
NGFG_00413	0.1250	0.4730	0.7620	0.0931	0.5940	0.8470	-0.4080	0.0194	0.1540
NGFG_00414	1.4700	0.0000	0.0000	0.7180	0.0037	0.0985	0.0902	0.7170	0.9050
NGFG_00415	0.9380	0.0000	0.0000	0.3280	0.0418	0.2870	-0.1310	0.4160	0.7470
NGFG_00416	0.1950	0.2490	0.5710	0.0967	0.5680	0.8260	-0.1430	0.3980	0.7330
NGFG_00417	-0.0705	0.7280	0.9000	-0.0172	0.9320	0.9850	0.0218	0.9140	0.9750
NGFG_00418	0.3370	0.0315	0.2330	0.2100	0.1800	0.5040	-0.3050	0.0513	0.2720
NGFG_00419	-0.1750	0.2020	0.5100	-0.1720	0.2070	0.5420	0.0341	0.8020	0.9370
NGFG_00422	-0.2440	0.0694	0.3180	-0.1840	0.1700	0.4950	-0.0048	0.9710	0.9940
NGFG_00423	0.1660	0.1750	0.4790	0.2010	0.1010	0.4070	-0.5740	0.0000	0.0002
NGFG_00424	-0.1140	0.3930	0.7070	-0.1130	0.3980	0.7360	0.0209	0.8750	0.9650
NGFG_00425	0.2080	0.2040	0.5130	0.2310	0.1590	0.4860	-0.2380	0.1470	0.4700
NGFG_00426	0.0328	0.7590	0.9100	0.0241	0.8220	0.9500	-0.0596	0.5760	0.8380
NGFG_00427	0.2280	0.0636	0.3010	0.1520	0.2160	0.5550	-0.2610	0.0336	0.2180
NGFG_00428	-0.3060	0.1820	0.4870	-0.1850	0.4170	0.7500	0.2900	0.2030	0.5570
NGFG_00429	#NV			#NV			-0.0122	0.9250	0.9790
NGFG_00430	0.0894	0.5990	0.8230	0.0004	0.9980	0.9990	-0.0987	0.5620	0.8340
NGFG_00432	-0.0098	0.9360	0.9790	-0.0443	0.7160	0.9020	0.1800	0.1380	0.4510
NGFG_00433	-0.2880	0.0588	0.2920	-0.2560	0.0926	0.3930	0.0847	0.5760	0.8380
NGFG_00435	0.0396	0.7270	0.9000	0.0216	0.8490	0.9610	-0.0121	0.9140	0.9750
NGFG_00439	0.0759	0.5890	0.8190	0.0927	0.5090	0.7960	-0.0782	0.5770	0.8380
NGFG_00440	0.0099	0.9340	0.9790	0.0058	0.9610	0.9940	0.0072	0.9520	0.9910
NGFG_00441	0.4370	0.0004	0.0252	0.3400	0.0058	0.1210	-0.1470	0.2320	0.5910
NGFG_00442	0.3830	0.0054	0.0968	0.5010	0.0003	0.0221	-0.0053	0.9690	0.9940
NGFG_00443	0.5060	0.0023	0.0631	0.4700	0.0047	0.1110	-0.0201	0.9040	0.9720

NGFG_00444	0.1150	0.3710	0.6850	0.0342	0.7910	0.9340	0.1620	0.2110	0.5680
NGFG_00445	0.1580	0.3780	0.6920	0.0746	0.6770	0.8850	-0.0839	0.6390	0.8730
NGFG_00446	-0.4190	0.0328	0.2350	-0.3030	0.1220	0.4430	0.5110	0.0092	0.0938
NGFG_00447	0.0895	0.7000	0.8830	#NV			0.8350	0.0005	0.0118
NGFG_00448	0.1500	0.4300	0.7270	0.0044	0.9810	0.9990	0.7490	0.0001	0.0035
NGFG_00449	0.0946	0.3260	0.6420	0.0280	0.7720	0.9270	0.1790	0.0628	0.3090
NGFG_00450	0.1390	0.4030	0.7110	0.3340	0.0437	0.2890	-0.0148	0.9290	0.9810
NGFG_00451	0.3540	0.0591	0.2920	0.1930	0.3030	0.6610	-0.2050	0.2750	0.6280
NGFG_00452	0.6240	0.0011	0.0429	0.1350	0.4860	0.7900	0.1540	0.4310	0.7600
NGFG_00453	#NV			#NV			-0.0353	0.8680	0.9630
NGFG_00454	-0.1930	0.1860	0.4930	-0.2950	0.0445	0.2910	0.3110	0.0329	0.2150
NGFG_00455	-0.2050	0.1540	0.4570	-0.2640	0.0665	0.3440	-0.0089	0.9500	0.9910
NGFG_00458	0.0814	0.5070	0.7840	0.0658	0.5920	0.8460	0.1980	0.1070	0.3910
NGFG_00459	-0.1620	0.2480	0.5700	-0.0008	0.9950	0.9990	0.0195	0.8890	0.9680
NGFG_00460	-0.1820	0.2530	0.5770	-0.2120	0.1840	0.5090	0.0439	0.7830	0.9320
NGFG_00461	0.0486	0.7410	0.9000	-0.0147	0.9200	0.9820	-0.1870	0.2030	0.5570
NGFG_00462	-0.0664	0.7580	0.9100	-0.1100	0.6110	0.8480	-0.1670	0.4370	0.7610
NGFG_00463	0.0883	0.5350	0.7990	0.0141	0.9210	0.9820	-0.3880	0.0056	0.0678
NGFG_00464	-0.5860	0.0018	0.0556	-0.5000	0.0078	0.1430	0.3410	0.0692	0.3220
NGFG_00466	-0.1520	0.5240	0.7930	#NV			0.4810	0.0446	0.2520
NGFG_00467	-0.3690	0.0885	0.3550	-0.0655	0.7610	0.9230	0.5030	0.0202	0.1590
NGFG_00468	0.0537	0.6910	0.8790	0.0461	0.7330	0.9110	0.1030	0.4440	0.7670
NGFG_00469	-0.2610	0.1770	0.4830	-0.2410	0.2130	0.5530	0.5360	0.0056	0.0677
NGFG_00470	-0.4790	0.0048	0.0904	-0.4460	0.0086	0.1430	0.3190	0.0580	0.2930
NGFG_00471	-0.6100	0.0070	0.1100	-0.6180	0.0062	0.1260	0.6190	0.0060	0.0704
NGFG_00472	-0.1300	0.5820	0.8160	#NV			0.6320	0.0084	0.0891
NGFG_00473	0.1210	0.5320	0.7960	-0.0979	0.6140	0.8480	-0.1770	0.3600	0.7050
NGFG_00474	0.0230	0.9060	0.9630	0.1930	0.3190	0.6800	0.2160	0.2640	0.6190
NGFG_00475	0.0168	0.9170	0.9690	0.0427	0.7910	0.9340	-0.1360	0.3950	0.7310
NGFG_00477	0.3950	0.0479	0.2720	0.3580	0.0724	0.3550	-0.1500	0.4530	0.7720
NGFG_00478	-0.3500	0.0579	0.2920	-0.2980	0.1060	0.4170	0.2920	0.1120	0.4030
NGFG_00479	0.0792	0.6810	0.8720	0.1470	0.4430	0.7670	0.3090	0.1090	0.3970
NGFG_00480	0.0264	0.8840	0.9570	-0.0344	0.8490	0.9610	0.8440	0.0000	0.0002
NGFG_00482	0.0988	0.5700	0.8160	-0.0310	0.8590	0.9690	0.1420	0.4140	0.7450
NGFG_00483	0.3310	0.0539	0.2860	0.1870	0.2750	0.6300	0.0058	0.9730	0.9940
NGFG_00486	0.0208	0.8980	0.9600	0.1160	0.4740	0.7870	-0.0949	0.5560	0.8320
NGFG_00487	-0.4920	0.0270	0.2190	-0.5230	0.0190	0.2070	0.3760	0.0875	0.3600
NGFG_00488	-0.1070	0.4570	0.7500	-0.0729	0.6120	0.8480	0.0150	0.9170	0.9760
NGFG_00489	-0.0298	0.8470	0.9430	0.1080	0.4830	0.7900	0.3010	0.0516	0.2720
NGFG_00490	0.2210	0.2260	0.5390	0.1970	0.2790	0.6340	-0.3860	0.0344	0.2200
NGFG_00491	-0.1070	0.6450	0.8520	-0.0897	0.6990	0.8940	0.3030	0.1920	0.5420
NGFG_00492	-0.1400	0.5550	0.8100	0.0380	0.8720	0.9720	-0.0453	0.8470	0.9550
NGFG_00495	0.0857	0.4730	0.7620	0.0824	0.4900	0.7910	0.1150	0.3340	0.6810
NGFG_00496	0.0715	0.5320	0.7960	-0.1150	0.3170	0.6750	0.0947	0.4080	0.7410
NGFG_00498	0.0086	0.9570	0.9870	-0.0149	0.9250	0.9830	-0.1200	0.4490	0.7700
NGFG_00499	-0.1630	0.2970	0.6140	-0.1330	0.3940	0.7360	0.0970	0.5350	0.8150
NGFG_00500	-0.0283	0.8590	0.9470	0.0384	0.8090	0.9470	-0.1060	0.5050	0.8000

NGFG_00501	0.0613	0.6160	0.8310	0.0117	0.9230	0.9820	-0.3170	0.0092	0.0938
NGFG_00502	0.0868	0.4360	0.7310	0.0807	0.4680	0.7830	-0.1140	0.3040	0.6540
NGFG_00503	0.2250	0.1610	0.4660	0.3580	0.0253	0.2330	0.0672	0.6750	0.8930
NGFG_00504	0.0022	0.9830	0.9950	-0.0422	0.6800	0.8850	0.1100	0.2830	0.6320
NGFG_00505	-0.1740	0.1410	0.4380	-0.1320	0.2630	0.6150	0.2370	0.0445	0.2520
NGFG_00506	-0.0535	0.7900	0.9150	-0.0237	0.9060	0.9820	0.3860	0.0547	0.2810
NGFG_00507	-0.2400	0.1590	0.4630	-0.2960	0.0821	0.3670	0.8270	0.0000	0.0001
NGFG_00508	0.1360	0.5810	0.8160	#NV			0.1920	0.4350	0.7610
NGFG_00509	0.2470	0.1140	0.3970	0.3200	0.0403	0.2870	-0.1020	0.5140	0.8020
NGFG_00510	-0.2100	0.1540	0.4570	-0.1550	0.2900	0.6450	0.0405	0.7810	0.9320
NGFG_00511	0.0234	0.7760	0.9130	0.0011	0.9890	0.9990	-0.2230	0.0067	0.0766
NGFG_00512	0.0826	0.4830	0.7670	0.0209	0.8590	0.9690	-0.0478	0.6850	0.8970
NGFG_00513	0.1640	0.1490	0.4520	0.0461	0.6860	0.8860	-0.1310	0.2500	0.6060
NGFG_00514	0.2050	0.2260	0.5390	0.1020	0.5480	0.8170	0.1600	0.3460	0.6910
NGFG_00515	-0.0569	0.7750	0.9120	-0.0581	0.7710	0.9260	0.4350	0.0301	0.2030
NGFG_00516	-0.0456	0.8000	0.9210	0.1440	0.4230	0.7510	0.2650	0.1410	0.4590
NGFG_00517	#NV			#NV			0.5030	0.0115	0.1100
NGFG_00518	-0.1580	0.1570	0.4600	-0.0853	0.4440	0.7670	-0.1590	0.1510	0.4770
NGFG_00519	0.2230	0.2900	0.6070	0.0731	0.7280	0.9080	-0.0651	0.7570	0.9190
NGFG_00520	0.3760	0.1180	0.4020	0.2670	0.2680	0.6220	0.1900	0.4300	0.7600
NGFG_00521	-0.2700	0.1240	0.4110	-0.2930	0.0959	0.3990	-0.1020	0.5610	0.8340
NGFG_00522	-0.3930	0.0089	0.1200	-0.3610	0.0159	0.1930	-0.0437	0.7660	0.9240
NGFG_00523	0.2370	0.1070	0.3870	0.1400	0.3420	0.6950	-0.1370	0.3510	0.6950
NGFG_00524	0.3200	0.0826	0.3470	0.3370	0.0668	0.3440	0.1390	0.4510	0.7710
NGFG_00525	0.1950	0.2740	0.5980	0.1430	0.4220	0.7510	0.0563	0.7520	0.9180
NGFG_00526	0.2290	0.0695	0.3180	0.1340	0.2890	0.6420	-0.2540	0.0436	0.2500
NGFG_00527	0.4530	0.0093	0.1230	0.3530	0.0427	0.2870	-0.3920	0.0244	0.1810
NGFG_00528	0.0775	0.6430	0.8500	0.0345	0.8370	0.9540	0.1410	0.3990	0.7340
NGFG_00529	-0.4780	0.0376	0.2480	-0.4750	0.0387	0.2830	0.4050	0.0760	0.3370
NGFG_00530	0.0123	0.9610	0.9890	#NV			-0.0805	0.7490	0.9160
NGFG_00531	-0.3510	0.0128	0.1470	-0.2940	0.0362	0.2770	0.0575	0.6770	0.8930
NGFG_00532	0.1230	0.5250	0.7930	0.0624	0.7470	0.9170	-0.1370	0.4740	0.7850
NGFG_00533	0.0105	0.9520	0.9850	0.1610	0.3590	0.7120	0.0067	0.9700	0.9940
NGFG_00534	0.1230	0.2830	0.6040	0.0596	0.6050	0.8480	-0.0979	0.3940	0.7310
NGFG_00535	-0.1730	0.2340	0.5500	-0.0365	0.8010	0.9420	0.0307	0.8310	0.9520
NGFG_00536	-0.0423	0.8210	0.9320	0.0238	0.8990	0.9800	0.2110	0.2590	0.6150
NGFG_00537	0.0705	0.5220	0.7920	0.0161	0.8830	0.9750	-0.1510	0.1710	0.5160
NGFG_00538	0.0081	0.9550	0.9870	-0.1280	0.3780	0.7220	0.2280	0.1160	0.4110
NGFG_00539	-0.1640	0.2480	0.5700	-0.1200	0.3990	0.7360	0.3000	0.0341	0.2190
NGFG_00541	0.3240	0.0355	0.2430	0.2810	0.0682	0.3470	-0.1700	0.2710	0.6250
NGFG_00542	-0.1200	0.5140	0.7870	-0.1810	0.3270	0.6860	-0.0735	0.6890	0.8970
NGFG_00543	-0.2380	0.3000	0.6160	-0.1950	0.3950	0.7360	0.0900	0.6930	0.8970
NGFG_00544	-0.5330	0.0030	0.0752	-0.4480	0.0122	0.1700	0.2840	0.1080	0.3940
NGFG_00545	-0.1310	0.4940	0.7740	-0.1090	0.5680	0.8260	0.0328	0.8630	0.9620
NGFG_00546	0.1950	0.2200	0.5330	0.2390	0.1330	0.4540	-0.1710	0.2800	0.6320
NGFG_00547	-0.1880	0.2090	0.5190	-0.2010	0.1800	0.5040	-0.1740	0.2370	0.5960
NGFG_00548	-0.3110	0.0551	0.2890	-0.2810	0.0833	0.3680	0.3850	0.0174	0.1430

NGFG_00550	-0.0803	0.4770	0.7630	-0.0923	0.4140	0.7500	-0.1920	0.0885	0.3610
NGFG_00551	-0.0045	0.9630	0.9900	-0.0117	0.9050	0.9820	-0.3110	0.0016	0.0278
NGFG_00554	0.2930	0.0591	0.2920	0.1900	0.2210	0.5640	-0.4340	0.0051	0.0652
NGFG_00555	-0.1310	0.2350	0.5510	-0.0961	0.3830	0.7270	-0.1270	0.2460	0.6030
NGFG_00556	-0.3500	0.0046	0.0889	-0.3000	0.0150	0.1890	-0.0697	0.5680	0.8370
NGFG_00557	0.2170	0.0750	0.3310	0.1310	0.2850	0.6390	-0.4180	0.0006	0.0134
NGFG_00558	-0.0047	0.9780	0.9950	-0.1150	0.4970	0.7940	-0.1150	0.4920	0.7950
NGFG_00559	0.1750	0.2650	0.5900	0.1430	0.3630	0.7140	-0.1540	0.3240	0.6700
NGFG_00562	-0.0579	0.6130	0.8290	-0.0689	0.5470	0.8170	-0.0423	0.7100	0.9010
NGFG_00563	-0.2660	0.2380	0.5560	-0.0246	0.9130	0.9820	0.3270	0.1450	0.4670
NGFG_00564	0.0895	0.6870	0.8770	0.0400	0.8570	0.9680	0.2910	0.1890	0.5390
NGFG_00565	-0.2300	0.2320	0.5460	-0.2240	0.2440	0.5910	-0.0146	0.9390	0.9860
NGFG_00566	-0.1960	0.1950	0.5020	-0.1950	0.1980	0.5310	0.0190	0.9000	0.9720
NGFG_00567	-0.0847	0.5260	0.7940	-0.0291	0.8270	0.9500	-0.1560	0.2400	0.5970
NGFG_00568	-0.3330	0.0087	0.1200	-0.3070	0.0153	0.1900	-0.0321	0.7980	0.9360
NGFG_00569	-0.2400	0.0644	0.3030	-0.2840	0.0284	0.2490	0.0270	0.8340	0.9520
NGFG_00570	0.1140	0.5230	0.7920	0.1070	0.5500	0.8170	0.0175	0.9220	0.9780
NGFG_00571	0.0380	0.7880	0.9150	0.0349	0.8050	0.9460	-0.0672	0.6340	0.8700
NGFG_00574	-0.0028	0.9860	0.9950	-0.1150	0.4720	0.7860	0.1780	0.2630	0.6190
NGFG_00575	-0.1110	0.4930	0.7740	-0.1320	0.4170	0.7500	-0.1230	0.4470	0.7690
NGFG_00576	-0.2730	0.1120	0.3930	-0.3870	0.0247	0.2330	0.0894	0.5980	0.8490
NGFG_00577	0.0548	0.7530	0.9080	0.0008	0.9960	0.9990	-0.1630	0.3490	0.6940
NGFG_00578	0.0471	0.6700	0.8670	0.0169	0.8790	0.9740	-0.0751	0.4970	0.7960
NGFG_00580	0.0041	0.9730	0.9940	-0.0619	0.6130	0.8480	-0.0626	0.6080	0.8580
NGFG_00582	#NV			#NV			0.0914	0.3160	0.6640
NGFG_00583	-0.0056	0.9820	0.9950	#NV			0.2270	0.3690	0.7140
NGFG_00584	-0.1620	0.5230	0.7920	#NV			0.1370	0.5890	0.8450
NGFG_00585	-0.2030	0.2080	0.5190	-0.0255	0.8730	0.9720	0.0290	0.8550	0.9580
NGFG_00586	-0.2240	0.2130	0.5240	-0.2050	0.2530	0.6020	0.1330	0.4570	0.7740
NGFG_00587	-0.2740	0.0269	0.2190	-0.2350	0.0572	0.3240	0.0131	0.9150	0.9750
NGFG_00588	-0.1270	0.3600	0.6750	-0.1600	0.2510	0.6000	0.0194	0.8890	0.9680
NGFG_00590	-0.2130	0.0334	0.2350	-0.0791	0.4280	0.7550	0.0352	0.7230	0.9070
NGFG_00591	-0.3100	0.0152	0.1610	-0.2910	0.0226	0.2250	-0.1350	0.2860	0.6340
NGFG_00592	-0.1280	0.3950	0.7080	-0.4020	0.0084	0.1430	-0.2380	0.1070	0.3910
NGFG_00593	-0.1980	0.2230	0.5360	-0.0826	0.6100	0.8480	0.1070	0.5070	0.8010
NGFG_00594	-0.0768	0.5470	0.8060	-0.0506	0.6920	0.8910	0.2210	0.0841	0.3530
NGFG_00595	0.4720	0.0160	0.1650	0.4140	0.0343	0.2750	-0.0808	0.6800	0.8930
NGFG_00596	0.2280	0.1700	0.4750	0.0351	0.8330	0.9530	-0.1940	0.2420	0.5970
NGFG_00597	-0.1560	0.1790	0.4870	-0.1170	0.3130	0.6710	-0.0437	0.7060	0.9010
NGFG_00598	-0.2190	0.3010	0.6160	-0.1640	0.4390	0.7650	0.0270	0.8980	0.9720
NGFG_00600	-0.4940	0.0530	0.2840	-0.3860	0.1300	0.4520	0.3260	0.2010	0.5560
NGFG_00601	0.3230	0.1130	0.3970	0.2840	0.1640	0.4920	-0.0928	0.6490	0.8790
NGFG_00602	0.2000	0.3230	0.6380	0.3060	0.1310	0.4520	0.2340	0.2480	0.6040
NGFG_00603	0.1010	0.4590	0.7520	0.1540	0.2580	0.6100	-0.3440	0.0116	0.1110
NGFG_00605	-0.2360	0.0622	0.2980	-0.1830	0.1490	0.4720	0.0861	0.4960	0.7960
NGFG_00606	0.0358	0.8220	0.9320	0.1430	0.3660	0.7140	-0.0767	0.6280	0.8680
NGFG_00607	0.2450	0.2000	0.5100	0.2620	0.1700	0.4950	-0.1030	0.5890	0.8450

NGFG_00608	0.1830	0.3330	0.6490	0.1280	0.4990	0.7940	0.1190	0.5290	0.8130
NGFG_00609	0.2020	0.2690	0.5940	0.1560	0.3940	0.7360	0.1480	0.4190	0.7510
NGFG_00610	0.2570	0.1380	0.4360	0.2260	0.1920	0.5200	0.2190	0.2060	0.5640
NGFG_00611	0.0894	0.6860	0.8770	0.1030	0.6410	0.8630	0.2430	0.2770	0.6290
NGFG_00614	-0.2530	0.2620	0.5870	-0.2510	0.2660	0.6220	0.1380	0.5360	0.8150
NGFG_00615	0.1170	0.2670	0.5920	0.1560	0.1390	0.4640	0.0330	0.7540	0.9190
NGFG_00616	0.2810	0.0167	0.1680	0.3290	0.0051	0.1150	-0.0118	0.9200	0.9780
NGFG_00617	0.5360	0.0001	0.0100	0.4670	0.0006	0.0303	-0.1150	0.3990	0.7340
NGFG_00618	-0.1940	0.3990	0.7090	-0.0382	0.8680	0.9720	0.1810	0.4300	0.7600
NGFG_00619	0.2830	0.1550	0.4570	0.1270	0.5250	0.8040	-0.3300	0.0952	0.3680
NGFG_00620	-0.1480	0.4780	0.7640	0.0807	0.6960	0.8920	-0.0424	0.8370	0.9520
NGFG_00621	-0.0716	0.7770	0.9130	-0.1330	0.5990	0.8480	0.0932	0.7130	0.9020
NGFG_00622	-0.1030	0.6560	0.8580	#NV			0.4730	0.0390	0.2330
NGFG_00623	-0.3680	0.1490	0.4530	#NV			0.5390	0.0348	0.2210
NGFG_00626	-0.2330	0.3540	0.6700	#NV			0.3680	0.1440	0.4670
NGFG_00627	0.4820	0.0052	0.0951	0.5000	0.0037	0.0985	-0.2790	0.1050	0.3900
NGFG_00628	0.0466	0.8030	0.9240	0.0950	0.6120	0.8480	-0.2110	0.2590	0.6150
NGFG_00629	0.0025	0.9890	0.9950	0.0234	0.8980	0.9800	0.2440	0.1810	0.5320
NGFG_00630	0.3580	0.0878	0.3540	0.2830	0.1770	0.5010	-0.2490	0.2350	0.5960
NGFG_00631	-0.2880	0.2580	0.5820	#NV			0.6560	0.0100	0.0995
NGFG_00632	#NV			#NV			-0.0180	0.9150	0.9750
NGFG_00633	-0.2470	0.3310	0.6470	#NV			0.3460	0.1730	0.5180
NGFG_00634	-0.6970	0.0047	0.0898	#NV			0.4630	0.0627	0.3090
NGFG_00637	#NV			#NV			0.0797	0.5000	0.7980
NGFG_00638	#NV			#NV			-0.3370	0.0530	0.2760
NGFG_00639	0.1450	0.5160	0.7880	#NV			0.1230	0.5820	0.8390
NGFG_00640	-0.1820	0.4640	0.7560	#NV			-0.0807	0.7470	0.9160
NGFG_00641	-0.2990	0.2100	0.5210	#NV			0.3320	0.1620	0.5010
NGFG_00643	#NV			#NV			-0.1180	0.4480	0.7700
NGFG_00646	-0.4380	0.0242	0.2090	-0.1900	0.3240	0.6830	-0.0304	0.8730	0.9630
NGFG_00647	-0.1900	0.4550	0.7490	#NV			0.0367	0.8850	0.9670
NGFG_00648	-0.1370	0.5720	0.8160	#NV			0.0612	0.8010	0.9370
NGFG_00649	-0.0066	0.9790	0.9950	#NV			-0.0110	0.9650	0.9940
NGFG_00651	-0.1970	0.3060	0.6220	-0.0543	0.7770	0.9300	0.1340	0.4840	0.7900
NGFG_00652	0.0467	0.8340	0.9360	-0.0285	0.8990	0.9800	0.4240	0.0584	0.2950
NGFG_00653	0.3400	0.1330	0.4280	0.1420	0.5310	0.8100	0.1800	0.4260	0.7560
NGFG_00654	-0.0202	0.8820	0.9570	-0.1740	0.2010	0.5350	0.0363	0.7900	0.9340
NGFG_00656	0.4330	0.0019	0.0566	0.3860	0.0056	0.1170	0.1510	0.2790	0.6310
NGFG_00657	0.2380	0.0345	0.2400	0.1490	0.1880	0.5160	-0.1810	0.1080	0.3930
NGFG_00658	0.3780	0.0005	0.0277	0.2220	0.0416	0.2870	0.4870	0.0000	0.0008
NGFG_00659	-0.2140	0.1900	0.4970	-0.1260	0.4390	0.7650	-0.0528	0.7460	0.9150
NGFG_00661	0.2730	0.2180	0.5300	0.1890	0.3920	0.7360	0.3840	0.0836	0.3510
NGFG_00662	0.1340	0.4730	0.7620	0.0186	0.9210	0.9820	0.5670	0.0026	0.0419
NGFG_00664	0.3670	0.0580	0.2920	0.4090	0.0347	0.2750	0.5680	0.0039	0.0563
NGFG_00666	0.0789	0.5250	0.7930	0.1030	0.4040	0.7400	0.4520	0.0003	0.0089
NGFG_00667	0.3970	0.0521	0.2840	0.4670	0.0224	0.2240	0.4050	0.0489	0.2670
NGFG_00670	0.2340	0.3120	0.6290	0.1000	0.6650	0.8780	0.7690	0.0009	0.0190

NGFG_00671	0.1650	0.4240	0.7230	0.1570	0.4460	0.7680	0.6820	0.0011	0.0217
NGFG_00672	0.1140	0.3870	0.7010	0.0995	0.4500	0.7700	0.0532	0.6870	0.8970
NGFG_00673	0.1110	0.4640	0.7560	0.0007	0.9960	0.9990	-0.3780	0.0110	0.1070
NGFG_00674	-0.0565	0.6730	0.8690	-0.0091	0.9460	0.9900	-0.1210	0.3650	0.7120
NGFG_00675	0.2000	0.3160	0.6330	0.1520	0.4470	0.7680	0.0855	0.6710	0.8890
NGFG_00676	0.3490	0.0814	0.3450	0.2050	0.3070	0.6630	-0.4330	0.0300	0.2030
NGFG_00678	-0.0177	0.8770	0.9540	-0.0449	0.6930	0.8910	-0.3150	0.0050	0.0644
NGFG_00679	-0.0155	0.8730	0.9510	-0.1410	0.1470	0.4700	-0.0147	0.8790	0.9650
NGFG_00682	-0.0840	0.5280	0.7960	-0.2140	0.1100	0.4210	-0.2170	0.0989	0.3750
NGFG_00683	-0.0447	0.8060	0.9240	-0.0051	0.9780	0.9980	-0.1810	0.3190	0.6660
NGFG_00684	-0.0741	0.6390	0.8470	-0.1010	0.5230	0.8030	-0.0907	0.5620	0.8340
NGFG_00686	-0.5230	0.0386	0.2520	#NV			0.2140	0.3960	0.7310
NGFG_00687	-0.4070	0.0743	0.3290	#NV			0.5100	0.0253	0.1850
NGFG_00688	-0.3280	0.1270	0.4180	-0.3090	0.1510	0.4720	0.2010	0.3460	0.6910
NGFG_00691	0.4110	0.0483	0.2720	0.2610	0.2120	0.5500	-0.3480	0.0948	0.3680
NGFG_00692	-0.0832	0.7300	0.9000	#NV			0.1030	0.6680	0.8870
NGFG_00693	0.0266	0.8550	0.9460	-0.0242	0.8680	0.9720	0.0604	0.6780	0.8930
NGFG_00694	0.2850	0.0374	0.2470	0.1900	0.1640	0.4920	-0.1310	0.3380	0.6840
NGFG_00695	-0.0664	0.6980	0.8810	-0.0494	0.7730	0.9270	-0.1500	0.3800	0.7230
NGFG_00696	0.0550	0.6060	0.8250	-0.0245	0.8190	0.9500	-0.1280	0.2270	0.5880
NGFG_00698	0.0051	0.9610	0.9890	-0.0780	0.4480	0.7680	-0.1570	0.1220	0.4250
NGFG_00699	-0.4210	0.0454	0.2690	-0.4490	0.0330	0.2670	0.8670	0.0000	0.0021
NGFG_00701	-0.2240	0.3790	0.6930	#NV			-0.1140	0.6530	0.8800
NGFG_00703	-0.5880	0.0000	0.0030	-0.4910	0.0003	0.0237	0.3350	0.0129	0.1180
NGFG_00704	-0.1930	0.1630	0.4680	-0.1400	0.3120	0.6700	-0.0761	0.5800	0.8390
NGFG_00705	0.0026	0.9870	0.9950	-0.1010	0.5130	0.8000	-0.1180	0.4440	0.7670
NGFG_00707	-0.0824	0.6040	0.8240	-0.0650	0.6820	0.8850	0.0916	0.5630	0.8340
NGFG_00708	-0.4230	0.0020	0.0584	-0.4130	0.0025	0.0785	0.5790	0.0000	0.0012
NGFG_00709	-0.0634	0.7740	0.9120	-0.0657	0.7660	0.9240	-0.1190	0.5890	0.8450
NGFG_00711	-0.0156	0.9050	0.9630	0.0175	0.8940	0.9800	-0.2130	0.1050	0.3900
NGFG_00712	0.0772	0.5870	0.8170	0.1280	0.3690	0.7150	-0.2780	0.0499	0.2700
NGFG_00713	0.1790	0.4040	0.7110	0.0024	0.9910	0.9990	0.1920	0.3680	0.7140
NGFG_00715	-0.4840	0.0563	0.2900	#NV			0.0692	0.7840	0.9320
NGFG_00717	#NV			#NV			0.1140	0.3310	0.6780
NGFG_00718	#NV			#NV			0.0214	0.7900	0.9340
NGFG_00719	#NV			#NV			0.0729	0.5560	0.8320
NGFG_00720	-0.1610	0.4260	0.7230	-0.0797	0.6940	0.8910	0.8780	0.0000	0.0010
NGFG_00721	0.1010	0.5950	0.8230	-0.0110	0.9540	0.9930	0.9420	0.0000	0.0001
NGFG_00723	0.0272	0.8940	0.9600	-0.0281	0.8900	0.9780	0.2400	0.2400	0.5970
NGFG_00724	-0.4760	0.0623	0.2980	#NV			0.2800	0.2720	0.6250
NGFG_00725	0.0423	0.8660	0.9490	#NV			0.1630	0.5180	0.8040
NGFG_00727	-0.1260	0.5740	0.8160	-0.2710	0.2270	0.5720	0.3400	0.1290	0.4340
NGFG_00728	-0.0567	0.8190	0.9310	#NV			0.1390	0.5740	0.8370
NGFG_00729	0.0264	0.8890	0.9590	-0.0819	0.6650	0.8780	0.2840	0.1340	0.4450
NGFG_00730	0.3970	0.0702	0.3190	0.4100	0.0617	0.3340	-0.0259	0.9060	0.9720
NGFG_00731	0.0552	0.7140	0.8930	-0.1470	0.3320	0.6900	0.1690	0.2630	0.6190
NGFG_00732	0.0788	0.7150	0.8940	-0.0912	0.6750	0.8850	-0.1040	0.6270	0.8680

NGFG_00733	0.1290	0.4310	0.7270	0.0030	0.9850	0.9990	0.1080	0.5120	0.8020
NGFG_00734	-0.1740	0.2850	0.6060	-0.0967	0.5520	0.8190	0.0562	0.7290	0.9110
NGFG_00735	-0.0722	0.5080	0.7840	-0.1860	0.0876	0.3810	-0.0889	0.4140	0.7450
NGFG_00736	-0.2120	0.1520	0.4550	-0.1060	0.4720	0.7860	0.1210	0.4080	0.7410
NGFG_00739	0.2310	0.1390	0.4360	0.1770	0.2580	0.6100	0.1110	0.4800	0.7860
NGFG_00740	-0.3840	0.0666	0.3120	-0.2380	0.2530	0.6020	-0.1030	0.6190	0.8640
NGFG_00741	-0.0970	0.6390	0.8470	-0.1530	0.4590	0.7760	-0.0305	0.8820	0.9650
NGFG_00742	-0.1080	0.4590	0.7520	-0.2360	0.1070	0.4170	-0.1010	0.4860	0.7910
NGFG_00743	-0.3930	0.0166	0.1680	-0.3220	0.0492	0.3050	-0.0324	0.8410	0.9530
NGFG_00744	-0.4160	0.0407	0.2600	-0.3370	0.0951	0.3980	0.0887	0.6540	0.8800
NGFG_00745	0.0868	0.5890	0.8190	0.1300	0.4180	0.7510	-0.4470	0.0053	0.0660
NGFG_00746	-0.3420	0.0513	0.2830	-0.2220	0.2060	0.5390	0.3370	0.0545	0.2810
NGFG_00750	-0.1100	0.5810	0.8160	-0.1510	0.4500	0.7700	0.4970	0.0136	0.1230
NGFG_00751	-0.4400	0.0327	0.2350	-0.3110	0.1300	0.4520	0.3500	0.0888	0.3610
NGFG_00752	-0.0400	0.8640	0.9490	0.1510	0.5170	0.8030	-0.0395	0.8660	0.9620
NGFG_00754	0.1390	0.5110	0.7850	0.1220	0.5620	0.8240	0.1270	0.5470	0.8240
NGFG_00755	0.1020	0.5830	0.8160	0.0751	0.6860	0.8860	0.1070	0.5630	0.8340
NGFG_00756	0.0314	0.8300	0.9350	0.0488	0.7390	0.9140	-0.3020	0.0368	0.2280
NGFG_00757	-0.0783	0.5200	0.7920	-0.0585	0.6310	0.8600	0.1560	0.2000	0.5540
NGFG_00759	-0.1430	0.4880	0.7700	-0.0187	0.9270	0.9830	-0.0179	0.9300	0.9820
NGFG_00760	0.0740	0.7700	0.9110	#NV			-0.2280	0.3650	0.7120
NGFG_00761	0.0354	0.7370	0.9000	0.0514	0.6260	0.8540	-0.0880	0.4020	0.7370
NGFG_00762	-0.0623	0.6630	0.8620	-0.0583	0.6830	0.8850	-0.0447	0.7530	0.9180
NGFG_00763	-0.0959	0.5790	0.8160	-0.1680	0.3310	0.6900	0.0388	0.8220	0.9490
NGFG_00764	-0.1160	0.6030	0.8240	-0.1520	0.4950	0.7940	-0.2570	0.2390	0.5960
NGFG_00765	0.0762	0.6270	0.8380	0.0170	0.9140	0.9820	-0.5290	0.0007	0.0159
NGFG_00766	-0.0662	0.7450	0.9030	-0.3110	0.1290	0.4520	0.0696	0.7310	0.9110
NGFG_00768	-0.0369	0.7960	0.9190	0.1200	0.3990	0.7360	0.0934	0.5120	0.8020
NGFG_00770	0.1180	0.4570	0.7500	0.1640	0.3020	0.6600	-0.0225	0.8870	0.9680
NGFG_00772	-0.1600	0.2540	0.5770	-0.1180	0.3980	0.7360	-0.1260	0.3670	0.7130
NGFG_00773	-0.2190	0.2370	0.5530	-0.2290	0.2160	0.5550	-0.0823	0.6530	0.8800
NGFG_00774	-0.3060	0.0339	0.2360	-0.2650	0.0655	0.3440	0.0538	0.7050	0.9010
NGFG_00775	-0.1250	0.4060	0.7120	-0.2620	0.0828	0.3680	0.1070	0.4770	0.7860
NGFG_00777	0.2400	0.1340	0.4300	0.3120	0.0513	0.3090	-0.1510	0.3440	0.6900
NGFG_00779	0.3470	0.0240	0.2080	0.3000	0.0505	0.3080	-0.5580	0.0003	0.0083
NGFG_00780	0.1700	0.5050	0.7820	#NV			0.3050	0.2290	0.5880
NGFG_00782	0.1110	0.4040	0.7110	0.1040	0.4360	0.7610	-0.1450	0.2740	0.6270
NGFG_00785	0.3750	0.0177	0.1740	0.4720	0.0028	0.0831	0.1380	0.3860	0.7260
NGFG_00786	0.0588	0.7210	0.8950	-0.0014	0.9930	0.9990	-0.2280	0.1650	0.5060
NGFG_00787	-0.1160	0.5530	0.8100	-0.0757	0.6990	0.8940	-0.0078	0.9680	0.9940
NGFG_00789	-0.2910	0.0079	0.1150	-0.1980	0.0697	0.3490	0.0329	0.7590	0.9210
NGFG_00790	-0.0361	0.8580	0.9470	0.0070	0.9720	0.9960	-0.0243	0.9030	0.9720
NGFG_00791	-0.6180	0.0099	0.1280	-0.5040	0.0352	0.2750	0.0614	0.7950	0.9350
NGFG_00792	-0.4590	0.0686	0.3170	#NV			0.1380	0.5820	0.8390
NGFG_00794	-0.3100	0.1900	0.4970	0.0884	0.7060	0.8960	-0.0104	0.9640	0.9940
NGFG_00795	0.0642	0.6480	0.8530	0.1350	0.3360	0.6900	-0.1400	0.3170	0.6640
NGFG_00798	0.0895	0.5660	0.8160	0.0726	0.6420	0.8630	-0.1470	0.3450	0.6900

NGFG_00799	-0.3060	0.0629	0.2990	-0.2580	0.1170	0.4370	0.1880	0.2530	0.6090
NGFG_00800	0.0077	0.9750	0.9940	0.1780	0.4590	0.7760	-0.1120	0.6410	0.8730
NGFG_00801	0.2080	0.2850	0.6060	0.1610	0.4100	0.7470	-0.3490	0.0723	0.3260
NGFG_00802	0.0498	0.7650	0.9100	0.2320	0.1590	0.4860	0.2550	0.1300	0.4350
NGFG_00803	0.2790	0.2730	0.5960	#NV			-0.1490	0.5570	0.8330
NGFG_00804	0.1010	0.6070	0.8250	0.0317	0.8710	0.9720	-0.0186	0.9240	0.9790
NGFG_00807	-0.0598	0.5250	0.7930	-0.1290	0.1700	0.4950	0.0696	0.4590	0.7740
NGFG_00811	0.1110	0.4030	0.7110	0.0525	0.6910	0.8910	-0.2890	0.0283	0.1970
NGFG_00812	0.1070	0.5470	0.8060	0.0278	0.8760	0.9740	-0.1120	0.5270	0.8120
NGFG_00813	-0.0737	0.6480	0.8530	-0.0431	0.7890	0.9340	0.0259	0.8720	0.9630
NGFG_00814	0.2130	0.2060	0.5160	-0.3530	0.0362	0.2770	0.8950	0.0000	0.0000
NGFG_00815	0.1420	0.4230	0.7230	-0.0097	0.9560	0.9930	-0.1140	0.5210	0.8060
NGFG_00816	0.1600	0.3710	0.6850	0.0528	0.7680	0.9250	-0.0066	0.9710	0.9940
NGFG_00817	0.1390	0.4260	0.7230	0.0832	0.6350	0.8600	0.0990	0.5720	0.8370
NGFG_00818	0.0864	0.6760	0.8710	0.1030	0.6160	0.8480	0.1000	0.6270	0.8680
NGFG_00819	0.2680	0.0842	0.3500	0.0888	0.5670	0.8260	0.2520	0.1040	0.3870
NGFG_00820	0.4290	0.0059	0.0995	0.1890	0.2250	0.5700	0.1260	0.4200	0.7510
NGFG_00821	0.3500	0.1300	0.4220	0.2930	0.2040	0.5380	0.4720	0.0451	0.2530
NGFG_00822	0.2290	0.1200	0.4040	0.1120	0.4510	0.7700	0.1280	0.3890	0.7280
NGFG_00823	0.1710	0.3200	0.6350	0.0862	0.6160	0.8480	-0.3240	0.0598	0.2990
NGFG_00824	0.0685	0.6360	0.8450	0.0165	0.9090	0.9820	-0.5730	0.0001	0.0031
NGFG_00825	0.3580	0.0974	0.3750	0.3280	0.1290	0.4520	-0.6910	0.0014	0.0256
NGFG_00826	-0.0131	0.9410	0.9820	-0.0525	0.7650	0.9240	-0.0358	0.8370	0.9520
NGFG_00827	-0.4100	0.0470	0.2700	-0.3280	0.1100	0.4210	0.1620	0.4210	0.7510
NGFG_00828	-0.1780	0.3620	0.6770	-0.0342	0.8600	0.9690	-0.2310	0.2260	0.5880
NGFG_00829	-0.0679	0.7330	0.9000	-0.0628	0.7520	0.9210	-0.1340	0.5010	0.7980
NGFG_00831	-0.2090	0.1840	0.4900	-0.3280	0.0368	0.2780	0.5320	0.0007	0.0164
NGFG_00836	0.2850	0.1880	0.4940	0.4810	0.0251	0.2330	-0.2540	0.2390	0.5960
NGFG_00839	-0.4580	0.0014	0.0476	-0.3440	0.0159	0.1930	0.1650	0.2480	0.6040
NGFG_00840	0.4410	0.0628	0.2990	0.4520	0.0565	0.3230	-0.2680	0.2590	0.6150
NGFG_00841	0.0267	0.8460	0.9430	0.0926	0.4990	0.7940	-0.2590	0.0578	0.2930
NGFG_00843	0.0992	0.5290	0.7960	0.1200	0.4440	0.7670	-0.2700	0.0854	0.3550
NGFG_00844	-0.1630	0.4430	0.7380	-0.1310	0.5380	0.8110	0.1040	0.6230	0.8650
NGFG_00845	-0.6990	0.0061	0.1010	#NV			0.4660	0.0671	0.3170
NGFG_00847	-0.5660	0.0225	0.2000	#NV			0.5600	0.0243	0.1810
NGFG_00848	0.2430	0.2870	0.6070	0.1300	0.5710	0.8280	-0.0899	0.6930	0.8970
NGFG_00851	-0.1470	0.5520	0.8090	-0.1970	0.4250	0.7540	0.1520	0.5370	0.8150
NGFG_00852	-0.0242	0.9190	0.9700	0.0531	0.8240	0.9500	0.0949	0.6910	0.8970
NGFG_00853	0.0698	0.6140	0.8300	0.0209	0.8800	0.9740	-0.1930	0.1630	0.5030
NGFG_00854	0.2940	0.1100	0.3910	0.2570	0.1620	0.4910	-0.2100	0.2530	0.6090
NGFG_00855	0.0349	0.8310	0.9350	0.0201	0.9020	0.9810	-0.0325	0.8420	0.9530
NGFG_00856	-0.3180	0.0164	0.1680	-0.2910	0.0279	0.2480	-0.0910	0.4840	0.7900
NGFG_00857	-0.1260	0.4680	0.7580	-0.0726	0.6740	0.8840	-0.0858	0.6110	0.8590
NGFG_00858	0.0347	0.7870	0.9150	-0.0576	0.6550	0.8730	-0.1260	0.3270	0.6730
NGFG_00859	0.0386	0.8060	0.9240	0.2720	0.0805	0.3640	0.1370	0.3840	0.7240
NGFG_00862	0.1810	0.4080	0.7140	-0.0116	0.9580	0.9930	0.3260	0.1360	0.4490
NGFG_00863	0.1990	0.1190	0.4040	0.0205	0.8730	0.9720	0.3650	0.0044	0.0590

NGFG_00866	#NV			#NV			0.1330	0.4890	0.7940
NGFG_00867	0.5200	0.0251	0.2100	0.6490	0.0052	0.1150	-0.1000	0.6660	0.8870
NGFG_00868	0.2590	0.0306	0.2320	0.1820	0.1300	0.4520	-0.3360	0.0050	0.0644
NGFG_00869	0.1490	0.4460	0.7410	0.3560	0.0687	0.3470	0.2200	0.2610	0.6180
NGFG_00870	0.4490	0.0244	0.2090	0.3160	0.1130	0.4300	0.1660	0.4050	0.7390
NGFG_00871	-0.0984	0.4920	0.7740	-0.0351	0.8060	0.9470	0.2310	0.1060	0.3910
NGFG_00872	0.0115	0.9410	0.9820	0.0443	0.7750	0.9280	-0.1150	0.4570	0.7740
NGFG_00873	0.0341	0.8850	0.9580	#NV			0.0740	0.7550	0.9190
NGFG_00874	-0.1850	0.3390	0.6540	-0.0421	0.8260	0.9500	0.5310	0.0064	0.0746
NGFG_00877	#NV			#NV			0.0273	0.7680	0.9240
NGFG_00878	-0.1910	0.0568	0.2900	-0.1870	0.0619	0.3340	0.0781	0.4340	0.7610
NGFG_00879	-0.0490	0.7190	0.8940	-0.0916	0.5020	0.7940	-0.2760	0.0377	0.2300
NGFG_00880	-0.0115	0.9540	0.9870	-0.0821	0.6820	0.8850	-0.2580	0.1980	0.5500
NGFG_00881	-0.3470	0.0008	0.0372	-0.3800	0.0003	0.0221	0.3530	0.0007	0.0153
NGFG_00882	0.0663	0.6990	0.8820	0.0078	0.9640	0.9940	-0.0305	0.8590	0.9600
NGFG_00883	0.0728	0.6050	0.8250	0.0625	0.6570	0.8750	0.0062	0.9650	0.9940
NGFG_00884	-0.0449	0.8180	0.9310	-0.0734	0.7070	0.8960	0.1140	0.5580	0.8330
NGFG_00886	-0.2930	0.0352	0.2430	-0.2930	0.0348	0.2750	-0.1130	0.4060	0.7390
NGFG_00888	-0.1510	0.4210	0.7230	-0.1130	0.5450	0.8150	-0.0037	0.9840	0.9960
NGFG_00889	0.0449	0.8410	0.9400	0.1820	0.4150	0.7500	-0.3780	0.0907	0.3620
NGFG_00892	-0.0377	0.7840	0.9140	-0.1880	0.1730	0.4950	-0.1540	0.2550	0.6120
NGFG_00893	-0.0106	0.9520	0.9850	0.0764	0.6650	0.8780	-0.5940	0.0006	0.0137
NGFG_00894	0.0637	0.7110	0.8910	0.1050	0.5400	0.8120	-0.3140	0.0671	0.3170
NGFG_00895	0.0562	0.7350	0.9000	-0.0135	0.9350	0.9860	-0.2780	0.0918	0.3630
NGFG_00896	-0.3660	0.0041	0.0841	-0.2050	0.1050	0.4170	0.1070	0.3930	0.7310
NGFG_00897	-0.3800	0.0024	0.0642	-0.4320	0.0006	0.0294	0.0577	0.6400	0.8730
NGFG_00898	-0.2590	0.0961	0.3710	-0.2130	0.1710	0.4950	-0.0012	0.9940	1.0000
NGFG_00899	-0.2050	0.1170	0.4020	-0.1680	0.1970	0.5300	0.3070	0.0187	0.1510
NGFG_00900	0.1040	0.4750	0.7620	0.0730	0.6170	0.8480	-0.0399	0.7850	0.9320
NGFG_00901	0.2240	0.2080	0.5190	0.1820	0.3070	0.6620	-0.3860	0.0297	0.2020
NGFG_00903	0.0315	0.8240	0.9320	0.1370	0.3340	0.6900	-0.1940	0.1680	0.5110
NGFG_00905	0.1250	0.5100	0.7850	0.1780	0.3490	0.7010	-0.2500	0.1880	0.5390
NGFG_00906	0.2080	0.1010	0.3780	0.1710	0.1770	0.5010	-0.4070	0.0012	0.0229
NGFG_00907	-0.1690	0.2140	0.5250	-0.1490	0.2750	0.6300	0.0596	0.6610	0.8840
NGFG_00908	-0.3440	0.0545	0.2880	-0.2010	0.2600	0.6100	0.3700	0.0381	0.2300
NGFG_00909	-0.0969	0.4750	0.7620	-0.1270	0.3510	0.7020	-0.1130	0.3980	0.7330
NGFG_00910	0.1500	0.5410	0.8020	#NV			-0.0920	0.7080	0.9010
NGFG_00911	-0.0389	0.8520	0.9450	0.0492	0.8130	0.9480	0.0634	0.7590	0.9210
NGFG_00912	0.2400	0.1670	0.4710	0.2430	0.1630	0.4920	-0.0561	0.7470	0.9160
NGFG_00913	0.0785	0.5220	0.7920	0.0112	0.9270	0.9830	-0.0493	0.6870	0.8970
NGFG_00914	-0.3140	0.0472	0.2700	-0.2670	0.0918	0.3920	0.1640	0.2990	0.6480
NGFG_00918	-0.2010	0.2240	0.5370	-0.2260	0.1730	0.4950	-0.0444	0.7880	0.9330
NGFG_00919	-0.4560	0.0583	0.2920	-0.4830	0.0449	0.2910	0.3240	0.1770	0.5230
NGFG_00920	-0.6240	0.0137	0.1540	#NV			0.5210	0.0406	0.2400
NGFG_00921	-0.5220	0.0404	0.2590	#NV			0.3820	0.1340	0.4450
NGFG_00922	-0.6110	0.0154	0.1620	#NV			0.0941	0.7060	0.9010
NGFG_00923	-0.3580	0.1290	0.4220	#NV			0.1660	0.4750	0.7850

NGFG_00924	-0.2260	0.1630	0.4680	0.1280	0.4180	0.7510	-0.0455	0.7730	0.9240
NGFG_00925	-0.2950	0.0868	0.3530	-0.2050	0.2300	0.5740	-0.2750	0.0963	0.3710
NGFG_00926	-0.1470	0.2650	0.5900	-0.1590	0.2280	0.5730	0.1930	0.1430	0.4620
NGFG_00928	0.2570	0.0228	0.2000	0.1750	0.1200	0.4400	0.0733	0.5160	0.8040
NGFG_00930	-0.1110	0.5220	0.7920	-0.1060	0.5390	0.8110	0.0655	0.7050	0.9010
NGFG_00931	-0.2020	0.2040	0.5130	-0.2230	0.1600	0.4860	-0.0487	0.7570	0.9190
NGFG_00932	0.0456	0.8470	0.9430	0.1350	0.5660	0.8260	-0.0655	0.7810	0.9320
NGFG_00933	0.4550	0.0091	0.1220	0.3040	0.0811	0.3640	-0.3110	0.0749	0.3350
NGFG_00934	0.4120	0.0311	0.2330	0.3340	0.0809	0.3640	-0.2520	0.1870	0.5390
NGFG_00936	0.1360	0.4630	0.7560	0.0103	0.9560	0.9930	-0.0452	0.8070	0.9390
NGFG_00937	-0.2950	0.0676	0.3150	-0.3200	0.0471	0.2980	0.2690	0.0934	0.3660
NGFG_00938	-0.3450	0.1530	0.4570	-0.1930	0.4230	0.7510	0.2570	0.2830	0.6320
NGFG_00940	0.1430	0.2580	0.5820	0.1330	0.2920	0.6460	-0.1200	0.3390	0.6850
NGFG_00941	0.5700	0.0000	0.0038	0.4890	0.0003	0.0221	-0.0081	0.9520	0.9910
NGFG_00942	0.0998	0.5300	0.7960	0.2870	0.0683	0.3470	-0.2330	0.1380	0.4510
NGFG_00943	-0.0451	0.8060	0.9240	-0.1620	0.3800	0.7240	-0.1570	0.3870	0.7260
NGFG_00945	0.2780	0.2300	0.5420	0.0886	0.7030	0.8960	-0.0628	0.7860	0.9330
NGFG_00946	0.0463	0.8530	0.9450	#NV			0.3850	0.1250	0.4280
NGFG_00947	-0.1540	0.5320	0.7960	#NV			0.2570	0.2960	0.6470
NGFG_00949	0.2720	0.1910	0.4970	0.3220	0.1200	0.4400	0.0941	0.6520	0.8800
NGFG_00950	0.4490	0.0126	0.1470	0.3290	0.0679	0.3470	-0.1480	0.4130	0.7450
NGFG_00952	-0.2800	0.1660	0.4710	-0.2330	0.2500	0.5990	0.8640	0.0000	0.0012
NGFG_00953	-0.5360	0.0152	0.1610	-0.4630	0.0359	0.2770	0.7310	0.0009	0.0191
NGFG_00954	0.2200	0.3900	0.7040	#NV			0.2180	0.3930	0.7310
NGFG_00955	-0.0041	0.9850	0.9950	0.1100	0.6130	0.8480	-0.0142	0.9480	0.9900
NGFG_00956	-0.1410	0.4690	0.7590	-0.0860	0.6600	0.8760	0.1540	0.4320	0.7600
NGFG_00958	-0.3210	0.1200	0.4040	-0.4350	0.0355	0.2760	0.5480	0.0080	0.0870
NGFG_00959	-0.1400	0.5840	0.8160	#NV			0.1400	0.5830	0.8390
NGFG_00960	0.1540	0.3910	0.7060	0.2650	0.1390	0.4640	0.0240	0.8940	0.9710
NGFG_00961	0.2180	0.1910	0.4970	0.1650	0.3230	0.6830	-0.0036	0.9830	0.9960
NGFG_00962	-0.0429	0.6970	0.8810	-0.0409	0.7110	0.8970	0.4490	0.0000	0.0022
NGFG_00963	-0.2140	0.2980	0.6150	-0.1070	0.6030	0.8480	0.6160	0.0029	0.0442
NGFG_00964	0.1370	0.5780	0.8160	#NV			0.1910	0.4380	0.7620
NGFG_00966	-0.1260	0.6060	0.8250	-0.1260	0.6040	0.8480	0.1600	0.5120	0.8020
NGFG_00967	0.1220	0.5730	0.8160	0.1200	0.5790	0.8360	0.0469	0.8280	0.9510
NGFG_00968	-0.1250	0.6220	0.8340	#NV			0.2820	0.2680	0.6220
NGFG_00969	0.1910	0.2490	0.5710	0.1990	0.2290	0.5740	-0.2380	0.1480	0.4720
NGFG_00970	0.5270	0.0056	0.0983	0.4270	0.0254	0.2330	-0.0113	0.9530	0.9910
NGFG_00971	-0.2790	0.1490	0.4520	-0.2850	0.1410	0.4650	0.7490	0.0001	0.0043
NGFG_00972	-0.0293	0.8850	0.9580	-0.1340	0.5070	0.7950	0.3390	0.0944	0.3670
NGFG_00973	0.0672	0.5870	0.8170	0.0616	0.6190	0.8490	0.3190	0.0099	0.0988
NGFG_00974	0.3450	0.0596	0.2920	0.2940	0.1090	0.4200	-0.0512	0.7800	0.9310
NGFG_00975	0.4090	0.0299	0.2320	0.3530	0.0610	0.3320	0.0009	0.9960	1.0000
NGFG_00976	0.1930	0.2620	0.5870	0.2250	0.1910	0.5200	0.3390	0.0488	0.2670
NGFG_00978	0.1420	0.5750	0.8160	#NV			0.1910	0.4520	0.7710
NGFG_00979	0.2010	0.2170	0.5300	0.1070	0.5130	0.8000	0.2720	0.0977	0.3730
NGFG_00980	-0.4010	0.0691	0.3180	-0.3750	0.0893	0.3850	0.4840	0.0283	0.1970

NGFG_00981	-0.5270	0.0248	0.2100	-0.4820	0.0401	0.2870	0.8390	0.0004	0.0100
NGFG_00982	0.2580	0.1480	0.4510	0.1350	0.4470	0.7680	-0.0624	0.7260	0.9100
NGFG_00983	0.4400	0.0110	0.1370	0.5310	0.0020	0.0707	-0.3790	0.0277	0.1960
NGFG_00984	0.1140	0.4660	0.7570	0.1360	0.3840	0.7270	-0.1720	0.2670	0.6210
NGFG_00985	0.0922	0.6680	0.8650	0.0264	0.9020	0.9810	-0.0444	0.8360	0.9520
NGFG_00986	0.2480	0.1910	0.4970	0.3460	0.0670	0.3440	-0.3140	0.0944	0.3670
NGFG_00987	0.1310	0.4630	0.7560	0.0590	0.7410	0.9140	-0.1270	0.4700	0.7830
NGFG_00988	0.2090	0.3820	0.6940	#NV			-0.2790	0.2450	0.6010
NGFG_00991	0.1500	0.4070	0.7120	0.2930	0.1030	0.4140	-0.0640	0.7230	0.9070
NGFG_00992	#NV			#NV			0.1650	0.3110	0.6610
NGFG_00993	0.0458	0.8240	0.9320	0.0775	0.7050	0.8960	-0.2790	0.1690	0.5110
NGFG_00994	-0.0926	0.6130	0.8290	0.0227	0.9010	0.9810	-0.1290	0.4750	0.7850
NGFG_00995	0.0881	0.6750	0.8700	0.0088	0.9670	0.9950	-0.1170	0.5740	0.8370
NGFG_00996	0.0852	0.7380	0.9000	#NV			0.0315	0.9020	0.9720
NGFG_00997	0.1780	0.4730	0.7620	#NV			0.4030	0.0996	0.3770
NGFG_00998	#NV			#NV			-0.1480	0.5080	0.8020
NGFG_01000	0.0112	0.9490	0.9830	0.2340	0.1790	0.5030	0.4780	0.0070	0.0779
NGFG_01001	-0.1200	0.6100	0.8280	-0.0127	0.9570	0.9930	0.2170	0.3560	0.7000
NGFG_01002	0.1820	0.3040	0.6200	0.0743	0.6760	0.8850	0.0947	0.5940	0.8470
NGFG_01003	0.1080	0.4660	0.7580	0.0178	0.9050	0.9820	0.1100	0.4590	0.7740
NGFG_01004	0.1770	0.2810	0.6010	0.2140	0.1910	0.5200	0.4420	0.0076	0.0843
NGFG_01008	-0.0133	0.9390	0.9810	-0.0027	0.9870	0.9990	-0.1110	0.5210	0.8060
NGFG_01009	-0.2610	0.1810	0.4870	-0.1040	0.5940	0.8470	0.0444	0.8200	0.9470
NGFG_01010	-0.0004	0.9980	0.9990	-0.0013	0.9920	0.9990	-0.0107	0.9330	0.9830
NGFG_01011	-0.0282	0.8310	0.9350	-0.0959	0.4680	0.7830	0.1590	0.2290	0.5880
NGFG_01012	0.5140	0.0088	0.1200	0.6840	0.0005	0.0292	0.0906	0.6440	0.8760
NGFG_01014	0.1290	0.4820	0.7660	0.0490	0.7890	0.9340	0.1350	0.4590	0.7740
NGFG_01015	0.1310	0.4550	0.7490	0.1010	0.5640	0.8250	-0.1990	0.2570	0.6130
NGFG_01016	-0.2850	0.1040	0.3850	-0.2690	0.1230	0.4460	0.1610	0.3520	0.6960
NGFG_01018	-0.3090	0.0228	0.2000	-0.3410	0.0119	0.1700	0.0727	0.5900	0.8450
NGFG_01019	-0.3760	0.0046	0.0889	-0.3530	0.0076	0.1420	0.1530	0.2440	0.6000
NGFG_01020	-0.1650	0.0710	0.3190	-0.1830	0.0458	0.2930	-0.0191	0.8330	0.9520
NGFG_01022	-0.0439	0.8350	0.9360	0.2010	0.3380	0.6910	-0.1410	0.5040	0.8000
NGFG_01023	0.0196	0.8980	0.9600	-0.0790	0.6050	0.8480	0.0061	0.9680	0.9940
NGFG_01024	-0.0149	0.9220	0.9710	-0.0871	0.5680	0.8260	-0.1760	0.2480	0.6040
NGFG_01025	-0.3540	0.0529	0.2840	-0.3210	0.0790	0.3640	0.2980	0.1030	0.3850
NGFG_01026	-0.0430	0.6480	0.8530	-0.0705	0.4540	0.7720	-0.1130	0.2280	0.5880
NGFG_01027	-0.3930	0.0017	0.0523	-0.4670	0.0002	0.0199	0.0700	0.5720	0.8370
NGFG_01028	-0.3060	0.0843	0.3500	-0.1500	0.3940	0.7360	0.3890	0.0278	0.1960
NGFG_01029	-0.2640	0.1030	0.3820	-0.2510	0.1200	0.4400	0.1010	0.5280	0.8130
NGFG_01030	0.1320	0.4700	0.7590	0.2020	0.2670	0.6220	-0.4260	0.0191	0.1530
NGFG_01031	#NV			#NV			0.1080	0.5520	0.8270
NGFG_01032	0.1660	0.2830	0.6040	0.0700	0.6500	0.8680	-0.1210	0.4330	0.7600
NGFG_01033	0.1960	0.1200	0.4040	0.0738	0.5600	0.8220	-0.2230	0.0766	0.3370
NGFG_01034	-0.1890	0.3930	0.7070	-0.0661	0.7650	0.9240	-0.0914	0.6780	0.8930
NGFG_01035	-0.0873	0.5970	0.8230	0.0164	0.9210	0.9820	-0.0931	0.5700	0.8370
NGFG_01036	0.3220	0.0540	0.2860	0.3310	0.0473	0.2980	-0.4040	0.0149	0.1270

NGFG_01037	-0.0631	0.7420	0.9010	-0.1900	0.3230	0.6830	0.0551	0.7720	0.9240
NGFG_01038	-0.1410	0.4750	0.7620	-0.1540	0.4350	0.7600	-0.0078	0.9680	0.9940
NGFG_01039	-0.0246	0.8920	0.9600	-0.0017	0.9920	0.9990	-0.1930	0.2810	0.6320
NGFG_01040	0.1930	0.3110	0.6280	0.0597	0.7540	0.9220	-0.4660	0.0142	0.1250
NGFG_01041	0.1220	0.6250	0.8360	#NV			-0.0724	0.7730	0.9240
NGFG_01043	-0.2770	0.0713	0.3190	-0.2620	0.0876	0.3810	-0.0082	0.9560	0.9940
NGFG_01044	-0.0360	0.8620	0.9490	0.0157	0.9400	0.9870	-0.0906	0.6610	0.8840
NGFG_01045	-0.1410	0.4090	0.7150	-0.1350	0.4290	0.7550	0.0409	0.8100	0.9400
NGFG_01046	-0.6390	0.0009	0.0376	-0.6020	0.0018	0.0702	0.4230	0.0263	0.1880
NGFG_01048	-0.2380	0.1330	0.4290	-0.1860	0.2380	0.5880	0.2340	0.1380	0.4520
NGFG_01051	0.3960	0.0073	0.1110	0.3590	0.0151	0.1890	-0.2150	0.1450	0.4670
NGFG_01052	-0.1090	0.5780	0.8160	-0.1300	0.5070	0.7950	0.0462	0.8110	0.9400
NGFG_01053	#NV			#NV			0.0147	0.8260	0.9500
NGFG_01056	-0.4040	0.0786	0.3380	-0.1190	0.6010	0.8480	0.3980	0.0811	0.3470
NGFG_01058	#NV			#NV			0.2550	0.1850	0.5380
NGFG_01059	#NV			#NV			0.1820	0.4130	0.7450
NGFG_01060	-0.4910	0.0491	0.2750	#NV			0.3630	0.1480	0.4710
NGFG_01062	-0.3380	0.1840	0.4900	#NV			0.0524	0.8370	0.9520
NGFG_01063	0.1070	0.6540	0.8550	0.1770	0.4560	0.7730	-0.2740	0.2460	0.6030
NGFG_01064	0.1980	0.4190	0.7230	#NV			-0.0245	0.9200	0.9780
NGFG_01068	0.0175	0.9080	0.9650	0.2370	0.1180	0.4370	-0.0192	0.8990	0.9720
NGFG_01069	-0.0435	0.8160	0.9290	-0.3360	0.0781	0.3640	0.0627	0.7370	0.9110
NGFG_01070	0.0998	0.5000	0.7790	0.0074	0.9600	0.9940	0.0548	0.7110	0.9010
NGFG_01072	0.0180	0.9070	0.9640	-0.0428	0.7810	0.9320	-0.1350	0.3810	0.7230
NGFG_01073	-0.1200	0.4240	0.7230	-0.0811	0.5890	0.8430	0.0114	0.9390	0.9860
NGFG_01074	-0.0842	0.5510	0.8090	-0.0727	0.6060	0.8480	-0.1240	0.3800	0.7230
NGFG_01075	-0.1440	0.3760	0.6910	-0.2380	0.1430	0.4670	-0.1090	0.5030	0.8000
NGFG_01076	0.2150	0.2920	0.6100	0.2180	0.2850	0.6390	-0.4970	0.0146	0.1270
NGFG_01077	-0.1440	0.3560	0.6700	-0.1210	0.4400	0.7650	-0.0930	0.5510	0.8270
NGFG_01078	0.0665	0.7700	0.9110	-0.0279	0.9030	0.9810	-0.0348	0.8790	0.9650
NGFG_01080	0.3090	0.0359	0.2440	0.3770	0.0102	0.1590	-0.1680	0.2530	0.6090
NGFG_01081	-0.0069	0.9710	0.9930	0.1210	0.5180	0.8030	0.0128	0.9450	0.9880
NGFG_01083	0.2470	0.2550	0.5800	0.5260	0.0142	0.1830	-0.1240	0.5660	0.8360
NGFG_01084	-0.1960	0.3240	0.6390	-0.1940	0.3300	0.6890	0.5420	0.0068	0.0771
NGFG_01088	0.0668	0.7400	0.9000	-0.0276	0.8910	0.9780	0.1370	0.4970	0.7960
NGFG_01091	0.4850	0.0263	0.2160	0.5600	0.0103	0.1600	0.0046	0.9830	0.9960
NGFG_01092	0.3650	0.0760	0.3320	0.4990	0.0150	0.1890	0.3740	0.0701	0.3250
NGFG_01093	0.4140	0.0075	0.1120	0.3700	0.0169	0.1990	-0.0149	0.9240	0.9790
NGFG_01094	0.4520	0.0411	0.2600	0.3460	0.1190	0.4390	-0.0653	0.7680	0.9240
NGFG_01095	0.2630	0.1220	0.4070	0.1910	0.2600	0.6110	-0.2590	0.1270	0.4340
NGFG_01096	-0.2200	0.2110	0.5210	-0.1610	0.3600	0.7120	0.0886	0.6120	0.8590
NGFG_01099	0.0156	0.9360	0.9790	0.1090	0.5750	0.8330	0.2660	0.1710	0.5170
NGFG_01100	-0.0298	0.8460	0.9430	-0.0231	0.8810	0.9740	0.4400	0.0044	0.0590
NGFG_01104	-0.3750	0.0729	0.3250	-0.3460	0.0971	0.4010	0.4400	0.0344	0.2200
NGFG_01105	-0.5270	0.0216	0.1950	-0.3280	0.1490	0.4720	-0.0309	0.8900	0.9690
NGFG_01106	-0.2100	0.3460	0.6620	#NV			0.3630	0.1020	0.3850
NGFG_01107	-0.0693	0.6820	0.8730	-0.0382	0.8210	0.9500	0.0906	0.5920	0.8470

NGFG_01108	0.0817	0.3890	0.7040	0.1020	0.2810	0.6350	-0.0807	0.3940	0.7310
NGFG_01109	-0.0001	0.9990	0.9990	0.0394	0.7820	0.9320	0.1470	0.3030	0.6530
NGFG_01110	0.3170	0.0470	0.2700	0.2350	0.1410	0.4660	-0.1670	0.2960	0.6470
NGFG_01112	-0.2700	0.0362	0.2440	-0.2290	0.0750	0.3610	0.0418	0.7430	0.9140
NGFG_01113	-0.2140	0.0958	0.3710	-0.3000	0.0201	0.2090	0.0281	0.8250	0.9500
NGFG_01114	-0.1790	0.1170	0.4020	-0.1070	0.3480	0.7010	-0.1510	0.1760	0.5210
NGFG_01115	-0.0024	0.9890	0.9950	-0.1840	0.2790	0.6340	-0.0082	0.9610	0.9940
NGFG_01116	-0.1060	0.5530	0.8090	-0.0582	0.7430	0.9150	-0.1500	0.3940	0.7310
NGFG_01117	0.2550	0.1470	0.4500	0.2020	0.2520	0.6010	-0.5040	0.0042	0.0579
NGFG_01118	-0.4820	0.0068	0.1080	-0.4200	0.0181	0.2060	0.2350	0.1860	0.5390
NGFG_01119	-0.0226	0.9160	0.9690	-0.0487	0.8200	0.9500	-0.2560	0.2280	0.5880
NGFG_01120	-0.0576	0.7850	0.9140	-0.1440	0.4960	0.7940	0.0971	0.6450	0.8760
NGFG_01121	0.1770	0.2740	0.5970	0.0809	0.6170	0.8480	0.1200	0.4590	0.7740
NGFG_01122	0.4970	0.0002	0.0160	0.3870	0.0040	0.1000	-0.0858	0.5240	0.8090
NGFG_01123	0.2240	0.1470	0.4500	0.1250	0.4190	0.7510	-0.3160	0.0404	0.2400
NGFG_01125	-0.1460	0.3770	0.6910	-0.1050	0.5250	0.8040	0.2810	0.0887	0.3610
NGFG_01127	-0.4420	0.0417	0.2600	-0.3440	0.1120	0.4270	0.2340	0.2780	0.6310
NGFG_01128	-0.4060	0.0108	0.1340	-0.1830	0.2450	0.5930	0.1020	0.5120	0.8020
NGFG_01129	-0.0483	0.7450	0.9030	-0.1960	0.1880	0.5150	0.1090	0.4600	0.7740
NGFG_01131	0.2950	0.1010	0.3790	0.3260	0.0699	0.3490	-0.3500	0.0510	0.2720
NGFG_01132	-0.0953	0.3760	0.6910	-0.1610	0.1350	0.4580	-0.0249	0.8170	0.9450
NGFG_01133	0.0247	0.8520	0.9450	0.0766	0.5630	0.8250	-0.2570	0.0512	0.2720
NGFG_01134	-0.2530	0.2990	0.6160	0.2270	0.3470	0.7010	-0.1610	0.5040	0.8000
NGFG_01135	-0.1150	0.5640	0.8160	-0.1370	0.4900	0.7910	0.1440	0.4670	0.7800
NGFG_01136	-0.0715	0.5840	0.8160	-0.1070	0.4120	0.7500	-0.0781	0.5470	0.8240
NGFG_01137	0.0897	0.4290	0.7260	-0.0267	0.8140	0.9480	-0.1300	0.2520	0.6090
NGFG_01138	-0.1400	0.4260	0.7230	-0.2610	0.1380	0.4640	0.2160	0.2180	0.5800
NGFG_01139	-0.0740	0.7130	0.8930	0.1340	0.5030	0.7940	0.0777	0.6980	0.8980
NGFG_01141	-0.1910	0.3330	0.6490	-0.3100	0.1170	0.4360	0.0792	0.6870	0.8970
NGFG_01143	0.0973	0.4930	0.7740	-0.0325	0.8190	0.9500	0.2440	0.0862	0.3570
NGFG_01144	-0.5450	0.0114	0.1390	-0.4500	0.0365	0.2770	0.4500	0.0358	0.2250
NGFG_01145	0.0874	0.5740	0.8160	0.0960	0.5360	0.8110	-0.2470	0.1100	0.3980
NGFG_01146	0.6330	0.0009	0.0376	0.3990	0.0377	0.2800	-0.9640	0.0000	0.0000
NGFG_01148	0.1440	0.4670	0.7580	0.2890	0.1440	0.4670	-0.2240	0.2580	0.6130
NGFG_01149	-0.0514	0.7370	0.9000	-0.0021	0.9890	0.9990	0.0183	0.9040	0.9720
NGFG_01150	-0.3690	0.0363	0.2440	-0.3070	0.0810	0.3640	0.2820	0.1100	0.3980
NGFG_01152	0.3110	0.0812	0.3450	0.2110	0.2360	0.5860	-0.2600	0.1440	0.4670
NGFG_01153	-0.3320	0.1630	0.4680	-0.1210	0.6100	0.8480	0.4000	0.0932	0.3660
NGFG_01154	-0.1240	0.4320	0.7270	-0.1590	0.3120	0.6700	-0.0923	0.5550	0.8310
NGFG_01155	0.1960	0.1100	0.3910	0.1480	0.2260	0.5710	-0.2740	0.0248	0.1830
NGFG_01156	0.0835	0.6630	0.8620	0.0698	0.7160	0.9020	-0.0400	0.8350	0.9520
NGFG_01157	0.3050	0.0471	0.2700	0.1760	0.2530	0.6020	0.1690	0.2750	0.6280
NGFG_01158	-0.3410	0.0937	0.3690	-0.4880	0.0168	0.1990	0.3310	0.1030	0.3860
NGFG_01160	0.6960	0.0007	0.0342	0.5710	0.0054	0.1170	0.1980	0.3350	0.6810
NGFG_01161	0.0650	0.6490	0.8530	0.0483	0.7360	0.9110	-0.1400	0.3270	0.6730
NGFG_01163	-0.8390	0.0009	0.0376	-0.6910	0.0063	0.1260	0.8980	0.0004	0.0105
NGFG_01164	-0.0945	0.5450	0.8050	-0.1500	0.3370	0.6900	0.2380	0.1270	0.4340

NGFG_01165	0.5360	0.0092	0.1220	0.4240	0.0398	0.2870	-0.1250	0.5470	0.8240
NGFG_01166	0.0384	0.8130	0.9260	0.0092	0.9550	0.9930	0.5250	0.0013	0.0242
NGFG_01167	0.2100	0.2610	0.5870	0.1850	0.3240	0.6830	-0.1870	0.3160	0.6640
NGFG_01168	0.1010	0.5990	0.8230	-0.0047	0.9800	0.9980	0.0175	0.9280	0.9800
NGFG_01169	-0.2350	0.3530	0.6700	#NV			0.4180	0.0998	0.3780
NGFG_01170	-0.1660	0.4780	0.7640	-0.3490	0.1380	0.4640	0.2750	0.2410	0.5970
NGFG_01171	-0.1590	0.2110	0.5220	-0.1390	0.2740	0.6300	-0.1540	0.2240	0.5860
NGFG_01172	-0.1010	0.4690	0.7590	-0.1620	0.2440	0.5910	-0.0484	0.7250	0.9100
NGFG_01173	-0.0555	0.7830	0.9140	-0.0867	0.6670	0.8780	-0.0752	0.7080	0.9010
NGFG_01175	-0.3060	0.0457	0.2690	-0.2970	0.0521	0.3120	0.0968	0.5230	0.8090
NGFG_01176	-0.4440	0.0002	0.0144	-0.3360	0.0041	0.1000	0.1010	0.3830	0.7240
NGFG_01181	0.5170	0.0106	0.1330	0.3290	0.1060	0.4170	-0.2790	0.1690	0.5110
NGFG_01182	0.3280	0.0029	0.0751	0.2300	0.0372	0.2790	-0.0688	0.5330	0.8150
NGFG_01183	0.1460	0.5360	0.8000	#NV			-0.2480	0.2960	0.6470
NGFG_01184	0.3290	0.0498	0.2770	0.1970	0.2390	0.5880	-0.3570	0.0334	0.2170
NGFG_01185	0.1020	0.4990	0.7790	0.0620	0.6830	0.8850	-0.3260	0.0315	0.2080
NGFG_01186	0.2400	0.2180	0.5300	0.2370	0.2240	0.5700	-0.3920	0.0438	0.2500
NGFG_01187	-0.0489	0.7240	0.8980	-0.0146	0.9160	0.9820	-0.1490	0.2760	0.6280
NGFG_01188	-0.3210	0.1080	0.3890	-0.1210	0.5430	0.8140	0.0715	0.7180	0.9050
NGFG_01189	0.0418	0.7660	0.9100	0.1690	0.2270	0.5720	-0.0744	0.5930	0.8470
NGFG_01190	-0.1920	0.4510	0.7470	#NV			0.4360	0.0872	0.3600
NGFG_01192	0.1670	0.2220	0.5350	0.2310	0.0922	0.3920	0.1670	0.2260	0.5880
NGFG_01193	-0.0552	0.7650	0.9100	-0.1230	0.5080	0.7950	-0.1630	0.3710	0.7160
NGFG_01194	0.0207	0.9030	0.9620	-0.0413	0.8070	0.9470	0.0797	0.6380	0.8730
NGFG_01195	0.1080	0.3590	0.6730	-0.0673	0.5680	0.8260	-0.0549	0.6420	0.8730
NGFG_01196	0.3100	0.1540	0.4570	0.4230	0.0507	0.3080	-0.1910	0.3800	0.7230
NGFG_01198	0.1550	0.3040	0.6200	0.0889	0.5570	0.8210	-0.1140	0.4480	0.7700
NGFG_01199	-0.0280	0.8500	0.9450	0.0180	0.9030	0.9810	-0.1490	0.3120	0.6610
NGFG_01200	0.1970	0.3230	0.6380	0.1490	0.4550	0.7730	-0.3660	0.0662	0.3160
NGFG_01201	-0.0465	0.7180	0.8940	-0.0831	0.5180	0.8030	-0.0226	0.8600	0.9610
NGFG_01202	0.1760	0.1380	0.4360	0.0602	0.6120	0.8480	-0.2780	0.0184	0.1500
NGFG_01203	0.1260	0.3560	0.6700	0.0553	0.6870	0.8870	-0.0969	0.4790	0.7860
NGFG_01204	0.5400	0.0000	0.0025	0.4910	0.0001	0.0125	-0.2620	0.0346	0.2200
NGFG_01205	0.3900	0.0075	0.1120	0.3310	0.0232	0.2280	-0.2300	0.1150	0.4100
NGFG_01206	-0.2160	0.1810	0.4870	-0.2050	0.2040	0.5380	0.1180	0.4630	0.7780
NGFG_01207	0.0622	0.6260	0.8370	0.0533	0.6760	0.8850	0.2200	0.0853	0.3550
NGFG_01208	0.1110	0.5390	0.8020	0.0822	0.6470	0.8670	0.3860	0.0321	0.2110
NGFG_01210	-0.2550	0.0804	0.3430	-0.2690	0.0651	0.3440	0.2840	0.0511	0.2720
NGFG_01211	-0.2000	0.1900	0.4970	-0.2110	0.1670	0.4940	0.4380	0.0041	0.0579
NGFG_01212	0.0911	0.5590	0.8120	0.1110	0.4770	0.7870	0.0928	0.5520	0.8270
NGFG_01215	0.4310	0.0686	0.3170	#NV			-0.2730	0.2500	0.6060
NGFG_01216	0.1770	0.0996	0.3770	0.0950	0.3780	0.7220	-0.3290	0.0022	0.0368
NGFG_01217	-0.0555	0.6150	0.8310	-0.0902	0.4140	0.7500	0.0032	0.9770	0.9940
NGFG_01220	-0.4300	0.0365	0.2440	-0.3820	0.0627	0.3380	0.3260	0.1110	0.4010
NGFG_01222	0.2730	0.0556	0.2900	0.2240	0.1150	0.4350	-0.2740	0.0528	0.2750
NGFG_01223	0.2890	0.0240	0.2080	0.2240	0.0807	0.3640	-0.2200	0.0845	0.3540
NGFG_01224	0.0676	0.4090	0.7150	0.0092	0.9110	0.9820	-0.1640	0.0449	0.2530

NGFG_01225	-0.0646	0.5940	0.8230	-0.1520	0.2110	0.5490	-0.3380	0.0052	0.0657
NGFG_01227	-0.0786	0.6530	0.8550	-0.1280	0.4650	0.7820	0.0058	0.9740	0.9940
NGFG_01228	-0.1420	0.4160	0.7200	-0.2490	0.1550	0.4800	0.0340	0.8450	0.9550
NGFG_01229	-0.1310	0.4630	0.7560	-0.3440	0.0560	0.3220	-0.0028	0.9870	0.9980
NGFG_01230	-0.2430	0.3160	0.6330	-0.0260	0.9140	0.9820	0.3830	0.1140	0.4070
NGFG_01231	0.0161	0.8840	0.9570	-0.0213	0.8460	0.9610	-0.1210	0.2700	0.6220
NGFG_01232	0.0020	0.9920	0.9960	-0.0220	0.9170	0.9820	-0.0834	0.6940	0.8970
NGFG_01233	-0.1540	0.5080	0.7840	-0.1590	0.4940	0.7940	-0.0748	0.7480	0.9160
NGFG_01236	0.1830	0.2290	0.5410	0.1380	0.3670	0.7140	-0.1150	0.4490	0.7700
NGFG_01240	0.3290	0.0871	0.3530	0.1620	0.4020	0.7390	-0.3240	0.0912	0.3620
NGFG_01242	-0.1270	0.5550	0.8100	-0.3680	0.0889	0.3840	0.5260	0.0148	0.1270
NGFG_01243	-0.0948	0.6040	0.8240	-0.2830	0.1240	0.4460	-0.1870	0.2980	0.6470
NGFG_01244	0.2810	0.0289	0.2280	0.2310	0.0723	0.3550	-0.3210	0.0123	0.1160
NGFG_01245	-0.4180	0.0194	0.1830	-0.3230	0.0698	0.3490	-0.0024	0.9890	0.9980
NGFG_01246	0.2190	0.0605	0.2930	0.1490	0.2030	0.5380	-0.0888	0.4470	0.7690
NGFG_01247	0.0418	0.7340	0.9000	-0.0474	0.7020	0.8950	-0.2730	0.0244	0.1810
NGFG_01248	-0.0879	0.6680	0.8650	-0.1060	0.6070	0.8480	0.1230	0.5480	0.8250
NGFG_01249	-0.2250	0.2270	0.5400	-0.0384	0.8360	0.9540	-0.0405	0.8270	0.9500
NGFG_01250	-0.0526	0.7500	0.9060	-0.0785	0.6350	0.8600	-0.1280	0.4350	0.7610
NGFG_01251	0.1750	0.3560	0.6700	0.0591	0.7560	0.9230	-0.2500	0.1880	0.5390
NGFG_01252	0.1060	0.5150	0.7870	-0.0195	0.9040	0.9820	-0.1630	0.3140	0.6630
NGFG_01253	-0.2250	0.2720	0.5960	-0.2020	0.3240	0.6830	0.1260	0.5360	0.8150
NGFG_01254	-0.0544	0.7280	0.9000	-0.0730	0.6410	0.8630	0.0164	0.9160	0.9760
NGFG_01255	-0.0350	0.7790	0.9130	-0.0845	0.4990	0.7940	-0.1270	0.3030	0.6540
NGFG_01256	0.1590	0.2950	0.6120	0.1450	0.3380	0.6910	-0.2510	0.0959	0.3700
NGFG_01257	0.3240	0.0736	0.3270	0.3180	0.0799	0.3640	-0.1250	0.4910	0.7950
NGFG_01259	0.0446	0.6730	0.8690	0.0096	0.9280	0.9830	-0.1070	0.3110	0.6610
NGFG_01260	-0.1350	0.2800	0.6010	-0.2240	0.0742	0.3580	0.3420	0.0063	0.0732
NGFG_01262	-0.3930	0.1200	0.4040	#NV			0.2650	0.2930	0.6430
NGFG_01264	-0.0269	0.8720	0.9510	0.0237	0.8870	0.9770	0.1180	0.4790	0.7860
NGFG_01265	-0.1260	0.5310	0.7960	-0.1950	0.3330	0.6900	0.0397	0.8420	0.9530
NGFG_01266	-0.1430	0.4130	0.7190	-0.1110	0.5230	0.8030	0.0331	0.8470	0.9550
NGFG_01268	-0.1040	0.3140	0.6300	-0.1080	0.2960	0.6530	-0.0349	0.7340	0.9110
NGFG_01269	0.0567	0.6420	0.8490	0.1260	0.3000	0.6600	0.0739	0.5430	0.8220
NGFG_01270	-0.1400	0.2860	0.6060	-0.0537	0.6810	0.8850	0.0476	0.7160	0.9040
NGFG_01272	-0.1540	0.2750	0.5980	-0.0355	0.8000	0.9420	-0.2080	0.1290	0.4340
NGFG_01273	-0.1650	0.3630	0.6770	-0.0787	0.6640	0.8780	0.3920	0.0305	0.2040
NGFG_01274	-0.6250	0.0102	0.1300	-0.4670	0.0545	0.3180	0.2860	0.2390	0.5960
NGFG_01275	#NV			#NV			0.0623	0.7110	0.9010
NGFG_01277	-0.1100	0.6670	0.8650	#NV			-0.2060	0.4200	0.7510
NGFG_01278	-0.4330	0.0769	0.3340	#NV			0.1640	0.5090	0.8020
NGFG_01279	-0.1300	0.5850	0.8160	#NV			0.1480	0.5340	0.8150
NGFG_01280	-0.2840	0.2470	0.5700	#NV			0.0077	0.9750	0.9940
NGFG_01281	-0.1360	0.3630	0.6770	-0.0753	0.6140	0.8480	-0.1760	0.2360	0.5960
NGFG_01283	-0.3290	0.1940	0.5000	#NV			0.1220	0.6290	0.8680
NGFG_01284	#NV			#NV			0.1630	0.4600	0.7740
NGFG_01285	0.1590	0.4790	0.7640	0.4190	0.0595	0.3290	-0.4230	0.0562	0.2870

NGFG_01287	-0.0680	0.7410	0.9010	-0.1080	0.5980	0.8480	0.1400	0.4980	0.7960
NGFG_01288	-0.2750	0.1840	0.4900	-0.1310	0.5290	0.8060	0.2680	0.1960	0.5500
NGFG_01289	-0.6350	0.0002	0.0160	-0.4190	0.0139	0.1830	0.2980	0.0785	0.3410
NGFG_01290	-0.5880	0.0142	0.1580	-0.6060	0.0115	0.1670	0.3210	0.1790	0.5270
NGFG_01291	-0.2710	0.2880	0.6070	#NV			0.3260	0.2010	0.5550
NGFG_01292	-0.5660	0.0207	0.1880	-0.5530	0.0239	0.2310	0.6640	0.0066	0.0765
NGFG_01293	-0.6800	0.0064	0.1030	#NV			0.3720	0.1340	0.4450
NGFG_01294	-0.4400	0.0770	0.3340	#NV			0.0324	0.8970	0.9720
NGFG_01295	-0.4110	0.0398	0.2570	#NV			0.1000	0.6200	0.8640
NGFG_01296	-0.5010	0.0308	0.2330	#NV			0.2750	0.2420	0.5970
NGFG_01297	#NV			#NV			0.2430	0.0820	0.3490
NGFG_01298	-0.7610	0.0022	0.0615	#NV			0.1060	0.6650	0.8870
NGFG_01299	0.1060	0.6500	0.8530	0.1020	0.6630	0.8780	-0.2840	0.2220	0.5840
NGFG_01300	-0.5090	0.0327	0.2350	-0.3610	0.1290	0.4520	0.4410	0.0630	0.3090
NGFG_01301	-0.1940	0.4070	0.7120	-0.2180	0.3520	0.7020	0.0923	0.6910	0.8970
NGFG_01302	-0.4400	0.0600	0.2920	#NV			0.5120	0.0289	0.2000
NGFG_01303	-0.4290	0.0044	0.0879	-0.2890	0.0543	0.3180	0.7100	0.0000	0.0002
NGFG_01304	0.2120	0.2610	0.5870	0.1700	0.3670	0.7140	0.0860	0.6490	0.8790
NGFG_01305	0.1490	0.5590	0.8120	#NV			-0.2550	0.3180	0.6650
NGFG_01308	#NV			#NV			-0.2860	0.1630	0.5020
NGFG_01309	-0.5680	0.0223	0.1990	#NV			0.4870	0.0513	0.2720
NGFG_01311	-0.7610	0.0026	0.0688	#NV			0.8160	0.0013	0.0247
NGFG_01312	0.2940	0.1430	0.4440	0.2890	0.1490	0.4720	-0.0060	0.9760	0.9940
NGFG_01313	0.1430	0.3970	0.7080	0.0276	0.8710	0.9720	0.0369	0.8270	0.9500
NGFG_01315	-0.1560	0.3860	0.6990	-0.2580	0.1510	0.4730	0.5390	0.0028	0.0438
NGFG_01316	-0.2870	0.0182	0.1760	-0.2230	0.0657	0.3440	0.0426	0.7250	0.9100
NGFG_01318	#NV			#NV			-0.0044	0.9650	0.9940
NGFG_01319	-0.0646	0.7790	0.9130	#NV			0.0880	0.7030	0.9010
NGFG_01320	-0.2400	0.2440	0.5680	#NV			0.1260	0.5460	0.8240
NGFG_01322	0.1750	0.3100	0.6280	0.1360	0.4300	0.7550	-0.3120	0.0675	0.3180
NGFG_01323	0.2610	0.0503	0.2790	0.1600	0.2310	0.5750	-0.4660	0.0004	0.0113
NGFG_01324	0.1240	0.2640	0.5880	0.1220	0.2710	0.6250	-0.3110	0.0048	0.0620
NGFG_01325	0.1600	0.1700	0.4750	0.0466	0.6910	0.8910	-0.1830	0.1170	0.4110
NGFG_01326	0.5230	0.0136	0.1530	0.2800	0.1880	0.5150	-0.0350	0.8700	0.9630
NGFG_01327	0.2300	0.2610	0.5870	0.2140	0.2940	0.6500	-0.3340	0.1010	0.3820
NGFG_01328	-0.1580	0.3810	0.6940	-0.1630	0.3650	0.7140	-0.0138	0.9380	0.9860
NGFG_01329	-0.1980	0.2580	0.5820	-0.1110	0.5270	0.8050	-0.0742	0.6710	0.8890
NGFG_01330	0.0061	0.9570	0.9870	-0.0390	0.7330	0.9110	-0.1870	0.0978	0.3730
NGFG_01331	0.0569	0.6810	0.8720	0.0416	0.7640	0.9240	-0.3630	0.0080	0.0870
NGFG_01332	0.2420	0.0959	0.3710	0.1240	0.3960	0.7360	-0.2890	0.0465	0.2570
NGFG_01334	-0.0411	0.7820	0.9140	-0.1640	0.2700	0.6240	0.1340	0.3650	0.7120
NGFG_01335	-0.4000	0.0052	0.0951	-0.3880	0.0067	0.1300	0.1160	0.4100	0.7440
NGFG_01336	0.1130	0.5450	0.8050	0.0857	0.6450	0.8660	-0.0954	0.6080	0.8580
NGFG_01337	-0.0715	0.5390	0.8020	-0.0319	0.7840	0.9320	0.0088	0.9390	0.9860
NGFG_01338	0.2160	0.1660	0.4710	0.1360	0.3840	0.7270	-0.1340	0.3890	0.7280
NGFG_01339	0.0444	0.8200	0.9320	0.0483	0.8050	0.9460	0.0644	0.7420	0.9140
NGFG_01340	0.1680	0.3480	0.6650	0.1300	0.4670	0.7830	0.2820	0.1160	0.4110

NGFG_01341	0.0581	0.8030	0.9240	#NV			0.4610	0.0500	0.2700
NGFG_01343	0.2270	0.2670	0.5920	0.2090	0.3060	0.6620	0.2550	0.2130	0.5710
NGFG_01345	0.2410	0.2080	0.5190	0.1230	0.5200	0.8030	0.4730	0.0149	0.1270
NGFG_01346	0.1040	0.5700	0.8160	0.0694	0.7050	0.8960	0.4100	0.0271	0.1930
NGFG_01347	0.2910	0.1140	0.3970	0.4290	0.0197	0.2080	0.1980	0.2850	0.6340
NGFG_01348	0.0594	0.7590	0.9100	-0.0720	0.7110	0.8970	0.5100	0.0088	0.0925
NGFG_01349	0.3520	0.1230	0.4080	0.1410	0.5380	0.8110	0.8540	0.0002	0.0064
NGFG_01350	0.1950	0.1760	0.4820	0.2740	0.0576	0.3240	-0.3120	0.0297	0.2020
NGFG_01351	-0.1700	0.2130	0.5240	-0.1750	0.2010	0.5350	-0.4100	0.0020	0.0342
NGFG_01353	0.4250	0.0729	0.3250	0.8930	0.0002	0.0173	-0.8020	0.0007	0.0161
NGFG_01354	0.1160	0.4250	0.7230	0.0599	0.6790	0.8850	-0.4260	0.0032	0.0472
NGFG_01355	-0.0411	0.8120	0.9260	0.0374	0.8290	0.9500	-0.0480	0.7810	0.9320
NGFG_01356	0.1270	0.2820	0.6040	0.1600	0.1740	0.4970	-0.4100	0.0004	0.0113
NGFG_01357	0.5680	0.0022	0.0615	0.4360	0.0189	0.2070	-0.0935	0.6140	0.8600
NGFG_01360	-0.0094	0.9330	0.9790	0.0459	0.6790	0.8850	0.0505	0.6480	0.8790
NGFG_01361	0.2110	0.2450	0.5690	0.3620	0.0456	0.2930	0.0945	0.6030	0.8550
NGFG_01362	-0.0750	0.3130	0.6290	-0.1030	0.1660	0.4930	-0.1490	0.0435	0.2500
NGFG_01366	-0.6120	0.0060	0.0995	-0.2000	0.3600	0.7120	0.1260	0.5630	0.8340
NGFG_01367	-0.1760	0.1230	0.4090	-0.2020	0.0770	0.3640	-0.0049	0.9660	0.9940
NGFG_01368	-0.0595	0.7540	0.9080	0.0220	0.9080	0.9820	-0.1300	0.4930	0.7950
NGFG_01369	-0.4980	0.0001	0.0099	-0.3340	0.0079	0.1430	0.2440	0.0519	0.2730
NGFG_01370	-0.2520	0.1100	0.3910	-0.2680	0.0888	0.3840	0.2970	0.0586	0.2950
NGFG_01373	-0.2980	0.1410	0.4400	-0.3640	0.0719	0.3550	0.5380	0.0079	0.0862
NGFG_01374	-0.1390	0.3000	0.6160	-0.0677	0.6130	0.8480	-0.0021	0.9880	0.9980
NGFG_01375	-0.4300	0.0279	0.2220	-0.4050	0.0386	0.2830	0.2920	0.1350	0.4460
NGFG_01376	-0.0208	0.9280	0.9760	-0.1010	0.6590	0.8750	-0.0672	0.7700	0.9240
NGFG_01377	0.2100	0.1680	0.4730	0.0242	0.8740	0.9720	0.3750	0.0141	0.1250
NGFG_01378	-0.0576	0.8050	0.9240	0.1440	0.5350	0.8110	0.0568	0.8070	0.9390
NGFG_01379	-0.2140	0.0323	0.2350	-0.2000	0.0443	0.2910	0.0153	0.8770	0.9650
NGFG_01380	-0.0607	0.6890	0.8790	-0.1480	0.3300	0.6890	0.0448	0.7670	0.9240
NGFG_01381	0.1430	0.2000	0.5100	0.0377	0.7360	0.9110	-0.0185	0.8690	0.9630
NGFG_01382	-0.0178	0.8890	0.9590	0.0061	0.9620	0.9940	0.2880	0.0240	0.1800
NGFG_01383	0.0868	0.6040	0.8240	0.1260	0.4510	0.7700	-0.2800	0.0907	0.3620
NGFG_01384	-0.3160	0.0560	0.2900	-0.0902	0.5830	0.8400	0.1370	0.4050	0.7390
NGFG_01385	-0.1240	0.4860	0.7690	-0.2270	0.2010	0.5350	-0.0540	0.7600	0.9210
NGFG_01386	0.0372	0.7890	0.9150	-0.0246	0.8600	0.9690	0.0784	0.5740	0.8370
NGFG_01387	-0.1410	0.0914	0.3650	-0.1540	0.0644	0.3430	0.0747	0.3700	0.7150
NGFG_01388	-0.0694	0.5660	0.8160	-0.1290	0.2870	0.6400	0.0145	0.9040	0.9720
NGFG_01389	0.2670	0.0481	0.2720	0.2000	0.1390	0.4640	-0.1110	0.4120	0.7450
NGFG_01390	0.0169	0.8540	0.9460	-0.0030	0.9740	0.9960	-0.1200	0.1900	0.5410
NGFG_01391	0.3570	0.0326	0.2350	0.4310	0.0097	0.1520	-0.2780	0.0949	0.3680
NGFG_01392	0.2980	0.0166	0.1680	0.3180	0.0106	0.1600	-0.0125	0.9200	0.9780
NGFG_01393	0.3560	0.0076	0.1120	0.2170	0.1050	0.4170	0.0523	0.6960	0.8980
NGFG_01394	0.1340	0.3990	0.7100	0.0752	0.6360	0.8600	0.0531	0.7380	0.9110
NGFG_01395	0.1840	0.0957	0.3710	0.2290	0.0382	0.2820	0.0826	0.4560	0.7740
NGFG_01396	-0.0568	0.6900	0.8790	-0.0822	0.5640	0.8250	0.1510	0.2880	0.6370
NGFG_01397	-0.0489	0.6600	0.8600	0.0205	0.8540	0.9650	-0.1990	0.0720	0.3260

NGFG_01398	-0.0360	0.8240	0.9320	-0.0173	0.9150	0.9820	-0.1190	0.4580	0.7740
NGFG_01399	0.0797	0.4560	0.7500	-0.1400	0.1950	0.5260	0.0570	0.5940	0.8470
NGFG_01400	0.1050	0.4740	0.7620	0.0731	0.6170	0.8480	-0.1200	0.4120	0.7450
NGFG_01401	0.2150	0.0593	0.2920	0.1530	0.1800	0.5040	-0.1230	0.2810	0.6320
NGFG_01402	0.1620	0.1500	0.4530	0.1770	0.1160	0.4360	-0.0466	0.6790	0.8930
NGFG_01403	-0.0158	0.9350	0.9790	-0.2600	0.1820	0.5060	0.1010	0.6040	0.8550
NGFG_01404	-0.4870	0.0055	0.0976	-0.4830	0.0059	0.1220	0.6690	0.0001	0.0053
NGFG_01405	-0.1720	0.3780	0.6920	-0.0475	0.8070	0.9470	0.3160	0.1060	0.3910
NGFG_01406	-0.2890	0.2000	0.5100	-0.2320	0.3030	0.6610	0.2030	0.3650	0.7120
NGFG_01407	-0.6660	0.0002	0.0160	-0.6800	0.0001	0.0160	0.6690	0.0002	0.0056
NGFG_01408	-0.2840	0.1540	0.4570	-0.4480	0.0259	0.2360	0.5170	0.0099	0.0986
NGFG_01409	-0.2960	0.1710	0.4750	-0.4450	0.0409	0.2870	0.4720	0.0295	0.2020
NGFG_01411	-0.7680	0.0000	0.0012	-0.7620	0.0000	0.0016	0.9320	0.0000	0.0000
NGFG_01412	-0.1420	0.1600	0.4650	-0.1640	0.1070	0.4170	-0.1390	0.1640	0.5050
NGFG_01413	-0.1990	0.2160	0.5280	-0.0380	0.8130	0.9480	0.2480	0.1240	0.4270
NGFG_01414	-0.2760	0.1710	0.4750	-0.1910	0.3440	0.6970	0.0987	0.6220	0.8650
NGFG_01415	0.1220	0.3710	0.6850	0.1270	0.3510	0.7020	-0.3730	0.0056	0.0677
NGFG_01416	-0.2280	0.1320	0.4270	-0.3610	0.0175	0.2040	-0.1380	0.3560	0.7000
NGFG_01417	-0.1930	0.3210	0.6350	-0.3510	0.0721	0.3550	0.1500	0.4370	0.7610
NGFG_01418	-0.2600	0.0571	0.2910	-0.2060	0.1310	0.4520	0.0929	0.4920	0.7950
NGFG_01419	-0.1900	0.3390	0.6540	0.0518	0.7920	0.9350	-0.0478	0.8060	0.9390
NGFG_01420	-0.3910	0.0035	0.0783	-0.2470	0.0648	0.3440	-0.0258	0.8460	0.9550
NGFG_01421	-0.2950	0.0767	0.3340	-0.2950	0.0767	0.3640	0.1110	0.5050	0.8000
NGFG_01422	-0.4690	0.0012	0.0448	-0.3750	0.0095	0.1510	0.1130	0.4330	0.7600
NGFG_01423	-0.1740	0.1720	0.4750	-0.2860	0.0253	0.2330	0.0811	0.5240	0.8090
NGFG_01424	-0.1890	0.2830	0.6040	-0.3080	0.0807	0.3640	0.0926	0.5980	0.8490
NGFG_01425	-0.1170	0.5800	0.8160	-0.1870	0.3750	0.7210	0.1880	0.3710	0.7160
NGFG_01426	-0.2640	0.0852	0.3510	-0.1470	0.3340	0.6900	0.0297	0.8440	0.9550
NGFG_01427	-0.2070	0.0567	0.2900	-0.1820	0.0930	0.3930	-0.0710	0.5090	0.8020
NGFG_01428	0.2420	0.1650	0.4700	0.1750	0.3150	0.6730	-0.3670	0.0350	0.2220
NGFG_01429	-0.2100	0.3210	0.6350	-0.3490	0.0990	0.4030	-0.0027	0.9900	0.9980
NGFG_01430	-0.4120	0.0449	0.2690	-0.1860	0.3610	0.7120	0.0092	0.9640	0.9940
NGFG_01431	-0.0866	0.5470	0.8060	-0.1150	0.4230	0.7510	-0.0381	0.7910	0.9340
NGFG_01432	0.1070	0.4870	0.7700	-0.0093	0.9520	0.9930	0.0107	0.9440	0.9880
NGFG_01435	0.1490	0.1840	0.4900	0.0799	0.4760	0.7870	-0.1460	0.1910	0.5410
NGFG_01436	-0.0626	0.7550	0.9080	0.0200	0.9210	0.9820	0.5090	0.0114	0.1100
NGFG_01437	-0.2830	0.0187	0.1800	-0.2730	0.0230	0.2280	0.1730	0.1500	0.4740
NGFG_01438	-0.3380	0.0332	0.2350	-0.1850	0.2420	0.5900	0.2920	0.0655	0.3150
NGFG_01439	0.0219	0.8800	0.9560	-0.0413	0.7770	0.9300	-0.0745	0.6090	0.8590
NGFG_01440	0.3210	0.0303	0.2320	0.4230	0.0042	0.1030	-0.0302	0.8390	0.9530
NGFG_01441	0.1410	0.4060	0.7120	0.1540	0.3650	0.7140	0.0309	0.8560	0.9580
NGFG_01442	0.2650	0.1140	0.3970	0.2380	0.1560	0.4820	-0.0945	0.5730	0.8370
NGFG_01443	0.3400	0.0102	0.1300	0.3250	0.0142	0.1830	-0.0721	0.5860	0.8420
NGFG_01444	0.1840	0.0350	0.2420	0.2100	0.0160	0.1930	-0.1880	0.0307	0.2050
NGFG_01445	-0.0033	0.9780	0.9950	0.1570	0.1980	0.5310	0.3930	0.0014	0.0255
NGFG_01446	0.3970	0.0133	0.1510	0.4240	0.0082	0.1430	-0.0004	0.9980	1.0000
NGFG_01447	0.2900	0.0592	0.2920	0.2820	0.0663	0.3440	0.1900	0.2180	0.5800

NGFG_01452	0.1260	0.3540	0.6700	0.3340	0.0129	0.1760	0.1470	0.2820	0.6320
NGFG_01453	0.2010	0.1300	0.4220	0.1530	0.2490	0.5990	0.0474	0.7210	0.9070
NGFG_01455	0.2230	0.1040	0.3850	0.1310	0.3400	0.6920	-0.2360	0.0852	0.3550
NGFG_01457	0.2520	0.0877	0.3540	0.2700	0.0666	0.3440	-0.2680	0.0680	0.3190
NGFG_01458	0.2010	0.2610	0.5870	0.1410	0.4310	0.7550	-0.3690	0.0389	0.2330
NGFG_01459	-0.2800	0.0847	0.3510	-0.1450	0.3720	0.7190	0.1600	0.3240	0.6700
NGFG_01460	-0.4710	0.0045	0.0889	-0.3910	0.0185	0.2060	0.2170	0.1890	0.5390
NGFG_01461	-0.3070	0.0033	0.0780	-0.2280	0.0289	0.2510	0.1080	0.2960	0.6470
NGFG_01464	0.0511	0.8120	0.9260	-0.0465	0.8290	0.9500	0.0234	0.9130	0.9750
NGFG_01466	0.0048	0.9750	0.9940	0.0458	0.7610	0.9230	-0.1490	0.3210	0.6690
NGFG_01467	-0.1420	0.4010	0.7100	-0.1880	0.2680	0.6230	-0.0578	0.7330	0.9110
NGFG_01468	0.0755	0.7110	0.8920	0.0210	0.9180	0.9820	0.0309	0.8790	0.9650
NGFG_01469	-0.0772	0.7370	0.9000	0.0977	0.6700	0.8810	-0.0005	0.9980	1.0000
NGFG_01470	-0.1930	0.2410	0.5600	0.0280	0.8640	0.9700	0.2950	0.0719	0.3260
NGFG_01471	0.3410	0.0034	0.0783	0.3630	0.0019	0.0704	-0.3850	0.0009	0.0191
NGFG_01472	-0.4070	0.0088	0.1200	-0.2430	0.1150	0.4350	-0.0234	0.8780	0.9650
NGFG_01476	-0.3350	0.0087	0.1200	-0.3370	0.0083	0.1430	0.0614	0.6290	0.8680
NGFG_01478	0.4070	0.0313	0.2330	0.4140	0.0285	0.2490	-0.3760	0.0463	0.2570
NGFG_01479	-0.3030	0.1320	0.4270	-0.1100	0.5820	0.8390	0.0117	0.9530	0.9910
NGFG_01480	-0.2550	0.1200	0.4040	-0.2650	0.1070	0.4170	0.2980	0.0693	0.3220
NGFG_01481	-0.1870	0.1770	0.4830	-0.2290	0.0976	0.4020	0.2350	0.0895	0.3620
NGFG_01482	-0.1070	0.4600	0.7520	-0.1010	0.4870	0.7900	-0.0043	0.9760	0.9940
NGFG_01483	-0.4480	0.0034	0.0780	-0.4020	0.0084	0.1430	0.0782	0.6070	0.8570
NGFG_01485	0.3300	0.0691	0.3180	0.3930	0.0307	0.2560	0.1030	0.5700	0.8370
NGFG_01486	-0.0291	0.7490	0.9050	-0.0298	0.7420	0.9150	-0.3030	0.0008	0.0170
NGFG_01488	-0.1820	0.4150	0.7200	-0.1720	0.4410	0.7650	0.1500	0.4990	0.7980
NGFG_01490	0.4030	0.0024	0.0646	0.2890	0.0295	0.2510	-0.1930	0.1450	0.4670
NGFG_01491	-0.6750	0.0014	0.0476	-0.6280	0.0029	0.0855	0.8770	0.0000	0.0018
NGFG_01492	-0.1530	0.4720	0.7620	-0.3150	0.1420	0.4660	0.3230	0.1290	0.4340
NGFG_01493	0.0497	0.7980	0.9200	0.1670	0.3890	0.7320	0.1980	0.3070	0.6570
NGFG_01495	-0.0750	0.4920	0.7740	-0.0991	0.3640	0.7140	-0.0479	0.6600	0.8840
NGFG_01496	-0.0210	0.8250	0.9330	-0.0485	0.6110	0.8480	-0.1630	0.0837	0.3510
NGFG_01497	0.3550	0.0099	0.1280	0.3680	0.0075	0.1420	-0.4370	0.0015	0.0271
NGFG_01498	0.0196	0.8870	0.9590	-0.0968	0.4860	0.7900	0.1410	0.3080	0.6570
NGFG_01499	-0.1860	0.2940	0.6110	-0.1150	0.5170	0.8030	0.2690	0.1290	0.4340
NGFG_01500	#NV			#NV			-0.0068	0.9460	0.9880
NGFG_01501	0.1490	0.2280	0.5400	0.0833	0.5020	0.7940	-0.1690	0.1720	0.5170
NGFG_01502	0.2250	0.1460	0.4490	0.2150	0.1650	0.4920	-0.1230	0.4270	0.7560
NGFG_01503	0.2760	0.0411	0.2600	0.2380	0.0780	0.3640	-0.2140	0.1130	0.4040
NGFG_01504	0.1020	0.4540	0.7480	0.0299	0.8260	0.9500	-0.1630	0.2300	0.5890
NGFG_01505	0.1380	0.2840	0.6050	0.2050	0.1120	0.4270	-0.1100	0.3930	0.7310
NGFG_01506	0.0752	0.5140	0.7870	0.0473	0.6820	0.8850	-0.1310	0.2540	0.6100
NGFG_01507	0.1610	0.1810	0.4870	0.1790	0.1380	0.4640	-0.2790	0.0206	0.1610
NGFG_01509	-0.0667	0.7260	0.8990	0.0013	0.9950	0.9990	0.1660	0.3810	0.7230
NGFG_01510	0.0305	0.8550	0.9460	0.0463	0.7810	0.9320	-0.0775	0.6390	0.8730
NGFG_01511	0.2740	0.2280	0.5400	0.3140	0.1660	0.4930	-0.3100	0.1720	0.5170
NGFG_01512	0.1010	0.6070	0.8250	-0.1350	0.4950	0.7940	0.2540	0.1970	0.5500

NGFG_01513	0.2850	0.1510	0.4530	0.1720	0.3850	0.7270	0.3440	0.0832	0.3510
NGFG_01514	0.3470	0.0900	0.3600	0.0930	0.6490	0.8670	1.1500	0.0000	0.0000
NGFG_01515	-0.1930	0.1670	0.4720	-0.1210	0.3850	0.7270	0.0668	0.6330	0.8690
NGFG_01516	-0.1880	0.2870	0.6070	-0.1080	0.5380	0.8110	-0.6280	0.0003	0.0081
NGFG_01517	-0.2640	0.0752	0.3310	-0.2260	0.1280	0.4520	0.0397	0.7850	0.9320
NGFG_01519	0.0152	0.9460	0.9830	-0.2640	0.2420	0.5900	-0.1320	0.5510	0.8270
NGFG_01520	-0.4430	0.0273	0.2200	-0.2900	0.1460	0.4680	0.2310	0.2410	0.5970
NGFG_01521	-0.1160	0.5400	0.8020	-0.2570	0.1760	0.5010	-0.0595	0.7500	0.9160
NGFG_01522	-0.2540	0.1940	0.5000	-0.0967	0.6190	0.8490	0.1610	0.4080	0.7410
NGFG_01523	0.4730	0.0117	0.1420	0.4030	0.0316	0.2610	-0.3740	0.0460	0.2570
NGFG_01524	-0.2220	0.0393	0.2560	-0.2110	0.0504	0.3080	0.1810	0.0907	0.3620
NGFG_01526	0.1380	0.4810	0.7660	0.1540	0.4310	0.7550	0.3880	0.0477	0.2620
NGFG_01527	0.2870	0.0559	0.2900	0.1880	0.2110	0.5500	0.3600	0.0170	0.1410
NGFG_01528	0.2750	0.0948	0.3700	0.3360	0.0409	0.2870	0.5520	0.0009	0.0191
NGFG_01529	0.2260	0.2220	0.5340	0.1670	0.3670	0.7140	0.4690	0.0114	0.1100
NGFG_01531	0.0480	0.8060	0.9240	0.1360	0.4880	0.7900	0.5360	0.0061	0.0716
NGFG_01532	0.1130	0.5710	0.8160	0.0471	0.8140	0.9480	0.5410	0.0069	0.0779
NGFG_01533	#NV			#NV			0.1760	0.1510	0.4770
NGFG_01536	0.2730	0.1810	0.4870	0.2990	0.1440	0.4670	0.7550	0.0002	0.0076
NGFG_01537	0.0179	0.8930	0.9600	-0.0665	0.6190	0.8490	-0.2350	0.0765	0.3370
NGFG_01538	0.4260	0.0268	0.2190	0.3830	0.0466	0.2960	-0.4540	0.0182	0.1490
NGFG_01539	0.1450	0.1720	0.4750	0.1850	0.0810	0.3640	-0.1210	0.2500	0.6060
NGFG_01540	-0.2140	0.1490	0.4520	-0.2180	0.1420	0.4660	0.0472	0.7490	0.9160
NGFG_01541	-0.0036	0.9840	0.9950	-0.0013	0.9940	0.9990	0.0683	0.6920	0.8970
NGFG_01542	0.0145	0.9160	0.9690	-0.0860	0.5340	0.8100	0.1380	0.3180	0.6650
NGFG_01543	0.2970	0.0415	0.2600	0.1100	0.4520	0.7700	-0.1780	0.2220	0.5840
NGFG_01544	0.1610	0.2060	0.5160	0.0450	0.7250	0.9070	-0.5530	0.0000	0.0008
NGFG_01545	#NV			#NV			-0.0615	0.7340	0.9110
NGFG_01546	0.0526	0.7340	0.9000	-0.0046	0.9770	0.9980	-0.3190	0.0390	0.2330
NGFG_01547	0.0959	0.5670	0.8160	0.0723	0.6660	0.8780	-0.2300	0.1690	0.5110
NGFG_01548	0.0567	0.7190	0.8940	0.0121	0.9390	0.9870	-0.3930	0.0128	0.1170
NGFG_01549	0.1690	0.3330	0.6490	-0.1230	0.4840	0.7900	-0.0358	0.8370	0.9520
NGFG_01550	-0.1530	0.3980	0.7090	-0.2220	0.2200	0.5620	-0.0463	0.7970	0.9350
NGFG_01551	0.1880	0.2950	0.6120	0.1440	0.4220	0.7510	0.3730	0.0379	0.2300
NGFG_01552	0.2610	0.2060	0.5160	-0.0045	0.9830	0.9990	0.3540	0.0910	0.3620
NGFG_01553	0.0358	0.7950	0.9190	-0.0480	0.7280	0.9080	0.2530	0.0665	0.3160
NGFG_01554	0.0139	0.9330	0.9790	-0.0461	0.7820	0.9320	-0.0602	0.7180	0.9050
NGFG_01555	0.0862	0.5700	0.8160	0.0175	0.9080	0.9820	-0.0685	0.6520	0.8800
NGFG_01556	0.0577	0.7050	0.8870	-0.0190	0.9010	0.9810	-0.0769	0.6140	0.8600
NGFG_01558	-0.0433	0.8390	0.9390	0.1710	0.4210	0.7510	-0.2040	0.3350	0.6810
NGFG_01559	-0.2840	0.0483	0.2720	-0.3820	0.0082	0.1430	0.3990	0.0054	0.0669
NGFG_01560	#NV			#NV			0.1460	0.4800	0.7860
NGFG_01561	0.0354	0.8580	0.9470	-0.1450	0.4630	0.7800	0.0850	0.6670	0.8870
NGFG_01562	-0.2350	0.0334	0.2350	-0.2550	0.0210	0.2160	-0.0556	0.6090	0.8590
NGFG_01564	0.3240	0.0202	0.1850	0.3300	0.0177	0.2040	-0.5020	0.0003	0.0087
NGFG_01565	-0.1210	0.4990	0.7790	0.0101	0.9550	0.9930	-0.1020	0.5680	0.8370
NGFG_01566	-0.1950	0.1500	0.4530	-0.3330	0.0143	0.1830	0.3020	0.0255	0.1850

NGFG_01567	-0.3620	0.0009	0.0376	-0.3370	0.0020	0.0707	-0.0767	0.4750	0.7850
NGFG_01568	-0.4690	0.0003	0.0232	-0.4590	0.0004	0.0267	-0.0308	0.8100	0.9400
NGFG_01569	-0.6520	0.0004	0.0271	-0.5320	0.0038	0.0990	0.2840	0.1150	0.4100
NGFG_01571	-0.4530	0.0009	0.0376	-0.2250	0.0971	0.4010	-0.2220	0.0976	0.3730
NGFG_01572	-0.0365	0.8520	0.9450	0.2230	0.2550	0.6050	-0.1050	0.5910	0.8450
NGFG_01573	-0.1230	0.3550	0.6700	-0.0851	0.5210	0.8030	-0.1140	0.3860	0.7260
NGFG_01574	-0.1770	0.2270	0.5390	-0.1750	0.2300	0.5740	-0.1310	0.3680	0.7130
NGFG_01575	-0.1410	0.1830	0.4880	-0.1490	0.1570	0.4830	-0.0397	0.7050	0.9010
NGFG_01576	-0.2130	0.1540	0.4570	-0.1010	0.4980	0.7940	-0.1520	0.3010	0.6510
NGFG_01577	-0.0663	0.7640	0.9100	-0.1570	0.4780	0.7870	0.1120	0.6120	0.8590
NGFG_01578	-0.1060	0.2170	0.5300	-0.1160	0.1780	0.5010	-0.0223	0.7930	0.9340
NGFG_01579	-0.1620	0.2720	0.5960	-0.1340	0.3640	0.7140	0.1090	0.4570	0.7740
NGFG_01580	-0.3590	0.0530	0.2840	-0.3180	0.0871	0.3810	0.1310	0.4800	0.7860
NGFG_01581	-0.4120	0.0015	0.0501	-0.2610	0.0425	0.2870	0.1960	0.1220	0.4250
NGFG_01582	-0.1720	0.3150	0.6320	-0.1980	0.2490	0.5990	0.1620	0.3450	0.6900
NGFG_01583	0.1920	0.0283	0.2240	0.1540	0.0779	0.3640	-0.2440	0.0052	0.0656
NGFG_01584	0.0986	0.4680	0.7580	0.0753	0.5790	0.8360	-0.1310	0.3340	0.6810
NGFG_01585	-0.2190	0.1500	0.4530	-0.1060	0.4840	0.7900	0.2970	0.0511	0.2720
NGFG_01586	-0.4730	0.0036	0.0783	-0.4240	0.0089	0.1450	0.0695	0.6660	0.8870
NGFG_01587	0.4170	0.0124	0.1460	0.4530	0.0066	0.1290	-0.1080	0.5170	0.8040
NGFG_01588	-0.1870	0.1900	0.4970	-0.1290	0.3640	0.7140	0.0998	0.4810	0.7880
NGFG_01589	-0.3560	0.0055	0.0972	-0.4000	0.0018	0.0704	0.1470	0.2480	0.6040
NGFG_01590	-0.1140	0.4750	0.7620	-0.1130	0.4780	0.7870	-0.0269	0.8660	0.9620
NGFG_01591	0.1210	0.4820	0.7660	0.1120	0.5160	0.8030	-0.3530	0.0400	0.2380
NGFG_01592	-0.1600	0.4880	0.7700	-0.4230	0.0677	0.3470	0.6040	0.0090	0.0936
NGFG_01593	-0.0073	0.9670	0.9910	0.0069	0.9690	0.9960	0.1300	0.4640	0.7780
NGFG_01594	-0.0831	0.6820	0.8730	-0.2650	0.1940	0.5240	-0.0233	0.9080	0.9730
NGFG_01595	-0.1010	0.4310	0.7270	-0.1400	0.2750	0.6300	-0.0405	0.7500	0.9160
NGFG_01596	0.0758	0.5580	0.8120	0.0355	0.7840	0.9320	-0.2000	0.1200	0.4210
NGFG_01597	-0.0014	0.9870	0.9950	-0.0855	0.3500	0.7010	0.0024	0.9790	0.9950
NGFG_01598	-0.2010	0.2130	0.5240	-0.1480	0.3580	0.7100	0.2740	0.0896	0.3620
NGFG_01599	-0.1040	0.6010	0.8240	-0.2430	0.2220	0.5660	0.0761	0.7020	0.9010
NGFG_01600	-0.1020	0.5140	0.7870	-0.1330	0.3960	0.7360	0.0567	0.7160	0.9040
NGFG_01601	-0.1810	0.2870	0.6070	-0.1530	0.3660	0.7140	0.2380	0.1590	0.4950
NGFG_01602	-0.4090	0.0802	0.3420	#NV			0.4120	0.0764	0.3370
NGFG_01603	-0.1420	0.4250	0.7230	-0.1410	0.4270	0.7540	0.1820	0.3050	0.6540
NGFG_01605	-0.2910	0.0746	0.3300	-0.3000	0.0662	0.3440	0.1950	0.2310	0.5900
NGFG_01606	-0.1930	0.2880	0.6070	-0.1160	0.5220	0.8030	0.3260	0.0721	0.3260
NGFG_01607	-0.0518	0.7510	0.9060	0.0337	0.8370	0.9540	-0.0674	0.6800	0.8930
NGFG_01608	-0.1200	0.2480	0.5700	-0.1200	0.2500	0.5990	-0.0497	0.6300	0.8680
NGFG_01609	0.2160	0.1140	0.3970	0.0732	0.5930	0.8470	-0.2520	0.0642	0.3120
NGFG_01610	-0.0572	0.6310	0.8420	-0.0789	0.5080	0.7950	-0.0400	0.7370	0.9110
NGFG_01611	0.1750	0.0925	0.3670	0.1660	0.1100	0.4210	0.1260	0.2250	0.5870
NGFG_01612	0.0307	0.8740	0.9510	0.1440	0.4560	0.7730	-0.1680	0.3840	0.7240
NGFG_01613	-0.0247	0.7550	0.9080	-0.0669	0.3990	0.7360	-0.0614	0.4360	0.7610
NGFG_01614	0.0958	0.5540	0.8100	0.2010	0.2150	0.5550	-0.2350	0.1470	0.4700
NGFG_01615	0.0431	0.8420	0.9410	0.1360	0.5280	0.8060	-0.2050	0.3400	0.6850

NGFG_01616	0.0486	0.8350	0.9360	0.2880	0.2140	0.5530	-0.2460	0.2880	0.6370
NGFG_01617	-0.3000	0.0399	0.2570	-0.1220	0.3980	0.7360	-0.2050	0.1460	0.4680
NGFG_01618	0.4330	0.0097	0.1260	0.5510	0.0010	0.0452	-0.3640	0.0297	0.2020
NGFG_01619	-0.4000	0.0057	0.0983	-0.2390	0.0974	0.4020	0.0132	0.9260	0.9800
NGFG_01620	0.0384	0.7640	0.9100	0.0141	0.9120	0.9820	-0.2210	0.0811	0.3470
NGFG_01621	0.0525	0.6120	0.8290	0.0235	0.8210	0.9500	-0.0783	0.4470	0.7690
NGFG_01622	-0.0382	0.8360	0.9360	-0.0292	0.8740	0.9720	-0.1140	0.5340	0.8150
NGFG_01623	-0.1590	0.4220	0.7230	-0.1220	0.5380	0.8110	0.1780	0.3670	0.7130
NGFG_01624	-0.0976	0.4390	0.7330	-0.0946	0.4530	0.7720	-0.0057	0.9640	0.9940
NGFG_01625	-0.0587	0.7550	0.9080	-0.0644	0.7320	0.9100	-0.0827	0.6600	0.8840
NGFG_01626	0.0217	0.8140	0.9270	0.0024	0.9800	0.9980	-0.1770	0.0548	0.2810
NGFG_01627	-0.0676	0.4510	0.7470	-0.0402	0.6530	0.8710	-0.2190	0.0138	0.1240
NGFG_01628	-0.0073	0.9720	0.9930	0.0357	0.8620	0.9700	-0.1410	0.4930	0.7950
NGFG_01630	-0.0456	0.7390	0.9000	0.0052	0.9700	0.9960	0.1060	0.4370	0.7610
NGFG_01631	-0.3120	0.0470	0.2700	-0.2310	0.1410	0.4650	0.0736	0.6350	0.8710
NGFG_01632	-0.1230	0.5850	0.8160	-0.0626	0.7820	0.9320	-0.0894	0.6920	0.8970
NGFG_01633	-0.2580	0.0454	0.2690	-0.1940	0.1310	0.4520	-0.1530	0.2310	0.5890
NGFG_01634	-0.0525	0.6750	0.8700	-0.1470	0.2400	0.5900	0.0266	0.8310	0.9520
NGFG_01635	-0.1730	0.3590	0.6730	-0.1400	0.4590	0.7760	-0.2000	0.2860	0.6340
NGFG_01636	-0.1250	0.4940	0.7740	-0.1330	0.4680	0.7830	-0.3790	0.0341	0.2190
NGFG_01637	-0.3200	0.0874	0.3530	-0.2480	0.1830	0.5070	-0.0025	0.9890	0.9980
NGFG_01638	-0.3260	0.0592	0.2920	-0.2960	0.0864	0.3790	0.3790	0.0283	0.1970
NGFG_01639	-0.5230	0.0147	0.1610	-0.4630	0.0309	0.2560	0.4210	0.0493	0.2670
NGFG_01640	0.2720	0.1070	0.3870	0.2750	0.1030	0.4130	-0.4410	0.0089	0.0934
NGFG_01641	-0.4410	0.0198	0.1850	-0.2620	0.1640	0.4920	0.1490	0.4270	0.7560
NGFG_01642	#NV			#NV			0.0105	0.9580	0.9940
NGFG_01643	-0.1850	0.0500	0.2780	-0.1830	0.0528	0.3130	0.1150	0.2220	0.5840
NGFG_01644	-0.3030	0.2100	0.5210	-0.3590	0.1380	0.4640	0.2410	0.3170	0.6640
NGFG_01645	-0.0910	0.7210	0.8950	#NV			-0.0016	0.9950	1.0000
NGFG_01646	-0.2370	0.1540	0.4570	-0.4050	0.0154	0.1900	-0.1280	0.4400	0.7640
NGFG_01647	-0.0769	0.6180	0.8310	-0.0266	0.8630	0.9700	-0.0139	0.9280	0.9800
NGFG_01648	0.0471	0.7120	0.8920	0.1250	0.3270	0.6860	-0.1790	0.1600	0.4960
NGFG_01649	0.0934	0.5100	0.7850	0.1700	0.2310	0.5750	-0.2380	0.0927	0.3650
NGFG_01652	0.1680	0.2150	0.5270	0.2040	0.1320	0.4540	-0.2190	0.1060	0.3910
NGFG_01653	0.0989	0.5090	0.7840	0.0873	0.5600	0.8220	-0.3030	0.0419	0.2440
NGFG_01654	0.0332	0.7870	0.9150	0.1110	0.3670	0.7140	-0.2810	0.0216	0.1670
NGFG_01655	0.1980	0.2060	0.5170	0.1460	0.3490	0.7010	-0.4410	0.0047	0.0615
NGFG_01656	0.1260	0.3640	0.6780	0.1290	0.3530	0.7040	-0.2800	0.0431	0.2500
NGFG_01657	-0.1430	0.2740	0.5980	-0.1800	0.1690	0.4950	-0.3000	0.0213	0.1660
NGFG_01659	-0.1170	0.3270	0.6430	-0.0920	0.4400	0.7650	-0.3360	0.0044	0.0593
NGFG_01660	0.0986	0.5310	0.7960	-0.0509	0.7460	0.9170	-0.3970	0.0112	0.1090
NGFG_01661	-0.0534	0.7660	0.9100	-0.0322	0.8570	0.9680	-0.2240	0.2110	0.5690
NGFG_01662	0.1860	0.2330	0.5480	0.1610	0.3010	0.6600	-0.3660	0.0187	0.1510
NGFG_01663	0.0246	0.8710	0.9510	-0.0265	0.8610	0.9690	-0.3470	0.0209	0.1630
NGFG_01664	-0.0338	0.8680	0.9500	0.2200	0.2780	0.6340	0.0748	0.7120	0.9020
NGFG_01665	0.3430	0.0053	0.0953	0.3890	0.0016	0.0664	-0.1870	0.1270	0.4340
NGFG_01666	0.0944	0.5740	0.8160	0.2770	0.0989	0.4030	0.0784	0.6410	0.8730

NGFG_01667	-0.2290	0.1450	0.4490	-0.3330	0.0347	0.2750	0.0528	0.7350	0.9110
NGFG_01668	-0.2580	0.2760	0.5980	#NV			0.0601	0.7970	0.9350
NGFG_01669	-0.0133	0.9350	0.9790	-0.0334	0.8370	0.9540	-0.2800	0.0828	0.3510
NGFG_01670	#NV			#NV			0.4740	0.0183	0.1490
NGFG_01671	0.1480	0.5580	0.8120	#NV			-0.2800	0.2640	0.6190
NGFG_01672	-0.0863	0.5180	0.7900	-0.1310	0.3280	0.6880	-0.2420	0.0677	0.3180
NGFG_01673	0.1680	0.4320	0.7270	0.3620	0.0898	0.3850	0.0839	0.6940	0.8970
NGFG_01674	0.0885	0.6250	0.8360	0.0715	0.6930	0.8910	-0.0332	0.8550	0.9580
NGFG_01676	-0.0728	0.6570	0.8580	0.1230	0.4500	0.7700	-0.0976	0.5470	0.8240
NGFG_01677	-0.2000	0.2510	0.5740	-0.0683	0.6930	0.8910	-0.0075	0.9650	0.9940
NGFG_01678	0.1400	0.5150	0.7870	0.0490	0.8200	0.9500	0.0150	0.9440	0.9880
NGFG_01680	0.0567	0.8240	0.9320	0.1200	0.6370	0.8600	-0.3910	0.1260	0.4310
NGFG_01681	0.0640	0.7170	0.8940	-0.0068	0.9690	0.9960	-0.1140	0.5200	0.8060
NGFG_01682	-0.2070	0.1930	0.5000	-0.1760	0.2680	0.6220	-0.0465	0.7640	0.9240
NGFG_01684	-0.2430	0.0064	0.1030	-0.2750	0.0020	0.0707	-0.0878	0.3220	0.6690
NGFG_01685	-0.4600	0.0361	0.2440	-0.3240	0.1400	0.4650	0.3870	0.0775	0.3390
NGFG_01686	-0.2260	0.0317	0.2330	-0.2530	0.0160	0.1930	0.1980	0.0574	0.2920
NGFG_01687	-0.3850	0.0995	0.3770	-0.1620	0.4870	0.7900	0.5350	0.0221	0.1690
NGFG_01688	-0.1010	0.4790	0.7640	-0.1200	0.3990	0.7370	0.0528	0.7090	0.9010
NGFG_01689	-0.3550	0.0767	0.3340	-0.4620	0.0214	0.2180	0.3770	0.0597	0.2990
NGFG_01690	0.1010	0.5760	0.8160	0.0529	0.7710	0.9260	-0.0770	0.6710	0.8890
NGFG_01691	-0.1740	0.4360	0.7310	0.1330	0.5480	0.8170	0.2020	0.3650	0.7120
NGFG_01692	-0.0780	0.7180	0.8940	-0.1060	0.6240	0.8520	0.0896	0.6780	0.8930
NGFG_01695	-0.3020	0.0618	0.2980	-0.2090	0.1960	0.5270	0.1920	0.2290	0.5880
NGFG_01696	-0.1760	0.1070	0.3870	-0.0795	0.4650	0.7820	-0.0610	0.5730	0.8370
NGFG_01697	-0.2580	0.0435	0.2660	-0.2610	0.0405	0.2870	-0.2300	0.0711	0.3250
NGFG_01698	-0.2350	0.0456	0.2690	-0.3710	0.0017	0.0676	0.0227	0.8450	0.9550
NGFG_01699	0.0431	0.7680	0.9110	-0.0051	0.9720	0.9960	0.0179	0.9020	0.9720
NGFG_01700	-0.2620	0.0522	0.2840	-0.3110	0.0214	0.2180	0.2430	0.0715	0.3260
NGFG_01701	-0.1730	0.4140	0.7190	-0.1480	0.4850	0.7900	0.0961	0.6470	0.8780
NGFG_01703	-0.1590	0.4200	0.7230	-0.1630	0.4090	0.7460	0.0662	0.7360	0.9110
NGFG_01704	-0.2310	0.1050	0.3870	-0.1470	0.3010	0.6600	0.0185	0.8950	0.9720
NGFG_01705	-0.1330	0.5960	0.8230	#NV			0.2600	0.2980	0.6480
NGFG_01706	-0.3620	0.0385	0.2520	-0.2940	0.0921	0.3920	0.2130	0.2170	0.5800
NGFG_01707	-0.1210	0.5810	0.8160	-0.1140	0.6040	0.8480	0.2640	0.2300	0.5880
NGFG_01708	0.1740	0.3740	0.6890	0.1060	0.5890	0.8430	-0.0532	0.7850	0.9320
NGFG_01709	0.2260	0.1660	0.4710	0.2170	0.1820	0.5060	-0.1520	0.3500	0.6950
NGFG_01710	0.1970	0.1740	0.4780	0.1260	0.3860	0.7270	-0.6190	0.0000	0.0011
NGFG_01711	0.0574	0.5310	0.7960	-0.0328	0.7210	0.9050	-0.2890	0.0016	0.0278
NGFG_01712	0.0079	0.9440	0.9830	-0.0030	0.9790	0.9980	-0.1240	0.2680	0.6220
NGFG_01713	-0.0636	0.6500	0.8530	-0.0733	0.6010	0.8480	-0.1120	0.4220	0.7510
NGFG_01714	0.0311	0.7920	0.9170	0.0231	0.8450	0.9600	-0.0856	0.4680	0.7800
NGFG_01715	0.1270	0.2270	0.5400	0.0728	0.4880	0.7900	-0.3870	0.0002	0.0073
NGFG_01716	0.0251	0.8640	0.9490	-0.0670	0.6480	0.8670	-0.2100	0.1510	0.4770
NGFG_01717	-0.2210	0.0435	0.2660	-0.1560	0.1550	0.4800	-0.0085	0.9380	0.9860
NGFG_01718	0.0025	0.9870	0.9950	0.0688	0.6520	0.8700	-0.0363	0.8120	0.9400
NGFG_01719	0.1950	0.2370	0.5530	0.1360	0.4120	0.7490	0.4320	0.0094	0.0947

NGFG_01720	0.2910	0.0702	0.3190	0.1980	0.2190	0.5610	-0.3600	0.0249	0.1830
NGFG_01721	-1.6300	0.0000	0.0000	-1.8800	0.0000	0.0000	2.6900	0.0000	0.0000
NGFG_01722	-0.8940	0.0000	0.0000	-1.0900	0.0000	0.0000	1.6900	0.0000	0.0000
NGFG_01723	-0.2300	0.2560	0.5800	-0.2330	0.2500	0.5990	0.0094	0.9630	0.9940
NGFG_01724	0.0738	0.6030	0.8240	-0.0042	0.9760	0.9980	0.0918	0.5170	0.8040
NGFG_01725	0.3130	0.0189	0.1810	0.2770	0.0376	0.2800	-0.1160	0.3840	0.7240
NGFG_01726	0.2890	0.0543	0.2880	0.2470	0.0999	0.4050	-0.2480	0.0981	0.3730
NGFG_01727	0.6610	0.0002	0.0160	0.5470	0.0022	0.0727	-0.6220	0.0005	0.0123
NGFG_01728	0.6220	0.0003	0.0186	0.5690	0.0008	0.0392	-0.5700	0.0008	0.0175
NGFG_01729	0.4230	0.0123	0.1460	0.5120	0.0024	0.0762	-0.3750	0.0262	0.1880
NGFG_01730	0.4460	0.0023	0.0631	0.4720	0.0013	0.0564	0.1110	0.4490	0.7700
NGFG_01731	0.3980	0.0050	0.0937	0.4100	0.0039	0.0990	0.1020	0.4710	0.7840
NGFG_01732	0.4550	0.0011	0.0413	0.4750	0.0006	0.0303	-0.0692	0.6180	0.8630
NGFG_01734	0.3850	0.0178	0.1740	0.4890	0.0026	0.0808	-0.0445	0.7840	0.9320
NGFG_01735	0.2160	0.1390	0.4360	0.3210	0.0280	0.2480	0.0841	0.5640	0.8350
NGFG_01736	0.1870	0.2000	0.5100	0.2130	0.1460	0.4670	0.1190	0.4160	0.7470
NGFG_01737	0.3960	0.1000	0.3780	0.4320	0.0729	0.3550	-0.1170	0.6290	0.8680
NGFG_01738	0.4190	0.0074	0.1110	0.3660	0.0194	0.2070	-0.0931	0.5530	0.8280
NGFG_01739	0.3470	0.0203	0.1850	0.2870	0.0549	0.3180	-0.0344	0.8180	0.9460
NGFG_01741	0.3520	0.0228	0.2000	0.3000	0.0523	0.3120	-0.0015	0.9920	0.9990
NGFG_01742	0.3870	0.0176	0.1740	0.2420	0.1390	0.4640	0.0196	0.9050	0.9720
NGFG_01743	0.3780	0.0201	0.1850	0.3910	0.0163	0.1950	-0.0308	0.8500	0.9570
NGFG_01744	0.3370	0.0314	0.2330	0.3460	0.0270	0.2420	0.0171	0.9130	0.9750
NGFG_01745	0.3530	0.0129	0.1470	0.2730	0.0546	0.3180	-0.0223	0.8750	0.9650
NGFG_01746	0.3470	0.0072	0.1110	0.4150	0.0013	0.0577	0.0541	0.6750	0.8930
NGFG_01747	0.3840	0.0304	0.2320	0.3400	0.0555	0.3200	0.0977	0.5820	0.8390
NGFG_01748	0.3200	0.0414	0.2600	0.2940	0.0604	0.3300	0.1650	0.2920	0.6430
NGFG_01749	0.2930	0.0641	0.3020	0.2250	0.1550	0.4800	0.0982	0.5350	0.8150
NGFG_01750	0.3980	0.0022	0.0615	0.3190	0.0141	0.1830	0.0417	0.7490	0.9160
NGFG_01751	0.3930	0.0077	0.1120	0.2780	0.0593	0.3280	0.0745	0.6130	0.8600
NGFG_01752	0.2980	0.1310	0.4240	0.1900	0.3360	0.6900	0.0139	0.9440	0.9880
NGFG_01753	0.1330	0.5620	0.8160	0.0177	0.9380	0.9870	0.1140	0.6200	0.8640
NGFG_01754	0.1170	0.5830	0.8160	0.0012	0.9960	0.9990	0.1620	0.4450	0.7670
NGFG_01755	0.0100	0.9660	0.9910	-0.1030	0.6580	0.8750	0.2510	0.2790	0.6310
NGFG_01756	0.0002	0.9990	0.9990	-0.0472	0.7950	0.9370	0.3050	0.0926	0.3650
NGFG_01757	0.2830	0.1540	0.4570	0.2320	0.2420	0.5900	0.0665	0.7380	0.9110
NGFG_01758	0.4300	0.0160	0.1650	0.3380	0.0584	0.3240	-0.0736	0.6800	0.8930
NGFG_01759	0.4060	0.0149	0.1610	0.4400	0.0084	0.1430	-0.1070	0.5200	0.8060
NGFG_01761	-0.1350	0.5030	0.7800	0.0194	0.9230	0.9820	-0.0569	0.7750	0.9260
NGFG_01762	#NV			#NV			-0.0439	0.6920	0.8970
NGFG_01763	-0.0893	0.7210	0.8950	#NV			0.2780	0.2660	0.6190
NGFG_01764	#NV			#NV			0.2380	0.2350	0.5960
NGFG_01766	-0.3650	0.0041	0.0841	-0.3660	0.0040	0.1000	0.0127	0.9200	0.9780
NGFG_01767	0.2670	0.1590	0.4640	0.3640	0.0548	0.3180	0.1710	0.3660	0.7120
NGFG_01768	0.2540	0.1270	0.4170	0.3110	0.0614	0.3340	0.2420	0.1450	0.4670
NGFG_01770	0.5030	0.0005	0.0297	0.5030	0.0005	0.0294	-0.0682	0.6390	0.8730
NGFG_01771	0.5280	0.0005	0.0272	0.5330	0.0004	0.0259	-0.2850	0.0591	0.2970

NGFG_01772	0.4090	0.0006	0.0335	0.4560	0.0001	0.0160	-0.0999	0.4040	0.7390
NGFG_01773	0.3260	0.0710	0.3190	0.3860	0.0325	0.2640	-0.0842	0.6420	0.8730
NGFG_01774	-0.0248	0.8910	0.9600	0.0086	0.9620	0.9940	0.3320	0.0685	0.3200
NGFG_01775	-0.5510	0.0045	0.0889	-0.5090	0.0086	0.1430	0.1250	0.5110	0.8020
NGFG_01776	#NV			#NV			-0.0348	0.8760	0.9650
NGFG_01779	0.1140	0.4280	0.7250	0.0728	0.6120	0.8480	-0.2990	0.0367	0.2280
NGFG_01780	0.0382	0.7470	0.9040	0.0325	0.7840	0.9320	-0.3410	0.0035	0.0516
NGFG_01781	-0.1810	0.1990	0.5100	-0.1230	0.3850	0.7270	-0.0744	0.5960	0.8490
NGFG_01782	-0.1270	0.1910	0.4970	-0.2020	0.0368	0.2780	-0.1910	0.0461	0.2570
NGFG_01783	-0.2360	0.0807	0.3430	-0.1710	0.2060	0.5390	0.0158	0.9060	0.9720
NGFG_01784	-0.1730	0.2180	0.5300	0.0200	0.8860	0.9770	-0.0213	0.8780	0.9650
NGFG_01785	-0.2380	0.0337	0.2360	-0.1690	0.1300	0.4520	0.0168	0.8800	0.9650
NGFG_01786	-0.0939	0.6010	0.8240	-0.1080	0.5460	0.8150	0.0998	0.5780	0.8380
NGFG_01787	0.0880	0.5010	0.7790	-0.0091	0.9440	0.9890	-0.2110	0.1060	0.3910
NGFG_01788	0.1170	0.5080	0.7840	0.0843	0.6350	0.8600	0.0151	0.9320	0.9830
NGFG_01790	-0.1710	0.2790	0.6010	-0.2160	0.1720	0.4950	-0.0192	0.9020	0.9720
NGFG_01791	-0.2050	0.3190	0.6340	-0.1650	0.4220	0.7510	0.1410	0.4920	0.7950
NGFG_01792	-0.3570	0.0354	0.2430	-0.3450	0.0421	0.2870	0.1710	0.3130	0.6610
NGFG_01793	-0.1550	0.2520	0.5750	-0.1790	0.1860	0.5130	-0.1190	0.3700	0.7150
NGFG_01794	-0.2630	0.2930	0.6110	#NV			0.1560	0.5320	0.8150
NGFG_01796	-0.2170	0.1170	0.4020	-0.1780	0.1980	0.5310	-0.1190	0.3870	0.7260
NGFG_01797	-0.1910	0.4180	0.7210	-0.0717	0.7610	0.9230	-0.0857	0.7150	0.9030
NGFG_01798	-0.1990	0.2800	0.6010	-0.1450	0.4300	0.7550	-0.0633	0.7290	0.9110
NGFG_01799	-0.0363	0.8320	0.9350	-0.1140	0.5050	0.7950	0.1080	0.5270	0.8120
NGFG_01801	0.0475	0.7820	0.9140	-0.1100	0.5230	0.8030	-0.0738	0.6670	0.8870
NGFG_01802	-0.0658	0.5810	0.8160	-0.1220	0.3060	0.6620	-0.1270	0.2850	0.6340
NGFG_01803	0.4410	0.0072	0.1110	0.2500	0.1270	0.4510	0.3260	0.0474	0.2610
NGFG_01805	0.2380	0.2920	0.6100	0.2060	0.3630	0.7140	0.2670	0.2370	0.5960
NGFG_01806	0.3540	0.0441	0.2680	0.3150	0.0727	0.3550	0.0155	0.9300	0.9820
NGFG_01809	0.1450	0.3620	0.6770	0.1260	0.4280	0.7550	-0.2740	0.0830	0.3510
NGFG_01810	-0.0166	0.8980	0.9600	-0.0069	0.9570	0.9930	-0.5250	0.0000	0.0017
NGFG_01811	0.0818	0.6650	0.8630	0.0149	0.9370	0.9870	-0.3430	0.0653	0.3150
NGFG_01812	-0.0713	0.6630	0.8620	0.0006	0.9970	0.9990	-0.3530	0.0273	0.1940
NGFG_01813	0.1240	0.4220	0.7230	0.1940	0.2080	0.5430	-0.3320	0.0301	0.2030
NGFG_01814	0.4180	0.0016	0.0523	0.3390	0.0107	0.1600	-0.3100	0.0193	0.1540
NGFG_01815	-0.2140	0.0491	0.2750	-0.1600	0.1410	0.4650	-0.1040	0.3360	0.6820
NGFG_01816	-0.1130	0.5260	0.7940	-0.1870	0.2960	0.6530	-0.0681	0.7020	0.9010
NGFG_01817	0.0449	0.7390	0.9000	0.0552	0.6820	0.8850	-0.3070	0.0220	0.1690
NGFG_01818	0.1410	0.2950	0.6120	0.0457	0.7360	0.9110	-0.1600	0.2330	0.5920
NGFG_01821	0.1480	0.5470	0.8060	#NV			0.7320	0.0028	0.0438
NGFG_01822	-0.2920	0.0361	0.2440	-0.2920	0.0360	0.2770	0.0545	0.6950	0.8970
NGFG_01824	-0.2320	0.0945	0.3700	-0.2320	0.0951	0.3980	0.0734	0.5940	0.8470
NGFG_01825	-0.0659	0.6520	0.8550	-0.1700	0.2460	0.5950	0.0396	0.7860	0.9330
NGFG_01826	0.1160	0.4430	0.7380	0.0883	0.5590	0.8220	-0.0654	0.6640	0.8870
NGFG_01827	0.0525	0.7740	0.9120	0.0181	0.9210	0.9820	-0.1760	0.3350	0.6810
NGFG_01828	-0.1010	0.5790	0.8160	0.1500	0.4030	0.7400	-0.2020	0.2570	0.6130
NGFG_01829	0.0033	0.9870	0.9950	-0.1020	0.6230	0.8510	-0.2740	0.1840	0.5340

NGFG_01830	0.0285	0.8820	0.9570	0.0898	0.6400	0.8630	-0.4720	0.0125	0.1160
NGFG_01831	-0.2620	0.1360	0.4350	-0.1800	0.3050	0.6620	-0.0975	0.5720	0.8370
NGFG_01832	0.0399	0.8120	0.9260	0.1130	0.5010	0.7940	-0.1180	0.4770	0.7860
NGFG_01834	-0.2310	0.3330	0.6490	#NV			-0.3180	0.1730	0.5170
NGFG_01836	-0.1740	0.3470	0.6640	-0.1230	0.5060	0.7950	-0.1280	0.4860	0.7910
NGFG_01837	-0.2670	0.1730	0.4760	-0.1680	0.3910	0.7350	-0.1290	0.5070	0.8010
NGFG_01839	0.0517	0.7400	0.9000	-0.0315	0.8400	0.9570	-0.2110	0.1740	0.5180
NGFG_01840	0.2050	0.1610	0.4660	0.2550	0.0811	0.3640	-0.2530	0.0835	0.3510
NGFG_01841	-0.1200	0.6360	0.8450	#NV			0.3980	0.1180	0.4160
NGFG_01842	-0.8780	0.0000	0.0042	-0.8360	0.0001	0.0119	0.7730	0.0002	0.0064
NGFG_01843	-0.4400	0.0519	0.2840	-0.3300	0.1440	0.4670	0.3210	0.1560	0.4880
NGFG_01844	-0.4250	0.0952	0.3710	-0.3090	0.2260	0.5710	0.3770	0.1390	0.4540
NGFG_01845	-0.2750	0.0536	0.2860	-0.3270	0.0217	0.2190	0.0979	0.4910	0.7950
NGFG_01846	-0.4560	0.0568	0.2900	-0.2860	0.2320	0.5760	0.1710	0.4730	0.7850
NGFG_01847	-0.3700	0.0022	0.0615	-0.2430	0.0425	0.2870	-0.0353	0.7640	0.9240
NGFG_01848	-0.1820	0.1080	0.3900	-0.0757	0.5030	0.7940	-0.2080	0.0628	0.3090
NGFG_01849	-0.5510	0.0117	0.1420	-0.4440	0.0416	0.2870	0.3920	0.0716	0.3260
NGFG_01850	-0.1180	0.3170	0.6330	-0.2120	0.0729	0.3550	-0.0054	0.9630	0.9940
NGFG_01851	-0.1220	0.2810	0.6010	-0.1970	0.0807	0.3640	0.0742	0.5100	0.8020
NGFG_01852	0.3110	0.0407	0.2600	0.3080	0.0426	0.2870	-0.1970	0.1950	0.5500
NGFG_01853	0.1930	0.1490	0.4520	0.1950	0.1440	0.4670	-0.0698	0.6010	0.8530
NGFG_01854	-0.0054	0.9670	0.9910	-0.0020	0.9880	0.9990	-0.1250	0.3420	0.6880
NGFG_01856	-0.1510	0.3020	0.6160	-0.0731	0.6150	0.8480	0.3330	0.0224	0.1700
NGFG_01859	0.2380	0.1930	0.5000	0.2670	0.1450	0.4670	-0.1440	0.4320	0.7600
NGFG_01860	0.1510	0.3770	0.6910	0.2090	0.2220	0.5660	-0.1670	0.3290	0.6760
NGFG_01861	0.0471	0.7680	0.9110	-0.0840	0.6000	0.8480	-0.2220	0.1580	0.4930
NGFG_01862	0.0231	0.9140	0.9690	-0.0579	0.7860	0.9330	-0.2240	0.2920	0.6430
NGFG_01863	-0.0308	0.8490	0.9450	-0.0358	0.8250	0.9500	-0.3670	0.0232	0.1760
NGFG_01864	0.0448	0.7830	0.9140	0.0509	0.7540	0.9220	-0.4010	0.0135	0.1230
NGFG_01865	0.0703	0.5130	0.7870	0.0936	0.3840	0.7270	-0.3180	0.0030	0.0453
NGFG_01868	0.2830	0.0532	0.2850	0.2500	0.0877	0.3810	-0.1980	0.1750	0.5190
NGFG_01869	0.2560	0.0333	0.2350	0.3570	0.0030	0.0873	-0.2820	0.0193	0.1540
NGFG_01870	-0.3210	0.0850	0.3510	-0.1430	0.4420	0.7660	-0.0707	0.7030	0.9010
NGFG_01872	0.0542	0.7370	0.9000	0.0956	0.5540	0.8190	-0.2020	0.2090	0.5660
NGFG_01873	0.0542	0.7860	0.9150	0.1690	0.3970	0.7360	-0.1740	0.3830	0.7240
NGFG_01874	-0.0164	0.9390	0.9810	0.0238	0.9110	0.9820	-0.0940	0.6590	0.8840
NGFG_01875	-0.4180	0.0036	0.0783	-0.3520	0.0143	0.1830	0.0941	0.5110	0.8020
NGFG_01876	-0.4560	0.0190	0.1810	-0.4090	0.0351	0.2750	0.1290	0.5040	0.8000
NGFG_01877	-0.4170	0.0860	0.3520	-0.3070	0.2050	0.5380	0.3100	0.2010	0.5550
NGFG_01878	-0.3990	0.0990	0.3770	-0.2040	0.3980	0.7360	0.1620	0.5020	0.8000
NGFG_01879	-0.5580	0.0201	0.1850	#NV			0.5000	0.0380	0.2300
NGFG_01880	-0.3400	0.1680	0.4720	-0.2360	0.3390	0.6910	0.2560	0.2970	0.6470
NGFG_01883	-0.0492	0.7890	0.9150	-0.0759	0.6800	0.8850	0.0003	0.9980	1.0000
NGFG_01884	-0.3180	0.1230	0.4080	-0.2080	0.3130	0.6710	0.2700	0.1890	0.5390
NGFG_01885	-0.2500	0.2180	0.5300	-0.1000	0.6220	0.8510	0.2910	0.1510	0.4770
NGFG_01886	0.0135	0.9150	0.9690	0.0642	0.6130	0.8480	-0.1020	0.4180	0.7500
NGFG_01887	-0.0276	0.7950	0.9190	-0.0350	0.7410	0.9140	-0.1270	0.2290	0.5880

NGFG_01888	0.0539	0.7690	0.9110	-0.0443	0.8090	0.9470	-0.2150	0.2400	0.5970
NGFG_01889	-0.1690	0.2700	0.5940	-0.1890	0.2170	0.5580	0.1240	0.4140	0.7450
NGFG_01890	-0.2220	0.3550	0.6700	-0.1600	0.5050	0.7950	0.0697	0.7700	0.9240
NGFG_01891	0.0260	0.8580	0.9470	-0.1550	0.2910	0.6450	-0.2220	0.1230	0.4250
NGFG_01892	0.0642	0.4440	0.7380	0.0549	0.5130	0.8000	-0.0671	0.4220	0.7510
NGFG_01893	0.1970	0.2630	0.5870	0.1420	0.4200	0.7510	0.1870	0.2890	0.6380
NGFG_01894	0.2620	0.0818	0.3450	0.2490	0.0988	0.4030	-0.0324	0.8290	0.9520
NGFG_01895	-0.0168	0.8860	0.9580	-0.0602	0.6080	0.8480	-0.1090	0.3510	0.6950
NGFG_01897	-0.2090	0.1720	0.4750	-0.2250	0.1400	0.4650	0.4750	0.0019	0.0322
NGFG_01898	-0.4170	0.0255	0.2130	-0.4340	0.0202	0.2090	0.6270	0.0008	0.0175
NGFG_01899	-0.2740	0.1090	0.3910	-0.0840	0.6220	0.8510	0.2910	0.0886	0.3610
NGFG_01900	-0.2760	0.0277	0.2220	-0.2320	0.0640	0.3420	0.0176	0.8870	0.9680
NGFG_01901	0.0044	0.9840	0.9950	-0.0199	0.9260	0.9830	-0.0716	0.7380	0.9110
NGFG_01902	-0.2210	0.3430	0.6600	-0.3300	0.1580	0.4840	0.0669	0.7720	0.9240
NGFG_01903	-0.0748	0.7360	0.9000	-0.1520	0.4950	0.7940	-0.0085	0.9690	0.9940
NGFG_01904	0.3010	0.1040	0.3850	0.2550	0.1670	0.4940	-0.4770	0.0098	0.0982
NGFG_01905	0.2900	0.0952	0.3710	0.2320	0.1820	0.5060	-0.1550	0.3730	0.7170
NGFG_01906	0.1690	0.2710	0.5950	-0.0232	0.8800	0.9740	-0.2520	0.1010	0.3820
NGFG_01907	-0.0194	0.9290	0.9760	-0.0660	0.7610	0.9230	0.0860	0.6910	0.8970
NGFG_01908	-0.2850	0.1100	0.3910	-0.1630	0.3590	0.7120	-0.2330	0.1870	0.5390
NGFG_01909	0.0709	0.7600	0.9100	0.3700	0.1080	0.4200	-0.3550	0.1230	0.4260
NGFG_01910	-0.0167	0.9180	0.9690	-0.0605	0.7100	0.8970	0.1300	0.4240	0.7530
NGFG_01911	0.4190	0.0126	0.1470	0.3700	0.0275	0.2450	-0.2340	0.1630	0.5030
NGFG_01912	0.2500	0.1610	0.4660	0.1200	0.5010	0.7940	0.1570	0.3810	0.7230
NGFG_01914	0.2540	0.2020	0.5100	0.2640	0.1860	0.5120	0.3010	0.1310	0.4380
NGFG_01915	0.1120	0.4620	0.7560	0.0711	0.6400	0.8630	0.0034	0.9820	0.9960
NGFG_01916	#NV			#NV			0.0079	0.8730	0.9630
NGFG_01917	0.2190	0.3050	0.6210	0.1960	0.3600	0.7120	0.1660	0.4370	0.7610
NGFG_01919	0.3120	0.1140	0.3970	0.3500	0.0754	0.3620	0.4870	0.0140	0.1240
NGFG_01922	0.3050	0.1550	0.4570	0.3760	0.0792	0.3640	0.2160	0.3150	0.6640
NGFG_01923	0.2080	0.3710	0.6850	0.3540	0.1270	0.4510	0.3170	0.1750	0.5190
NGFG_01924	0.1150	0.4880	0.7700	0.0268	0.8720	0.9720	-0.2770	0.0954	0.3680
NGFG_01925	-0.0157	0.9160	0.9690	0.0427	0.7740	0.9280	-0.3710	0.0120	0.1140
NGFG_01926	-0.0147	0.9420	0.9820	-0.0204	0.9190	0.9820	-0.1790	0.3730	0.7170
NGFG_01927	0.1090	0.5910	0.8190	0.0402	0.8440	0.9590	-0.0066	0.9740	0.9940
NGFG_01928	0.2640	0.2390	0.5560	0.4490	0.0434	0.2880	-0.4820	0.0291	0.2010
NGFG_01929	0.3010	0.2100	0.5210	0.2110	0.3800	0.7240	-0.0413	0.8640	0.9620
NGFG_01931	0.2220	0.1120	0.3930	0.1850	0.1860	0.5120	-0.0999	0.4740	0.7850
NGFG_01933	0.0435	0.7880	0.9150	0.0999	0.5380	0.8110	-0.0546	0.7360	0.9110
NGFG_01934	-0.3410	0.0030	0.0752	-0.2320	0.0431	0.2880	-0.0028	0.9810	0.9960
NGFG_01935	-0.3030	0.0007	0.0342	-0.2510	0.0050	0.1150	-0.0651	0.4650	0.7790
NGFG_01937	-0.0044	0.9800	0.9950	-0.3640	0.0324	0.2640	0.9030	0.0000	0.0000
NGFG_01939	-0.2590	0.0593	0.2920	-0.3580	0.0091	0.1460	0.1770	0.1960	0.5500
NGFG_01940	-0.0178	0.8970	0.9600	-0.0427	0.7570	0.9230	-0.0277	0.8400	0.9530
NGFG_01941	-0.0400	0.7610	0.9100	0.0942	0.4730	0.7860	-0.4940	0.0001	0.0053
NGFG_01942	0.0222	0.9040	0.9630	0.1230	0.5060	0.7950	-0.1780	0.3350	0.6810
NGFG_01943	-0.2270	0.1800	0.4870	-0.2990	0.0776	0.3640	-0.2090	0.2120	0.5710

NGFG_01944	-0.0226	0.9220	0.9710	-0.0499	0.8300	0.9500	-0.0285	0.9020	0.9720
NGFG_01945	0.0636	0.6980	0.8820	0.1470	0.3680	0.7140	-0.0908	0.5770	0.8380
NGFG_01946	0.1240	0.5470	0.8060	0.1310	0.5250	0.8040	0.0622	0.7630	0.9240
NGFG_01947	0.4130	0.0121	0.1450	0.3250	0.0489	0.3040	-0.1540	0.3520	0.6960
NGFG_01948	0.1470	0.3750	0.6900	-0.0181	0.9130	0.9820	0.3260	0.0514	0.2720
NGFG_01949	-0.0042	0.9730	0.9940	-0.0025	0.9840	0.9990	0.1500	0.2170	0.5800
NGFG_01950	0.3550	0.0300	0.2320	0.3100	0.0581	0.3240	-0.1570	0.3360	0.6820
NGFG_01951	0.2790	0.0993	0.3770	0.2940	0.0818	0.3660	0.0533	0.7550	0.9190
NGFG_01952	0.3210	0.0996	0.3770	0.2890	0.1370	0.4640	-0.0072	0.9710	0.9940
NGFG_01953	0.3280	0.1160	0.4010	0.2190	0.2940	0.6500	0.0156	0.9410	0.9870
NGFG_01954	0.3320	0.0413	0.2600	0.2380	0.1440	0.4670	0.0906	0.5780	0.8380
NGFG_01955	-0.0506	0.6580	0.8590	-0.0363	0.7510	0.9210	0.4710	0.0000	0.0020
NGFG_01956	0.1050	0.3180	0.6340	0.0719	0.4930	0.7940	0.4940	0.0000	0.0002
NGFG_01957	-0.0132	0.9330	0.9790	0.0242	0.8780	0.9740	-0.0638	0.6820	0.8940
NGFG_01958	0.1660	0.3740	0.6890	0.1480	0.4270	0.7540	-0.2110	0.2580	0.6130
NGFG_01959	-0.2430	0.0620	0.2980	-0.2840	0.0293	0.2510	-0.0519	0.6870	0.8970
NGFG_01960	-0.0494	0.6930	0.8800	-0.0710	0.5720	0.8290	0.1070	0.3900	0.7290
NGFG_01961	-0.0713	0.6220	0.8340	-0.1170	0.4200	0.7510	-0.0819	0.5660	0.8360
NGFG_01962	-0.0443	0.7500	0.9060	-0.0979	0.4820	0.7900	-0.0767	0.5810	0.8390
NGFG_01963	-0.2070	0.1710	0.4750	-0.1230	0.4150	0.7500	-0.1170	0.4370	0.7610
NGFG_01964	-0.2040	0.2680	0.5930	-0.0033	0.9860	0.9990	-0.4030	0.0254	0.1850
NGFG_01965	-0.0199	0.9020	0.9620	-0.1670	0.3040	0.6610	0.0908	0.5740	0.8370
NGFG_01968	0.1240	0.3340	0.6490	0.1640	0.2010	0.5350	-0.1370	0.2840	0.6320
NGFG_01969	0.2260	0.2340	0.5500	0.3860	0.0414	0.2870	-0.1870	0.3230	0.6700
NGFG_01970	0.2110	0.1390	0.4360	0.1920	0.1770	0.5010	-0.2480	0.0809	0.3470
NGFG_01971	-0.2440	0.0417	0.2600	-0.2200	0.0665	0.3440	0.0977	0.4140	0.7450
NGFG_01972	0.3160	0.0237	0.2070	0.2800	0.0451	0.2910	-0.0865	0.5360	0.8150
NGFG_01973	-0.1460	0.3290	0.6440	-0.0154	0.9180	0.9820	0.2290	0.1240	0.4280
NGFG_01974	-0.4910	0.0043	0.0866	-0.4050	0.0182	0.2060	0.1110	0.5140	0.8020
NGFG_01975	-0.0893	0.4060	0.7120	-0.1170	0.2760	0.6300	-0.2640	0.0136	0.1230
NGFG_01977	-0.0909	0.3680	0.6830	-0.0971	0.3360	0.6900	-0.1040	0.3000	0.6480
NGFG_01978	-0.2740	0.1630	0.4680	-0.2100	0.2840	0.6390	-0.0122	0.9500	0.9910
NGFG_01979	-0.1030	0.3950	0.7080	-0.0998	0.4110	0.7480	-0.1020	0.4020	0.7370
NGFG_01980	-0.3130	0.0222	0.1990	-0.1870	0.1730	0.4950	0.1750	0.2010	0.5550
NGFG_01981	-0.1970	0.2010	0.5100	-0.1280	0.4040	0.7410	-0.1360	0.3720	0.7160
NGFG_01982	-0.3780	0.0699	0.3180	-0.4540	0.0299	0.2530	0.0286	0.8880	0.9680
NGFG_01983	-0.0895	0.4020	0.7110	-0.0737	0.4900	0.7910	-0.1260	0.2300	0.5890
NGFG_01984	-0.0643	0.7170	0.8940	-0.1370	0.4410	0.7650	0.3630	0.0409	0.2410
NGFG_01986	0.1310	0.4930	0.7740	0.1090	0.5680	0.8260	0.2920	0.1310	0.4370
NGFG_01987	0.1720	0.3920	0.7070	0.3820	0.0580	0.3240	-0.2340	0.2440	0.6010
NGFG_01988	-0.2480	0.0158	0.1650	-0.2090	0.0420	0.2870	0.0097	0.9240	0.9790
NGFG_01989	0.1330	0.4950	0.7750	0.1390	0.4760	0.7870	0.0511	0.7940	0.9340
NGFG_01990	-0.1520	0.5170	0.7890	-0.1650	0.4830	0.7900	0.4350	0.0647	0.3140
NGFG_01992	-0.0858	0.6960	0.8810	-0.1460	0.5050	0.7950	-0.1360	0.5330	0.8150
NGFG_01993	-0.2700	0.1190	0.4040	-0.1550	0.3690	0.7150	0.2300	0.1840	0.5340
NGFG_01994	-0.3840	0.0458	0.2690	-0.5240	0.0065	0.1290	0.5290	0.0059	0.0703
NGFG_01996	-0.2660	0.1480	0.4510	-0.3830	0.0379	0.2810	0.0498	0.7850	0.9320

NGFG_01997	-0.1160	0.5380	0.8020	-0.0502	0.7890	0.9340	0.1910	0.3090	0.6590
NGFG_01999	-0.0527	0.8220	0.9320	0.0600	0.7970	0.9390	-0.3190	0.1680	0.5110
NGFG_02000	0.2510	0.0918	0.3660	0.2710	0.0687	0.3470	-0.3840	0.0093	0.0941
NGFG_02001	0.1280	0.5410	0.8020	0.1470	0.4820	0.7900	-0.2270	0.2760	0.6280
NGFG_02002	-0.1710	0.3510	0.6680	-0.2960	0.1070	0.4170	-0.1360	0.4530	0.7720
NGFG_02003	-0.0644	0.5970	0.8230	0.0361	0.7660	0.9240	-0.0227	0.8510	0.9570
NGFG_02004	0.3700	0.1010	0.3780	0.4030	0.0738	0.3580	0.2750	0.2230	0.5850
NGFG_02005	0.3680	0.0112	0.1380	0.3260	0.0247	0.2330	-0.0576	0.6910	0.8970
NGFG_02006	0.1010	0.2880	0.6070	-0.0162	0.8660	0.9710	-0.1340	0.1560	0.4880
NGFG_02007	0.0070	0.9550	0.9870	0.1870	0.1340	0.4580	-0.1590	0.1990	0.5540
NGFG_02008	-0.2050	0.0937	0.3690	-0.1670	0.1710	0.4950	-0.1280	0.2820	0.6320
NGFG_02010	-0.3240	0.1310	0.4240	-0.2450	0.2530	0.6020	0.2960	0.1670	0.5110
NGFG_02011	0.2930	0.0781	0.3370	0.3350	0.0445	0.2910	-0.0959	0.5640	0.8350
NGFG_02012	-0.3140	0.0584	0.2920	-0.3760	0.0237	0.2290	0.1150	0.4870	0.7910
NGFG_02013	0.5530	0.0038	0.0805	0.3090	0.1100	0.4210	0.0427	0.8270	0.9500
NGFG_02014	0.0128	0.9220	0.9710	-0.0439	0.7350	0.9110	0.1670	0.1970	0.5500
NGFG_02015	0.0378	0.7850	0.9140	-0.0141	0.9190	0.9820	-0.0779	0.5710	0.8370
NGFG_02016	0.0826	0.3790	0.6930	0.0656	0.4850	0.7900	-0.1740	0.0635	0.3100
NGFG_02017	0.0553	0.5870	0.8170	0.1300	0.2030	0.5380	-0.1110	0.2760	0.6280
NGFG_02018	-0.1090	0.5080	0.7840	-0.0782	0.6340	0.8600	0.0906	0.5810	0.8390
NGFG_02019	0.4750	0.0272	0.2200	0.4300	0.0452	0.2910	-0.5590	0.0092	0.0938
NGFG_02020	0.0562	0.7650	0.9100	0.1030	0.5850	0.8400	-0.0865	0.6450	0.8760
NGFG_02022	0.1210	0.4520	0.7480	0.0643	0.6880	0.8880	-0.2180	0.1720	0.5170
NGFG_02023	-0.0990	0.4530	0.7480	-0.1160	0.3790	0.7230	-0.1900	0.1480	0.4720
NGFG_02024	-0.2370	0.0706	0.3190	-0.2010	0.1250	0.4490	-0.1210	0.3520	0.6960
NGFG_02025	-0.3490	0.1110	0.3930	-0.0240	0.9120	0.9820	0.3370	0.1230	0.4250
NGFG_02027	0.0786	0.5700	0.8160	0.1330	0.3340	0.6900	0.0331	0.8110	0.9400
NGFG_02029	-0.2640	0.1820	0.4880	-0.2700	0.1720	0.4950	0.3070	0.1200	0.4200
NGFG_02030	-0.2330	0.2520	0.5750	-0.1690	0.4050	0.7410	0.0727	0.7190	0.9050
NGFG_02031	-0.0611	0.6800	0.8720	-0.1310	0.3770	0.7220	0.1540	0.2990	0.6480
NGFG_02032	0.0048	0.9720	0.9930	-0.0463	0.7300	0.9080	-0.0222	0.8690	0.9630
NGFG_02033	0.0574	0.7850	0.9140	0.0657	0.7550	0.9220	0.1210	0.5630	0.8340
NGFG_02034	-0.1050	0.5780	0.8160	-0.1830	0.3320	0.6900	0.4110	0.0298	0.2020
NGFG_02035	-0.0829	0.4540	0.7480	-0.0018	0.9870	0.9990	-0.0325	0.7680	0.9240
NGFG_02036	-0.0493	0.6170	0.8310	-0.0082	0.9340	0.9850	-0.1150	0.2380	0.5960
NGFG_02037	-0.1350	0.4530	0.7480	-0.1430	0.4290	0.7550	0.1240	0.4930	0.7950
NGFG_02038	-0.0340	0.8260	0.9340	-0.0509	0.7430	0.9150	-0.2040	0.1870	0.5390
NGFG_02039	0.5060	0.0001	0.0099	0.3940	0.0021	0.0717	-0.6740	0.0000	0.0000
NGFG_02040	0.5620	0.0005	0.0272	0.4990	0.0019	0.0707	-0.6670	0.0000	0.0017
NGFG_02041	0.3260	0.0129	0.1470	0.2600	0.0475	0.2980	-0.8930	0.0000	0.0000
NGFG_02042	0.1390	0.3470	0.6640	0.2080	0.1610	0.4870	-1.0600	0.0000	0.0000
NGFG_02043	0.1990	0.3700	0.6850	0.2320	0.2950	0.6510	-0.2690	0.2240	0.5860
NGFG_02044	0.3820	0.0035	0.0783	0.2930	0.0247	0.2330	-0.6210	0.0000	0.0002
NGFG_02045	0.4280	0.0073	0.1110	0.4660	0.0034	0.0962	-0.4190	0.0086	0.0913
NGFG_02046	0.0330	0.8720	0.9510	-0.0792	0.6980	0.8940	0.0846	0.6780	0.8930
NGFG_02047	-0.0028	0.9900	0.9950	0.0203	0.9290	0.9830	0.0816	0.7210	0.9070
NGFG_02048	0.0733	0.7720	0.9120	0.0000	1.0000	1.0000	-0.0109	0.9660	0.9940

NGFG_02049	0.0026	0.9900	0.9950	-0.3130	0.1500	0.4720	0.8540	0.0001	0.0037
NGFG_02050	0.0151	0.9450	0.9830	-0.3220	0.1450	0.4670	0.6940	0.0018	0.0312
NGFG_02052	-0.0764	0.6360	0.8450	-0.2670	0.0999	0.4050	0.3380	0.0369	0.2280
NGFG_02053	0.0520	0.7430	0.9020	-0.0057	0.9710	0.9960	0.3300	0.0375	0.2300
NGFG_02054	-0.0250	0.8780	0.9550	0.0219	0.8930	0.9790	0.0696	0.6680	0.8870
NGFG_02055	-0.0263	0.8680	0.9500	-0.0533	0.7360	0.9110	0.1140	0.4700	0.7830
NGFG_02056	0.1600	0.4240	0.7230	0.2530	0.2060	0.5390	-0.7030	0.0004	0.0113
NGFG_02057	0.1120	0.3640	0.6780	0.1680	0.1730	0.4950	-0.3940	0.0013	0.0253
NGFG_02058	0.0914	0.4960	0.7750	0.1370	0.3060	0.6620	0.3770	0.0050	0.0644
NGFG_02061	-0.1020	0.4150	0.7200	-0.0532	0.6700	0.8810	0.1370	0.2730	0.6260
NGFG_02062	-0.0094	0.9570	0.9870	-0.1060	0.5380	0.8110	-0.0397	0.8180	0.9460
NGFG_02065	0.2740	0.0852	0.3510	0.2880	0.0707	0.3520	-0.6380	0.0001	0.0026
NGFG_02066	-0.0478	0.6870	0.8770	0.0277	0.8150	0.9480	-0.4400	0.0002	0.0064
NGFG_02067	0.0024	0.9890	0.9950	0.0134	0.9380	0.9870	-0.1900	0.2690	0.6220
NGFG_02068	-0.1240	0.5980	0.8230	-0.0564	0.8110	0.9470	-0.1140	0.6280	0.8680
NGFG_02069	0.0270	0.8800	0.9560	-0.0744	0.6780	0.8850	0.3360	0.0611	0.3040
NGFG_02070	0.2400	0.1880	0.4940	0.2780	0.1270	0.4510	-0.4370	0.0156	0.1310
NGFG_02071	-0.0234	0.9040	0.9630	0.0073	0.9700	0.9960	-0.2470	0.1960	0.5500
NGFG_02073	0.3460	0.0171	0.1700	0.2550	0.0791	0.3640	-0.0774	0.5940	0.8470
NGFG_02074	0.2550	0.3170	0.6340	#NV			0.0877	0.7310	0.9110
NGFG_02075	-0.0994	0.6190	0.8310	-0.1600	0.4230	0.7510	-0.0584	0.7680	0.9240
NGFG_02076	0.4180	0.1010	0.3790	#NV			-0.1900	0.4560	0.7740
NGFG_02077	0.0961	0.7010	0.8840	#NV			0.1200	0.6330	0.8690
NGFG_02078	-0.2670	0.2670	0.5930	-0.2550	0.2890	0.6420	0.3660	0.1280	0.4340
NGFG_02079	0.0851	0.7310	0.9000	#NV			0.3220	0.1920	0.5420
NGFG_02080	0.2490	0.0818	0.3450	0.1990	0.1650	0.4920	-0.1690	0.2370	0.5960
NGFG_02081	0.0023	0.9860	0.9950	0.0334	0.7930	0.9360	-0.2050	0.1060	0.3910
NGFG_02082	-0.1080	0.3510	0.6680	-0.2280	0.0495	0.3060	-0.1390	0.2260	0.5880
NGFG_02084	-0.1190	0.6090	0.8270	0.1570	0.4980	0.7940	0.2030	0.3820	0.7240
NGFG_02085	-0.0306	0.8340	0.9360	-0.0844	0.5620	0.8240	-0.1940	0.1820	0.5340
NGFG_02086	-0.0406	0.8310	0.9350	-0.0957	0.6150	0.8480	-0.1950	0.3040	0.6540
NGFG_02087	-0.2000	0.2630	0.5870	-0.2080	0.2430	0.5900	-0.0581	0.7430	0.9140
NGFG_02088	-0.3140	0.1080	0.3910	-0.2720	0.1630	0.4920	0.0973	0.6110	0.8590
NGFG_02089	-0.0403	0.8210	0.9320	-0.1720	0.3360	0.6900	0.1110	0.5320	0.8150
NGFG_02090	0.0713	0.6190	0.8320	-0.0780	0.5880	0.8430	0.4590	0.0015	0.0271
NGFG_02092	-0.0344	0.7380	0.9000	-0.1240	0.2290	0.5740	0.0744	0.4670	0.7800
NGFG_02093	-0.2120	0.2890	0.6070	-0.2490	0.2140	0.5530	-0.0071	0.9710	0.9940
NGFG_02094	-0.0269	0.8830	0.9570	0.1160	0.5220	0.8030	-0.0323	0.8590	0.9600
NGFG_02095	-0.3950	0.0724	0.3240	-0.2100	0.3360	0.6900	-0.0333	0.8780	0.9650
NGFG_02097	-0.2150	0.3960	0.7080	#NV			-0.0842	0.7390	0.9110
NGFG_02098	-0.6750	0.0039	0.0819	-0.4380	0.0598	0.3290	0.2620	0.2550	0.6120
NGFG_02100	-0.4870	0.0431	0.2660	-0.2470	0.3030	0.6610	0.4210	0.0796	0.3430
NGFG_02102	-0.7040	0.0002	0.0160	-0.6440	0.0006	0.0303	1.1000	0.0000	0.0000
NGFG_02103	-0.1870	0.4290	0.7260	-0.0842	0.7210	0.9050	0.4170	0.0782	0.3400
NGFG_02104	-0.0652	0.6890	0.8790	-0.1000	0.5380	0.8110	0.2100	0.1970	0.5500
NGFG_02105	0.2120	0.0758	0.3320	0.0701	0.5580	0.8210	0.0020	0.9860	0.9980
NGFG_02106	0.5540	0.0000	0.0049	0.4260	0.0015	0.0636	-0.1340	0.3180	0.6650

NGFG_02107	0.7000	0.0000	0.0011	0.5450	0.0004	0.0249	-0.1950	0.2020	0.5560
NGFG_02108	0.2650	0.0517	0.2840	0.3740	0.0061	0.1250	0.0345	0.8010	0.9370
NGFG_02109	0.0066	0.9660	0.9910	0.2230	0.1450	0.4670	0.1100	0.4730	0.7850
NGFG_02111	1.1700	0.0000	0.0000	1.0900	0.0000	0.0000	-0.5870	0.0014	0.0256
NGFG_02112	0.0798	0.5510	0.8090	0.0803	0.5490	0.8170	-0.2390	0.0736	0.3290
NGFG_02113	0.2050	0.2760	0.5980	0.3130	0.0956	0.3990	-0.1100	0.5600	0.8340
NGFG_02115	0.1840	0.2620	0.5870	0.1930	0.2390	0.5880	-0.4530	0.0056	0.0677
NGFG_02116	-0.0633	0.7070	0.8880	-0.0395	0.8140	0.9480	0.0545	0.7450	0.9150
NGFG_02117	0.1490	0.2780	0.6000	0.1260	0.3580	0.7100	-0.3050	0.0259	0.1880
NGFG_02118	-0.1920	0.1460	0.4490	-0.0693	0.5980	0.8480	-0.0929	0.4780	0.7860
NGFG_02119	0.0363	0.7400	0.9000	0.0255	0.8160	0.9480	0.0185	0.8660	0.9620
NGFG_02120	0.1930	0.1060	0.3870	0.1850	0.1210	0.4410	0.0574	0.6310	0.8690
NGFG_02121	-0.0744	0.5140	0.7870	0.0183	0.8720	0.9720	0.1290	0.2570	0.6130
NGFG_02122	-0.0048	0.9690	0.9930	0.0386	0.7530	0.9220	0.2120	0.0865	0.3580
NGFG_02123	-0.1180	0.1190	0.4040	-0.1070	0.1570	0.4830	0.0724	0.3400	0.6850
NGFG_02124	0.0606	0.6600	0.8600	0.0493	0.7200	0.9050	-0.1030	0.4520	0.7710
NGFG_02125	-0.0225	0.8630	0.9490	-0.0562	0.6670	0.8780	-0.0722	0.5790	0.8390
NGFG_02126	0.1580	0.4540	0.7480	0.3190	0.1310	0.4520	-0.0941	0.6560	0.8820
NGFG_02127	0.5210	0.0059	0.0995	0.3800	0.0448	0.2910	-0.3630	0.0551	0.2820
NGFG_02128	0.2330	0.0970	0.3730	0.1250	0.3740	0.7210	-0.1860	0.1840	0.5340
NGFG_02129	0.2500	0.2230	0.5350	0.0430	0.8340	0.9540	0.3490	0.0885	0.3610
NGFG_02130	0.1000	0.5970	0.8230	0.3710	0.0501	0.3080	0.5020	0.0081	0.0870
NGFG_02134	0.1250	0.5700	0.8160	0.1110	0.6130	0.8480	0.3910	0.0770	0.3380
NGFG_02135	0.0237	0.8940	0.9600	0.0631	0.7230	0.9060	0.4700	0.0089	0.0934
NGFG_02136	-0.1130	0.3900	0.7040	-0.1080	0.4080	0.7460	-0.1450	0.2640	0.6190
NGFG_02137	-0.2160	0.1910	0.4970	-0.3490	0.0354	0.2760	0.1440	0.3810	0.7240
NGFG_02138	-0.2010	0.1780	0.4830	-0.1940	0.1910	0.5200	0.0993	0.5010	0.7990
NGFG_02140	0.1300	0.3380	0.6540	0.2270	0.0950	0.3980	0.0033	0.9810	0.9960
NGFG_02141	-0.1890	0.3380	0.6540	0.1410	0.4720	0.7860	0.0256	0.8960	0.9720
NGFG_02142	0.0608	0.6500	0.8530	0.0077	0.9540	0.9930	-0.2310	0.0821	0.3490
NGFG_02143	-0.0331	0.8040	0.9240	-0.0953	0.4750	0.7870	0.0713	0.5900	0.8450
NGFG_02144	-0.0320	0.7620	0.9100	-0.0966	0.3610	0.7120	-0.3720	0.0004	0.0104
NGFG_02147	0.1190	0.4990	0.7790	0.1710	0.3300	0.6890	0.0999	0.5710	0.8370
NGFG_02148	-0.3880	0.0622	0.2980	0.0126	0.9510	0.9930	0.5990	0.0041	0.0579
NGFG_02149	0.1620	0.5190	0.7910	#NV			0.4700	0.0636	0.3100
NGFG_02151	0.0146	0.9470	0.9830	0.0789	0.7220	0.9050	-0.1700	0.4410	0.7640
NGFG_02152	-0.2000	0.1350	0.4340	-0.2170	0.1060	0.4170	-0.1610	0.2180	0.5800
NGFG_02153	0.2510	0.0438	0.2680	0.2590	0.0371	0.2790	-0.7620	0.0000	0.0000
NGFG_02154	-0.1810	0.3210	0.6350	-0.0486	0.7890	0.9340	-0.6310	0.0004	0.0113
NGFG_02155	-0.3310	0.0697	0.3180	-0.2180	0.2310	0.5750	0.1730	0.3380	0.6840
NGFG_02156	0.0908	0.4050	0.7120	0.0411	0.7060	0.8960	-0.1460	0.1790	0.5270
NGFG_02157	0.0281	0.7820	0.9140	0.0037	0.9710	0.9960	0.0789	0.4360	0.7610
NGFG_02160	-0.3940	0.0784	0.3380	-0.3430	0.1250	0.4490	0.0929	0.6760	0.8930
NGFG_02161	-0.3710	0.0861	0.3520	-0.3730	0.0842	0.3720	0.1930	0.3720	0.7160
NGFG_02162	-0.3630	0.0249	0.2100	-0.3820	0.0183	0.2060	0.1530	0.3440	0.6900
NGFG_02163	-0.1590	0.2290	0.5410	-0.1410	0.2840	0.6380	0.1010	0.4390	0.7630
NGFG_02164	-0.1200	0.4210	0.7230	0.0379	0.7990	0.9410	0.0576	0.6980	0.8980

NGFG_02165	-0.1720	0.2260	0.5390	-0.0118	0.9340	0.9850	0.1230	0.3850	0.7240
NGFG_02166	0.1750	0.1270	0.4170	0.1750	0.1270	0.4510	-0.0857	0.4550	0.7740
NGFG_02167	0.0249	0.8350	0.9360	0.0013	0.9910	0.9990	-0.1310	0.2700	0.6220
NGFG_02170	0.0404	0.7840	0.9140	0.0319	0.8290	0.9500	0.9070	0.0000	0.0000
NGFG_02171	0.0377	0.7800	0.9140	0.0173	0.8980	0.9800	0.4810	0.0004	0.0104
NGFG_02173	0.1620	0.1640	0.4680	0.0445	0.7010	0.8950	0.1730	0.1370	0.4490
NGFG_02174	0.3240	0.0354	0.2430	0.2960	0.0548	0.3180	-0.0882	0.5680	0.8370
NGFG_02175	0.1370	0.2630	0.5880	0.1340	0.2730	0.6290	-0.0397	0.7450	0.9150
NGFG_02176	0.0823	0.6910	0.8790	0.0122	0.9530	0.9930	0.2190	0.2910	0.6420
NGFG_02180	-0.1140	0.5740	0.8160	-0.2010	0.3220	0.6830	0.5000	0.0140	0.1250
NGFG_02184	0.5260	0.0063	0.1030	0.5190	0.0070	0.1340	-0.1910	0.3230	0.6700
NGFG_02185	-0.6490	0.0103	0.1300	#NV			0.6060	0.0165	0.1380
NGFG_02188	-0.1650	0.3260	0.6410	-0.2130	0.2030	0.5380	0.2540	0.1280	0.4340
NGFG_02189	#NV			#NV			0.4290	0.0368	0.2280
NGFG_02190	-0.5370	0.0316	0.2330	#NV			0.7180	0.0041	0.0579
NGFG_02191	-0.0619	0.6270	0.8370	-0.0485	0.7030	0.8960	0.1770	0.1650	0.5060
NGFG_02192	-0.0765	0.6770	0.8720	-0.2150	0.2420	0.5900	0.1140	0.5340	0.8150
NGFG_02194	-0.0414	0.8660	0.9490	-0.0455	0.8530	0.9650	-0.0639	0.7930	0.9340
NGFG_02196	0.5210	0.0222	0.1990	0.5940	0.0091	0.1460	-0.1430	0.5330	0.8150
NGFG_02197	0.0446	0.8500	0.9450	0.1650	0.4840	0.7900	0.0622	0.7920	0.9340
NGFG_02198	-0.0108	0.9640	0.9900	#NV			-0.3630	0.1230	0.4260
NGFG_02199	-0.3660	0.0335	0.2350	-0.2020	0.2380	0.5880	0.1110	0.5130	0.8020
NGFG_02200	0.1460	0.4840	0.7670	-0.0108	0.9590	0.9930	0.1950	0.3540	0.6980
NGFG_02203	0.3570	0.0938	0.3690	0.3950	0.0632	0.3380	0.3220	0.1310	0.4380
NGFG_02204	0.1950	0.3420	0.6590	0.1220	0.5530	0.8190	0.6930	0.0008	0.0170
NGFG_02205	-0.0695	0.6800	0.8720	-0.1010	0.5500	0.8170	0.5860	0.0005	0.0128
NGFG_02206	-0.3450	0.1520	0.4550	#NV			0.4330	0.0727	0.3270
NGFG_02207	-0.3850	0.1210	0.4050	#NV			0.3090	0.2110	0.5690
NGFG_02208	#NV			#NV			0.0076	0.9720	0.9940
NGFG_02209	-0.3770	0.0842	0.3500	-0.5120	0.0192	0.2070	0.6630	0.0024	0.0402
NGFG_02213	-0.4870	0.0523	0.2840	#NV			0.0868	0.7270	0.9100
NGFG_02217	0.0912	0.5770	0.8160	0.1340	0.4130	0.7500	0.0761	0.6410	0.8730
NGFG_02219	0.1450	0.3940	0.7070	0.1090	0.5220	0.8030	0.0632	0.7090	0.9010
NGFG_02222	0.0860	0.5750	0.8160	0.1170	0.4460	0.7680	0.4320	0.0054	0.0664
NGFG_02225	-0.2800	0.2700	0.5940	#NV			0.4040	0.1110	0.4010
NGFG_02226	-0.2840	0.2560	0.5800	#NV			-0.2320	0.3490	0.6940
NGFG_02228	0.2060	0.1170	0.4020	0.1450	0.2720	0.6280	-0.3340	0.0107	0.1050
NGFG_02229	0.4450	0.0167	0.1680	0.3500	0.0597	0.3290	-0.0386	0.8350	0.9520
NGFG_02231	#NV			#NV			-0.0969	0.6600	0.8840
NGFG_02232	-0.1530	0.5230	0.7920	#NV			0.2080	0.3860	0.7260
NGFG_02233	-0.4600	0.0713	0.3190	#NV			0.4570	0.0733	0.3290
NGFG_02234	-0.2220	0.3810	0.6940	#NV			0.4580	0.0704	0.3250
NGFG_02237	-0.8120	0.0013	0.0450	#NV			0.7720	0.0021	0.0363
NGFG_02238	-0.2350	0.1710	0.4750	-0.0788	0.6460	0.8660	0.4650	0.0069	0.0776
NGFG_02239	0.2590	0.2500	0.5730	0.2220	0.3240	0.6830	-0.0786	0.7270	0.9100
NGFG_02243	0.2350	0.3510	0.6680	#NV			-0.4200	0.0972	0.3730
NGFG_02244	0.2070	0.3300	0.6470	-0.0112	0.9580	0.9930	0.1240	0.5610	0.8340

NGFG_02245	#NV			#NV			0.1230	0.4750	0.7850
NGFG_02247	-0.1740	0.3560	0.6700	-0.0173	0.9270	0.9830	0.6210	0.0011	0.0216
NGFG_02248	-0.0023	0.9930	0.9960	#NV			0.3900	0.1070	0.3910
NGFG_02253	0.0787	0.6900	0.8790	-0.1580	0.4260	0.7540	0.4200	0.0352	0.2220
NGFG_02254	#NV			#NV			0.2320	0.2970	0.6470
NGFG_02255	0.1530	0.4910	0.7730	0.1220	0.5840	0.8400	-0.2320	0.2930	0.6430
NGFG_02257	-0.3020	0.0796	0.3410	-0.2360	0.1710	0.4950	0.2900	0.0915	0.3620
NGFG_02258	-0.0221	0.8930	0.9600	-0.1170	0.4770	0.7870	-0.0554	0.7360	0.9110
NGFG_02259	0.2330	0.1700	0.4750	0.1680	0.3250	0.6830	-0.4990	0.0033	0.0493
NGFG_02260	-0.2190	0.3000	0.6160	-0.2150	0.3080	0.6640	0.0822	0.6950	0.8970
NGFG_02262	-0.1520	0.4860	0.7690	0.1130	0.6020	0.8480	-0.2590	0.2300	0.5890
NGFG_02263	0.5530	0.0004	0.0238	0.6110	0.0001	0.0127	-0.4610	0.0029	0.0452
NGFG_02264	-0.1980	0.4060	0.7120	#NV			-0.1910	0.4140	0.7450
NGFG_02265	-0.2180	0.0564	0.2900	-0.2480	0.0308	0.2560	0.0123	0.9130	0.9750
NGFG_02266	0.0458	0.7440	0.9020	0.0848	0.5450	0.8150	-0.0251	0.8570	0.9590
NGFG_02267	0.0551	0.8060	0.9240	-0.1140	0.6130	0.8480	-0.0390	0.8610	0.9610
NGFG_02268	-0.2400	0.2950	0.6120	-0.1670	0.4660	0.7820	0.0459	0.8400	0.9530
NGFG_02269	-0.0077	0.9600	0.9890	0.0199	0.8970	0.9800	0.1080	0.4850	0.7910
NGFG_02270	0.3330	0.1470	0.4500	0.2760	0.2280	0.5730	0.4810	0.0362	0.2270
NGFG_02271	-0.0673	0.6300	0.8410	-0.1910	0.1720	0.4950	0.2370	0.0896	0.3620
NGFG_02272	-0.3880	0.0038	0.0805	-0.4230	0.0016	0.0664	0.0744	0.5730	0.8370
NGFG_02273	0.1980	0.2460	0.5690	0.2300	0.1780	0.5010	-0.3430	0.0442	0.2510
NGFG_02274	-0.1150	0.5670	0.8160	-0.0694	0.7290	0.9080	0.0971	0.6270	0.8680
NGFG_02275	-0.1900	0.1490	0.4520	-0.1240	0.3460	0.6990	-0.1360	0.2970	0.6470
NGFG_02276	-0.2930	0.0863	0.3520	-0.2500	0.1430	0.4670	-0.1010	0.5420	0.8210
NGFG_02277	0.0506	0.8300	0.9350	-0.0352	0.8820	0.9740	-0.0397	0.8660	0.9620
NGFG_02278	-0.2950	0.2040	0.5130	-0.1030	0.6570	0.8750	0.2040	0.3800	0.7230
NGFG_02279	#NV			#NV			-0.0047	0.9640	0.9940
NGFG_02280	0.1000	0.5130	0.7870	0.0245	0.8740	0.9720	-0.3000	0.0464	0.2570
NGFG_02281	-0.0007	0.9960	0.9980	-0.0678	0.6660	0.8780	0.0131	0.9330	0.9830
NGFG_02282	-0.2050	0.2100	0.5210	-0.2650	0.1060	0.4170	0.0590	0.7180	0.9050
NGFG_02284	-0.2580	0.0596	0.2920	-0.2930	0.0325	0.2640	0.5540	0.0001	0.0025
NGFG_02285	#NV			#NV			0.1110	0.5750	0.8370
NGFG_02286	-0.5100	0.0453	0.2690	#NV			0.6110	0.0163	0.1370
NGFG_02287	#NV			#NV			0.2710	0.1480	0.4720
NGFG_02288	-0.4240	0.0959	0.3710	#NV			0.4940	0.0525	0.2750
NGFG_02289	#NV			#NV			-0.0225	0.9130	0.9750
NGFG_02290	-0.3230	0.2010	0.5100	#NV			0.6160	0.0145	0.1270
NGFG_02291	-0.1510	0.5020	0.7800	-0.0215	0.9240	0.9820	0.2500	0.2650	0.6190
NGFG_02292	#NV			#NV			0.2450	0.0887	0.3610
NGFG_02294	-0.1820	0.4740	0.7620	#NV			0.1270	0.6160	0.8620
NGFG_02295	-0.2580	0.3110	0.6280	#NV			0.3360	0.1870	0.5390
NGFG_02296	-0.6690	0.0082	0.1170	#NV			0.3250	0.2020	0.5560
NGFG_02297	#NV			#NV			0.1700	0.1430	0.4620
NGFG_02298	#NV			#NV			0.1890	0.4050	0.7390
NGFG_02299	#NV			#NV			0.0795	0.7190	0.9050
NGFG_02300	0.2250	0.2890	0.6070	0.2390	0.2590	0.6100	-0.2140	0.3120	0.6610

NGFG_02301	-0.2680	0.1060	0.3870	-0.0140	0.9320	0.9850	0.1220	0.4570	0.7740
NGFG_02302	0.1800	0.3370	0.6530	0.2690	0.1500	0.4720	-0.0848	0.6500	0.8800
NGFG_02303	-0.2020	0.2180	0.5300	-0.1370	0.4040	0.7400	0.0797	0.6230	0.8650
NGFG_02304	0.0863	0.7170	0.8940	0.1190	0.6170	0.8480	-0.0877	0.7120	0.9010
NGFG_02305	-0.2220	0.2630	0.5870	-0.0599	0.7610	0.9230	0.1660	0.4000	0.7350
NGFG_02306	0.3930	0.0573	0.2910	0.4020	0.0515	0.3090	-0.5070	0.0137	0.1230
NGFG_02307	-0.3140	0.0525	0.2840	-0.3120	0.0541	0.3180	0.3540	0.0282	0.1970
NGFG_02309	-0.1030	0.5900	0.8190	0.0302	0.8740	0.9720	-0.0754	0.6920	0.8970
NGFG_02310	0.2460	0.2250	0.5390	0.2910	0.1500	0.4720	-0.2740	0.1740	0.5180
NGFG_02311	-0.0732	0.7630	0.9100	#NV			0.3880	0.1120	0.4020
NGFG_02312	-0.1680	0.5100	0.7850	#NV			-0.2750	0.2810	0.6320
NGFG_02313	-0.2400	0.1280	0.4190	-0.1750	0.2630	0.6160	0.0295	0.8490	0.9560
NGFG_02314	-0.1780	0.2390	0.5560	-0.0230	0.8780	0.9740	0.1290	0.3890	0.7280
NGFG_02315	-0.3160	0.1750	0.4790	-0.0156	0.9460	0.9900	0.0557	0.8090	0.9400
NGFG_02316	-0.0252	0.8620	0.9490	-0.0978	0.5000	0.7940	0.3220	0.0267	0.1910
NGFG_02317	-0.0420	0.8640	0.9490	#NV			0.1010	0.6800	0.8930
NGFG_02318	0.2270	0.3080	0.6250	0.2760	0.2160	0.5550	0.2090	0.3480	0.6940
NGFG_02319	0.2960	0.1950	0.5020	0.4210	0.0651	0.3440	0.2240	0.3320	0.6780
NGFG_02320	-0.0053	0.9800	0.9950	0.0889	0.6770	0.8850	0.2710	0.2050	0.5610
NGFG_02321	-0.1990	0.3950	0.7080	-0.1120	0.6320	0.8600	0.2750	0.2410	0.5970
NGFG_02322	-0.3350	0.0443	0.2680	-0.2610	0.1160	0.4360	0.1270	0.4410	0.7640
NGFG_02323	-0.1350	0.4940	0.7740	-0.0898	0.6490	0.8670	0.3130	0.1140	0.4060
NGFG_02324	-0.0253	0.9150	0.9690	#NV			0.0887	0.7070	0.9010
NGFG_02325	0.3510	0.0369	0.2460	0.1970	0.2440	0.5910	-0.3070	0.0664	0.3160
NGFG_02326	-0.4010	0.1040	0.3850	#NV			0.2700	0.2700	0.6220
NGFG_02328	0.2170	0.1830	0.4890	0.1650	0.3110	0.6700	0.0447	0.7850	0.9320
NGFG_02329	0.3270	0.0414	0.2600	0.2270	0.1570	0.4830	-0.0991	0.5370	0.8150
NGFG_02330	-0.1040	0.5280	0.7960	-0.0475	0.7740	0.9280	-0.0114	0.9450	0.9880
NGFG_02331	-0.4800	0.0194	0.1830	-0.4220	0.0395	0.2870	0.5550	0.0068	0.0776
NGFG_02333	#NV			#NV			-0.0012	0.9810	0.9960
NGFG_02334	-0.2130	0.1870	0.4930	-0.1100	0.4930	0.7940	0.1040	0.5130	0.8020
NGFG_02335	0.1010	0.6530	0.8550	0.0123	0.9560	0.9930	-0.0378	0.8660	0.9620
NGFG_02336	-0.1540	0.5440	0.8050	#NV			0.4350	0.0869	0.3590
NGFG_02337	-0.2180	0.2240	0.5370	-0.2280	0.2050	0.5380	-0.0150	0.9330	0.9830
NGFG_02338	-0.0135	0.9550	0.9870	#NV			-0.0179	0.9400	0.9860
NGFG_02339	0.3330	0.0941	0.3690	0.2760	0.1650	0.4920	-0.0443	0.8240	0.9500
NGFG_02340	#NV			#NV			0.0419	0.8390	0.9530
NGFG_02342	0.1150	0.5940	0.8230	0.0352	0.8700	0.9720	0.9630	0.0000	0.0006
NGFG_02343	-0.4710	0.0121	0.1450	-0.4690	0.0124	0.1730	1.1100	0.0000	0.0000
NGFG_02344	0.2740	0.1390	0.4360	0.4230	0.0219	0.2200	0.4350	0.0195	0.1540
NGFG_02345	0.3180	0.1110	0.3930	0.1520	0.4470	0.7680	0.7530	0.0002	0.0064
NGFG_02346	0.1320	0.2930	0.6110	0.0898	0.4770	0.7870	0.1250	0.3230	0.6700
NGFG_02347	0.0620	0.7790	0.9130	-0.1130	0.6130	0.8480	0.4510	0.0436	0.2500
NGFG_02348	0.4400	0.0145	0.1600	0.3430	0.0567	0.3230	0.8360	0.0000	0.0004
NGFG_02349	0.2010	0.3000	0.6160	0.1140	0.5560	0.8210	0.9500	0.0000	0.0002
NGFG_02350	0.1820	0.4010	0.7100	0.0752	0.7290	0.9080	0.3080	0.1560	0.4880
NGFG_02351	0.2870	0.0920	0.3660	0.2540	0.1370	0.4640	-0.3290	0.0537	0.2780

NGFG_02352	-0.4380	0.0260	0.2140	-0.1170	0.5480	0.8170	-0.1640	0.3930	0.7310
NGFG_02353	#NV			#NV			-0.0628	0.7600	0.9210
NGFG_02354	-0.2270	0.3650	0.6790	#NV			-0.0404	0.8710	0.9630
NGFG_02355	#NV			#NV			0.4150	0.0625	0.3090
NGFG_02356	0.0282	0.9120	0.9680	#NV			0.0381	0.8810	0.9650
NGFG_02357	0.0849	0.7320	0.9000	#NV			-0.1980	0.4270	0.7560
NGFG_02358	-0.3350	0.1550	0.4570	#NV			0.4780	0.0423	0.2460
NGFG_02359	-0.1340	0.5980	0.8230	#NV			0.3280	0.1980	0.5500
NGFG_02361	#NV			#NV			0.3310	0.0965	0.3710
NGFG_02362	-0.0059	0.9810	0.9950	-0.0726	0.7640	0.9240	0.3870	0.1110	0.4000
NGFG_02363	-0.3240	0.1660	0.4710	-0.3910	0.0955	0.3990	0.6990	0.0030	0.0453
NGFG_02364	-0.1560	0.5350	0.7990	#NV			0.3410	0.1770	0.5210
NGFG_02365	#NV			#NV			0.1340	0.4860	0.7910
NGFG_02366	#NV			#NV			-0.0310	0.8820	0.9650
NGFG_02367	-0.4870	0.0564	0.2900	-0.5950	0.0197	0.2080	0.4520	0.0763	0.3370
NGFG_02368	#NV			#NV			0.1160	0.5290	0.8130
NGFG_02369	#NV			#NV			-0.0107	0.8320	0.9520
NGFG_02370	-0.4260	0.0335	0.2350	-0.5130	0.0105	0.1600	0.1380	0.4880	0.7930
NGFG_02371	-0.1420	0.5740	0.8160	#NV			0.4640	0.0651	0.3150
NGFG_02372	0.1450	0.3850	0.6980	0.1220	0.4660	0.7830	0.0805	0.6310	0.8690
NGFG_02373	-0.0411	0.7770	0.9130	-0.0866	0.5500	0.8170	0.4160	0.0042	0.0579
NGFG_02374	0.4280	0.0469	0.2700	0.4380	0.0420	0.2870	-0.2650	0.2200	0.5830
NGFG_02376	0.3800	0.0468	0.2700	0.3830	0.0445	0.2910	-0.5420	0.0042	0.0579
NGFG_02377	0.3770	0.1370	0.4360	#NV			-0.2840	0.2620	0.6190
NGFG_02378	-0.0354	0.8370	0.9370	-0.0870	0.6140	0.8480	0.1390	0.4200	0.7510
NGFG_02379	0.0173	0.9230	0.9710	-0.0754	0.6720	0.8830	0.3020	0.0902	0.3620
NGFG_02380	0.4090	0.0442	0.2680	0.4560	0.0246	0.2330	0.0079	0.9690	0.9940
NGFG_02381	0.1210	0.4330	0.7270	0.2230	0.1460	0.4670	-0.3230	0.0338	0.2180
NGFG_02382	0.0918	0.6750	0.8700	0.0680	0.7560	0.9230	-0.3740	0.0806	0.3460
NGFG_02383	0.2420	0.0556	0.2900	0.3160	0.0120	0.1700	-0.2050	0.1020	0.3850
NGFG_02384	0.3220	0.1420	0.4410	0.1940	0.3770	0.7220	-0.1100	0.6180	0.8630
NGFG_02385	-0.0313	0.9000	0.9610	#NV			-0.0466	0.8520	0.9570
NGFG_02386	0.1160	0.5630	0.8160	0.0257	0.8980	0.9800	-0.1510	0.4500	0.7700
NGFG_02387	0.3950	0.0932	0.3680	0.2570	0.2770	0.6320	0.0524	0.8250	0.9500
NGFG_02388	0.1890	0.4010	0.7100	0.2540	0.2580	0.6100	-0.0383	0.8650	0.9620
NGFG_02389	-0.2040	0.3690	0.6840	-0.1080	0.6340	0.8600	0.1150	0.6110	0.8590
NGFG_02391	0.1020	0.5550	0.8100	0.3230	0.0605	0.3300	-0.0319	0.8530	0.9570
NGFG_02392	-0.3830	0.0705	0.3190	-0.3560	0.0928	0.3930	0.3300	0.1160	0.4110
NGFG_02393	-0.0039	0.9830	0.9950	-0.0996	0.5770	0.8340	0.4050	0.0235	0.1770
NGFG_02394	-0.1300	0.5380	0.8010	-0.1140	0.5890	0.8430	0.1130	0.5890	0.8450
NGFG_02395	-0.2170	0.1930	0.5000	-0.1320	0.4260	0.7540	0.1310	0.4270	0.7560
NGFG_02396	-0.1560	0.2700	0.5940	0.0241	0.8650	0.9700	-0.0525	0.7090	0.9010
NGFG_02397	-0.0883	0.5830	0.8160	-0.0981	0.5420	0.8140	0.1510	0.3460	0.6910
NGFG_02398	0.0120	0.9490	0.9830	-0.1320	0.4850	0.7900	0.3540	0.0609	0.3040
NGFG_02399	0.3220	0.0998	0.3770	0.2100	0.2860	0.6400	-0.0970	0.6210	0.8640
NGFG_02400	0.2550	0.1660	0.4710	0.1230	0.5060	0.7950	-0.4450	0.0148	0.1270
NGFG_02401	0.0122	0.9620	0.9890	#NV			-0.0172	0.9460	0.9880

NGFG_02402	0.3770	0.0152	0.1610	0.2300	0.1390	0.4640	-0.0849	0.5850	0.8420
NGFG_02403	0.4590	0.0447	0.2690	0.1460	0.5250	0.8040	-0.0997	0.6640	0.8870
NGFG_02404	0.0419	0.8100	0.9260	0.0802	0.6450	0.8660	-0.0715	0.6800	0.8930
NGFG_02405	0.3700	0.1180	0.4030	0.3390	0.1520	0.4730	0.3070	0.1970	0.5500
NGFG_02406	-0.2890	0.0493	0.2760	-0.2730	0.0631	0.3380	0.1640	0.2630	0.6190
NGFG_02407	-0.0012	0.9920	0.9960	0.0858	0.4720	0.7860	-0.4410	0.0002	0.0068
NGFG_02408	-0.0002	0.9990	0.9990	0.2500	0.1700	0.4950	-0.0234	0.8980	0.9720
NGFG_02409	0.1800	0.1310	0.4240	0.2950	0.0133	0.1800	-0.2340	0.0490	0.2670
NGFG_02410	-0.2670	0.0601	0.2920	-0.1890	0.1820	0.5060	0.0344	0.8050	0.9390
NGFG_02411	-0.4050	0.0035	0.0783	-0.0594	0.6640	0.8780	0.1350	0.3230	0.6700
NGFG_02412	-0.1290	0.5520	0.8090	-0.1930	0.3740	0.7210	0.3240	0.1360	0.4490
NGFG_02414	#NV			#NV			-0.0712	0.7380	0.9110
NGFG_02415	-0.0212	0.9180	0.9690	0.1430	0.4860	0.7900	1.3300	0.0000	0.0000
NGFG_02416	0.2400	0.1620	0.4660	0.1310	0.4440	0.7670	0.1900	0.2680	0.6220
NGFG_02417	0.3660	0.1370	0.4360	0.1140	0.6440	0.8660	0.4030	0.1040	0.3890
NGFG_02418	-0.0198	0.9180	0.9690	-0.0638	0.7410	0.9140	0.4640	0.0162	0.1360
NGFG_02419	0.1200	0.3010	0.6160	0.1880	0.1060	0.4170	-0.4500	0.0001	0.0033
NGFG_02420	-0.0712	0.7040	0.8860	-0.0280	0.8810	0.9740	-0.0836	0.6510	0.8800
NGFG_02421	-0.0384	0.8650	0.9490	0.0832	0.7100	0.8970	-0.5030	0.0217	0.1670
NGFG_02422	0.0820	0.5400	0.8020	0.1120	0.4030	0.7400	-0.1020	0.4420	0.7640
NGFG_02423	-0.0090	0.9470	0.9830	-0.0210	0.8770	0.9740	0.0361	0.7900	0.9340
NGFG_02424	-0.2160	0.0760	0.3320	-0.2570	0.0351	0.2750	0.0894	0.4590	0.7740
NGFG_02425	0.2250	0.2380	0.5560	0.1230	0.5210	0.8030	-0.2570	0.1760	0.5210
NGFG_02426	-0.8820	0.0004	0.0238	-0.9670	0.0001	0.0135	0.5310	0.0310	0.2050
NGFG_02428	0.2460	0.1950	0.5010	0.2440	0.1990	0.5330	0.1750	0.3560	0.7000
NGFG_02429	-0.1480	0.5510	0.8090	#NV			0.5630	0.0244	0.1810
NGFG_02430	-0.0822	0.7400	0.9000	#NV			-0.1320	0.5980	0.8490
NGFG_02431	-0.2930	0.2470	0.5700	#NV			-0.0113	0.9640	0.9940
NGFG_02432	-0.1280	0.4640	0.7560	-0.0524	0.7650	0.9240	0.0819	0.6400	0.8730
NGFG_02434	#NV			#NV			0.4260	0.0333	0.2170
NGFG_02435	0.1220	0.5000	0.7790	0.0649	0.7190	0.9050	-0.0394	0.8270	0.9500
NGFG_02437	-0.0400	0.8280	0.9350	0.0838	0.6480	0.8670	0.0269	0.8830	0.9660
NGFG_02438	-0.1350	0.5630	0.8160	-0.1150	0.6200	0.8490	-0.0773	0.7380	0.9110
NGFG_02439	0.2050	0.3380	0.6540	0.3070	0.1500	0.4720	0.6750	0.0022	0.0371
NGFG_02440	0.1890	0.2800	0.6010	0.0188	0.9140	0.9820	0.2020	0.2480	0.6040
NGFG_02441	0.3220	0.0843	0.3500	0.1660	0.3750	0.7210	-0.1070	0.5660	0.8360
NGFG_02442	#NV			#NV			0.1620	0.1490	0.4730
NGFG_02443	-0.2180	0.2920	0.6100	-0.1260	0.5430	0.8140	0.0773	0.7060	0.9010
NGFG_02444	-0.4140	0.0989	0.3770	#NV			0.2660	0.2860	0.6340
NGFG_02445	-0.2570	0.1810	0.4870	-0.1980	0.3010	0.6600	0.1400	0.4630	0.7780
NGFG_02446	-0.4090	0.0998	0.3770	#NV			0.5170	0.0375	0.2300
NGFG_02447	0.0724	0.7750	0.9120	#NV			0.3440	0.1750	0.5190
NGFG_02448	#NV			#NV			0.0907	0.6320	0.8690
NGFG_02449	-0.1050	0.6790	0.8720	#NV			0.1660	0.5120	0.8020
NGFG_02450	-0.0132	0.9430	0.9830	-0.1080	0.5570	0.8210	0.3320	0.0709	0.3250
NGFG_02452	0.3360	0.1110	0.3930	0.3270	0.1210	0.4410	-0.1220	0.5630	0.8340
NGFG_02453	-0.0548	0.8290	0.9350	#NV			0.1840	0.4660	0.7800

NGFG_02454	0.2750	0.1170	0.4020	0.0471	0.7890	0.9340	-0.1470	0.4020	0.7370
NGFG_02455	-0.0601	0.7880	0.9150	-0.0536	0.8100	0.9470	0.2590	0.2470	0.6040
NGFG_02456	-0.3230	0.0250	0.2100	-0.2210	0.1240	0.4470	0.0135	0.9250	0.9790
NGFG_02457	-0.1960	0.1400	0.4360	-0.1090	0.4070	0.7440	-0.0453	0.7290	0.9110
NGFG_02458	0.1280	0.3040	0.6200	0.2200	0.0756	0.3620	-0.2570	0.0376	0.2300
NGFG_02459	#NV			#NV			0.1700	0.3340	0.6810
NGFG_02460	0.1740	0.3720	0.6870	0.2110	0.2810	0.6350	0.2330	0.2370	0.5960
NGFG_02461	#NV			#NV			-0.0100	0.8380	0.9520
NGFG_02463	-0.0573	0.7680	0.9110	-0.0727	0.7080	0.8970	0.7040	0.0003	0.0089
NGFG_02464	#NV			#NV			0.1450	0.2020	0.5560
NGFG_02465	0.3160	0.0840	0.3500	0.2330	0.2020	0.5380	-0.0672	0.7130	0.9020
NGFG_02466	0.2840	0.0862	0.3520	0.2170	0.1910	0.5200	-0.0711	0.6680	0.8870
NGFG_02467	-0.0343	0.8560	0.9460	-0.0240	0.8990	0.9800	-0.0553	0.7690	0.9240
NGFG_02468	0.2370	0.2810	0.6010	0.5170	0.0177	0.2040	-0.0990	0.6530	0.8800
NGFG_02469	0.1910	0.3540	0.6700	0.0632	0.7590	0.9230	0.3970	0.0542	0.2800
NGFG_02470	0.2630	0.1060	0.3870	0.2930	0.0719	0.3550	-0.0669	0.6810	0.8930
NGFG_02471	0.2380	0.0657	0.3080	0.3010	0.0200	0.2090	-0.2640	0.0407	0.2400
NGFG_02472	-0.0370	0.8840	0.9570	#NV			-0.0653	0.7970	0.9350
NGFG_02473	-0.0368	0.8160	0.9290	-0.0016	0.9920	0.9990	-0.1730	0.2720	0.6250
NGFG_02475	-0.0321	0.8720	0.9510	0.0395	0.8420	0.9580	0.0235	0.9050	0.9720
NGFG_02476	0.1460	0.3180	0.6340	0.2530	0.0833	0.3680	0.0268	0.8550	0.9580
NGFG_02477	-0.0162	0.9130	0.9680	0.0605	0.6810	0.8850	0.2090	0.1570	0.4890
NGFG_02478	0.0621	0.6340	0.8440	0.0653	0.6170	0.8480	0.1720	0.1860	0.5390
NGFG_02479	#NV			#NV			-0.0037	0.9670	0.9940
NGFG_02480	-0.0289	0.8970	0.9600	0.0274	0.9020	0.9810	0.2890	0.1970	0.5500
NGFG_02481	-0.1960	0.4240	0.7230	#NV			0.4670	0.0575	0.2930
NGFG_02482	-0.0168	0.9470	0.9830	#NV			-0.0411	0.8710	0.9630
NGFG_02483	0.0226	0.8900	0.9600	-0.0501	0.7590	0.9230	-0.1930	0.2380	0.5960
NGFG_02484	-0.3180	0.1470	0.4500	-0.4000	0.0690	0.3470	0.3910	0.0735	0.3290
NGFG_02485	-0.0874	0.6930	0.8800	0.0603	0.7840	0.9320	0.0416	0.8500	0.9570
NGFG_02486	0.2960	0.0522	0.2840	0.2500	0.1010	0.4070	-0.0954	0.5310	0.8150
NGFG_02487	-0.1680	0.4540	0.7480	-0.3430	0.1290	0.4520	0.5640	0.0125	0.1160
NGFG_02488	-0.1550	0.4390	0.7330	-0.1600	0.4240	0.7520	0.0580	0.7690	0.9240
NGFG_02489	#NV			#NV			-0.0393	0.4980	0.7960
NGFG_02490	-0.0947	0.5970	0.8230	-0.1410	0.4320	0.7560	-0.1150	0.5150	0.8030
NGFG_02491	0.1850	0.3360	0.6530	0.2740	0.1530	0.4770	-0.0572	0.7660	0.9240
NGFG_02492	-0.6520	0.0086	0.1200	-0.4540	0.0665	0.3440	0.5120	0.0385	0.2320
NGFG_02496	0.6670	0.0010	0.0413	0.5100	0.0122	0.1700	0.1130	0.5770	0.8380
NGFG_02497	-0.5180	0.0091	0.1220	-0.4340	0.0285	0.2490	0.5570	0.0049	0.0630
NGFG_02498	-0.3040	0.1500	0.4530	-0.4030	0.0574	0.3240	0.5520	0.0092	0.0938
NGFG_02499	-0.5130	0.0193	0.1830	-0.5600	0.0108	0.1600	0.7800	0.0004	0.0105
NGFG_02500	-0.6940	0.0011	0.0417	-0.6330	0.0029	0.0852	0.8130	0.0001	0.0050
NGFG_06000	-0.2550	0.2300	0.5420	#NV			0.1430	0.5060	0.8000
NGFG_06001	#NV			#NV			0.0267	0.7900	0.9340
NGFG_06002	0.2180	0.3490	0.6670	-0.0320	0.8920	0.9780	-0.0297	0.8990	0.9720
NGFG_06003	#NV			#NV			-0.0882	0.4290	0.7580
NGFG_06004	-0.1590	0.3960	0.7080	-0.0705	0.7060	0.8960	0.3870	0.0395	0.2360

NGFG_06005	#NV			#NV			-0.0552	0.6920	0.8970
NGFG_06006	#NV			#NV			0.0079	0.8730	0.9630
NGFG_06007	#NV			#NV			-0.0763	0.4590	0.7740
NGFG_06008	#NV			#NV			0.3120	0.0661	0.3160
NGFG_06009	#NV			#NV			-0.0507	0.6570	0.8840
NGFG_06010	-0.0104	0.9640	0.9900	-0.2020	0.3850	0.7270	0.6410	0.0060	0.0703
NGFG_06011	0.2450	0.2940	0.6110	0.0322	0.8900	0.9780	0.1520	0.5160	0.8040
NGFG_06012	-0.1680	0.4210	0.7230	-0.1700	0.4150	0.7500	0.6080	0.0037	0.0538
NGFG_06013	-0.3590	0.1570	0.4600	#NV			0.6860	0.0070	0.0779
NGFG_06014	-0.6220	0.0127	0.1470	#NV			0.9720	0.0001	0.0042
NGFG_06015	0.2340	0.2680	0.5930	0.0240	0.9100	0.9820	-0.1850	0.3790	0.7230
NGFG_06018	#NV			#NV			-0.0213	0.9080	0.9730
NGFG_06019	#NV			#NV			-0.0722	0.7470	0.9160
NGFG_06021	-0.4020	0.1090	0.3910	-0.8870	0.0004	0.0259	0.8360	0.0009	0.0185
NGFG_06022	#NV			#NV			0.0079	0.8730	0.9630
NGFG_06023	#NV			#NV			0.1670	0.3960	0.7310
NGFG_06024	-0.4040	0.0754	0.3320	-0.8580	0.0002	0.0173	0.7350	0.0012	0.0235
NGFG_06025	#NV			#NV			0.2290	0.2300	0.5880
NGFG_06026	-0.2340	0.2850	0.6060	-0.1510	0.4910	0.7920	0.7280	0.0009	0.0191
NGFG_06027	-0.2100	0.3280	0.6430	-0.3090	0.1490	0.4720	0.7910	0.0002	0.0073
NGFG_06028	-0.5220	0.0147	0.1610	-0.3320	0.1200	0.4400	0.8370	0.0001	0.0039
NGFG_06029	-0.1150	0.6480	0.8530	#NV			0.2940	0.2420	0.5970
NGFG_06030	-0.3770	0.1010	0.3790	-0.3710	0.1070	0.4170	0.7100	0.0022	0.0363
NGFG_06032	-0.3790	0.1250	0.4130	-0.9000	0.0003	0.0221	0.8460	0.0006	0.0145
NGFG_06033	-1.3100	0.0000	0.0000	-1.2700	0.0000	0.0000	1.7200	0.0000	0.0000
NGFG_06034	#NV			#NV			0.1190	0.4820	0.7880
NGFG_06035	-0.3430	0.1290	0.4220	-0.8740	0.0001	0.0149	0.7050	0.0018	0.0315
NGFG_06036	#NV			#NV			0.1040	0.5330	0.8150
NGFG_06037	-0.2120	0.3990	0.7100	#NV			-0.0773	0.7570	0.9200
NGFG_06038	-0.0200	0.9370	0.9800	#NV			-0.0097	0.9700	0.9940
NGFG_06039	#NV			#NV			-0.1290	0.4660	0.7800
NGFG_06040	-0.1340	0.5710	0.8160	#NV			0.3710	0.1160	0.4110
NGFG_06041	0.2120	0.3550	0.6700	0.1440	0.5300	0.8080	-0.0225	0.9220	0.9780
NGFG_06042	-0.0202	0.9330	0.9790	#NV			-0.0412	0.8620	0.9620
NGFG_06044	-0.3340	0.1260	0.4160	-0.7850	0.0003	0.0237	0.6930	0.0015	0.0277
NGFG_06045	#NV			#NV			0.0210	0.7010	0.9010
NGFG_06046	#NV			#NV			0.1690	0.3240	0.6700
NGFG_06047	-0.2840	0.1820	0.4870	-0.7350	0.0006	0.0294	0.6090	0.0042	0.0579
NGFG_06048	-0.1750	0.4430	0.7380	-0.1240	0.5860	0.8410	0.6790	0.0030	0.0453
NGFG_06049	-0.4380	0.0856	0.3510	#NV			0.4630	0.0696	0.3230
NGFG_06050	-0.2170	0.3840	0.6980	#NV			0.4990	0.0455	0.2550
NGFG_06051	-0.1350	0.5780	0.8160	#NV			0.3220	0.1830	0.5340
NGFG_06052	#NV			#NV			-0.0021	0.9750	0.9940
NGFG_06053	0.2050	0.4160	0.7200	#NV			-0.2540	0.3130	0.6610
NGFG_06054	#NV			#NV			0.0669	0.6040	0.8550
NGFG_06056	-0.0487	0.8360	0.9360	0.0108	0.9630	0.9940	0.1470	0.5290	0.8130
NGFG_06058	-0.3700	0.1380	0.4360	-0.8940	0.0003	0.0237	0.8790	0.0004	0.0113

NGFG_06059	-1.2900	0.0000	0.0000	-1.4600	0.0000	0.0000	1.8000	0.0000	0.0000
NGFG_06060	#NV			#NV			0.2280	0.1720	0.5170
NGFG_06061	-0.3090	0.1650	0.4710	-0.8160	0.0002	0.0221	0.6650	0.0028	0.0441
NGFG_06062	0.0724	0.7280	0.9000	0.0949	0.6490	0.8670	0.0634	0.7610	0.9220
NGFG_06063	-0.2390	0.3230	0.6380	#NV			0.2470	0.3110	0.6610
NGFG_06065	-0.3940	0.1170	0.4020	#NV			0.5060	0.0442	0.2510
NGFG_06066	#NV			#NV			0.1680	0.2080	0.5660
NgncR_001	0.6710	0.0072	0.1110	#NV			0.2330	0.3570	0.7000
NgncR_002	-0.2110	0.2040	0.5130	-0.0075	0.9640	0.9940	0.1290	0.4330	0.7600
NgncR_003	-0.0415	0.8000	0.9210	-0.0373	0.8200	0.9500	-0.0406	0.8030	0.9370
NgncR_004	-0.3100	0.1060	0.3870	-0.2660	0.1650	0.4920	0.3870	0.0431	0.2500
NgncR_005	0.2130	0.1520	0.4550	0.0212	0.8870	0.9770	-0.4430	0.0026	0.0419
NgncR_006	-0.4130	0.0473	0.2700	-0.2990	0.1500	0.4720	0.4820	0.0204	0.1610
NgncR_008	-0.2840	0.0598	0.2920	-0.1180	0.4290	0.7550	0.1960	0.1880	0.5390
NgncR_009	-0.1020	0.6900	0.8790	#NV			0.0032	0.9900	0.9980
NgncR_010	-0.1400	0.5670	0.8160	#NV			0.2730	0.2650	0.6190
NgncR_011	#NV			#NV			-0.0045	0.9630	0.9940
NgncR_012	-0.0070	0.9750	0.9940	-0.0772	0.7290	0.9080	0.3520	0.1170	0.4110
NgncR_014	-0.1820	0.4370	0.7320	-0.0707	0.7620	0.9230	0.2340	0.3150	0.6640
NgncR_015	0.2760	0.1700	0.4750	0.2010	0.3170	0.6750	0.3060	0.1280	0.4340
NgncR_018	0.0759	0.7490	0.9050	0.2260	0.3390	0.6910	0.1990	0.4020	0.7370
NgncR_020	#NV			#NV			0.1720	0.2370	0.5960
NgncR_022	0.4210	0.0552	0.2890	0.6170	0.0046	0.1110	-0.1880	0.3930	0.7310
NgncR_023	#NV			#NV			0.1440	0.5000	0.7980
NgncR_024	0.5590	0.0081	0.1160	0.5250	0.0128	0.1760	-0.1390	0.5130	0.8020
NgncR_027	-0.1690	0.4490	0.7460	#NV			-0.0003	0.9990	1.0000
NgncR_032	#NV			#NV			0.0393	0.8650	0.9620
NgncR_033	-0.0188	0.9280	0.9760	0.2000	0.3280	0.6870	0.1830	0.3750	0.7210
NgncR_036	-0.0598	0.8090	0.9260	-0.0027	0.9910	0.9990	0.3940	0.1130	0.4030
NgncR_037	#NV			#NV			0.0439	0.6860	0.8970
NgncR_038	#NV			#NV			0.5360	0.0127	0.1170
NgncR_044	0.3020	0.0464	0.2700	0.2660	0.0803	0.3640	-0.0964	0.5260	0.8120
NgncR_045	-0.0759	0.7610	0.9100	#NV			0.0377	0.8800	0.9650
NgncR_047	-0.3930	0.1220	0.4080	#NV			0.5980	0.0188	0.1510
NgncR_049	#NV			#NV			0.0873	0.6650	0.8870
NgncR_053	-0.1960	0.4240	0.7230	#NV			0.7010	0.0045	0.0603
NgncR_054	#NV			#NV			0.1600	0.4370	0.7610
NgncR_055	0.3230	0.1930	0.5000	#NV			0.1960	0.4260	0.7560
NgncR_057	-0.4770	0.0199	0.1850	-0.3660	0.0725	0.3550	0.0597	0.7660	0.9240
NgncR_059	0.3630	0.1190	0.4040	#NV			-0.5990	0.0091	0.0938
NgncR_060	0.2230	0.2120	0.5230	0.1980	0.2690	0.6230	-0.0520	0.7710	0.9240
NgncR_062	0.1120	0.5310	0.7960	0.1290	0.4700	0.7850	-0.0963	0.5890	0.8450
NgncR_063	0.0780	0.5790	0.8160	0.1070	0.4450	0.7680	0.0072	0.9590	0.9940
NgncR_064	0.4130	0.0012	0.0450	0.3390	0.0079	0.1430	-0.0186	0.8840	0.9670
NgncR_065	0.1100	0.6400	0.8470	#NV			-0.0588	0.8010	0.9370
NgncR_066	0.0875	0.6400	0.8470	0.1630	0.3830	0.7270	-0.2450	0.1880	0.5390
NgncR_068	0.2140	0.2660	0.5910	0.4270	0.0250	0.2330	0.2450	0.2090	0.5660

NgncR_070	0.4960	0.0057	0.0983	0.4540	0.0115	0.1670	-0.4740	0.0083	0.0887
NgncR_072	0.2530	0.1070	0.3870	0.2110	0.1780	0.5010	0.3840	0.0167	0.1390
NgncR_073	0.2560	0.2900	0.6070	#NV			-0.0962	0.6910	0.8970
NgncR_075	0.0826	0.6310	0.8420	0.0418	0.8080	0.9470	0.0563	0.7430	0.9140
NgncR_076	-0.1220	0.6250	0.8360	#NV			0.3050	0.2220	0.5840
NgncR_077	0.1490	0.5030	0.7800	0.1680	0.4480	0.7680	0.2300	0.3040	0.6540
NgncR_078-Y2	-0.0167	0.9460	0.9830	#NV			0.1220	0.6180	0.8630
NgncR_079	-0.2370	0.3430	0.6600	#NV			0.1760	0.4830	0.7890
NgncR_082	0.2410	0.2020	0.5100	0.1340	0.4760	0.7870	0.1290	0.4960	0.7960
NgncR_088	#NV			#NV			0.0647	0.5830	0.8390
NgncR_089	#NV			#NV			0.0892	0.3310	0.6780
NgncR_093	0.3090	0.2260	0.5390	#NV			-0.0251	0.9220	0.9780
NgncR_094	#NV			#NV			0.2820	0.1210	0.4230
NgncR_095	-0.0291	0.8970	0.9600	-0.0503	0.8240	0.9500	0.5820	0.0109	0.1070
NgncR_096	#NV			#NV			0.0308	0.8370	0.9520
NgncR_097	#NV			#NV			0.0863	0.6650	0.8870
NgncR_098	-0.0638	0.8030	0.9240	#NV			0.4610	0.0704	0.3250
NgncR_099	-0.1070	0.6660	0.8650	#NV			0.2700	0.2790	0.6310
NgncR_100	0.3570	0.0675	0.3150	0.3430	0.0792	0.3640	-0.2140	0.2730	0.6260
NgncR_101	0.1150	0.3120	0.6290	0.0724	0.5250	0.8040	0.1910	0.0937	0.3670
NgncR_102	0.1820	0.3270	0.6420	0.2450	0.1850	0.5120	0.0546	0.7690	0.9240
NgncR_105	-0.2490	0.2780	0.6010	-0.3870	0.0915	0.3920	0.4260	0.0634	0.3100
NgncR_106	0.0348	0.8900	0.9590	#NV			0.3770	0.1330	0.4430
NgncR_107	-0.2350	0.3500	0.6680	#NV			0.2210	0.3800	0.7230
NgncR_109	-0.0606	0.7750	0.9120	#NV			0.2240	0.2900	0.6410
NgncR_110	0.1340	0.5770	0.8160	#NV			0.3700	0.1250	0.4280
NgncR_112	-0.4280	0.0874	0.3530	#NV			0.3070	0.2180	0.5800
NgncR_113	#NV			#NV			0.0274	0.7620	0.9230
NgncR_114	-0.0013	0.9960	0.9980	#NV			0.0956	0.6980	0.8980
NgncR_115	-0.2250	0.2800	0.6010	-0.1150	0.5810	0.8370	0.2250	0.2790	0.6310
NgncR_117	0.0473	0.8290	0.9350	0.1300	0.5520	0.8190	0.0429	0.8440	0.9550
NgncR_118	-0.0498	0.7610	0.9100	-0.0135	0.9340	0.9850	0.4960	0.0025	0.0409
NgncR_119	0.2410	0.1710	0.4750	0.1150	0.5130	0.8000	0.3420	0.0531	0.2760
NgncR_120	#NV			#NV			0.0434	0.8410	0.9530
NgncR_121	-0.0369	0.8740	0.9510	-0.0355	0.8780	0.9740	0.1980	0.3940	0.7310
NgncR_122	-0.2180	0.3920	0.7070	#NV			0.4460	0.0801	0.3450
NgncR_125	#NV			#NV			0.0901	0.3200	0.6660
NgncR_126	-0.3140	0.2140	0.5250	#NV			0.6690	0.0082	0.0877
NgncR_127	-0.2310	0.3630	0.6770	#NV			0.3220	0.2060	0.5640
NgncR_128	-0.2510	0.2790	0.6010	0.0258	0.9110	0.9820	0.4530	0.0507	0.2720
NgncR_129	-0.3590	0.0586	0.2920	-0.3710	0.0504	0.3080	0.4260	0.0245	0.1810
NgncR_130	-0.5740	0.0197	0.1850	#NV			0.4810	0.0526	0.2750
NgncR_131	#NV			#NV			-0.0018	0.9770	0.9940
NgncR_133	#NV			#NV			0.1900	0.1340	0.4450
NgncR_136	-0.5670	0.0258	0.2140	#NV			0.8450	0.0009	0.0185
NgncR_137	0.1650	0.4020	0.7110	0.0085	0.9660	0.9950	0.0622	0.7530	0.9180
NgncR_140	0.2960	0.1680	0.4730	0.2160	0.3150	0.6730	0.2440	0.2560	0.6120

NgncR_144	#NV			#NV			0.1190	0.4050	0.7390
NgncR_147	-0.0401	0.8560	0.9460	-0.0184	0.9340	0.9850	0.1090	0.6230	0.8650
NgncR_148	0.2670	0.1620	0.4670	0.2490	0.1920	0.5200	0.0924	0.6280	0.8680
NgncR_152	-0.0275	0.8900	0.9590	-0.1910	0.3390	0.6910	0.3390	0.0903	0.3620
NgncR_154	#NV			#NV			0.0796	0.6710	0.8890
NgncR_155	0.2910	0.1100	0.3910	0.5050	0.0051	0.1150	-0.2220	0.2210	0.5830
NgncR_156	0.1630	0.3450	0.6620	0.2600	0.1320	0.4530	-0.0126	0.9420	0.9880
NgncR_161	0.0314	0.8990	0.9610	#NV			0.1280	0.6050	0.8550
NgncR_162	#NV			#NV			-0.0554	0.7360	0.9110
NgncR_163	0.4710	0.0448	0.2690	#NV			-0.8840	0.0002	0.0073
NgncR_164	#NV			#NV			0.0294	0.8530	0.9570
NgncR_165	-0.0888	0.6930	0.8800	-0.0440	0.8450	0.9600	0.0265	0.9060	0.9720
NgncR_166	#NV			#NV			0.5550	0.0077	0.0843
NgncR_167	-0.1150	0.6170	0.8310	#NV			0.1310	0.5690	0.8370
NgncR_169	#NV			#NV			0.1170	0.3870	0.7260
NgncR_173	-0.2900	0.2190	0.5320	#NV			0.3670	0.1210	0.4230
NgncR_176	-0.1460	0.5580	0.8120	#NV			0.2940	0.2400	0.5970
NgncR_177	0.1310	0.6010	0.8240	#NV			0.0801	0.7500	0.9160
NgncR_179	0.4430	0.0784	0.3380	0.5490	0.0291	0.2510	-0.0993	0.6940	0.8970
NgncR_180	#NV			#NV			-0.0172	0.9150	0.9760
NgncR_181	-0.1670	0.4180	0.7210	0.0219	0.9150	0.9820	0.2520	0.2200	0.5830
NgncR_182	0.1410	0.5010	0.7790	0.1280	0.5410	0.8120	0.2800	0.1830	0.5340
NgncR_184	-0.5020	0.0294	0.2310	-0.2980	0.1940	0.5240	0.2390	0.2950	0.6470
NgncR_185	#NV			#NV			-0.0100	0.8380	0.9520
NgncR_186	#NV			#NV			0.2620	0.2270	0.5880
NgncR_189	0.2060	0.4130	0.7190	#NV			-0.1710	0.4970	0.7960
NgncR_191	-0.7990	0.0017	0.0523	#NV			0.9860	0.0001	0.0042
NgncR_193	-0.1990	0.2220	0.5340	-0.2140	0.1880	0.5160	0.1780	0.2710	0.6250
NgncR_198	-0.3710	0.1170	0.4020	#NV			0.3010	0.2080	0.5660
NgncR_199	-0.3740	0.1420	0.4410	#NV			0.9360	0.0002	0.0076
NgncR_200	-0.0999	0.6180	0.8310	-0.0013	0.9950	0.9990	-0.1950	0.3190	0.6660
NgncR_201	-0.8830	0.0002	0.0160	-1.1700	0.0000	0.0002	1.5500	0.0000	0.0000
NgncR_203	#NV			#NV			0.0721	0.6930	0.8970
NgncR_205	0.1890	0.2220	0.5340	0.2730	0.0770	0.3640	-0.0769	0.6190	0.8640
NgncR_206	-0.2420	0.3180	0.6340	-0.0171	0.9440	0.9890	0.5540	0.0227	0.1730
NgncR_207	-0.3360	0.1810	0.4870	#NV			0.0281	0.9100	0.9740
NgncR_209	0.1410	0.5630	0.8160	#NV			-0.1890	0.4410	0.7640
NgncR_210	-0.2370	0.2560	0.5800	-0.1610	0.4390	0.7650	0.7850	0.0002	0.0064
NgncR_211	#NV			#NV			-0.0508	0.5230	0.8090
NgncR_212	#NV			#NV			-0.1360	0.5060	0.8000
NgncR_213	#NV			#NV			-0.0208	0.7670	0.9240
NgncR_214	0.4690	0.0032	0.0769	0.3930	0.0135	0.1810	-0.0808	0.6110	0.8590
NgncR_218	-0.3050	0.2280	0.5400	#NV			0.2240	0.3770	0.7220
NgncR_221	-0.4770	0.0613	0.2960	#NV			0.2480	0.3310	0.6780
NgncR_223	0.0998	0.5900	0.8190	0.3050	0.0981	0.4020	0.0900	0.6280	0.8680
NgncR_224	-0.3410	0.1810	0.4870	#NV			0.2060	0.4190	0.7510
NgncR_225	0.1510	0.4840	0.7670	0.2330	0.2800	0.6340	0.1030	0.6320	0.8690

NgncR_227	0.2900	0.0933	0.3680	0.2570	0.1370	0.4640	-0.3110	0.0707	0.3250
NgncR_229	0.4350	0.0304	0.2320	0.3830	0.0568	0.3230	0.2270	0.2630	0.6190
NgncR_230-	#NV			#NV			-0.0100	0.8380	0.9520
NgncR_231	0.1920	0.4140	0.7190	0.2310	0.3250	0.6830	0.1520	0.5180	0.8040
NgncR_232	0.3180	0.1710	0.4750	0.2510	0.2800	0.6340	0.3350	0.1520	0.4770
NgncR_236	0.8270	0.0001	0.0110	0.5660	0.0086	0.1430	-0.3000	0.1660	0.5070
NgncR_237	0.2800	0.0398	0.2570	0.2690	0.0490	0.3040	-0.2370	0.0823	0.3500
NgncR_238	0.0541	0.7710	0.9110	-0.2000	0.2820	0.6350	-0.2070	0.2630	0.6190
NgncR_239	0.0823	0.7340	0.9000	#NV			0.1740	0.4730	0.7850
NgncR_241	#NV			#NV			-0.0089	0.9500	0.9910
NgncR_242	-0.0651	0.7680	0.9110	-0.0659	0.7660	0.9240	-0.0067	0.9760	0.9940
NgncR_247	0.2470	0.1110	0.3930	0.3620	0.0189	0.2070	0.0331	0.8310	0.9520
NgncR_249	-0.0311	0.8510	0.9450	0.1760	0.2870	0.6400	0.1710	0.3010	0.6510
NgncR_250	-0.4650	0.0167	0.1680	-0.5670	0.0036	0.0979	0.9120	0.0000	0.0002
NgncR_251	#NV			#NV			0.0206	0.8910	0.9700

Table A.3: Composition of chemically defined media [g/l]

	Hepes	RPMI	Graver-Wade	CDM-10
Inorganic salts				
$CaCl_2$ x $2H_2O$	0.01128	-	0.1333	0.02775
$Ca(NO_3)_2$	-	0.1	-	-
$FeCl_3$	-	-	-	-
$Fe(NO_3)_3$ x 9 H_2O	0.004	-	0.0005	0.004
KCl	-	0.4	0.2667	-
KH_2PO_4	-	-	-	0.272
K_2HPO_4	-	-	-	0.348
$MgCl_2$ x 7 H_2O	0.5	-	-	0.02
$MgSO_4$	-	0.1	0.0645	-
K_2SO_4	-	-	-	1.0
Na-acetate	3.4	-	0.7	-
$(NH_4)HCO_3$	-	-	1.3333	-
$(NH_4)Cl$	-	-	-	0.22
$NaHCO_3$	-	2	-	0.168
NaCl	5	5.5	4.5333	5.845
Na_2HPO_4	-	0.8	-	-
NaH_2PO_4	-	-	0.0813	-
Na_2EDTA	-	-	-	0.003
Amino acids				
L-alanine	0.1	-	0.0167	0.1
L-alanyl-glutamine	-	0.446	-	-
L-arginine	0.15	0.2	0.1133	0.15
L-asparagine	0.025	0.05	-	0.025
L-aspartic acid	-	0.02	0.02	0.5
L-cystine	0.036	0.05	0.0001	0.035
L-cysteine	0.061	-	0.0173	0.055
L-glutamic acid	-	0.02	0.0445	1.3
L-glutamine	0.05	-	0.5	0.05
Glycine	0.025	0.01	0.0333	0.025
L-histidine	0.018	0.015	0.0146	0.025
Hydroxy-L-proline	-	0.02	0.0067	-
L-isoleucine	-	0.05	0.0133	0.03
L-leucine	-	0.05	0.04	0.09
L-lysine	0.05	0.04	0.0467	0.05

L-methionine	0.015	0.015	0.01	0.015
L-phenylalanine	-	0.015	0.0167	0.025
L-ornithine	-	-	0.0067	-
L-proline	0.05	0.02	0.0267	0.05
L-serine	0.05	0.03	0.0167	0.05
L-threonine	0.05	0.02	0.02	0.05
L-tryptophan	-	0.005	0.0067	0.08
L-tyrosine	-	0.02	0.0384	0.07
L-valine	-	0.02	0.0167	0.06
Vitamins				
Ascorbic acid	-	-	0.0004	-
D-Biotin	0.004	0.0002	0.00001	0.003
Calciferol	-	-	0.0001	-
Choline chloride	-	0.003	0.0003	-
Cobalamin	-	0.000005	-	-
Folic acid	-	0.001	0.00001	-
Inositol	-	0.035	0.00003	-
Menadion	-	-	0.00001	-
Nicotinamide	-	0.001	0.00002	-
NAD	0.00825	-	0.0067	-
Nicotinic acid	-	-	0.00002	-
p-Amino benzoic acid	-	0.001	0.00003	-
Pantothenic acid	0.00825	0.00025	0.00001	0.0019
Pyridoxal x HCl	-	-	0.00002	-
Pyridoxine x HCl	-	0.001	0.00002	-
Retinyl acetate	-	-	0.0001	-
Riboflavin	-	0.0002	0.00001	-
DL-Tocopherol phosphate	-	-	0.00001	-
Thiamine x HCl	0.00825	0.001	0.0333	0.002
Thiaminepyrophosphate	0.00825	-	-	0.0005
Others				
Adenine sulfate	-	-	0.0067	-
Adenosine triphosphate	-	-	0.0007	-
Adenosine monophosphate	-	-	0.0002	-
Cholesterol	-	-	0.0001	-
Deoxyribose	-	-	0.0003	-
Glucose	7.5	2	7.3333	5
Gluthation (red.)	0.046	0.001	0.00003	0.025
Glycerol	0.91968	-	-	-
Guanine	-	-	0.0002	-
HEPES	2.38	5.985	-	10
Hypoxanthine	0.003245	-	0.0335	0.05
Na-lactate	0.2502	-	1	-
Oxalacetate	0.0825	-	0.0333	-
Phenol red	-	0.005	-	-
Ribose	-	-	0.0003	-
Spermidine	-	-	0.1333	-
Thymine	-	-	0.0002	-
TWEEN 80	-	-	0.0133	-
Uracil	0.008	-	0.0335	0.05
Xanthine	-	-	0.0002	-

Table A.4: TargetRNA2 Screen of NgncR_237 on *N. gonorrhoeae* FA1090

Rank	Gene	Energy	p-value	sRNA start	sRNA stop	mRNA start	mRNA stop
1	NGO2088	-21.57	0.000	79	93	-55	-41
2	NGO0484	-17.41	0.000	66	86	-17	4
3	NGO1111	-17.41	0.000	66	86	-17	4
4	NGO0759	-17.4	0.000	76	93	2	19
5	NGO1088	-17.25	0.000	67	83	-80	-66
6	NGO1325	-16.79	0.000	80	92	6	18
7	NGO0632	-16.63	0.000	80	93	-59	-46
8	NGO0368	-16.53	0.000	77	92	-40	-25
9	NGO0979	-16.29	0.000	78	93	-45	-28
10	NGO0187	-16.09	0.000	78	88	-9	2
11	NGO0083	-15.63	0.000	80	96	-78	-62
12	NGO0783	-15.46	0.000	50	65	-12	4
13	NGO2070	-14.68	0.001	79	93	-36	-21
14	NGO0578	-13.82	0.002	80	93	2	16
15	NGO2160	-13.63	0.002	80	92	-22	-10
16	NGO1632	-13.54	0.002	78	98	-4	16
17	NGO0611	-13.32	0.003	81	93	-52	-40
18	NGO1819	-13.18	0.003	78	93	-49	-35
19	NGO0265	-13.18	0.003	76	91	1	16
20	NGO1521	-13.06	0.004	57	72	-51	-36
21	NGO0063	-12.6	0.005	63	72	-78	-69
22	NGO1800	-12.52	0.005	78	92	-33	-18
23	NGO1767	-12.51	0.005	80	95	-49	-35
24	NGO0364	-12.21	0.007	42	52	-11	-1
25	NGO0481	-11.8	0.009	78	98	-4	16
26	NGO1113	-11.8	0.009	78	98	-4	16
27	NGO0765	-11.74	0.009	58	73	-71	-57
28	NGO2116	-11.51	0.010	80	93	-24	-10
29	NGO2078	-11.43	0.011	59	72	-56	-43
30	NGO1976	-11.16	0.013	57	72	-76	-61
31	NGO0605	-11.13	0.013	58	72	-44	-30
32	NGO2124	-11.13	0.013	76	95	-13	8
33	NGO1376	-11.07	0.013	57	72	-21	-7
34	NGO0798	-11.01	0.014	80	92	-49	-38
35	NGO1189	-10.9	0.015	79	93	-71	-59
36	NGO0173	-10.82	0.015	80	98	-30	-14
37	NGO0226	-10.71	0.016	75	88	-66	-52
38	NGO2077	-10.7	0.016	56	73	-1	17
39	NGO1337	-10.56	0.018	80	96	2	17
40	NGO0419	-10.51	0.018	80	91	-35	-24
41	NGO1220	-10.49	0.018	63	72	-55	-46
42	NGO0257	-10.45	0.019	74	88	-21	-7
43	NGO1598	-10.15	0.022	43	54	-29	-18
44	NGO1475	-9.89	0.025	64	76	-16	-4
45	NGO0491	-9.86	0.025	65	80	-80	-61
46	NGO1056	-9.27	0.033	66	80	-22	-8
47	NGO1565	-9.16	0.035	63	72	-68	-59
48	NGO1942	-9.1	0.036	58	73	-74	-59
49	NGO0500	-8.94	0.038	79	94	-62	-47
50	NGO1237	-8.85	0.040	52	66	-75	-61
51	NGO1047	-8.7	0.042	49	65	-12	5
52	NGO0530	-8.67	0.043	80	93	-28	-14
53	NGO1754	-8.67	0.043	85	99	3	18
54	NGO0138	-8.65	0.043	63	72	-46	-37
55	NGO0319	-8.64	0.043	63	72	-15	-6
56	NGO1704	-8.61	0.044	80	99	-4	17

Table A.5: Complete list of the results of the RNAseq screen on Δ237 237AlE versus Δ237

Locus Tag	logFC	p-value	Adjusted p-value	Locus Tag	logFC	p-value	Adjusted p-value
NGFG_00001	0.1040	0.6220	0.9140	NGFG_00058	-0.0633	0.7470	0.9560
NGFG_00002	0.3340	0.0868	0.5030	NGFG_00062	-0.1200	0.4350	0.8540
NGFG_00003	0.3110	0.2200	0.7080	NGFG_00063	-0.2390	0.2110	0.6930
NGFG_00006	0.0128	0.9580	0.9960	NGFG_00064	-0.0855	0.4330	0.8530
NGFG_00007	0.2310	0.3570	0.8020	NGFG_00065	-0.0049	0.9730	0.9960
NGFG_00008	0.2840	0.2590	0.7410	NGFG_00067	-0.3100	0.0383	0.3830
NGFG_00009	0.0070	0.9780	0.9960	NGFG_00068	-0.2720	0.2360	0.7210
NGFG_00010	0.3450	0.1650	0.6280	NGFG_00069	-0.4050	0.0164	0.2740
NGFG_00014	-0.2700	0.1270	0.5710	NGFG_00070	-0.2240	0.1110	0.5490
NGFG_00017	0.0201	0.8800	0.9810	NGFG_00071	-0.1060	0.5050	0.8760
NGFG_00018	-0.2050	0.2110	0.6930	NGFG_00072	-0.0312	0.8130	0.9720
NGFG_00021	0.1170	0.5140	0.8780	NGFG_00073	-0.1050	0.4930	0.8700
NGFG_00022	-0.1160	0.5920	0.9080	NGFG_00074	-0.0598	0.6550	0.9230
NGFG_00023	-0.0664	0.6650	0.9240	NGFG_00075	-0.1410	0.3600	0.8020
NGFG_00024	-0.1540	0.4370	0.8540	NGFG_00076	-0.3480	0.0758	0.4850
NGFG_00025	-0.2700	0.0250	0.3370	NGFG_00077	-0.0772	0.6760	0.9300
NGFG_00027	0.1760	0.4630	0.8640	NGFG_00078	-0.0676	0.5770	0.9010
NGFG_00028	-0.0680	0.6440	0.9210	NGFG_00081	0.4900	0.0248	0.3370
NGFG_00029	-0.1930	0.1600	0.6220	NGFG_00082	0.4720	0.0282	0.3410
NGFG_00030	0.1130	0.5390	0.8860	NGFG_00083	0.1470	0.2100	0.6930
NGFG_00031	-0.0652	0.5470	0.8870	NGFG_00084	-0.0344	0.8560	0.9740
NGFG_00032	0.1830	0.3870	0.8180	NGFG_00085	-0.0203	0.9240	0.9920
NGFG_00033	0.2550	0.0068	0.1820	NGFG_00087	-0.1710	0.2280	0.7170
NGFG_00034	-0.0662	0.6520	0.9210	NGFG_00088	0.0973	0.5100	0.8780
NGFG_00035	0.1240	0.5070	0.8760	NGFG_00089	-0.0072	0.9650	0.9960
NGFG_00036	-0.1760	0.4690	0.8640	NGFG_00091	-0.0791	0.5530	0.8900
NGFG_00037	-0.1550	0.3810	0.8140	NGFG_00092	0.1870	0.2590	0.7410
NGFG_00038	-0.2370	0.1290	0.5740	NGFG_00093	0.0050	0.9660	0.9960
NGFG_00039	0.0140	0.9480	0.9960	NGFG_00094	0.1030	0.5410	0.8860
NGFG_00041	-0.1560	0.2670	0.7510	NGFG_00095	-0.2580	0.0032	0.1420
NGFG_00042	-0.0845	0.6330	0.9200	NGFG_00097	-0.0347	0.8810	0.9810
NGFG_00043	0.3480	0.0462	0.4100	NGFG_00098	0.0909	0.5250	0.8830
NGFG_00044	0.1280	0.4630	0.8640	NGFG_00099	0.1040	0.5820	0.9030
NGFG_00045	0.2530	0.1380	0.5970	NGFG_00100	0.2640	0.1110	0.5490
NGFG_00046	0.1870	0.3510	0.8020	NGFG_00101	0.2090	0.1180	0.5560
NGFG_00048	-0.0755	0.5450	0.8860	NGFG_00102	0.1720	0.1680	0.6330
NGFG_00049	-0.0554	0.8100	0.9720	NGFG_00103	0.1410	0.2120	0.6930
NGFG_00050	0.1960	0.3150	0.7770	NGFG_00104	0.2040	0.2190	0.7070
NGFG_00051	0.3220	0.0811	0.5020	NGFG_00105	0.2560	0.1290	0.5740
NGFG_00052	-0.1160	0.4380	0.8540	NGFG_00106	-0.1390	0.3730	0.8080
NGFG_00054	-0.1140	0.4380	0.8540	NGFG_00107	-0.1250	0.4360	0.8540
NGFG_00055	0.1870	0.3410	0.7940	NGFG_00109	-0.0616	0.6600	0.9240
NGFG_00056	0.0273	0.8380	0.9730	NGFG_00110	-0.1500	0.2320	0.7210

NGFG_00116	-0.0774	0.5220	0.8830	NGFG_00178	0.0900	0.6970	0.9350
NGFG_00117	-0.0173	0.9310	0.9950	NGFG_00180	-0.1240	0.2500	0.7350
NGFG_00118	-0.0194	0.8860	0.9820	NGFG_00181	-0.0284	0.8640	0.9750
NGFG_00119	-0.0523	0.8070	0.9720	NGFG_00182	0.1670	0.4250	0.8490
NGFG_00120	-0.1240	0.4960	0.8700	NGFG_00183	0.2470	0.2600	0.7410
NGFG_00121	-0.2650	0.0504	0.4150	NGFG_00184	-0.1840	0.2870	0.7660
NGFG_00124	-0.0041	0.9820	0.9960	NGFG_00186	-0.3650	0.0107	0.2150
NGFG_00125	-0.0617	0.6960	0.9350	NGFG_00187	-0.1210	0.5660	0.8980
NGFG_00126	-0.1500	0.2130	0.6940	NGFG_00189	-0.0809	0.6030	0.9080
NGFG_00127	0.2740	0.2110	0.6930	NGFG_00190	0.1120	0.6260	0.9150
NGFG_00128	0.2260	0.1330	0.5830	NGFG_00192	-0.0403	0.8580	0.9740
NGFG_00129	0.0933	0.6130	0.9120	NGFG_00193	0.0547	0.7340	0.9490
NGFG_00130	0.2780	0.0249	0.3370	NGFG_00194	-0.1350	0.4390	0.8540
NGFG_00131	0.0568	0.5170	0.8800	NGFG_00195	-0.0254	0.8680	0.9760
NGFG_00133	-0.1420	0.4980	0.8710	NGFG_00196	-0.0569	0.7260	0.9460
NGFG_00134	-0.3500	0.0072	0.1830	NGFG_00197	0.0070	0.9540	0.9960
NGFG_00135	0.2760	0.2750	0.7560	NGFG_00199	0.0466	0.8050	0.9720
NGFG_00137	-0.1260	0.4480	0.8580	NGFG_00200	-0.0777	0.4620	0.8640
NGFG_00138	0.0461	0.6470	0.9210	NGFG_00203	-0.0240	0.8560	0.9740
NGFG_00139	-0.0399	0.8440	0.9730	NGFG_00204	0.0165	0.8340	0.9730
NGFG_00140	0.0245	0.9060	0.9870	NGFG_00207	-0.0696	0.6960	0.9350
NGFG_00143	-0.0607	0.7200	0.9450	NGFG_00208	-0.0973	0.3590	0.8020
NGFG_00149	-0.0611	0.7700	0.9600	NGFG_00209	-0.2050	0.2590	0.7410
NGFG_00152	-0.1050	0.5310	0.8830	NGFG_00214	-0.2350	0.0173	0.2810
NGFG_00153	-0.1870	0.1860	0.6520	NGFG_00217	0.2340	0.3590	0.8020
NGFG_00154	-0.2210	0.3540	0.8020	NGFG_00218	-0.2460	0.1130	0.5520
NGFG_00155	-0.0063	0.9630	0.9960	NGFG_00219	-0.2750	0.0562	0.4290
NGFG_00156	-0.0116	0.9580	0.9960	NGFG_00220	-0.2150	0.1420	0.6000
NGFG_00157	-0.0587	0.6980	0.9350	NGFG_00221	-0.2660	0.0782	0.4920
NGFG_00158	-0.3090	0.0919	0.5120	NGFG_00222	-0.3430	0.0407	0.3870
NGFG_00159	0.0035	0.9880	0.9960	NGFG_00223	-0.2160	0.0955	0.5140
NGFG_00160	-0.0302	0.8900	0.9820	NGFG_00224	-0.1710	0.2940	0.7700
NGFG_00161	-0.1050	0.4600	0.8640	NGFG_00225	-0.1080	0.6310	0.9200
NGFG_00162	-0.4190	0.0005	0.0547	NGFG_00226	0.0215	0.9240	0.9920
NGFG_00163	-0.3890	0.0682	0.4700	NGFG_00227	0.0149	0.8990	0.9840
NGFG_00164	-0.0698	0.6880	0.9340	NGFG_00230	-0.0726	0.7020	0.9350
NGFG_00165	-0.1390	0.2920	0.7700	NGFG_00231	-0.3530	0.0102	0.2100
NGFG_00166	0.1750	0.4340	0.8530	NGFG_00232	-0.1120	0.5030	0.8760
NGFG_00167	-0.1180	0.5660	0.8980	NGFG_00233	-0.3050	0.0303	0.3540
NGFG_00169	-0.1890	0.0773	0.4910	NGFG_00234	-0.3090	0.0861	0.5030
NGFG_00170	-0.3340	0.0522	0.4150	NGFG_00235	-0.1840	0.2310	0.7210
NGFG_00171	-0.2280	0.0366	0.3710	NGFG_00236	-0.0738	0.6690	0.9280
NGFG_00172	0.0524	0.7790	0.9650	NGFG_00237	0.3310	0.0088	0.1920
NGFG_00174	-0.0614	0.5250	0.8830	NGFG_00238	0.0585	0.6980	0.9350
NGFG_00175	0.0086	0.9540	0.9960	NGFG_00239	-0.0615	0.7420	0.9540
NGFG_00176	0.1290	0.5410	0.8860	NGFG_00240	0.0724	0.4920	0.8700
NGFG_00177	-0.1000	0.5830	0.9040	NGFG_00241	0.2300	0.0164	0.2740

NGFG_00242	0.1580	0.3260	0.7810	NGFG_00306	-0.0488	0.8390	0.9730
NGFG_00243	0.0572	0.6950	0.9350	NGFG_00307	-0.3680	0.0158	0.2740
NGFG_00245	-0.0087	0.9540	0.9960	NGFG_00308	0.0029	0.9880	0.9960
NGFG_00246	-0.0918	0.5120	0.8780	NGFG_00309	0.0890	0.5650	0.8980
NGFG_00247	-0.0644	0.7570	0.9570	NGFG_00310	-0.1390	0.3560	0.8020
NGFG_00249	0.5900	0.0037	0.1520	NGFG_00311	-0.2060	0.3660	0.8060
NGFG_00250	-0.3040	0.2310	0.7210	NGFG_00313	-0.4140	0.0076	0.1850
NGFG_00251	-0.3070	0.0826	0.5020	NGFG_00314	-0.2940	0.0120	0.2320
NGFG_00252	-0.4620	0.0001	0.0268	NGFG_00316	0.0323	0.8400	0.9730
NGFG_00253	0.0439	0.8330	0.9730	NGFG_00317	-0.1460	0.5660	0.8980
NGFG_00254	-0.2150	0.1460	0.6100	NGFG_00318	-0.2280	0.0962	0.5140
NGFG_00255	-0.2970	0.0087	0.1920	NGFG_00319	0.1250	0.3460	0.7960
NGFG_00256	-0.0980	0.5860	0.9060	NGFG_00320	0.1730	0.1950	0.6700
NGFG_00257	-0.1130	0.6490	0.9210	NGFG_00321	0.1480	0.3720	0.8070
NGFG_00259	0.1890	0.3110	0.7770	NGFG_00322	-0.1080	0.4900	0.8700
NGFG_00260	0.2390	0.3040	0.7770	NGFG_00323	0.0767	0.6840	0.9340
NGFG_00262	0.0432	0.7610	0.9570	NGFG_00324	0.0407	0.8140	0.9720
NGFG_00263	0.3780	0.1100	0.5490	NGFG_00325	-0.1760	0.3110	0.7770
NGFG_00264	0.0056	0.9810	0.9960	NGFG_00326	0.0849	0.6640	0.9240
NGFG_00266	-0.0622	0.5450	0.8860	NGFG_00327	0.1410	0.2330	0.7210
NGFG_00267	-0.0840	0.5860	0.9060	NGFG_00328	0.1930	0.1890	0.6570
NGFG_00268	-0.2160	0.1040	0.5330	NGFG_00329	-0.1880	0.4250	0.8490
NGFG_00269	-0.2330	0.0571	0.4320	NGFG_00330	0.0081	0.9220	0.9910
NGFG_00270	0.0592	0.6970	0.9350	NGFG_00331	0.0992	0.3440	0.7960
NGFG_00271	0.0875	0.5590	0.8950	NGFG_00332	0.1470	0.3150	0.7770
NGFG_00272	-0.1540	0.4300	0.8530	NGFG_00333	0.1580	0.1010	0.5270
NGFG_00273	-0.0317	0.7640	0.9570	NGFG_00334	0.4180	0.0041	0.1620
NGFG_00275	-0.2080	0.0676	0.4700	NGFG_00335	0.0288	0.8800	0.9810
NGFG_00276	-0.5290	0.0041	0.1620	NGFG_00336	-0.0886	0.5750	0.9000
NGFG_00277	0.2630	0.2730	0.7560	NGFG_00337	-0.1040	0.3980	0.8260
NGFG_00281	0.0800	0.4480	0.8580	NGFG_00338	-0.0957	0.5740	0.9000
NGFG_00282	-0.1550	0.3280	0.7830	NGFG_00339	-0.1640	0.3080	0.7770
NGFG_00283	-0.2210	0.3250	0.7810	NGFG_00340	-0.1210	0.2760	0.7560
NGFG_00284	-0.0673	0.6710	0.9280	NGFG_00341	-0.0104	0.9430	0.9960
NGFG_00286	-0.4630	0.0081	0.1870	NGFG_00343	0.1650	0.3700	0.8070
NGFG_00287	-0.0090	0.9580	0.9960	NGFG_00345	-0.0007	0.9960	0.9970
NGFG_00289	-0.1730	0.2890	0.7670	NGFG_00346	-0.0611	0.7320	0.9490
NGFG_00291	-0.0709	0.6750	0.9300	NGFG_00347	-0.1170	0.6080	0.9090
NGFG_00292	-0.3520	0.0134	0.2420	NGFG_00348	-0.0557	0.8130	0.9720
NGFG_00293	0.0977	0.5240	0.8830	NGFG_00349	-0.1160	0.5790	0.9030
NGFG_00295	-0.1290	0.4680	0.8640	NGFG_00350	0.1230	0.5960	0.9080
NGFG_00297	-0.0817	0.6280	0.9170	NGFG_00351	-0.0355	0.8460	0.9730
NGFG_00300	0.3050	0.2150	0.6980	NGFG_00352	0.0122	0.9300	0.9940
NGFG_00301	0.3810	0.1220	0.5670	NGFG_00353	-0.1030	0.6370	0.9210
NGFG_00302	0.2360	0.3070	0.7770	NGFG_00355	-0.3740	0.0889	0.5040
NGFG_00303	0.1250	0.6100	0.9100	NGFG_00356	-0.0757	0.7240	0.9450
NGFG_00305	-0.1160	0.6030	0.9080	NGFG_00357	-0.2580	0.2360	0.7210

NGFG_00358	-0.2790	0.0678	0.4700	NGFG_00417	0.0293	0.8850	0.9820
NGFG_00359	0.0181	0.9360	0.9960	NGFG_00418	-0.1200	0.4440	0.8550
NGFG_00360	-0.3000	0.1400	0.5990	NGFG_00419	-0.0538	0.6950	0.9350
NGFG_00361	-0.2690	0.1840	0.6520	NGFG_00422	-0.3210	0.0167	0.2740
NGFG_00362	0.2680	0.0540	0.4170	NGFG_00423	-0.1440	0.2230	0.7110
NGFG_00363	0.4580	0.0509	0.4150	NGFG_00424	-0.0401	0.7630	0.9570
NGFG_00364	0.6020	0.0083	0.1880	NGFG_00425	-0.0625	0.7020	0.9350
NGFG_00366	0.6090	0.0060	0.1810	NGFG_00426	0.1530	0.1500	0.6160
NGFG_00368	0.0908	0.6470	0.9210	NGFG_00427	0.0878	0.4740	0.8640
NGFG_00369	-0.2740	0.1580	0.6220	NGFG_00428	0.2870	0.2130	0.6940
NGFG_00371	-0.0496	0.8050	0.9720	NGFG_00429	-0.0922	0.4730	0.8640
NGFG_00372	-0.0870	0.5940	0.9080	NGFG_00430	-0.1340	0.4320	0.8530
NGFG_00373	0.0477	0.7650	0.9580	NGFG_00432	-0.0679	0.5720	0.9000
NGFG_00374	-0.4000	0.0060	0.1810	NGFG_00433	-0.2750	0.0718	0.4780
NGFG_00375	-0.1250	0.3620	0.8030	NGFG_00435	0.0044	0.9690	0.9960
NGFG_00376	-0.2070	0.0961	0.5140	NGFG_00439	0.0446	0.7510	0.9570
NGFG_00377	-0.0711	0.6390	0.9210	NGFG_00440	0.0901	0.4520	0.8590
NGFG_00378	-0.1780	0.3340	0.7900	NGFG_00441	0.2130	0.0834	0.5030
NGFG_00379	-0.0376	0.8260	0.9720	NGFG_00442	0.2830	0.0400	0.3870
NGFG_00381	-0.1380	0.2140	0.6960	NGFG_00443	0.4640	0.0053	0.1660
NGFG_00383	0.0535	0.7510	0.9570	NGFG_00444	0.1620	0.2110	0.6930
NGFG_00384	0.0689	0.7210	0.9450	NGFG_00445	0.2820	0.1120	0.5500
NGFG_00385	0.0134	0.8920	0.9820	NGFG_00446	0.3200	0.1040	0.5330
NGFG_00386	-0.0275	0.8780	0.9800	NGFG_00447	0.3930	0.0996	0.5230
NGFG_00387	0.2600	0.2830	0.7610	NGFG_00448	0.4060	0.0328	0.3580
NGFG_00390	0.1260	0.4850	0.8670	NGFG_00449	0.1680	0.0813	0.5020
NGFG_00391	0.0492	0.7700	0.9600	NGFG_00450	0.1730	0.2970	0.7700
NGFG_00392	-0.3270	0.0565	0.4290	NGFG_00451	0.2680	0.1520	0.6160
NGFG_00393	-0.1650	0.5060	0.8760	NGFG_00452	0.5550	0.0044	0.1620
NGFG_00396	-0.1030	0.5270	0.8830	NGFG_00453	0.0777	0.7130	0.9410
NGFG_00398	0.0056	0.9760	0.9960	NGFG_00454	-0.2090	0.1570	0.6220
NGFG_00400	-0.1950	0.1650	0.6280	NGFG_00455	-0.2290	0.1090	0.5490
NGFG_00401	-0.3230	0.0620	0.4490	NGFG_00458	-0.0298	0.8090	0.9720
NGFG_00402	-0.1440	0.4730	0.8640	NGFG_00459	-0.0987	0.4800	0.8650
NGFG_00403	-0.2180	0.0821	0.5020	NGFG_00460	-0.0928	0.5600	0.8960
NGFG_00405	-0.0643	0.7250	0.9460	NGFG_00461	-0.2810	0.0553	0.4240
NGFG_00406	-0.1250	0.4240	0.8490	NGFG_00462	-0.0968	0.6520	0.9210
NGFG_00407	-0.2160	0.1710	0.6370	NGFG_00463	-0.1900	0.1810	0.6480
NGFG_00408	-0.2240	0.0966	0.5140	NGFG_00464	-0.1430	0.4470	0.8580
NGFG_00409	-0.1120	0.5670	0.8980	NGFG_00466	-0.2530	0.2950	0.7700
NGFG_00410	-0.1860	0.2600	0.7410	NGFG_00467	0.0157	0.9430	0.9960
NGFG_00411	-0.0410	0.7880	0.9680	NGFG_00468	-0.0394	0.7710	0.9600
NGFG_00412	-0.0893	0.5210	0.8830	NGFG_00469	0.4290	0.0266	0.3410
NGFG_00413	-0.2240	0.1990	0.6770	NGFG_00470	-0.0433	0.8040	0.9720
NGFG_00414	-0.1080	0.6660	0.9250	NGFG_00471	-0.1470	0.5230	0.8830
NGFG_00415	-0.0639	0.6920	0.9350	NGFG_00472	-0.2030	0.4090	0.8370
NGFG_00416	-0.0436	0.7970	0.9690	NGFG_00473	0.0626	0.7470	0.9560

NGFG_00474	0.3830	0.0481	0.4140	NGFG_00528	-0.1270	0.4470	0.8580
NGFG_00475	-0.1700	0.2910	0.7700	NGFG_00529	-0.0082	0.9720	0.9960
NGFG_00477	0.2250	0.2590	0.7410	NGFG_00530	0.0582	0.8180	0.9720
NGFG_00478	-0.0227	0.9030	0.9850	NGFG_00531	-0.0176	0.9010	0.9840
NGFG_00479	0.2280	0.2390	0.7260	NGFG_00532	0.1290	0.5050	0.8760
NGFG_00480	0.5540	0.0024	0.1270	NGFG_00533	0.1520	0.3900	0.8190
NGFG_00482	-0.2980	0.0872	0.5030	NGFG_00534	0.0675	0.5570	0.8930
NGFG_00483	-0.0887	0.6060	0.9080	NGFG_00535	-0.2050	0.1590	0.6220
NGFG_00486	-0.2140	0.1840	0.6520	NGFG_00536	0.1320	0.4800	0.8650
NGFG_00487	-0.0546	0.8070	0.9720	NGFG_00537	0.0043	0.9690	0.9960
NGFG_00488	-0.0414	0.7730	0.9620	NGFG_00538	-0.0695	0.6330	0.9200
NGFG_00489	0.0585	0.7030	0.9360	NGFG_00539	0.0518	0.7160	0.9420
NGFG_00490	-0.0326	0.8580	0.9740	NGFG_00541	-0.0697	0.6510	0.9210
NGFG_00491	0.0502	0.8290	0.9720	NGFG_00542	-0.2850	0.1190	0.5580
NGFG_00492	0.0532	0.8210	0.9720	NGFG_00543	-0.1320	0.5620	0.8970
NGFG_00495	0.1080	0.3650	0.8060	NGFG_00544	-0.2610	0.1380	0.5960
NGFG_00496	-0.0008	0.9940	0.9970	NGFG_00545	-0.2540	0.1770	0.6450
NGFG_00498	-0.1480	0.3490	0.8010	NGFG_00546	-0.1440	0.3640	0.8050
NGFG_00499	-0.0153	0.9220	0.9910	NGFG_00547	-0.1690	0.2540	0.7410
NGFG_00500	-0.0755	0.6340	0.9210	NGFG_00548	0.0364	0.8230	0.9720
NGFG_00501	-0.0739	0.5440	0.8860	NGFG_00550	-0.0634	0.5740	0.9000
NGFG_00502	-0.1100	0.3200	0.7780	NGFG_00551	-0.0624	0.5250	0.8830
NGFG_00503	0.1680	0.2950	0.7700	NGFG_00554	-0.0754	0.6270	0.9170
NGFG_00504	0.0193	0.8520	0.9740	NGFG_00555	-0.0906	0.4080	0.8360
NGFG_00505	-0.0524	0.6610	0.9240	NGFG_00556	-0.2430	0.0473	0.4140
NGFG_00506	0.2900	0.1500	0.6160	NGFG_00557	-0.0745	0.5370	0.8860
NGFG_00507	0.4500	0.0095	0.1970	NGFG_00558	-0.0870	0.6040	0.9080
NGFG_00508	0.4220	0.0884	0.5030	NGFG_00559	-0.5450	0.0005	0.0596
NGFG_00509	0.1620	0.2960	0.7700	NGFG_00562	-0.2180	0.0565	0.4290
NGFG_00510	0.0270	0.8540	0.9740	NGFG_00563	0.0173	0.9380	0.9960
NGFG_00511	0.0028	0.9730	0.9960	NGFG_00564	0.3540	0.1110	0.5490
NGFG_00512	0.1250	0.2880	0.7670	NGFG_00565	-0.2020	0.2920	0.7700
NGFG_00513	0.0570	0.6150	0.9140	NGFG_00566	-0.0339	0.8220	0.9720
NGFG_00514	0.3180	0.0618	0.4490	NGFG_00567	-0.2030	0.1260	0.5710
NGFG_00515	0.3650	0.0689	0.4720	NGFG_00568	-0.3620	0.0042	0.1620
NGFG_00516	0.3240	0.0733	0.4820	NGFG_00569	-0.2080	0.1100	0.5490
NGFG_00517	0.2830	0.1480	0.6130	NGFG_00570	0.1530	0.3930	0.8210
NGFG_00518	-0.2300	0.0384	0.3830	NGFG_00571	0.0830	0.5570	0.8930
NGFG_00519	-0.0908	0.6650	0.9240	NGFG_00574	-0.1400	0.3810	0.8140
NGFG_00520	0.2670	0.2670	0.7510	NGFG_00575	-0.2470	0.1250	0.5710
NGFG_00521	-0.2360	0.1770	0.6450	NGFG_00576	-0.2280	0.1810	0.6480
NGFG_00522	-0.1750	0.2340	0.7210	NGFG_00577	-0.1580	0.3660	0.8060
NGFG_00523	0.1630	0.2690	0.7530	NGFG_00578	-0.0647	0.5580	0.8930
NGFG_00524	0.4810	0.0090	0.1930	NGFG_00580	-0.1330	0.2780	0.7580
NGFG_00525	0.2010	0.2590	0.7410	NGFG_00583	-0.2290	0.3550	0.8020
NGFG_00526	-0.1030	0.4120	0.8370	NGFG_00584	0.0696	0.7850	0.9680
NGFG_00527	-0.1590	0.3610	0.8030	NGFG_00585	0.0577	0.7180	0.9430

NGFG_00586	-0.2410	0.1800	0.6480	NGFG_00646	-0.2690	0.1570	0.6220
NGFG_00587	-0.2720	0.0284	0.3410	NGFG_00647	-0.0836	0.7430	0.9540
NGFG_00588	-0.0112	0.9360	0.9960	NGFG_00648	-0.2980	0.2190	0.7070
NGFG_00590	-0.1530	0.1270	0.5710	NGFG_00649	0.2220	0.3820	0.8140
NGFG_00591	-0.2710	0.0318	0.3570	NGFG_00651	-0.2620	0.1870	0.6520
NGFG_00592	-0.1750	0.2440	0.7310	NGFG_00652	0.1950	0.3840	0.8160
NGFG_00593	0.0443	0.7850	0.9680	NGFG_00653	-0.2530	0.2650	0.7490
NGFG_00594	0.0629	0.6220	0.9140	NGFG_00654	-0.1800	0.1870	0.6520
NGFG_00595	0.0919	0.6390	0.9210	NGFG_00656	0.3880	0.0053	0.1660
NGFG_00596	-0.0547	0.7420	0.9540	NGFG_00657	0.0075	0.9470	0.9960
NGFG_00597	-0.1180	0.3100	0.7770	NGFG_00658	0.2770	0.0131	0.2390
NGFG_00598	-0.1580	0.4560	0.8610	NGFG_00659	-0.2220	0.1750	0.6430
NGFG_00600	-0.3000	0.2400	0.7260	NGFG_00661	0.4800	0.0306	0.3540
NGFG_00601	0.0113	0.9560	0.9960	NGFG_00662	0.6110	0.0012	0.0917
NGFG_00602	0.3500	0.0848	0.5030	NGFG_00664	0.7190	0.0003	0.0410
NGFG_00603	-0.0541	0.6920	0.9350	NGFG_00666	0.2290	0.0698	0.4760
NGFG_00605	-0.1960	0.1220	0.5670	NGFG_00667	0.6970	0.0007	0.0682
NGFG_00606	-0.5110	0.0013	0.0917	NGFG_00670	0.4860	0.0359	0.3700
NGFG_00607	-0.0542	0.7760	0.9650	NGFG_00671	0.2830	0.1740	0.6430
NGFG_00608	0.0624	0.7420	0.9540	NGFG_00672	-0.0030	0.9820	0.9960
NGFG_00609	0.1010	0.5800	0.9030	NGFG_00673	-0.1810	0.2120	0.6940
NGFG_00610	0.2960	0.0874	0.5030	NGFG_00674	-0.1620	0.2240	0.7110
NGFG_00611	0.0100	0.9650	0.9960	NGFG_00675	0.1750	0.3790	0.8130
NGFG_00614	-0.2720	0.2410	0.7260	NGFG_00676	-0.2400	0.2300	0.7210
NGFG_00615	-0.0083	0.9370	0.9960	NGFG_00678	-0.1430	0.1970	0.6750
NGFG_00616	0.0661	0.5740	0.9000	NGFG_00679	-0.1090	0.2620	0.7410
NGFG_00617	0.1860	0.1750	0.6430	NGFG_00682	-0.1010	0.4410	0.8540
NGFG_00618	0.2260	0.3270	0.7830	NGFG_00683	-0.0473	0.7950	0.9690
NGFG_00619	-0.1420	0.4750	0.8640	NGFG_00684	-0.2020	0.2030	0.6850
NGFG_00620	-0.0952	0.6460	0.9210	NGFG_00686	-0.5600	0.0276	0.3410
NGFG_00621	0.0325	0.8980	0.9840	NGFG_00687	-0.4370	0.0614	0.4490
NGFG_00622	-0.2070	0.3560	0.8020	NGFG_00688	-0.3750	0.0791	0.4950
NGFG_00623	-0.2090	0.4120	0.8370	NGFG_00691	-0.0626	0.7650	0.9580
NGFG_00626	0.2460	0.3210	0.7780	NGFG_00692	0.0352	0.8830	0.9820
NGFG_00627	-0.1570	0.3620	0.8030	NGFG_00693	-0.2230	0.1270	0.5710
NGFG_00628	-0.3770	0.0437	0.4010	NGFG_00694	-0.1050	0.4410	0.8540
NGFG_00629	0.2000	0.2750	0.7560	NGFG_00695	-0.1220	0.4720	0.8640
NGFG_00630	0.1720	0.4100	0.8370	NGFG_00696	-0.0768	0.4680	0.8640
NGFG_00631	0.0799	0.7520	0.9570	NGFG_00698	-0.2340	0.0217	0.3170
NGFG_00632	-0.0082	0.9610	0.9960	NGFG_00699	0.1400	0.5260	0.8830
NGFG_00633	0.1060	0.6770	0.9300	NGFG_00701	-0.1610	0.5280	0.8830
NGFG_00634	-0.1270	0.6050	0.9080	NGFG_00703	-0.3160	0.0217	0.3170
NGFG_00638	0.0315	0.8520	0.9740	NGFG_00704	-0.0990	0.4710	0.8640
NGFG_00639	0.1480	0.5070	0.8760	NGFG_00705	-0.0569	0.7100	0.9400
NGFG_00640	-0.2530	0.3100	0.7770	NGFG_00707	0.2030	0.1980	0.6760
NGFG_00641	-0.3990	0.0947	0.5140	NGFG_00708	-0.0278	0.8410	0.9730
NGFG_00643	0.2840	0.0688	0.4720	NGFG_00709	-0.0856	0.6990	0.9350

NGFG_00711	-0.1290	0.3250	0.7810	NGFG_00774	-0.4140	0.0043	0.1620
NGFG_00712	-0.1090	0.4410	0.8540	NGFG_00775	-0.1760	0.2460	0.7310
NGFG_00713	0.2740	0.2010	0.6790	NGFG_00777	0.0746	0.6410	0.9210
NGFG_00715	-0.2000	0.4340	0.8530	NGFG_00779	-0.1970	0.1990	0.6770
NGFG_00719	0.0096	0.9370	0.9960	NGFG_00780	0.0779	0.7590	0.9570
NGFG_00720	0.3130	0.1250	0.5710	NGFG_00782	-0.1430	0.2800	0.7580
NGFG_00721	0.3420	0.0723	0.4790	NGFG_00785	0.3170	0.0462	0.4100
NGFG_00723	-0.1840	0.3820	0.8140	NGFG_00786	-0.0997	0.5440	0.8860
NGFG_00724	-0.2260	0.3760	0.8110	NGFG_00787	-0.1140	0.5580	0.8930
NGFG_00725	-0.2630	0.2910	0.7700	NGFG_00789	0.0032	0.9760	0.9960
NGFG_00727	-0.2920	0.1990	0.6770	NGFG_00790	-0.0755	0.6980	0.9350
NGFG_00728	0.0141	0.9550	0.9960	NGFG_00791	0.0113	0.9620	0.9960
NGFG_00729	-0.0516	0.7890	0.9690	NGFG_00792	-0.0824	0.7440	0.9540
NGFG_00730	0.4110	0.0611	0.4490	NGFG_00794	0.1450	0.5360	0.8860
NGFG_00731	0.0597	0.6980	0.9350	NGFG_00795	-0.2150	0.1260	0.5710
NGFG_00732	0.0017	0.9940	0.9970	NGFG_00798	-0.2000	0.2000	0.6770
NGFG_00733	0.0054	0.9740	0.9960	NGFG_00799	-0.1470	0.3690	0.8070
NGFG_00734	-0.0842	0.6040	0.9080	NGFG_00800	-0.2570	0.2870	0.7670
NGFG_00735	-0.1110	0.3090	0.7770	NGFG_00801	-0.2480	0.2080	0.6930
NGFG_00736	-0.1980	0.1780	0.6470	NGFG_00802	0.0716	0.6710	0.9280
NGFG_00739	0.2160	0.1680	0.6340	NGFG_00803	0.1900	0.4530	0.8590
NGFG_00740	-0.1620	0.4360	0.8540	NGFG_00804	0.0489	0.8020	0.9720
NGFG_00741	-0.1060	0.6080	0.9090	NGFG_00807	0.0988	0.2940	0.7700
NGFG_00742	-0.1620	0.2620	0.7410	NGFG_00811	-0.0995	0.4510	0.8590
NGFG_00743	-0.2610	0.1140	0.5520	NGFG_00812	0.0338	0.8490	0.9740
NGFG_00744	-0.3600	0.0752	0.4850	NGFG_00813	-0.0149	0.9260	0.9920
NGFG_00745	-0.2050	0.2010	0.6790	NGFG_00814	-0.0602	0.7220	0.9450
NGFG_00746	-0.0366	0.8360	0.9730	NGFG_00815	-0.0115	0.9480	0.9960
NGFG_00750	0.3890	0.0531	0.4150	NGFG_00816	-0.0366	0.8380	0.9730
NGFG_00751	-0.0402	0.8470	0.9730	NGFG_00817	-0.0653	0.7090	0.9400
NGFG_00752	-0.0946	0.6860	0.9340	NGFG_00818	0.0981	0.6350	0.9210
NGFG_00754	0.2760	0.1910	0.6620	NGFG_00819	0.1570	0.3110	0.7770
NGFG_00755	0.2480	0.1800	0.6480	NGFG_00820	0.0611	0.6950	0.9350
NGFG_00756	-0.2040	0.1700	0.6360	NGFG_00821	0.5160	0.0285	0.3410
NGFG_00757	0.1800	0.1400	0.5980	NGFG_00822	0.2370	0.1100	0.5490
NGFG_00759	-0.0327	0.8710	0.9770	NGFG_00823	0.0235	0.8910	0.9820
NGFG_00760	0.6250	0.0130	0.2390	NGFG_00824	-0.1780	0.2160	0.7010
NGFG_00761	-0.0554	0.5960	0.9080	NGFG_00825	-0.2620	0.2250	0.7130
NGFG_00762	-0.0199	0.8880	0.9820	NGFG_00826	-0.3930	0.0253	0.3380
NGFG_00763	-0.0900	0.6010	0.9080	NGFG_00827	0.0205	0.9190	0.9910
NGFG_00764	-0.1240	0.5730	0.9000	NGFG_00828	-0.0957	0.6160	0.9140
NGFG_00765	-0.1570	0.3160	0.7770	NGFG_00829	-0.0871	0.6600	0.9240
NGFG_00766	-0.0484	0.8100	0.9720	NGFG_00831	0.0967	0.5400	0.8860
NGFG_00768	0.0045	0.9750	0.9960	NGFG_00836	0.1550	0.4710	0.8640
NGFG_00770	0.1470	0.3500	0.8010	NGFG_00839	-0.1210	0.3970	0.8260
NGFG_00772	-0.2190	0.1150	0.5520	NGFG_00840	-0.0741	0.7550	0.9570
NGFG_00773	-0.2480	0.1790	0.6480	NGFG_00841	-0.0064	0.9620	0.9960

NGFG_00843	0.0334	0.8310	0.9730	NGFG_00906	-0.2550	0.0409	0.3870
NGFG_00844	0.2410	0.2610	0.7410	NGFG_00907	-0.1050	0.4420	0.8540
NGFG_00845	0.2210	0.3870	0.8180	NGFG_00908	0.2630	0.1450	0.6090
NGFG_00847	-0.0255	0.9170	0.9910	NGFG_00909	0.0853	0.5300	0.8830
NGFG_00848	0.0229	0.9200	0.9910	NGFG_00910	0.1490	0.5420	0.8860
NGFG_00851	-0.2610	0.2930	0.7700	NGFG_00911	0.2560	0.2260	0.7150
NGFG_00852	0.0160	0.9460	0.9960	NGFG_00912	0.0624	0.7170	0.9430
NGFG_00853	-0.0874	0.5250	0.8830	NGFG_00913	0.1440	0.2420	0.7260
NGFG_00854	0.0718	0.6960	0.9350	NGFG_00914	0.0016	0.9920	0.9960
NGFG_00855	-0.0125	0.9390	0.9960	NGFG_00918	-0.0572	0.7290	0.9470
NGFG_00856	-0.2460	0.0602	0.4450	NGFG_00919	-0.2500	0.3060	0.7770
NGFG_00857	0.1830	0.2710	0.7550	NGFG_00920	0.0738	0.7700	0.9600
NGFG_00858	-0.0095	0.9410	0.9960	NGFG_00921	-0.0100	0.9680	0.9960
NGFG_00859	-0.1350	0.3910	0.8190	NGFG_00922	-0.4540	0.0722	0.4790
NGFG_00862	0.3800	0.0823	0.5020	NGFG_00923	-0.3320	0.1710	0.6370
NGFG_00863	0.0311	0.8090	0.9720	NGFG_00924	-0.4360	0.0045	0.1620
NGFG_00866	0.0194	0.9190	0.9910	NGFG_00925	-0.1850	0.2710	0.7550
NGFG_00867	0.4880	0.0352	0.3680	NGFG_00926	0.0920	0.4850	0.8670
NGFG_00868	-0.0785	0.5120	0.8780	NGFG_00928	0.2480	0.0284	0.3410
NGFG_00869	0.2940	0.1340	0.5840	NGFG_00930	0.1590	0.3580	0.8020
NGFG_00870	0.4440	0.0262	0.3410	NGFG_00931	-0.1600	0.3050	0.7770
NGFG_00871	0.2100	0.1440	0.6040	NGFG_00932	-0.0058	0.9800	0.9960
NGFG_00872	-0.3400	0.0283	0.3410	NGFG_00933	-0.0236	0.8930	0.9820
NGFG_00873	-0.0500	0.8330	0.9730	NGFG_00934	-0.1190	0.5340	0.8850
NGFG_00874	-0.1520	0.4430	0.8540	NGFG_00936	0.0744	0.6880	0.9340
NGFG_00878	-0.0356	0.7210	0.9450	NGFG_00937	-0.0576	0.7150	0.9420
NGFG_00879	-0.0969	0.4770	0.8640	NGFG_00938	-0.2340	0.3260	0.7810
NGFG_00880	-0.1060	0.5960	0.9080	NGFG_00940	0.1840	0.1400	0.5990
NGFG_00881	-0.0490	0.6390	0.9210	NGFG_00941	0.2640	0.0497	0.4150
NGFG_00882	0.0099	0.9540	0.9960	NGFG_00942	0.0225	0.8850	0.9820
NGFG_00883	0.1510	0.2800	0.7580	NGFG_00943	0.1390	0.4520	0.8590
NGFG_00884	0.0974	0.6170	0.9140	NGFG_00945	0.2310	0.3190	0.7780
NGFG_00886	-0.2590	0.0620	0.4490	NGFG_00946	0.2090	0.4060	0.8330
NGFG_00888	-0.2440	0.1870	0.6520	NGFG_00947	0.2720	0.2680	0.7510
NGFG_00889	-0.3570	0.1100	0.5490	NGFG_00949	0.1850	0.3770	0.8120
NGFG_00892	-0.2220	0.1020	0.5270	NGFG_00950	0.3470	0.0534	0.4150
NGFG_00893	-0.3260	0.0588	0.4380	NGFG_00952	0.2470	0.2320	0.7210
NGFG_00894	-0.2870	0.0930	0.5120	NGFG_00953	0.2130	0.3380	0.7910
NGFG_00895	-0.0961	0.5570	0.8930	NGFG_00954	-0.0659	0.7960	0.9690
NGFG_00896	-0.0354	0.7790	0.9650	NGFG_00955	0.4740	0.0306	0.3540
NGFG_00897	-0.2800	0.0265	0.3410	NGFG_00956	0.2450	0.2110	0.6930
NGFG_00898	-0.2460	0.1150	0.5520	NGFG_00958	0.0303	0.8860	0.9820
NGFG_00899	-0.1020	0.4410	0.8540	NGFG_00959	0.2930	0.2500	0.7350
NGFG_00900	-0.0443	0.7620	0.9570	NGFG_00960	0.1260	0.4860	0.8670
NGFG_00901	-0.2370	0.1820	0.6520	NGFG_00961	-0.0586	0.7270	0.9460
NGFG_00903	-0.0361	0.7980	0.9690	NGFG_00962	0.1780	0.1080	0.5490
NGFG_00905	-0.0631	0.7390	0.9530	NGFG_00963	0.4840	0.0210	0.3100

NGFG_00964	0.1340	0.5890	0.9080	NGFG_01022	0.0025	0.9910	0.9960
NGFG_00966	-0.1010	0.6810	0.9340	NGFG_01023	-0.0270	0.8610	0.9750
NGFG_00967	0.2060	0.3420	0.7940	NGFG_01024	-0.2430	0.1110	0.5490
NGFG_00968	0.6200	0.0146	0.2620	NGFG_01025	-0.0438	0.8110	0.9720
NGFG_00969	0.1100	0.5120	0.8780	NGFG_01026	-0.0297	0.7520	0.9570
NGFG_00970	0.4630	0.0170	0.2770	NGFG_01027	-0.1450	0.2490	0.7350
NGFG_00971	0.3470	0.0732	0.4820	NGFG_01028	0.0081	0.9640	0.9960
NGFG_00972	0.3650	0.0719	0.4780	NGFG_01029	0.1960	0.2240	0.7110
NGFG_00973	0.3690	0.0029	0.1370	NGFG_01030	-0.0704	0.6980	0.9350
NGFG_00974	0.4200	0.0219	0.3180	NGFG_01031	-0.0575	0.7490	0.9570
NGFG_00975	0.5150	0.0063	0.1810	NGFG_01032	0.0339	0.8270	0.9720
NGFG_00976	0.4410	0.0104	0.2110	NGFG_01033	-0.0284	0.8230	0.9720
NGFG_00978	0.3990	0.1170	0.5560	NGFG_01034	-0.0427	0.8460	0.9730
NGFG_00979	0.2840	0.0871	0.5030	NGFG_01035	-0.3560	0.0338	0.3640
NGFG_00980	0.2490	0.2610	0.7410	NGFG_01036	0.0275	0.8680	0.9760
NGFG_00981	0.1960	0.4060	0.8330	NGFG_01037	-0.0510	0.7930	0.9690
NGFG_00982	0.1960	0.2710	0.7550	NGFG_01038	-0.0003	0.9990	1.0000
NGFG_00983	-0.0776	0.6520	0.9210	NGFG_01039	-0.2430	0.1800	0.6480
NGFG_00984	0.1180	0.4490	0.8590	NGFG_01040	-0.2800	0.1410	0.6000
NGFG_00985	0.1130	0.6000	0.9080	NGFG_01041	-0.3040	0.2240	0.7110
NGFG_00986	-0.1390	0.4600	0.8640	NGFG_01043	-0.1750	0.2510	0.7360
NGFG_00987	-0.1040	0.5650	0.8980	NGFG_01044	-0.0527	0.7980	0.9690
NGFG_00988	-0.1650	0.4870	0.8670	NGFG_01045	-0.0680	0.6890	0.9340
NGFG_00991	-0.1590	0.3830	0.8140	NGFG_01046	-0.0532	0.7860	0.9680
NGFG_00992	-0.1480	0.3590	0.8020	NGFG_01048	-0.1640	0.3130	0.7770
NGFG_00993	0.0777	0.7020	0.9350	NGFG_01051	0.2080	0.1650	0.6280
NGFG_00994	-0.1860	0.3140	0.7770	NGFG_01052	-0.2400	0.2300	0.7210
NGFG_00995	-0.0648	0.7600	0.9570	NGFG_01056	-0.1640	0.4930	0.8700
NGFG_00996	0.5440	0.0329	0.3580	NGFG_01058	-0.1920	0.3070	0.7770
NGFG_00997	-0.0422	0.8640	0.9750	NGFG_01059	-0.0044	0.9840	0.9960
NGFG_00998	-0.0166	0.9400	0.9960	NGFG_01060	0.1510	0.5440	0.8860
NGFG_01000	0.0289	0.8720	0.9770	NGFG_01062	0.5600	0.0282	0.3410
NGFG_01001	0.2270	0.3390	0.7940	NGFG_01063	0.0412	0.8600	0.9750
NGFG_01002	0.1530	0.3920	0.8190	NGFG_01064	0.1080	0.6570	0.9240
NGFG_01003	0.1910	0.2040	0.6860	NGFG_01068	-0.2100	0.1760	0.6430
NGFG_01004	0.1940	0.2460	0.7310	NGFG_01069	0.0785	0.6890	0.9340
NGFG_01008	-0.2310	0.1830	0.6520	NGFG_01070	0.1460	0.3330	0.7890
NGFG_01009	-0.1740	0.3720	0.8070	NGFG_01072	0.0915	0.5510	0.8900
NGFG_01010	0.1130	0.3770	0.8120	NGFG_01073	0.0028	0.9850	0.9960
NGFG_01011	0.0622	0.6380	0.9210	NGFG_01074	-0.0154	0.9130	0.9880
NGFG_01012	0.4920	0.0121	0.2320	NGFG_01075	-0.0361	0.8240	0.9720
NGFG_01014	0.1450	0.4280	0.8510	NGFG_01076	-0.0057	0.9780	0.9960
NGFG_01015	-0.1530	0.3870	0.8180	NGFG_01077	-0.0065	0.9670	0.9960
NGFG_01016	-0.2360	0.1830	0.6520	NGFG_01078	-0.0730	0.7480	0.9570
NGFG_01018	-0.0997	0.4620	0.8640	NGFG_01080	0.2690	0.0681	0.4700
NGFG_01019	-0.0085	0.9480	0.9960	NGFG_01081	-0.1180	0.5360	0.8860
NGFG_01020	-0.0349	0.6990	0.9350	NGFG_01083	0.0917	0.6670	0.9250

NGFG_01084	0.2650	0.1920	0.6630	NGFG_01148	-0.1480	0.4540	0.8590
NGFG_01088	0.3060	0.1290	0.5740	NGFG_01149	-0.0346	0.8180	0.9720
NGFG_01091	0.4490	0.0397	0.3870	NGFG_01150	0.3520	0.0455	0.4100
NGFG_01092	0.7090	0.0006	0.0606	NGFG_01152	0.0035	0.9840	0.9960
NGFG_01093	0.2690	0.0825	0.5020	NGFG_01153	0.4030	0.0921	0.5120
NGFG_01094	0.4100	0.0640	0.4550	NGFG_01154	-0.0558	0.7210	0.9450
NGFG_01095	-0.1800	0.2900	0.7700	NGFG_01155	-0.0896	0.4640	0.8640
NGFG_01096	0.0307	0.8600	0.9750	NGFG_01156	-0.2130	0.2740	0.7560
NGFG_01099	0.2200	0.2590	0.7410	NGFG_01157	0.1830	0.2400	0.7260
NGFG_01100	0.2750	0.0752	0.4850	NGFG_01158	-0.1970	0.3400	0.7940
NGFG_01104	-0.1240	0.5630	0.8970	NGFG_01160	0.7610	0.0002	0.0371
NGFG_01105	-0.0460	0.8420	0.9730	NGFG_01161	0.0802	0.5750	0.9000
NGFG_01106	-0.0467	0.8290	0.9720	NGFG_01163	-0.0476	0.8520	0.9740
NGFG_01107	-0.0326	0.8480	0.9730	NGFG_01164	-0.1650	0.2960	0.7700
NGFG_01108	-0.0835	0.3790	0.8130	NGFG_01165	-0.1180	0.5740	0.9000
NGFG_01109	0.0604	0.6720	0.9280	NGFG_01166	0.0017	0.9920	0.9960
NGFG_01110	0.0787	0.6220	0.9140	NGFG_01167	-0.1690	0.3660	0.8060
NGFG_01112	-0.1450	0.2580	0.7410	NGFG_01168	-0.1230	0.5250	0.8830
NGFG_01113	-0.0346	0.7870	0.9680	NGFG_01169	0.0240	0.9250	0.9920
NGFG_01114	-0.3310	0.0036	0.1520	NGFG_01170	-0.2130	0.3710	0.8070
NGFG_01115	-0.1860	0.2740	0.7560	NGFG_01171	-0.2590	0.0414	0.3870
NGFG_01116	0.0283	0.8720	0.9770	NGFG_01172	-0.1160	0.4010	0.8300
NGFG_01117	-0.0614	0.7270	0.9460	NGFG_01173	0.1220	0.5410	0.8860
NGFG_01118	-0.2790	0.1180	0.5560	NGFG_01175	-0.0053	0.9720	0.9960
NGFG_01119	-0.0142	0.9460	0.9960	NGFG_01176	-0.3130	0.0077	0.1850
NGFG_01120	-0.0941	0.6550	0.9230	NGFG_01181	-0.1380	0.4950	0.8700
NGFG_01121	0.0931	0.5650	0.8980	NGFG_01182	0.1260	0.2520	0.7380
NGFG_01122	0.1920	0.1540	0.6200	NGFG_01183	-0.1250	0.5960	0.9080
NGFG_01123	0.0021	0.9890	0.9960	NGFG_01184	-0.0822	0.6240	0.9140
NGFG_01125	0.0000	1.0000	1.0000	NGFG_01185	-0.2130	0.1600	0.6220
NGFG_01127	-0.1820	0.4040	0.8330	NGFG_01186	-0.3380	0.0826	0.5020
NGFG_01128	-0.1820	0.2530	0.7380	NGFG_01187	-0.2680	0.0528	0.4150
NGFG_01129	0.1070	0.4660	0.8640	NGFG_01188	-0.1520	0.4470	0.8580
NGFG_01131	-0.1950	0.2780	0.7580	NGFG_01189	-0.0614	0.6620	0.9240
NGFG_01132	-0.1440	0.1870	0.6520	NGFG_01190	0.1790	0.4820	0.8650
NGFG_01133	0.0635	0.6300	0.9190	NGFG_01192	0.2320	0.0902	0.5080
NGFG_01134	0.1650	0.4940	0.8700	NGFG_01193	0.0811	0.6610	0.9240
NGFG_01135	0.1930	0.3300	0.7850	NGFG_01194	0.0891	0.5990	0.9080
NGFG_01136	-0.1710	0.1860	0.6520	NGFG_01195	0.0131	0.9110	0.9870
NGFG_01137	-0.0253	0.8240	0.9720	NGFG_01196	0.1330	0.5300	0.8830
NGFG_01138	0.0725	0.6810	0.9340	NGFG_01198	0.1190	0.4330	0.8530
NGFG_01139	-0.0571	0.7740	0.9620	NGFG_01199	-0.1340	0.3620	0.8030
NGFG_01141	0.0725	0.7110	0.9400	NGFG_01200	-0.1940	0.3290	0.7850
NGFG_01143	0.1990	0.1600	0.6220	NGFG_01201	-0.1020	0.4270	0.8490
NGFG_01144	-0.0524	0.8090	0.9720	NGFG_01202	-0.1650	0.1600	0.6220
NGFG_01145	-0.0873	0.5730	0.9000	NGFG_01203	-0.0960	0.4820	0.8650
NGFG_01146	0.1470	0.4310	0.8530	NGFG_01204	0.2270	0.0667	0.4670

NGFG_01205	0.0699	0.6320	0.9200	NGFG_01269	0.1860	0.1270	0.5710
NGFG_01206	-0.1130	0.4840	0.8650	NGFG_01270	-0.1220	0.3520	0.8020
NGFG_01207	0.1970	0.1220	0.5670	NGFG_01272	-0.2170	0.1350	0.5870
NGFG_01208	0.3490	0.0531	0.4150	NGFG_01273	0.1940	0.2860	0.7660
NGFG_01210	0.0536	0.7140	0.9420	NGFG_01274	0.0314	0.8980	0.9840
NGFG_01211	-0.0223	0.8840	0.9820	NGFG_01275	-0.0044	0.9790	0.9960
NGFG_01212	0.1350	0.3870	0.8180	NGFG_01277	-0.0377	0.8820	0.9820
NGFG_01215	0.1790	0.4420	0.8540	NGFG_01278	-0.1090	0.6560	0.9240
NGFG_01216	-0.0246	0.8190	0.9720	NGFG_01279	0.1640	0.4960	0.8700
NGFG_01217	-0.1150	0.2970	0.7700	NGFG_01280	-0.6700	0.0063	0.1810
NGFG_01220	-0.3200	0.1220	0.5670	NGFG_01281	-0.1070	0.4690	0.8640
NGFG_01222	0.0321	0.8170	0.9720	NGFG_01283	-0.3050	0.2280	0.7170
NGFG_01223	0.0156	0.9030	0.9850	NGFG_01284	0.0892	0.6870	0.9340
NGFG_01224	0.0395	0.6290	0.9180	NGFG_01285	-0.0393	0.8580	0.9740
NGFG_01225	-0.2030	0.0949	0.5140	NGFG_01287	0.1330	0.5170	0.8800
NGFG_01227	-0.1920	0.2770	0.7570	NGFG_01288	-0.1140	0.5810	0.9030
NGFG_01228	-0.2930	0.0945	0.5140	NGFG_01289	-0.4140	0.0163	0.2740
NGFG_01229	-0.1090	0.5430	0.8860	NGFG_01290	-0.6400	0.0081	0.1870
NGFG_01230	0.1110	0.6460	0.9210	NGFG_01291	0.1020	0.6870	0.9340
NGFG_01231	0.0339	0.7580	0.9570	NGFG_01292	-0.0760	0.7590	0.9570
NGFG_01232	0.2440	0.2490	0.7350	NGFG_01293	-0.0435	0.8630	0.9750
NGFG_01233	0.0447	0.8480	0.9730	NGFG_01294	-0.1030	0.6730	0.9290
NGFG_01236	0.1610	0.2930	0.7700	NGFG_01295	-0.1420	0.4750	0.8640
NGFG_01240	-0.0650	0.7320	0.9490	NGFG_01296	0.2540	0.2640	0.7460
NGFG_01242	-0.0080	0.9700	0.9960	NGFG_01297	0.0818	0.5490	0.8880
NGFG_01243	-0.0044	0.9810	0.9960	NGFG_01298	-0.3320	0.1860	0.6520
NGFG_01244	-0.0277	0.8290	0.9720	NGFG_01299	-0.0715	0.7620	0.9570
NGFG_01245	-0.0727	0.6850	0.9340	NGFG_01300	0.0442	0.8540	0.9740
NGFG_01246	0.1900	0.0983	0.5200	NGFG_01301	0.2850	0.2350	0.7210
NGFG_01247	-0.0634	0.6010	0.9080	NGFG_01302	0.1540	0.5020	0.8760
NGFG_01248	0.1160	0.5720	0.9000	NGFG_01303	0.1480	0.3370	0.7910
NGFG_01249	-0.3350	0.0709	0.4780	NGFG_01304	0.1730	0.3590	0.8020
NGFG_01250	-0.0516	0.7530	0.9570	NGFG_01305	0.1550	0.5440	0.8860
NGFG_01251	-0.1970	0.3000	0.7750	NGFG_01308	0.2270	0.2730	0.7560
NGFG_01252	0.0025	0.9880	0.9960	NGFG_01309	-0.1980	0.4180	0.8430
NGFG_01253	-0.1480	0.4770	0.8640	NGFG_01311	-0.0184	0.9410	0.9960
NGFG_01254	-0.0840	0.5900	0.9080	NGFG_01312	0.2240	0.2650	0.7490
NGFG_01255	-0.0722	0.5570	0.8930	NGFG_01313	-0.1860	0.2800	0.7580
NGFG_01256	-0.0120	0.9370	0.9960	NGFG_01315	0.0606	0.7370	0.9500
NGFG_01257	0.1810	0.3170	0.7770	NGFG_01316	-0.2420	0.0462	0.4100
NGFG_01259	-0.1560	0.1410	0.5990	NGFG_01319	0.1750	0.4330	0.8530
NGFG_01260	-0.1480	0.2490	0.7350	NGFG_01320	0.0030	0.9880	0.9960
NGFG_01262	-0.2880	0.2560	0.7410	NGFG_01322	-0.2440	0.1570	0.6220
NGFG_01264	-0.0346	0.8370	0.9730	NGFG_01323	-0.1360	0.3070	0.7770
NGFG_01265	0.0422	0.8330	0.9730	NGFG_01324	-0.0860	0.4380	0.8540
NGFG_01266	-0.2360	0.1590	0.6220	NGFG_01325	-0.1170	0.3190	0.7780
NGFG_01268	-0.0729	0.4790	0.8650	NGFG_01326	-0.2320	0.2740	0.7560

NGFG_01327	-0.0954	0.6400	0.9210	NGFG_01385	-0.2090	0.2390	0.7260
NGFG_01328	-0.2260	0.2050	0.6890	NGFG_01386	-0.0644	0.6460	0.9210
NGFG_01329	-0.1160	0.5050	0.8760	NGFG_01387	-0.1620	0.0519	0.4150
NGFG_01330	-0.0906	0.4240	0.8490	NGFG_01388	-0.1520	0.2070	0.6910
NGFG_01331	-0.2890	0.0341	0.3650	NGFG_01389	-0.1090	0.4200	0.8440
NGFG_01332	-0.2810	0.0536	0.4160	NGFG_01390	-0.2020	0.0269	0.3410
NGFG_01334	-0.3120	0.0377	0.3790	NGFG_01391	-0.0063	0.9690	0.9960
NGFG_01335	-0.2270	0.1090	0.5490	NGFG_01392	0.1150	0.3570	0.8020
NGFG_01336	-0.0221	0.9050	0.9860	NGFG_01393	0.1370	0.3100	0.7770
NGFG_01337	-0.0198	0.8630	0.9750	NGFG_01394	-0.0067	0.9660	0.9960
NGFG_01338	0.1400	0.3690	0.8070	NGFG_01395	0.0371	0.7360	0.9500
NGFG_01339	0.0857	0.6610	0.9240	NGFG_01396	0.0540	0.7040	0.9360
NGFG_01340	0.4860	0.0070	0.1820	NGFG_01397	-0.1760	0.1110	0.5490
NGFG_01341	0.4110	0.0815	0.5020	NGFG_01398	-0.0166	0.9180	0.9910
NGFG_01343	0.4050	0.0477	0.4140	NGFG_01399	-0.2090	0.0503	0.4150
NGFG_01345	0.6640	0.0006	0.0606	NGFG_01400	-0.1050	0.4730	0.8640
NGFG_01346	0.6170	0.0010	0.0878	NGFG_01401	-0.0204	0.8580	0.9740
NGFG_01347	0.4880	0.0081	0.1870	NGFG_01402	0.0612	0.5870	0.9070
NGFG_01348	0.3680	0.0600	0.4450	NGFG_01403	0.1130	0.5610	0.8970
NGFG_01349	0.3250	0.1550	0.6220	NGFG_01404	0.0228	0.8990	0.9840
NGFG_01350	0.0337	0.8140	0.9720	NGFG_01405	-0.1640	0.4220	0.8470
NGFG_01351	-0.2490	0.0581	0.4360	NGFG_01406	-0.0607	0.7930	0.9690
NGFG_01353	0.0059	0.9800	0.9960	NGFG_01407	-0.1510	0.4170	0.8400
NGFG_01354	-0.3130	0.0296	0.3510	NGFG_01408	0.0736	0.7240	0.9450
NGFG_01355	-0.1090	0.5280	0.8830	NGFG_01409	0.0964	0.6620	0.9240
NGFG_01356	-0.1970	0.0927	0.5120	NGFG_01411	-0.2760	0.1300	0.5790
NGFG_01357	0.1350	0.4680	0.8640	NGFG_01412	-0.2500	0.0123	0.2320
NGFG_01360	0.0875	0.4330	0.8530	NGFG_01413	-0.1130	0.4820	0.8650
NGFG_01361	0.3200	0.0784	0.4920	NGFG_01414	-0.0767	0.7020	0.9350
NGFG_01362	-0.1420	0.0547	0.4210	NGFG_01415	-0.0694	0.6040	0.9080
NGFG_01366	-0.0362	0.8690	0.9760	NGFG_01416	-0.3270	0.0310	0.3570
NGFG_01367	-0.2290	0.0463	0.4100	NGFG_01417	-0.2020	0.3020	0.7770
NGFG_01368	-0.2360	0.2130	0.6940	NGFG_01418	-0.0900	0.5070	0.8760
NGFG_01369	-0.3700	0.0036	0.1520	NGFG_01419	0.1780	0.3580	0.8020
NGFG_01370	-0.1780	0.2590	0.7410	NGFG_01420	-0.2020	0.1310	0.5790
NGFG_01373	0.1220	0.5490	0.8870	NGFG_01421	-0.1650	0.3210	0.7780
NGFG_01374	-0.0635	0.6360	0.9210	NGFG_01422	-0.2160	0.1370	0.5930
NGFG_01375	-0.2480	0.2090	0.6930	NGFG_01423	-0.0845	0.5060	0.8760
NGFG_01376	-0.0277	0.9040	0.9860	NGFG_01424	-0.1710	0.3280	0.7830
NGFG_01377	0.0054	0.9720	0.9960	NGFG_01425	-0.0658	0.7550	0.9570
NGFG_01378	0.0525	0.8210	0.9720	NGFG_01426	0.0539	0.7220	0.9450
NGFG_01379	-0.1630	0.1020	0.5280	NGFG_01427	-0.1390	0.1950	0.6700
NGFG_01380	-0.0846	0.5770	0.9010	NGFG_01428	-0.1200	0.4910	0.8700
NGFG_01381	-0.0894	0.4240	0.8490	NGFG_01429	-0.2490	0.2360	0.7210
NGFG_01382	0.1790	0.1600	0.6220	NGFG_01430	-0.3950	0.0505	0.4150
NGFG_01383	-0.2200	0.1870	0.6520	NGFG_01431	-0.1260	0.3800	0.8130
NGFG_01384	0.0563	0.7320	0.9490	NGFG_01432	-0.0527	0.7330	0.9490

NGFG_01435	0.1130	0.3100	0.7770	NGFG_01499	-0.2430	0.1750	0.6430
NGFG_01436	0.3030	0.1310	0.5790	NGFG_01501	0.1210	0.3250	0.7810
NGFG_01437	0.0292	0.8080	0.9720	NGFG_01502	0.1490	0.3310	0.7870
NGFG_01438	-0.0410	0.7960	0.9690	NGFG_01503	0.1500	0.2620	0.7410
NGFG_01439	-0.0097	0.9470	0.9960	NGFG_01504	0.0629	0.6410	0.9210
NGFG_01440	0.2140	0.1530	0.6160	NGFG_01505	0.1570	0.2230	0.7110
NGFG_01441	0.0368	0.8280	0.9720	NGFG_01506	-0.0695	0.5450	0.8860
NGFG_01442	0.0624	0.7090	0.9400	NGFG_01507	-0.1080	0.3700	0.8070
NGFG_01443	0.0934	0.4790	0.8650	NGFG_01509	-0.2790	0.1400	0.5980
NGFG_01444	-0.0528	0.5450	0.8860	NGFG_01510	-0.2940	0.0758	0.4850
NGFG_01445	0.3480	0.0046	0.1620	NGFG_01511	-0.1450	0.5240	0.8830
NGFG_01446	0.2290	0.1530	0.6160	NGFG_01512	-0.1230	0.5330	0.8850
NGFG_01447	0.3580	0.0201	0.3010	NGFG_01513	0.0162	0.9350	0.9960
NGFG_01452	0.3810	0.0050	0.1660	NGFG_01514	0.2160	0.2910	0.7700
NGFG_01453	0.1850	0.1640	0.6280	NGFG_01515	-0.2210	0.1140	0.5520
NGFG_01455	0.2470	0.0708	0.4780	NGFG_01516	-0.0991	0.5560	0.8930
NGFG_01457	0.1640	0.2570	0.7410	NGFG_01517	0.0081	0.9560	0.9960
NGFG_01458	0.1330	0.4560	0.8610	NGFG_01519	-0.3910	0.0821	0.5020
NGFG_01459	-0.1190	0.4680	0.8640	NGFG_01520	-0.0550	0.7840	0.9680
NGFG_01460	-0.1350	0.4190	0.8430	NGFG_01521	-0.1190	0.5240	0.8830
NGFG_01461	-0.0744	0.4760	0.8640	NGFG_01522	0.0686	0.7230	0.9450
NGFG_01464	-0.1650	0.4420	0.8540	NGFG_01523	-0.0524	0.7800	0.9660
NGFG_01466	0.0017	0.9910	0.9960	NGFG_01524	-0.3360	0.0019	0.1070
NGFG_01467	-0.1720	0.3080	0.7770	NGFG_01526	0.4170	0.0329	0.3580
NGFG_01468	-0.1760	0.3700	0.8070	NGFG_01527	0.3970	0.0085	0.1910
NGFG_01469	0.3490	0.1270	0.5710	NGFG_01528	0.5870	0.0004	0.0547
NGFG_01470	0.3450	0.0356	0.3700	NGFG_01529	0.4400	0.0176	0.2820
NGFG_01471	0.1920	0.0984	0.5200	NGFG_01531	0.4090	0.0362	0.3700
NGFG_01472	-0.0441	0.7750	0.9640	NGFG_01532	0.4800	0.0166	0.2740
NGFG_01476	-0.1380	0.2800	0.7580	NGFG_01533	0.0488	0.6820	0.9340
NGFG_01478	-0.0142	0.9400	0.9960	NGFG_01536	0.6420	0.0019	0.1070
NGFG_01479	-0.8170	0.0001	0.0230	NGFG_01537	-0.3450	0.0093	0.1960
NGFG_01480	0.0258	0.8750	0.9780	NGFG_01538	0.0288	0.8810	0.9810
NGFG_01481	-0.0312	0.8220	0.9720	NGFG_01539	-0.0340	0.7490	0.9570
NGFG_01482	-0.1830	0.2060	0.6910	NGFG_01540	-0.1110	0.4540	0.8590
NGFG_01483	-0.2250	0.1390	0.5970	NGFG_01541	0.0801	0.6440	0.9210
NGFG_01485	0.4560	0.0122	0.2320	NGFG_01542	0.1300	0.3540	0.8020
NGFG_01486	-0.0624	0.4910	0.8700	NGFG_01543	-0.2840	0.0527	0.4150
NGFG_01488	-0.1730	0.4410	0.8540	NGFG_01544	-0.2500	0.0489	0.4150
NGFG_01490	-0.0346	0.7940	0.9690	NGFG_01545	0.0009	0.9960	0.9970
NGFG_01491	0.1360	0.5270	0.8830	NGFG_01546	-0.0915	0.5530	0.8900
NGFG_01492	0.0878	0.6830	0.9340	NGFG_01547	0.0774	0.6410	0.9210
NGFG_01493	0.1820	0.3480	0.8010	NGFG_01548	-0.0502	0.7500	0.9570
NGFG_01495	-0.0451	0.6800	0.9340	NGFG_01549	-0.0452	0.7950	0.9690
NGFG_01496	-0.1880	0.0485	0.4140	NGFG_01550	-0.1080	0.5490	0.8870
NGFG_01497	-0.1490	0.2800	0.7580	NGFG_01551	0.3590	0.0462	0.4100
NGFG_01498	0.0938	0.5040	0.8760	NGFG_01552	0.4350	0.0410	0.3870

NGFG_01553	0.0905	0.5170	0.8800	NGFG_01603	-0.0378	0.8320	0.9730
NGFG_01554	0.0455	0.7840	0.9680	NGFG_01605	-0.0290	0.8580	0.9740
NGFG_01555	0.0951	0.5310	0.8830	NGFG_01606	-0.1800	0.3260	0.7810
NGFG_01556	0.0908	0.5510	0.8900	NGFG_01607	-0.1180	0.4710	0.8640
NGFG_01558	-0.3930	0.0619	0.4490	NGFG_01608	-0.2110	0.0397	0.3870
NGFG_01559	-0.0091	0.9520	0.9960	NGFG_01609	0.0216	0.8720	0.9770
NGFG_01560	0.0072	0.9720	0.9960	NGFG_01610	-0.1190	0.3180	0.7770
NGFG_01561	-0.2760	0.1640	0.6280	NGFG_01611	0.1770	0.0907	0.5090
NGFG_01562	-0.2250	0.0394	0.3870	NGFG_01612	-0.1190	0.5390	0.8860
NGFG_01564	0.1820	0.1800	0.6480	NGFG_01613	-0.0846	0.2830	0.7610
NGFG_01565	-0.3460	0.0520	0.4150	NGFG_01614	-0.1010	0.5320	0.8830
NGFG_01566	0.0030	0.9830	0.9960	NGFG_01615	-0.0626	0.7690	0.9600
NGFG_01567	-0.2370	0.0275	0.3410	NGFG_01616	0.0002	0.9990	1.0000
NGFG_01568	-0.3620	0.0052	0.1660	NGFG_01617	-0.5750	0.0000	0.0193
NGFG_01569	-0.5030	0.0076	0.1850	NGFG_01618	0.1140	0.4910	0.8700
NGFG_01571	-0.3830	0.0047	0.1620	NGFG_01619	-0.2770	0.0523	0.4150
NGFG_01572	-0.2090	0.2830	0.7610	NGFG_01620	-0.1160	0.3550	0.8020
NGFG_01573	-0.1590	0.2290	0.7200	NGFG_01621	-0.0412	0.6870	0.9340
NGFG_01574	-0.0609	0.6760	0.9300	NGFG_01622	-0.0905	0.6220	0.9140
NGFG_01575	-0.2080	0.0474	0.4140	NGFG_01623	-0.1060	0.5890	0.9080
NGFG_01576	-0.1100	0.4510	0.8590	NGFG_01624	-0.0685	0.5860	0.9060
NGFG_01577	-0.1180	0.5920	0.9080	NGFG_01625	-0.1040	0.5810	0.9030
NGFG_01578	-0.1200	0.1560	0.6220	NGFG_01626	-0.1650	0.0737	0.4820
NGFG_01579	0.0209	0.8880	0.9820	NGFG_01627	-0.0933	0.2960	0.7700
NGFG_01580	-0.0430	0.8170	0.9720	NGFG_01628	-0.0949	0.6440	0.9210
NGFG_01581	-0.1340	0.2970	0.7700	NGFG_01630	-0.0508	0.7120	0.9400
NGFG_01582	0.0122	0.9430	0.9960	NGFG_01631	-0.1500	0.3330	0.7880
NGFG_01583	0.0968	0.2680	0.7510	NGFG_01632	-0.0636	0.7780	0.9650
NGFG_01584	-0.1050	0.4380	0.8540	NGFG_01633	-0.2520	0.0479	0.4140
NGFG_01585	0.0174	0.9090	0.9870	NGFG_01634	-0.0297	0.8140	0.9720
NGFG_01586	-0.2980	0.0648	0.4580	NGFG_01635	-0.2570	0.1710	0.6390
NGFG_01587	0.0138	0.9340	0.9960	NGFG_01636	-0.4310	0.0185	0.2830
NGFG_01588	-0.2580	0.0735	0.4820	NGFG_01637	-0.2910	0.1230	0.5680
NGFG_01589	-0.2110	0.1010	0.5270	NGFG_01638	-0.1710	0.3260	0.7810
NGFG_01590	-0.0637	0.6880	0.9340	NGFG_01639	-0.2840	0.1900	0.6580
NGFG_01591	-0.0911	0.5960	0.9080	NGFG_01640	-0.2600	0.1230	0.5680
NGFG_01592	-0.1720	0.4570	0.8620	NGFG_01641	-0.0944	0.6180	0.9140
NGFG_01593	-0.0605	0.7330	0.9490	NGFG_01642	0.0885	0.6510	0.9210
NGFG_01594	-0.1440	0.4730	0.8640	NGFG_01643	-0.0186	0.8430	0.9730
NGFG_01595	-0.0556	0.6640	0.9240	NGFG_01644	-0.0596	0.8040	0.9720
NGFG_01596	-0.1780	0.1650	0.6280	NGFG_01645	-0.2570	0.3120	0.7770
NGFG_01597	-0.0329	0.7170	0.9430	NGFG_01646	-0.0767	0.6430	0.9210
NGFG_01598	-0.0076	0.9630	0.9960	NGFG_01647	-0.0108	0.9440	0.9960
NGFG_01599	-0.2550	0.2010	0.6790	NGFG_01648	0.0411	0.7460	0.9560
NGFG_01600	-0.2310	0.1490	0.6140	NGFG_01649	0.0567	0.6880	0.9340
NGFG_01601	-0.0685	0.6960	0.9350	NGFG_01652	0.0407	0.7630	0.9570
NGFG_01602	-0.2640	0.2700	0.7530	NGFG_01653	-0.1060	0.4720	0.8640

NGFG_01654	-0.1070	0.3790	0.8130	NGFG_01708	0.0594	0.7610	0.9570
NGFG_01655	-0.1580	0.3090	0.7770	NGFG_01709	0.0038	0.9820	0.9960
NGFG_01656	-0.0051	0.9710	0.9960	NGFG_01710	-0.1680	0.2470	0.7340
NGFG_01657	-0.2910	0.0252	0.3380	NGFG_01711	-0.1380	0.1320	0.5790
NGFG_01659	-0.3750	0.0014	0.0954	NGFG_01712	0.0177	0.8740	0.9780
NGFG_01660	-0.3010	0.0534	0.4150	NGFG_01713	0.0218	0.8760	0.9790
NGFG_01661	-0.2820	0.1150	0.5520	NGFG_01714	0.0597	0.6120	0.9120
NGFG_01662	-0.2000	0.1970	0.6750	NGFG_01715	-0.1640	0.1180	0.5560
NGFG_01663	-0.2650	0.0751	0.4850	NGFG_01716	-0.0732	0.6160	0.9140
NGFG_01664	0.0430	0.8310	0.9730	NGFG_01717	-0.0937	0.3900	0.8190
NGFG_01665	0.0920	0.4540	0.8590	NGFG_01718	-0.1250	0.4140	0.8380
NGFG_01666	0.1420	0.3980	0.8260	NGFG_01719	0.3030	0.0704	0.4780
NGFG_01667	-0.3940	0.0112	0.2230	NGFG_01720	0.0407	0.8000	0.9700
NGFG_01668	-0.1260	0.6000	0.9080	NGFG_01721	0.0176	0.9120	0.9870
NGFG_01669	-0.2180	0.1750	0.6430	NGFG_01722	-0.0102	0.9410	0.9960
NGFG_01670	-0.0891	0.6490	0.9210	NGFG_01723	-0.1340	0.5080	0.8760
NGFG_01671	-0.0595	0.8120	0.9720	NGFG_01724	0.0365	0.7990	0.9700
NGFG_01672	-0.3880	0.0031	0.1420	NGFG_01725	0.0376	0.7780	0.9650
NGFG_01673	0.3220	0.1320	0.5790	NGFG_01726	0.1860	0.2170	0.7010
NGFG_01674	0.0608	0.7370	0.9500	NGFG_01727	0.1960	0.2710	0.7550
NGFG_01676	-0.2090	0.1950	0.6710	NGFG_01728	0.1410	0.4060	0.8330
NGFG_01677	-0.2610	0.1320	0.5790	NGFG_01729	0.1840	0.2760	0.7560
NGFG_01678	0.2080	0.3350	0.7900	NGFG_01730	0.5120	0.0005	0.0547
NGFG_01680	-0.2240	0.3790	0.8130	NGFG_01731	0.4530	0.0014	0.0954
NGFG_01681	-0.0403	0.8190	0.9720	NGFG_01732	0.3920	0.0048	0.1620
NGFG_01682	0.0970	0.5330	0.8850	NGFG_01734	0.4070	0.0123	0.2320
NGFG_01684	-0.2140	0.0153	0.2700	NGFG_01735	0.4550	0.0018	0.1070
NGFG_01685	-0.0166	0.9400	0.9960	NGFG_01736	0.4810	0.0010	0.0881
NGFG_01686	0.0095	0.9280	0.9940	NGFG_01737	0.6000	0.0120	0.2320
NGFG_01687	-0.1880	0.4210	0.8460	NGFG_01738	0.4580	0.0032	0.1420
NGFG_01688	-0.2190	0.1160	0.5520	NGFG_01739	0.3540	0.0178	0.2830
NGFG_01689	0.1310	0.5130	0.8780	NGFG_01741	0.3020	0.0507	0.4150
NGFG_01690	0.1490	0.4100	0.8370	NGFG_01742	0.3600	0.0270	0.3410
NGFG_01691	-0.0439	0.8420	0.9730	NGFG_01743	0.2540	0.1180	0.5560
NGFG_01692	-0.0071	0.9740	0.9960	NGFG_01744	0.3300	0.0352	0.3680
NGFG_01695	-0.2170	0.1810	0.6480	NGFG_01745	0.3720	0.0088	0.1920
NGFG_01696	-0.0820	0.4510	0.8590	NGFG_01746	0.4930	0.0001	0.0286
NGFG_01697	-0.1150	0.3680	0.8070	NGFG_01747	0.4750	0.0075	0.1850
NGFG_01698	-0.0933	0.4270	0.8490	NGFG_01748	0.4240	0.0068	0.1820
NGFG_01699	-0.0125	0.9320	0.9960	NGFG_01749	0.3730	0.0184	0.2830
NGFG_01700	-0.0318	0.8130	0.9720	NGFG_01750	0.3460	0.0078	0.1860
NGFG_01701	-0.0354	0.8670	0.9760	NGFG_01751	0.3660	0.0131	0.2390
NGFG_01703	-0.1740	0.3750	0.8110	NGFG_01752	0.2280	0.2490	0.7350
NGFG_01704	-0.2030	0.1460	0.6110	NGFG_01753	0.1880	0.4130	0.8370
NGFG_01705	0.1240	0.6190	0.9140	NGFG_01754	0.2490	0.2410	0.7260
NGFG_01706	0.0102	0.9540	0.9960	NGFG_01755	0.2130	0.3570	0.8020
NGFG_01707	0.1120	0.6100	0.9100	NGFG_01756	0.2540	0.1610	0.6250

NGFG_01757	0.3360	0.0904	0.5080	NGFG_01816	0.1670	0.3550	0.8020
NGFG_01758	0.3290	0.0659	0.4640	NGFG_01817	-0.1910	0.1580	0.6220
NGFG_01759	0.1420	0.3940	0.8220	NGFG_01818	-0.0633	0.6490	0.9210
NGFG_01761	-0.1490	0.4650	0.8640	NGFG_01821	1.3300	0.0000	0.0000
NGFG_01763	-0.0143	0.9540	0.9960	NGFG_01822	-0.2490	0.0742	0.4840
NGFG_01764	-0.0366	0.8570	0.9740	NGFG_01824	0.1230	0.3710	0.8070
NGFG_01766	-0.0130	0.9190	0.9910	NGFG_01825	0.0965	0.5070	0.8760
NGFG_01767	0.5760	0.0024	0.1270	NGFG_01826	0.1830	0.2230	0.7110
NGFG_01768	0.5250	0.0016	0.0987	NGFG_01827	0.1180	0.5170	0.8800
NGFG_01770	0.3930	0.0069	0.1820	NGFG_01828	-0.1760	0.3120	0.7770
NGFG_01771	0.3380	0.0246	0.3370	NGFG_01829	-0.0731	0.7220	0.9450
NGFG_01772	0.3810	0.0014	0.0954	NGFG_01830	-0.1200	0.5260	0.8830
NGFG_01773	0.5030	0.0053	0.1660	NGFG_01831	-0.3380	0.0515	0.4150
NGFG_01774	-0.0403	0.8260	0.9720	NGFG_01832	-0.2110	0.2090	0.6930
NGFG_01775	-0.2850	0.1430	0.6030	NGFG_01834	-0.2740	0.2390	0.7260
NGFG_01776	0.0916	0.6840	0.9340	NGFG_01836	-0.2190	0.2350	0.7210
NGFG_01779	-0.0308	0.8290	0.9720	NGFG_01837	-0.1770	0.3590	0.8020
NGFG_01780	-0.1940	0.1000	0.5240	NGFG_01839	-0.1260	0.4150	0.8390
NGFG_01781	0.0431	0.7600	0.9570	NGFG_01840	-0.1940	0.1810	0.6490
NGFG_01782	-0.1040	0.2820	0.7610	NGFG_01841	-0.3960	0.1180	0.5560
NGFG_01783	-0.0186	0.8900	0.9820	NGFG_01842	-0.2040	0.3550	0.8020
NGFG_01784	0.0123	0.9300	0.9940	NGFG_01843	-0.1550	0.4930	0.8700
NGFG_01785	-0.0142	0.8990	0.9840	NGFG_01844	-0.0837	0.7430	0.9540
NGFG_01786	0.0763	0.6710	0.9280	NGFG_01845	-0.4280	0.0027	0.1350
NGFG_01787	-0.1030	0.4310	0.8530	NGFG_01846	-0.5160	0.0320	0.3580
NGFG_01788	-0.3030	0.0874	0.5030	NGFG_01847	-0.3700	0.0020	0.1080
NGFG_01790	-0.0340	0.8280	0.9720	NGFG_01848	-0.1770	0.1150	0.5520
NGFG_01791	-0.0027	0.9890	0.9960	NGFG_01849	0.1440	0.5120	0.8780
NGFG_01792	-0.0067	0.9680	0.9960	NGFG_01850	-0.0370	0.7510	0.9570
NGFG_01793	-0.2090	0.1230	0.5680	NGFG_01851	0.0623	0.5810	0.9030
NGFG_01794	-0.1100	0.6610	0.9240	NGFG_01852	-0.0222	0.8840	0.9820
NGFG_01796	-0.1400	0.3120	0.7770	NGFG_01853	0.0088	0.9480	0.9960
NGFG_01797	-0.3080	0.1920	0.6630	NGFG_01854	-0.2190	0.0954	0.5140
NGFG_01798	-0.1430	0.4390	0.8540	NGFG_01856	-0.0251	0.8640	0.9750
NGFG_01799	0.1720	0.3180	0.7770	NGFG_01859	0.1320	0.4700	0.8640
NGFG_01801	-0.0359	0.8360	0.9730	NGFG_01860	-0.0446	0.7940	0.9690
NGFG_01802	-0.0624	0.6020	0.9080	NGFG_01861	-0.1360	0.3950	0.8230
NGFG_01803	0.2480	0.1310	0.5790	NGFG_01862	-0.0827	0.6970	0.9350
NGFG_01805	0.2790	0.2180	0.7040	NGFG_01863	-0.2290	0.1560	0.6220
NGFG_01806	0.3160	0.0719	0.4780	NGFG_01864	-0.1420	0.3810	0.8140
NGFG_01809	0.0150	0.9250	0.9920	NGFG_01865	-0.0761	0.4980	0.8710
NGFG_01810	-0.1080	0.3880	0.8180	NGFG_01868	0.2550	0.0815	0.5020
NGFG_01811	0.1150	0.5340	0.8850	NGFG_01869	0.1680	0.1620	0.6250
NGFG_01812	-0.3480	0.0345	0.3660	NGFG_01870	-0.1390	0.4530	0.8590
NGFG_01813	-0.0540	0.7280	0.9470	NGFG_01872	0.0218	0.8920	0.9820
NGFG_01814	0.1520	0.2510	0.7360	NGFG_01873	0.1200	0.5480	0.8870
NGFG_01815	-0.2620	0.0160	0.2740	NGFG_01874	0.0867	0.6860	0.9340

NGFG_01875	-0.1890	0.1870	0.6520	NGFG_01931	0.1960	0.1600	0.6220
NGFG_01876	-0.2310	0.2350	0.7210	NGFG_01933	0.1330	0.4120	0.8370
NGFG_01877	0.0722	0.7660	0.9580	NGFG_01934	-0.1440	0.2080	0.6930
NGFG_01878	-0.0325	0.8930	0.9830	NGFG_01935	-0.2100	0.0185	0.2830
NGFG_01879	0.1270	0.5940	0.9080	NGFG_01937	0.1560	0.3630	0.8040
NGFG_01880	-0.2700	0.2750	0.7560	NGFG_01939	-0.1820	0.1850	0.6520
NGFG_01883	0.0602	0.7430	0.9540	NGFG_01940	-0.2080	0.1270	0.5710
NGFG_01884	-0.0339	0.8690	0.9760	NGFG_01941	-0.7310	0.0000	0.0000
NGFG_01885	-0.0763	0.7070	0.9400	NGFG_01942	-0.4130	0.0250	0.3370
NGFG_01886	-0.1220	0.3350	0.7900	NGFG_01943	-0.3700	0.0274	0.3410
NGFG_01887	-0.1520	0.1510	0.6160	NGFG_01944	-0.0067	0.9770	0.9960
NGFG_01888	-0.0501	0.7850	0.9680	NGFG_01945	-0.0916	0.5820	0.9030
NGFG_01889	-0.0105	0.9450	0.9960	NGFG_01946	-0.2290	0.2570	0.7410
NGFG_01890	0.1950	0.4140	0.8380	NGFG_01947	0.0220	0.8960	0.9840
NGFG_01891	-0.1440	0.3180	0.7770	NGFG_01948	0.6420	0.0001	0.0268
NGFG_01892	0.0182	0.8270	0.9720	NGFG_01949	0.3140	0.0093	0.1960
NGFG_01893	0.3770	0.0327	0.3580	NGFG_01950	0.0493	0.7630	0.9570
NGFG_01894	0.1030	0.4950	0.8700	NGFG_01951	0.0445	0.7980	0.9690
NGFG_01895	-0.1360	0.2420	0.7260	NGFG_01952	0.0924	0.6350	0.9210
NGFG_01897	0.2390	0.1190	0.5580	NGFG_01953	0.0375	0.8580	0.9740
NGFG_01898	0.1880	0.3180	0.7770	NGFG_01954	0.2350	0.1490	0.6140
NGFG_01899	-0.0397	0.8180	0.9720	NGFG_01955	0.2360	0.0405	0.3870
NGFG_01900	-0.2090	0.0949	0.5140	NGFG_01956	0.2570	0.0156	0.2730
NGFG_01901	-0.1230	0.5630	0.8970	NGFG_01957	-0.1090	0.4790	0.8650
NGFG_01902	-0.2200	0.3500	0.8010	NGFG_01958	0.0368	0.8440	0.9730
NGFG_01903	-0.2950	0.1830	0.6520	NGFG_01959	-0.0894	0.4890	0.8690
NGFG_01904	-0.0039	0.9830	0.9960	NGFG_01960	0.1250	0.3200	0.7780
NGFG_01905	-0.3450	0.0479	0.4140	NGFG_01961	0.0546	0.7000	0.9350
NGFG_01906	-0.2730	0.0759	0.4850	NGFG_01962	-0.1250	0.3660	0.8060
NGFG_01907	-0.1890	0.3850	0.8180	NGFG_01963	-0.1590	0.2940	0.7700
NGFG_01908	-0.3790	0.0324	0.3580	NGFG_01964	-0.6780	0.0002	0.0371
NGFG_01909	-0.3630	0.1120	0.5500	NGFG_01965	-0.3000	0.0661	0.4640
NGFG_01910	-0.0115	0.9440	0.9960	NGFG_01968	-0.0158	0.9010	0.9840
NGFG_01911	0.0859	0.6090	0.9100	NGFG_01969	-0.0835	0.6610	0.9240
NGFG_01912	-0.0607	0.7340	0.9490	NGFG_01970	-0.0015	0.9920	0.9960
NGFG_01914	0.4350	0.0292	0.3480	NGFG_01971	-0.1050	0.3800	0.8130
NGFG_01915	0.0568	0.7090	0.9400	NGFG_01972	0.3010	0.0314	0.3570
NGFG_01917	0.4530	0.0344	0.3660	NGFG_01973	0.2130	0.1570	0.6220
NGFG_01919	0.4710	0.0179	0.2830	NGFG_01974	0.1730	0.3130	0.7770
NGFG_01922	0.4390	0.0408	0.3870	NGFG_01975	-0.0563	0.5970	0.9080
NGFG_01923	0.5130	0.0279	0.3410	NGFG_01977	-0.1450	0.1510	0.6160
NGFG_01924	-0.0547	0.7420	0.9540	NGFG_01978	-0.0397	0.8390	0.9730
NGFG_01925	-0.2500	0.0925	0.5120	NGFG_01979	-0.2690	0.0263	0.3410
NGFG_01926	-0.1240	0.5360	0.8860	NGFG_01980	-0.1860	0.1740	0.6430
NGFG_01927	0.1880	0.3460	0.7960	NGFG_01981	-0.2630	0.0878	0.5030
NGFG_01928	-0.0213	0.9220	0.9910	NGFG_01982	0.1020	0.6230	0.9140
NGFG_01929	-0.0061	0.9790	0.9960	NGFG_01983	-0.1240	0.2440	0.7310

NGFG_01984	0.0461	0.7960	0.9690	NGFG_02039	0.0038	0.9770	0.9960
NGFG_01986	0.2970	0.1280	0.5720	NGFG_02040	-0.0206	0.8970	0.9840
NGFG_01987	-0.1580	0.4330	0.8530	NGFG_02041	-0.0823	0.5230	0.8830
NGFG_01988	-0.1210	0.2350	0.7210	NGFG_02042	-0.0337	0.8190	0.9720
NGFG_01989	0.0709	0.7200	0.9450	NGFG_02043	0.0407	0.8540	0.9740
NGFG_01990	0.2430	0.3070	0.7770	NGFG_02044	-0.1820	0.1630	0.6270
NGFG_01992	-0.0960	0.6580	0.9240	NGFG_02045	-0.0504	0.7520	0.9570
NGFG_01993	0.0045	0.9790	0.9960	NGFG_02046	-0.1080	0.5960	0.9080
NGFG_01994	0.0219	0.9100	0.9870	NGFG_02047	-0.1590	0.4870	0.8670
NGFG_01996	-0.1670	0.3670	0.8060	NGFG_02048	-0.0589	0.8160	0.9720
NGFG_01997	-0.1880	0.3240	0.7810	NGFG_02049	-0.0997	0.6480	0.9210
NGFG_01999	-0.3830	0.0967	0.5140	NGFG_02050	0.2200	0.3440	0.7960
NGFG_02000	-0.1970	0.1770	0.6450	NGFG_02052	0.3090	0.0576	0.4340
NGFG_02001	0.0412	0.8430	0.9730	NGFG_02053	0.3950	0.0129	0.2390
NGFG_02002	-0.1470	0.4150	0.8390	NGFG_02054	-0.0088	0.9560	0.9960
NGFG_02003	-0.1660	0.1690	0.6350	NGFG_02055	0.0051	0.9750	0.9960
NGFG_02004	0.4590	0.0420	0.3910	NGFG_02056	-0.5120	0.0104	0.2110
NGFG_02005	0.0897	0.5360	0.8860	NGFG_02057	-0.3000	0.0148	0.2620
NGFG_02006	-0.1310	0.1670	0.6330	NGFG_02058	0.3810	0.0046	0.1620
NGFG_02007	-0.1110	0.3690	0.8070	NGFG_02061	-0.0648	0.6040	0.9080
NGFG_02008	-0.1810	0.1360	0.5910	NGFG_02062	0.0289	0.8670	0.9760
NGFG_02010	0.0250	0.9070	0.9870	NGFG_02065	-0.1520	0.3360	0.7910
NGFG_02011	0.2410	0.1480	0.6130	NGFG_02066	-0.1790	0.1250	0.5710
NGFG_02012	-0.1370	0.4050	0.8330	NGFG_02067	0.0439	0.7950	0.9690
NGFG_02013	0.3620	0.0526	0.4150	NGFG_02068	0.0703	0.7650	0.9580
NGFG_02014	0.0567	0.6620	0.9240	NGFG_02069	0.3330	0.0636	0.4550
NGFG_02015	0.0559	0.6840	0.9340	NGFG_02070	-0.0485	0.7880	0.9680
NGFG_02016	-0.0229	0.8080	0.9720	NGFG_02071	-0.0020	0.9920	0.9960
NGFG_02017	-0.0752	0.4590	0.8640	NGFG_02073	0.2470	0.0887	0.5030
NGFG_02018	-0.0281	0.8640	0.9750	NGFG_02074	0.0814	0.7500	0.9570
NGFG_02019	-0.3110	0.1480	0.6130	NGFG_02075	0.1470	0.4670	0.8640
NGFG_02020	-0.0411	0.8250	0.9720	NGFG_02076	0.4600	0.0710	0.4780
NGFG_02022	-0.0174	0.9130	0.9880	NGFG_02077	0.1170	0.6440	0.9210
NGFG_02023	-0.1240	0.3410	0.7940	NGFG_02078	0.1270	0.5990	0.9080
NGFG_02024	-0.3430	0.0089	0.1920	NGFG_02079	-0.0223	0.9280	0.9940
NGFG_02025	0.1820	0.4010	0.8300	NGFG_02080	0.1440	0.3100	0.7770
NGFG_02027	-0.1970	0.1560	0.6220	NGFG_02081	-0.2750	0.0301	0.3540
NGFG_02029	-0.0853	0.6650	0.9240	NGFG_02082	-0.1910	0.0972	0.5160
NGFG_02030	-0.1390	0.4940	0.8700	NGFG_02084	0.1020	0.6580	0.9240
NGFG_02031	-0.0021	0.9890	0.9960	NGFG_02085	-0.0753	0.6050	0.9080
NGFG_02032	-0.0242	0.8570	0.9740	NGFG_02086	0.1230	0.5160	0.8800
NGFG_02033	0.0435	0.8360	0.9730	NGFG_02087	-0.0412	0.8150	0.9720
NGFG_02034	-0.0074	0.9690	0.9960	NGFG_02088	-0.1440	0.4720	0.8640
NGFG_02035	-0.1140	0.2980	0.7700	NGFG_02089	0.1800	0.3150	0.7770
NGFG_02036	-0.0400	0.6830	0.9340	NGFG_02090	0.1980	0.1750	0.6430
NGFG_02037	-0.1170	0.5190	0.8820	NGFG_02092	-0.1250	0.2340	0.7210
NGFG_02038	-0.0030	0.9850	0.9960	NGFG_02093	-0.0230	0.9080	0.9870

NGFG_02094	-0.1530	0.4060	0.8330	NGFG_02153	0.2100	0.0849	0.5030
NGFG_02095	-0.0338	0.8780	0.9800	NGFG_02154	-0.3970	0.0241	0.3370
NGFG_02097	-0.0978	0.6990	0.9350	NGFG_02155	-0.3630	0.0455	0.4100
NGFG_02098	-0.0332	0.8890	0.9820	NGFG_02156	0.1850	0.0865	0.5030
NGFG_02100	0.1050	0.6660	0.9250	NGFG_02157	0.0535	0.5970	0.9080
NGFG_02102	0.1950	0.3080	0.7770	NGFG_02160	-0.0649	0.7700	0.9600
NGFG_02103	0.0331	0.8890	0.9820	NGFG_02161	0.0272	0.9000	0.9840
NGFG_02104	0.1170	0.4730	0.8640	NGFG_02162	0.0212	0.8960	0.9840
NGFG_02105	0.1200	0.3180	0.7770	NGFG_02163	-0.1590	0.2260	0.7150
NGFG_02106	0.3060	0.0224	0.3230	NGFG_02164	-0.0546	0.7090	0.9400
NGFG_02107	0.4200	0.0061	0.1810	NGFG_02165	0.0014	0.9920	0.9960
NGFG_02108	0.1970	0.1490	0.6140	NGFG_02166	0.0810	0.4820	0.8650
NGFG_02109	0.2100	0.1720	0.6420	NGFG_02167	-0.1550	0.1940	0.6680
NGFG_02111	0.2680	0.1440	0.6040	NGFG_02170	0.5460	0.0002	0.0371
NGFG_02112	-0.1000	0.4540	0.8590	NGFG_02171	0.4420	0.0011	0.0917
NGFG_02113	0.1330	0.4760	0.8640	NGFG_02173	0.1080	0.3520	0.8020
NGFG_02115	-0.1370	0.4020	0.8310	NGFG_02174	0.0975	0.5260	0.8830
NGFG_02116	0.0966	0.5650	0.8980	NGFG_02175	0.1690	0.1620	0.6270
NGFG_02117	-0.0983	0.4730	0.8640	NGFG_02176	0.3190	0.1220	0.5670
NGFG_02118	-0.0990	0.4490	0.8590	NGFG_02180	0.3650	0.0777	0.4910
NGFG_02119	-0.4550	0.0000	0.0181	NGFG_02184	0.4400	0.0248	0.3370
NGFG_02120	-0.0632	0.5950	0.9080	NGFG_02185	-0.1960	0.4430	0.8540
NGFG_02121	-0.0974	0.3910	0.8190	NGFG_02188	-0.1180	0.4820	0.8650
NGFG_02122	0.0302	0.8080	0.9720	NGFG_02189	-0.1110	0.5770	0.9010
NGFG_02123	-0.2460	0.0012	0.0917	NGFG_02190	0.3470	0.1680	0.6330
NGFG_02124	-0.0425	0.7580	0.9570	NGFG_02191	0.1550	0.2210	0.7090
NGFG_02125	-0.1090	0.4050	0.8330	NGFG_02192	-0.0836	0.6480	0.9210
NGFG_02126	-0.1010	0.6330	0.9200	NGFG_02194	-0.1140	0.6380	0.9210
NGFG_02127	0.0880	0.6420	0.9210	NGFG_02196	0.5360	0.0184	0.2830
NGFG_02128	-0.1520	0.2780	0.7580	NGFG_02197	0.2650	0.2600	0.7410
NGFG_02129	0.5610	0.0062	0.1810	NGFG_02198	0.1270	0.5940	0.9080
NGFG_02130	0.5350	0.0047	0.1620	NGFG_02199	0.0025	0.9880	0.9960
NGFG_02134	-0.2270	0.3110	0.7770	NGFG_02200	0.1270	0.5530	0.8900
NGFG_02135	0.2100	0.2450	0.7310	NGFG_02203	0.5780	0.0068	0.1820
NGFG_02136	-0.1870	0.1520	0.6160	NGFG_02204	0.5550	0.0071	0.1830
NGFG_02137	-0.2330	0.1580	0.6220	NGFG_02205	0.3050	0.0718	0.4780
NGFG_02138	-0.1720	0.2500	0.7350	NGFG_02206	-0.0460	0.8440	0.9730
NGFG_02140	-0.2540	0.0622	0.4500	NGFG_02207	0.0933	0.7100	0.9400
NGFG_02141	-0.0606	0.7580	0.9570	NGFG_02208	0.0497	0.8090	0.9720
NGFG_02142	-0.0958	0.4740	0.8640	NGFG_02209	0.1090	0.6230	0.9140
NGFG_02143	-0.1350	0.3240	0.7810	NGFG_02213	-0.1810	0.4710	0.8640
NGFG_02144	-0.1780	0.0882	0.5030	NGFG_02217	-0.0507	0.7560	0.9570
NGFG_02147	0.0916	0.6220	0.9140	NGFG_02219	-0.0447	0.7920	0.9690
NGFG_02148	0.4160	0.0508	0.4150	NGFG_02222	0.1250	0.4300	0.8530
NGFG_02149	0.5380	0.0336	0.3630	NGFG_02225	0.3450	0.1690	0.6350
NGFG_02151	-0.2280	0.2970	0.7700	NGFG_02226	-0.1760	0.4810	0.8650
NGFG_02152	-0.2730	0.0361	0.3700	NGFG_02228	-0.1250	0.3390	0.7940

NGFG_02229	0.2470	0.1840	0.6520	NGFG_02291	-0.3780	0.0931	0.5120
NGFG_02231	-0.1840	0.3910	0.8190	NGFG_02292	0.1590	0.2560	0.7410
NGFG_02232	-0.2360	0.3160	0.7770	NGFG_02294	0.1150	0.6520	0.9210
NGFG_02233	0.2570	0.3120	0.7770	NGFG_02295	-0.2720	0.2830	0.7610
NGFG_02234	0.0053	0.9840	0.9960	NGFG_02296	-0.1830	0.4680	0.8640
NGFG_02237	0.3070	0.2270	0.7160	NGFG_02298	-0.0867	0.7010	0.9350
NGFG_02238	0.1150	0.5100	0.8780	NGFG_02299	-0.2780	0.2010	0.6790
NGFG_02239	0.2400	0.2840	0.7630	NGFG_02300	-0.0479	0.8200	0.9720
NGFG_02243	0.1890	0.4540	0.8590	NGFG_02301	-0.1710	0.3080	0.7770
NGFG_02244	0.1080	0.6140	0.9140	NGFG_02302	0.1780	0.3400	0.7940
NGFG_02245	0.1210	0.4750	0.8640	NGFG_02303	-0.1610	0.3350	0.7900
NGFG_02247	0.6210	0.0012	0.0917	NGFG_02304	0.1200	0.6170	0.9140
NGFG_02248	0.2040	0.4010	0.8300	NGFG_02305	0.1050	0.5980	0.9080
NGFG_02253	-0.0707	0.7300	0.9480	NGFG_02306	-0.0540	0.7920	0.9690
NGFG_02254	0.0776	0.7240	0.9450	NGFG_02307	-0.2420	0.1410	0.5990
NGFG_02255	0.1450	0.5130	0.8780	NGFG_02309	0.0092	0.9610	0.9960
NGFG_02257	0.1060	0.5390	0.8860	NGFG_02310	0.1320	0.5130	0.8780
NGFG_02258	-0.0329	0.8420	0.9730	NGFG_02311	0.2030	0.4120	0.8370
NGFG_02259	-0.3660	0.0315	0.3570	NGFG_02312	0.2030	0.4270	0.8490
NGFG_02260	0.0134	0.9500	0.9960	NGFG_02313	-0.2300	0.1530	0.6160
NGFG_02262	-0.3020	0.1640	0.6280	NGFG_02314	-0.1800	0.2350	0.7210
NGFG_02263	0.3040	0.0497	0.4150	NGFG_02315	-0.1990	0.3880	0.8180
NGFG_02264	0.0340	0.8840	0.9820	NGFG_02316	0.2990	0.0411	0.3870
NGFG_02265	-0.2120	0.0649	0.4580	NGFG_02317	0.3080	0.2110	0.6930
NGFG_02266	-0.0286	0.8380	0.9730	NGFG_02318	0.5940	0.0079	0.1870
NGFG_02267	-0.2170	0.3330	0.7880	NGFG_02319	0.5430	0.0191	0.2900
NGFG_02268	0.0223	0.9210	0.9910	NGFG_02320	0.2240	0.2940	0.7700
NGFG_02269	-0.1890	0.2340	0.7210	NGFG_02321	0.2960	0.2070	0.6920
NGFG_02270	0.3950	0.0854	0.5030	NGFG_02322	-0.2270	0.1760	0.6450
NGFG_02271	0.0600	0.6610	0.9240	NGFG_02323	0.1090	0.5930	0.9080
NGFG_02272	-0.3220	0.0161	0.2740	NGFG_02324	0.1600	0.5080	0.8770
NGFG_02273	-0.1980	0.2440	0.7310	NGFG_02325	-0.0276	0.8710	0.9770
NGFG_02274	-0.0836	0.6740	0.9300	NGFG_02326	0.1710	0.4870	0.8670
NGFG_02275	-0.1330	0.3110	0.7770	NGFG_02328	0.0671	0.6890	0.9340
NGFG_02276	-0.2760	0.1080	0.5490	NGFG_02329	0.0035	0.9840	0.9960
NGFG_02277	-0.0524	0.8230	0.9720	NGFG_02330	-0.2590	0.1180	0.5560
NGFG_02278	-0.0076	0.9740	0.9960	NGFG_02331	-0.0124	0.9520	0.9960
NGFG_02280	-0.0775	0.6020	0.9080	NGFG_02334	-0.1610	0.3190	0.7780
NGFG_02281	-0.0923	0.5520	0.8900	NGFG_02335	-0.1760	0.4290	0.8530
NGFG_02282	0.0626	0.7020	0.9350	NGFG_02336	0.0787	0.7560	0.9570
NGFG_02284	0.1600	0.2460	0.7310	NGFG_02337	-0.2840	0.1130	0.5520
NGFG_02285	0.0468	0.8100	0.9720	NGFG_02338	0.2230	0.3570	0.8020
NGFG_02286	0.1350	0.5970	0.9080	NGFG_02339	0.3050	0.1250	0.5710
NGFG_02287	-0.0482	0.7910	0.9690	NGFG_02340	0.1290	0.5300	0.8830
NGFG_02288	0.2200	0.3890	0.8180	NGFG_02342	0.3740	0.0854	0.5030
NGFG_02289	0.1280	0.5300	0.8830	NGFG_02343	0.4430	0.0244	0.3370
NGFG_02290	0.1230	0.6220	0.9140	NGFG_02344	0.6620	0.0004	0.0514

NGFG_02345	0.8110	0.0001	0.0224	NGFG_02396	-0.0083	0.9530	0.9960
NGFG_02346	0.0560	0.6580	0.9240	NGFG_02397	-0.1010	0.5380	0.8860
NGFG_02347	0.2020	0.3740	0.8110	NGFG_02398	0.3100	0.1020	0.5270
NGFG_02348	0.3770	0.0432	0.4000	NGFG_02399	0.1800	0.3500	0.8010
NGFG_02349	0.4230	0.0348	0.3670	NGFG_02400	-0.1400	0.4470	0.8580
NGFG_02350	0.4330	0.0465	0.4100	NGFG_02401	0.2630	0.3010	0.7770
NGFG_02351	-0.1470	0.3890	0.8180	NGFG_02402	0.2740	0.0777	0.4910
NGFG_02352	-0.1010	0.6060	0.9080	NGFG_02403	0.4340	0.0583	0.4370
NGFG_02353	0.1310	0.5260	0.8830	NGFG_02404	0.0463	0.7940	0.9690
NGFG_02354	-0.1740	0.4910	0.8700	NGFG_02405	0.4100	0.0884	0.5030
NGFG_02355	-0.1590	0.4660	0.8640	NGFG_02406	-0.1750	0.2340	0.7210
NGFG_02356	0.0460	0.8570	0.9740	NGFG_02407	-0.2040	0.0843	0.5030
NGFG_02357	-0.0276	0.9110	0.9870	NGFG_02408	0.1230	0.5040	0.8760
NGFG_02358	0.0475	0.8370	0.9730	NGFG_02409	-0.0568	0.6380	0.9210
NGFG_02359	-0.0560	0.8260	0.9720	NGFG_02410	-0.3300	0.0210	0.3100
NGFG_02361	-0.0046	0.9810	0.9960	NGFG_02411	-0.1180	0.3990	0.8290
NGFG_02362	-0.1580	0.5230	0.8830	NGFG_02412	0.1720	0.4260	0.8490
NGFG_02363	0.4040	0.0963	0.5140	NGFG_02414	0.2090	0.3120	0.7770
NGFG_02364	0.2890	0.2560	0.7410	NGFG_02415	0.6360	0.0028	0.1350
NGFG_02365	0.0651	0.7260	0.9460	NGFG_02416	0.2140	0.2120	0.6930
NGFG_02366	0.1360	0.5050	0.8760	NGFG_02417	0.2470	0.3220	0.7790
NGFG_02367	-0.0786	0.7580	0.9570	NGFG_02418	0.3800	0.0491	0.4150
NGFG_02368	-0.0374	0.8360	0.9730	NGFG_02419	-0.1620	0.1520	0.6160
NGFG_02370	-0.1220	0.5460	0.8870	NGFG_02420	-0.0643	0.7340	0.9490
NGFG_02371	0.1710	0.4970	0.8700	NGFG_02421	-0.2080	0.3450	0.7960
NGFG_02372	0.0457	0.7830	0.9680	NGFG_02422	-0.2250	0.0935	0.5120
NGFG_02373	0.2860	0.0495	0.4150	NGFG_02423	0.0269	0.8430	0.9730
NGFG_02374	0.3790	0.0769	0.4900	NGFG_02424	-0.2550	0.0372	0.3760
NGFG_02376	-0.0217	0.9090	0.9870	NGFG_02425	-0.1360	0.4670	0.8640
NGFG_02377	0.0418	0.8690	0.9760	NGFG_02426	-0.0538	0.8290	0.9720
NGFG_02378	-0.1800	0.3080	0.7770	NGFG_02428	0.5600	0.0031	0.1420
NGFG_02379	0.2840	0.1130	0.5520	NGFG_02429	0.2370	0.3450	0.7960
NGFG_02380	0.1990	0.3180	0.7770	NGFG_02430	-0.1190	0.6350	0.9210
NGFG_02381	-0.0856	0.5740	0.9000	NGFG_02431	0.2310	0.3640	0.8050
NGFG_02382	0.1220	0.5800	0.9030	NGFG_02432	-0.0538	0.7590	0.9570
NGFG_02383	0.2010	0.1100	0.5490	NGFG_02434	0.1730	0.3700	0.8070
NGFG_02384	0.2290	0.2970	0.7700	NGFG_02435	0.0135	0.9410	0.9960
NGFG_02385	0.0250	0.9200	0.9910	NGFG_02437	0.1030	0.5750	0.9000
NGFG_02386	0.1860	0.3540	0.8020	NGFG_02438	-0.1290	0.5740	0.9000
NGFG_02387	0.0265	0.9100	0.9870	NGFG_02439	0.3040	0.1750	0.6430
NGFG_02388	0.1610	0.4750	0.8640	NGFG_02440	0.3850	0.0279	0.3410
NGFG_02389	0.1330	0.5660	0.8980	NGFG_02441	0.2660	0.1550	0.6210
NGFG_02391	-0.0030	0.9860	0.9960	NGFG_02443	-0.1740	0.4130	0.8370
NGFG_02392	-0.2300	0.2890	0.7670	NGFG_02444	-0.0447	0.8580	0.9740
NGFG_02393	0.3060	0.0868	0.5030	NGFG_02445	-0.0310	0.8730	0.9780
NGFG_02394	-0.3090	0.1520	0.6160	NGFG_02446	-0.0130	0.9580	0.9960
NGFG_02395	-0.2380	0.1670	0.6330	NGFG_02447	0.0460	0.8570	0.9740

NGFG_02448	-0.1160	0.5420	0.8860	NGFG_06008	-0.0457	0.7830	0.9680
NGFG_02449	-0.2090	0.4110	0.8370	NGFG_06010	0.4960	0.0359	0.3700
NGFG_02450	0.2670	0.1470	0.6110	NGFG_06011	0.4610	0.0498	0.4150
NGFG_02452	0.1780	0.4070	0.8330	NGFG_06012	0.2200	0.3040	0.7770
NGFG_02453	0.0268	0.9160	0.9910	NGFG_06013	0.5760	0.0240	0.3370
NGFG_02454	0.3890	0.0274	0.3410	NGFG_06014	0.4730	0.0627	0.4510
NGFG_02455	0.3770	0.0944	0.5140	NGFG_06015	0.1940	0.3550	0.8020
NGFG_02456	-0.0757	0.5930	0.9080	NGFG_06018	-0.1170	0.5190	0.8820
NGFG_02457	-0.1410	0.2760	0.7560	NGFG_06019	0.2700	0.2210	0.7090
NGFG_02458	-0.1340	0.2860	0.7660	NGFG_06021	0.1360	0.5870	0.9070
NGFG_02459	0.0360	0.8350	0.9730	NGFG_06023	0.0316	0.8670	0.9760
NGFG_02460	0.2430	0.2240	0.7110	NGFG_06024	0.0994	0.6610	0.9240
NGFG_02463	0.5310	0.0067	0.1820	NGFG_06025	-0.0077	0.9670	0.9960
NGFG_02465	0.1810	0.3210	0.7780	NGFG_06026	0.1920	0.3890	0.8190
NGFG_02466	0.1570	0.3420	0.7940	NGFG_06027	0.4160	0.0529	0.4150
NGFG_02467	-0.0747	0.6930	0.9350	NGFG_06028	0.3670	0.0892	0.5040
NGFG_02468	-0.1530	0.5060	0.8760	NGFG_06029	0.1330	0.5940	0.9080
NGFG_02469	0.3260	0.1160	0.5520	NGFG_06030	0.1020	0.6620	0.9240
NGFG_02470	0.0857	0.5990	0.9080	NGFG_06032	0.1140	0.6440	0.9210
NGFG_02471	-0.0932	0.4750	0.8640	NGFG_06033	0.7130	0.0027	0.1350
NGFG_02472	-0.1070	0.6700	0.9280	NGFG_06034	0.0669	0.6880	0.9340
NGFG_02473	-0.2310	0.1390	0.5970	NGFG_06035	0.1420	0.5290	0.8830
NGFG_02475	0.1800	0.3600	0.8020	NGFG_06036	0.1950	0.2340	0.7210
NGFG_02476	-0.0409	0.7810	0.9660	NGFG_06037	-0.2220	0.3750	0.8110
NGFG_02477	0.2950	0.0462	0.4100	NGFG_06038	0.0317	0.9000	0.9840
NGFG_02478	0.0652	0.6170	0.9140	NGFG_06039	0.0331	0.8510	0.9740
NGFG_02480	-0.0675	0.7670	0.9580	NGFG_06040	0.0847	0.7150	0.9420
NGFG_02481	0.0913	0.7120	0.9400	NGFG_06041	-0.1730	0.4560	0.8610
NGFG_02482	-0.1270	0.6180	0.9140	NGFG_06042	0.0594	0.8060	0.9720
NGFG_02483	-0.3520	0.0317	0.3570	NGFG_06044	0.0594	0.7860	0.9680
NGFG_02484	0.3390	0.1350	0.5880	NGFG_06046	0.1290	0.4390	0.8540
NGFG_02485	0.1540	0.4870	0.8670	NGFG_06047	0.1090	0.6070	0.9080
NGFG_02486	0.2620	0.0856	0.5030	NGFG_06048	0.4000	0.0850	0.5030
NGFG_02487	-0.0474	0.8370	0.9730	NGFG_06049	0.2430	0.3420	0.7940
NGFG_02488	-0.1700	0.4030	0.8330	NGFG_06050	-0.5870	0.0182	0.2830
NGFG_02490	-0.0118	0.9460	0.9960	NGFG_06051	0.1190	0.6200	0.9140
NGFG_02491	0.1390	0.4720	0.8640	NGFG_06053	0.1430	0.5720	0.9000
NGFG_02492	0.0206	0.9340	0.9960	NGFG_06054	0.2390	0.0634	0.4550
NGFG_02496	0.3510	0.0848	0.5030	NGFG_06056	0.4820	0.0437	0.4010
NGFG_02497	-0.1790	0.3770	0.8120	NGFG_06058	0.1230	0.6220	0.9140
NGFG_02498	-0.0839	0.7010	0.9350	NGFG_06059	0.7160	0.0016	0.0998
NGFG_02499	-0.0466	0.8390	0.9730	NGFG_06060	0.1800	0.2740	0.7560
NGFG_02500	0.1260	0.5730	0.9000	NGFG_06061	0.0598	0.7880	0.9680
NGFG_06000	-0.1440	0.4950	0.8700	NGFG_06062	0.0245	0.9060	0.9870
NGFG_06002	0.0299	0.8980	0.9840	NGFG_06063	-0.3810	0.1070	0.5450
NGFG_06004	0.3570	0.0682	0.4700	NGFG_06065	0.0154	0.9510	0.9960
NGFG_06005	0.0673	0.6210	0.9140	NGFG_06066	-0.1080	0.4080	0.8360

NgncR_001	0.9020	0.0003	0.0513	NgncR_082	0.0120	0.9500	0.9960
NgncR_002	0.1970	0.2410	0.7260	NgncR_088	0.1300	0.2720	0.7550
NgncR_003	-0.2380	0.1430	0.6030	NgncR_093	0.0249	0.9220	0.9910
NgncR_004	-0.0159	0.9340	0.9960	NgncR_094	-0.0140	0.9380	0.9960
NgncR_005	0.0837	0.5680	0.8990	NgncR_095	0.3660	0.1150	0.5520
NgncR_006	0.0598	0.7780	0.9650	NgncR_096	-0.0461	0.7580	0.9570
NgncR_008	0.1340	0.3830	0.8140	NgncR_097	-0.1870	0.3450	0.7960
NgncR_009	-0.0631	0.8040	0.9720	NgncR_098	0.0228	0.9290	0.9940
NgncR_010	0.0096	0.9690	0.9960	NgncR_099	0.0138	0.9560	0.9960
NgncR_012	-0.2640	0.2550	0.7410	NgncR_100	0.1110	0.5710	0.9000
NgncR_014	0.3750	0.1130	0.5520	NgncR_101	0.0798	0.4880	0.8680
NgncR_015	0.3970	0.0484	0.4140	NgncR_102	0.3130	0.0930	0.5120
NgncR_018	0.3990	0.0910	0.5090	NgncR_105	0.3780	0.0998	0.5230
NgncR_020	-0.0750	0.6050	0.9080	NgncR_106	0.4100	0.1040	0.5330
NgncR_022	0.5090	0.0200	0.3010	NgncR_107	0.1780	0.4830	0.8650
NgncR_023	0.1120	0.5970	0.9080	NgncR_109	0.0415	0.8460	0.9730
NgncR_024	0.0463	0.8280	0.9720	NgncR_110	0.4130	0.0853	0.5030
NgncR_027	0.3590	0.1120	0.5500	NgncR_112	-0.1160	0.6470	0.9210
NgncR_032	-0.2840	0.2110	0.6930	NgncR_114	-0.1560	0.5290	0.8830
NgncR_033	0.1000	0.6430	0.9210	NgncR_115	0.1420	0.5140	0.8780
NgncR_036	0.6730	0.0069	0.1820	NgncR_117	0.0830	0.7090	0.9400
NgncR_037	0.0758	0.4810	0.8650	NgncR_118	0.2910	0.0760	0.4850
NgncR_038	0.0035	0.9870	0.9960	NgncR_119	0.5080	0.0044	0.1620
NgncR_044	-0.1440	0.3490	0.8010	NgncR_120	-0.0396	0.8520	0.9740
NgncR_045	0.0787	0.7550	0.9570	NgncR_121	-0.1680	0.4680	0.8640
NgncR_047	-0.0367	0.8860	0.9820	NgncR_122	0.2200	0.3880	0.8180
NgncR_049	0.0388	0.8460	0.9730	NgncR_126	0.1180	0.6440	0.9210
NgncR_053	0.2840	0.2540	0.7410	NgncR_127	0.0155	0.9510	0.9960
NgncR_054	0.1940	0.3420	0.7940	NgncR_128	0.2340	0.3120	0.7770
NgncR_055	0.1620	0.5140	0.8780	NgncR_129	0.0812	0.6690	0.9270
NgncR_057	-0.1480	0.4720	0.8640	NgncR_130	0.0849	0.7290	0.9470
NgncR_059	-0.2550	0.2790	0.7580	NgncR_133	-0.0171	0.8920	0.9820
NgncR_060	0.2050	0.2510	0.7360	NgncR_136	-0.0287	0.9090	0.9870
NgncR_062	-0.3660	0.0413	0.3870	NgncR_137	0.3570	0.0801	0.5000
NgncR_063	-0.3170	0.0266	0.3410	NgncR_140	0.4600	0.0324	0.3580
NgncR_064	0.1830	0.1530	0.6160	NgncR_144	0.0219	0.8780	0.9800
NgncR_065	-0.0138	0.9540	0.9960	NgncR_147	0.0402	0.8560	0.9740
NgncR_066	0.0313	0.8660	0.9760	NgncR_148	0.3820	0.0451	0.4100
NgncR_068	0.0480	0.8110	0.9720	NgncR_152	0.0539	0.7900	0.9690
NgncR_070	-0.0188	0.9170	0.9910	NgncR_154	0.1410	0.4470	0.8580
NgncR_072	0.3300	0.0401	0.3870	NgncR_155	0.4190	0.0230	0.3290
NgncR_073	0.0791	0.7430	0.9540	NgncR_156	0.3210	0.0638	0.4550
NgncR_075	-0.0920	0.5950	0.9080	NgncR_161	0.7880	0.0015	0.0958
NgncR_076	0.1130	0.6520	0.9210	NgncR_162	0.2820	0.0990	0.5220
NgncR_077	0.2720	0.2240	0.7120	NgncR_163	0.0322	0.8960	0.9840
NgncR_078-Y2	0.1170	0.6370	0.9210	NgncR_164	0.2090	0.1870	0.6520
NgncR_079	0.1220	0.6240	0.9140	NgncR_165	-0.0398	0.8620	0.9750

NgncR_166	0.0855	0.6750	0.9300
NgncR_167	-0.1380	0.5470	0.8870
NgncR_169	0.0233	0.8640	0.9750
NgncR_173	0.1150	0.6230	0.9140
NgncR_176	0.2670	0.2860	0.7660
NgncR_177	0.2440	0.3300	0.7850
NgncR_179	0.4000	0.1100	0.5490
NgncR_180	-0.0760	0.6290	0.9180
NgncR_181	0.2280	0.2680	0.7510
NgncR_182	0.1090	0.6040	0.9080
NgncR_184	-0.0928	0.6890	0.9340
NgncR_186	0.3070	0.1450	0.6090
NgncR_189	0.2030	0.4210	0.8460
NgncR_191	0.0529	0.8330	0.9730
NgncR_193	-0.0989	0.5440	0.8860
NgncR_198	-0.0718	0.7540	0.9570
NgncR_199	0.2560	0.3140	0.7770
NgncR_200	-0.0284	0.8900	0.9820
NgncR_201	0.6640	0.0063	0.1810
NgncR_203	-0.0009	0.9960	0.9970
NgncR_205	0.2660	0.0830	0.5020
NgncR_206	0.2360	0.3320	0.7870
NgncR_207	0.2960	0.2410	0.7260
NgncR_209	-0.2320	0.3370	0.7910
NgncR_210	0.2460	0.2490	0.7350
NgncR_212	0.0520	0.8000	0.9700
NgncR_214	0.4270	0.0072	0.1830
NgncR_218	-0.0345	0.8910	0.9820
NgncR_221	-0.0662	0.7950	0.9690
NgncR_223	0.1120	0.5400	0.8860
NgncR_224	0.0326	0.8980	0.9840
NgncR_225	0.2070	0.3360	0.7910
NgncR_227	0.0271	0.8750	0.9780
NgncR_229	0.1720	0.3950	0.8230
NgncR_231	0.4080	0.0837	0.5030
NgncR_232	0.4770	0.0412	0.3870
NgncR_236	0.4650	0.0316	0.3570
NgncR_237	1.2400	0.0000	0.0000
NgncR_238	-0.0932	0.6180	0.9140
NgncR_239	0.3950	0.1040	0.5330
NgncR_241	0.2010	0.1650	0.6280
NgncR_242	-0.1090	0.6210	0.9140
NgncR_247	0.1050	0.4960	0.8700
NgncR_249	0.1510	0.3580	0.8020
NgncR_250	0.0025	0.9900	0.9960
NgncR_251	0.2840	0.0589	0.4380

Table A.6: Results from the CopraRNA Screen of NgncR_237

Rank	CopraRNA p-value	CopraRNA fdr value	Locus Tag	Energy [kcal/mol]	IntaRNA p-value	Position mRNA	Position sRNA
1	6,67E-03	0.007633	ngfg_rs01395	-18.50	0.000163	40 -- 57	45 -- 62
2	9,96E-03	0.007633	ngfg_rs11490	-13.30	0.016568	160 -- 212	14 -- 61
3	0.0001109	0.05666	ngfg_rs03535	-16.44	0.001388	236 -- 254	45 -- 62
4	0.00105	0.3942	ngfg_rs06565	-12.65	0.025454	271 -- 280	49 -- 58
5	0.001635	0.3942	ngfg_rs11310	-15.82	0.002397	40 -- 90	43 -- 92
6	0.001756	0.3942	ngfg_rs11775	-13.19	0.017835	269 -- 285	44 -- 60
7	0.0018	0.3942	ngfg_rs11900	-8.99	0.190587	7 -- 16	51 -- 61
8	0.00284	0.4985	ngfg_rs04550	-15.83	0.002392	24 -- 44	2 -- 22
9	0.003599	0.4985	ngfg_rs04165	-13.71	0.012430	191 -- 203	51 -- 63
10	0.003709	0.4985	ngfg_rs03515	-13.90	0.010886	75 -- 120	49 -- 92
11	0.003815	0.4985	ngfg_rs08335	-11.96	0.039299	116 -- 143	43 -- 74
12	0.003902	0.4985	ngfg_rs08060	-14.14	0.009104	240 -- 258	47 -- 61
13	0.00481	0.5348	ngfg_rs05805	-13.61	0.013359	192 -- 249	2 -- 62
14	0.004884	0.5348	ngfg_rs04625	-13.25	0.017070	192 -- 203	51 -- 62
15	0.005379	0.5498	ngfg_rs02435	-12.60	0.026207	188 -- 198	43 -- 53
16	0.005765	0.5524	ngfg_rs06605	-13.32	0.016266	71 -- 84	44 -- 60
17	0.006663	0.5814	ngfg_rs10900	-12.92	0.021336	248 -- 259	43 -- 54
18	0.00721	0.5814	ngfg_rs09215	-12.76	0.023684	178 -- 193	48 -- 63
19	0.00735	0.5814	ngfg_rs00470	-19.74	0.000033	173 -- 204	52 -- 92
20	0.008377	0.5814	ngfg_rs05665	-10.47	0.091560	167 -- 177	52 -- 62
21	0.008379	0.5814	ngfg_rs01735	-11.20	0.061459	185 -- 227	49 -- 97
22	0.008957	0.5814	ngfg_rs12945	-12.06	0.036981	78 -- 89	45 -- 60
23	0.009033	0.5814	ngfg_rs13415	-16.35	0.001505	251 -- 267	45 -- 62
24	0.009983	0.5814	ngfg_rs08205	-12.93	0.021271	10 -- 20	43 -- 53
25	0.01005	0.5814	ngfg_rs00155	-11.54	0.050258	21 -- 28	44 -- 51
26	0.01014	0.5814	ngfg_rs03440	-13.88	0.011010	58 -- 70	46 -- 58
27	0.01024	0.5814	ngfg_rs09160	-12.71	0.024461	225 -- 239	43 -- 58
28	0.011	0.5928	ngfg_rs03160	-12.27	0.032292	189 -- 220	32 -- 62
29	0.0118	0.5928	ngfg_rs03225	-8.92	0.197572	248 -- 273	45 -- 60
30	0.01215	0.5928	ngfg_rs11445	-12.20	0.033758	36 -- 46	49 -- 59
31	0.01293	0.5928	ngfg_rs01860	-12.44	0.029156	294 -- 300	47 -- 53
32	0.01298	0.5928	ngfg_rs11675	-14.17	0.008960	147 -- 172	56 -- 92
33	0.01376	0.5928	ngfg_rs12505	-12.20	0.033844	140 -- 154	49 -- 63
34	0.014	0.5928	ngfg_rs03790	-8.87	0.201311	1 -- 16	45 -- 61
35	0.01415	0.5928	ngfg_rs08570	-12.03	0.037460	273 -- 281	43 -- 51
36	0.01449	0.5928	ngfg_rs05995	-11.13	0.063718	137 -- 156	43 -- 62
37	0.01462	0.5928	ngfg_rs10355	-11.60	0.048711	87 -- 96	44 -- 53
38	0.01484	0.5928	ngfg_rs00975	-14.30	0.008128	164 -- 219	51 -- 98
39	0.01527	0.5928	ngfg_rs05415	-12.35	0.030811	188 -- 198	43 -- 53
40	0.01547	0.5928	ngfg_rs04790	-12.90	0.021586	44 -- 61	47 -- 63
41	0.01598	0.5977	ngfg_rs09465	-11.63	0.047698	183 -- 192	48 -- 58
42	0.01672	0.6056	ngfg_rs08465	-13.15	0.018297	131 -- 142	50 -- 61
43	0.01699	0.6056	ngfg_rs04590	-12.93	0.021179	65 -- 75	43 -- 53

44	0.01787	0.6226	ngfg_rs05865	-8.98	0.191627	9 -- 25	43 -- 59
45	0.01899	0.6333	ngfg_rs00225	-9.76	0.132164	265 -- 280	9 -- 24
46	0.02085	0.6333	ngfg_rs12340	-13.01	0.020147	1 -- 10	48 -- 57
47	0.02132	0.6333	ngfg_rs10325	-10.98	0.069529	239 -- 254	47 -- 60
48	0.02169	0.6333	ngfg_rs01565	-9.82	0.128025	28 -- 44	43 -- 58
49	0.02184	0.6333	ngfg_rs00855	-9.03	0.187472	152 -- 198	44 -- 92
50	0.02188	0.6333	ngfg_rs11320	-11.48	0.052051	99 -- 116	43 -- 60
51	0.02211	0.6333	ngfg_rs00425	-12.61	0.026161	223 -- 239	43 -- 58
52	0.02278	0.6333	ngfg_rs09200	-11.66	0.047062	128 -- 144	47 -- 62
53	0.02383	0.6333	ngfg_rs03000	-10.72	0.079918	182 -- 195	44 -- 57
54	0.02443	0.6333	ngfg_rs09625	-14.34	0.007864	148 -- 195	43 -- 92
55	0.02489	0.6333	ngfg_rs07995	-11.45	0.053049	189 -- 207	44 -- 62
56	0.02497	0.6333	ngfg_rs10675	-11.45	0.053244	238 -- 246	45 -- 53
57	0.02586	0.6333	ngfg_rs00195	-11.38	0.055370	3 -- 15	45 -- 59
58	0.02588	0.6333	ngfg_rs10785	-11.04	0.066985	158 -- 166	45 -- 53
59	0.02601	0.6333	ngfg_rs04060	-10.27	0.101651	263 -- 276	50 -- 63
60	0.02668	0.6333	ngfg_rs02155	-10.77	0.078070	189 -- 198	43 -- 52
61	0.02673	0.6333	ngfg_rs09895	-11.86	0.041690	290 -- 296	48 -- 54
62	0.02679	0.6333	ngfg_rs00355	-10.87	0.073841	234 -- 244	51 -- 61
63	0.02788	0.6333	ngfg_rs00440	-13.45	0.014944	78 -- 122	2 -- 54
64	0.02794	0.6333	ngfg_rs00325	-9.34	0.162271	182 -- 200	44 -- 61
65	0.02803	0.6333	ngfg_rs09540	-12.91	0.021498	108 -- 118	49 -- 59
66	0.02844	0.6333	ngfg_rs00585	-11.45	0.053086	117 -- 128	45 -- 55
67	0.02849	0.6333	ngfg_rs03480	-11.14	0.063268	209 -- 227	43 -- 60
68	0.02888	0.6333	ngfg_rs03230	-10.32	0.099337	171 -- 192	44 -- 63
69	0.02905	0.6333	ngfg_rs08855	-13.14	0.018423	173 -- 182	44 -- 53
70	0.02942	0.6333	ngfg_rs11270	-10.13	0.109767	270 -- 299	44 -- 62
71	0.02948	0.6333	ngfg_rs05460	-14.02	0.009991	1 -- 17	45 -- 61
72	0.03001	0.6333	ngfg_rs04815	-9.71	0.135544	43 -- 89	47 -- 92
73	0.03015	0.6333	ngfg_rs12085	-12.19	0.034128	243 -- 254	46 -- 61
74	0.03092	0.6359	ngfg_rs11035	-11.33	0.057075	135 -- 145	51 -- 61
75	0.03111	0.6359	ngfg_rs07340	-7.04	0.418383	184 -- 193	75 -- 84
76	0.03249	0.6481	ngfg_rs03025	-11.94	0.039574	1 -- 10	44 -- 53
77	0.03287	0.6481	ngfg_rs08455	-13.06	0.019507	162 -- 218	1 -- 54
78	0.03333	0.6481	ngfg_rs03120	-11.00	0.068665	107 -- 120	47 -- 60
79	0.03371	0.6481	ngfg_rs03510	-10.76	0.078189	192 -- 198	45 -- 51
80	0.03417	0.6481	ngfg_rs01805	-10.24	0.103489	110 -- 125	43 -- 58
81	0.03424	0.6481	ngfg_rs07550	-11.63	0.047735	29 -- 35	47 -- 53
82	0.03503	0.655	ngfg_rs00170	-9.56	0.145925	231 -- 248	43 -- 61
83	0.03585	0.6621	ngfg_rs02165	-9.31	0.164445	263 -- 279	45 -- 62
84	0.03632	0.6629	ngfg_rs07675	-10.90	0.072580	86 -- 103	43 -- 63
85	0.03685	0.6647	ngfg_rs11220	-10.86	0.074066	74 -- 94	45 -- 61
86	0.03994	0.6914	ngfg_rs07470	-10.47	0.091487	118 -- 132	43 -- 60
87	0.04056	0.6914	ngfg_rs02420	-9.96	0.119617	171 -- 191	40 -- 62
88	0.04062	0.6914	ngfg_rs04495	-10.48	0.091345	182 -- 197	45 -- 60
89	0.04064	0.6914	ngfg_rs09235	-12.10	0.036007	266 -- 288	16 -- 39
90	0.04078	0.6914	ngfg_rs11020	-10.81	0.076064	120 -- 126	47 -- 53

91	0.04111	0.6914	ngfg_rs00100	-13.40	0.015475	145 -- 211	9 -- 62
92	0.04157	0.6914	ngfg_rs04500	-10.10	0.111477	91 -- 108	48 -- 63
93	0.04194	0.6914	ngfg_rs01340	-9.65	0.139247	258 -- 271	47 -- 59
94	0.04341	0.7075	ngfg_rs03125	-9.52	0.148843	81 -- 100	9 -- 26
95	0.04393	0.7075	ngfg_rs00175	-7.08	0.413267	192 -- 223	32 -- 62
96	0.04473	0.7075	ngfg_rs11015	-9.95	0.119856	152 -- 164	50 -- 62
97	0.04481	0.7075	ngfg_rs10595	-11.32	0.057184	194 -- 210	43 -- 60
98	0.04579	0.7075	ngfg_rs00525	-10.35	0.097580	185 -- 192	47 -- 54
99	0.04707	0.7075	ngfg_rs08170	-10.43	0.093868	246 -- 252	47 -- 53
100	0.04732	0.7075	ngfg_rs09950	-9.95	0.120268	43 -- 60	44 -- 61
101	0.04764	0.7075	ngfg_rs08575	-10.57	0.087018	187 -- 199	50 -- 62
102	0.04946	0.7075	ngfg_rs01730	-10.95	0.070678	1 -- 12	46 -- 56
103	0.05009	0.7075	ngfg_rs02430	-11.94	0.039605	63 -- 77	47 -- 62
104	0.05048	0.7075	ngfg_rs03495	-9.69	0.136988	286 -- 295	51 -- 60
105	0.05103	0.7075	ngfg_rs11715	-11.04	0.067177	9 -- 17	45 -- 53
106	0.05155	0.7075	ngfg_rs11655	-6.70	0.469011	67 -- 107	50 -- 92
107	0.05158	0.7075	ngfg_rs10045	-9.42	0.156155	282 -- 293	47 -- 58
108	0.05236	0.7075	ngfg_rs11580	-7.91	0.303426	131 -- 150	43 -- 61
109	0.05267	0.7075	ngfg_rs06985	-10.50	0.090014	194 -- 207	47 -- 60
110	0.05278	0.7075	ngfg_rs11820	-10.71	0.080601	1 -- 15	43 -- 58
111	0.05371	0.7075	ngfg_rs11240	-10.50	0.090380	51 -- 66	47 -- 62
112	0.05413	0.7075	ngfg_rs01595	-10.34	0.098375	265 -- 281	20 -- 35
113	0.0545	0.7075	ngfg_rs00700	-10.52	0.089485	279 -- 296	40 -- 54
114	0.05457	0.7075	ngfg_rs01445	-9.50	0.150374	46 -- 105	37 -- 93
115	0.05473	0.7075	ngfg_rs05010	-11.01	0.068347	283 -- 300	43 -- 62
116	0.05477	0.7075	ngfg_rs01855	-9.01	0.189600	28 -- 38	52 -- 62
117	0.05478	0.7075	ngfg_rs11150	-9.73	0.134460	66 -- 73	46 -- 53
118	0.05482	0.7075	ngfg_rs01930	-10.18	0.106770	1 -- 29	14 -- 53
119	0.05518	0.7075	ngfg_rs01875	-10.06	0.113680	101 -- 130	43 -- 62
120	0.05559	0.7075	ngfg_rs03595	-9.70	0.135895	177 -- 200	43 -- 63
121	0.05617	0.7075	ngfg_rs08245	-8.61	0.225929	179 -- 232	51 -- 97
122	0.0563	0.7075	ngfg_rs05135	-10.48	0.091360	50 -- 61	52 -- 63
123	0.05689	0.709	ngfg_rs01240	-10.50	0.090173	203 -- 213	51 -- 61
124	0.05788	0.7133	ngfg_rs09955	-9.99	0.117700	191 -- 212	1 -- 22
125	0.05816	0.7133	ngfg_rs03355	-10.15	0.108672	40 -- 61	43 -- 61
126	0.0592	0.7203	ngfg_rs01115	-10.72	0.080119	138 -- 153	45 -- 62
127	0.06064	0.732	ngfg_rs05590	-9.52	0.148655	221 -- 231	74 -- 84
128	0.0622	0.7384	ngfg_rs08775	-9.25	0.169585	253 -- 267	46 -- 58
129	0.06235	0.7384	ngfg_rs09475	-10.84	0.074983	115 -- 129	43 -- 58
130	0.0629	0.7384	ngfg_rs04635	-10.12	0.109886	231 -- 249	45 -- 61
131	0.0631	0.7384	ngfg_rs07325	-10.12	0.109869	21 -- 52	43 -- 61
132	0.06395	0.7427	ngfg_rs11145	-8.60	0.227300	220 -- 231	49 -- 59
133	0.06584	0.7526	ngfg_rs04035	-10.68	0.081776	148 -- 156	45 -- 53
134	0.06679	0.7526	ngfg_rs11330	-12.23	0.033302	63 -- 78	48 -- 63
135	0.06809	0.7526	ngfg_rs03460	-8.67	0.220057	135 -- 142	46 -- 53
136	0.06835	0.7526	ngfg_rs00430	-7.71	0.328250	28 -- 37	52 -- 61
137	0.06838	0.7526	ngfg_rs05420	-9.92	0.122167	147 -- 157	52 -- 62

138	0.06838	0.7526	ngfg_rs11605	-9.94	0.120683	243 -- 249	45 -- 51
139	0.06904	0.7526	ngfg_rs05350	-10.35	0.097894	60 -- 79	43 -- 61
140	0.06969	0.7526	ngfg_rs11325	-8.35	0.253656	25 -- 36	50 -- 61
141	0.0697	0.7526	ngfg_rs03985	-7.33	0.377626	70 -- 91	34 -- 57
142	0.06972	0.7526	ngfg_rs02910	-9.12	0.180041	94 -- 105	43 -- 53
143	0.07262	0.7711	ngfg_rs02840	-7.19	0.398317	256 -- 267	47 -- 58
144	0.07278	0.7711	ngfg_rs06760	-10.72	0.079966	264 -- 281	46 -- 61
145	0.07454	0.7711	ngfg_rs08745	-7.76	0.321639	104 -- 115	50 -- 63
146	0.07469	0.7711	ngfg_rs10615	-11.70	0.045836	195 -- 222	33 -- 59
147	0.07492	0.7711	ngfg_rs10660	-9.60	0.142948	14 -- 67	51 -- 95
148	0.07638	0.7711	ngfg_rs05630	-7.01	0.422766	18 -- 29	51 -- 62
149	0.07698	0.7711	ngfg_rs08750	-11.24	0.059971	156 -- 171	49 -- 63
150	0.07733	0.7711	ngfg_rs01740	-10.45	0.092570	175 -- 200	44 -- 61
151	0.07735	0.7711	ngfg_rs08030	-9.78	0.130736	133 -- 151	38 -- 54
152	0.07781	0.7711	ngfg_rs01760	-9.66	0.138837	239 -- 250	51 -- 62
153	0.07883	0.7711	ngfg_rs08835	-11.98	0.038786	86 -- 93	45 -- 52
154	0.07887	0.7711	ngfg_rs10200	-10.06	0.113854	56 -- 68	41 -- 52
155	0.08013	0.7711	ngfg_rs09715	-5.81	0.607423	140 -- 187	13 -- 61
156	0.08052	0.7711	ngfg_rs03090	-8.28	0.261206	1 -- 17	43 -- 57
157	0.08065	0.7711	ngfg_rs07450	-10.24	0.103527	138 -- 144	47 -- 53
158	0.08106	0.7711	ngfg_rs01160	-9.40	0.157496	9 -- 17	52 -- 60
159	0.08116	0.7711	ngfg_rs01060	-9.64	0.140064	18 -- 27	47 -- 58
160	0.08124	0.7711	ngfg_rs09490	-10.26	0.102682	276 -- 292	44 -- 60
161	0.08187	0.7711	ngfg_rs11120	-7.03	0.419816	87 -- 117	43 -- 64
162	0.08198	0.7711	ngfg_rs09640	-8.14	0.276125	10 -- 47	13 -- 64
163	0.0839	0.7711	ngfg_rs05075	-10.15	0.108493	72 -- 82	48 -- 58
164	0.08431	0.7711	ngfg_rs11025	-9.80	0.129314	24 -- 33	52 -- 61
165	0.08452	0.7711	ngfg_rs07430	-11.76	0.044215	208 -- 222	49 -- 61
166	0.08503	0.7711	ngfg_rs09825	-9.49	0.151236	17 -- 24	44 -- 51
167	0.08542	0.7711	ngfg_rs00310	-11.73	0.044981	12 -- 19	46 -- 53
168	0.08571	0.7711	ngfg_rs01565	-9.82	0.128025	28 -- 44	43 -- 58
169	0.08654	0.7711	ngfg_rs01440	-9.06	0.184840	137 -- 204	29 -- 99
170	0.08664	0.7711	ngfg_rs05295	-10.13	0.109365	183 -- 200	42 -- 58
171	0.08669	0.7711	ngfg_rs09520	-9.96	0.119485	166 -- 230	54 -- 92
172	0.08842	0.7711	ngfg_rs09525	-8.94	0.195394	106 -- 116	51 -- 62
173	0.08863	0.7711	ngfg_rs01575	-10.64	0.083598	26 -- 39	45 -- 57
174	0.08871	0.7711	ngfg_rs00495	-9.42	0.156381	114 -- 121	46 -- 53
175	0.08887	0.7711	ngfg_rs07925	-9.29	0.166350	270 -- 281	13 -- 24
176	0.08909	0.7711	ngfg_rs03720	-7.37	0.372607	184 -- 195	43 -- 60
177	0.08938	0.7711	ngfg_rs01775	-9.59	0.143895	194 -- 233	4 -- 62
178	0.0921	0.7711	ngfg_rs12110	-9.52	0.148489	3 -- 14	43 -- 53
179	0.09267	0.7711	ngfg_rs06040	-9.09	0.182068	286 -- 295	44 -- 53
180	0.09307	0.7711	ngfg_rs06620	-9.07	0.184280	177 -- 196	43 -- 61
181	0.0932	0.7711	ngfg_rs03240	-6.76	0.460828	36 -- 49	44 -- 58
182	0.09343	0.7711	ngfg_rs00145	-9.81	0.129085	125 -- 134	49 -- 58
183	0.09364	0.7711	ngfg_rs01295	-8.87	0.201559	196 -- 209	43 -- 61
184	0.09395	0.7711	ngfg_rs03050	-10.02	0.116125	13 -- 44	36 -- 62

185	0.09408	0.7711	ngfg_rs06585	-9.31	0.164399	3 -- 21	47 -- 63
186	0.09519	0.7711	ngfg_rs11060	-9.59	0.144065	215 -- 239	43 -- 63
187	0.09528	0.7711	ngfg_rs06425	-10.44	0.093208	150 -- 162	47 -- 58
188	0.09722	0.7711	ngfg_rs03330	-8.40	0.247711	3 -- 49	50 -- 96
189	0.09724	0.7711	ngfg_rs01840	-8.27	0.261385	203 -- 213	52 -- 62
190	0.09863	0.7711	ngfg_rs06880	-8.03	0.289463	1 -- 13	50 -- 63
191	0.09994	0.7711	ngfg_rs04695	-9.98	0.118583	181 -- 191	50 -- 60
192	0.1002	0.7711	ngfg_rs07835	-8.32	0.256016	188 -- 200	52 -- 63
193	0.1012	0.7711	ngfg_rs05050	-7.76	0.321562	226 -- 248	1 -- 24
194	0.1012	0.7711	ngfg_rs11045	-9.56	0.145782	80 -- 90	49 -- 59
195	0.1017	0.7711	ngfg_rs00830	-12.05	0.037011	177 -- 226	9 -- 58
196	0.1043	0.7711	ngfg_rs00515	-9.52	0.149097	186 -- 222	33 -- 59
197	0.1044	0.7711	ngfg_rs07575	-4.77	0.764053	137 -- 143	49 -- 55
198	0.1051	0.7711	ngfg_rs00985	-8.97	0.192404	193 -- 205	49 -- 61
199	0.1054	0.7711	ngfg_rs02400	-10.70	0.080860	226 -- 234	50 -- 58
200	0.1063	0.7711	ngfg_rs03235	-7.68	0.332299	103 -- 112	24 -- 33

DANKSAGUNG

An dieser Stelle möchte ich mich bei allen bedanken, die zum Entstehen dieser Thesis beigetragen haben.

Ein großer Dank an Dagmar Beier, für die Betreuung in den letzten Jahren und für die viele Zeit, die du in mein Projekt investiert hast.
Auch möchte ich mich bei Thomas Rudel bedanken, für die Ideen zu meinem Projekt und dass ich die Möglichkeit bekommen habe, noch ein halbes Jahr länger am Lehrstuhl zu bleiben.
Mein Dank gilt auch Cynthia Sharma, für die Übernahme des Zweitgutachtens und die wertvollen Beiträge im Rahmen der Thesis Committee Meetings.

Weiterhin möchte ich mich bei Utz Fischer und Archana Prusty dafür bedanken, das Isotopenlabor der Biochemie während der Umbauarbeiten mitnutzen zu können und bei Claudia Höbartner und Carolin Scheitl dafür, dass ich ihren Phosphor-Imager nutzen konnte, als unserer ausgefallen ist.
Ein Dank gilt auch meinen Kooperationspartnern für die gute Zusammenarbeit, Bruno Hüttel für die Transkriptomanalyse und Wolfgang Eisenreich und Thomas Steiner für die Metabolom-Untersuchung.

Ganz herzlich möchte ich mich beim gesamten Lehrstuhl für Mikrobiologie bedanken, es war schön mit euch zusammenzuarbeiten! Dabei möchte ich erst einmal Susi Bauer hervorheben, die mir mit Rat und Tat immer zur Seite stand. Meine Studenten, Julia, Eva-Maria, Johannes und Katharina, die fleißig meine Arbeit unterstützt haben und mit denen ich gerne mein Labor geteilt habe. Dann ganz besonders die Görlz und Bois – ohne euch wäre es nie so schön gewesen, deshalb danke Adriana, Franzi, Kathrin, Max, Micha, Naddl, Pargev, Regi, Sophie und Tobi!

Mein abschließender Dank gilt meiner Familie. Insbesondere meinen Eltern, meinen Schwestern und meiner Tante Ines. Danke für eure Liebe und Unterstützung, eure Zeit und nicht zu vergessen das gute Essen ;)

EIDESSTATTLICHE ERKLÄRUNG

Eidesstattliche Erklärungen nach §7 Abs. 2 Satz 3, 4, 5
der Promotionsordnung der Fakultät für Biologie

Eidesstattliche Erklärung

Hiermit erkläre ich an Eides statt, die Dissertation: „Funktionelle Charakterisierung kleiner nicht-kodierender RNAs in Neisseria gonorrhoeae“, eigenständig, d. h. insbesondere selbständig und ohne Hilfe eines kommerziellen Promotionsberaters, angefertigt und keine anderen, als die von mir angegebenen Quellen und Hilfsmittel verwendet zu haben.

Ich erkläre außerdem, dass die Dissertation weder in gleicher noch in ähnlicher Form bereits in einem anderen Prüfungsverfahren vorgelegen hat.

Weiterhin erkläre ich, dass bei allen Abbildungen und Texten bei denen die Verwertungsrechte (Copyright) nicht bei mir liegen, diese von den Rechtsinhabern eingeholt wurden und die Textstellen bzw. Abbildungen entsprechend den rechtlichen Vorgaben gekennzeichnet sind sowie bei Abbbildungen, die dem Internet entnommen wurden, der entsprechende Hypertextlink angegeben wurde.

Affidavit

I hereby declare that my thesis entitled: „Functional characterization of small non-coding RNAs of Neisseria gonorrhoeae” is the result of my own work. I did not receive any help or support from commercial consultants. All sources and / or materials applied are listed and specified in the thesis.

Furthermore I verify that the thesis has not been submitted as part of another examination process neither in identical nor in similar form.

Besides I declare that if I do not hold the copyright for figures and paragraphs, I obtained it from the rights holder and that paragraphs and figures have been marked according to law or for figures taken from the internet the hyperlink has been added accordingly.

Würzburg, den